Metals at
High Temperatures

By
FRANCES HURD CLARK
U. S. Navy Material Catalog Office

Contents

Preface

In the preparation of this book, my intention has been simply to compile the information recently made available on the properties of metals at elevated temperatures. Especially since the last World War engaged metallurgical interest in the gas turbine, these data have been forthcoming at a rapid rate. It is therefore now timely to assemble the observations of many laboratories for comparison and reference.

At high temperatures, the significant deformations of stressed machine parts are plastic in nature. If an adequate analytic description of the plastic behavior of materials existed, there would be little reason for the detailed examination of so many metals and alloys under particular states of stress and temperature. However, the theoretical prediction of plastic behavior is still very uncertain and no simple formula can be offered to forecast the flow of materials subjected to stress at temperatures approaching the melting point.

To present the data in a revealing light, it has seemed wise to include a chapter on the phenomenological aspects of plastic flow. This chapter, Chapter 1 of the text, surveys the theoretical attempts to discover the laws governing plastic behavior. This necessarily involves rather more of an excursion into the fields of elasticity and viscoelasticity than would ordinarily be found in a metallurgical text. For this reason, Chapter 1, on the theoretical aspects of plasticity, is somewhat expanded in content.

In the preparation of the material, I was generously assisted by the staffs of the professional societies, notably the American Society for Testing Materials, the American Society of Mechanical Engineers, the American Institute of Mining and Metallurgical Engineers, and the American Society for Metals. An appreciation is also offered here of the many contributions of the industrial research organizations which have for so many years devoted their facilities to the examination of the high temperature properties of metals, with prompt dissemination of the findings for public use. Their efforts have resulted, incidentally, in the data presented here, and, more importantly, in the consequent development of many new alloys of remarkable temperature resistant properties. In particular, I am grateful to the following organizations for useful material and helpful suggestions: the International Nickel Company, the Westinghouse Electric Corp., the Baldwin-Southwark Division of the Baldwin Locomotive Works, Gebrüder Sulzer, the Timken Roller Bearing Company, the Babcock and Wilcox Tube Company, the M. W. Kellogg Company, the American Brakeshoe Company, the Haynes-Stellite Company, and the high temperature research laboratory under the direction of Professor Nicholas Grant at the Massachusetts Institute of Technology.

Chapter 1

Introduction and Theoretical Aspects

A. INTRODUCTION

This book treats of the mechanical and metallurgical properties of metals and alloys at elevated temperatures. Industrial uses of metals at high temperatures have greatly increased and the temperatures required for many operations are steadily rising. The chemical and petroleum industries utilize low alloy steels and stainless steels at moderately elevated temperatures below 538°C (1000°F) under severely corrosive conditions. Industrial furnaces operating in the neighborhood of 1000°C (1832°F) consume a large quantity of heat-resistant alloys. These furnace parts must resist oxidation under conditions of relatively low loading. The more recent development of the gas turbine has very greatly sharpened metallurgical interest in high temperature properties. The gas turbine demands materials operating in the neighborhood of 815°C (1500°F) but at high stresses due primarily to centrifugal forces. Efficient operation of gas turbines demands an ever-increasing gas inlet temperature for successful competition with other means of providing power.

It is the purpose of this book to present currently available information on the properties of metallic materials at elevated temperatures for the use of the design engineer. Up to the present such data have not been available in any single source. For such readers, it is hoped that the text will serve as a useful reference.

In high-temperature operation, the behavior of metallic parts depends more upon their plastic properties than upon the elastic properties which dominate their behavior at low temperatures. The plastic properties are more difficult to characterize, since the plastic deformations are not proportional to the applied loads. In the high temperature regime, a part may creep under constant load so that in time the plastic deformation much exceeds the elastic strain. The tendency of the part to flow, the deformation continuously increasing in time, is a high temperature property of immediate concern to design engineers. Metallurgists recognize additional properties necessary to successful operation at high temperature.

The decisive characteristics of metals at elevated temperatures are their resistance to surface changes and their resistance to flow. The tendency

toward scale formation of the metal under the condition of no load must be evaluated at the temperature and in the atmosphere selected for service. One chapter of this book is devoted to the factors involved in scaling and to data on the depth of scale formation occurring in certain heat-resistant alloys. The other characteristic—that of flow—is of importance in all industrial applications where metals are subjected to loading at elevated temperatures. The main portion of this text is directed to the phenomenon of flow in metallic systems, to methods of measuring flow, and to the results of flow tests on many metals and alloys.

I. Historical

In the early history of creep testing, investigators reported the effect of stressing metals for long periods at room temperature or for short periods at high temperatures. In 1885, copper wires and silver wires were stressed at room temperature by Howe for as much as 6500 hours at 60, 70, and 80 per cent of the breaking load. Recordings were made of the stretch of the wires as a function of time[23]. Other early creep tests on copper, iron, tin, and lead were reported by Andrade in 1911 and by Chevenard in 1919[2,9]. Constant-stress measurements were made by Andrade in 1914, but their full significance was not appreciated until recently after many years of experimental work with constant-load conditions[2].

To explain the fracture of tin alloys close to the melting point, it was suggested in 1912 by Rosenhain and Ewen that metals, when stressed at high temperature, pass through a critical range where the nature of the fracture changes from transcrystalline to intercrystalline. Because of grain boundary sliding, the metal loses its ability to deform and breaks in a brittle manner. The temperature at which this occurs was called the equicohesive temperature[40]. Later, Jeffries and Archer observed a similar effect in steels after prolonged heating at high temperature[24].

Early work on rapid testing of steel at elevated temperature was reported in 1921 by Dupuy, but no creep values were given[11]. However, by 1922, Dupuy published tests on nickel and its alloys at high temperature[9]. In 1924 actual measurements of the creep of a chromium steel and a chromium-nickel steel when stressed at 8.5 tons per square inch over a temperature range of about 600 to 900°C were reported by Dickenson[10]. At about this time, the industrial use of metals stressed at high temperature was expanding rapidly, and it was suggested by French that allowance must be made by design engineers for creep of metals under such service conditions[13].

II. Arrangement of Data

The emphasis of this book has been placed on the high-temperature properties of plain-carbon steels, alloy steels, and the special heat-resistant alloys (Co-Ni-Cr-Mo, etc.) developed for turbine applications. A smaller

part is devoted to the lower-melting metals, especially Al and Mg alloys, which have important commercial uses at moderately high temperatures. In the course of two decades, the results of a great many tests have been published. The data presented here have been selected on the basis of most recent observations, provided that a comprehensive history of the material under test has been recorded.

In addition, Chapter 2 describes test methods and equipment for high-temperature investigations. There is also a chapter (9) on manufacturing processes and their relation to the high-temperature properties of the product. The results of tests on scaling of certain oxidation resistant alloys are given in Chapter 11. Also, there will be found in the extension to this chapter a phenomenological account of the plastic behavior of metallic materials.

In the selection of the data to be presented, an effort has been made to include the method of manufacture and heat treatment as the prior history of the material influences the resistance of the metal to flow. The room-temperature strength properties are given for certain alloys where such information is not readily available elsewhere. The high-temperature strength properties are presented in the general order of the short-time tensile strength, the stress-rupture strength, and the creep resistance. These are followed by other high-temperature properties from such tests as hot fatigue, hot impact, and hot hardness. Not all tests have been conducted for all materials listed. Classification is in general arranged in the following sequence.

Tables of High Temperature Properties

1. Chemical composition
2. Processing data
3. Room temperature properties compared to high temperature properties
4. Short time tensile strength
5. Stress rupture strength
6. Creep strength
7. Design data
8. Hot fatigue strength
9. Hot impact strength
10. Change in the elastic constants with temperature
11. Change in the coefficients of thermal expansion
12. Change in the thermal conductivity
13. Hot hardness
14. Relaxation tests
15. Influence of combined stresses

B. Theoretical Aspects

I. The Solid and the Fluid States

As the operating temperature approaches the melting point, metals enter upon the shadowy middle ground wherein the distinction between the solid and the fluid states loses its sharpness. The distinction comes out of the observation that in the fluid states, material is incapable, or almost incapable, of supporting any shearing stress. Having this property, fluid material may be deformed in shape, without any change in volume, by the expenditure of little or no work. Such deformations may be classified as *permanent*, since they persist after removing the applied force.

Permanent deformations are to be distinguished from *reversible* strains, which do disappear upon removal of the applied forces. Even in fluids, an actual deformation is usually a composite of both types. A perfect liquid is supposed to sustain no shearing stress whatsoever, and so may be deformed in shape without work. A perfect liquid can, however, sustain the stress system of simple hydrostatic pressure, the corresponding strain being a change in volume, finite although often very small. The applied forces do work in compressing the liquid; this work is stored in the material as the potential energy of the strain and is returned to the environment when the forces are removed, as the material returns to its original volume. That is to say, the liquid behaves elastically under hydrostatic pressure.

Of course, actual fluids are imperfect. They exhibit a viscous resistance in shear which allows them to sustain some shearing stress by flowing. To this degree, they partake of the cohesive properties of solids. Solids, on the other hand, exhibit a weakness in shear which at higher temperatures becomes increasingly fluid-like. The fluid-like properties of metals, which largely determine their engineering usefulness in high-temperature applications, are the principal concern of the studies reported in the following chapters. Unfortunately, the description of the fluid behavior of metals is much less simple than the description of the viscous behavior of fluids. The properties of metals come into sharper focus, however, if viewed in the light of the relatively uncomplicated theory of viscosity.

II. The Viscosity of Fluids

The nature of viscous flow is most vividly portrayed in a model of simple geometry, as illustrated by Fig. 1-1. Here a volume of fluid is confined between parallel plates. We can suppose the bottom plate to be fixed and identify its surface with the plane $y = 0$ of a rectangular coordinate system. If now the upper plate, whose surface is the plane $y = y_0$, is displaced by the distance u_0 in the x direction, the confined fluid experiences a deformation in simple shear. As the layer of fluid in contact with the upper plate moves through the distance u_0 along with the plate, the layer in contact

with the bottom plate remains at rest, while a layer at height y above the bottom moves through the distance $u = (u_0/y_0)y$.

Thus layers at different heights move different distances, the relative displacement of layers separated in height by dy being $du = (u_0/y_0)dy$. The relative displacement for unit separation in height, *i.e.*, u_0/y_0, is the shearing strain, γ. In a deformation of this kind, particles of the fluid which lay in a plane before the displacement also lie in a plane after the displacement; an element of the material which had initially a rectangular cross-section accordingly passes into an element whose cross-section is the oblique parallelogram of the figure.

It would not be easy to set up an experiment on the model of Fig. 1-1 to determine the relation between the applied forces F, and the rate of deformation of the fluid. Among other difficulties, the material could not be in torsional equilibrium under the action of the forces F alone. In addition, the plates must exert normal forces upon the material, to prevent rotation of the whole. We may, however, suppose these to be small
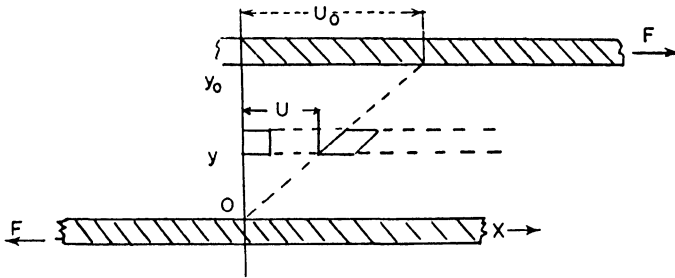
Fig. 1-1. Schematic representation of viscous flow.

enough so that their effect in compressing the fluid is insignificant. The hypothetical experiment may then at least be envisaged. It would be observed that the rate of simple shear depends on the tangential force per unit area, that is, the shearing stress $\tau = F/A$, where A is the total area of the plates. This tangential stress is transmitted throughout the bulk of the fluid, being exerted along every plane parallel to the plates.

The strain rate, $d\gamma/dt \equiv \dot{\gamma}$, would be found in this hypothetical experiment to be constant if τ is constant, and so can be written as

$$\dot{\gamma} = \frac{1}{\eta}\tau \tag{1}$$

where the coefficient of viscosity η measures the frictional resistance at the applied stress. For many fluids (and most solid materials), η cannot be taken as a constant, but rather must be regarded as dependent on the strain rate.

For certain fluids deforming at rates so low that the flow is laminar and free from turbulence, η *is* approximately constant over a considerable

range in γ. In this case the flow is described as Newtonian or truly viscous. The dotted line in Fig. 1-2 describes this linear relation between stress and strain rate. The behavior of other fluids and nearly all solids is less simple, a typical dependence of strain rate upon stress being indicated by the solid line in Fig. 1-2. Such a nonlinear relationship is perhaps most simply formulated in the empirical expression

$$\dot{\gamma} = k(\tau - \tau_0)^n \tag{2}$$

for which the three constants τ_0, k, n must be determined. Flow of this type is described as quasi-viscous. The nonlinear dependence of strain rate upon stress creates formidable mathematical difficulties in using
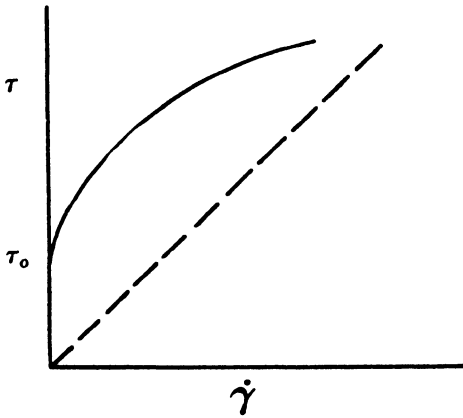
Fig. 1-2. Stress (τ) versus strain rate ($\dot{\gamma}$). The broken line represents viscous flow. The solid curve represents an empirical relation $\dot{\gamma} = k(\tau - \tau_0)^n$ or quasi-viscous flow. The stress (τ_0) is the value for instantaneous strain.

observations made in simple shear for the prediction of the behavior of quasi-viscous materials under other stress systems.

If the material is Newtonian, on the other hand, knowledge of the behavior in simple shear suffices for the easy prediction of the behavior in different circumstances. This may be illustrated by considering the steady flow of a viscous substance in a capillary tube. It is by this means that viscosity is measured practically.

Suppose the tube to be of radius R and length L, with the pressure P_1 maintained at the upper end, and $P_2 < P_1$ at the lower, as in Fig. 1-3. In steady flow, any coaxial cylinder of radius r, say, is in equilibrium under the forces acting on it. The unbalanced force acting on the end faces of such a cylinder is $\pi r^2 (P_1 - P_2)$. This force must therefore be equilibrated by the tangential force exerted on the lateral surface of the cylinder by the fluid outside, that is, by the viscous drag.

For the typical volume element, take a cylindrical shell of radius r, thickness dr. On a lateral surface of this element, the tangential force

per unit area is $r(P_1 - P_2)/2L$, since the total force is $\pi r^2(P_1 - P_2)$ and the total area is $2\pi rL$. The fluid outside the shell flows more slowly, and exerts an upward drag on its outer surface. Inside the shell, the fluid is moving more rapidly, and the tangential force on the inner surface is
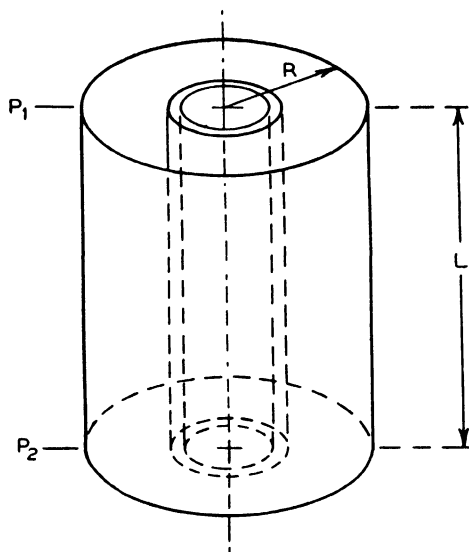
Fig. 1-3. Flow in a capillary tube.

directed downward. Therefore, the fluid contained in the shell is in shear, the stress being

$$\tau = r(P_1 - P_2)/2L.$$

The strain is measured by the displacement of the fluid along the inner surface relative to that at the outer. If we call the fluid velocity at distance r from the axis $v(r)$ then the strain rate $\dot\gamma$ is dv/dr. But $\dot\gamma = (1/\eta)\tau$, so that

$$\frac{dv}{dr} = \frac{r(P_1 - P_2)}{2L\eta}.$$

The velocity within the shell is found by integrating this equation. Since the fluid in contact with the wall of the tube is stationary,

$$v(r) \equiv \int_R^r \frac{dv}{dr}\,dr = \frac{(P_1 - P_2)}{2L\eta} \int_R^r r\,dr = \frac{(P_1 - P_2)}{4L\eta}\,(r^2 - R^2),$$

which shows that the distribution of velocity within the tube is parabolic. The total rate of discharge is found, by summing the contributions from all the elementary shells, to be

$$V = \int_0^R v(r)2\pi r\,dr = \frac{\pi R^4(P_1 - P_2)}{8L\eta},$$

which is Poiseuille's Law.   In the common apparatus for the measurement of viscosity, V is noted for a given tube and pressure difference, and η determined by the formula.

The formula also illustrates the useful fact that wherever the relation between shear stress and shear strain (strain rate) is linear, the relation between uniaxial stress and strain (strain rate) is also linear.

Atomic Model of Viscosity. Fluid materials in both the gaseous and liquid states exhibit the phenomenon of viscosity.   In the gaseous state, which is distinguished by complete atomic or molecular disorder, the phenomenon has an easily apprehended explanation.   If we return to the model of simple shear presented in Fig. 1-1, we observe that, in a lamina of the fluid at the height y, the average particle velocity in the x direction exceeds that in the next lamina below, and is itself exceeded by the mean particle velocity in the next lamina above.   On account of thermal diffusion, some of the particles from the y lamina will wander into the lamina above, where, on the average, their lower velocities will bring them into collision with the faster-moving particles of the upper lamina in such a way as to convert some of the transport momentum of these particles into the random motions of heat vibration.   Thus to sustain a higher velocity in the upper lamina, the applied force must continuously do work.   The particles of the y lamina which diffuse into the lower lamina also contribute to the resistance of the liquid to shear.   In collision with the slower-moving particles, they induce an increase in momentum which must be resisted by the shearing force.

The diffusion model of viscosity is less satisfactory for liquids and unacceptable for solids.   In both states the constituent particles are more densely packed, so that the motion of any particle is intimately dependent upon that of its neighbors.   Close packing implies a certain degree of order in the molecular array which, in the extreme case of crystalline solids, extends to easily measurable distances through the material.   In the case of liquids and amorphous solids, the structure is less systematic; in liquids, certainly, disorder in the aggregation is so conspicuous that any order is difficult to discern.   Nevertheless, if a point in a fluid could be examined sufficiently closely, there would be found a partial order of the molecules of the sort depicted schematically in Fig. 1-4.   Herein the molecules are for the most part closely packed, the array being disturbed by the presence of a hole.   In solids, such imperfections are comparatively few and far between, so that the motion of any molecule entrains the motion of many others.   In liquids, we must consider that the holes are very numerous, so that the regions of even semi-ordered structure are quite localized.   In this event, a particle may be free to slip into an adjacent hole without any

disturbance to the molecular arrangement more than a few angstroms distant.

With this model, we can suppose that at any instant a typical particle in a fluid is constrained by the action of its neighbors to an equilibrium position of minimum potential energy about which it executes only small vibrations according to its thermal energy. An average particle is as likely to have a hole to its right as to its left, so that we can make a repre-
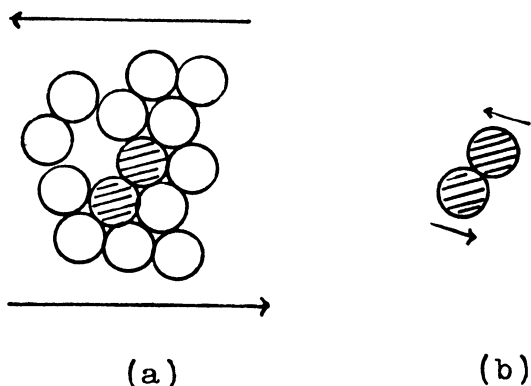
Fig. 1.4. Atoms subjected to a shear stress.
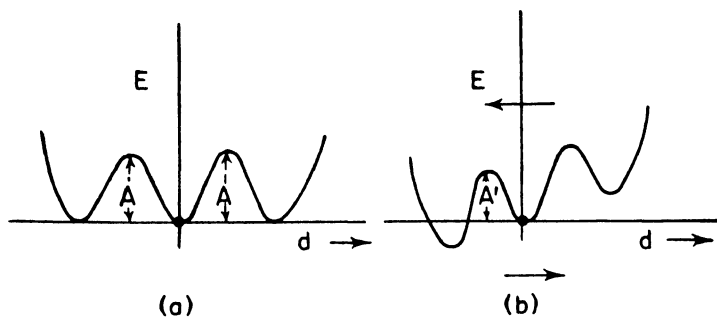
Fig. 1-5. Potential energy for a particle adjacent to holes before and after the application of shearing stress. d—displacement; E—energy.

sentation of the variation in its potential energy with displacement in this horizontal direction as in Fig. 1-5a. The drawing implies that the typical particle occupies a position of relatively close packing when the displacement *d* is zero. To move from this position, it must displace slightly the close packed particles in the neighborhood, storing some energy in a local elastic strain. The presence of nearby holes is indicated by the other potential minima to the right and left. If *d* becomes so great as to exceed

the potential maximum, the particle drops into the next hole.   The original closeness of packing is recovered, and the stored energy is reconverted to the kinetic energy of thermal vibration.

The thermal energy of the typical particle is continually being altered by contributions from the random thermal motion of its neighbors.   In time, its thermal energy may surpass the "activation energy" A, and it will slip into an adjoining hole.   In the case depicted, a transition in either direction is equally likely, and on the average no deformation of the material occurs.   If, however, there is superposed a shearing stress, the potential barrier in the favored direction is lowered while that in the contrary direction is raised, as shown in Fig. 1-5b.   Since the typical particle achieves high thermal energies only infrequently and lower thermal energies relatively often, there is a higher probability that the transition, if it occurs, will be in the preferred direction.   Ordinarily, a particular particle would not in fact have a hole on either side; rather, there would only be found as many particles favorably situated for shear in one direction as another.   In the illustration of Fig. 1-4, the shaded particles are favorably situated for microscopic shear in the direction of the arrows, which occurs whenever the upper particle achieves sufficient thermal energy to displace elastically the obstructing atom.   In the following, a hole will be considered an imperfection only in respect of the particle for which it affords a possible transition in the preferred direction.

This model can be given a quantitative interpretation with the help of the Einstein-Boltzmann equation for the frequency of local fluctuations in thermal energy.   This equation states that

$$\nu_i = Ce^{-(A_i/kT)}$$

where ν_i is the number of times per second that the thermal energy within an elementary volume, V_i, of the material is expected to exceed the activation energy A_i at that point.   In this expression, k is Boltzmann's constant, T is the absolute temperature, and C is a constant of proportionality.   Whenever this occurs, an elementary shear strain in the volume V_i results.   The rate at which the volume V_i is contributing to the gross strain of the material is

$$\Delta_i\dot{\gamma} = \nu_i\Delta_i\gamma$$

where $\Delta_i\gamma$ is the contribution of the microscopic transition in V_i to the macroscopic strain.   If we suppose these to be independent, then the macroscopic strain rate is

$$\dot{\gamma} = \sum_i \Delta_i\dot{\gamma}$$

or

$$\dot{\gamma} = C \sum e^{-(A_i/kT)}\Delta_i\gamma. \tag{3}$$

In the absence of any applied stress, the macroscopic shear strain vanishes or

$$\dot{\gamma} = C \sum_i e^{-(A_i/kT)} \Delta_i \gamma = 0. \tag{4}$$

In the presence of an applied shearing stress, the activation energies in the favored direction will be reduced from the values A_i to smaller values A_i'. For very viscous fluids and particularly for solids, the bias due to the applied stress is very slight. One would therefore expect that such reduction in the activation energies might be expressed by the linear approximation,

$$A_i' = A_i - a_i \tau \tag{5}$$

where τ is the applied stress. It will follow directly that this approximation implies Newtonian flow. For non-Newtonian fluids and solids, the linear approximation does not hold.

Replacing the A_i of the unstressed material in Eq. (3) by the reduced values given by Eq. (5), we have for the strain rate in the preferred direction

$$\dot{\gamma} = C \sum_i e^{-(A_i - a_i \tau)/kT} \Delta_i \gamma. \tag{6}$$

This equality is unaffected if, by Eq. (4), we subtract

$$C \sum_i e^{-(A_i/kT)} \Delta_i \gamma = 0$$

obtaining

$$\dot{\gamma} = C \sum_i e^{-(A_i/kT)} (e^{a_i \tau/kT} - 1) \Delta_i \gamma. \tag{7}$$

Since the reduction in activation energy by the stress field is small, $\exp(a_i\tau/kT)$ is approximately $1 + a_i\tau/kT$, and the parenthesis in Eq. (7), collapses to $a_i\tau/kT$. Furthermore, the activation energy A_i is unlikely to vary much from point to point in the material. Little error is introduced by replacing A_i by its mean value A in each term of summation, so that

$$\dot{\gamma} = \tau \left(\frac{C'}{kT} \right) e^{-(A/kT)}$$

where

$$C' = C \sum_i a_i \Delta_i \gamma$$

is a constant of the material. This is the equation of viscous flow

$$\dot{\gamma} = \frac{1}{\eta} \tau \tag{1}$$

with the coefficient of viscosity given by

$$\frac{1}{\eta} = \frac{C'}{kT} e^{-(A/kT)}. \tag{8}$$

Thus the mechanical model yields the prediction that strain rate is approximately proportional to stress which, as has been said, is not always characteristic even of fluids, and which is seldom characteristic of solids.

The mechanical model has, however, predicted the variation of viscosity with temperature in a way which is qualitatively correct. The predicted rapid decay of viscosity with increasing temperature is a matter of common experience. For many substances, this description of the temperature dependence of viscosity is also *quantitatively* reliable over a considerable range in temperature.
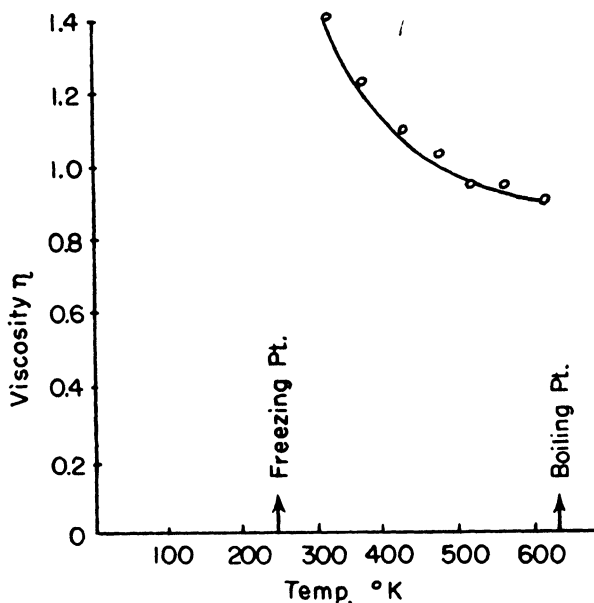
Fig. 1-6. Variation of viscosity (centipoises) with temperature for mercury from 50 to 350°C. The dots record the measured values; the solid curve is a graph of the formula $\eta = (kT/C')$ exp (A/kT).

For example, the dots of Fig. 1-6 record measured values of the viscosity of liquid mercury over almost the complete temperature range between freezing and boiling. The solid curve is a graph of the formula $\eta = (kT/C')\exp(A/kT)$ with the constants C' and A evaluated to match the data at the extremes of the range. The deviations of the measured values are small, and it is evident that the relation affords a useful approximation in this case. For other fluids, the agreement is less satisfactory. In any event, the formula must necessarily fail at the temperatures for which change of state occurs.

III. Stress and Strain

In the following, it will be helpful to have in mind the description of stress and strain which is conventional in the theory of elasticity. In general, the description of the state of stress at a point P in the material requires the specification of six independent components of a stress tensor. Similarly, the state of strain is described by specifying six independent components of a strain tensor. The behavior of the material is characterized by a set of stress-strain relations, which express the components of stress in terms of the components of strain, or vice versa. The physical
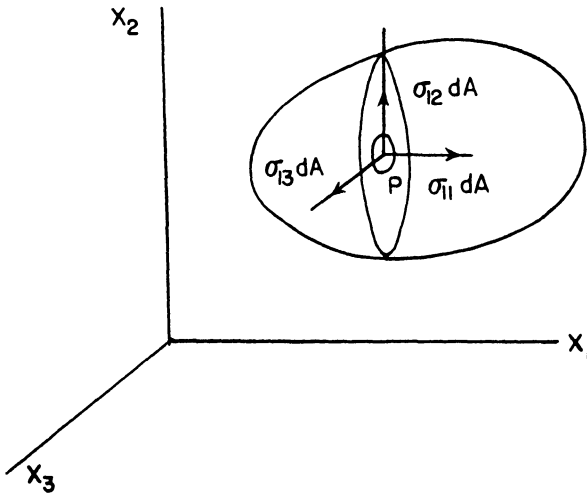
Fig. 1-7. Stress components at a point P for the orthogonal axes X_1 and X_2.

significance of the stress and strain components, and of the relations between them, will be examined in this section.*

Analysis of Stress. Consider a solid body which is in equilibrium under external forces applied at the boundary surface. Suppose, as in Fig. 1-7, that an interior point P is located by coordinates x_1, x_2, x_3 in respect to a rectangular system of reference axes, of arbitrary orientation. Through P pass a plane normal to the x_1 axis, dividing the body into a left-hand part and a right-hand part. Ordinarily, the left-hand part will not be in equilibrium under the external forces alone, but will also be acted on by the right-hand part, the interior forces being transmitted through the dividing plane.

* The material of the section is taken from lecture notes of Professor W. Prager of Brown University.

Let dA be an elementary area of this plane containing the point P. The force exerted through dA on the left-hand part need not be normal to dA. If it has a normal component, call it $\sigma_{11}dA$, where σ_{11} is the normal force per unit area. The tangential component of the force may itself be resolved into components parallel to the x_2 and x_3 axes. Call these $\sigma_{12}dA$ and $\sigma_{13}dA$, respectively. The three numbers σ_{11}, σ_{12}, σ_{13} define the *stress vector* at P for dA oriented normal to the x_1 axis, as indicated by the leading subscript.

Next let the dividing plane be rotated about P until it is normal to the x_2 axis. The force now exerted through the elementary area dA upon the lower part of the body will ordinarily be different from the force described in the preceding paragraph, which was exerted by the right part upon the left part. We can characterize this new force by the normal component $\sigma_{22}dA$, and the tangential components, $\sigma_{21}dA$ and $\sigma_{23}dA$. The leading subscript indicates that for this stress vector, dA is taken normal to the x_2 axis; the second subscript identifies the direction of the component.

The *state of stress* at P is completely determined if the force transmitted through dA is specified for three orthogonal orientations of the dividing plane. So finally, rotate the plane until it is normal to the x_3 axis, and note the components $\sigma_{31}dA$, $\sigma_{32}dA$, and $\sigma_{33}dA$. This set of nine stress components serves to determine the force transmitted through dA, regardless of its orientation.

However, not all of these nine components are independent. The material in the vicinity of P is in equilibrium; if we were to consider the forces acting on an elementary cube containing P, it would appear that moment equilibrium for the cube requires $\sigma_{ij} = \sigma_{ji}$. Therefore, the 3×3 array of stress components is symmetrical, the values of three off-diagonal elements being determined by the other three.

To determine the force transmitted through an element dA of the dividing plane, when this has an arbitrary orientation, we can consider the equilibrium of an elementary tetrahedron containing P. Take three of the faces of this tetrahedron parallel to the coordinate planes, and the fourth as the dividing plane, as in Fig. 1-8. Suppose the dividing plane is normal to a unit vector $\mathbf{n}$, whose projections n_1, n_2, n_3 on the coordinate axes are its direction cosines in this reference system. Locate the dividing plane on this normal so that the area of the slant face of the tetrahedron is dA. Then the areas of the other three faces are n_1dA, n_2dA, and n_3dA, respectively, and the forces transmitted through them are in proportion, the constants of proportionality being the σ's. Equilibrium of the tetrahedron requires that the stress vector $\mathbf{S}_n$ on the oblique face have components in the coordinate directions which equilibrate corresponding

components of the forces on the other three faces. Therefore, we have immediately,

$$\left.\begin{array}{l} S_{n_1} = n_1\sigma_{11} + n_2\sigma_{21} + n_3\sigma_{31} \\ S_{n_2} = n_1\sigma_{12} + n_2\sigma_{22} + n_3\sigma_{32} \\ S_{n_3} = n_1\sigma_{13} + n_2\sigma_{23} + n_3\sigma_{33} \end{array}\right\} \tag{9}$$

Evidently, for a given state of stress, the values of the several stress components depend upon the arbitrary orientation of the reference axes. To find the way in which these components vary as the reference axes are rotated, we need next to find the projection of the stress vector $\mathbf{S}_n$ on an arbitrary direction determined by the unit vector $\mathbf{m}$, say, whose direction cosines relative to the given reference axes are m_1, m_2, m_3. This is
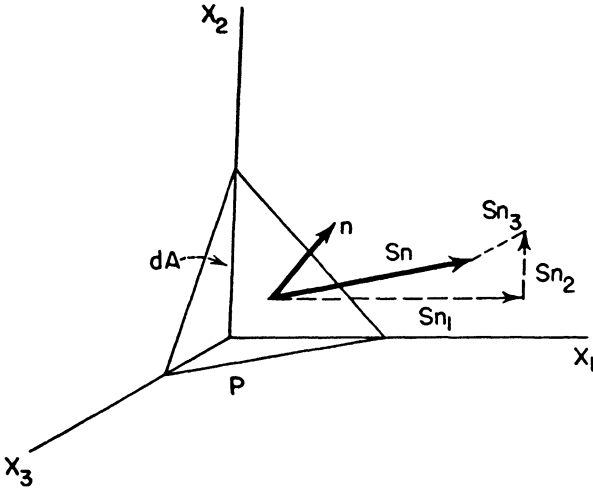
Fig. 1-8. Stress on an inclined plane.

easily accomplished by summing the projections of the three components on the m direction:

$$S_{nm} = S_{n_1} m_1 + S_{n_2} m_2 + S_{n_3} m_3.$$

When by Eq. (9) the S's are evaluated in terms of the σ's, the expression is less simple, *viz.*,

$$\left.\begin{array}{l} S_{nm} = \sigma_{11}n_1m_1 + \sigma_{21}n_2m_1 + \sigma_{31}n_3m_1 \\ \quad + \sigma_{12}n_1m_2 + \sigma_{22}n_2m_2 + \sigma_{32}n_3m_2 \\ \quad + \sigma_{13}n_1m_3 + \sigma_{23}n_2m_3 + \sigma_{33}n_3m_3 \end{array}\right\} \tag{10}$$

Now suppose that the original reference axes are rotated into a new orientation, referred to which the coordinates of P are x_1', x_2', x_3'. Let

the direction cosines of the axes in the new orientation referred to the old be

$$\alpha_{ip} = \cos(x_i, x_p'), \quad i, p = 1, 2, 3. \tag{11}$$

Then to find σ_{11}', the force in the x_1' direction exerted across unit area normal to this direction, we must in Eq. (10) identify n_1 and m_1 with α_{11}, n_2 and m_2 with α_{12}, and n_3 and m_3 with α_{13}. This gives

$$\begin{aligned}
\sigma_{11}' = {} & \sigma_{11}\alpha_{11}^2 + \sigma_{21}\alpha_{12}\alpha_{11} + \sigma_{31}\alpha_{13}\alpha_{11} \\
& + \sigma_{12}\alpha_{11}\alpha_{12} + \sigma_{22}\alpha_{12}^2 + \sigma_{32}\alpha_{13}\alpha_{12} \\
& + \sigma_{13}\alpha_{11}\alpha_{13} + \sigma_{23}\alpha_{12}\alpha_{13} + \sigma_{33}\alpha_{13}^2 .
\end{aligned}$$

To find σ_{12}', the force in the x_2' direction exerted across unit area normal to the x_1' direction, we should identify n_1, n_2, n_3 as before, but take $m_1 = \alpha_{12}$, $m_2 = \alpha_{22}$, $m_3 = \alpha_{32}$. In this way, we can write out all six independent components of stress, referred to the primed axial system. Obviously, a more condensed notation would be desirable. If account is taken of symmetry, it is seen that in general,

$$\sigma_{pq}' = \sum_{i=1}^{3} \sum_{j=1}^{3} \alpha_{ip}\alpha_{jq}\sigma_{ij} . \tag{12}$$

Under a common convention that affixes appearing twice in the typical term necessarily denote summation on those indices, the summation signs are often omitted. Physical quantities which depend in this way upon rotation of the reference axes are tensors, and the set of stress components which, for a fixed orientation, specifies the state of stress at the point P constitutes the *stress tensor*.

Principal Axes. Returning to the general tetrahedron of Fig. 1-8, we next inquire if the direction vector **n** may be so chosen that the stress vector $\mathbf{S}_n$ coincides with **n**, or so that the force on dA is normal. For this purpose, we must resolve $\mathbf{S}_n$ into a component S_{nn} normal to dA, and a component S_{nt} tangential to dA, as in Fig. 1-9. It must then be determined if the tangential component vanishes for any orientation of **n**.

The normal component is easily computed by summing the projections on **n** of the x_1, x_2, x_3 components of $\mathbf{S}_n$, as given by Eq. (9); that is,

$$S_{nn} = n_1 S_{n1} + n_2 S_{n2} + n_3 S_{n3} . \tag{13}$$

This quantity will recur frequently in the subsequent discussion; henceforth we shall represent it for short simply by σ. The components of σ along the coordinate axes are $n_1\sigma$, $n_2\sigma$, and $n_3\sigma$, respectively.

The tangential component of the stress vector has components in the coordinate directions which are the components of $\mathbf{S}_n$ diminished by the

components of σ, or $S_{n_1} - n_1\sigma$, $S_{n_2} - n_2\sigma$, $S_{n_3} - n_3\sigma$. These all vanish if S_{nt} is zero, so that $\mathbf{S}_n$ is normal to dA and has the magnitude σ. If the values of the S_{ni} are substituted from Eq. (9), setting equal to zero the three components of the tangential stress yields the equations

$$
\left.
\begin{aligned}
(\sigma_{11} - \sigma)n_1 + \sigma_{21}n_2 + \sigma_{31}n_3 &= 0 \\
\sigma_{12}n_1 + (\sigma_{22} - \sigma)n_2 + \sigma_{32}n_3 &= 0 \\
\sigma_{13}n_1 + \sigma_{23}n_2 + (\sigma_{33} - \sigma)n_3 &= 0
\end{aligned}
\right\}
\tag{14}
$$

to determine the components n_1, n_2, n_3 of the desired unit vector $\mathbf{n}$. These linear equations are homogeneous in the unknowns, and so have a solution if the determinant of the coefficients vanishes. This determinant
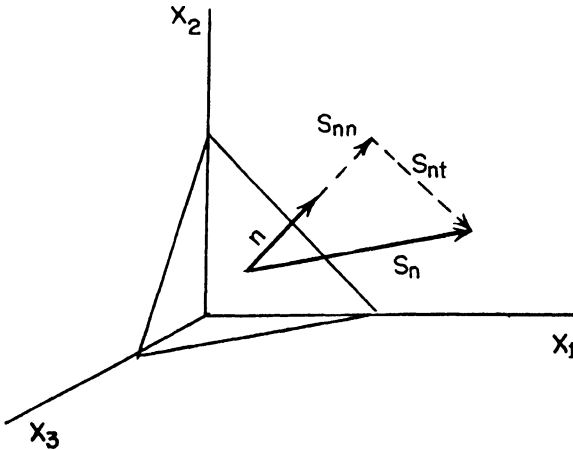
Fig. 1-9. Normal and tangential components of stress.

is a cubic polynomial in the normal stress, σ, and the condition may be written

$$
\sigma^3 - J_1'\sigma^2 - J_2'\sigma - J_3' = 0
\tag{15}
$$

where

$$
\left.
\begin{aligned}
J_1' &= \sigma_{11} + \sigma_{22} + \sigma_{33}\,, \\
J_2' &= -\begin{vmatrix} \sigma_{11} & \sigma_{21} \\ \sigma_{12} & \sigma_{22} \end{vmatrix} - \begin{vmatrix} \sigma_{22} & \sigma_{32} \\ \sigma_{23} & \sigma_{33} \end{vmatrix} - \begin{vmatrix} \sigma_{11} & \sigma_{31} \\ \sigma_{13} & \sigma_{33} \end{vmatrix} \\
J_3' &= \begin{vmatrix} \sigma_{11} & \sigma_{21} & \sigma_{31} \\ \sigma_{12} & \sigma_{22} & \sigma_{32} \\ \sigma_{13} & \sigma_{23} & \sigma_{33} \end{vmatrix}
\end{aligned}
\right\}
\tag{16}
$$

It can be demonstrated by an argument rather too lengthy for inclusion here that the roots of Eq. (15), σ_1 , σ_2 , σ_3 , say, are all *real*.   If the roots are distinct, and σ_1 is put for σ in the equations (14), the determinant of the coefficients is zero and the equations may be solved for the ratios $n_1:n_2:n_3$. Together with $n_1^2 + n_2^2 + n_3^2 = 1$, since $\mathbf{n}$ is a unit vector, the solution fixes an orientation of dA for which the stress vector is normal, and of magnitude σ_1 .

Using in succession $\sigma = \sigma_2$ and $\sigma = \sigma_3$ in (14), we can determine two other directions for which the stress vector is normal to dA.   It is another demonstrable property of the stress tensor that the three directions so determined are mutually orthogonal.   They are called the *principal directions* of stress.   If the axes of reference are rotated into the principal directions, they become *principal* axes.   For principal axes, the tangential tensor components σ'_{ij} ($i \neq j$) are of course zero, while the normal components σ'_{ii} are σ_1 , σ_2 , σ_3 , respectively.   These are the three *principal stresses*.   We shall use a single subscript to identify the principal stresses.

It was hypothesized above that the roots σ_1 , σ_2 , σ_3 were distinct.   The discriminantal equation may have multiple roots.   If σ_1 is distinct, but σ_2 and σ_3 are equal, then only one principal direction is determined uniquely. Any direction normal to this is also a principal direction, and the stress tensor is invariant to rotation of the reference system about the x'_1 axis. If all three roots are equal, every direction is a principal direction and the stress tensor is diagonal for any orientation of axes whatsoever.   In this case, which corresponds to simple hydrostatic pressure, the stress tensor is described as "spherical".   In the degenerative cases in which two or more of the principal stresses are equal, less than six numbers are required to specify the state of stress at a point in the body.   Otherwise, three numbers are required to locate the principal directions at that point, and three to specify the principal stresses.

For a given state of stress, the discriminantal equation (15) determines the principal stresses regardless of the orientation of the original reference axes.   Therefore, the coefficients of the polynomial must be invariant to rotations of the reference system.   When the reference axes are principal axes the off-diagonal terms vanish, and the stress invariants become

$$\left.\begin{array}{l} J'_1 = \sigma_1 + \sigma_2 + \sigma_3 \\[4pt] J'_2 = -\sigma_1\sigma_2 - \sigma_2\sigma_3 - \sigma_3\sigma_1 \\[4pt] J'_3 = \sigma_1\sigma_2\sigma_3 \end{array}\right\} \tag{17}$$

all symmetric functions of the principal stresses.

The Deviatoric Stress Tensor.   We shall find it useful to decompose the general stress tensor into two parts, one of which is associated with a

change of shape only, and the other with a change of volume only. The *mean normal stress* at the point P is

$$\sigma_0 = \tfrac{1}{3} (\sigma_{11} + \sigma_{22} + \sigma_{33}). \tag{18}$$

The components of the *deviatoric stress tensor* are taken as

$$\left.\begin{array}{ll} s_{ii} = \sigma_{ii} - \sigma_0 , & i = 1, 2, 3 \\ s_{ij} = \sigma_{ij} , & i \neq j. \end{array}\right\} \tag{19}$$

If to the deviatoric tensor there is added a spherical tensor whose nonvanishing (*i.e.*, diagonal) elements are σ_0, the general stress tensor is recovered. The spherical part of the state of stress corresponds to hydrostatic pressure, and induces a change in volume of the material. Since the sum of the s_{ii} is identically zero, the deviatoric part of the stress induces only a shape change at constant volume.

The deviatoric tensor has the same principal directions as the stress tensor and its principal values, s_1, s_2, s_3 may be found from σ_1, σ_2, σ_3 simply by subtracting from each $\sigma_0 = \tfrac{1}{3}(\sigma_1 + \sigma_2 + \sigma_3)$. Alternately, we can determine the principal directions from the deviatoric tensor itself, starting from the equations (14) with the σ's replaced by s's. This leads to a discriminantal equation

$$s^3 - J_1 s^2 - J_2 s - J_3 = 0 \tag{15'}$$

whose roots are s_1, s_2, s_3. The coefficients are given by the equations (16) with the σ's replaced by s's. But since the sum $s_{11} + s_{22} + s_{33}$ is zero, J_1 necessarily vanishes.

Moreover, with the help of this relation, the deviatoric stress invariants J_2 and J_3 may be formulated somewhat more perspicaciously. Expressed in terms of the principal stress deviations, they may be found from equations (17) by substituting s_i for σ_i. But also by using $J_1 = 0$ together with the identity

$$s_1 s_2 + s_2 s_3 + s_3 s_1 = \tfrac{1}{2}\{s_1(s_2 + s_3) + s_2(s_1 + s_3) + s_3(s_1 + s_2)\}$$

we can put J_2 in the form,

$$J_2 = \tfrac{1}{2}(s_1^2 + s_2^2 + s_3^2).$$

Thus, in a sense, J_2 provides a measure of the intensity of the deviatoric stress at P. In a similar way, it is found that

$$J_3 = \tfrac{1}{3}(s_1^3 + s_2^3 + s_3^3).$$

Principal Shearing Stresses. The stress deviation at the point P may be described in a different way by giving the values of the maximum shear-

ing stresses.   Suppose the plane of the elementary area dA is rotated about one of the principal directions of stress, say the direction of σ_1.   When the plane is aligned with the direction of σ_2 or σ_3, the tangential component of stress transmitted through dA vanishes.   For intermediate positions, the tangential component is finite.   As the rotation proceeds from the second toward the third principal direction, this component increases in absolute value to a maximum attained at the 45° point, and thereafter decays to zero.   The value of this maximum is

$$\tau_1 = \tfrac{1}{2} \mid \sigma_2 - \sigma_3 \mid \tag{20}$$

which is the same as

$$\tfrac{1}{2} \mid s_2 - s_3 \mid .$$

Likewise, if the plane of dA were to be rotated about the second principal direction, the tangential stress component would be greatest when the angle between the other principal directions was bisected.   The absolute value of this shearing stress is

$$\tau_2 = \tfrac{1}{2} \mid \sigma_3 - \sigma_1 \mid = \tfrac{1}{2} \mid s_3 - s_1 \mid . \tag{20}$$

Finally, a rotation about the third principal direction gives

$$\tau_3 = \tfrac{1}{2} \mid \sigma_1 - \sigma_2 \mid = \tfrac{1}{2} \mid s_1 - s_2 \mid . \tag{20}$$

The normal stresses at these three orientations are $\tfrac{1}{2}(\sigma_2 + \sigma_3)$, $\tfrac{1}{2}(\sigma_3 + \sigma_1)$, and $\tfrac{1}{2}(\sigma_1 + \sigma_2)$, respectively.

The set τ_1, τ_2, τ_3 constitutes the triple of *principal shearing stresses*. This set serves also to determine the deviatoric invariant J_2, since

$$\tau_1^2 + \tau_2^2 + \tau_3^2 = \tfrac{1}{4} \{(s_2 - s_3)^2 + (s_3 - s_1)^2 + (s_1 - s_2)^2\}$$

$$= \tfrac{1}{2} \{(s_1^2 + s_2^2 + s_3^2) - (s_1 s_2 + s_2 s_3 + s_3 s_1)\}$$

$$= \tfrac{3}{2} J_2 .$$

Analysis of Strain.   During the deformation of a solid body the material near a typical point P, having initially the coordinates x_i, undergoes a displacement $\mathbf{u}$ to a point P', having the coordinates $x_i + u_i$.   Such a displacement, illustrated by Fig. 1-10, consists in part of a rigid body displacement, and in part of a pure deformation.   The latter part is measured by the *state of strain* at P, a tensor having the components

$$\epsilon_{ij} = \frac{1}{2}\left(\frac{du_i}{dx_j} + \frac{du_j}{dx_i}\right). \tag{21}$$

Of these, the *normal strains* ϵ_{ii} represent the unit extensions in the direction of the reference axes; the off-diagonal components $\epsilon_{ij} = \epsilon_{ji}$, $(i \neq j)$,

represent changes of shape. These tensor components are related to the *shearing strains* γ_{ij} according to

$$\gamma_{ij} = 2\epsilon_{ij}. \tag{22}$$
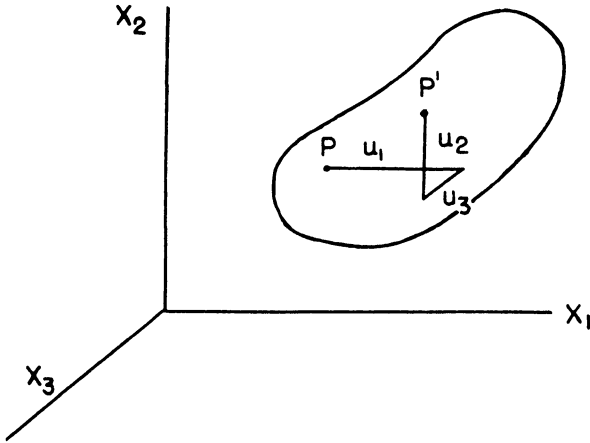
Fig. 1-10. Displacement of a point P of an elemental surface to P' by an amount u_1 on the X_1 axis, u_2 on the X_2 axis, and u_3 on the X_3 axis.
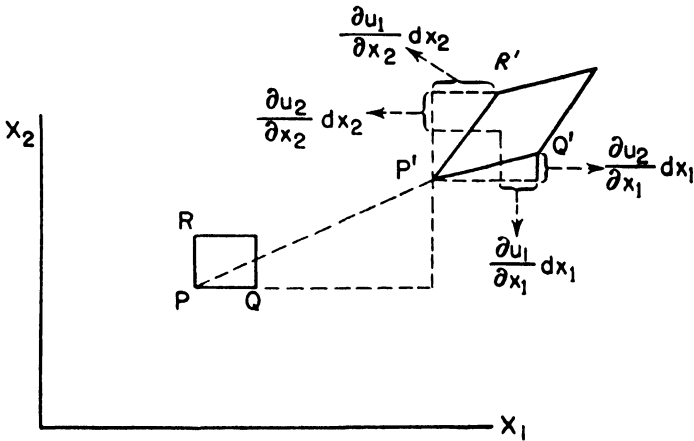
Fig. 1-11. Two-dimensional view of the displacement of a volume element.

The significance of this description is made clear by examination of Fig. 1-11, which shows for two-dimensional strain the displacement of a volume element having originally a rectangular cross-section, the sides parallel to the coordinate axes being of length dx_1 and dx_2, respectively. The deformation carries the point P into the point P'. If the material were

rigid, the adjoining vertices Q and R would experience equal displacements, the volume element going into an element having the dotted cross-section of the figure. If the material is elastic, however, the neighboring points Q and R will undergo displacements slightly different from the displacement of P. Their displacements may to the first order be found from the displacement at point P by

$$\left.\begin{aligned}
u_1^Q &= u_1^P + \frac{\partial u_1}{\partial x_1} dx_1 & u_1^R &= u_1^P + \frac{\partial u_1}{\partial x_2} dx_2 \\
u_2^Q &= u_2^P + \frac{\partial u_2}{\partial x_1} dx_1 & u_2^R &= u_2^P + \frac{\partial u_2}{\partial x_2} dx_2
\end{aligned}\right\} \tag{23}$$
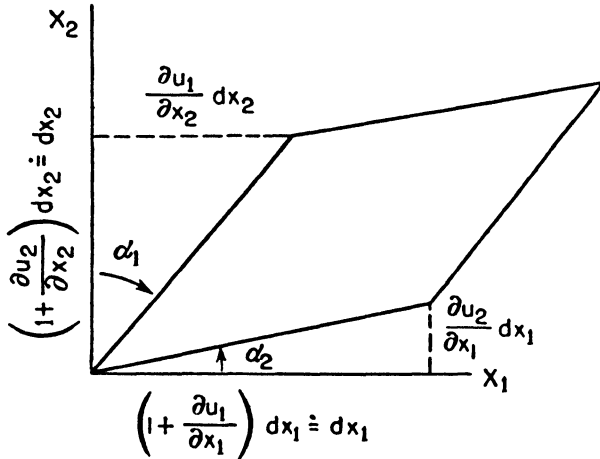
Fig. 1-12. The closing of originally perpendicular planes during shear.

where $\partial u_1/\partial x_1$ is the rate at which displacement of the material in the x_1 direction varies in the x_1 direction, and so forth. When these rates are all positive, the equations define final positions for the points Q and R, as indicated in the figure.

Evidently, $\partial u_1/\partial x_1$ and $\partial u_2/\partial x_2$, that is, ϵ_{11} and ϵ_{22}, measure the percentage extension of the volume element in the respective coordinate directions. We suppose that the displacement of R differs but little from that of P, so that their final separation in the x_1 direction, $(1 + \partial u_1/\partial x_1)dx_1$ is only slightly different from dx_1. For clarity in the drawing, this difference has been greatly exaggerated. Under the assumption of small strains, it is seen from Fig. 1-12 that $\partial u_2/\partial x_1$ measures the rotation of the side originally parallel to the x_1 axis, while $\partial u_1/\partial x_2$ measures the rotation of the side originally parallel to the x_2 axis. The angle through which the

originally perpendicular sides have closed during the deformation is the sum

$$\alpha_1 + \alpha_2 = \frac{\partial u_1}{\partial x_2} + \frac{\partial u_2}{\partial x_1}.$$

This angle is the shearing strain $\gamma_{12} = 2\epsilon_{12}$.

It is easily seen that this description of shear is equivalent to the description of simple shear which we invoked in Section II. There the shearing strain was described as the unit lateral displacement of parallel planes. For infinitesimal strain, this is also given by $\alpha_1 + \alpha_2$. For, in Fig. 1-13, we can approximate to dl with dx_2 so that

$$\frac{ds}{dl} = \cot\left(\frac{\pi}{2} - \alpha_1 - \alpha_2\right) = \tan(\alpha_1 + \alpha_2) \doteq \alpha_1 + \alpha_2.$$

Fig. 1-13. Lateral displacement of parallel planes during shear.
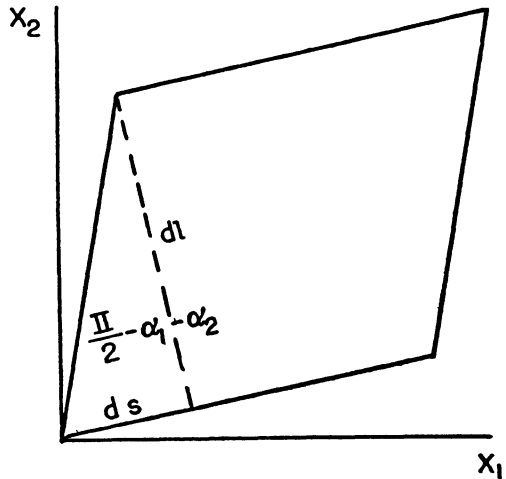
Throughout the following sections, the simplifications due to the presumption of small strains will be retained. Elastic strains are in fact so small that the infinitesimal approximation is very good. Although the plastic deformations which we must consider later are frequently very great, we shall nevertheless not undertake to introduce into our analysis the nonlinearities associated with finite strain.*

* For specimens elongated in simple tension, it is sometimes attempted to accommodate the nonlinearities of finite strain by writing

$$\epsilon = \int_{l_0}^{l} \frac{dl}{l} = \log\frac{l}{l_0}.$$

When the final length l does not greatly exceed the original length l_0 , this expression reduces to the conventional definition of infinitesimal strain.

Exactly as for the components of the stress tensor, the components of the strain tensor depend for their values upon the orientation of the reference axes. For the strain tensor, there likewise exists a set of three orthogonal reference directions for which the strain is normal. These directions remain orthogonal throughout the deformation. These are the *principal directions of strain*. The normal components of strain in these directions ϵ_1, ϵ_2, ϵ_3 are found as the roots of the discriminantal equation analogous to Eq. (15) in which the σ's are replaced by ϵ's. These are the *principal strains*.

Similarly, the strain tensor may be decomposed into a deviatoric tensor describing change of shape and a spherical tensor describing change of volume. By the *strain deviation*, we shall mean

$$\left.\begin{array}{l} e_{ii} = \epsilon_{ii} - \epsilon_0 \\ e_{ij} = \epsilon_{ij}, \quad i \neq j \end{array}\right\} \tag{24}$$

where ϵ_0 is the *mean normal strain*;

$$\epsilon_0 = \tfrac{1}{3}(\epsilon_{11} + \epsilon_{22} + \epsilon_{33}).$$

This decomposition of the stress and strain tensors leads to particularly simple stress-strain relationships in the special case of isotropic substances. This case is of particular interest since, unlike single crystals, engineering materials may often be characterized to a satisfactory approximation as free from preferred directions of strain.

Finally, the deviatoric strain may be represented by three principal shearing strains. Among all directions normal to a principal direction of strain, the maximum value of shear is attained on the plane which bisects the two other principal directions. There is one such plane for each of the three principal directions. The absolute values of shearing strains referred to such a triple of planes are given by

$$\gamma_1 = |e_2 - e_3|, \quad \gamma_2 = |e_3 - e_1|, \quad \gamma_3 = |e_1 - e_2|. \tag{25}$$

From these expressions, the factor $\tfrac{1}{2}$ which appeared in Eq. (20) is missing because of the relation between shearing strain and the strain tensor components.

Stress-Strain Relations of Elasticity. In order to predict the deformation of a solid body under external load, it is necessary to join with the conditions of equilibrium and compatibility, the relations between stress and strain for the material. These are simplest when the deformations are entirely elastic. But even when material obeys Hooke's law, the characterization of its behavior requires much data. In general, each component of stress is a linear function of all the components of strain Generally, we must write

$$\epsilon_{ij} = \sum_{p=1}^{3} \sum_{q=1}^{3} C_{ij}^{pq} \sigma_{pq}. \tag{26}$$

This generalized form of Hooke's law thus requires a 9×9 array of elastic constants C_{ij}^{pq} to relate the nine components of strain to the nine components of stress. Because of symmetries, only twenty-one of the elastic constants are independent. However, the twenty-one independent values are not purely constants of the material, but depend also upon the orientation of the reference axes in respect, say, to the crystallographic planes of the substance.

If the material is isotropic, the relation between stress and strain is tremendously simplified. In this event, the orientation of the reference axes in respect to the material is indifferent; the principal directions of strain coincide with the principal directions of stress; and the number of independent elastic constants reduces to two. Even in this case, there is no one-to-one correspondence between the components of stress and the corresponding strains. If, for example, a specimen is subjected to simple tension in the x_1 direction, the corresponding elongation ϵ_{11} is accompanied by contractions ϵ_{22} and ϵ_{33} in the two orthogonal directions. With the reference axes oriented in principal directions, we have in general for the isotropic substance

$$
\left.
\begin{aligned}
e_1 &= \frac{1}{E}[\sigma_1 - \nu(\sigma_2 + \sigma_3)] \\
e_2 &= \frac{1}{E}[\sigma_2 - \nu(\sigma_3 + \sigma_1)] \\
e_3 &= \frac{1}{E}[\sigma_3 - \nu(\sigma_1 + \sigma_2)]
\end{aligned}
\right\}
\qquad (27)
$$

where the two independent elastic constants are E, the Young's modulus and ν, Poisson's ratio between the percentage lateral contraction and the percentage longitudinal elongation. It is easily verified that a value of 0.5 for Poisson's ratio corresponds to elongation at constant volume. Many materials, for example steels, exhibit some diminution in volume under elongation, being characterized by a Poisson's ratio of about 0.3.

For an isotropic material, a one-to-one correspondence between stress and strain components may be achieved by decomposition of the general tensors into deviatoric and spherical parts. If this be done, the relation between a stress deviation and the corresponding strain deviation is found to be

$$
e_{ij} = \frac{1}{2G} s_{ij}
\qquad (28)
$$

where G, the modulus of rigidity, is related to the Young's modulus and Poisson's ratio by

$$
G = \frac{E}{2(1 + \nu)}.
\qquad (29)
$$

The relation between the components of the hydrostatic stress and strain tensors is

$$\sigma_0 = 3K\epsilon_0 \tag{30}$$

where K is the bulk modulus, equal to

$$K = \frac{E}{3(1 - 2\nu)}. \tag{31}$$

This decomposition provides the handiest formulation of the relation between stress and small strain for isotropic materials. As we will see in the following sections, the usefulness of the decomposition extends beyond the elastic case here considered. The part of a general deformation which involves a change of volume can be regarded as entirely elastic, and so is entirely contained in Eq. (30) with K constant. The shape change described by Eq. (28) can usually be regarded as occurring at constant volume, although it be in part elastic and in part plastic. Of course, in so far as the deformation is elastic, G likewise is constant; to accommodate plastic effects, we shall need to assign a generalized meaning to this factor.

IV. The Stress-Strain Relations of Viscoelasticity

There is a class of solid materials, including glasses and the high polymers, which are capable of supporting elastic shearing stresses but which also exhibit a tendency to flow continuously under the applied stress. Such a material may be regarded as a complex of ordered elastic regions intermixed with disordered viscous regions. If the flow in the viscous regions is Newtonian, so that a linear relation obtains between the local stress and the strain rate, then the elastic equations of the preceding section may be rather easily extended to account for the combined effects.

To do this it is necessary to invoke two assumptions which in actual cases are seldom fulfilled exactly. For one, let us suppose that the material is isotropic, so that the components of the deviatoric stress tensor depend uniquely on the corresponding components of the deviatoric strain tensor. For the other, we suppose that the strains remain small so that the nonlinearities associated with finite strains are not introduced. Actually, in steady flow, the observed strains may in time become very great. The analysis of finite strains is extraordinarily difficult and far beyond our scope.

The simplest combination of an elastic domain and a viscous domain which we can conceive is represented by the mechanical model of Fig. 1-14.

For this arrangement, which is sometimes called the Maxwell element, the applied stress is transmitted through the spring to the dash pot and the resultant strain is the sum of the elastic and the plastic strains. If constant stress is suddenly applied at the initial instant, the spring deforms instantaneously and the dash pot begins to pull out at a uniform rate. When the stress is removed at time t_c , the elastic strain immediately disappears and the plastic strain persists, as shown to the right of the figure.
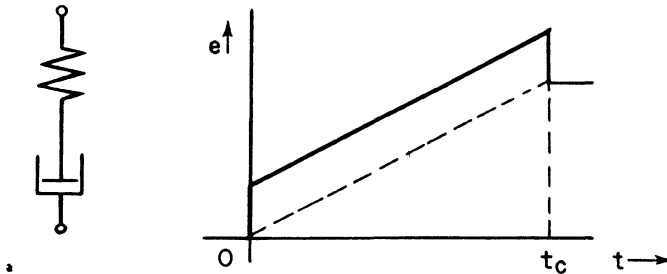
Fig. 1-14. Response of series combination of spring and dash pot. Extension under constant load applied at t = 0, removed at t = t_c.

The stress-strain relations describing this behavior are found simply by adding the elastic and plastic parts of the strain. The elastic contribution to the strain rate can be written

$$2\dot{e}' = \frac{\dot{s}}{G}$$

while the viscous part is given by

$$2\dot{e}'' = \frac{s}{\eta}$$

so that the total strain $e = e' + e''$ is

$$2\dot{e} = \frac{\dot{s}}{G} + \frac{s}{\eta}. \tag{32}$$

If, at the instant of starting, the value of the stress is raised from zero to the constant value s_0 , the equation prescribes initially an infinite rate of strain. Subsequently, the strain increases at the constant rate prescribed by the coefficient of viscosity as shown in Fig. 1-14.

A second possible arrangement of a single elastic domain and a single plastic domain is shown in Fig. 1-15. In this case the dash pot and the spring deform together, the applied stress being supported in part by one and in part by the other. This is a so-called Voigt element. If the constant stress s_0 be suddenly applied at the initial instant, it is at first

entirely expended in pulling out the dash pot since the unextended spring supports no force. As the deformation proceeds, the spring extends, assuming more and more of the load and reducing the part available for maintaining the strain rate. The strain rate tends toward zero as the spring approaches the steady state extension which equilibriates the stress. This behavior is shown on Fig. 1-15. If at the instant t_c the stress be removed, the process is reversed, the potential energy stored in the spring being slowly expended in reducing the extension of the dash pot to zero. This phenomenon is sometimes called "retarded elasticity".
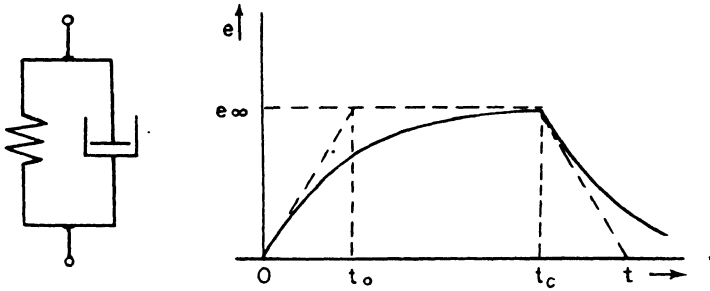
Fig. 1-15. Response of parallel combination of spring and dash pot. Extension under constant load applied at t = 0, removed at t = t_c.

For this case, the stress-strain relations are found simply by adding the part of the stress supported by the spring to the part supported by the dash pot. The elastic stress is

$$s' = 2Ge$$

while the viscous part is

$$s'' = 2\eta \dot{e}$$

so that the total stress is

$$s = 2Ge + 2\eta \dot{e}. \tag{33}$$

If this combination is loaded in the same way as the other, the integral of this equation, subject to the initial conditions $e = \dot{e} = 0$ for $t = 0$, is

$$e = \frac{s_0}{2G}(1 - \epsilon^{-t/t_0}),$$

where $t_0 = \eta/G$ is the "relaxation time" of the combination. This is the equation plotted in Fig. 1-15.

These simple combinations do not generally suffice to describe the behavior even of linear materials. However, they are easily extended to a very general model by combining a Maxwell element with a number of Voigt elements each characterized by its own relaxation time. This

arrangement is shown in Fig. 1-16.   By an extension of Eqs. (32) and (33), we can see that the stress-strain relations for the general model have the form

$$Ps = 2Qe \tag{34}$$

where P is the differential operator

$$P_0 + P_1 \frac{d}{dt} + P_2 \frac{d^2}{dt^2} + \cdots + P_n \frac{d^n}{dt^n}$$

and Q is the operator

$$Q_0 + Q_1 \frac{d}{dt} + Q_2 \frac{d^2}{dt^2} + \cdots + Q_n \frac{d^n}{dt^n}$$

the coefficients P_i, Q_i being constant.   These linear equations can be integrated to fit boundary and initial conditions in all cases for which the solution to the purely elastic problem is known.
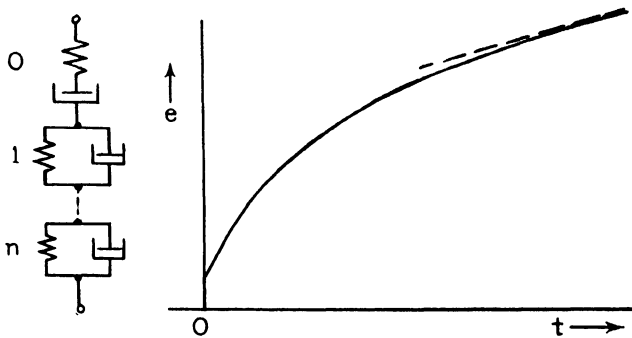
Fig. 1-16. Multiple arrangement of springs and dash pots for general case.

In certain respects, the predicted behavior resembles the reaction of metals at elevated temperatures.   However, on closer examination, it is evident that the behavior of metals is much more complicated than the behavior of viscoelastic materials and is, in fact, highly nonlinear.   The next section deals with the aspects of metals in which the observed behavior does differ from the viscoelastic phenomena.

V. Plastic Behavior of Metals

The observed behavior of metals is not predicted, even approximately, by the linear relations of viscoelasticity described in the preceding section. There is, however, a superficial resemblance between the mechanical behavior of metallic materials and the behavior of viscoelastic substances which becomes closer at higher operating temperatures.

What must be regarded as a high operating temperature depends on the material. Plastic flow increases as the melting point is approached. Different engineering materials behave in a roughly similar way at temperatures which are the same fraction of the melting point in degrees Kelvin. The ratio of the absolute operating temperature to the absolute temperature of melting for the material will be called θ, the homologous temperature. Generally speaking, a value for θ exceeding 0.5 corresponds to a high operating temperature for the material. This is not necessarily a high actual temperature. For lead and its alloys, room temperature corresponds to a value of θ equal to 0.5. For aluminum and its alloys, a high operating temperature is approached at 200°C, whereas for a high-nickel alloy, such as "Inconel", the value θ equal to 0.5 is reached at 600°C. In this section, an examination will be made of the observed plastic behavior of typical materials at the higher operating temperatures, that is, at values of θ between 0.5 and unity.

Suppose that a specimen at a high temperature is suddenly loaded in pure tension and a record made of the relative elongation as a function of the time after loading. If precautions are taken to insure constancy of θ and constancy of the tensile stress σ, the record of the strain ϵ will appear as in Fig. 1-17. The strain is observed to increase sharply at the initial instant. The strain rate remains high for some time but gradually subsides into a substantially constant rate which is quite reminiscent of viscous flow.

It is not to be supposed that the simple behavior indicated in Fig. 1-17 can be observed without very special precautions to insure that the stress is in fact maintained constant during the deformation. If the test were to have been conducted at constant load, the stress would increase as the cross sectional area diminished during the extension. This condition leads to an acceleration of the strain rate at high strains, generally followed quickly by fracture. For a test at constant load, where the nominal stress, σ_0, is taken as the ratio of load to initial area, the record would appear as in Fig. 1-18. At short times and small strains, the observations would be nearly identical with those recorded in Fig. 1-17. For some combinations of σ_0 and θ, the strain might be observed to settle into a constant creep rate for some time, but sooner or later, the increase of actual stress with decreasing cross-section of the specimen results in an acceleration of the strain rate, followed shortly by necking and resulting finally in rupture. For some combinations of σ_0 and θ, no interval of constant creep is observed, the linear segment of the graph shrinking into a point of inflection. A test at constant load may very well correspond more exactly to the actual service conditions for which the material is intended. Nevertheless the added complication of changing stress during

the experiment greatly confuses the discussion of the theoretical behavior of materials. In the following, it is supposed that the experiments are
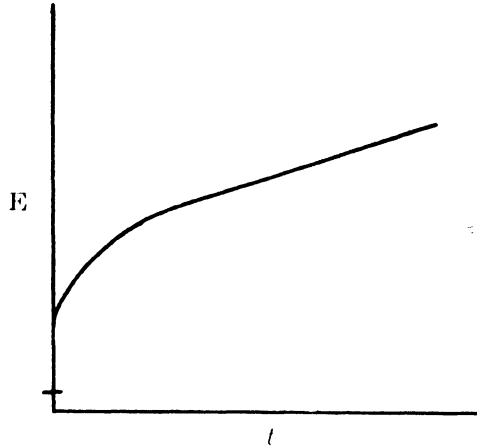
Fig. 1-17. Strain versus time under tensile load with temperature and stress constant.
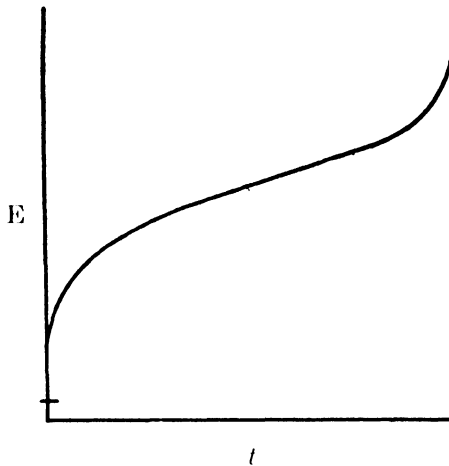
Fig. 1-18. Strain versus time under tensile load with temperature and load constant.

performed with constant stress. Means for preserving constancy of true stress are described in Chapter 2.

The strain-time curve at constant true stress (Fig. 1-17) may be resolved into the components illustrated by Fig. 1-19. The total strain is

observed to be a compound of a usually small elastic strain, instantaneous and reversible, and two plastic components which do not disappear when the specimen is unloaded. Of these, one is a steady flow of the type exhibited by viscous liquids. The case of metals is distinguished by the appearance. of a new strain component, called in Fig. 1-19 the initial plastic strain. This may be itself a compound containing a part which appears suddenly upon the imposition of the stress, blending imperceptibly into a part which, starting at an infinite rate of increase, subsides in time into a constant final value.

It is noticed that the high-temperature strain depends on the time of exposure to the stress. Evidently, it depends as well upon the temperature and upon the constant stress. The dependence upon the stress will next be examined. If the experiment which produced the record of Fig. 1-17, is repeated, with the temperature maintained constant at the same
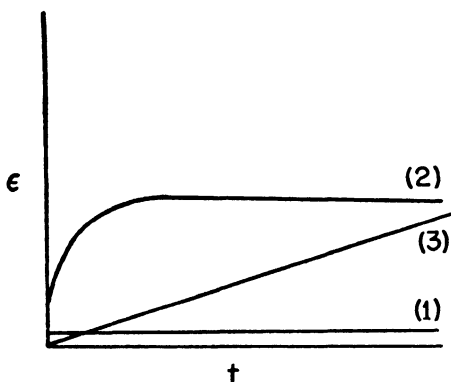
Fig. 1-19. Decomposition of strain-time curve at constant stress of Fig. 1-17 into (1) a small elastic strain, (2) the initial plastic strain and (3) steady state creep.

value of θ, but with suddenly applied constant stresses of differing magnitude, a family of strain-time records similar to those of Fig. 1-20 is obtained. If the stress is progressively increased from the constant value σ to the value σ', and to σ'', etc., the steady state component of the creep is found to increase very rapidly. A measure of the rate of increase is obtained by estimating the final strain rate from the linear parts of the record and plotting them against the corresponding stress. When this is done for the curves of Fig. 1-20, which incidentally are typical of the behavior of lead at room temperature, the variation shown by Fig. 1-21 is obtained. If the material were viscous, the dependence of strain rate upon stress would conform to the dashed line drawn on the figure. It is evident that for actual metals the relationship is highly nonlinear so that the steady flow can be at most described as "quasi-viscous".

It remains to consider the dependence of the strain-time record upon the

operating temperature. If the experiment which produced Fig. 1–17 is repeated keeping the true stress constant at the value σ, but progressively reducing θ, from the constant value θ', to θ'', etc., a family of curves similar to those of Fig. 1-22 is obtained for a typical material. From this figure, it is observed that the steady creep decreases very rapidly with decreasing temperature and may become entirely negligible at values of θ below 0.5.
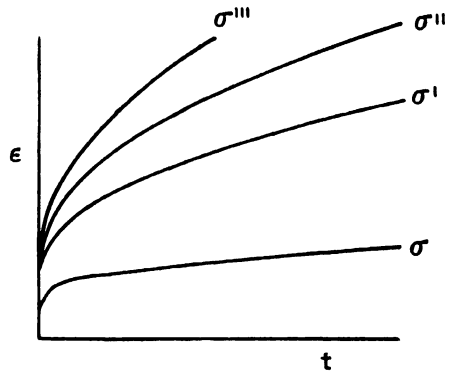
Fig. 1-20. Strain-time curves at various constant stress levels, all for constant temperature.
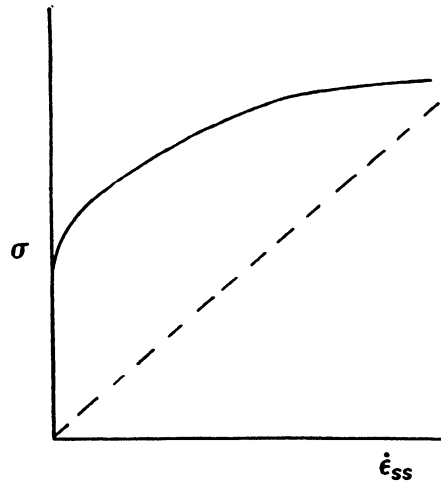
Fig. 1-21. Plot of steady state strain rate against stress for quasi-viscous flow. The dashed line corresponds to viscous flow.

A representative graph of the final steady creep rate against temperature is presented in Fig. 1-23. The initial plastic deformation subsides to final values which also decrease with temperature, although, if σ is great, it may remain large relative to the elastic strain. Moreover, the time required for the initial plastic strain to settle on its final value shortens notably as the temperature lowers. The combination of these two effects allows the

time of exposure to be eliminated as a parameter in the determination of the strain at low temperatures, such as θ''' of Fig. 1-22, provided the stress is not varied too rapidly.

From the foregoing, it is seen that a very high steady creep rate will be observed only under conditions in which both homologous temperature and the stress are great. However, even the smallest tendency of a material to elongate continuously under constant stress has tremendous
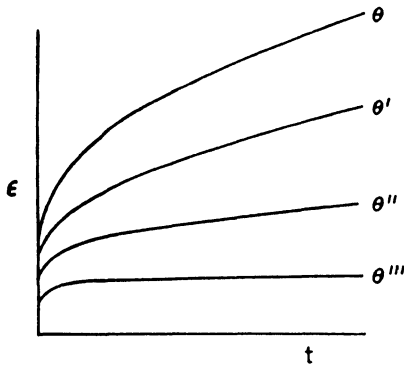
Fig. 1-22. Strain-time curves at various constant temperature levels, all at constant stress.
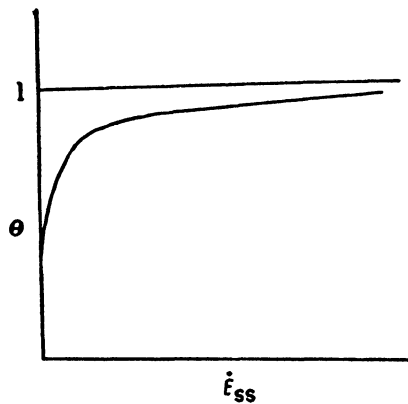
Fig. 1-23. Plot of steady state creep rate against temperature at constant stress.

implications for engineering design. Therefore, creep tests are often extended over many thousands of hours so as to detect even the smallest steady strain rates. On such a time scale, the initial plastic deformation appears to be instantaneous. The results of many such tests will be reported in the subsequent chapters. Perhaps regrettably, practically all the experiments have been conducted at constant load rather than constant stress, and so involve the complication of increasing strain rate with increasing strains. This effect appears more quickly the higher the

stress. In the so-called stress rupture test, the load is adjusted to produce fracture within a few hundred hours.

VI. Low-Temperature Plasticity

At temperatures so low that steady flow is negligble, the time can be eliminated as a parameter. An ordinary tensile test may be substituted for the creep test, the specimen being loaded in simple tension by successive increments, and a record kept of the corresponding extensions. When the temperature is not high, these will ordinarily settle to a steady value very shortly after each change of load. Tensile test data are presented as the stress-strain curve for the material, an example of which is portrayed by Fig. 1-24. For small stresses, the specimen extends elastically along the straight line portion of the curve, the slope of which is the Young's modulus. For higher stresses, the observed extension exceeds the elastic strain as the material begins to yield plastically. Sometimes the point at which the stress-strain curve begins to depart from the elastic line is quite clearly marked. More often the departure is very gradual and the *yield stress, k*, is taken as the stress required to produce a permanent strain of 0.2 per cent.*

The variables used in Fig. 1-24 to describe the behavior of the material are the strain

$$\epsilon = \frac{\Delta l}{l_0}$$

where l_0 is the original length of the specimen and Δl the increase in length, and

$$\sigma = \frac{P}{A}$$

where P is the load and A is the cross-section at that load. These definitions suppose a homogeneous state of stress in the elongating specimen, and fail when local necking begins.

A somewhat different description of the behavior is obtained if the true stress σ is replaced by the nominal stress σ_0 defined by

$$\sigma_0 = \frac{P}{A_0}$$

where A_0 is the original cross-section of the material. Since the actual cross-section diminishes with increasing extension, the nominal stress is an underestimate of the true stress in the material. Fig. 1-25 illustrates the nominal stress-strain curve of Fig. 1-24. In consequence of the increase in true stress as the cross-sectional area decreases, the curve of Fig. 1-25

* The stress so defined is sometimes called the proof stress.

reaches a maximum value of nominal stress. At greater extensions, the specimen can only support lower loads. The maximum value of nominal stress is called the *ultimate strength* of the material. After the maximum has been passed, the observed stress-strain curve is likely to be perturbed by local inhomogeneities in the stress due to the beginning of necking.
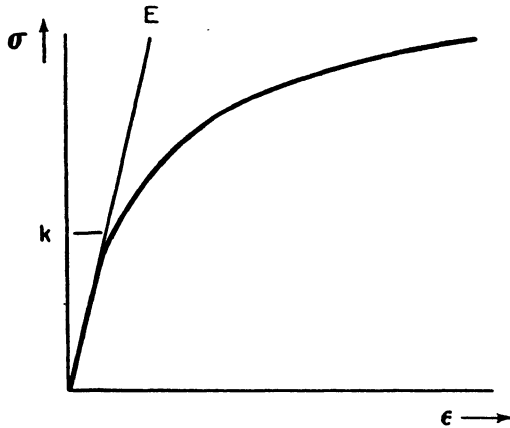
Fig. 1-24. True stress-strain curve.
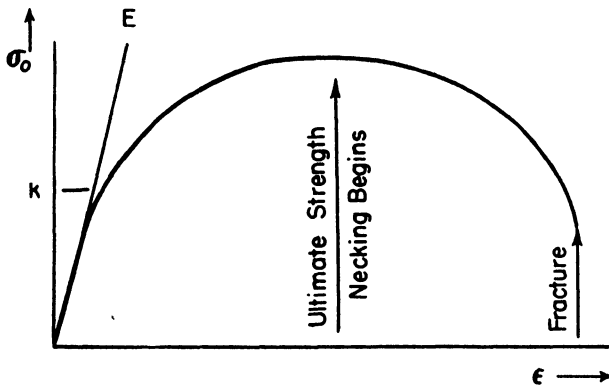
Fig. 1-25. Nominal stress-strain curve.

If, nevertheless, the test be continued until the specimen fails, the *elongation at fracture* can be obtained as a further useful measure of the plastic properties of the material.

As long as the stress remains homogeneous, the true stress-strain curve is simply related to the nominal stress-strain curve. It is necessary only to suppose that the strain is mostly plastic and, accordingly, at constant

volume. In this case, the cross-sectional area at any extension is related to the original area by

$$\frac{A_0}{A} = \frac{l}{l_0} = \frac{l_0 + \Delta l}{l_0} = 1 + \epsilon$$

so that, if

$$\sigma = \frac{P}{A} \quad \text{and} \quad \sigma_0 = \frac{P}{A_0}$$

then

$$\frac{\sigma}{\sigma_0} = 1 + \epsilon .$$
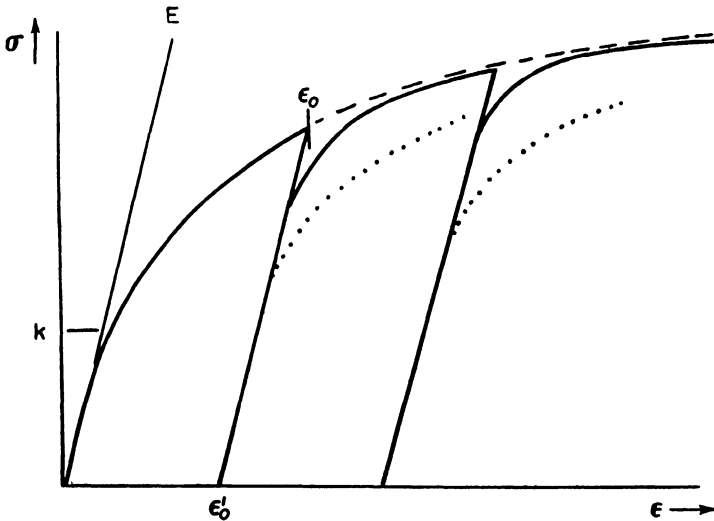
Fig. 1-26. Cyclic loading.

With the help of this equation, the true stress-strain curve can be easily constructed from the nominal stress-strain curve up to the point at which necking begins. In the following, it will be supposed that the elongation is referred to the true stress, for the same reasons that control in the case of creep.

Fig. 1-26 is the true stress-strain curve for a virgin specimen which under increasing load has been extended to the elongation ϵ_0. If at this point, the load is then reduced, the specimen will be found to contract along the line $\epsilon_0 - \epsilon_0'$, having also the slope E. By the time the load is completely removed, the strain is reduced to the permanent set ϵ_0'. If then the specimen be immediately loaded, the strain is found to increase

at the elastic rate. The curve, however, follows the line $\epsilon_0 - \epsilon_0'$ until a stress considerably greater than the initial yield stress k is attained. That is, the specimen has been work-hardened. If not very much time has elapsed in the unloading and subsequent reloading, the stress-strain curve rejoins the dashed curve obtained by continuously increasing the load. Additional cycles of loading and unloading result in similar behavior as indicated by the figure.

During the unloading along the line $\epsilon_0 - \epsilon_0'$, the stress increment is related to the strain increment according to the elastic law

$$\Delta\sigma = E\Delta\epsilon .$$

This equality is unaffected if both sides of the equation are divided by Δt, in which case it becomes in the limit

$$\dot\sigma = E\dot\epsilon . \tag{35}$$

This generalization of Hooke's law provides a succinct formulation of the differential relationship, making the rate of variation independent of the absolute value of the strain. However, the homogeneous relation between stress rate and strain rate implies no flow in the sense of viscous flow.

If, after the initial loading and unloading, the specimen is allowed to remain in the unloaded condition for an extended period, a different behavior will be observed on subsequent reloading. A part of the work hardening will be found to have disappeared, the strain varying with increasing stress according to the dotted curve of Fig. 1-26. This phenomenon of resoftening in time is known as *recovery*. At very low temperatures, it is insignificant, but it becomes more evident as the rest temperature of the specimen approaches $\theta = 0.5$. At about this homologous temperature, the process of recovery is much hastened by *recrystallization* of the material.

VII. Stress-Strain Relations of Low-Temperature Plasticity

In the elastic, isotropic case, simple tensile tests of the type considered, serve to provide values for the two material constants, however these are chosen. Observations of the gage length and cross-section of the specimen as the load increases determine immediately the modulus of elasticity E and Poisson's ratio ν. In the elastic case, this pair determines the modulus of rigidity G and the bulk modulus K through the equations (29) and (31) of Section III. These data enable the prediction of elastic deformation of engineering parts of complicated geometry variously loaded.

When the yield stress of the material is exceeded, the case is more difficult. The resulting deformation is compounded of usually small elastic

strains and often great plastic strains.* To predict such deformations of engineering parts, it is necessary to generalize the stress-strain relations of elasticity to include the plastic component of strain. Also, it is necessary to decide what elementary experiments yield a description of the plastic behavior appropriate to the generalized stress-strain relations. In the plastic case, the easy relation between the behavior in simple tension and the behavior in simple shear is missing. Although the results of tensile tests were used above to illustrate the general nature of plastic behavior, the basic description of the material is derived from shearing tests.

For plastic deformation takes place by shear, just as in the phenomenon of viscous flow. One process by which such deformation occurs in metals is *slip*, which is readily observed in single crystals. This process takes place by glide on preferred slip planes, which are crystal planes of high atomic density. Fig. 1-27 is a schematic diagram of slip in a crystal having
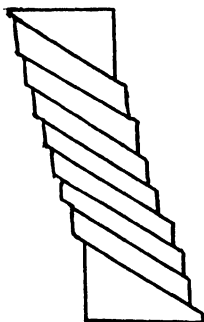
Fig. 1-27. Deformation of a single crystal of zinc.

a unique slip plane. Such a material is zinc, the hexagonal crystal lattice of which has but one plane of high atomic density, the basal plane. If a single crystal of zinc be stressed in simple tension, the deformation produced is a relative displacement along slip planes, as evidenced by the appearance of visible *slip bands* on the surface of the strained specimen, in the manner suggested by the figure. The slip bands are found to coincide with the basal planes of the crystal.

Ordinarily, in a tensile test, the ends of the specimen would be constrained, and lateral motion inhibited. In this event, the slip planes rotate under increasing elongation. Near the ends, there is local bending of the slip planes and a nonhomogeneous state of stress.

* The plastic strains resulting, for example, from forming operations and rupture tests may be very large. In the following, consideration is limited to permanent strains which, while very much greater than elastic strains, are still small enough to be regarded as infinitesimal.

Other crystal lattices have several planes of high atomic density on which slip may occur. Whether or not they become slip planes is determined by the value of the resolved shearing stress for these planes. Crystals having a face-centered cubic lattice, for example, may slip on any of the several octahedral planes. The existence of many slip planes in the face centered cubic lattice accounts for the ductility of such metals as copper and aluminum.

Engineering materials are polycrystalline aggregates generally isotropic in nature and accordingly without preferred planes of specially high atomic density. In such materials, slip is observed to occur along the planes of maximum shearing stress. In a simple tensile test, such planes are inclined at 45° to the axis of the stress. That slip along these planes does in fact occur during extension is sometimes evidenced by the appearance of Luder's lines on the strained material.
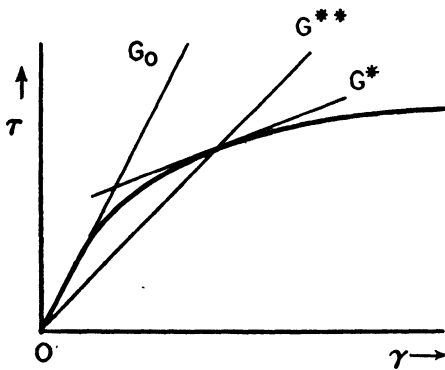
Fig. 1-28. Typical stress-strain curve.

Thus the evidence supports the view that the permanent plastic strain observed in engineering materials results from a mechanism very like the mechanism of viscous flow considered in Section II. Accordingly, the plastic strains are expected to be shape changes purely, unaccompanied by any volume changes in the material. Finally, since the basic mechanism is shear, it is to be expected that the essential experimental data should describe the nonlinear behavior of the material in shear rather than in tension.

Experimental procedures for the determination of the plastic behavior of a metal in shear are easily devised. An approximation to a state of simple shearing stress is obtained from a thin walled tube loaded in torsion. As shown above, the state of simple shearing stress exists only as an approximation since additional stresses are required for the satisfaction of the equilibrium conditions. In a well designed experiment, the stress

component of simple shear is made dominant and homogeneous over most of the volume of the specimen. From such a test is obtained a stress-strain curve for the material in which the dominant stress is the shearing stress τ and the corresponding strain the shear, γ. For low values of stress and strain, the elastic relationship is measured by the shear modulus G. This measures the slope of the line to which the observed stress-strain curve is tangent at low strains as in Fig. 1-28. Observed stress-strain curves depart from elastic behavior at higher strains in the shearing experiment in a way qualitatively identical with the behavior in tension. The permanent plastic yield is measured by the departure of the observed curve to the right of the elastic line. The effect of work-hardening is revealed by the continued upward slope of the recorded observations, there being no point at which the material can yield freely under constant stress.

The behavior illustrated in Fig. 1-28 implies a continuously decreasing value of the differential ratio

$$\frac{d\tau}{d\gamma} = G(\tau) \ . \tag{36}$$

The modulus G is of course nothing but the slope of the stress-strain curve at the point whose ordinate is τ. As τ decreases, $G(\tau)$ tends toward the elastic modulus of rigidity. This limiting value will henceforth be designated G_0. To indicate G specifically as a function of τ, the notation G^* will be used. This is usually called the *tangent modulus* and describes the nonlinear behavior of the material under simple shear. Fig. 1-28 is drawn for positive values of τ; this suffices for the isotropic materials considered here, since a reversal in the sign of τ implies merely a reversal in the sign of γ. If one wished, one could imply such symmetry by writing G^* as a function of τ^2 rather than τ.

A second quantity describing the nonlinear behavior of the material is sometimes of interest. This measures the slope of the line drawn from the origin to the point on the stress-strain curve corresponding to a given ordinate τ. The slope is the *secant modulus* which will be designated by $G^{**}(\tau^2)$. A typical line of which G^{**} is the slope is also shown on Fig. 1-28. For the secant modulus, the defining equation is

$$\frac{\tau}{\gamma} = G^{**}(\tau^2) \ . \tag{37}$$

Thus, if G^{**} is given as a function of τ, the corresponding strain is immediately found as the ratio τ/G^{**}.

The observed plastic behavior of engineering materials in simple shear does not permit of very easy analytical formulation. A popular approxi-

mation to the behavior is represented by Fig. 1-29.   A material conform-
ing to this representation is described as a "perfect plastic." For a
perfectly plastic material, the elastic law is obeyed up to a well defined
yield stress $\tau = k$.   The material is supposed to be incapable of supporting
any shear stresses greater than k and, accordingly, yields to effect stress
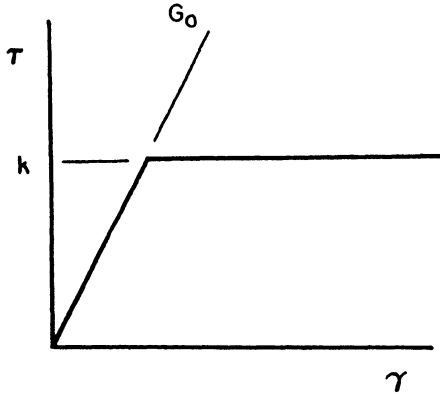
Fig. 1-29. The stress-strain curve of
perfect plasticity.
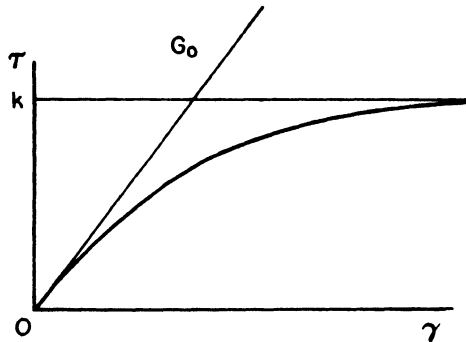
Fig. 1-30. The hyperbolic tangent approximation.

relief in any region throughout which the elastic stress would exceed k.
In this approximation,

$$G^* = G_0 \text{ , for } \tau^2 < k^2 \text{ , and}$$

$$G^* = 0, \text{ for } \tau^2 > k^2.$$

The simplicity of this analytical formulation of plastic behavior has made
possible mathematical solutions to physical problems of extraordinary
interest.   It is immediately evident, however, that engineering materials
do not conform very exactly to the assumptions of perfect plasticity.

A somewhat improved analytical formulation is to be had from the familiar hyperbolic tangent relationship between strain and stress. If this be written as

$$\gamma = \frac{k}{G_0} \operatorname{argtanh} \frac{\tau}{k}$$

illustrated by Fig. 1-30, it is seen that the behavior at low stress conforms to the identification of G_0 with the elastic modulus. This simple shear stress-simple shear strain relation provides a continuous transition from the elastic to the plastic regime, and accounts for work-hardening at all stresses inferior to the limiting stress taken here as k. As the shear stress k is approached, the representation makes the material tend toward perfect plasticity. In this limit the tangent modulus G^* tends toward zero. In actual materials, the effects of work-hardening do not disappear quite so fast with increasing stress. The approximation, however, allows an easy analytical evaluation of the tangent modulus as a function of stress, namely,

$$\frac{1}{G^*} = \frac{d\gamma}{d\tau} = \frac{k}{G_0} \frac{d}{d\tau} \left(\operatorname{argtanh} \frac{\tau}{k} \right)$$

$$= \frac{k^2}{G_0} \frac{1}{k^2 - \tau^2} .$$

To anticipate somewhat the formulation of the general stress-strain relations under combined stresses, it can be noted now that the stress invariant J_2 in the case of simple shear becomes nothing but τ^2. Accordingly, for simple shear the expression above can be written as

$$\frac{G_0}{G^*} = \frac{k^2}{k^2 - J_2}$$

and

$$\frac{G_0}{G^*} - 1 = \frac{J_2}{k^2 - J_2} . \tag{38}$$

This equation will later on be helpful in understanding Prager's generalization of the relationship.

The following paragraphs review some of the efforts to extend the analysis to the case of combined stresses. It is of course desirable that the behavior of the material be expressed in the generalized case by the constants obtained from simple tests of the type described above. It is then necessary to decide what measure of the intensity of the combined stress system will be used as the equivalent of the simple shearing stress τ approximated to in the test. Tresca's yield condition stipulates that the greatest principal shearing stress determines the plastic behavior of the specimen[51].

This conceptually simple condition is extremely awkward to express analytically. If the principal directions of stress are chosen so that $\sigma_1 > \sigma_2 > \sigma_3$, then the greatest principal shearing stress, taken by Tresca as equivalent to the simple shear stress, is

$$\tau = \tfrac{1}{2}(\sigma_1 - \sigma_3)$$

But if the principal directions are not so ordered, or if the orientation of the reference system is arbitrary, the equivalence is much more difficult to express. However, Von Mises has shown that the Tresca condition is very nearly the same as the identification

$$\tau = \sqrt{J_2}$$

where the invariant J_2 is independent of the reference coordinate system[31]. Then for a state of combined stress, J_2 may replace τ^2 in the arguments of $G^*(\tau^2)$ and $G^{**}(\tau^2)$ obtained from tests in simple shear.

In the generalization to combined stress, use can be made of the restriction to isotropic materials so that, even in plastic deformation, the directions of principal strain coincide with the directions of principal stress. This is Nadai's first rule.

Nadai's second rule states that the permanent deformations are at constant volume. This imposes on the principal components of strain the relation

$$\epsilon_1 + \epsilon_2 + \epsilon_3 = 0. \tag{39}$$

Otherwise, we can note that plastic deformations are deviatoric in character and so separate out the hydrostatic component of the stress and strain tensors. It is supposed that the elastic compressibility relation,

$$(\sigma_{11} + \sigma_{22} + \sigma_{33}) = 3K(\epsilon_{11} + \epsilon_{22} + \epsilon_{33}) \tag{30}$$

where K is the bulk modulus, obtains also throughout the plastic range. The shape changes defined by relations between the deviatoric strain components e_{ij} and the stress components s_{ij} are then necessarily at constant volume and so satisfy Eq. (39). The e_{ij} corresponding to a given state of stress may, however, contain reversible elastic components proportional to the s_{ij} along with permanent components which are more complicated functions of the entire stress system and perhaps as well of the strain history.

In formulating his third rule of plastic deformation, Nadai ignored the dependence on the past history of strain. To his rule on isotropy and his rule on incompressibility, Nadai adds the rule that the principal components of plastic strain be in the proportion of the principal components of stress. If the general stress-strain relations are written to conform with Nadai's third rule, they are found to describe the observed behavior of plastic materials when specialized to the easily measurable cases of pure

tension, pure compression, and pure shear. Suppose that the principal components of stress are σ_1, σ_2, σ_3, the corresponding principal components of strain being ϵ_1, ϵ_2, ϵ_3, so that the principal shearing stresses and principal shearing strains are given by

$$\gamma_1 = \epsilon_2 - \epsilon_3 \qquad\qquad \tau_1 = \frac{\sigma_2 - \sigma_3}{2}$$

$$\gamma_2 = \epsilon_3 - \epsilon_1 \qquad\qquad \tau_2 = \frac{\sigma_3 - \sigma_1}{2}$$

$$\gamma_3 = \epsilon_1 - \epsilon_2 \qquad\qquad \tau_3 = \frac{\sigma_1 - \sigma_2}{2}$$

Then Nadai's third rule states

$$\gamma_1 : \gamma_2 : \gamma_3 = \tau_1 : \tau_2 : \tau_3 \tag{40}$$

On account of the identities,

$$\gamma_1 + \gamma_2 + \gamma_3 = 0 \quad\text{and}\quad \tau_1 + \tau_2 + \tau_3 = 0$$

only one of the ratios (40) is independent. When written in terms of the principal components of stress and strain, the third rule is rather more complicated; in these terms the two ratios (40) are

$$\frac{\epsilon_2 - \epsilon_3}{\epsilon_3 - \epsilon_1} = \frac{\sigma_2 - \sigma_3}{\sigma_3 - \sigma_1} \quad\text{and}\quad \frac{\epsilon_1 - \epsilon_2}{\epsilon_3 - \epsilon_1} = \frac{\sigma_1 - \sigma_2}{\sigma_3 - \sigma_1}$$

The difference of these two equations is the ratio

$$\frac{\epsilon_2 - \epsilon_3 - \epsilon_1 + \epsilon_2}{\epsilon_3 - \epsilon_1} = \frac{\sigma_2 - \sigma_3 - \sigma_1 + \sigma_2}{\sigma_3 - \sigma_1} \tag{41}$$

which, along with the equivalent relations obtained by cyclic permutation of subscripts, constitutes the condition on the principal stresses and strains given by (40). When expressed in terms of the principal deviatoric strain and stress components, Eq. (41) reduces to

$$\frac{e_2}{e_3 - e_1} = \frac{s_2}{s_3 - s_1} \tag{42}$$

The relation (Eq. 42), and the similar relations, can obviously be satisfied simultaneously if each principal strain is related to the corresponding principal stress by

$$e_i = \left(\frac{1}{2G}\right) s_i$$

where the factor $(1/2G)$ is the same for all i. Taking account of the 2:1 relation between the shear strains and the tensor components, we can

identify the G in this expression with the factor relating γ to τ in Eq. (37). G is therefore the secant modulus G^{**} of the simple shear experiment, and is itself a function of the shearing stress, or of J_2 in the case of combined stresses. Moreover, by the first rule, the principal strain e_i is linearly related to the general deviatoric strain components e_{ij} in the same way that the principal stress s_i is related to the general deviatoric stress components s_{ij}. Therefore, one could write as well

$$e_{ij} = \frac{s_{ij}}{2G^{**}(J_2)}. \tag{43}$$

Eq. (43) illustrates what has been called the "deformation type" of general stress-strain relations for plasticity. In this type the strain is uniquely determined by the stress, although the relationship is by no means simple. The transition from the elastic to the plastic range accompanies the gradual decay of the function G^{**} as the stress intensity increases. For a given material, this decay is determined from observation by a test in simple shear. One source of nonlinearity in Eq. (43) is thus the physical behavior of the material. A second source of nonlinearity is concealed in the argument J_2 at which G^{**} is evaluated. This stress invariant is of course a quadratic function involving all stress components s_{ij}, $i, j = 1, 2, 3$. Thus, even for the isotropic materials, a particular e_{ij} in the plastic case depends not only upon the corresponding s_{ij}, but also upon a highly nonlinear function of all the stress components.

For very small values of J_2, the deformations are essentially elastic, G^{**} approaching the constant value G_0, the modulus of rigidity. At this extreme, the nonlinearities disappear from the relationship. At greater values of J_2, the predicted strains e_{ij} are a compound of reversible elastic extensions and permanent plastic strains. To isolate the residual strains, it is necessary to substitute for Eq. (43) a different relationship during the period of unloading. The behavior is to a close approximation elastic during unloading and for $\dot{J}_2 < 0$, we can, as in the last section, replace Eq. (43) by the differential relationship

$$de_{ij} = \frac{ds_{ij}}{2G_0}. \tag{44}$$

This prescribes that the slope of the unloading curve will be the same as the slope along the elastic part of the stress-strain curve during the initial loading. Integration of the differential relation results in the elastic stress-strain relationship except for a constant of integration which fits the relation to the strain at which unloading commences. This constant also measures the permanent strain remaining after all stresses have been removed.

Also, as mentioned in Section VI, the nomenclature can be made more compact by dividing Eq. (44) on both sides by the differential, dt. This in no way effects the equality, but allows one to write the relation as

$$\dot{e}_{ij} = \frac{\dot{s}_{ij}}{2G_0} \qquad \dot{J}_2 < 0 \tag{45}$$

in conformity with the usual convention by which the dot denotes time differentiation. In this homogeneous relation, no actual dependence on the time is implied.

Taking the strain history more generally into account involves a considerable increase in complexity. This leads to a type of stress-strain relationship which might be well called the "differential type", although it is designated by its originators, namely, W. Prager and his students, as the "flow type". This expression follows naturally from the use of the compact notation mentioned in the above paragraph, although no "flow" in the sense of continuously increasing viscous displacement under constant stress is intended. In the flow type of relation, the physical behavior of the material is measured by the factor which in simple shear is the tangent modulus G^*, although this is not immediately evident from the form in which the general relations are presented. These are given as

$$\dot{e}_{ij} = \frac{1}{2G_0}\left(\dot{s}_{ij} + \frac{1}{2}\frac{\dot{J}_2}{k^2 - J_2}s_{ij}\right). \tag{46}$$

In this expression, the first term on the right accounts for the elastic component of the strain. The second term accounts for the permanent component of strain, the homogeneity of the relation in respect to time being preserved by the factor $\dot{J}_2$. But the factor s_{ij} makes the plastic strain dependent upon the strain history of the specimen.

We can see this by specializing to the case of simple shear, and invoking the approximation of Eq. (38), by which

$$\frac{1}{k^2 - J_2} = \left(\frac{G_0}{G^*} - 1\right)\frac{1}{J_2}. \tag{38}$$

In simple shear, we can identify $2e_{ij}$ with γ and s_{ij} with τ, so that (46) becomes

$$\dot{\gamma} = \frac{1}{G_0}\left[\dot{\tau} + \frac{1}{2}\left(\frac{G_0}{G^*} - 1\right)\frac{\dot{J}_2}{J_2}\gamma\right]$$

But in simple shear, J_2 is nothing but τ^2, so that $\dot{J}_2$ is $2\tau\dot{\tau}$. Making these substitutions, we have

$$\dot{\gamma} = \frac{1}{G_0}\left[\dot{\tau} + \frac{1}{2}\left(\frac{G_0}{G^*} - 1\right)\frac{2\tau\dot{\tau}}{\tau^2}\tau\right] = \frac{1}{G^*}\dot{\tau}$$

which by Eq. (36) is only the definition of the tangent modulus G^* for the particular combination of stress and strain experienced in the specimen. The dependence of G^* upon the strain history (for the initial loading only) is seen in Fig. 1-36.

At the time being it appears that the differential relations are somewhat more flexible in meeting the compatibility conditions than the deformation relations advanced earlier. It is to be emphasized, however, that they are also highly nonlinear in character and lead to insuperable mathematical difficulties except in problems of particularly simple geometry. Despite the appearance of the rates $\dot{e}$ and $\dot{s}$ in these homogeneous relations, it should be recalled that they read only on the case of ordinary low temperature plasticity from which time variations are excluded, the deformations being supposed all to occur instantaneously. Thus, even before the high temperature phenomenon of creep is included, the mathematics has failed. Not even for the systems of ordinary plasticity can one repeat the statement made in Section IV for linear viscoelastic systems that the general solution can be found if the purely elastic solution can be found.

VIII. Time Effects in Plasticity

The assumptions of low temperature plasticity, which suppose the plastic deformation to be instantaneous, are an idealization of the actual behavior of material. Even at quite low temperature, the plastic deformation does in fact take some time to complete. There is a range of moderately high temperatures for which the steady state component of creep is small enough to ignore but for which the duration of the initial transient creep is appreciable as at θ''' of Fig. 1-22. In this case the stress-strain curve, alike in tension or shear, observed in a test of the material, will depend somewhat upon the rate of strain. If, at such a temperature, the specimen is suddenly subjected to a constant stress, the resulting strain will be observed to increase as time goes on, finally approaching a constant limiting value. If the value of the strain at successive equal increments of time be noted down, the results of the test may be represented as in Fig. 1-31.* Actually, such a record would be impossible to obtain. Even if the apparatus could maintain the true stress constant under increasing deformation, in any event, the instantaneous deformation would be controlled by the inertia of the machine. Nevertheless this presentation helps in visualizing the relationship. One can imagine the test repeated for different values of the constant imposed stress and the whole family of stress-strain curves obtained by linking the observations corresponding to the same times. Such a family of "isochronous" curves is exhibited in Fig. 1-32.

* This representation and its subsequent development in this section were suggested by unpublished papers of F. R. Shanley. See also Reference 30.

These curves make it possible to investigate the dependence of the behavior upon the strain rate. If for example the specimen is strained very slowly, the dashed limit curve to the right of Fig. 1-32 is obtained. The behavior at higher strain rates can be estimated by supposing the specimen to be subjected to shear by equal increments at the beginning of each time interval. By choosing both the strain increment $\Delta\gamma$ and the time incre-
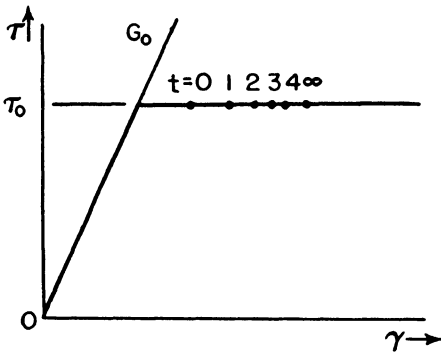
Fig. 1-31. Strain γ at succesive time intervals under constant stress τ_0. The modulus of rigidity G_0 is the slope of the elastic stress-strain curve.
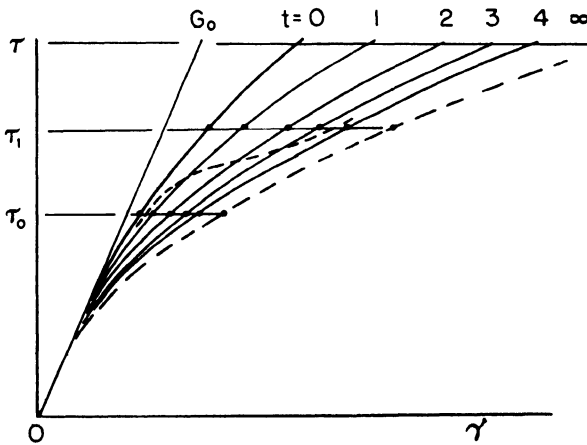
Fig. 1-32 Family of isochronous curves.

ment Δt sufficiently small, one can approximate closely to a continuous strain rate. The stress increment corresponding to each incremental strain is a compound of the elastic component predicted by the modulus of rigidity and a plastic component dependent upon both the total strain and strain rate, that is, upon γ and Δt. Suppose, as in Fig. 1-33, that a number of incremental strains have accumulated to the total strain γ and the stress τ. For this condition, there occurs during the next time interval

the plastic strain $\Delta\gamma'$. Then the stress increment corresponding to the forced shear $\Delta\gamma$ is the elastic stress corresponding to the strain $\Delta\gamma - \Delta\gamma'$, or $\Delta\tau = G_0(\Delta\gamma - \Delta\gamma')$. A continuation of this step-wise process extends the stress-strain curve which would be observed at the given strain rate. The dashed curve to the left in Fig. 1-32, corresponding to a high constant strain rate, was obtained in this way.

The step-wise approximation is easily adapted to situations in which the strain rate is not constant. For example, if the specimen is suddenly deformed to the strain γ, which is thereafter held constant, the method
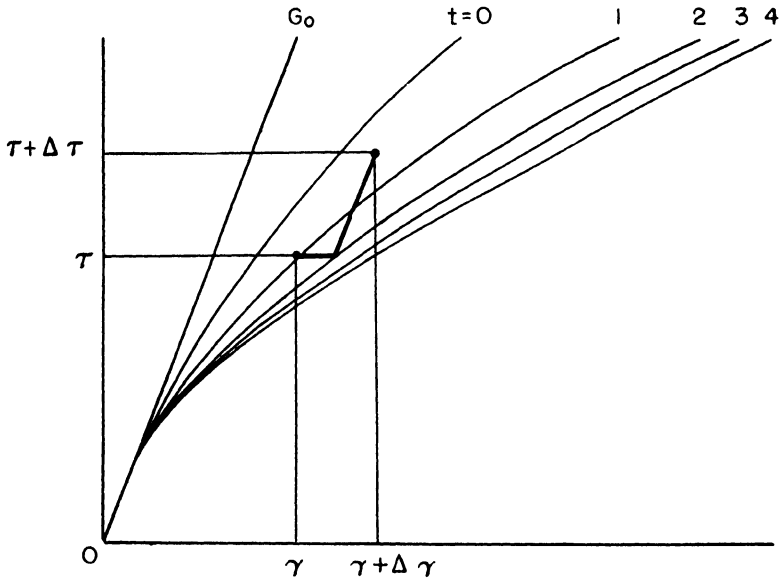
Fig. 1-33.

yields the relaxation curve of Fig. 1-34. To delineate the behavior, it is necessary to use in the step-wise approximation a time interval smaller than that for which the stress-strain curves are sketched. This can always be done; in the drawing, the ratio of these time intervals is 1:4. In this way, the precision of the approximation can be improved as needed, and the procedure adapted to any controlled variation in the rate of strain. Also, the procedure may be modified in an obvious way to predict behavior observed under controlled rates of stressing.

It is interesting to note that for certain materials the stress-strain curves obtained at controlled strain rate may be remarkably unlike any in the family of Fig. 1-32. Steels, for example, when stressed at room tempera-

ture exhibit a significant dependence upon strain rate, the part of the plastic deformation which is truly instantaneous, being small. Fig. 1-35 is the analogue of Fig. 1-32 for such a material in simple tension. It shows also the step-wise calculation of the predicted behavior when this material is tested at a high strain rate. The familiar sharply marked upper and lower yield points are properly indicated. Since the plastic deformation is relatively slow, in the early stages of the test, a high elastic stress is established. By the end of the fourth time interval, the slow yield begins to relieve the established stress and a temporary relaxation occurs. Beyond the lower yield point, work-hardening effects become dominant. Since the method of approximation over-estimates the stress
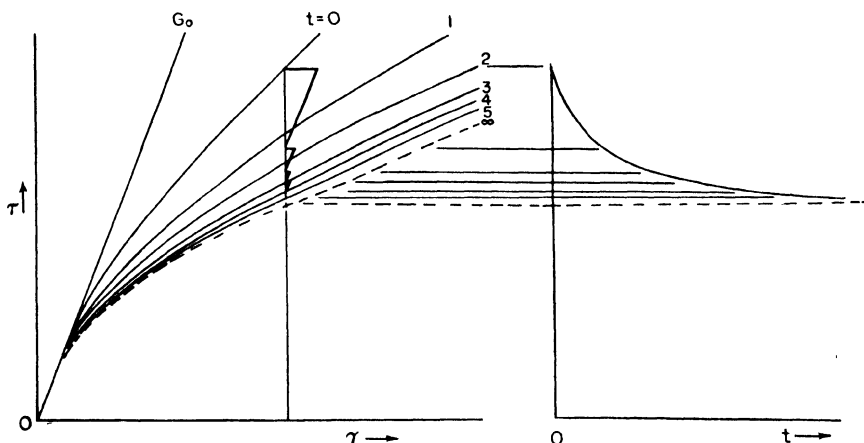
Fig. 1-34. Fast extension followed by relaxation.

when the stress is increasing, and underestimates it in the contrary circumstance, the actual variation would be found—by reducing the step interval —to conform to the solid curve of the figure. Of course, experimental stress-strain curves for steels do not conform exactly to this simple model, since with ordinary testing equipment the operator has control over neither the stress rate nor the strain rate but only over a complicated combination of the two.

The stress-strain relations for temperature ranges in which time effects become significant are evidently vastly more complicated than those described in the preceding section. In this case, the modulus G^* which relates the stress increment $\Delta\tau$ to the strain increment $\Delta\gamma$ can no longer be expressed as a function of the stress alone. The curves of Fig. 1-36 illustrate the behavior of a material in which the stress has been estab-
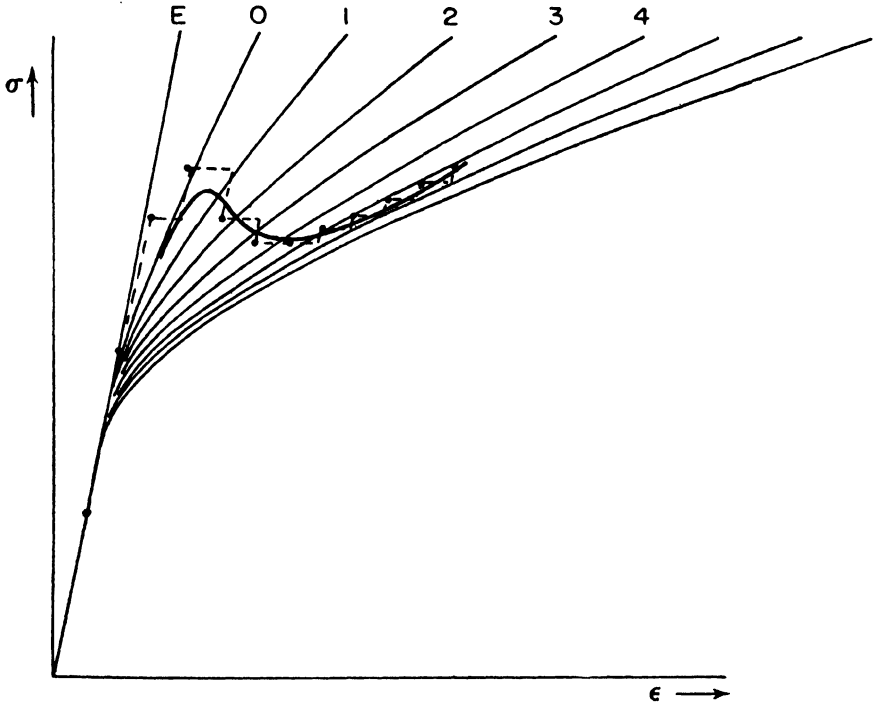
Fig. 1-35. Upper and lower yield stress.
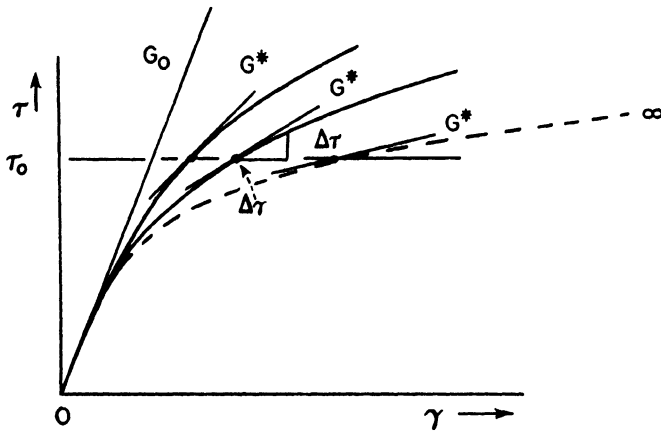
Fig. 1-36

lished through different constant rates of deformation.   The limiting curve
to the right corresponds to deformation at a very low strain rate and so is

identical with the limiting curve of Fig. 1-32. The bounding curve to the left is supposed to correspond to a very great rate of deformation and the remaining curves to typical intermediate values. The effect of the strain history is revealed in two ways. First, different values of the strain correspond to the same stress τ_0 depending upon the past rate of strain. Second, the slope G^* at the stress τ_0 varies widely between the value obtained at high strain rates, perhaps only slightly less than the elastic modulus, and the much lower value obtained at low rates of deformation. Thus, for any condition of the specimen, the rate of change of stress with strain must be considered as a function of the strain as well as of the stress.

No entirely satisfactory formulation of this relationship has been achieved. An interesting attempt is represented by Holloman's mechanical equation of state[20]. In a much more elementary way, some account can be taken of the strain history merely by estimating the value of G^* appropriate to each combination of τ, γ by scrutiny of experimental records of the type exemplified by Fig. 1-36.

IX. An Atomistic Model for Creep; Transient Creep

In high-temperature metallurgy, there is added to the considerations of the preceding sections the further complication of steady state creep, that is, the steady flow of the material under load resulting in deformations continuously increasing with time. Even though the steady creep rate be very small, nevertheless the resulting deformation during the service life of a part stressed at high temperature may be so great as to dominate all other effects. In fact the determination of the steady state creep rate is the primary concern of high-temperature metallurgy and most of the material testing described in the following chapters is directed toward this end.

The phenomenon is like the viscous flow of liquids in that the strain rate is determined by the stress. In an earlier section, it was distinguished from the phenomena of low-temperature plasticity, in which the stress-strain relations are homogeneous, so that the strain rate is determined by the stress rate. The steady creep of metals is distinguished from viscous flow in liquids and amorphous solids primarily by this, that in no case is the flow Newtonian, or even approximately proportionate to the applied stress. For metals the typical dependence of strain rate upon stress was illustrated in Fig. 1-2. If, as is usual in metals, the strain rate is constant under constant stress, although not proportional, the flow is described as quasi-viscous. A satisfactory rationalization of this behavior has yet to be brought forth.

Very little of the available creep data have been obtained at constant stress; technical creep tests are conducted at constant load and necessarily exhibit the acceleration in creep rate due to diminution in cross section

of the specimen. But if this rather trivial effect could be sorted out, so that the quasi-viscous component could be ascertained merely by waiting until transient effects had subsided, still it would be found that metals do not always tend toward a constant creep rate under constant stress. The reason for this is, of course, change of state. If, during the period of exposure to stress and temperature, the material changes phase through recrystallization (or otherwise changes structure through the precipitation or diffusion of microconstituents) the steady creep rate can alter even though stress and temperature are held scrupulously constant. The recommended range of operating temperature for any material is ordinarily adjusted so that such structural changes are not likely to occur. They are not further considered here; however, the possibility of their occurrence should be held in mind whenever creep data are to be interpreted.

The atomistic model already used in Section II for the prediction of viscosity in liquids can be made to serve for the prediction of the steady creep of metals. In the solid state, it must be supposed that the ordered regions of close packing are relatively extensive, with the "holes" or disordered regions localized and sparsely distributed. These holes are characterized exactly as in Fig. 1-3. Even though the local imperfections of structure be separated by many atomic distances, so that they are nearly independent one of the other, it is still possible that in the aggregate they are very numerous, so that the total population of soft points is not seriously depleted by the occasional successful transitions. If it is supposed that the potential barriers to transition for the several imperfections are all high, then one has a model for a state of aggregation which can support elastic shearing stresses. By the same premises, the imposed stress field makes only a small modification of the activation energies at the soft points, giving a slight bias in favor of transitions in the preferred direction. Wherever through thermal fluctuation the free energy in the neighborhood of an imperfection surpasses the least potential barrier, a transition in the preferred direction occurs. Under the assumption of high barriers these are infrequent, and, under the assumption of independence, these make equal contribution to the macroscopic strain. This combination of assumptions leads to a formulation of the dependence of strain rate upon stress and temperature identical to that adduced for the viscous flow of fluids in Section II, *viz.*,

$$\dot{\gamma} = \frac{1}{\eta}\tau \tag{1}$$

where $\dot{\gamma}$ is here only the steady state component of the creep. Quantitatively, the relative freedom of solid materials from loose points would indicate a greatly reduced rate of strain, which is of course observed. But

again, the model gives no indication of the dependence of activation energies upon the applied stress, and the same assumption of linearity yields the Newtonian case. An improvement of the model to account for the observed nonlinearities of quasi-viscous creep would seem to be the first priority task of high-temperature metallurgy.

The atomic model used for the (rather imperfect) prediction of the steady state component of creep is certainly inadequate for the prediction of the transient component, characterized by a very high initial rate of deformation and a subsequent rapid deceleration. The refinement of the model to account for this effect has received attention from Andrade, Becker, Orowan and their co-workers[2, 4, 36]. It is necessary to consider that in the early stages of the deformation, the material contains loose points, or imperfections of very low activation energies, which are by no means infinitely numerous, but which are, to the contrary, rapidly used up. Then for the deformation to proceed, higher energy barriers must be surpassed. In this view, work-hardening is equivalent to the elimination from the material of the imperfections of low activation energies.

When the virgin material is subjected to stress, the energy stored elastically modifies the potential barriers, reducing the activation energies required for transitions in the preferred direction. Wherever in the virgin material the potential barriers were sufficiently low, they are extinguished by the application of the load and the transitions occur instantaneously. This accounts for the instantaneous component of the plastic deformation. At other imperfections, the potential barrier in the preferred direction is only reduced to a value which may occasionally be exceeded in the course of thermal fluctuations in the local energy. The progressive elimination of such imperfections accounts for the time dependent—initial creep.

To improve the mechanical model, one should know the distribution of the A_i, where A_i is the activation energy for the imperfection located at point i in a typical slip plane of the virgin material. One should further know the modified values A_i' to which the A_i's are reduced by the applied stress for transitions in the slip directions. Such information would permit the prediction of the shearing rate as a function of load and temperature. Actually, these distributions can only be inferred from observations of the macroscopic behavior, and we undertake only to evaluate statistical averages. We can form a first estimate of the way in which the mean activation energy A' necessary to continued deformation increases, as the loose spots are exhausted, by examination of Fig. 1-37. In this figure, the curve, which is identical with the left-hand curve of Fig. 1-32, measures the distribution of activation energies in the virgin material. The suddenly applied stress τ_0, which produces immediately the elastic strain γ''', also reduces to negative values of A_i' a sufficient proportion of the A_i

to produce instantaneously the macroscopic plastic deformation γ''. As time goes on, the specimen creeps under constant stress to the deformation γ_1, exceeding the instantaneous γ_0 by the creep strain γ'. It is supposed that this time is taken short enough that the quasi-viscous component of the creep is inconsiderable.

The deformation γ_1 might have been produced instantaneously by the imposition of the stress τ_1. That is, a suddenly applied stress τ_1 reduces to negative values the proportion of the A_i corresponding to the
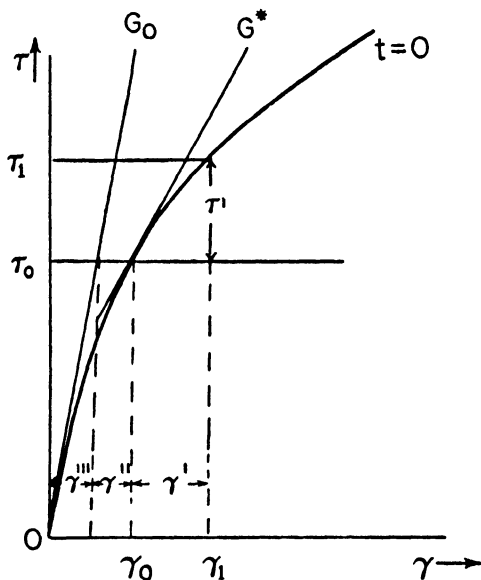
Fig. 1-37. τ' = Activation stress;
γ' = Transient creep strain;
γ'' = Instantaneous plastic strain;
γ''' = Elastic strain;
$G^* = \lim\limits_{t \to 0} \dfrac{\tau'}{\gamma'}.$

macroscopic strain γ_1. Thus the difference $\tau' = \tau_1 - \tau_0$ provides a measure of the proportion of imperfections eliminated during the creep γ'. One can call τ' the "activation" stress corresponding to the applied stress τ_0 and the strain $\gamma_1 = \gamma_0 + \gamma'$. It is observed to increase with increasing creep. Initially it is quite small; correspondingly, the material contains imperfections for which the potential barriers, being reduced very nearly to zero by the applied stress τ_0, are exceeded by the smallest thermal fluctuations. Since these occur very frequently, the time rate of deforma-

tion is high. As creep proceeds, the loose spots are eliminated, and large, infrequent fluctuations are required to exceed the remaining potential barriers; this corresponds to greater values for τ' and slower rates of deformation. For γ' not too large, the activation stress is given approximately by

$$\tau' = G^*\gamma' \tag{47}$$

where the modulus G^* is to be evaluated at $\tau = \tau_0$ on the stress-strain curve for $t = 0$.

The so-called activation stress τ', as here defined, provides only a crude measure of the disorder remaining in the material after the creep strain γ'. The definition implies that during the creep γ', following the instantaneous deformation γ_0, the same set of microscopic transitions is successfully achieved as would be achieved if the total deformation γ_1 were accomplished instantly. This is hardly to be expected, since during creep at the constant applied stress τ_0, the surpassing of the potential barrier at any particular imperfection is entirely a matter of chance fluctuation in the local energy. On the contrary, in the distribution of activation energies for the imperfections remaining after the strain γ_1, one should anticipate differences depending upon the way in which γ_1 has been established; that is, differences dependent upon the strain history of the material. Careful measurements have established quite conclusively that such differences do exist, although they may be relatively unimportant[26]. The absence of these differences implies the existence of a "mechanical equation of state". The presence of these differences implies that one's estimate could be improved by the substitution for G^* in Eq. (47) of a different constant dependent upon the strain history as well as upon τ_0. In this connection, the issue is of trifling importance, since G^* is not itself a measurable quantity, and whatever proportionality constant is to appear in Eq. (47) must be determined by an empirical fit to observed creep data.

In order to obtain a useful characterization of transient creep one needs to convert the activation stress τ' into the corresponding value for the mean of the activation energies A_i appearing in the Einstein-Boltzmann relation

$$\nu_i \propto e^{(-A_i/kT)} \tag{48}$$

so as to evaluate at least the mean frequency of transitions due to thermal fluctuation. In this calculation, the A_i should be distinguished from the activation energies at imperfections in the virgin material. Rather, one wishes i to range only over the imperfections surviving after the specimen has deformed to the strain γ_1, say; and moreover the A_i must, like the A_i', reflect the reduction of the potential barriers in the slip direction due

to the imposed constant stress τ_0. From the average of this distribution one could predict the rate of creep under stress τ_0 at strain γ_1.

Under this interpretation, Becker's formula gives the activation energy A within an average volume element V of the material as the following function of the activation stress:

$$A = \frac{(\tau')^2}{2G_0} V \tag{49}$$

where G_0 is the elastic modulus of rigidity. Using this value for A, one finds for the average frequency of successful transitions within V,

$$\nu \propto e^{-(\tau'^2/2G_0 kT)V} = e^{-(B/T)\tau'^2} \tag{50}$$

To obtain a formula for strain rate, it remains only to evaluate the contribution of a successful transition to the macroscopic strain. If it were assumed, as for the case of viscous flow, that each transition made the same contribution to the observed shear, the strain rate would also be given by the formula (Eq. 50). But in the early stages of transient creep, the material is rich in imperfections. These are so closely spaced that the effect of a single transition upon the local stress field extends to neighboring loose points, lowering the barriers to transitions there. In transient creep, inhomogeneities in the stress field, and interaction between transitions, cannot be ignored. Thus, the stress relief achieved by a successful thermal fluctuation at the point i may redistribute the stress field at neighboring imperfections in such a way as to trigger off a whole chain of transitions. That this interdependence actually exists is evidenced by the observed initial rate of transient creep, which does not seem to be finite but which, to the contrary, appears smoothly to continue the instantaneous deformation.

For such reasons, the hypothesis that successful fluctuations make equal contributions to the macroscopic strain is untenable in transient creep. Orowan conjectured that the interdependence effect might be accounted for by taking the strain rate proportionate not to ν, but to $(1/\tau')^2\nu$, where $(1/\tau')^2$ is to be regarded as an empirical factor[36]. He wrote

$$\dot{\gamma}' = \frac{C}{\tau'^2} e^{-(B/T)\tau'^2} \tag{51}$$

as a simple, but surprisingly adequate characterization of transient creep. The activation stress being zero at the commencement of transient creep, the formula correctly predicts the infinite initial rate of creep strain. Moreover, as the material hardens under continued deformation (and τ' increases), the density of imperfections (and accordingly the interaction effect) decays in a way which is at least superficially consistent with the formula.

When the activation stress is expressed in terms of the creep strain, Eq. (51) becomes

$$\dot{\gamma}' = \frac{C}{(G^*\gamma')^2} e^{-(B/T)(G^*\gamma')^2} \tag{52}$$

where G^* contains the dependence upon the applied stress, and perhaps also on the strain history. Since the instantaneous stress-strain curve, which provides the estimate of G^*, depends on the temperature, G^* is temperature-dependent as well. In fact, it is the G^* which mainly determines the temperature dependence of transient creep. For the exponential factor of Eq. (52), in which T appears explicitly, is only a small correction, serving to hasten the deceleration in transient creep rate at large strains. For all the materials studied, the multiplier BG^{*2}/T is so small that the exponential departs but little from unity during the principal part of the deformation. This accounts for the marked difference in the variation with temperature of the transient and steady components of creep. The quasi-viscous component, being more nearly an exponential function of $-(1/T)$, disappears quickly as the temperature is lowered. The transient component, being dependent more upon G^*, persists as the temperature is lowered, being observed even at temperatures close to absolute zero, although at such temperatures the duration of the transient becomes very brief.

If the exponential factor of Eq. (51) is approximated by unity, the resulting equation integrates to

$$\gamma' \propto t^{1/3} \tag{53}$$

which is Andrade's early formula for the transient component of creep. In the present notation, the constant of proportionality is $(3C)^{1/3}(G^*)^{-(2/3)}$. This remarkable general result stipulates that for all materials, however stressed at whatever temperature, the variation of creep strain with time is in the early stages, represented by curves of the same slope, all cubic parabolas. Since these form a one-parameter family, it should be possible to find, for any material, combinations of applied stress and temperature which determine a particular curve in that family, or, what is the same thing, which correspond to the same constant of proportionality. This possibility has been confirmed by Los, whose measurements on copper and aluminum at appropriately selected values of temperature and stress are given in Fig. 1-38. The measurements yielded the variation of total strain with time; to obtain the creep component, the observed strains were reduced by the instantaneous strains, the values of which were chosen for best fit. The agreement among the three sets of observations is dramatic, but not superior to other cases not illustrated here.

The smooth curve upon which the observations fall departs significantly from the cubic parabola at times greater than about 15 minutes. The smooth curve was calculated by mechanical integration of Eq. (52), after best choice of the constant BG^{*2} and therefore reflects also the exponential reduction in strain rate at large strains.

The transient component of creep is thus fairly well predicted by a very crude model, making only the most general assumptions regarding the state of aggregation of the material. It may well be expected that sharper results will flow from a closer examination of the molecular structure and the nature of the imperfections. A tool for such an investigation is provided by the theory of dislocations, which is briefly reviewed in the following section.
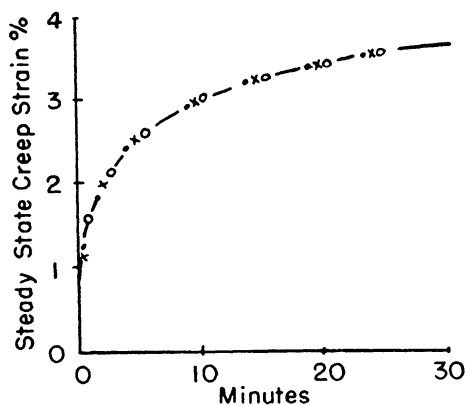
Fig. 1-38. Steady state creep strain (%) versus time (minutes) of the following:
○ Cu at 100°C; mean stress 2485 kg/cm².
✕ Cu at 230°C; mean stress 1990 kg/cm².
● Al at 15°C; mean stress 735 kg/cm². (After Orowan)

X. Dislocation Theory

In the preceding discussions, a point of looseness or imperfection in the material was envisaged as a hole into which an adjoining particle might rather easily slip under the influence of thermal fluctuations or external load. This model has a certain plausibility for liquids but is somewhat strained in its application to polycrystalline metals and fails completely in application to single crystals. Single crystals also deform plastically by slip in a way which cannot be explained on the hypothesis of a perfectly uniform crystalline structure. It must be supposed that single crystals contain imperfections. The model proposed by Volterra for such imperfections was called by Love a dislocation. This model has served in a qualitative, and even semi-quantitative way to explain the plastic behavior of single crystals, as is witnessed for instance by the soap bubble experiments of Sir Lawrence Bragg. Moreover, useful models of more complicated states of aggregation, such as polycrystalline materials, may be constructed as arrays of dislocations.

In Fig. 1-39, the small drawing (a) represents a section through a perfect crystal having a simple cubic lattice. The small drawing (b) shows a section through the crystal after the atoms above the dashed line have slipped one atomic distance to the right. It is supposed that the arrangement of atoms on every parallel section through the crystal is identical. The displacement of the upper left hand atoms has resulted in a line of dislocation (normal to the plane of the drawing) where a vertical plane of atoms terminates on the slip plane. The adjoining "vertical" atomic planes are at least in approximate register as they intersect the horizontal
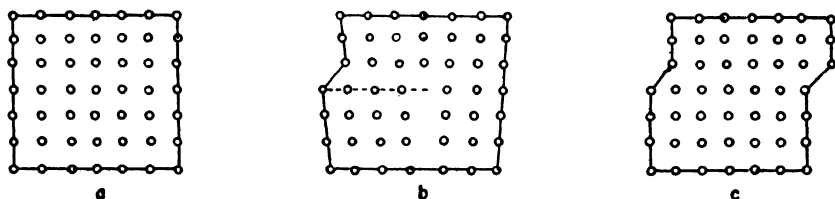
POSITIVE DISLOCATION
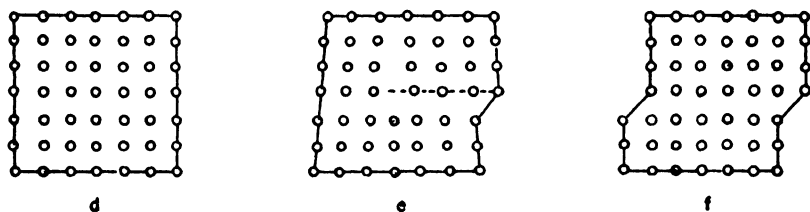
NEGATIVE DISLOCATION

Fig. 1-39. Propagation of a dislocation through a cubic lattice.

slip plane, but they are slightly deformed elastically, the material above the slip plane being in a state of compression in the neighborhood of the dislocation, whereas the material below is in tension. By convention, this configuration is described as a positive dislocation. If the plane of atoms to the right of the dislocation should divide on the slip plane, the lower half falling into register with the atoms of the terminated plane, the dislocation is propagated by one atomic distance, to the right. The continuation of this process to the boundary of the material relieves the elastic strain and results in a permanent slip deformation.

The same deformation can be obtained in a different way as illustrated

by the drawings (d), (e), (f) of Fig. 1-39. These show a displacement in the opposite sense of atomic planes. If this originates in the right hand boundary and is propagated to the left, the macroscopic shear is the same. In the neighborhood of this imperfection, the material above the slip plane is in tension, and that below in compression; it is a negative dislocation.

The work which must be done by the applied forces on a perfect crystal in order to produce a dislocation can be calculated from the elastic constants by determining the energy stored in the strained material nearby. Similarly, the work which must be done in order to propagate a dislocation by one atom distance may be calculated.

Since the atoms in the neighborhood of a dislocation are under considerable elastic stress, it requires only a small external force to produce a transition in the preferred direction. Therefore the energy expended in the propagation of a dislocation is small. The propagation of a dislocation across an entire slip plane through the body is easily shown to require the expenditure of relatively little energy. In fact, the energy is only a tiny fraction of the energy required to displace simultaneously the atoms above the slip plane of a perfect crystal to the neighboring equilibrium locations. In this way it is explained why the yield stress of single crystals is so very much less than would be required for the rigid displacement of parallel atomic planes.

To explain the observed shear of crystalline materials under applied stress, it does not suffice to assume that all the dislocations are generated by the action of the external forces; to explain observed behavior there must be many such imperfections present in the virgin crystal. Under initial loading, certain of these dislocations are eliminated through propagation to the boundary of the body and work-hardening results.

XI. Grain Boundaries, Fracture, Precipitation of Microconstituents

In the foregoing sections, the theory of plasticity of metals has been developed on the basis of homogeneity of structure without regard to the actual structure of polycrystalline substances, particularly grain boundaries. The existence of grain boundaries, segregation of impurities, and the possibility of other defects in the aggregate of metal crystals add enormously to the complexity of plastic behavior. Measurements of internal friction of single crystals of copper indicate that this material is fairly insensitive to mechanical shock. Polycrystalline copper, on the other hand, has a tenfold increase of internal friction under similar conditions of mechanical disturbance. Grain boundaries thus appear to be a source of dislocations[42].

Much has been written about viscous behavior of grain boundaries, and,

while there is evidence for support of this concept, it is really only necessary to assume that grain boundaries are areas of disorder. The effect of grain size in metals, when they are stressed at elevated temperature, is evident in that larger grains generally show greater creep resistance than very fine grains. This decrease in the grain boundary areas with increased creep resistance coincides with the requirements of disorder. Examples of this effect will be shown later under specific metallic systems.

In a characterization of metal fractures, a ductile failure is classed as one which necks down at fracture. Generally, in the vicinity of the fracture, deformed grains are visible under the microscope. The same metal may fail in a brittle manner with little or no necking down at the fracture and the grains are undistorted in the vicinity of the fracture. This description is obviously an idealized picture.
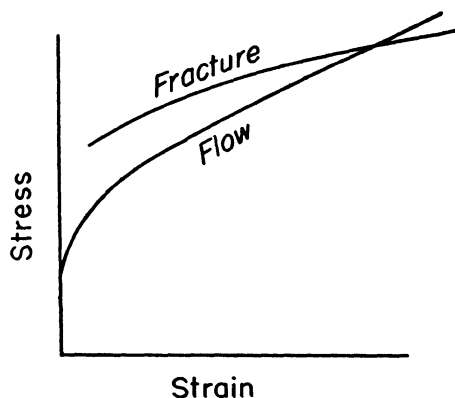
Fig. 1-40. Schematic curves for flow and fracture.

At room temperature, ductile metals may fail in a brittle manner under high-speed impact or other types of sudden shock. It is also true that metals which are ordinarily ductile at room temperature may fail with a brittle fracture when subjected to low temperatures. In the case of steels, there are many factors such as notch sensitivity to increase the probability of brittle failure.

To explain such ductile and brittle behavior, it is assumed that metals possess a fracture stress which is larger than that required for plastic flow.* Where the surfaces intersect, fracture of the metal occurs. It is also assumed that the fracture stress of the unbroken metal is dependent upon the amount of deformation that it has undergone. On a conventional stress-strain diagram, the curve for fracture stress appears above that of the curve for the flow stress as in Fig. 1-40. When the flow stress for a

* Flow stress is defined as the greatest principal stress during flow under any stress combination (McAdam).

metal is raised so that it equals the fracture strength, then fracture occurs. Or, stated another way, if the flow stress is less than the fracture stress, the metal can deform plastically until it is stopped by fracture.

If two samples of the same metal are alike in all particulars except that there is a large separation between the curves for flow and fracture of one of them, this sample then exhibits ductility. The converse is also true that slight separation between flow and fracture curves indicates brittleness. It is difficult to measure the fracture and flow stresses for a metal. If plastic deformation occurs, the fracture stress has changed; while if fracture occurs, further deformation cannot be measured. Low temperature experiments where brittleness can be induced are one method of determining fracture strength. For single crystals, the temperature does not influence the fracture stress, but there is a temperature effect for polycrystalline metals. Other variables which will change the flow and fracture of metallic structures are the stress system, strain rates, and the microstructure.

The type of fracture produced in a metal is strongly temperature dependent. The effect is readily observed in a type of fracture resulting from grain boundary sliding or intercrystalline fracture. In certain metals such as plain carbon steel, the transition to intercrystalline fracture occurs in a narrow temperature range which has been designated the equicohesive temperature. The occurrence of grain boundary sliding at fracture is also time dependent and is observed frequently after long creep test periods. This effect will be illustrated in later sections of the text.

The precipitation of microconstituents in a metal changes the resistance to creep. The presence of complex carbides in certain alloy steels may be largely responsible for their increase in creep resistance[22]. In heat-resistant alloys, the precipitation of microconstituents after prolonged heating at high temperature will also change the creep resistance. This reaction may or may not be detrimental to the load-carrying ability of the material.

References

1. Alfrey, T., "Mechanical Behavior of High Polymers," Interscience Publishers, Inc., New York (1948).
2. Andrade, E. N. daC., "On the Viscous Flow in Metals and Allied Phenomena," *Proc. Roy. Soc. (A)*, **84**, 1 (1911).
3. Andrade, E. N. daC., "Flow of Metals under Large Constant Stresses," *Proc. Roy. Soc.*, **90**, 329 (1914).
4. Becker, "Über die Plästizitat amorpher and kristalliner fester Korper," *Phys. Zeits.*, **26**, 919 (1925).
5. Boas, W., "Physics of Metals and Alloys," John Wiley & Sons, Inc. (1947).
6. Boas, W., and Schmid, E., "Concerning the Dependence of Crystal Plasticity upon Temperature," *Z. Physik*, **71**, 703 (1931).
7. Burghoff, H., and Mathewson, C. H., "Time and Temperature Effects in the

Deformation of Brass Crystals," *Trans. Am. Inst. Min. and Metallurgical Engrs.*, **143,** 45 (1941).

8. Carpenter, H. C., and Robertson, "Metals," Oxford University Press, London (1939).

9. Chevenard, P., *Comptes Rendus*, **169,** 712 (1919), **175,** 486 (1922).

10. Dickenson, J. H. S., "Flow of Steels at a Red Heat," *Engineering*, **114,** 326, 378 (1924).

11. Dupuy, E. L., "An Experimental Investigation of the Mechanical Properties of Steels at High Temperatures," *J. Iron and Steel Inst.*, **104,** II, 91 (1921).

12. Fahrenwald, F. A., "Some Principles underlying the Successful Use of Metals at High Temperatures," *Proc. Am. Soc. Testing Materials*, **24,** II 310 (1924).

13. French, H. J., and Tucker, W. A., "Available Data on the Properties of Irons and Steels at Various Temperatures," *Proc. Am. Soc. Testing Materials*, **24,** II, 56 (1924).

14. Gensamer, M., Saibel, E., Ransom, J. T., and Lowrie, R. E., "Fracture of Metals," Amer. Welding Soc. (1947).

15. Gillette, H. W., "Some Things We Don't Know about Creep," *Trans. Am. Inst. Min. and Metallurgical Engrs.*, **135,** 15 (1939).

16. Griffith, A. A., "Theory of Rupture," Proc. International Congress for Applied Mechanics, Delft, April (1924).

17. Hanffstengel, K. von, and Hannemann, H., "Mechanism of Creep and Fatigue Limit Investigated for Pb and Pb Alloys," *Z. f. Metallkunde*, **29,** 50 (1937).

18. Hanson, D., and Wheeler, M. A., "Deformation of Metals under Prolonged Loading, Part I. Flow and Fracture of Aluminum," *J. Inst. Metals*, **45,** 229 (1931).

19. Holloman, J. H., "Problem of Fracture," Am. Welding Soc. (1946).

20. Holloman, J. H., "Mechanical Equation of State," *Trans. Am. Inst. Min. and Metallurgical Engrs.*, **171,** 535 (1947).

21. Holloman, J. H., and Jaffe, "Ferrous Metallurgical Design," Macmillan Co., New York (1947).

22. Holloman, J. H., and Lubahn, J. D., "Flow of Metals at Elevated Temperatures," *Gen. Elec. Rev.*, **50,** 28, 44 (1947).

23. Howe, H. M., "Patience of Copper and Silver as Affected by Annealing," *Trans. Am. Inst. Min. and Metallurgical Engrs.*, **13,** 646 (1885).

24. Jeffries, Z., and Archer, R., "Science of Metals," McGraw-Hill Book Co., New York (1942).

25. Kanter, J. J., "Problem of Temperature Coefficient of Tensile Creep Rate," *Trans. Am. Inst. Min. and Metallurgical Engrs.*, **131,** 385 (1938).

26. Kochendörfer, A., "Plastische Eigenschaften von Kristallen und metallischen Werkstoffen," Springer Verlag, Berlin (1941).

27. Lea, F. C., "Effect of Low and High Temperatures on Materials," *Proc. Inst. Mech. Engrs.*, **2,** 1053 (1924).

28. Machlin, E. S., and Nowick, A. S., "Stress Rupture of Heat Resisting Alloys as a Rate Process," Nat. Advisory Com. for Aeronautics, Tech. Note No. 1126, Sept. (1946).

29. Malcolm, V. T., "Methods of Testing at Various Temperatures," *Proc. Am. Soc. Testing Materials*, **24,** II, 14 (1924).

30. McVetty, P. G., "Working Stresses for High Temperature Service," *Mechanical Engineering*, **56,** 149 (1934). "Predicting Creep Strength," *Metal Progress*, **51,** 959 (1947).

31. Mises, R. V., "Mechanik der festen Koerper in plastisch deformablen Zustand," *Goettinger Nachr., math phys.*, **K1**, 582 (1913).
32. Nadai, A., "On the Creep of Solids at Elevated Temperatures," *J. Applied Phys.*, **8,** 418 (1937).
33. Nadai, A., "Plasticity, a Mechanics of the Plastic State of Matter," McGraw-Hill Book Co., New York (1931).
34. Norton, F. H., "Creep of Steel at High Temperatures," McGraw-Hill Book Co., New York (1929).
35. Nowick, A. S., and Machlin, E. S., "Dislocation Theory as Applied by NACA to the Creep of Metals," *J. Applied Phys.*, **18,** 79 (1947).
36. Orowan, E., "Creep of Metals," West of Scotland Iron and Steel Inst., Febr. 14 (1947).
37. Prager, W., "Strain Hardening under Combined Stresses," *J. Applied Phys.*, **16,** 837 (1945).
38. Prager, W., "An Introduction to the Mathematical Theory of Plasticity," *J. Applied Phys.*, **18,** 375 (1947).
39. Rosenhain, W., "Deformation and Fracture in Iron and Steel," *J. Iron and Steel Inst.*, **70,** 189 (1906).
40. Rosenhain, W., and Ewen, D., "Intercrystalline Cohesion in Metals," *J. Inst. Metals*, 149 (1912); 119 (1913).
41. Rosenhain, W., and Humphrey, J., "Crystalline Structure of Iron at High Temperature," *Proc. Roy. Soc.*, **83,** 200 (1909).
42. Seitz, F., and Read, T. A., "Theory of the Plastic Properties of Solids," *J. Applied Phys.*, **12,** 100, 170, 470, 538 (1941).
43. Siebel, E., "Die Prüfung der Metallischen Werkstoffe," vol. 2, Springer Verlag, Berlin (1939).
44. Siebel, E., and Pomp, A., "Influence of Strain Rates on the Course of the Flow Curves of Metals," *Mitt. K. W. Inst. f. Eisenforschung*, **10,** 63 (1928).
45. Tapsell, H. J., "Creep of Metals," Oxford University Press (1931).
46. Taylor, G. I., "Mechanism of Plastic Deformation of Crystals, Part I. Theoretical," *Proc. Roy. Soc.*, **145-A,** 362 (1934).
47. Thielemann, R. H., "Correlation of High Temperature Creep and Rupture Test Results," *Trans. Am. Soc. Metals*, **29,** 355 (1941).
48. Thielemann, R. H., "Some effects of Composition and Heat Treatment on the High Temperature Rupture Properties of Ferrous Alloys," *Proc. Am. Soc. Testing Materials*, **40,** 788 (1940).
49. Thielemann, R. H., and Parker, E. R., "Fracture of Steels at Elevated Temperatures after Prolonged Loading," *Trans. Am. Inst. Min. and Metallurgical Engrs.*, **135.** 559 (1939).
50. Thurston, R. H., "Notes Relating to a Peculiarity Distinguishing Annealed from Unannealed Iron," *Science*, **1,** 418 (1883).
51. Tresca, H., "Mémoire sur l'écoulement des corps solides," *Mém. prés. par div. sav.*, **18,** 733 (1868).
52. Zener, C., "Anelasticity of Metals," *Am. Inst. Min. and Metallurgical Engrs.*, Tech. Paper 1992 (1946).

Chapter 2

Test Methods and Equipment for Elevated Temperature

A. OBJECT OF ELEVATED TEMPERATURE TESTING

Creep of metals is the continually increasing deformation which occurs when a metal is stressed at a constant load while held at a constant temperature. Creep tests are conducted to establish safe working stresses for materials subjected to loading sustained usually at elevated temperature. The object of the tests is to determine the deformation to be expected in the metal during a certain period of service. Creep tests are not suitable for acceptance tests since the time periods involved are too extensive.

It is convenient in investigating the creep of metals to apply a tensile load on the test specimen. Such a practice in general does not simulate actual service conditions, since shapes such as beams, pipes, shells, etc. are subjected to combined stresses. However, the centrifugal forces at the root of turbine blades rotating at constant speed without regard to other forces such as bending and vibrational stresses produce tensile stresses. Bolts are also subjected to tensile stresses.

I. Test Periods

The observed behavior of metals stressed at elevated temperature depends importantly on the length of the test period. The time factor is an economic problem, as long test periods are costly. Test periods less than 1 per cent of the expected life of the material are not significant[3]. Where possible, a test period of at least 10 per cent of the service life is preferred. The selection of a suitable test period for any material also depends on the structural changes that may occur in the material and may render extrapolation of the data on the time axis uncertain.

On the basis of length of the test period, elevated temperature testing can be classified as follows:

(1) Creep testing at small deformations and low stresses for several hundreds or thousands of hours at strain rates of the order of 10^{-10} sec^{-1}.

(2) Stress rupture testing at larger deformations and higher stresses for a few hundred hours at strain rates of the order of 10^{-7}sec^{-1}.

(3) Short time tensile tests conducted at large deformation and the high stresses encountered in the usual tension testing equipment at strain rates of the order of 10^{-5}sec^{-1}.

Since a great deal of the data available cover creep testing of metals, this long time testing will be considered first.

B. Tension Tests

I. Creep Tests at Constant Load

When a metal is submitted to creep testing, it is placed in a furnace and allowed to reach a uniform temperature. A zero reading of the length is taken, the load is applied, and another reading is taken within a few minutes of application of the load. Thereafter, subsequent readings are made at suitable intervals during the test. The data recorded comprise the length and the cross sectional area of the specimen, the load, temperature, and the time. Of these, the temperature and extension are the most difficult to measure.

Standards established for creep testing require an accuracy in recording the loading within 1 per cent[3]. Temperature variations over long test periods must be held to an accuracy as follows[3]:
For a specimen with less than a 5-inch gage length, the temperature over the gage length should be controlled to an accuracy of

$\pm1.5°C$ to 650°C ($\pm3°F$ to 1200°F),

$\pm3°C$ to 870°C ($\pm5°F$ to 1600°F), and

$\pm6°C$ to 1090°C ($\pm10°F$ to 2000°F).

The intervals of recording the extension under load of the specimen at the test temperature are selected to define the extension-time curve sufficiently accurately. This curve begins with a nearly instantaneous extension, part of which is elastic, and disappears upon removal of the load. The plastic recovery which occurs in the specimen over a longer time after unloading may also be recorded.

a. Object. The principal objective of the creep test is to ascertain the steady state creep rate $V_0 = d\epsilon/dt$ of Fig. 2-1 for the given conditions of temperature and stress. Under conditions of fairly low temperature or stress, the final value ϵ_0 of the initial transient creep is also important. Since most creep tests have been conducted under constant load, the steady state creep rate is not directly observed, since the creep rate is accelerated by the increase of true stress due to diminishing cross section. Accordingly, it is customary to identify the minimum observed creep rate with the steady state creep rate for that nominal stress. Unfortunately, the acceleration on account of diminishing cross section may sometimes mask variation in steady creep rate due to structural changes in the material.

b. Time versus Elongation Curves. Typical time-elongation tests on a 16 Cr-25 Ni-6 Mo alloy are shown in Fig. 2-2 and Fig. 2-3. The creep rate is determined by drawing the tangent to the curve or, if more convenient, by calculating the average creep over a small interval of time. From the time-elongation curves shown, the three stages of creep can be seen.

c. Stress versus Creep Rate Curve. When the constant minimum creep rate has been established for second stage creep, a more convenient method of representation is to plot this value against the applied stress that produced it on log-log coordinates. If the minimum creep rates established for several creep tests carried out at different stresses under constant temperature are thus plotted, often a fairly straight line relationship results, as shown in Fig. 2-4. From this curve, the stress to produce
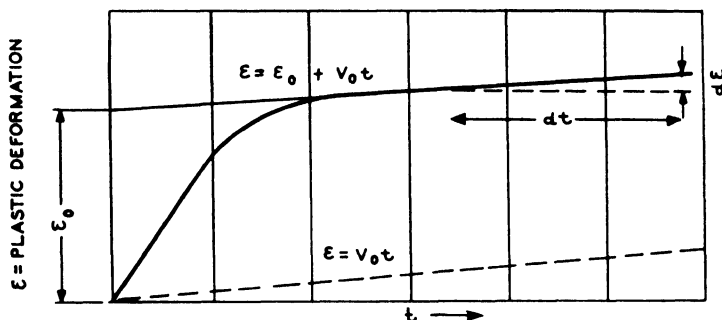
Fig. 2-1. Tension creep curve: Plastic deformation as a function of time. (After McVetty)

any desired stationary creep rate for the temperature of test can be selected. If structural changes take place, such a procedure is impossible.

d. Allowable Creep Rates. Materials for use at elevated temperatures are designed to allow for a certain minimum creep after a stated period. Certain designers of gas turbines have set a standard of 0.1 per cent creep in 10,000 hours as permissible for their service conditions. Other industries allow smaller or larger deformations in service. This value corresponds to 0.01 per cent in 1000 hours or to 0.1 millionth of an inch per inch per hour. The stress to produce the permissible creep rate (e.g. 0.1 per cent in 10,000 hours) is called the limiting creep stress.

The difficulties and expense of carrying out creep tests over very long periods are great. Short cuts to abbreviate the testing period are therefore very attractive. It is inviting to extrapolate into the future data which plot as straight lines on logarithmic stress and time scales. This practice is unsafe. The large amount of creep data available in recent years makes it evident that the facts generally do not admit of such a procedure.
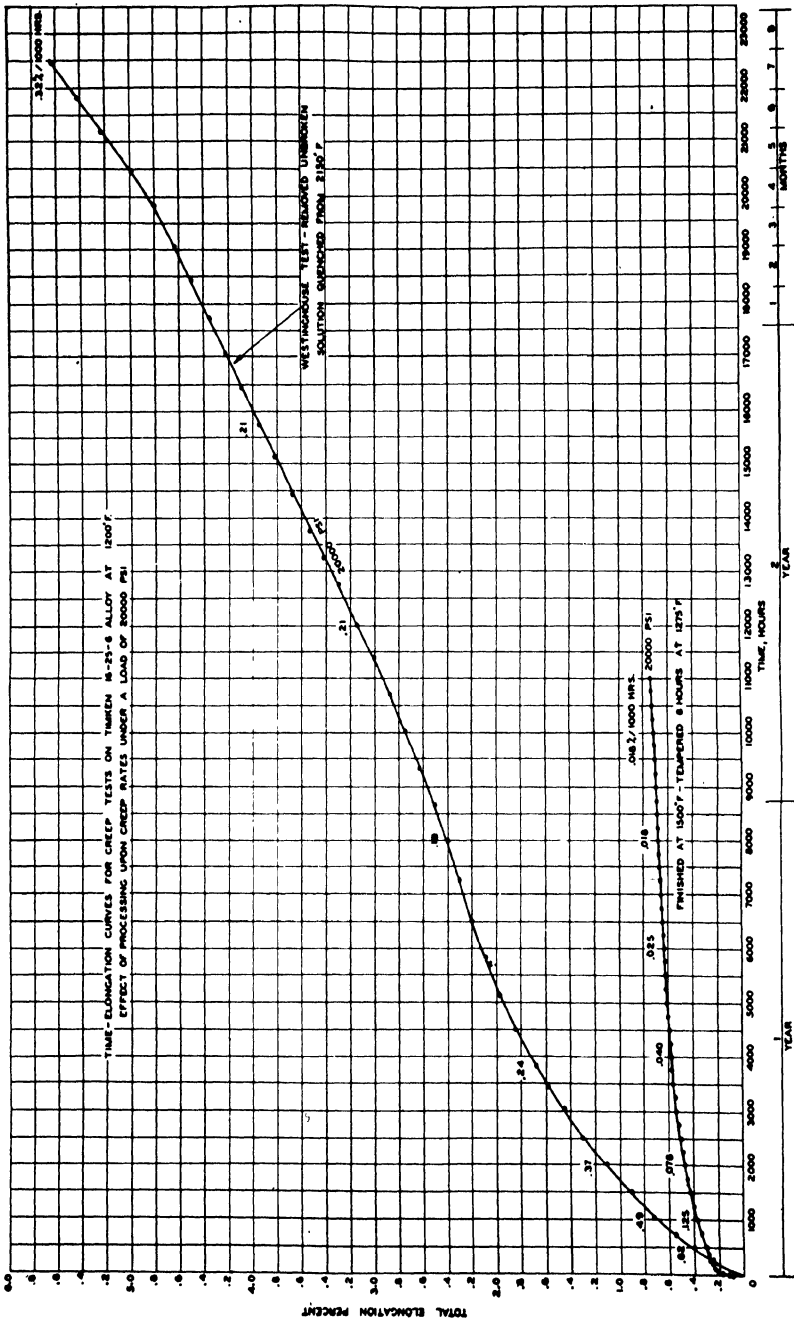
Fig. 2-2. Time-elongation curves for creep tests on Alloy 16-25-6 at 650°C (1200°F) under a load of 20,000 psi. The upper curve represents a heat treatment of solution quenching from 1176°C (2150°F); the lower curve represents material finished at 815°C (1500°F), followed by tempering at 690°C (1275°F) for 6 hrs.
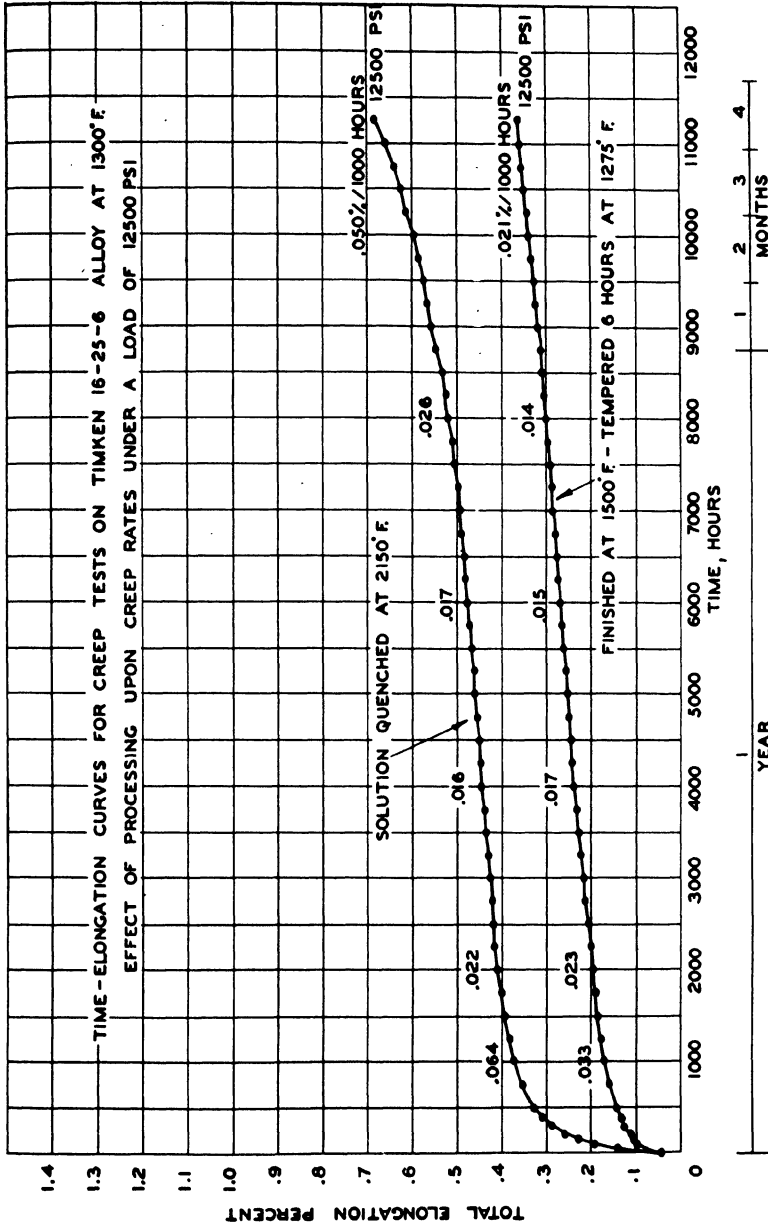
Fig. 2-3. Time-elongation curves for creep tests on Alloy 16-25-6 at 704°C (1300°F) under a load of 12,500 psi. The upper curve represents a heat treatment of solution quenching from 1176°C (2150°F); the lower curve represents a material finished at 815°C (1500°F), followed by tempering at 690°C (1275°F) for 6 hrs.

(Courtesy Timken Roller Bearing Co.)

e. Time to Fracture. Carrying out creep testing by measuring the strain and calculating the strain rate even over prolonged periods does not in itself give any indication as to when fracture of the specimen may occur in the future. This is more apparent if attempts are made to predict fracture by translating the effects of testing to lower stresses. The effect of time on the deformation of a material in relation to fracture is not simple. On the contrary, in general, all materials under load at high temperature show a decrease in ductility with time. Changes in the structure of the metal such as precipitation of micro-constituents result in lowering of the ductility. The effect of time in decreasing the ability of a metal to deform will be shown later in the text for many metallic systems.
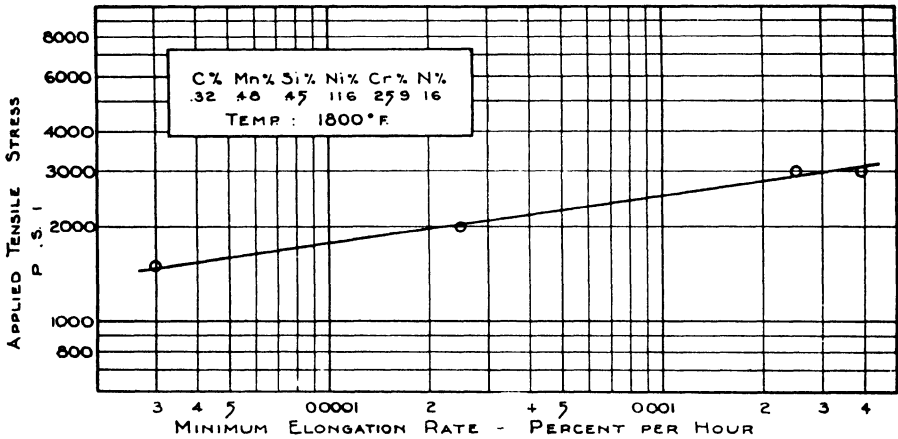
(*Courtesy American Brake Shoe and Foundry Co.*)

Fig. 2-4. Log-log plot of stress versus strain rate of cast Alloy 26-12 tested at 982°C (1800°F).

f. Increased Creep Rates due to Structural Changes. There are many changes occurring in a metal under load at elevated temperature which cause an increase in creep rates. The movements that take place in a crystal aggregate during recrystallization may produce creep or increase the creep rate. This is reported for lead which recrystallizes at room temperature, for brass when stressed above 370°C (700°F), and for steel heated from 315 to 538°C (600 to 1000°F) after deformation. In general, the transformations resulting in changes in the microstructure of a metal or alloy produce increased creep rates. The creep time-curve is also changed by spheroidization in steel and by localized flow by means of cracks as observed in lead.

g. Creep Testing Equipment. Creep testing equipment consists essen-
the other samples on test. The equipment is often set up as a battery of

tially of a device for applying a constant load over an extended time, a means of measuring the extension of the specimen very accurately, and a means of heating the specimen under closely controlled conditions. The development of creep testing over a period of many years has been largely devoted to increasing the accuracy of measuring small deformations, more
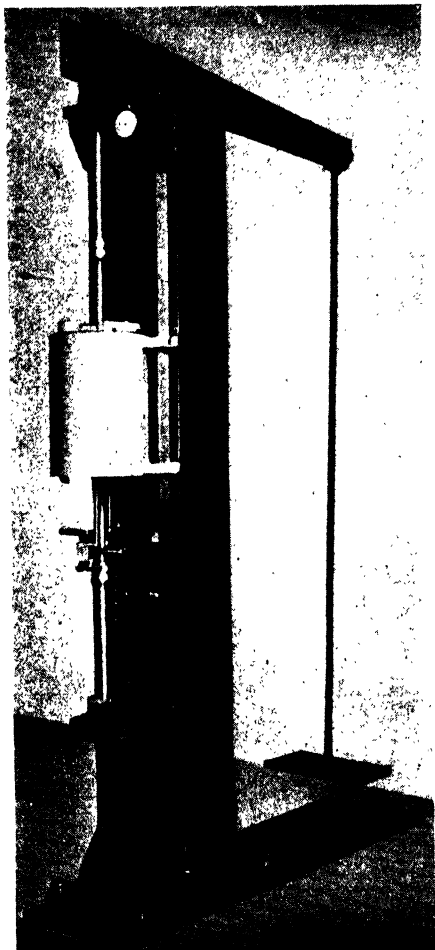
Fig. 2-5. Lever arm creep machine.

(*Courtesy Westinghouse Electric Corp. and Baldwin Locomotive Works.*)

rigorous temperature control, and increasing attention to the chemical composition, prior treatment, and other physical data of the test material.

1. Arrangement of Test Specimen. Most creep testing equipment is so arranged that each specimen is centered in its own furnace and held on an individual frame so that the jar of breaking a specimen does not disturb

$\frac{7}{16}''$ maximum elongation obtained at specimen for any particular setting of lower adjusting nut

Dial to check on elongation and vertical motion

Test specimen inside furnace

Clamp

Furnace (Slidable vertically to remove test piece)

Extensometer

Plug-in leads to thermocouples

Elongation indicator

Plug leads to thermocouples

Time indicator

Furnace controls

Spherical seat

Furnace voltage control

6'-1¾"

12"

(Courtesy Baldwin Locomotive Works.)

Fig. 2-6a. Lever arm creep machine.

the other samples on test.   The equipment is often set up as a battery of such units in conjunction with panels for instrument control.   A single unit[30] for creep testing is shown in Figs. 2-5 and 2-6.

Some creep testing furnaces are designed for multiple testing as in a recent installation[21] where 48 test bars are tested at the same temperature but with different loads.   Another arrangement provides 36 stations in the same furnace with individually adjustable loads.   The furnace and

the temperature controlling devices for this equipment are shown in Figs. 2-7 and 2-8. The machine is so constructed that 2 bars can be inserted
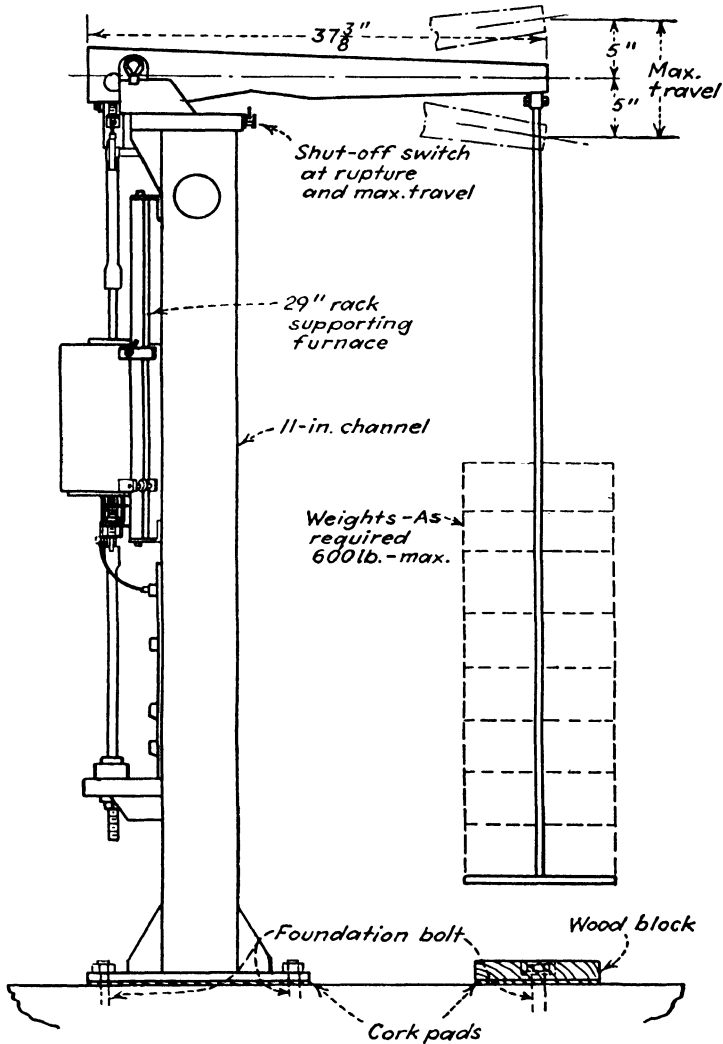
Fig. 2-6b.

at each station so that 72 specimens are tested at the same time, but the load must be the same for each pair. In this installation, the outer jacket revolves slowly to maintain a uniform temperature. Within the furnace, each specimen has its own additional heating unit. By this method, the temperature variation over the gage length of the specimen is exceedingly small.

2. Loading Mechanism. For simplicity and economy, the specimen is generally loaded through a lever arm by dead weights. It is often convenient to maintain a ratio of about 10:1 in the loading arm, and, by the

(*Courtesy Sulzer Brothers, Winterthur, Switzerland.*)

Fig. 2-7. Multiple creep testing unit with control panels.
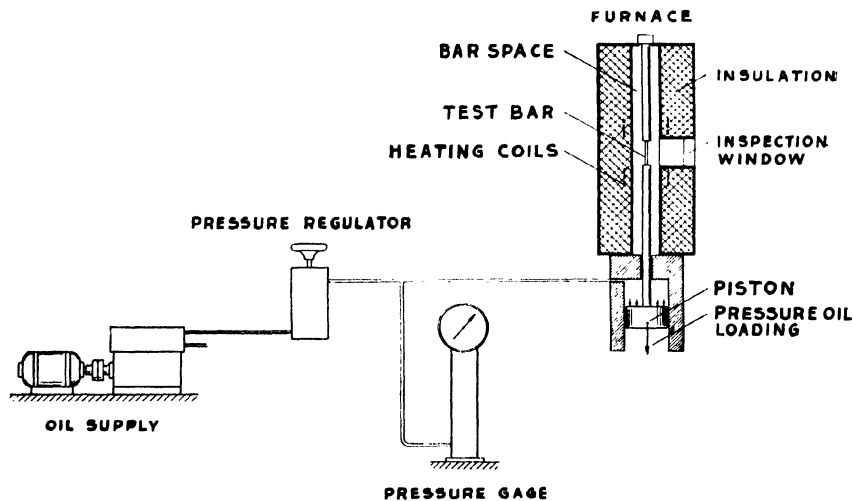
(*Courtesy Sulzer Brothers, Winterthur, Switzerland.*)

Fig. 2-8. Multiple creep testing unit showing the connection of a single specimen in furnace with the pressure regulator.

use of counterweights, to eliminate the tare[8]. In an individual case, a 10-gm weight placed on top of the specimen grip will balance a 1-gm weight attached to the loading shackle[8]. Under these conditions, the maximum error in loading is reported as 0.06 per cent. In other installations,

the lever arm ratio may be different, such as 20:1. The range of applied stress may be 50 to 50,000 psi in steps of 50 lbs[8].

In the installation for testing 36 and 72 specimens shown in Fig. 2-7, space saving requirements prevented the use of dead weight loading. A system using hydrostatic pressure from an oil reservoir operates a series
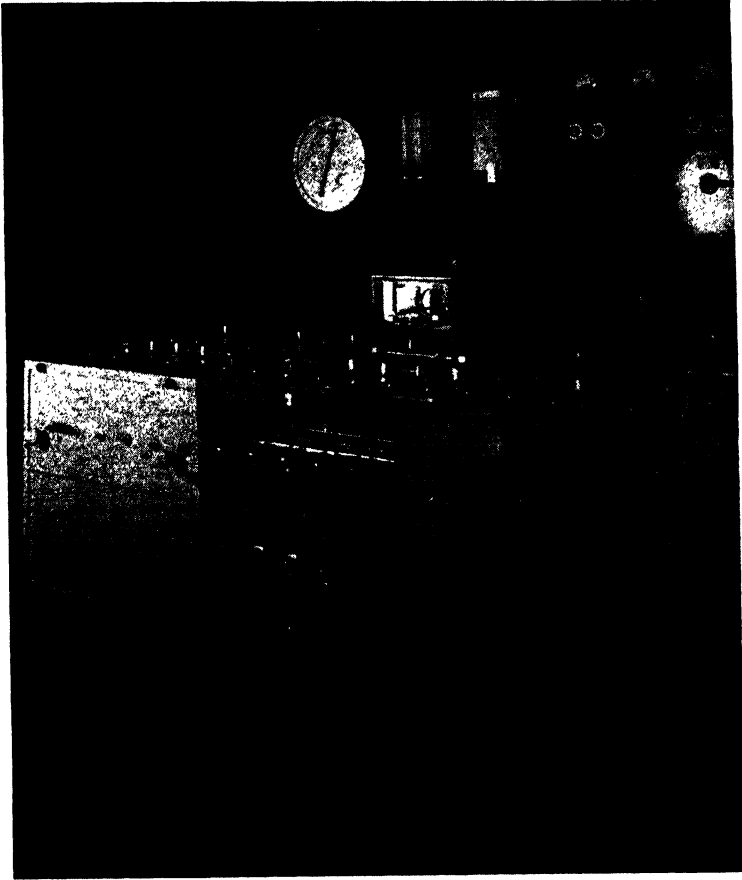
Fig. 2-9. Multiple creep testing unit showing loading mechanism.

of specially designed pressure regulators in conjunction with a servo-mechanism which controls accurately the load on the test piece. The system is conveniently operated from a central position and the load is applied by means of a hand wheel for each individual specimen as shown in Fig. 2-9.

The threaded ends of the test piece are held in grips of a heat resistant

alloy or of a ceramic material. Axial alignment is provided by crossed knife edges at the grip or by ball bearings at the points of leverage outside the furnace.

3. Temperature Control. In creep testing, the maintenance of uniform temperature over the gage length of the test piece is of utmost importance. Much of the earlier creep data are unreliable due to inadequate control in
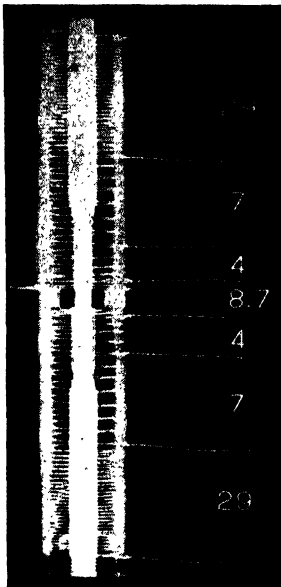
Fig. 2-10. Radiograph of winding.

(Courtesy American Brake Shoe and Foundry Co.)

this respect. To insure a uniform temperature over the gage length of the specimen, the winding of the furnace may be arranged as in the radiograph shown in Fig. 2-10. In this case, the leads are connected to shunts to provide more precise temperature adjustment for each individual test[8]. It is reported that, with this winding, the maximum temperature variation over the gage length is ±1°F. In all installations, the temperature control should be automatic-recording.

The temperature over the gage length of the specimen may be controlled by three thermocouples. In one arrangement, they are attached at five points by means of spot welding. After uniformity of temperature has been established, only the top, middle, and bottom couples are checked daily[8]. The maintenance of constant calibration is made difficult by contamination from oxides of chromium and iron which volatilize and condense on the thermocouple leads. Such effects may result in an error of 10°C (18°F). Temperature variations along the gage length of a test bar at 982°C (1800°F) and 760°C (1400°F) are shown in Fig. 2-11. Fluctu-

ations of temperature for a short period[8] and for a long period are shown in Figs. 2-12 and 2-13 in the installation shown in Fig. 2-10.

In a room filled with a group of creep testing furnaces, variations due
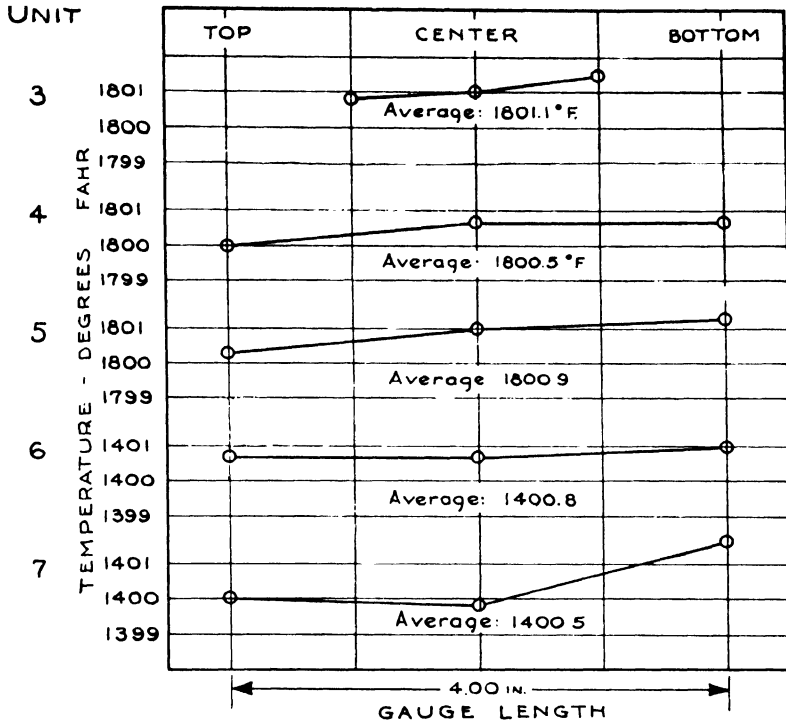
(Courtesy American Brake Shoe and Foundry Co.)

Fig. 2-11. Representative thermal gradients along test bar gage lengths.
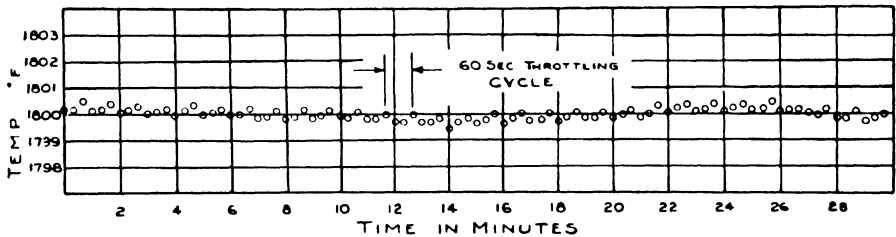
(Courtesy American Brake Shoe and Foundry Co.)

Fig. 2-12. Short time fluctuations in control temperature.

to temperature fluctuations in the Constantan resistance slide wires and in the batteries of pyrometers must be considered. In many instances, air conditioning has been used. Voltage regulation of the power supply

is also important; fluctuations should not exceed the order of ±1 per cent[3].

4. Effect of Temperature Variations. That the results of creep tests may be critically dependent upon the maintenance of uniform tempera-
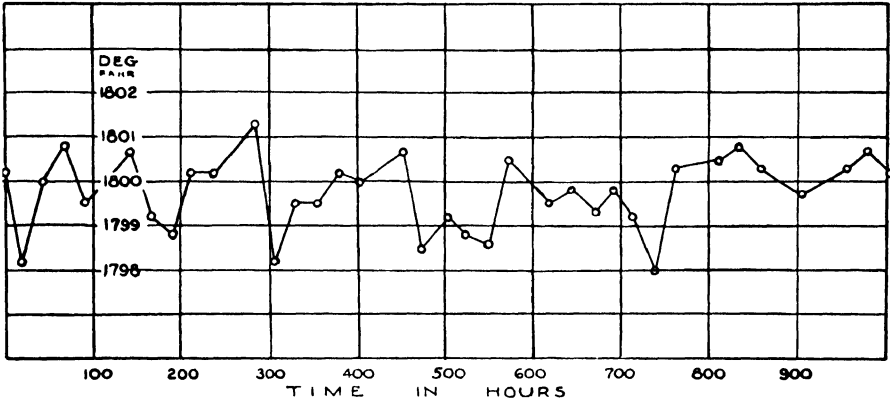
Fig. 2-13. Long time fluctuations in control temperature.
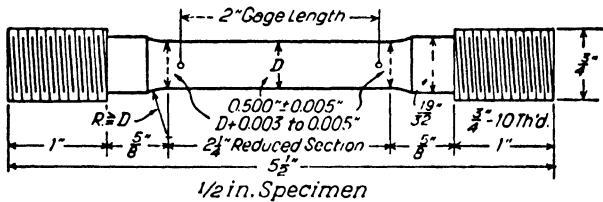
Fig. 2-14. Test bar for creep determinations.

ture is indicated by an interesting experiment[3] on two identical specimens of a cast 26 Cr-12 Ni steel having the following analysis:

Material				*Chemical Analysis*			
		C	Mn	Si	Ni	Cr	N
Cast 26-12		0.32	0.46	0.45	11.5	25.9	16

Bar	Stress psi	Temp (°C)	(°F)	Time (hrs)	Elong. % per 1000 hrs	Type of Test
A	3000	982	1800	530[a]	3.9	Standard
B	3000	982	1800	221[b]	26.0	20° F cycle

(a) Specimen broke.
(b) Test discontinued. Bar had 4.5 per cent residual elongation.

Both bars were subjected to the constant stress of 3000 psi at the average temperature of 982°C (1800°F). For bar A, the temperature was maintained constant at the average value and the steady creep rate of 3.9 per

cent per 1000 hours observed. For bar B, the temperature was varied by
±6°C (±10°F) about the average in a cyclic fluctuation of 7 minutes
period. In this case, the reported steady creep rate was more than 20
per cent per 1000 hours. This is very much greater than the rate corre-
sponding to the constant temperature equal to the peak value of 1810°F.

5. Test Specimens. The standard test bar recommended for use has a
uniform cross section accurate to ±0.5 per cent throughout the gage
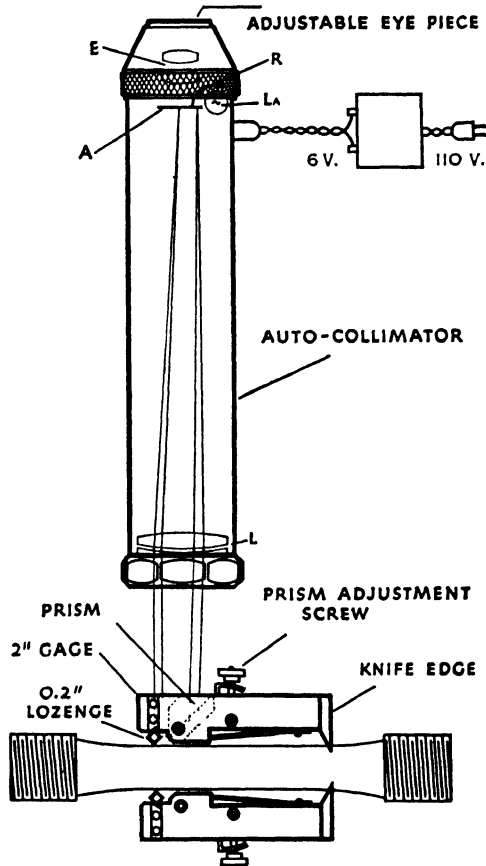
(*Courtesy American Instrument Co.*)

Fig. 2-15. Schematic drawing of Tuckermann strain gage.

length, which is at least 2 in[3, 8, 12, 14]. The diameters are often 0.505,
0.357, or 0.252, but the preference is 0.505 in, as shown in Fig. 2-14.

6. Extensometer Measurements. There are various methods for reading
elongations of the specimen. Extension arms attached to the specimen

protrude from the furnace and operate micrometer dial gages or optical levers. The Tuckermann optical strain gage consists of an extensometer attached to a test piece to measure an increase or decrease in length, and an auto-collimating tube with a reticle for reading the change in dimension. The tube is separate from the extensometer and may be adapted to reading more than one specimen. In Fig. 2-15, the optical system and arrangement of the parts are shown for measuring changes in length of a test piece
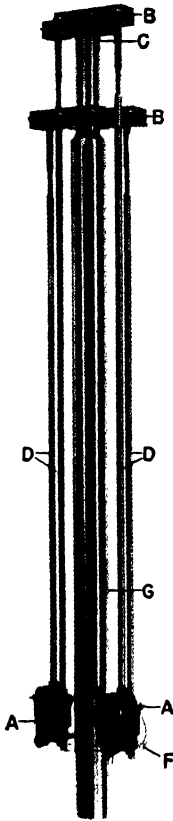
Fig. 2-16. Tuckermann strain gage.

at room temperature. Two extensometers may be attached to the specimen, one on each side, and the readings averaged. This arrangement automatically compensates for slight bending if it occurs in the test piece.

The extensometer carries a knife edge at one end mounted on the specimen for marking the gage length. A lozenge of ground and polished "Stellite" rests on the specimen and marks the other end of the gage length which for a 2-in section may be as accurate as ± 0.0002 in. As elongation

or contraction occurs in the test piece, the lozenge rocks on one edge and deflects a light beam reflected from the surface of a prism also shown in the drawing. The degree of rocking is measured in the auto-collimator. This optical strain gage measures changes in length with a sensitivity of 0.000002 in.
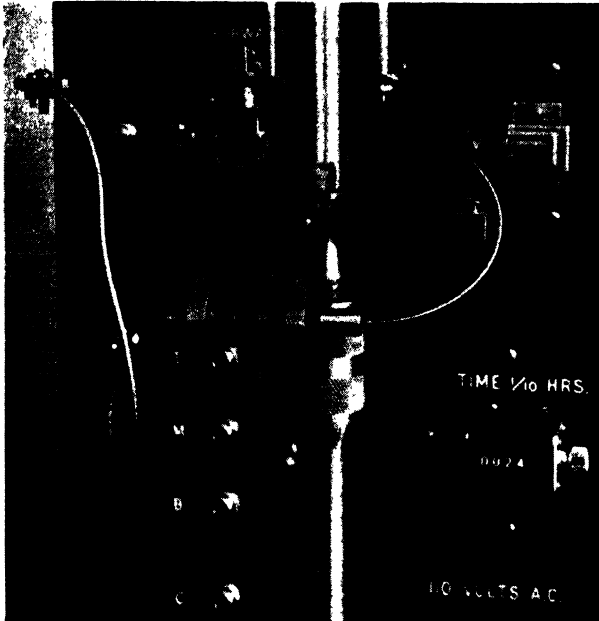
(Courtesy of Baldwin Locomotive Works)
Fig. 2-17. Unit for recording strain and time.

For elevated temperature service, it is necessary to place the extensometer outside the heated zone of the furnace. In Fig. 2-16, a typical arrangement is shown for attachment of the extensometer indicated by the letter A. The two adapters at B are clamped to the specimen C and mark the gage length. The rods D extend from the top and bottom adapters to the extensometer below. The upper portion of this apparatus operates in the heated zone of the furnace. From the illustration, it is evident that the two rods D which are attached to each extensometer transmit the dimensional changes in the gage length to the extensometers placed at either side to compensate for bending of the specimen. The extensometers rest on a metal plate F and are held flexibly against the rod G.

In the creep equipment shown in Fig. 2-5, automatic reading of the elongation of the specimen is provided by the unit shown in Fig. 2-17.

TABLE 2-1. FORM FOR REPORTING DATA AND RESULTS OF LONG-TIME HIGH TEMPERATURE TENSION TESTS METALLIC MATERIALS[3]

(IN ACCORDANCE WITH A.S.T.M. RECOMMENDED PRACTICE E22-41)

LABORATORY DESIGNATION:

               1st   2nd   3rd   4th

MATERIAL:
I. DESCRIPTION OF MATERIAL

Type   Wrought   Separately
       Cast   Integrally

Form of material   Dimensions
                Bars
                Tubes
                Plates
                Forgings
                Keel blocks
                Castings
                Longitudinal
                Transverse

Heat Treatment   Type
                 Temperature
                 Holding time
                 Size of material treated

Impact   Izod
        Charpy
        Specimen dimensions

Initial Micro-Structure

Hardness
   Brinell
   Rockwell B
   Rockwell C
   Others

×100

TABLE 2-1 (Cont'd)

FERROUS ALLOYS

Chemical Composition:

C   Mn   P   S   Si   Ni   Cr   W   V   Mo   Cu   Al   Others

Austenitic Grain Size Established: A.S.T.M. No.

  (a) by carburizing test (McQuaid-Ehn)
    (State whether case or core)

  (b) at final heat-treating tempera-
    ture above critical range. (State
    method used to reveal austenitic
    grain size)

Normality:

Grain Size in Specimen as Tested
  (State constituent rated)

NON-FERROUS ALLOYS

Chemical Composition

Cu   Sn   Zn   Pb   Ni   Fe   Al   P   Si   Mn   Others

Initial Physical Properties (all stresses in pounds per square inch)
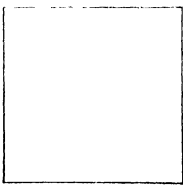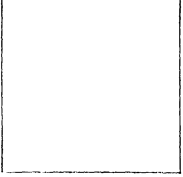
Temp °F	Tensile Strength	Yield Point	Yield Stress	Proportional Limit	Elonga- tion in 2 in %	Reduc- tion of Area %	Impact, ft-lb Charpy Izod	Modulus of Elas- ticity	Poisson's Ratio	Lateral Plastic Contraction
			0.2% Set							

TABLE 2-1 (Cont'd)

II. MANUFACTURING DATA:

Type furnace
  Acid or Basic
  Direct arc
  Indirect arc
  Induction
  Open hearth
  Open flame
  Crucible

Size melt
Size ingot
Size billet
Size finished product

Deoxidation
Straightening
Treatment

III. PROPERTIES OF SPECIMENS AFTER TESTS

Creep Testing					Tensile Strength	Yield Strength (Offset 0.2 %)	Prop Limit	Elonga-tion in 2 in, %	Reduction of Area, %	Impact, ft-lb Charpy Izod	Hardness
Temp °F	Stress	Time, hr	Temp °F								

Microstructure of Completed Long-Time Test Specimens

Temp	Time	Stress	Temp	Time	Stress	Temp	Time	Stress	Temp	Time	Stress

IV. CREEP CHARACTERISTICS:

Testing Temp °F	Stress Lb/Sq In	Total Time, Hr	Total Creep In/In	Average for Past Interval Millionth In/In/Hr	Tangent to Curve	Intercept, In/In	Temp	Time	Stress	Stress for Designated Creep Rate

The extensometer is attached to the specimen by pin holes drilled in the shoulder of the specimen[30]. As the specimen elongates, electrical contacts in a circuit become separated and the break excites an electric motor which drives a follow-up and closes the contacts again. The motor also operates a revolution counter whereby the elongation of the specimen is recorded. In this equipment, the revolution counter registers extensions in units of 0.000025 in. In another installation, the counters are photographed by a motion picture camera which takes a single exposure every 4 hrs[14].

7. Furnace Atmospheres. Some creep tests are equipped to operate in inert atmospheres, but, for the most part, tests are conducted in air[20]. Creep testing of aluminum alloys is carried out in furnaces immersed in liquids for maintenance of the temperature required. For lower temperatures, hot water under thermostatic control is satisfactory[10]. For temperatures up to 190°C (375°F), boiling glycol-water solutions recirculated by a reflux condenser maintain a temperature control of less than $\pm 1\frac{1}{2}$°F in the system.

8. Form for Reporting Data. A standard form for reporting creep measurements is shown in Table 2-1 which is recommended by several laboratories from many years of creep testing. Emphasis is placed on a complete description of the manufacturing procedure and the physical properties of the material prior to testing. Space is provided for the recording of the conditions of the creep test as temperature, load, elongation, and time. Subsequent to plotting of the elongation versus time, the tangent to the curve, the intercept, and the creep rates are recorded. After completion of the test, changes in the microstructure and physical properties due to stressing at elevated temperature may be noted.

II. Stress Rupture Tests (Creep Rupture Tests)

a. Object. Stress rupture tests (sometimes called sustained load tests) are conducted to estimate the ability of a metal to resist fracture under prolonged stressing at elevated temperature. They differ from creep tests in that stresses are raised sufficiently to cause failure in shorter periods usually not exceeding 1000 hrs. Many stress rupture tests are conducted in 10 to 400 hrs. For certain types of service it may be important to know the strain of the metal at the time of fracture. This is obtained from measurements of the specimen after fracture.

The data recorded from these tests are usually plotted in log-log coordinates of stress versus rupture time and the stress varied to produce rupture in 10, 100, and 1000 hrs. If no structural changes occur during the test period, a straight line relationship usually holds. For example, Fig. 2-18 shows the fracture time for different stresses at 982°C (1800°F) for a cast 25 Cr-12 Ni alloy[8].

While the principal objective of the creep rupture test is to determine the time to fracture, it is possible before fracture to determine the elongation as a function of the time, as in an ordinary creep test. From these additional data, the steady creep rate at very high stresses may also be estimated. The stress rupture data become more edifying if the creep data are also presented as in Fig. 2-18. For instance, if the permissible creep rate were as great as 0.0001 per cent per hour, the limiting stress at 982°C (1800°F) for the material would be determined by Fig. 2-18 as 2200 psi which corresponds on the figure to fracture in less than 5000 hours.
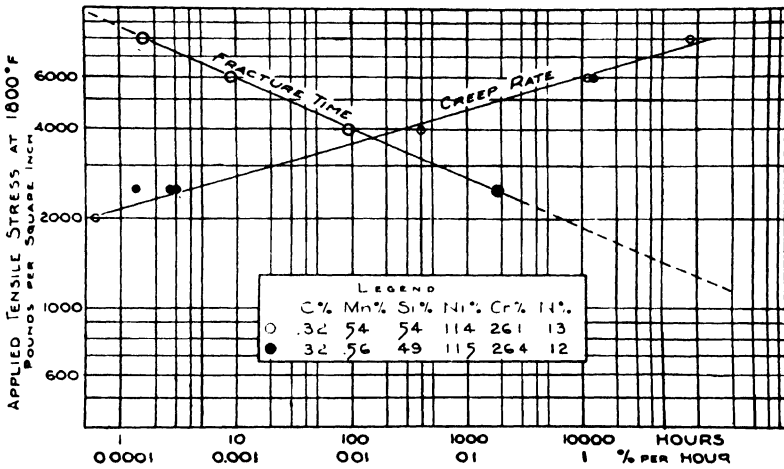
Fig. 2-18. Correlation of creep data with stress rupture data. (After Fellows, Cook, and Avery)

A warning must be given here against the practice of extrapolating the time-to-fracture curve to predict failure of materials at the low stresses and long periods encountered in creep testing. It must be remembered that overloading bars at high temperature and attempting to extrapolate these data to lower stresses may lead to many dangerous conclusions. However, stress rupture data yield useful information for limited service life, particularly for gas turbines operating in aircraft.

b. Design Curves. When the stress rupture test is conducted by measuring the elongation of the specimen at specified intervals, and the time and strain at fracture, another presentation of the data is often useful. This representation, known as a design curve, exhibits in a single drawing the results of stress rupture tests at many applied stresses as in Fig. 2-19. Here the time to rupture for the given material is exhibited as a function of the applied stress, the stress scale being linear and the time scale being

logarithmic. The strain at rupture is indicated for the several loads at which the tests were conducted. Additional information is given by curves showing the time to reach 0.2 and 0.3 per cent strain at various stresses. The curve for transition from second to third stage creep identifies the time and stress at which acceleration in the strain rate due to necking begins, the corresponding strains being recorded on the figure. The minimum creep rate as a function of the stress is represented by a curve referred to the upper scale.
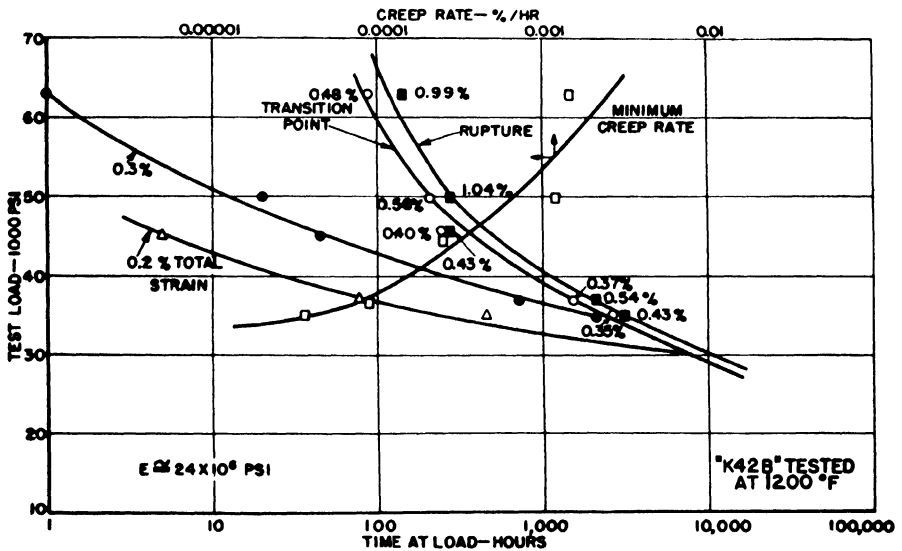
Fig. 2-19. Design curves for K42B* at 650°C (1200°F). Specimens machined from hot rolled bar stock. Heat treatment: Solution treatment 1065°C (1950°F), 1 hr.; oil quenched; aged 732°C (1350°F), 20 hrs. (After Scott and Gordon)

* See Chapter 5 for further description of this alloy.

c. Equipment. The equipment used in creep testing is suitable for stress rupture measurements if allowance is made for the difference in elongations which occur in stress rupture tests, since the stresses are much higher. The extensometer is therefore less sensitive in design and may read in ten-thousandths of an inch (0.010) for strains up to failure[14]. Since elongations are large the test specimen may be designed with a shorter gage length, such as 2 in.

Recent designs in equipment for conducting creep rupture tests incorporate some novel features for labor saving and space saving improvements. The machine shown in Figs. 2-20 and 2-21 does not use weights and lever arms for application of the load, but a motor driven screw jack loads the

specimen through a spring load weighing block.   Creep, or elongation, is measured by the travel of the screw jack while engaged in maintaining constant load on the specimen.   The deflection of the spring load weighing block is indicated by the dial gage which has been calibrated in pounds load on the specimen.   An electric contact on this dial gage controls the motor driving the jack to hold the load constant on the creeping specimen.
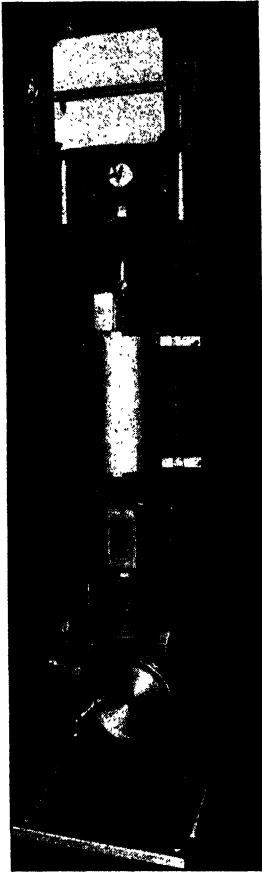
Fig. 2-20. Screw driven stress rupture machine.

(Courtesy Westinghouse Electric Corp. and Baldwin Locomotive Works.)

The capacity of this machine is 100,000 psi on a standard 0.505 in test piece. This screw driven type of stress rupture machine can also be adapted to short time tension tests and relaxation tests.

III. Short Time Tension Tests

Short time tension tests at elevated temperature are used to study the effect of heating a sample and testing under strain rates encountered in

ELONGATION COUNTER.

RECORDER
PANEL

ELECTRIC CLOCK DRIVES
PEN HORIZONTALLY GIVING
TIME COORDINATE

SPRING LOAD
WEIGHING BLOCK

DIAL·GAGE

CONTROL
PANEL

FLEXIBLE SHAFT OPERATES
ELONGATION COUNTER
AND DRIVES PEN
VERTICALLY GIVING
STRAIN COORDINATE

SPECIMEN
HOLDERS

SPECIMEN

FURNACE

FURNACE PANEL

HAND
WHEEL

SCREW JACK
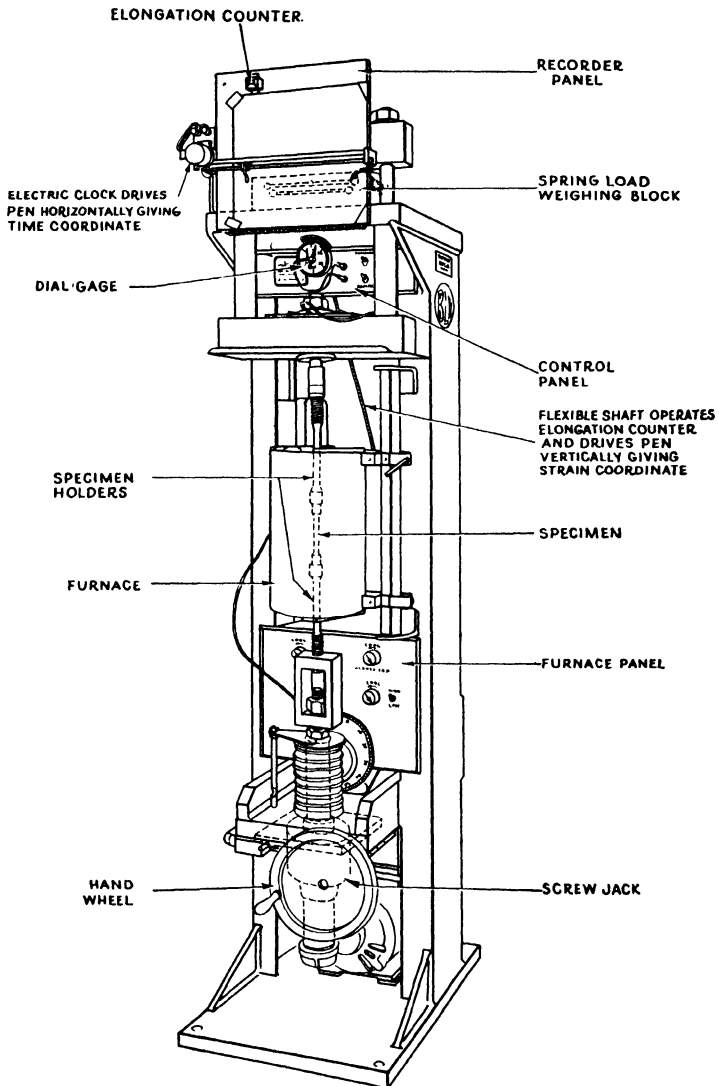
(Courtesy Westinghouse Electric Corp. and Baldwin Locomotive Works.)
Fig. 2-21. Schematic drawing of Screw Driven Stress Rupture Machine.

the ordinary tensile testing machine. These tests do not indicate the properties of a metal subjected to stressing at high temperature for long periods. They are, however, sometimes used for rapid estimation of materials which may warrant further study.

Short time tension tests are carried out in any standard tension testing machine with suitable arrangement for heating the specimen and holding the temperature constant for the short test period. An automatic stress strain recorder is convenient to use with this equipment. The arms of the extensometer which reach into the furnace may be made of some heat resistant alloy.

IV. Relaxation Tests

The phenomenon of relaxation is exhibited when a metal is stretched and held at a given elongation so that the strain remains constant. Under these conditions, creep begins at a rate dependent upon the stress in the test piece. Due to the restraint in the metal, a release of the load occurs, which is balanced by an elastic shortening of the material under test A schematic drawing of this phenomenon was shown in Chapter 1 (Fig. 1-34). Relaxation tests are especially useful for determining stresses suitable for materials to be used for bolts under conditions of high temperature. Relaxation tests can be conducted in several different ways. In one type of test, the sample is placed in the furnace cold and stressed to some predetermined value which is selected to give the maximum allowable deformation of a bolt in service. After a suitable time at test temperature, the creep rate is measured for this stress. The stress is then lowered a specified amount and the creep rate again measured. A record is maintained of the creep rates for the different stresses of this step down test. The residual stress may be taken at the end of, for example, 1000 and 10,000 hrs. Many heat resistant alloys are examined on the basis of the deformation resulting from an initial stress of 50,000 psi.

A relationship for the residual stress and relaxation creep data has been suggested by Robinson as follows[25]:

$$S = \sqrt[n-1]{\frac{bS_0^n}{(n-1)r_0Et}}$$

t = elapsed time (hr)
b = elastic ratio, total system to that of creep bar
n = % increase in creep rate per % increase in stress
     or the inverse slope of stress-rate curve for creep test ⸱
E = modulus of elasticity (psi)
r_0 = nominal creep rate (in/in/hr)
S_0 = nominal strength (psi to cause r_0)
S = residual stress (psi after time t)

V. Abridged Methods of Creep Testing

In the earlier investigations undertaken to establish creep data for metals at elevated temperature, numerous attempts were made to devise experiments to evaluate the long time behavior of the specimen from short

time tests. These depend on setting standards for allowable deformations at periods of only a few hours[3, 23, 24, 26]. The difficulties in such evaluations still remain, so that extrapolations on the time axis are uncertain. For short test periods, it is often impossible to establish second stage creep rates. Furthermore, short test periods do not take into account the possibility of structural changes in the material during its service life. For all creep testing, the great problem is the prediction of structural changes which may occur over long periods. A recent evaluation of several of the early standards for creep tests indicate some promise, and they are therefore given below[3].

a. Hatfield Time Yield. The Hatfield time-yield test is based on a total period of 72 hrs. The time-yield stress is defined as the maximum stress which produces a deformation not greater than 0.05 per cent during the first 24 hrs. This time-yield stress, moreover, during the next 48 hrs must not produce an average creep rate greater than 10^{-6} in per in per hr. The limiting creep stress has had several interpretations, such as the stress required to produce 0.048 per cent or 0.05 per cent elongation during the last 48 hrs. To conduct a time-yield test, the specimen is subjected to several different stresses and the deformation plotted against the time. Extrapolation of these values provides information on the stress required to obtain 0.0005-in deformation between the 24th and 72nd hour of test.

b. D.I.N. (D.V.M.) Method (German). This method likewise suggests a shortened test period, which is the stress required to produce a creep rate of 1 per cent per 1000 hrs between the 25th and 35th hour. The stress for this creep resistance is defined as the "conventional limit", and the test period is a total of 45 hours. The second requirement is that the permanent deformation should not exceed 0.2 per cent by the end of the 45th hour.

c. Barr and Bardgett Method. This test is an accelerated type of test lasting 48 hours; it depends on the relaxation or decrease in stress in a specimen over this period. A test piece 6 in long by 0.25 in diameter is fastened at both ends and stressed in axial tension in a heavy frame. The load is applied by means of a screw at the top of the specimen at some selected constant temperature. A weigh bar attached at the lower end of the specimen measures its extension by means of a dial gage. The elongation of the weigh bar is calibrated for various values of the load.

At the selected test temperature, an initial stress is applied to the specimen. During the 48 hour period, the specimen elongates and the decrease in stress is recorded at the end of the test. Several tests are conducted at the same temperature with different initial stresses. Curves are drawn to show the decrease of stress plotted against the initial stress. The "limiting creep stress" is defined as that stress which will not decrease

measurably for the 48 hour testing period, and is indicated by the intersection of the curve with the initial stress axis.

C. Creep Tests under Constant Stress

Creep tests carried out under constant stress require a device for maintaining the stress constant as the specimen elongates during the test. Under the assumption that the volume of the material remains substantially constant during the test,

$$\frac{A}{A_0} = \frac{l_0}{l}$$

where l_0 and A_0 are the length and cross-sectional area of the specimen at the moment of application of the load and l and A are the length and cross-sectional area at some subsequent period. Devices for constant stress tests consist of methods for decreasing the load on the specimen as it elongates since the force is inversely proportional to the elongation.

I. Device using V-Shaped Specimen[9]

One convenient arrangement utilizes a wire bent into a V-shape with the ends supported at the top and a stress applied at the vertex of the angle as shown in the inset of Fig. 2-22. As the legs of the V-shaped specimen elongate, the angle α_0 becomes smaller and the load decreases. If the force in the vertical plane is F_z, the load applied at the vertex is w, and the angle after closing is α, then

$$\frac{w}{2} = F_z = F \cos \frac{\alpha}{2}.$$

The stress S in each leg is expressed as,

$$S = \frac{F}{A} = \frac{w}{2A} \sec \frac{\alpha}{2}$$

At the time of starting,

$$S_0 = \frac{w}{2A_0} \sec \frac{\alpha_0}{2},$$

where S_0, α_0, and A_0 are initial values.
Then

$$\frac{S}{S_0} = \frac{A_0}{A} \frac{\cos \frac{\alpha_0}{2}}{\cos \frac{\alpha}{2}}.$$
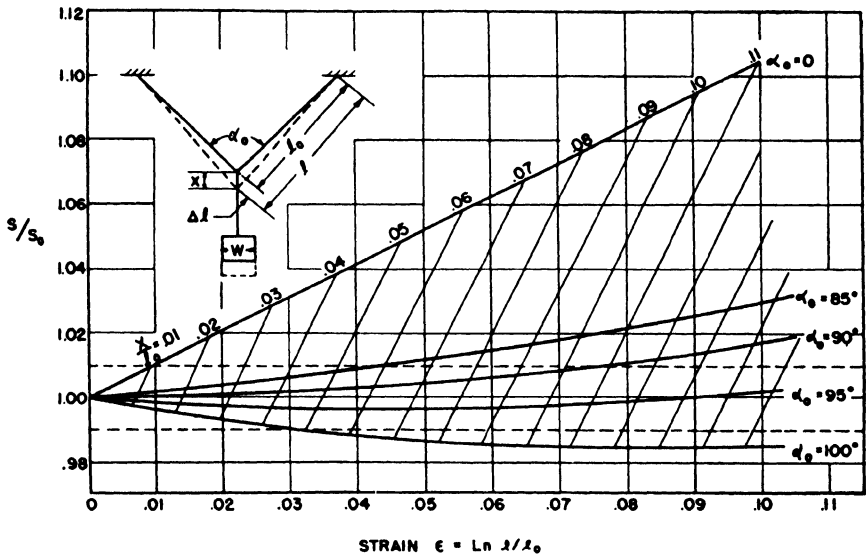
Fig. 2-22. Schematic drawing of V-shaped specimen for constant stress creep test. Curves show variation of stress with initial angle. (After Fisher and Carreker)

Since the elongation is at constant volume,

$$\frac{S}{S_0} = \frac{l}{l_0} \frac{\cos \dfrac{\alpha_0}{2}}{\cos \dfrac{\alpha}{2}}.$$

If the distance between the points of the supports is fixed,

$$\frac{\sin \dfrac{\alpha}{2}}{\sin \dfrac{\alpha_0}{2}} = \frac{l_0}{l}.$$

Eliminating α by this equation yields

$$\frac{S}{S_0} = \frac{\left(\dfrac{l}{l_0}\right)^2}{\sqrt{1 + \left[\left(\dfrac{l}{l_0}\right)^2 - 1\right] \sec^2 \dfrac{\alpha_0}{2}}}$$

If α_0 is made nearly equal to 90°, the stress S is found from this expression to vary but little with increasing elongation as illustrated by the figure. In this graph of S/S_0 versus the true strain ϵ, variations are shown for α_0

at 85, 90, 95, and 100°.   The two dashed lines indicate a small range for
the ratio S/S_0 from values of 0.99 to 1.01.   It is also possible to measure
the small increase x at the vertex during the test rather than the change
in length of the specimen.   The upper line in the figure marked $\alpha_0 = 0$
(specimen is a straight line) shows the relation to S/S_0 and the true strain
ϵ.   This method is suitable for testing small wires with a reasonable ac-
curacy.   It could be used with larger specimens with suitable grips for
holding the two rods at the vertex.

II. Device using a Weight Operating through a Linkage[1]

A more complicated and somewhat more accurate method than the one
described above maintains a tensile force on a horizontal specimen which is
pulled from both ends so that the center does not change its position.
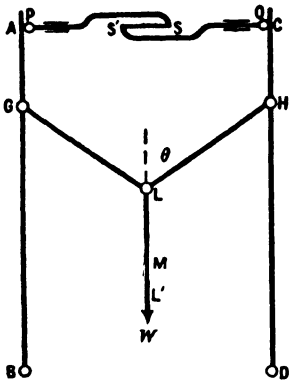
Fig. 2-23. Device for maintaining constant stress
on a rod operating through a linkage. (After
Andrade)

During the test, the pull diminishes as the specimen elongates and decreases
in cross-section.   In Fig. 2-23, a cylindrical specimen $S'S$ is attached at
either end to the rigid rods AB and CD which are pivoted at positions
B and D.   A weight placed at W applies a force at G and H which in turn
causes A and C to approach each other as the specimen increases in length.

From the geometry of the system,

$$\frac{AB}{GB} = \frac{CD}{HD}.$$

If $AG = c$, $GB = f$, and $r = \dfrac{CD}{HD}$, then

$$r = 1 + \frac{c}{f}$$

If $GL = HL = p$ and the angle subtended at $GLH = 2\theta$, the horizontal force at G is

$$F = \frac{1}{2}W \tan \theta.$$

The axial force is

$$F' = \frac{1}{2r} W \tan \theta.$$

Assume that at the time of starting, the length is l_0 and the angle θ_0, and at some subsequent time, the length is l and the angle θ. Then the specimen length l is

$$l = l_0 + 2pr(\sin \theta - \sin \theta_0).$$

If $c = 2pr/l_0$, it follows that

$$l = l_0[1 + c(\sin \theta - \sin \theta_0)].$$

It follows by an argument similar but more complicated than that outlined for the V-shape specimen that constancy of stress may be maintained within very close limits of accuracy. In fact, for a value of α of 8°, where $\alpha = \theta_0 - \theta$, a specimen which has been extended 30 per cent, may be held to a constancy of stress of 0.2 per cent. This linkage method of test offers an advantage in accuracy over the V-shaped specimen in that there are two parameters, c and θ_0, to adjust.

D. Torsion Creep Tests

Metals may be tested at elevated temperature in torsion with specimens in the shape of thin walled cylinders which provide a fairly uniform radial stress distribution depending upon the wall thickness and diameter of the test sample. However, the difficulty of manufacturing certain heat resistant alloys in tubular form may preclude this type of sample. One arrangement for creep testing in torsion has the lower end of a tubular specimen attached rigidly to a frame and twists the upper end through a constant torque[7]. Means are provided for heating the specimen at constant temperature and for reading the angle of twist to determine the shear strain.

A view of an installation for creep testing in torsion showing the furnace for heating the specimen and a wheel for application of the load in torsion is given in Fig. 2-24. This equipment is designed to test a solid cylinder utilizing a cylindrical specimen 22 in long and $\frac{7}{8}$ in diameter with a 2 in gage length of 0.75 in diameter.

The equipment may be utilized for a rapid twist test by means of a variable-speed D.C. motor. The displacement of a pendulum attached to

one end of the specimen indicates the maximum torque. Long-time torsion creep-testing is controlled by a constant load applied by a torque wheel. The equipment provides autographic recording of the load versus strain for the short-time twist test and for the strain versus time for the torsion creep test. With this arrangement graphs of torsion creep rate

(Courtesy M. W..Kellogg Co.)
Fig. 2-24. Equipment for creep testing in torsion.

versus the maximum fiber stress in torsion plotted on log-log coordinates appear to follow a straight line under the test conditions as reported.

To evaluate the tension and torsion creep test, a comparison is given in Table 2-2 of the results of creep in tension and creep in torsion of a steel tested in the form of a hollow cylinder. The analysis of the material is as follows[7]:

C .	Mn	S	P	Si	Mo
0.146	0.54	0.018	0.015	0.21	0.53

The steel was produced in a 60 ton open hearth furnace; the samples had a heat treatment of annealing at 732°C (1350°F) for 1 hr followed by furnace cooling 27°C (50°F) per hr to 593°C (1100°F), and were finally cooled in air.

Steels at room temperature have a ratio of yield point in shear to yield point in tension of about 0.6. From the results shown in Table 2-2, this ratio still holds at test conducted at 426°C (800°F). When the temperature is raised to 565°C (1050°F), the ratio of creep in torsion to creep in

TABLE 2-2. COMPARISON OF TORSION CREEP AND TENSION CREEP IN A
0.5 PER CENT MO STEEL

Temp (°C)	(°F)	Type of Test	Stress for Designated Creep Rate (psi) Rate % per 1000 Hrs at 0.01%	at 0.10%	Ratio Torsion Creep to Tension Creep at 0.01%	at 0.10%
426	800	Torsion	12,200	17,800	0.63	0.60
426	800	Tension	19,250	29,750		
565	1050	Torsion	4950	7500	0.80	0.59
565	1050	Tension	6200	12,800		

tension is 0.6 for the higher creep rate of 0.10 per cent per 1000 hours, but, at the lower creep rate of 0.01 per cent per 1000 hours, this ratio becomes 0.8.

E. COMBINED STRESS

I. Notched Specimens

The effect of combined stress in its relation to high temperature will next be examined. A state of stress represented by a triaxial stress system in which the mutually orthogonal principal stresses s_1, s_2, and s_3 have different values is difficult to obtain experimentally. A biaxial stress system where two of the principal stresses are equal is a simpler representation for the case where the principal stress s_1 is the greatest and the stresses s_2 and s_3 are equal. Combinations of the uniaxial stress systems and the torsion experiments described in the preceding sections of this chapter provide one means of establishing a biaxial stress system. Another experimental approximation to a biaxial stress system is a notched solid cylindrical rod in tension in which the principal stress s_1 operates along the axis of the specimen and the radial stress s_3, perpendicular to s_1 and algebraically less than s_1, occurs at the base of the notch where the cross section is a minimum. The radial tension at the minimum diameter is comprised of the two stresses s_2 and s_3, equal to each other, mutually perpendicular and rotatable around the axis of the specimen. In such a system, it is assumed that the radial stress is uniform. The distribution of the stress within the notch is controversial but it is sometimes considered as zero at the outer surface limited

by the boundary conditions and reaches a maximum at some interior position.

Tension tests on notched bars are effective in relating the influence of a biaxial stress system to the true breaking stress, the yield strength, and the true strain. The presence of the notch adds the variables of notch depth, notch angle, and radius at the base of the notch. The evaluation of the stress concentration factor is difficult but it is known to decrease during plastic deformation. The extent to which plastic deformation relieves the stress concentration at the base of the notch is large for certain metals as copper and less for many other metals.

Although the experimental results of the effects of biaxial stress systems on metals at room temperature have been investigated to a considerable degree, much less information is available for creep tests on notched specimens at high temperature. A few suggestive experiments are indicated in this section to show some of the trends that certain alloy steels exhibit. If notched bars are broken in a stress rupture test at elevated temperature, it is found that the existence of the radial stress component has sometimes increased and some times decreased the time to fracture, as compared to the effect of the same test on a smooth bar.

It is possible to compare the effect of different types of notches with unnotched specimens by conducting stress rupture and creep tests at elevated temperature and by evaluating the true stress and the reduction of area at the time of fracture of the specimen. The results of such a series of tests are shown for an austenitic steel with the following composition[29]:

Steel No. 1 Chemical Composition (%)

C	Mn	Si	Ni	Cr	W	V	Co	Cb
0.47	1.02	1.4	14.3	13.9	3.14	0.2	10.0	2.3

The test specimens consist of unnotched creep test pieces and of two types of notched bars, one with a sharp V notch with an angle of a 60° opening and one with a round notch of 1.5 mm radius of curvature. The results of testing at 650°C (1202°F) and 700°C (1292°F) for various periods of time from 2 minutes to 2350 hours are shown in Fig. 2-25. When the true stress in kg per sq mm measured at fracture is plotted against the per cent reduction in area on linear scales, an S-shaped curve can be drawn through the points at constant temperature to indicate the variation in the reduction of area or ductility.

The solid line in Fig. 2-25 shows the test results at 650°C (1202°F); the broken line shows the results at 700°C (1292°F). The reduction in area plotted against the true stress for the smooth bars follows the double S-shaped curve consistently. The minimum contraction is indicated at

about 169 hrs; the maximum contraction occurs at the opposite end of the second loop at 1673 hrs.

The position of the notched bars shown in Fig. 2-25 also follows a pattern in these tests. At 650°C, the bar with the sharp notch of 0.5-mm radius and a 60° angle broke in 35 hrs with a reduction in area of about 4 per cent. The bar with a round notch of 3-mm radius broke in 1012 hrs with a reduction in area of about 13 per cent.

The results of testing notched bars at 650°C suggest that the bar with the sharp notch failed in 35 hrs due to the greater stress concentration at
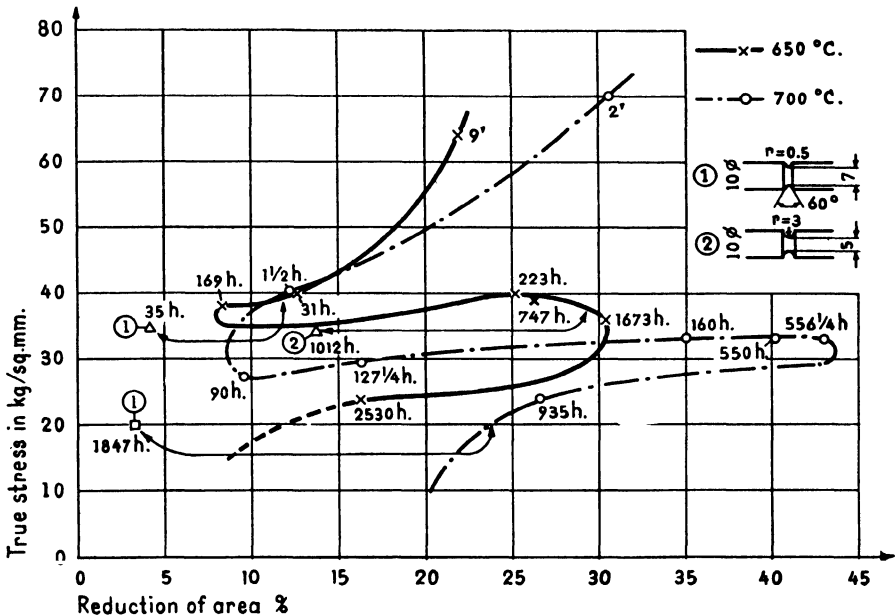
Fig. 2-25. True stress at fracture versus reduction in area for Steel No. 1 tested at 650 and 700°C. (After Siegfried)

the base of the notch. It is also in the region of the curve where the deformation capacity is lower. The other notched bar with a testing time of 1012 hrs has a lower stress concentration due to the rounded notch, and at the same time it is in the region of the curve where the deformation capacity at this loading period is greater.

From such curves it is evident that the deformation capacity of this steel varies considerably with time and may increase or decrease depending upon the course followed in the S-shaped curves. This method of showing the effect of true stress, reduction of area, and time has been duplicated for several steels and for tin alloys. It appears likely that the S-shaped curves exist for other metallic systems.

Fig. 2-26. Fractured test bar of Steel No. 2 for a rupture time of 55 hours at 650°C. (After Siegfried)
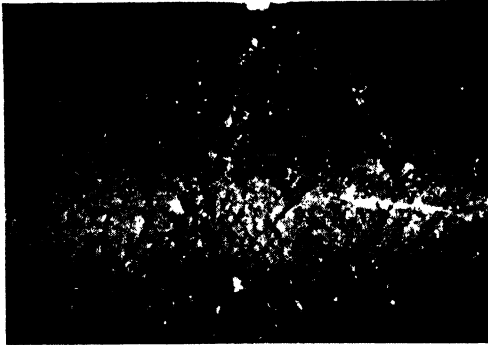
Fig. 2-27. Fractured test bar of Steel No. 2 for a rupture time of 2567 hrs. at 650°C. (After Siegfried)
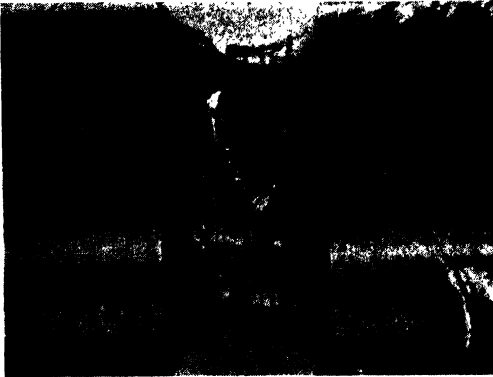
Fig. 2-28. Fractured test bar of Steel No. 2 for a rupture time of 150 hrs. at 650°C. (After Siegfried)

The type of fracture varies somewhat depending upon the position of the test specimen in relation to the S-shaped curves. In Figs. 2-26, 2-27, and 2-28, fractures at 650°C are shown for an austenitic steel of the following composition[29]:

Steel No. 2 Chemical Composition (%)

C	Mn	Si	Ni	Cr	W	Mo	Ti
0.15	1.3	0.86	31.34	15.35	1.06	1.0	0.52

The steel in Fig. 2-26 represents a fracture which occurred after 55 hrs and a reduction in area of 9.6 per cent. Although the graph of the S-shaped curve is not shown here, this steel represents the front portion of the S-curve where the deformation capacity is small. The fracture shown in Fig. 2-27 represents the same steel which failed after 2567 hrs at 650°C, with a reduction in area of 29.3 per cent. This steel on the S-shaped curve represents the area at the opposite end of the loop where the deformation capacity is high. However, the fracture in this case appears quite different from that of Fig. 2-26. In Fig. 2-27 the neck formation superimposes a radial stress which causes a general loosening of the crystalline structure and the formation of many fine cracks in the vicinity of the fracture. The fracture of this same steel is shown in Fig. 2-28 for a bar with a rounded notch of 1.5-mm radius of curvature. This specimen fractured after 150 hrs at 650°C. This steel also shows a large number of cracks which formed before fracture. The stress concentration in the round notch is not as severe as the sharp notch, but the radial stress that does exist tends to reduce the deformation capacity and cause extensive cracking before failure.

F. Hot Fatigue Tests

Hot fatigue tests involve holding a specimen at elevated temperatures under closely controlled conditions and subjecting it to alternating stresses. Most of the hot fatigue testing has been carried out with standard equipment of either the rotating beam or the tensile stress type. Such assemblies are modified by surrounding the specimen with a furnace for heating the test specimen to the desired temperature. Even with such arrangements dissatisfaction is expressed over the fact that laboratory test methods do not represent the actual stresses encountered in service conditions such as gas turbines. It is claimed that the impulses in turbines are characterized by a very high frequency and that bending stresses and torsional stresses are superimposed on the stresses derived from centrifugal forces.

It appears evident that heating of the test piece above 538°C (1000°F) results in a fatigue curve which does not have a true endurance limit. Furthermore, at a temperature of 871°C (1600°F), all special alloys for high-temperature service subjected to 100 million cycles of stress are annealed and fail at about the same stress, in the neighborhood of 10,000 psi.

One arrangement for hot fatigue testing of Ni alloys consists of a standard rotating-beam machine operating at 3450 rpm in which the test bar is 16 in long and has a turned-down section 10 in long in the center of the piece. The diameter of the bar is 0.350 in and the 3 in ends of the bar are held in

grips. A heating unit is slipped over the specimen in the 10-in section and heating of the gage length is conducted in air with a temperature control of $\pm 3°C$ ($\pm 5°F$).

G. HARDNESS TESTS

I. Room Temperature

Hardness testing at room temperature of certain alloys is used during the manufacturing process to indicate steps in solution heat treatment and subsequent precipitation hardening. The following conversion Table 2-3 is included here to indicate changes in hardness that may occur in such alloys

TABLE 2-3. RELATION OF ROCKWELL C TO DIAMOND PYRAMID HARDNESS (VICKERS)
FOR PRECIPITATION-HARDENED AUSTENITIC ALLOYS[27]

Diamond Pyramid (50-kg load)	Rockwell C	Rockwell C	Diamond Pyramid (50-kg load)
400	39.6	40	403
390	38.5	38	385
380	37.4	36	367
370	36.3	34	349
360	35.2	32	331
350	34.1	30	315
340	33.0	29	307
330	31.8	28	300
320	30.6	27	293
310	29.4	26	286
300	28.0	25	280
290	26.6	24	274
280	25.0	23	268
270	23.4	22	262
260	21.6	21	257
250	19.5	20	252
		19	248

as K42B, "Discaloy", and "Refractaloy" 26 during manufacturing[27]. The figures represent diamond pyramid hardness (DPH) under a 50-kg load converted to standard Rockwell C scale. These alloys are precipitation-hardened by titanium.

In general, hardness tests have not been correlated with the structure of alloys in the solution treated (quenched state) nor in the aged condition where many metals show precipitation of certain constituents over a period of time when exposed to elevated temperatures. Some changes in hardness do occur, but either they are not consistent or cannot be duplicated for various temperatures and times of exposure.

The microstructure of gas-turbine alloys consists of a relatively soft austenitic matrix through which is dispersed a network of hard complex carbides. The indenters used for both Rockwell and Brinell readings are too large to indicate small significant changes in hardness during aging.

The Knoop hardness tester, which indents on a microscale, can be centered on the austenitic matrix where precipitation is taking place. Hardness values obtained with the Knoop tester do show changes occurring in the austenite, but they are inconsistent due to a lack of uniformity in orientation of the austenite grain as a whole[12].

II. Hot Hardness Tests

(1) Static tests for hardness at elevated temperature are conducted by surrounding the specimen with a heating unit, placing it on an anvil, and then measuring its hardness by conventional methods. To protect the

(Courtesy of Climax Molybdenum Co.)

Fig. 2-29. Hot hardness testing equipment.

surface of the specimen from oxidation, it may be immersed in water, oil, or salt baths for measurements at moderate temperatures. At higher temperatures, the specimen may be prevented from oxidation by a controlled atmosphere such as nitrogen or by the use of an evacuation system maintained at 10^{-3} mm mercury or less.[5]

Due to the possibility of oxidation, a diamond indenter is required for hardness tests and, because of the time factor involved in static testing, the indenter must be at the same temperature as the specimen itself. Since a metal flows at elevated temperature, the time of testing should be kept constant if comparisons are to be made of different materials. An arrange-

Fig. 2-30. Hot hardness equipment showing position of specimen and furnace.

A	Vickers loading piston	M	Vickers stage
B	Flexible piston suspension	N	Heating coil
C	Piston (Invar)	O	Diamond indenter
D	Suspension collar	P	Specimen
E	Cylinder (stainless steel)	Q	Refractory tube
F	Top steel plate	R	Vacuum pump connection
G	Hold-down bolts	S	Refractory pusher rod
H	Steel cylinder	T	Brass cap screw holder
I	Sealed furnace leads	U	Thumb screw
J	Aluminum foil radiation shield	V	Bottom steel plate
K	Silica brick insulation	W	Thermocouple bead hot junction
L	Stainless steel anvil	X	Sealed thermocouple leads

ment for static hot hardness testing with an evacuation system is shown in Figs. 2-29 and 2-30[5].

The results of static hot hardness tests are valuable in a few instances. In the development of certain chromium base alloys, it is possible to set a minimum hardness requirement, in this case a value of 200 Vickers pyramid

hardness at 871° C (1600° F), to determine which compositions show promise of good creep strength[22]. However, static hot hardness tests do not indicate aging and diffusion consistently in steels or heat-resistant alloys. There is also no satisfactory correlation generally between static hot hardness and high-temperature strength or ductility.

(2) Dynamic hot hardness tests depend upon the indentation obtained by striking a specimen rapidly. The specimen is heated in a furnace for a specified period, removed and struck a blow within a short period of 1 to 1.5 sec. Since energy losses occur due to rebound of the blow, vibration of the specimen, and other losses, correlation of the dynamic test with other hardness tests is difficult. Certain advantages are, however, that the time element does not enter, since the blow struck is instantaneous. The test also permits the use of steel ball indenters and tests may be conducted with specimens held as high as 1204° C (2200° F).

In one design, a guillotine type of machine provides a drop hammer fitted with a removable steel ball of 10-mm diameter which moves between two polished steel slides and strikes a blow on the surface of the hot specimen. The diameter of the impression may be correlated with Brinell numbers also made on the same material. It is difficult to check hardness values obtained by different investigators in this type of dynamic testing. It is recommended that standard size specimens be used to minimize heat losses during the test[3].

Another arrangement for dynamic hot hardness testing consists of a spring-loaded center punch equipped with a high-speed steel indenter which transmits a blow to the sample during the tempering operation. This method is useful in obtaining information in martempering steels as the start of martensite formation is indicated in both air-hardening and oil-hardening steels[6].

H. Magnetic and Resistivity Tests

Magnetic tests at room temperature on alloys before and after exposure under load at elevated temperature do not show consistent results in changes that occur in the structure of the material with the possible exception of the austenitic 18-8 steels. These changes are likely to be precipitation, aging, and migration of certain microconstituents. Magnetic tests could be carried out at elevated temperature under certain conditions but there is little data available[12].

Tests on the electrical resistivity at room temperature of certain heat-resistant alloys before and after exposure under load at elevated temperature do show some promise in indicating changes occurring in the structure of the alloys under test. These changes will be discussed in later sections of the text.

I. Hot Impact Tests

Methods of conducting hot impact tests involve holding a specimen for several hours at a constant elevated temperature and breaking it in a standard Charpy or Izod impact-testing machine. The results of such tests will be reported in the text under the alloy system for which tests were made.

References

1. Andrade, E. N. daC., "Creep of Metals," Proc. Physical Soc. of London, **59,** 20 (1947); "New Device for Maintaining Constant Stress in a Rod undergoing Plastic Extension," *Proc. Physical Soc. London,* **60,** 304 (1948); Andrade, E. N. daC., and Chalmers, B., Resistivity of Polycrystalline Wires in Relation to Plastic Deformation and the Mechanism of Plastic Flow," *Proc. Roy. Soc., A,* **138,** 348 (1932).
2. Agnew, J. T., Hawkins, G. A., and Solberg, H. L., "Stress Rupture Characteristics of Various Steels in Steam at 1200° F," *Trans. Am. Soc. Mech. Engrs.,* **68,** 309 (1946).
3. Am. Soc. Testing Materials, Standards, E22-43, "Long-Time High Temperature Tension Tests of Metallic Materials," **46,** 735 (1946); "Short-Time," etc., E21-43, **43,** 204 (1943); **44,** 186 (1944).
4. Bailey, R. W., "Utilization of Creep Test Data in Engineering Design," Proc. Inst. Mech. Engrs., **131,** 131 (1935).
5. Bens, R. P., "Hardness Testing at Elevated Temperatures," Am. Soc. Metals, Preprint 3 (1946).
6. Enos, G. M., Peer, G. J., and Holzworth, J. C., "Dynamic Hot Hardness Testing," *Metal Progress,* **54,** 51 (1948).
7. Everett, F. L. and Clark, C. L., "Report on Torsion Creep Tests for Comparison with Tension on a Carbon-Molybdenum Steel," *Proc. A. S. T. M.,* **39,** 215 (1939).
8. Fellows, J. A., Cook, E., and Avery, H. S., "Precision in Creep Testing," *Trans. Am. Inst. Min. Metallurgical Engrs.,* **150,** 359 (1942).
9. Fisher, J., and Carreker, R. P., "Simple Constant Stress Creep Test," *J. Metals,* **1,** 178 (1949).
10. Flanigen, A. E., Tedsen, L. F., and Dorn, J. E., "Compressive Properties of Aluminum Alloy Sheet at Elevated Temperatures," A.S.T.M., Symposium on Materials for Gas Turbines, 161, June (1946). "Rupture and Creep Tests on Aluminum Alloy Sheet at Elevated Temperatures," *Am. Inst. Min. Metallurgical Engrs.,* **171,** 213 (1947).
11. Foley, F. B., "Interpretation of Creep and Stress Rupture Data," *Metal Progress,* **51,** 951 (1947).
12. Grant, N. J., Lane, J. R., and Taylor, M. E., "Aging Characteristics of Gas Turbine Alloys," Bur. Ships, Res. Memo., No. 1-47, Test B-3254 (1947). Grant, N. J., "Stress Rupture and Creep Properties of Heat-Resistant Alloys," Am. Soc. Metals, Preprint No. 2 (1946).
13. Jackson, L. R., Cross, H. C., and Berry, J. M., "Tensile, Fatigue, and Creep Properties of Forged Aluminum Alloys at Temperatures up to 800° F," Nat. Advisory Committee for Aeronautics, Tech. Note 1469 (Mar., 1948).
14. Manjoine, M. J., "New Machines for Creep and Creep-Rupture Tests," *Trans. Am. Soc. Mech. Engrs.,* **67,** 111 (1945).
15. Manjoine, M. J., "Screw-driven Creep Rupture-testing Machine," *Metal Progress,* **50,** 1100 (1946).

16. McVetty, P. G., "Interpretation of Creep Data," *Proc. A.S.T.M.*, **43, 707** (1943).

17. Mochel, N. L., "Relaxation Tests on .35 C Steel K20 at 850° F," *Trans. Am. Soc. Mech. Engrs.*, **59,** 453 (1937).

18. Nadai, A. and Boyd, J., "A New Automatic Relaxation Machine," *J. Applied Mechanics, Trans. Am. Soc. Mech. Engrs.*, **60,** A 118 (1938).

19. Nadai, A. and Manjoine, M. J., "High-speed Tension Tests at Elevated Temperatures. Part I," *Proc. A.S.T.M.*, **40, 822** (1940).

20. Nadai, A. and Manjoine, M. J., "High-speed Tension Tests at Elevated Temperatures. Parts II and III," *J. Applied Mechanics,* **63,** A-77 (1941).

21. Nisbet, J. D., "Rupture Testing in a 48-Bar Furnace," *Iron Age,* **161,** 81 (1948).

22. Parke, R. M. and Bens, F. P., "Chromium-base Alloys," A.S.T.M., Symposium on Materials for Gas Turbines, 80 (June, 1946).

23. Pomp, A. and Enders, W., "Accelerated Method for Determining Creep Limit," *Instruments,* **5** (7), 166 (1932).

24. Pomp, A. and Krisch, A., "Problem of Creep Resistance of High-temperature, High-strength Steels at 600, 700 and 800° C," *Mitt. K. W. Inst. Eisenforschung,* **12,** (9) 137 (1930).

25. Robinson, E. L., "Resistance to Relaxation of Materials at High Temperature," *Trans. Am. Soc. Mech. Engrs.*, **61,** 543 (1939).

26. Rosenhain, W., "Quick Determinations of Limiting Creep Stress," *Metal Progress,* **21–22,** 65 (1932).

27. Scott, H. and Gordon, R. B., "Precipitation-hardened Alloys for Gas Turbine Service. I," *Trans. Am. Soc. Mech. Engrs.*, **69,** 583 (1947).

28. Siegfried, W., "Failure from Creep as Influenced by the State of Stress,"*Sulzer Tech. Rev.*, No. 1, 43 (1945).

29. Siegfried, W., "Observations on Conducting and Evaluating Creep Tests," *J. Iron and Steel Inst.*, 189 (June, 1947).

30. Tatnall, F. G., "High-temperature Testing of Materials to be Used at Temperatures above 1200° F," Baldwin Locomotive Works, *Testing Topics,* 2 (Jul.–Aug.–Sept., 1947); **3** (Aug.–Sept.–Oct., 1948).

31. Trumpler, W. E. Jr., "Relaxation of Metals at High Temperatures," *J. Applied Physics,* **12,** 248 (1941).

32. Welch, W. P. and Wilson, W. A., "A New High-temperature Fatigue Machine," *Proc. A.S.T.M.*, **41,** 733 (1941).

33. White, A. E., Clark, C. L., and Hildorf, W. G., "Stress-rupture Tests for Heated Metal," *Metal Progress,* **33,** 266 (1938).

Chapter 3

Plain-carbon and Low-alloy Steels

A. PLAIN-CARBON STEELS

I. Elevated-temperature Properties

The flow of plain-C steels at high temperature is influenced by many factors, such as the method of manufacture, heat treatment, and previous deformation. At higher temperatures, recrystallization (if it occurs) and oxidation tend to lower creep resistance. The lower limit for the temperature of recrystallization of a low-C steel after cold-working is about 460° C (806° F). Physical properties determined at room temperature appear to provide little information concerning creep at high temperature, since plain-C steels with similar tensile properties and hardness at room temperature may display very different creep properties. It is also generally agreed that short-time tensile properties obtained at elevated temperatures have little relation to the creep properties of a steel.

Although plain-C steels are limited for many services at high temperature, a study of the structural changes taking place may lead to an understanding of changes occurring in highly alloyed, heat-resistant metals. Such factors are the precipitation of iron carbides, spheroidization of the carbides, and diffusion of these microconstituents through the grain.

There is available today a considerable body of literature on elevated-temperature properties of plain-C and low-alloy steels. Incorporated in the codes for boiler construction and pressure vessels are allowable working stresses for moderate-temperature requirements well below the recrystallization temperature of the steel. However, for higher temperatures flow properties must be evaluated on the basis of long time creep tests.

In Tables 3-1 and 3-2 the results of elevated-temperature tests at 454° C (850° F) and 538° C (1000° F) are shown for a plain-C steel with 0.35 per cent C and for a C-Mo steel with 0.16 per cent C and 0.53 per cent Mo (designated K20 and K22, respectively[3a]). The figures include short-time tension tests, stress-rupture tests, and several different creep tests, as described in the previous chapter. The results of hot hardness tests for these two steels are given in Table 3-3.

The strength values for S.A.E. 1035 steel (designated K20) are generally

much lower than for 0.5 per cent Mo steel (designated K22). At 454° C (850° F), the stress rupture for K20 steel after only 10 hrs is 33,000 psi; the creep strength of the same steel at 454° C (850° F) for a creep rate of 0.1 per cent per 1000 hrs is 7600 psi. Hot hardness tests on K20 steel show a decrease in Vickers hardness at 426° C (800° F).

The creep properties of three S.A.E. 1015 C steels are shown in Table 3-4[3]. These steels of close chemical analysis vary slightly in grain size; one has received a normalizing heat treatment and two have been annealed. The creep strength in all cases falls at test temperatures above 426° C (800° F).

a. Variations in Creep Strength. *1. Effect of C Content.* The influence of C content on the creep strength of steels at high temperature is more compli-

TABLE 3-1. COMPOSITION AND HEAT TREATMENT OF STEELS K 20 AND K 22[3a]

Steel	C	Mn	P	S	Si	Mo	Grain Size McQuaid-Ehn
K20	0.35	0.55	0.016	0.03	0.19	—	6 to 8
K22	0.16	0.66	0.015	0.027	0.24	0.53	6 to 8

Manufacturing Data

Both steels are representative of a 100-ton basic open-hearth heat.

K20: ladle deoxidation 50% ferrosilicon and 1.2 lb Al/ton

K22:   "   "   "   "   " 1.6 "   "   "

Both steels were rolled to 1 in bar stock and heat-treated as follows.

K20: Heated to 843° C (1550° F) in 2 hrs, held 1⅓ hr, furnace-cooled to 538° C (1000° F), then air-cooled. Reheated to 694° C (1280° F) in 4 hrs, held 2 hrs, furnace-cooled to 538° C (1000° F), then air-cooled. Cold-straightened and reheated to 510° C (950° F) and air-cooled.

K22: Heated to 900° C (1650° F), held 1¾ hr, air-cooled. Reheated to 650° C (1200° F), held 2 hrs, air-cooled. Machine-straightened, stress-relieved at 650° C (1200° F) 2 hrs, and air-cooled.

cated than the simpler relationship for room-temperature properties where an increase in C content increases the strength of the steel. The earlier evidence from creep testing is conflicting, as in some reports an increase in C content is beneficial in the temperature range of 400–538° C (750–1000° F) while in other cases the reverse appears true[19,23,30,33]. From Table 3-5, it is evident that an increase in C content improves the creep strength of steel at the lower temperatures where the carbides are present in lamellar form. At higher temperatures, where the carbides are spheroidized, the strength of the steel is decreased as C increases[13].

More recently, tests at 426° C on three steels of 0.23, 0.53, and 0.91 per cent C show increasing creep resistance with increase in C content, as shown in Fig. 3-1[5]. These same steels tested at 538° C do not show improved creep resistance with increase in C content.

TABLE 3-2. COMPARATIVE SHORT-TIME AND LONG-TIME (CREEP) TEST STRENGTH AT 454 °C (850 °F) AND 538 °C (1000 °F)

Test	Strength Values			Average Creep Strength 0.1 per cent per 1000 hr			Prediction Factor 0.01 per cent per 1000 hr		
	K20 850 F	K22 850 F	K22 1000 F	K20 850 F	K22 850 F	K22 1000 F	K20 850 F	K22 850 F	K22 1000 F
HOT HARDNESS TESTS									
(a) Dynamic (equivalent Brinell)	95	95	115	1.6	0.4	1.1	1.5	0.3	1.2
(b) Vickers, d.p.h.n.[a]	116	136	119	1.6	0.5	0.9	1.6	0.3	1.1
STANDARD SHORT-TIME TENSILE TESTS									
(a) Tensile strength (average)	44,060	58,060	47,360	1.6	0.6	0.9	1.6	0.4	1.1
(b) Yield strength (average)	19,640	27,500	28,210	1.4	0.6	1.0	1.4	0.3	1.3
CONSTANT STRAIN RATE TENSILE TEST									
(a) Ultimate strength for 0.1 per cent per 1000 hr strain rate[b]	7500	45,000	13,500	0.7	1.1	0.7			
		52,500	25,000		1.3	1.2			
(b) Ultimate strength for 0.01 per cent per 1000 hr strain rate[b]	2500	42,500	7000				0.3	1.0	0.6
		51,750	21,500					1.2	1.9
SUSTAINED LOAD TENSILE TEST									
(a) 0.1 per cent per 1000 hr creep strength[b]	8000	39,000	11,000	1.0	1.3	0.7	1.1	0.9	1.0
(b) 0.01 per cent per 1000 hr creep strength[b]	5400	28,000	7800						
STRESS RUPTURE TEST									
(a) 10 hr. rupture strength	33,000	56,000	42,000	1.4	0.7	0.9	1.4	0.4	1.2
HATFIELD TIME YIELD TEST									
(a) Time yield strength		17,000	6000		1.0	0.7		0.8	0.9
		18,000	10,000		1.0	1.2		0.8	1.6
DIN (DVM) TEST									
(a) Permissible stress		26,000			0.9			1.3	
BARR AND BARDGETT TEST									
(a) Stress for no relaxation after 48 hr	5500	13,400	6000	1.4	0.9	0.8	1.4	0.6	1.0
		11,100	9100		0.8	1.2		0.5	1.6
STEP-DOWN RELAXATION (FLOW RATE) TEST									
(a) Stress for creep rate of 0.1 per cent per 1000 hr	6200		9200	1.1		0.9			
(b) Stress for creep rate of 0.01 per cent per 1000 hr	3700		3500				1.2		0.8

CONSTANT STRAIN RELAXATION TESTS

(a) 50 hr Residual Stress

"Bolt" test............................	4875	....	....	0.9	....	....	0.9	....	....
Continuous test.......................	6500	....	....	1.2	....	....	1.2	....	....
Automatic test........................	6500	17,750	10,750	1.2	0.9	1.0	1.2	0.6	1.3
Automatic test........................	....	16,000	9600	....	0.8	0.9	....	0.5	1.2

(b) 1000 hr residual stress

"Bolt" test............................	4850	10,650	6600	1.4	0.8	1.0	1.5	0.6	1.4
Automatic test........................	3500	14,000	3800	1.0	1.1	0.6	1.1	0.8	0.8

CONSTANT STRESS CREEP TESTS (1000 hr)

(a) Stress for creep rate, 0.1 per cent per 1000 hr....	7600	28,500	15,000	....	....	....	....	....	....
(b) Stress for creep rate, 0.01 per cent per 1000 hr....	3400	20,000	5200	....	....	....	....	....	....

^{a} d.p.h.n. = diamond pyramid hardness number. ^{b} Obtained by considerable extrapolation.
Note: All stress values are in pounds per square inch. Two values for the same test represent results from different laboratories.

$$\text{Average creep strength prediction factor} = \frac{\text{test strength}}{\text{creep strength}} \div \text{Average ratio of test strengths to creep strengths}$$

For example, the factors for the standard short-time tensile strengths were calculated as follows: 1. Ratios of test strength to creep strengths:

(a) K20 at 850 F $= \dfrac{44060}{7600} = 5.8$ (b) K22 at 850 F $= \dfrac{58060}{28500} = 2.0$, (c) K22 at 1000 F $= \dfrac{47360}{15000} = 3.1$.

2. Average ratio of test strengths to creep strengths $= \dfrac{5.8 + 2.0 + 3.1}{3} = 3.633$.

3. Calculation of factors:

(a) K20 at 850 F $= \dfrac{5.8}{3.63} = 1.6$, (b) K22 at 850 F $= \dfrac{2.0}{3.63} = 0.6$, (c) K22 at 1000 F $= \dfrac{3.1}{3.63} = 0.9$.

2. Effect of Heat Treatment. For high-temperature service, normalizing is generally recommended as a heat treatment for plain-C steels. Variations in the normalizing temperature may result in steels with different creep properties, since a high temperature tends to produce a coarser grain or

TABLE 3-3. HOT HARDNESS OF STEELS K20 AND K22[3a]

Material	Type of Test	Temperature (°C)	(°F)	Hardness Number
K20	Dynamic	454	850	95 Equivalent Brinell
		482	900	95
		510	950	105
		538	1000	110
	Vickers	27	80	152 D.P.H.
		426	800	131
		454	850	120
		482	900	109
		510	950	93
		538	1000	82
		565	1050	74
		593	1100	67
		621	1150	60
		650	1200	56
		677	1250	49
		704	1300	43
		732	1350	39
K22	Dynamic	454	850	95 Equivalent Brinell
		482	900	105
		510	950	105
		538	1000	115
	Vickers	27	80	149 D.P.H.
		426	800	140
		454	850	134
		482	900	128
		510	950	126
		538	1000	119
		565	1050	111
		593	1100	103
		621	1150	95
		650	1200	86
		677	1250	74
		704	1300	63

may dissolve carbides which persist at lower normalizing temperatures[19]. If steels intended for high-temperature service are normalized and drawn, it is recommended that the drawing temperature should be 94° C (200° F) above the operating temperature[14]. Working or stress-relieving a steel after the normalizing treatment also changes the creep resistance.

Plain-C steels in the annealed condition are generally less stable than

TABLE 3-4. CREEP STRENGTH OF WROUGHT 0.10 TO 0.20 C STEELS[3]

(*Chemical Composition and Manufacturing Data*)

Sample No.	Chem. Composition					Heat Treatment (°F)	Brinell	Grain Size	Type Mat.	Type Fur.	Deox.	Temperature (°F)	Temperature (°C)	Creep Strength Stress (psi)	
	C	Mn	Si	S	P									0.10% per 1000 hours	0.01% per 1000 hours
2b	0.17	0.47	0.02	0.037	0.004	N. 1725	—	—	1⅛" bar	O.H.	open (rimmed)	288	550	26,500	—
												426	800	13,500	—
												538	1000	4300	—
												650	1200	740	—
3a	0.15	0.50	0.23	0.032	0.025	A. 1550	123	4-5	1" bar	E.F.	killed	426	800	27,000	18,200
												482	900	17,000	12,800
												538	1000	7200	2150
												593	1100	1800	850
												650	1200	620	295
3b	0.15	0.46	0.28	0.021	0.019	A. 1550	111	5-6	1" bar	O.H.	killed	426	800	17,000	12,000
												538	1000	3300	1800
												650	1200	5200	140

Note: All tests are 1000 hrs duration.
Grain size: McQuaid-Ehn.
N: Normalized.
A: Annealed.
O. H.: Open hearth.
E. F. Electric furnace.

those with normalized structures. Exposure of annealed steels to a temperature of 538° C (1000° F) shows a marked change of pearlite to a spheroidized condition[7, 41]. Creep resistance is lowered by such changes in the microstructure. Variations in the cooling rate through the tempering range during an annealing operation also influence the creep resistance, since these may change the structure of the steel.

TABLE 3-5. INFLUENCE OF C CONTENT ON CREEP RESISTANCE[13]

Steel	Temp. (°C)	(°F)	Stress psi for Designated Creep Rate % per 1000 Hrs		
			0.01	0.10	1.0
1015	426	800	12,000	17,200	25,500
1040	426	800	13,000	18,500	27,000
1015	538	1000	1800	3300	6000
1040	538	1000	2800	5500	9300
1015	650	1200	140	540	2100
1040	650	1200	140	860	2650

Note: Creep tests of 1000 hours duration.

Steel	C	Mn	Si	S	P	Brinell	Grain Size	Type Furnace
S.A.E. 1015	0.15	0.46	0.28	0.021	0.019	111	5–6	O.H.
S.A.E. 1040	0.43	0.67	0.20	0.033	0.035	167	4–5	O.H.

Note: Both steels annealed at 1550° F.
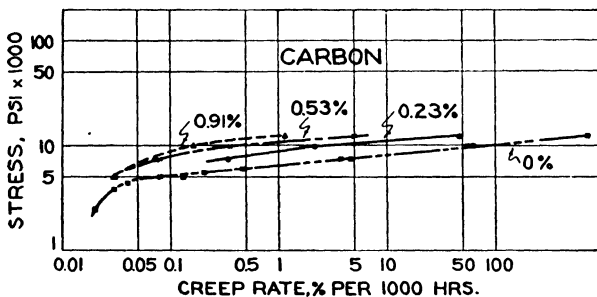
Fig. 3-1. Logarithmic plot showing relation between stress and strain rate for Fe-C alloys compared with commercially pure Fe at 426° C (800° F). (After Austin, St. John, and Lindsay)

The rate and extent of spheroidization in plain-C and low-alloy steels is important, since, as pointed out earlier, the occurrence of spheroidization decreases the creep resistance. Below the transformation temperature of steel, the relation between spheroidization rate, time and temperature according to Bailey and Roberts is expressed as follows[9]:

$$t = Ae^{b/T}$$

where t = time, T = temperature, and A and b are constants.

The equation is valid only for the same steel under identical conditions where only time and temperature are the variables. In this relationship, $1/T$ plotted against log t produces a straight line. Tests indicating the validity of this equation show that below the maximum temperature possible for spheroidization, the same degree of spheroidization is obtained at different temperatures but with a variation in the time required. With decrease in temperature, the time required for spheroidization increases. As an example, for a steel with 0.9 per cent C, heating for 278 hours at 600° C (1112° F) gives the same spheroidization as 2000 hrs at 560° C (1040° F).

TABLE 3-6. INFLUENCE OF HEAT TREATMENT ON CREEP CHARACTERISTICS
AT 538° C (1000° F) OF ELECTRIC AND OPEN HEARTH S.A.E. 1015
TYPE STEEL[14]

Steel		Stress psi for Designated Rate of Creep % per 1000 Hours		
		0.01	0.10	1.0
EF A	Hot-rolled	7000	12,800	15,800
OH A	Hot-rolled	6100	6800	7800
EF B	N.940(1725), D.650(1200*)	4900	9900	12,100
OH B	N.940(1725), D.650(1200*)	4000	5500	7700
EF C	Ann.843(1550)	3000	6200	12,900
OH C	Ann.843(1550)	2350	4500	6200
EF D	N.940(1725), D.650(1200†)	2750	5800	8200
OH D	N.940(1725), D.650(1200†)	2600	5300	7400

* Drawn 1 hour at 650° C (1200° F).
† Drawn 168 hours at 650° C (1200° F).
EF—Electric furnace heat.
OH—Open hearth heat.
Note: Creep tests of 1000 hours duration.
N: Normalized.

This equation is useful for temperatures as low as 398° C (750° F). At temperatures as high as 593 to 704° C (1100 to 1300° F) spheroidization rates for plain-C steels are rapid. The relationship does not hold for highly alloyed steels, probably because the composition of the complex carbides are changed by prolonged heating[9].

The rate of spheroidization in steels is influenced by many factors. Cold-working increases the rate of spheroidization. In general cast steels are difficult to spheroidize. Larger carbide lamellae take longer to spheroidize than finer particles which may account for the fact that annealed steels have somewhat lower spheroidization rates than normalized steels[29]. All these factors influence the creep resistance of a steel at elevated temperatures. It may be that the flow itself, occurring at the test temperature, although exceedingly small, may increase the rate of spheroidization.

In Table 3-6, a comparison is given of the creep strength at 538° C

(1000° F) of two steels, S.A.E. 1015, produced in heats from an electric furnace and an open hearth. The samples represent four different heat treatments as follows[14]: (1) hot rolling, (2) annealing at 843° C, (3) normalizing at 940° C, followed by drawing at 650° C, and (4) normalizing at 940° C and drawing at 650° C for 168 hrs to produce a spheroidized structure. At the test temperature of 538° C, the hot-rolled structure has the highest creep strength in both the electric and open-hearth furnace heats. The next most favorable treatment is that resulting from the normalized and drawn structure. In these tests, the electric furnace steel annealed is superior to the spheroidized structure. For the open-hearth steel, the reverse is true. These anomalous results indicate that many factors must be evaluated to determine the net results on creep resistance of even a simple C steel.

TABLE 3-7.   CREEP CHARACTERISTICS OF ELECTRIC AND OPEN HEARTH
S.A.E. 1015 TYPE STEELS (ANNEALED)[14]

Type Steel	Temp (°C)	(°F)	Stress psi for Designated Rate of Creep % per 1000 Hours		
			0.01	0.10	1.0
Electric	426	800	18,500	26,800	38,500
Open-hearth	426	800	12,000	17,200	25,000
Electric	482	900	12,800	16,900	22,100
Electric	538	1000	2700	5750	12,100
Open-hearth	538	1000	1800	3300	6000
Electric	593	1100	850	1800	3850
Electric	650	1200	290	620	1300
Open-hearth	650	1200	140	540	2100

All values based on tests of at least 1000 hours duration.

3. Effect of Melting Furnace. Two steels of the S.A.E. 1015 type melted under conditions to control the chemical composition closely in (1) an electric furnace and (2) in an open-hearth furnace, have creep strengths as shown in Table 3-7[14]. In this series of tests, there is no report available of the grain size of the two steels, and for this reason, the superior performance of the electric furnace product over that of the open hearth steel may depend on several factors not controlled under the test conditions. At 426° C (800° F), the electric furnace steel has a creep strength of 18,500 psi for a creep rate of 0.01 per cent per 1000 hrs while the open-hearth steel has a creep strength of 12,000 psi under the same conditions. The same general trend holds for the other temperatures investigated, namely, 538 and 650° C (1000 and 1200° F).

The factors involved in such a comparison must take into consideration the fact that open-hearth steels are more highly oxidized than electric furnace steels. Furthermore, the quality of a steel is dependent upon the degree of deoxidation and the subsequent effect on heat treatment. It is

more than likely that if both types of steel are produced to give a fine grain (McQuaid-Ehn grain size 6–8), their creep properties will closely resemble each other.

4. Effect of Melting Practice. The use of deoxidizers in steel melting influences creep strength. In many alloys, it is generally true that coarse grains have a higher creep strength than fine grains. The part played by the grain boundary itself in a coarse or fine grain structure was discussed in an earlier chapter. Since both Al and Si used for deoxidizing steel produce fine grains which also increase the rate of spheroidization, these deoxidizers are generally limited in their use. Thus it is recommended that steels for high-temperature service be limited to 0.5 lb of Al per ton of steel[29].

Creep tests on a killed and an open S.A.E. 1015 at 426° C (800° F), 482° C (900° F) and 538° C (1000° F) are shown in Table 3-8[14]. The amount of deoxidizer and the resulting grain size are not reported for these two

TABLE 3-8. CREEP CHARACTERISTICS OF KILLED AND OPEN* PLAIN-CARBON OPEN HEARTH STEEL S.A.E. 1015[14]

Type Steel	Temp (°C)	(°F)	Stress psi for Designated Rate of Creep % per 1000 Hours		
			0.01	0.10	1.0
Killed	426	800	13,000	18,000	25,000
Open	426	800	15,000	19,500	25,000
Killed	482	900	11,250	15,250	20,500
Open	482	900	5400	8000	11,500
Killed	538	1000	3200	6800	14,500
Open	538	1000	1800	3550	7000

Note: Creep tests of 500 hours duration.
* Open (rimmed steel).

steels. At 426° C, the killed steel is superior in creep strength. At 482° C and 538° C, the reverse is true. If there are more nonmetallic inclusions in the open steel, these may inhibit flow at the higher temperatures.

In an examination of a series of low C steels, containing 0.4 to 1.5 per cent Mn, 0.01 to 0.15 per cent Si, and 0 to 0.11 per cent Mo, it is reported that all steels which have abnormally high creep rates are fine-grained. The Al additions in these tests vary up to 3 lbs per ton of steel. To determine whether the steel has an abnormal creep rate, it is subjected to a stress of 8 tons per sq in at 450° C (842° F) for 5 days. The creep rate at the end of this period is taken as a value to establish the ability of a steel to withstand elevated temperature service. All steels in the test are normalized at 920° C (1688° F) previous to creep testing to give a comparable microstructure. The results of the tests indicate that abnormal creep due to the presence of Al is considerably reduced by the presence of Mn, Si, and Mo within the limits shown above. In general, it is recommended that Al additions for

these steels should be low enough to maintain a coarse-grained structure (McQuaid-Ehn grain size)[19].

5. Effect of Ingot Size. Variation in the type and size of an ingot has an influence on the creep properties of metals, since the change in cooling rates from the liquid state will influence the dendritic structure and the distribution of impurities. With increase in the size of the ingot, dendritic segregation increases. Both preheating and hot-working lower the tendency toward a banded or segregated structure. In actual manufacture, a small ingot may receive less reduction and therefore have considerable segregation. Tests on specimens from steel ingots ranging in size from 20 to 3800 lbs, stressed to produce a creep rate of 0.01 per cent per 1000 hrs, vary in creep resistance from 8200 to 12000 psi. The smaller ingots show a higher creep resistance[14,41]. The advantage shown by the smaller ingots is less marked at higher creep rates.

TABLE 3-9. EFFECT OF WORKING ON THE CREEP RATE OF S.A.E. 1040 STEEL[14]

Steel	Temp (°C)	(°F)	Creep Rate % per 1000 Hours
Hot-rolled	315	600	0.013
6% Elong.	315	600	0.018
12% Elong.	315	600	0.020
Hot-rolled	454	850	0.10
6% Elong.	454	850	0.198
12% Elong.	454	850	0.132
Hot-rolled	538	1000	0.132
6% Elong.	538	1000	0.374
12% Elong.	538	1000	0.323

6. Effect of Previous Deformation. A series of tests are reported on a 0.40 per cent C steel tested for creep in (a) the hot-rolled condition (b) cold-drawn to 6 per cent elongation and (c) cold-drawn to 12 per cent elongation. The results of creep-testing on these samples at constant load are shown in Table 3-9[14].

At each temperature of test, the hot-rolled steel shows the lowest creep rate, the samples with 6 per cent the next, and the samples with 12 per cent elongation the highest rate of creep. This difference is greater as the temperature increases. The hot-rolled condition is therefore the most stable of the three in these tests. As stated earlier, cold work increases the rate of spheroidization which in turn decreases creep resistance.

7. Effect of Time on Ductility. In low-C steels there is a definite temperature range and time of stressing where the type of fracture which occurs during a creep test changes from a brittle to a ductile type. This condition is termed the equicohesive temperature and in low-C steels it may well coincide with the temperature of recrystallization[13]. The type of fracture

in an electric furnace steel S.A.E. 1015 is changed by the following conditions indicated in Table 3-10.

The tests indicate that for a test temperature of 538° C (1000° F) an increase in testing time increases the tendency to brittleness.

8. Effect of Time on Structural Changes. Steels stressed at high temperature undergo changes in microstructure especially in regard to the carbides. For example, in a 1015 steel stressed at 538° C (1000° F), the pearlite laminations originally present will slowly become spherical and will migrate

TABLE 3-10. EFFECT OF TIME FOR FRACTURE FOR S.A.E. 1015 STEEL[13]

Short time tensile at 538° C (1000° F)	Ductile fracture, deformed grains
Failed after 6.4 hrs at 25,000 psi at 538° C (1000° F)	Ductile fracture, deformed grains
Failed after 1552 hrs at 12,000 psi at 538° C (1000° F)	Brittle fracture, non-deformed grains
Failed after 13,950.75 hrs at 6000 psi at 538° C (1000° F)	Brittle fracture, non-deformed grains

TABLE 3-11. MICROSTRUCTURAL CHANGES IN S.A.E. 1015 STEEL AT 538° C (1000° F)[13]

S.A.E. 1015 Steel	Microstructure
(a) Original condition as received	Pearlite not completely laminated
(b) Stressed at 9000 psi at 1000° F 4788.5 hrs	Appreciable spheroidization
(c) Stressed at 6000 psi at 13,950.75 hrs	Appreciable spheroidization and carbide migration

TABLE 3-12. IMPACT TESTS AT ELEVATED TEMPERATURE

Temp (°C)	(°F)	Charpy Impact Resistance (ft-lbs) Laboratory No. 1		Laboratory No. 2	
26	80	31.5	33.5	32	33
232	450	45.0	45.5	43	43
315	600	44.0	48.5	40	41
400	750	34.5	35.5	37	39
454	850	28.5	29.0	32	32
538	1000	23.0	26.0	22	24
650	1200	68.0	73.0	55	56

through the grain. This carbide migration and spheroidization is readily observed under the microscope under the conditions shown in Table 3-11[13].

Such movement of carbides is observed in low-alloy steels and highly alloyed austenitic structures when they are stressed at elevated temperature. This phenomenon is characteristic of changes occurring during creep tests, as will be shown later.

II. Hot Impact Tests

The results of hot impact tests are reported in Table 3-12 for the following 0.35 C steel[2a].

Chemical Analysis

C	Mn	P	S	Si
0.35	0.55	0.016	0.03	0.19

Manufacturing Data

Samples are representative of a heat from a 100-ton basic open hearth furnace. Deoxidation practice is 1.2 lb/ton of Al added to the ladle.

Heat Treatment

Heated in 2 hrs to 843° C (1550° F), held 1 hr, furnace-cooled to 538° C (1000° F), air-cooled. Reheated to 694° C (1280° F) in 4 hrs, held 2 hrs, cooled to 538° C (1000° F), air-cooled.

The results in Table 3-12 are duplicate tests carried out in two different laboratories. Specimens are held $1\frac{1}{2}$ hrs at temperature before breaking. Except for the values determined at 650° C (1200° F), the agreement is fairly good.

B. Low-Alloy Steels

At elevated temperature the creep resistance of steels, containing approximately 1 per cent of one or more alloying elements, is in general higher than that of plain-C steels. Increased oxidation and corrosion resistance of low-alloy steels add to their high-temperature stability. The fact that alloying elements raise the temperature at which the lowest temperature of recrystallization occurs also contributes to increased creep resistance.

In the absence of C, alloying elements added to ferrite up to approximately 1 per cent form solid solutions, regardless of whether they are considered as carbide formers or as elements entering into solid solution with iron. Some of these, notably Mo, are most effective in increasing creep resistance of pure iron. When C is added to ferrite and the alloying element maintained at a value low enough to keep the steel pearlitic, the effect of an alloying element as a carbide former is important. At test temperatures above the recrystallization temperature of the steel, the carbides present, especially those located in the vicinity of grain boundaries, increase high-temperature stability. Creep properties in these higher-temperature ranges are largely determined by grain boundary conditions, and it is probable that the carbides act as keyways to prevent flow[14].

I. Binary Ferrites

A comparison of the creep resistance at 426° C (800° F) and 538° C (1000° F) of a series of binary ferrites is presented to demonstrate the relative effectiveness of the several elements in combination with pure Fe. The constant-temperature tests are conducted by a method of stepped up loading as follows[4,5]: A load of 5000 psi is applied for 600 to 700 hrs, during

which the time versus the extension is measured. Then the load is given an increment of 2500 psi and again held for 600 to 700 hrs. This stepping up of the load in increments of 2500 psi is continued until failure of the specimen occurs.

At a test temperature of 426° C (800° F), the creep rates of several binary ferrites containing from ½ to 1½ per cent of alloying elements are plotted against the stress in Fig. 3-2. At the same temperature, the stress to produce three different creep rates, namely 0.05, 0.1 and 1.0 per cent, is shown for six binary ferrites containing 1 per cent by weight of each element in Fig. 3-3.

It is interesting to compare the effect of these binary ferrites in increasing room-temperature strength and creep resistance at 426° C (800° F) over
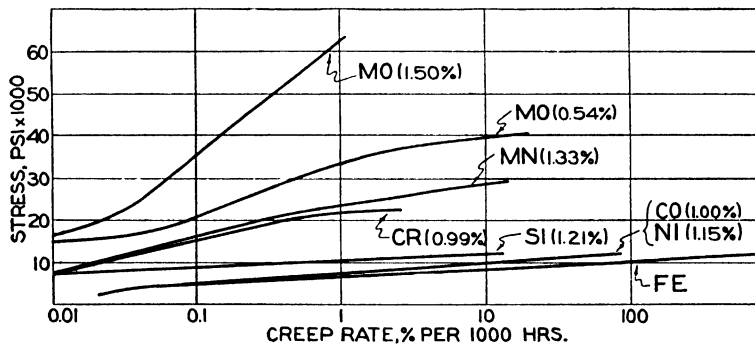
Fig. 3-2. Semilogarithmic plot showing comparison between behaviors of elements in ferritic solid solution at approximately one weight per cent at 426° C (800° F). (After Austin, St. John, and Lindsay)

ferrite in the absence of C. While both Ni and Si dissolved in Fe each increase the hardness and tensile strength of ferrite at room temperature, these two elements do not improve creep resistance of ferrite at high temperature. Mo strengthens ferrite at room temperature and is most effective in increasing creep resistance when added to ferrite. Mn is similar in its effect to Mo at both room temperature and high temperature, although to a more modest degree. The element Cr is unusual in that it does not change the room-temperature properties of ferrite, but does improve creep resistance. Co changes neither room-temperature nor elevated-temperature properties when added to ferrite to form a solid solution.

Another aspect of the effect of alloying elements on ferrite is the change due to cold work. Different elements have varying effects on the temperature of softening after ferrite is cold-worked. It appears that this factor bears some relation to creep resistance of the alloyed solid solution, accord-

ing to tests conducted at 426° C (800° F). Mo markedly opposes softening
of the solid solution after cold-working, which is in line with its effect in
improving creep resistance. Cr and Mn also oppose the softening tendency,
but to a lesser degree. Si is only slightly effective in this regard, and Ni and
Co have practically no effect.

In creep tests conducted at 538° C (1000° F), the only binary ferrite to
show any improved creep resistance is that containing 0.54 and 1.5 per
cent Mo. This may be due partly to the fact that the presence of this ele-
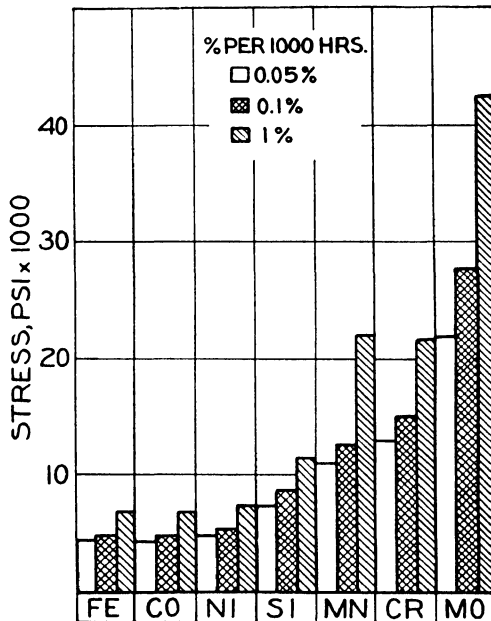
Fig. 3-3. Stresses causing indicated creep rates at 426° C (800° F) in ferritic solid
solutions containing one per cent by weight of each element. (After Austin, St. John,
and Lindsay)

ment in ferrite raises the softening temperature of the cold-worked material
well above 538° C (1000° F)[5].

II. C-Mo Steel (0.5% Mo)

In the presence of C, the addition of 0.5 per cent Mo is most effective in
increasing creep resistance compared with plain-C steel. At 482° C (900° F),
this alloy steel has about twice the creep resistance of plain-C steel.

The results of short-time tensile tests on a 0.2 per cent C, 0.5 per cent
Mo steel are shown in Table 3-13[6].

The creep properties of a steel with 0.1 per cent C and 0.5 per cent Mo

are shown in Table 3-14[3]. This steel retains its strength for a creep rate of 0.1 per cent per 1000 hrs fairly well at 482° C (900° F). The steels shown in Table 3-14 represent several analyses with varying manufacturing methods and heat treating conditions.

a. Effect of C on 0.5% Mo Steel. To investigate the effect of C content on a steel with 0.5 per cent Mo, a series of steels shown in Table 3-15 have a C content varying from 0.05 to 0.395 per cent. Steels A1 and A6 represent heats of 18 lbs from a high-frequency furnace and the other four steels, A2, A3, A4, and A5 are open-hearth products[20].

The samples represent 1-in diameter bars normalized at 950° C (1742° F), except sample A1 with 0.05 per cent C, which is normalized at 1000° C (1832° F) to obtain a structure similar to sample A2 with 0.09 per cent C. The results of creep tests on these samples are shown in Fig. 3-4 where the

TABLE 3-13. SHORT-TIME TENSILE TESTS OF C-Mo STEEL (0.5% Mo)[6]

C	Mn	S	P	Si	Mo
0.1–0.2	0.3–0.6	0.045	0.04	0.1–0.5	0.45–0.65

Temp (°C)	Temp (°F)	Tensile Strength (psi)	Elong. % in 2″	Reduction of Area (%)
426	800	70,500	28	72
482	900	63,500	28	76
538	1000	57,500	29	77
593	1100	45,100	38	84
650	1200	27,000	60	88
704	1300	16,200	83	94
760	1400	8700	94	86

total strain is plotted against time. The tests are conducted at a constant temperature of 600° C (1112° F) under a constant load of 4 tons per sq in. These curves indicate that the steels with the lower C contents deform less than the samples with the higher C contents in the early period of the test. It is also evident that steels A1 and A2 with the lowest C contents enter third-stage creep sooner than the other steels under these test conditions.

The effect of C content on deformation is more clearly seen in Fig. 3-5, where the per cent C is plotted against the time required to reach specific amounts of deformation. The lowest curve indicates 0.1 per cent strain, the next above 0.2 per cent strain, and the others in increasing amounts up to 0.6 per cent strain. At the lowest deformation, 0.1 per cent, the steel with the lowest C content takes the longest time to reach this value. With increasing deformation, the steel which takes longest to reach the specified deformation has an increasing C content. This value of C content reaches 0.2 to 0.25 per cent for the steel which takes the maximum time to reach 0.5 to 0.6 per cent strain. Thus, at small deformations, the low-C steels

TABLE 3-14. CREEP STRENGTH C-MO STEEL (0.5% Mo)*

Chemical Composition and Manufacturing Data
Wrought 0.20 C Max. 0.50 Mo Steel

Sampl No.	C	Mn	Si	S	P	Mo	Heat Treatment (°F)	Grain Size	Brinell	Type Mat.	Type Furn.	Temperature (°C) (°F)		Creep Strength Stress (psi) 0.10% per 1000 hours	0.01% per 100 hours?
3a	0.13	0.49	0.25	0.010	0.011	0.52	Ann. 1550	8 N	121	Bars	EF Basic	482	900	19,000	12,800
3d	0.11	0.19	1.35	0.012	0.010	0.50	Ann. 1550	6–8 N	146	Bars	EF Basic	426	800	29,500	18,400
												538	1000	9300	5000
4d	0.15	0.41	0.19	—	—	0.58	N. 1650, D. 1200	CG		Piping	OH Basic	495	925	17,100	13,000
6d	0.11	0.47	0.17	0.014	0.010	0.54	N. 1650 D. 1300, 5 hours	—	68.2*	Bars	OH Basic	593	1100	3500	1600

* Rockwell B scale
Note: All tests 1000 hrs duration.
EF: Electric furnace.
Ann: Annealed.
N: Normalized.
D: Drawn.

TABLE 3-15. MANUFACTURING DETAILS AND ANALYSIS OF 0.5% Mo
STEELS WITH VARYING C CONTENT[20]

Steel	Process	Method of Deoxidation	C	Si	S	P	Mn	Ni	Cr	Mo	Cu
A1	18 lb H.F.	FeMn and FeSi	0.055	0.16	0.032	0.018	0.48	0.10	0.04	0.50	0.08
A2	Basic O.H.	SiMn to ladle	.09	.22	.044	.013	.43	.09	.03	.51	.08
A3	Basic O.H.	SiMn to ladle	.145	.15	.030	.032	.56	.12	.01	.48	.06
A4	Basic O.H.	SiMn to ladle	.21	.17	.030	.029	.49	—	—	.55	—
A5	Acid O.H.	SiMn to ladle	.31	.18	.038	.040	.55	—	—	.52	—
A6	18 lb H.F.	FeMn and FeSi	.395	.14	.029	.018	.48	.11	.06	.48	.08

O.H. = Open hearth.
H.F. = High frequency.

Note: The above steels, in the form of 1 in diameter bars, are normalized from 950° C, with the exception of the 0.05 per cent C steel which is normalized from 1000° C to give a structure similar to that of the 0.09 per cent C open-hearth steel.
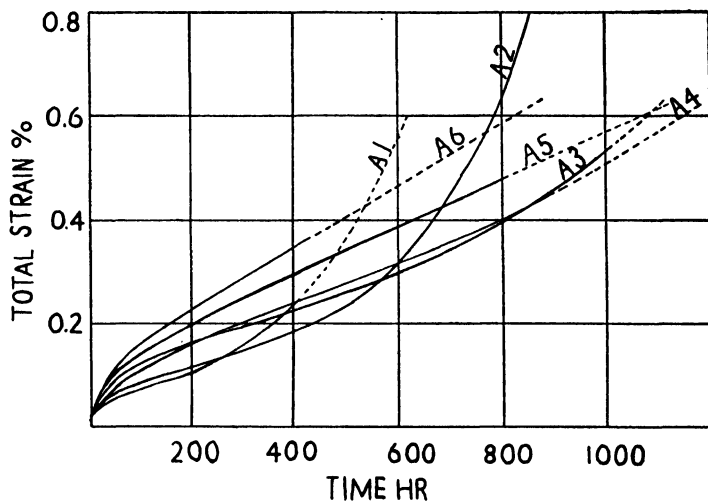
Fig. 3-4. Steel. Carbon content: A1—0.055%, A2—0.09%, A3—0.145%, A4—0.21%, A5—0.31%, A6—0.395%. Curves of creep tests on 0.5% Mo steels with various carbon contents. Stress 4 tons/sq inch; temperature 600 ° C. (After Glen)

are most effective in creep resistance, but at larger deformations steels with C contents of 0.2 to 0.25 per cent have the greater creep resistance. It is important to point out here that these results hold only for this particular test temperature of 1112° F (600° C).

b. Effect of Tempering 0.5% Mo Steel. Variation in the time of tempering a steel influences the amount of spheroidization of the carbides, which in turn affects creep resistance. This effect is reported for Steel A2 containing 0.09 per cent C, 0.51 per cent Mo, tempered at 650° C (1202° F) for periods of 5, 10, 20, 50 and 100 hrs followed by air-cooling. The increase in tempering time increases the amount of spheroidization. These samples tested for
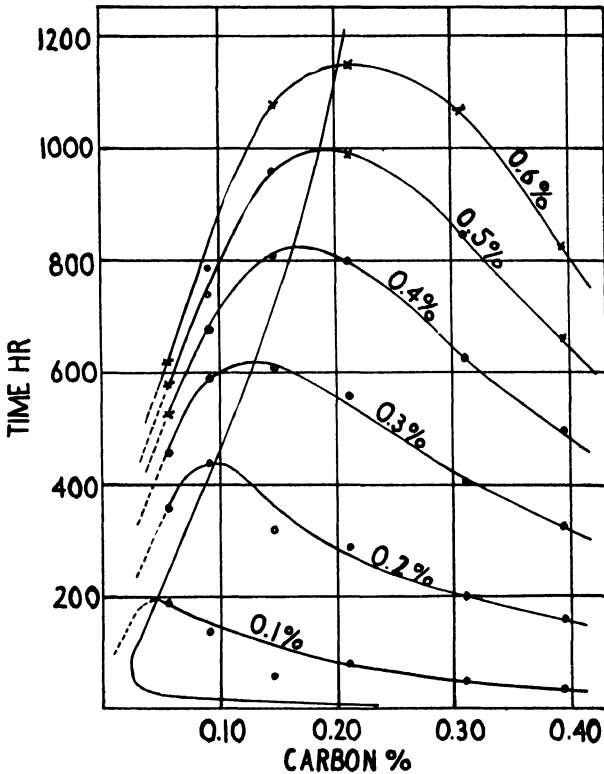
Fig. 3-5. Curves showing the effect of carbon content of 0.5% Mo steel on the time to reach the strains indicated. Derived from Figure 3-4. Stress 4 tons/sq inch, temperature 600° C. (After Glen)

creep at 550° C (1022° F) and at 6 tons per sq in display a decrease in creep strength with increase in tempering time. This deterioration in creep strength with increase in spheroidization is in accord with many observations for other steels. Creep tests conducted at higher temperatures, namely 650° C (1202° F) indicate that spheroidization is more important in the deterioration of steels containing 0.5 per cent Mo than scaling of the surface during the test[20].

c. Spheroidization. An interesting comparison of spheroidization of a C-Mo steel exposed in the laboratory to elevated temperature under no load is made with the same type of steel taken from actual service. The

Fig. 3-6. C-Mo steel before exposure. Magnification 1000×. (After Miller, Golaszewski, and Smith)
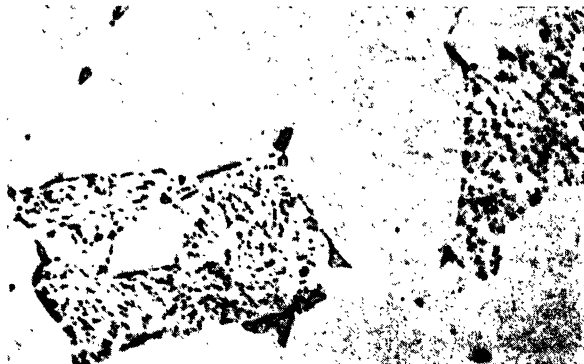
Fig. 3-7. C-Mo steel as shown in Figure 3-6 after exposure at 593° C (1100° F) for 3000 hrs. Magnification 1000×. (After Miller, Golaszewski, and Smith)

laboratory sample spheroidized under controlled conditions has the following analysis[30]:

C	Mn	P	S	Si	Mo	Al	Al$_2$O$_3$
0.14	0.55	0.016	0.023	0.15	0.53	0.02	0.026

It is a fine-grained steel produced with Si and about 1.5 lbs Al per ton of steel. The heat treatment before exposure to high temperature consists of normalizing for 30 min at 900° C (1650° F), as shown in Fig. 3-6 at 1000×.

This microstructure is typical of the analysis and treatment which the sample has received. The spheroidization which occurs when this steel is heated to 593° C (1100° F) for 3000 hrs is shown in Fig. 3-7. The globular form of the carbides is quite evident.

A steel of the same nominal composition in service for 30,000 hours at 593° C (1100° F) is shown in Fig. 3-8. The increase of exposure time by a factor of ten results in much greater spheroidization. It is interesting to observe here that neither of these steels reveals any evidence of graphitization with such long exposure times.

As pointed out earlier, temperature is the most important factor in increasing the rate of spheroidization. A few hours' exposure at 650 to 700° C produces more spheroidization than months or years at 480 to 538° C for

Fig. 3-8. C-Mo steel of the same general analysis as that in Figure 3-6 after a service life at 593° C (1100° F) of 30,000 hrs. Magnification 1000×. (After Miller, Golaszewski, and Smith)

plain-C and low-alloy steels[30]. In general, the deterioration in a normalized 0.5 per cent Mo steel exposed 10,000 hrs at 538° C (1000° F) is estimated to be a loss of $\frac{1}{2}$ of its initial creep strength[35].

d. Graphitization in Plain-C and C-Mo Steels. Prolonged exposure of plain-C steels containing 0.2 per cent C to the temperatures encountered in steam pipes may result in failure due to graphitization of the carbides originally present in the structure. The type of graphitization which is rather uniformly distributed through the grains is not necessarily harmful, but graphitization which is highly localized is believed to account for certain failures noted in service[17]. One of the factors contributing to localized graphitization is the occurrence of plastic deformation during exposure of the steel to elevated temperature. At the areas where graphitization has occurred, reduced ductility may well account for failure of the part.

Deoxidation practice is one of the major factors in determining the period of incubation before graphitization and the rate at which graphitization takes place. In 10,000 hours' exposure tests in a temperature range of 482 to 650° C (900 to 1200° F), all deoxidized C steels graphitize[40]. This tendency exists whether the deoxidized steel is an acid bessemer or basic open-hearth product. Undeoxidized steels are much more resistant to graphitization.

Mo added to low-C steels reduces the tendency to graphitization although, in amounts up to 0.5 per cent, this resistance is not marked in steels undergoing many years of service. The addition of Cr to 0.5 per cent Mo steels reduces the tendency toward graphitization, but there exists a minimum Cr content to prevent graphitization. A steel with 0.5 per cent Mo and 0.25 per cent Cr deoxidized with Si and a large amount of Al exhibits graphitization. However, a 0.5 per cent Mo steel with 0.5 per cent Cr, regardless of deoxidization practice, shows no graphitization after 10,000 hours' exposure at three different temperatures, 482° C (900° F), 565° C (1050° F), and 650° C (1200° F)[40].

Other compositions of steels of low alloy content show tendencies to graphitize as follows: (1) a steel with 1 per cent Mo graphitizes after 10,000 hours at 565° C (1050° F); (2) a steel with 1.5 per cent Mo and 0.16 per cent V graphitizes after 10,000 hours at 565° C (1050° F); (3) a steel with 3.7 per cent Ni graphitizes after 1000 hours at 565° C (1050° F); (4) a steel with 0.38 per cent C, 0.26 per cent Mo, and 1.7 per cent Ni graphitizes after 1000 hours at 565° C (1050° F); (5) a steel with 5.2 per cent Ni shows no graphitization after 1000 hours at 565° C (1050° F), but has large nodules of graphite after 10,000 hours' exposure[40]. With low-alloy steels in general, deoxidation practice should be such as to produce normal steels. Such a procedure decreases the possibility of graphitization in service when steels are exposed to high temperatures for long periods.

III. 0.8% Cr, 0.5% Mo Steel

Up to an amount of 1 per cent, the addition of Cr to steels containing 0.5 per cent Mo increases their creep resistance, but beyond this amount, the creep strength diminishes[19]. Steels of these analyses have a finer grain structure than those containing only Mo. In creep tests with C varying from 0.10, 0.145, to 0.22 per cent and Cr and Mo held to 0.8 and 0.5 per cent respectively, the higher C contents show greater creep strength[19].

Tempering this series of steels at 650° C (1202° F) for periods up to 100 hours shows a decreased creep strength with increase in tempering time, but the deterioration is not as marked even after 100 hours, as in the case of the straight C-Mo steels. It is evident that the presence of Cr has a stiffening effect on these compositions. In stress-rupture tests on these

same steels, where values of the stress are shown as a function of time on a log scale, a linear relation does not hold. The fact that the curves resulting from stress-rupture tests for the 0.8 per cent Cr, 0.5 per cent Mo steel falls below a straight line indicates that spheroidization is probably taking place.

IV. 0.3% V, 0.5% Mo Steels

The addition of 0.3 per cent V to a steel of 0.5 per cent Mo results in increased creep resistance over the straight C-Mo and the C-Mo steel with 0.8 per cent Cr[20]. In a series of analyses of the above V and Mo contents and with C varying from 0.08, to 0.13, to 0.19 per cent, the higher C content shows the best creep resistance in tests at 550° C (1022° F) under a load of 9 tons per sq in. Tempering the Mo-V at 650° C (1202° F) does not decrease the creep strength, while tempering at 690° C (1274° F) only slightly decreases it.

The addition of Al as a deoxidizer to the Mo-V steels is less detrimental than to plain-C steels, since deoxidation has already taken place due to the presence of the V. An amount of 0.1 per cent V added to a 0.5 per cent Mo steel is such a powerful deoxidizer that a fine grain of 6 to 8 results even when the normalizing temperature is high[20].

In stress-rupture tests of the 0.3 per cent V, 0.5 per cent Mo steels, a remarkable change occurs, in that the curve resulting from plotting the stress as a function of the time on a log scale actually rises above the straight line, indicating that this alloy is increasing in stiffness. Mo-V steel shows such marked superiority in stress-rupture and creep tests over C-Mo and Cr-Mo steels that it is recommended for service as steam pipes and superheater pipes[20].

C. 1.25 to 2.50% Cr Steel

Cr is the most effective single element for imparting corrosion- and scaling-resistant properties to steels for high-temperature service. Its presence in proportions as small as $1\frac{1}{4}$ per cent in combination with Si and/or Mo results in an alloy which is suitable for use in the temperature range of 482–538° C (900–1000° F). The presence of Mo decreases the tendency to brittleness at room temperature after prolonged heating. With the addition of 2 per cent Cr, corrosion resistance against crude oils at high temperature and pressure is noticeable[6]. These series of low-alloy pearlitic steels are widely used for tubing for moderately elevated temperatures.

The short-time, high-temperature tensile strength for the $1\frac{1}{4}$ per cent Cr steel is given in Table 3-16[6]. The strength of this alloy holds fairly well up to 538° C (1000° F).

The creep strength of the $1\frac{1}{4}$ per cent Cr alloy steel is given in Table 3-17, obtained from several different sources. Although the values do not

check too closely, it is evident that the creep strength of this steel falls off in the region of 538° C (1000° F).

The high-temperature properties of steels containing 2 per cent Cr with small amounts of Mo and Si are shown in Tables 3-19, 3-20, 3-21, and 3-22.

TABLE 3-16. SHORT-TIME, HIGH-TEMPERATURE TENSILE PROPERTIES OF STEEL (1.25% Cr, 0.50% Mo, 0.75% Si)[6]*

Temp. (°C)	(°F)	Ultimate Strength psi	Elong. % in 2"	Red. of Area (%)
426	800	69,250	27	68
482	900	67,500	26	66
538	1000	57,750	26	73
593	1100	47,500	31	83
650	1200	33,300	32	88
704	1300	22,800	62	95
760	1400	13,800	72	99

* "Croloy" 1¼, Courtesy Babcock and Wilcox Tube Co.

TABLE 3-17. CREEP STRENGTH OF 1¼% Cr STEELS

Sample No.	Steel	Temp. (°C)	(°F)	Stress (psi % per 1000 hrs) 0.1	.01
* 8b[3]	1.24 Cr	538	1000	14,700	8200
† Cr-Si-Mo[14]	1.24 Cr	426	800	28,000	20,000
		538	1000	24,000	15,000
		593	1100	6800	4300
		650	1200	3950	1950

| ⌐ Chemical Composition ⌐ | | | | | Heat | | Type | Type |
C	Mn	Si	Cr	Mo	Treatment (°F)	Brinell	Material	Furnace
*0.10	0.36	0.63	1.24	0.54	Ann. 1525	143	Tubes	E.F. Basic
†0.07	—	0.72	1.24	0.54				

Note: Test for No. 8b 1000 hours duration.

TABLE 3-18. THERMAL EXPANSION STEEL (1¼% Cr, 0.5% Mo)*

Temp (°F)	Mean Coefficient of Linear Expansion (In/In/°F × 10⁻⁶)
70–600	7.40
70–800	7.80
70–1000	8.20
70–1200	8.50

* "Croloy" 1¼, Courtesy Babcock and Wilcox Tube Co.

In the series of alloy steels with Cr varying from 1.25 to 2.50 per cent with less than 1 per cent Mo and Si, the microstructure consists of ferrite with the carbides in lamellar form. These low-alloy pearlitic steels have moderate air-hardening properties, which attain a maximum of 300 Brinell

TABLE 3-19. SHORT-TIME TENSILE STRENGTH STEEL (2.00% CR, 0.50% MO)*

Temp. (°C)	(°F)	Ultimate Strength (psi)	Elong. % in 2″	Red. of Area (%)
426	800	64,300	27	63
482	900	61,600	31	72
538	1000	55,300	35	77
593	1100	44,250	40	72
650	1200	30,850	58	88
704	1300	19,400	77	92
760	1400	10,500	86	98

* "Croloy" 2, Courtesy Babcock & Wilcox Tube Co.

TABLE 3-20. CREEP STRENGTH OF 2% CR STEELS[3]

Temp. (°C)	(°F)	Stress psi, %/1000 Hrs 0.1	0.01
482	900	20,000	14,300
538	1000	9000	5700
593	1100	6000	4000

⌐ Chemical Composition ⌐					Heat Treatment (°F)	Brinell	Grain Size	Type Material	Type Furnace
C	Mn	Si	Cr	Mo					
0.11	0.45	0.42	2.08	0.50	Ann. 1550	131	7–8	1 in Bar	E.F. Basic

Note: Test 1000 hours' duration.

TABLE 3-21. HOT IMPACT TESTS STEEL (2% CR)*

Temperature (°C)	(°F)	Charpy Impact (ft-lbs)	Temperature (°C)	(°F)	Charpy Impact (ft-lbs)
30	85	62	371	700	52
93	200	61	426	800	70
149	300	57	482	900	41
204	400	62	538	1000	40
260	500	59	593	1100	36
315	600	57	650	1200	38
			704	1300	65

* "Croloy" 2 annealed, Courtesy Babcock & Wilcox Tube Co. Drilled keyhole notch.

TABLE 3-22. THERMAL EXPANSION STEEL (2% CR, 0.5% MO)*

Temp. (°F)	Mean Coefficient of Linear Expansion (In/In/°F × 10⁻⁶)
70–450	7.45
70–750	˙ 7.78
70–1050	8.45
70–1150	8.50

* "Croloy" 2, Courtesy Babcock & Wilcox Tube Co.

on air-cooling a 2.50 per cent Cr steel from 982° C. When used as tubing for high-temperature service in oil refineries or boiler tubes, both economy and operating conditions determine selection of the most suitable material.

Common failures which occur in service are due to excessive temperature conditions accompanied by corrosion and scaling[6].

The high-temperature properties of several steels containing 2.25 to 2.50 per cent Cr with small percentages of Mo and Si are given in Tables 3-23, 3-24, 3-25, and 3-26.

The effect of heat treatment on a steel with 2.25 per cent Cr and 1 per cent Mo is shown in Table 3-26[27]. Air-cooling from 900° C followed by tempering at 750° C and furnace-cooling gives a creep strength of 13,300 psi for a creep rate of 0.1 per cent per 1000 hours at a test temperature of 538° C (1000° F). This same steel heat-treated by furnace-cooling from 900°C has a creep strength under the same conditions of 12,100 psi. These tests represent periods of creep-testing of 3000 hours.

TABLE 3-23. SHORT-TIME TENSILE STRENGTH STEEL (2.25% Cr, 1.00% Mo)*

Temp. (°C)	(°F)	Ultimate Strength (psi)	Elong. % in 2″	Red. of Area (%)
260	500	68,800	27	66
315	600	67,500	24	64
371	700	71,400	23	61
426	800	66,750	28	66
482	900	63,750	33	72
538	1000	49,750	35	82
593	1100	39,100	55	89
650	1200	31,250	57	93
704	1300	23,750	62	97
760	1400	13,650	76	100

* "Croloy" 2¼, Courtesy Babcock & Wilcox Tube Co.

D. 4-6% Cr Steel, Type 502

Seamless tubing of 5 per cent Cr steel finds extensive use in the petroleum industry because of its high strength and corrosion resistance against oils and crudes containing hydrogen sulphide and other corrosive agents. The addition of 0.5 per cent Mo decreases a tendency toward brittleness after operation in the service range of 426 to 538° C (800 to 1000° F). Steels containing 5 per cent Cr and 0.5 per cent Mo air-harden to a maximum of 328 Brinell on cooling from 955° C (1750° F)[6].

The elevated-temperature properties of several low-C steels with 5 per cent Cr are given in Tables 3-27, 3-28, 3-29, 3-30, and 3-31.

I. 4–6% Cr Steel with Ti

The addition of Ti to alloy steels containing 5 per cent Cr and 0.5 per cent Mo is advantageous in reducing the tendency of these steels to air-harden. Without the presence of Ti they must be annealed and cooled very slowly to prevent the appearance of martensite, which causes poor ma-

TABLE 3-24. CREEP STRENGTH OF 2¼ CR STEELS

	Temp.		Stress psi, %/1000 Hrs	
	(°C)	(°F)	0.1	0.01
* 2.50 Cr	426	800	26,000	23,000
	650	1200	2450	1000
† 2.50 Cr	426	800	27,000	22,000
	538	1000	9300	6100
	650	1200	2325	1000

Tests of 1000 hours' duration.

	⌐ Chemical Composition ⌐					Heat Treatment (°F)	Brinell	Grain Size	Type Material	Type Furnace
	C	Mn	Si	Cr	Mo					
* Ref. 3	0.11	0.41	0.78	2.50	0.50	Ann. 1550	143	7–8	1 in Bar	E.F. Basic
† Ref. 14	0.11		0.78	2.50	0.50					

TABLE 3-25. THERMAL EXPANSION STEEL (2.25% CR, 1.00% MO)*

Temp (°F)	Mean Coefficient of Linear Expansion (In/In/°F × 10⁻⁶)
73–402	6.90
73–609	7.21
73–809	7.54
73–1015	7.86
73–1207	8.09

* "Croloy" 2¼, Courtesy Babcock & Wilcox Tube Co.

TABLE 3-26. EFFECT OF HEAT TREATMENT ON 2.25% CR STEEL[27]

Steel	Nominal Composition	Heat Treatment (°C)	Creep Test Temp (°C)	(°F)	Creep Stress (psi)	Duration Creep Test (hrs)	Av. Creep Rate During Last 1000 Hrs (millionth in/in/hr)
B 2*	2.25 Cr-1 Mo	900 AC, 750 FC	538	1000	15,000	3000	1.47
B 2*	2.25 Cr-1 Mo	900 FC	538	1000	15,000	3000	7.45

	Modified 2/3 Size Charpy Impact Strength			Brinell		Amount of Change of Micro-structure during Creep	Stress for Creep Rate (millionth in/in/hr)
	Before Creep Test (ft-lbs)	After Creep Test (ft-lbs)		Before Creep	After Creep		
B 2	46	44		159	167	None	13,300
B 2	39	44		133	136	Slight	12,100

* Chemical Analysis Steel B 2 C 0.10, Mn 0.34, P 0.012, S 0.007, Si 0.12, Cr 2.26, Mo 1.06.

chinability and low ductility. After fabrication into tubes or after being welded, the steel with Ti is air-cooled. No perceptible air-hardening occurs

TABLE 3-27. SHORT-TIME TENSILE PROPERTIES STEEL (5% CR, 0.50% MO)*

Temp (°C)	Temp (°F)	Ultimate Strength (psi)	Elong. % in 2″	Reduction in Area (%)
93	200	62,900	37	74
150	300	60,700	35	73
204	400	58,300	34	72
260	500	56,000	33	73
315	600	55,400	30	68
371	700	55,600	28	66
426	800	54,200	29	67
482	900	53,350	37	74
538	1000	45,350	46	83
593	1100	31,700	60	90
650	1200	24,450	70	94
704	1300	17,800	79	97
760	1400	11,350	78	99
815	1500	11,900	23	74

* "Croloy"5, Courtesy Babcock & Wilcox Tube Co.

TABLE 3-28. CREEP STRENGTH WROUGHT 4–6% CR-MO STEEL[3]

Chemical Composition and Manufacturing Data

C	Mn	Si	S	P	Cr	Mo	Heat Treatment	Grain Size	Brinell	Type Material	Type Furnace
0.10	0.45	0.18	0.015	0.017	5.09	0.55	Ann. 1550°F	7	128	Bars	EF

Temperature (°C)	(°F)	Creep Strength Stress (psi) 0.10% per 1000 hours	0.01% per 1000 hours
426	800	22,000	14,300
482	900	15,200	11,600
538	1000	10,100	7700
593	1100	5900	3150
650	1200	2900	1720

Note: Tests 1000 hours' duration.

TABLE 3-29. THERMAL EXPANSION STEEL (5% CR, 0.50% MO)*

Temp (°F)	Mean Coefficient of Linear Expansion (In/In/°F × 10⁻⁶)
70–400	6.40
70–600	6.80
70–800	7.10
70–1000	7.20
70–1200	7.30

* "Croloy" 5, Courtesy Babcock & Wilcox Tube Co.

on air-cooling from temperatures as high as 1010° C. Recent work indicates that these Ti-bearing steels have advantages in improved creep resistance

under certain conditions[16]. The Ti-to-C ratio should be maintained at 3.8 to 5.1 per cent. Many commercial alloys of this class carrying Ti have a Ti-to-C ratio of 5 or more. The Si content is usually held to not more than 0.5 per cent. However, the Si can be increased to 1.20 per cent for improved creep properties[16]. The heat treatment usually applied to the Cr-Mo-Ti steel is annealing or normalizing. If hot-working is carried out, the temperature should be reasonably low to maintain a fine grain. Subsequently, the steel may be tempered at 1350° F (730° C).

TABLE 3-30. HOT IMPACT PROPERTIES STEEL (5% CR)*

Temperature (°C)	(°F)	Charpy Impact (ft-lbs)	Temperature (°C)	(°F)	Charpy Impact (ft-lbs)
29	85	81	371	700	75
93	200	68	426	800	87
150	300	68	482	900	65
204	400	64	538	1000	59
260	500	64	593	1100	54
315	600	73	650	1200	54
			704	1300	75

* "Croloy 5" annealed, Courtesy Babcock & Wilcox Tube Co. Drilled keyhole notch.

A comparison of the stress rupture values of two steels with 5 per cent Cr, with and without Ti, is shown as follows:

Material	At 650° C (1202° F) Stress Rupture (psi in 1000 hrs)
5% Cr, 0.5% Mo	7,000
C .08, Mn .30, Si .22, Ti .30 Ti/C ratio 3.8	10,000

This Ti-bearing steel maintained good impact properties at room temperature after being stressed 2000 hrs at 650° C (1202° F)[16].

E. 7–9% CR STEELS

This class of steel in the medium C range finds wide use in exhaust valves for many applications. A typical analysis is 0.4 to 0.5 per cent C, 3 to 3.5 per cent Si, and 8 to 9 per cent Cr. Steels of this general type are being replaced by austenitic alloys, since corrosion resistance in exhaust atmospheres is superior in the single phase austenitic alloys[22].

In the lower range of C, not exceeding 0.15 per cent, the 7 to 9 per cent Cr steels are widely used in tubing applications. Steels with Cr in the range of 7 to 9 per cent are suitable where corrosion resistance is more important than oxidation resistance as encountered in contact with hot petroleum products. Their composition places them nearer the outside of the gamma loop, and for maintenance of a single phase the Si and Al contents should

TABLE 3-31. EFFECT OF HEAT TREATMENT ON THE HIGH TEMPERATURE PROPERTIES OF A 5% CR STEEL.[27]

Nominal Composition	Heat Treatment (°C)	Creep Test Temp. (°C) (°F)	Creep Stress (psi)	Duration Creep Test (hrs)	Av. Creep Rate During Last 1000 Hrs (millionth in/in/hr)	Modified ½ Size Charpy Impact Strength		Brinell		Amount of Change of Microstructure during Creep	Stress for Creep Rate 0.1% per 1000 hours
						Before Creep Test (ft-lbs)	After Creep Test (ft-lbs)	Before Creep	After Creep		
5 Cr-1 Mo	900 AC 750 AC	538 1000	15,000	1000	7.9	39	33	202	174	None	10,800
5 Cr-1 Mo	900 FC	538 1000	15,000	500	39.8	29.5	29.5	140	138	None	8400 10,000
5 Cr-1 Mo	900 AC 750 FC	593 1100	8000	1000	17.5	39	30.5	181	158	Slight	4300 4900

Chemical Analysis Steel C 2 C 0.13, Mn 0.56, P 0.008, S 0.017, Si 0.38, Cr 5.66, Mo 0.98
AC: Air cooled.
FC: Furnace cooled.

TABLE 3-32. SHORT-TIME TENSILE STRENGTH STEEL (7% CR, 0.50% Mo, 0.50 TO 1.00% SI)*

Temp (°C)	(°F)	Ultimate Strength (psi)	Elong. % in 2″	Reduction in Area (%)
93	200	70,100	35	75
204	400	66,900	32	74
315	600	65,650	30	72
426	800	54,000	26	74
482	900	44,750	27	78
538	1000	33,100	27	82
593	1100	27,770	40	84
650	1200	17,350	38	77
704	1300	10,950	50	80
760	1400	7750	66	92
815	1500	5950	79	87
870	1600	8800	31	27

* "Croloy" 7, Courtesy Babcock & Wilcox Tube Co.

TABLE 3-33. THERMAL EXPANSION STEEL (7% CR, 0.5% Mo, 0.75% SI)*

Temp (°F)	Mean Coefficient of Linear Expansion (In/In/°F $\times$ 10^{-6})
70–400	6.28
70–800	6.74
70–1000	7.02
70–1200	7.20

* "Croloy" 7, Courtesy Babcock & Wilcox Tube Co.

TABLE 3-34. SHORT-TIME TENSILE STRENGTH STEEL (9% CR, 1.00% Mo).*

Temp (°C)	(°F)	Ultimate Strength (psi)	Elong. % in 2″	Reduction in Area (%)
482	900	52,850	34	75
538	1000	44,800	43	82
593	1100	35,800	46	86
650	1200	23,050	68	91
704	1300	15,950	87	91
760	1400	10,750	87	93

* "Croloy" 9M, Courtesy Babcock & Wilcox Tube Co.

TABLE 3-35. THERMAL EXPANSION STEEL (9% CR, 1.25% Mo)*

Temp (°F)	Mean Coefficient of Linear Expansion (In/In/°F $\times$ 10^{-6})
70–300	6.29
70–600	6.67
70–900	7.00
70–1200	7.30

* "Croloy" 9, Courtesy Babcock & Wilcox Tube Co.

be less than 1.0 per cent. Certain refineries report that 7 per cent Cr steel tubing has a corrosion resistance five times that of the 5 per cent Cr steel,

TABLE 3-36. ELEVATED-TEMPERATURE PROPERTIES OF STEELS (8 TO 9% CR)[27]

Steel	Nominal Composition	Heat Treatment (°C)	Creep Test Temp. (°C) (°F)	Creep Stress (psi)	Duration Creep Test (hrs)	Av. Creep Rate During Last 1000 Hrs (millionth in/in/hr)	Modified ⅓ Size Charpy Impact Strength Before Creep Test (ft-lbs)	After Creep Test (ft-lbs)	Brinell Before Creep	Brinell After Creep	Amount of Change of Microstructure during Creep	Stress for Creep Rate of 0.1% per 1000 hrs
D-1	8 Cr-Mo	926 FC	593 1100	4000	3000	0.20	23	28	145	141	None	5600
D-2	8 Cr-Mo-Cb	926 FC	593 1100	4000	3000	0.05	41	22.5	141	138	None	8000
D-3	9 Cr-Mo	926 FC	593 1100	4000	3000	0.22	23	22	144	143	None	5200

Chemical Composition:

	C	Mn	P	S	Si	Cr	Mo	Cb
D-1	0.10	0.36	0.011	0.009	0.31	8.04	1.04	—
D-2	0.09	0.56	—	—	0.33	8.15	0.91	0.59
D-3	0.12	0.43	0.011	0.015	0.43	9.47	1.04	—

Transformation Temperatures:

Steel	Approx A1 (°C) (°F)	Approx A3 (°C) (°F)
D-1	800 1475	871 1600
D-2	788 1450	900 1650
D-3	815 1500	871 1600

In order to dissolve the carbides in the austenite, these steels were heated 1 hr at 926 °C (1700 °F) and furnace-cooled at a rate of 50 °F per hr to prevent air hardening. Actually air hardening these steels produced the following results:

D-1 (8 Cr-Mo)—VPN 408
D-2 (8 Cr-Mo-Cb)—VPN 336
D-3 (9 Cr-Mo)—VPN 436

With such a high alloy content, some martensite forms at a cooling rate of 200° F per hour but none at 100° F per hour. At 593° C (1100° F), the 8 Cr-Mo steel has a creep strength of 5600 psi. The addition of 1 per cent Cr decreases this value to 5200 psi, but Cb increases the value to 8000 psi.

FC: Furnace cooled.

and 9 per cent Cr steel has a corrosion resistance six times that of 5 per cent Cr steel[12].

The elevated-temperature properties of several steels containing 7 to 9 per cent Cr are shown in Tables 3-32, 3-33, 3-34, and 3-35.

In steels D_1, D_2, and D_3 shown in Table 3-36, changes in impact strength are not exceptional nor are the hardness changes significant. In general the microstructures show evidence of spheroidization and agglomeration of the carbides. Neither furnace-cooling nor tempering shows a tendency toward greater stability of structure as regards the microconstituents[27].

F. Effect of Banding or Lack of Uniformity in Microstructure

The effect of a banded structure in a low-alloy steel containing small percentages of Ni, Cr, Mo, Mn, and/or Si indicates that creep strength is greatly lowered if this condition exists[42]. The results of creep tests conducted at 450° C (842° F) on two steels of nearly similar chemical composition, one uniform in structure and one severely segregated are shown as follows:

Type of Steel	C	Ni	Cr	Mo	Mn	Si	Stress (psi)
Uniform	0.35	1.91	0.85	0.46	0.56	—	36,000
Banded	0.37	1.78	0.77	0.36	0.55	0.16	11,500

In this method of rest, an initial load is applied to give a strain of 0.1 per cent in a period of several days and then the load is decreased to produce a creep rate of 1 per cent in 100,000 hours[15]. This method of test gives a much lower value for the segregated alloy than for the alloy with a uniform structure. The effect is great enough so that any advantage from alloying itself is lost.

References

1. Agnew, J. T., Hawkins, G. A., and Solberg, II. L., "Stress Rupture Characteristics of Various Steels in Steam at 1200° F," *Trans. Am. Soc. Mech. Engrs.*, **68**, 309 (1946).
2. Am. Soc. Mech. Engrs., Boiler Construction Code (1946); Code for Fired Pressure Vessels (1946); Code for Unfired Pressure Vessels (1946).
   (a) "Short-time Tensile Tests at 850° F of the 0.35 C Steel Material K20," *Trans. Am. Soc. Mech. Engrs.*, **58**, 97 (1936).
3. Am. Soc. Testing Materials, Compilation of Creep Data (1938).
   (a) "Correlation Short Time and Long Time Elevated Temperature Test Methods," *A.S.T.M.*, **44**, 186 (1944).
4. Austin, C. R. and Nickol, H. D., "Comparison of Tensile Deformation Characteristics of Alloys at Elevated Temperatures," *J. Iron and Steel Inst.*, No. 1, 177P (1938).
5. Austin, C. R., St. John, C. R., and Lindsay, R. W., "Creep Properties of Some Binary Solid Solutions of Ferrites," *Trans. Am. Inst. Min. Met. Engrs.*, **162**, 84 (1945).

6. Babcock and Wilcox Tube Co., Bulletin 6E (1948).

7. Bailey, R. W. and Roberts, A. M., "Testing of Materials for Service in High-temperature Steam Plant," *Engineering*, 133, 261 (1932).

8. Bailey, R. W., "Utilization of Creep Test Data," *Proc. Inst. Mech. Engrs.*, 131, 131 (1935).

9. Bailey, R. W. and Roberts, A. M., "Testing of Materials for Service in High-temperature Steam Plant," *Proc. Inst. Mech. Engrs.*, 122, 209 (1932).

10. Bibliography on Creep- and Heat-resisting Steels, 1937–1947, *J. Iron and Steel Inst.*, 156, 338 (1947).

11. Clark, C. L., "Requirements for High Temperature Service," *Metal Progress*, 50, 897 (1946).

12. Clark, C. L., "Alloy Steels Intermediate in Chromium," *Metal Progress*, 50, 1199 (1946).

13. Clark, C. L. and White, A. E., "Influence of Carbon Content on the High-temperature Properties of Steels," *Trans. Am. Soc. Metals*, 23, 995 (1935).

14. Clark, C. L. and White, A. E., "Creep Characteristics of Metals," *Trans. Am. Soc. Metals*, 24, 831 (1936).

15. Coffin, E. P. and Swisher, T. H., "Flow of Steels at Elevated Temperatures," *Trans. Am. Soc. Mech. Engrs.*, 54, 59 (1932).

16. Comstock, G. F., "Effect of Variations in Composition and Heat Treatment on Some Properties of 4 to 6 Per Cent Chromium Steel Containing Molybdenum and Titanium," *Trans. Am. Soc. Metals*, 36, 81 (1946).

17. Emerson, R. W. and Morrow, M., "Further Observations of Graphitization in Aluminum-killed Carbon-Molybdenum Steel Steam Piping," *Trans. Am. Soc. Mech. Engrs.*, 68, 597 (1946).

18. Fetz, E., "Dynamic Hardness Testing of Metals and Alloys at Elevated Temperatures," *Trans. Am. Soc. for Metals*, 30, 1419 (1942).

19. Glen, J., "Abnormal Creep in Carbon Steels," *J. Iron and Steel Inst.*, 155, 501 (Apr., 1947).

20. Glen, J., "Creep Properties of Molybdenum, Chronium-Molybdenum, and Molybdenum-Vanadium Steels," *J. Iron and Steel Inst.*, 158, 37 (1948).

21. Grün, von P., "Creep Strength of Steels as Dependent on Alloy and Heat Treatment," *Arch. Eisenhüttenwesen*, 8, 205 (1934).

22. Heron, S. D., Harder, O. E., and Nestor, M. R., "Valves and Valve Seat Material Data Sheet," *Metal Progress*, Data Sheet 103 (1946); 37–38, 541 (1940).

23. Jenkins, C. H. M., Mellor, G. A., and Jenkinson, E. A., "Investigation of the Behavior of Metals under Deformation at High Temperatures. Part II. Structural Changes in Carbon Steels caused by Creep and Graphitization," *J. Iron and Steel Inst.*, 145, 51 (1942).

24. Jenkins, C. H. M., Tapsell, H. J., Mellor, G. A., and Johnson, "Some Aspects of Carbon and Molybdenum Steels at High Temperature," World Power Conference, England (1936).

25. Juretzk and Sauerwald, "Creep Resistance of Structural Steel and a Simplified Testing Method," *Die Wärme*, 57, 267 (1934).

26. Miller, R. F., "Effect of Deoxidation Practice on Creep Strength of C-Mo Steel at 850 and 1000° F," *Trans. Am. Soc. Mech. Engrs.*, 65, 309 (1943).

27. Miller, R. F., Benz, W. G., and Unverzagt, W. E., "Creep Strength of 17 Low-alloy Steels at 1000° F," *Proc. A.S.T.M.*, 40, 771 (1940).

28. Miller, R. F., Benz, W. G., and Day, M. J., "Creep Strength, Stability of Microstructure and Oxidation of Cr-Mo and 18Cr-8Ni Steels," *Trans. Am. Soc. Metals*, 32, 381 (1944).

29. Miller, R. F., Campbell, R. F., Aborn, R. H., and Wright, E. C., "Influence of Heat Treatment on Creep of Carbon-Molybdenum and Chromium-Molybdenum-Silicon Steel," *Trans. Am. Soc. Metals*, **26**, 81 (1938).
30. Miller, R. F., Golaszewski, E. V., and Smith, G. V., "Spheroidization of Molybdenum Steel in High-temperature Service," *Metal Progress*, **53**, 83 (1948).
31. Norton, F. H., "Creep of Steel at High Temperatures," McGraw-Hill Book Co., Inc., New York, 1929.
32. Oertel, W. and Schepers, A., "Properties of Killed and Open Steels," *Stahl und Eisen*, **51**, 710 (1931).
33. Smith, G. V., Miller, R. F., and Tarr, C. O., "Structural Changes in Carbon and Molybdenum Steels during Prolonged Heating at 900 to 1100° F, as Affected by Deoxidation Practice," *Proc. A.S.T.M.*, **45**, 486 (1945).
34. Solberg, H. L., Potter, A. A., Hawkins, G. A., and Agnew, J. T., "Corrosion of Stressed Alloy Steel Bars by High-temperature Steam," *Trans. Am. Soc. Mech. Engrs.*, **65**, 47 (1943).
35. Weaver, S. H., "Effect of Carbide Spheroidization upon the Creep Strength of Carbon-Molybdenum Steel," *Proc. A.S.T.M.*, **41**, 608 (1941).
36. White, A. E., Clark, C. L., and Wilson, R. L., "Influence of Time on Creep of Steels," *Proc. A.S.T.M.*, **35**, II, 167 (1935).
37. White, A. E., Clark, C. L., and Wilson, R. L., "Influence of Time at 1000° F on Characteristics of Carbon Steel," *Proc. A.S.T.M.*, **36**, II, 139 (1936).
38. White, A. E., Clark, C. L., and Wilson, R. L., "Fracture of Carbon Steels at Elevated Temperatures," *Trans. Am. Soc. Metals*, **25**, 863 (1937).
39. White, A. E., Clark, C. L., and Wilson, R. L., "Rupture Strength of Steels at Elevated Temperatures," *Trans. Am. Soc. Metals*, **26**, 52 (1938).
40. Wilder, A. B. and Tyson, J. D., "Graphitization of Steel at Elevated Temperatures," *Trans. Am. Soc. Metals*, **40**, 233 (1948).
41. Wilson, R. L., "High-temperature Strength of Steels," *Metal Progress*, **33–34**, 499 (1938).
42. Wyman, L. L., "Creep of Steels as Influenced by Macrostructure," *Mech. Eng.*, **57**, 625 (1935).

Chapter 4

Chrome Irons, Moderately Alloyed Austenitic Steels

A. HIGH-CR IRONS

Alloys of Fe and Cr containing 13 to 27 per cent Cr find many uses due to their corrosion resistance at room temperature and scaling resistance at moderately elevated temperatures. Although Type 446 containing 23 to 27 per cent Cr resists oxidation up to 1176° C (2150° F), the Cr-Fe alloys in general do not maintain high strength above 676° C (1250° F). In spite of the fact that the Cr-Fe alloys at room temperature are somewhat notch-sensitive, they have a fairly high fatigue resistance.

I. Types 405, 410

The low-Cr alloys, Types 405 and 410, containing 11.5 to 13.5 per cent Cr, are very widely used in elevated-temperature service because of their good forming properties and reasonable cost compared to many of the more highly alloyed materials. Type 410 with 0.15 per cent C is martensitic and is hardened by oil-quenching. It is not subject to embrittlement from age-hardening when heated in the range of 371 to 538° C (700 to 1000° F) for long periods. Type 405 is similar to Type 410 except that it contains 0.1 –0.3 per cent Al, which prevents the formation of martensite and keeps the alloy ferritic. This alloy does not age-harden in the range of 38 to 538° C (100 to 1000° F) in laboratory tests of 1500 hrs duration[22]. Both Types 405 and 410 are too low in Cr to be susceptible to the appearance of the sigma phase from prolonged heating at 538 to 704° C (1000 to 1300° F).

Type 405 finds use as stationary blades for steam turbines operating at temperatures up to 523° C (975° F). These alloys are also used in this moderate-temperature range as blades for compressors which operate gas turbines. Type 405 is used in heat exchanger tubing in oil refineries and as corrosion-resistant liners in pressure vessels. It is suitable for welded construction because of its reduced hardenability on welding[22,27].

The elevated-temperature properties of the Cr-Fe alloys which follow represent annealed material and the values are therefore at a minimum. These are given in Tables 4-1 and 4-2.

II. Hardenable Cr-Fe Alloys

The Cr-Fe alloys containing 12 to 14 per cent Cr and medium or high C have excellent wear-resistant properties, good hot hardness and are corro-

145

sion-resistant at fairly high temperatures. These properties make them suitable for use in valves and valve trim under many highly corrosive conditions at elevated temperatures. Types 420 and 440 with varying amounts of C are used in the hardened condition in these applications. The composition of these alloys is as follows[1]:

Material	C	Cr	Mo
Type 420	More than 0.15	12–14	—
Type 440A	0.60–0.75	16–18	0.75 max

There are many other compositions for exhaust and intake valve steels, but these are alloyed with other elements and are therefore no longer ferritic. They will be listed under austenitic alloys in a later section of this chapter.

TABLE 4-1. CREEP STRENGTH STEEL TYPE 405[27]

Chemical Composition

C	Mn	Si	P	S	Cr	Other Elements
0.08 max	1.00	1.00	0.04 max	0.04 max	11.5–13.5	Al—0.10–0.3

Creep Strength

Type Steel Annealed	Temp. (°C)	Temp. (°F)	Stress (psi) for Designated Rate of Creep % per 1000 Hrs 0.01	0.10
405	426	800	30,000	—
405 + 0.5 Mo	426	800	18,000	—
405	482	900	17,500	43,000
405 + 0.5 Mo	482	900	11,750	18,000
405	538	1000	4500	8300
405 + 0.5 Mo	538	1000	5500	9000

III. 27 Cr Steel (Type 446)

The elevated-temperature properties of this steel are given in Table 4-3. Although it maintains excellent resistance to scaling up to 1176° C (2150° F), its creep strength is low compared to that of the austenitic alloys.

B. AUSTENITIC ALLOYS

I. Types 302, 303, 304

The austenitic steels show increased stability over the ferritic steels under load at elevated temperature due primarily to their oxidation resistance in many types of corrosive atmospheres. The fact that they consist of a single phase, austenite, through a wide temperature range and do not undergo a phase change, as in the case of the lower alloy steels, adds greatly to their higher creep strength.

a. Effect of Working. There are several means by which the hardness of

the austenitic alloys may be increased to insure that they will be less liable to creep when placed in high-temperature service. Cold-working is effective in producing uniform hardness in strip and bar stock, but for larger or

TABLE 4-2. ELEVATED TEMPERATURE PROPERTIES STEEL TYPE 410 (ANNEALED)[27]

Chemical Composition

C	Mn	Si	P	S	Cr
0.15 max	1.00	1.00	0.04 max	0.04 max	11.5–13.5

Short-time Tensile Properties

Temp. (°C)	(°F)	Tensile Strength (psi)	Yield Strength 0.1% offset	Elong % in 2″	Reduction in Area (%)
Room	Room	78,000	52,000	30.5	78.5
426	800	55,900	39,500	26.0	69.1
482	900	47,300	32,200	35.5	74.2
538	1000	40,500	29,000	43.5	75.8

Stress Rupture

Temp (°C)	(°F)		Stress (psi) for Fracture in Hrs			
		10	100	1000	10,000	100,0000
650	1200	10,100	7800	4800	2900	1750

Creep Strength

Temp (°C)	(°F)	Stress (psi) for Designated Rate of Creep % per 1000 Hrs	
		0.01	0.10
538	1000	—	13,000
593	1100	—	5000
650	1200	595	1400

Thermal Expansion

Temp (°F)	MeanCoefficient of Linear Expansion (In/In/°F × 10⁻⁶)
70–400	6.09
70–600	6.21
70–800	6.41
70–900	6.50
70–1000	6.59
70–1100	6.66
70–1200	6.71
70–1300	6.80
70–1400	6.88

Thermal Conductivity

Temp (°F)	Thermal Conductivity (BTU/Hr/Sq Ft/In/°F)
200	173
1000	199

irregularly shaped pieces, it is more difficult to procure uniformity in hardness by this method. Subjecting cold-worked parts to high temperature will cause softening and possible deformation if the temperature of use is above that required for recrystallization.

Hot working of austenitic alloys will also increase hardness if the temperature of hot-working is below the recrystallization temperature. Again the problem of uniformity of hardness becomes important especially in the case of large rotor disks where variations in hardness across the surface should be avoided[13,14].

b. Intergranular Corrosion. Stainless steels of the 18Cr-8Ni type and even those with higher alloy content as 18Cr-12Ni, 25Cr-12Ni, and 25Cr-20Ni, are subject to intergranular attack on exposure to elevated tempera-

TABLE 4-3. ELEVATED-TEMPERATURE PROPERTIES OF 27 CR STEEL TYPE 446[1]

Chemical Composition: C 0.35 max   Cr 23.0–27.0

Short Time Tensile Strength

Temp (°C)	Temp (°F)	Tensile Strength (psi)
Room	Room	83,000
426	800	68,500
482	900	66,000
538	1000	61,000
593	1100	43,500
650	1200	24,000
704	1300	17,000
760	1400	12,000

Rupture Strength

Temp (°C)	Temp (°F)	Stress (psi) for Rupture in 1000 Hrs
593	1100	6000
650	1200	4000
704	1300	2800
760	1400	1700

Creep Strength

Temp (°C)	Temp (°F)	Stress (psi) for 1% Creep in 10,000 hrs
538	1000	6000
593	1100	3000
650	1200	1500
704	1300	600

tures. The mechanism for this reaction is that C, which at ordinary temperatures is retained in supersaturated solution, becomes unstable at certain higher temperatures and is rejected from solid solution in the form of Cr-rich carbide. Adjacent areas are thus impoverished in Cr and the metal corrodes. The evidence of carbide precipitation is very often revealed by microscopic examination, especially the type of intergranular corrosion which appears at the grain boundaries.

Exposure of stainless steels of the 18Cr-8Ni type to elevated temperature

for long periods of time during creep tests often induces microstructural changes of carbide precipitation and movement of carbide particles to the grain boundaries. Stainless steel 18Cr-8Ni Type 304 is subject to carbide precipitation when exposed to temperatures above 400° C (750° F). As an example, the 18Cr-8Ni steel (E1) in Table 4-5 stressed at 13,000 psi at 593° C (1100° F) for 3000 hours shows a moderate change in microstructure due to this deterioration[19].

c. Elevated-temperature Properties. The elevated-temperature properties of steel Type 304 as shown in Table 4-4 indicate that this steel is stable at moderate temperatures, but that its strength deteriorates in the neighborhood of 538° C (1000° F).

TABLE 4-4. ELEVATED-TEMPERATURE PROPERTIES 18CR-8NI STEEL TYPE 304

Chemical Composition

C	Cr	Ni	Mn
0.08 max	18.0–20.0	8.00–11.00	2.00 max

Room-temperature Properties

Tensile Strength (psi)	Elong % in 2″
90,800	67

Short-time Tensile Strength[5]

Temp (°C)	(°F)	Tensile Strength (psi)	Elong % in 2 in.	Reduction in Area (%)
426	800	67,050	45	69
482	900	64,500	40	69
538	1000	61,500	45	69
593	1100	53,750	41	65
650	1200	44,400	47	64
704	1300	35,600	51	58

Rupture Strength[1]

Temp (°C)	(°F)	Stress psi for Rupture in 1000 hrs (psi)
593	1100	28,000
650	1200	15,000
704	1300	9000
760	1400	6000
815	1500	3700

Creep Strength

Temp (°C)	(°F)	Stress for 1% Creep in 10,000 hrs (psi)
538	1000	17,500
593	1100	12,000
650	1200	7000
704	1300	4000
760	1400	2500

TABLE 4-4.—*Continued*

Hot Fatigue Strength[1]

Condition: water-quenched from (2000° F)

Temp (°C)	Temp (°F)	Fatigue Strength (psi)
Room	Room	40,000
426	800	32,000
538	1000	32,000
650	1200	30,000

Note: At elevated temperatures, the S-N curve continues to slope downward at all reversals of stress investigated.

Hot Impact Properties[5]

Temp (°C)	Temp (°F)	Charpy Impact (ft-lbs)
29	85	71
260	500	93
315	600	96
371	700	99
426	800	93
482	900	86
538	1000	89
593	1100	91
650	1200	85
704	1300	78

Material: annealed
Specimens: drilled keyhole notch

Thermal Expansion[5] (0.007 C Max)

Temp (°F)	Mean Coefficient of Linear Expansion (In/In/°F $\times$ 10⁻⁶)
68–600	9.88
68–800	10.08
68–1000	10.20
68–1200	10.41
68–1292	10.50

Thermal Conductivity[5] (C 0.07, Mn 0.27, Cr 18.6, Ni 9.10)

Temp (°C)	Thermal Conductivity (watts/cm/°C)
100	0.164
200	0.177
300	0.190
400	0.203
500	0.216

d. Heat Treatment. For many services, the 18Cr-8Ni steels have the best resistance to intergranular corrosion when heated to 657 to 760° C (1250 to 1400° F). The temperature varies in this range depending on the degree of cold work which the material has received. However, for stainless steels

TABLE 4-5. CREEP TESTS ON AUSTENITIC STAINLESS STEELS[19]

Steel	Nominal Composition	Heat Treatment (°C)	Creep Test Temp (°C)	(°F)	Creep Stress (psi)	Duration Creep Test (hrs)	Av. Creep Rate During Last 1000 Hrs (millionth in/in/hr)	Modified ½ Size Charpy Impact Strength Before Creep Test (ft-lbs)	After Creep Test (ft-lbs)	Brinell Before Creep	After Creep	Amount of Change of Microstructure During Creep	Stress for Creep Rate Millionth in/in/hr (0.1% per 1000 hrs)
E-1	18-8	1037 WQ	593	1100	13,000	3000	0.79	56.5	42	153	155	Moderate	13,500
E-2	18-8 Ti	1037 AC	593	1100	13,000	3000	0.62	53	41	143	144	Slight	13,600
E-2	18-8 Ti	1037 AC 871 AC	593	1100	13,000	3000	1.66	50	43.5	141	147	None	12,600
E-3	18-8 Cb	1037 AC	593	1100	19,000	3000	0.29	42.5	34	165	172	Slight	22,200
E-3	18-8 Cb	1039 AC 871 AC	593	1100	19,000	3000	1.57	42.5	33	158	176	Slight	18,000

Chemical Composition:

	C	Mn	P	S	Si	Ni	Cr	Other
E-1	0.05	0.28	—	—	0.43	9.85	18.40	—
E-2	0.05	0.52	0.017	0.010	0.39	10.90	17.50	Ti 0.44
E-3	0.05	1.51	—	—	0.32	11.12	18.10	Cb 0.82

WQ: Water quenched.
AC: Air cooled.

The addition of Cb to the 18-8 series is a definite improvement and even though the stabilization heat treatment of heating to 871° C (1600° F) for 2 hrs and air cooling reduces the creep strength from 22,000 to 18,000 psi, it is still higher than the straight 18-8 (E1) and 18-8 Ti (E 2) steels.

exposed to temperatures in the neighborhood of 593° C, a heat treatment of water-quenching from 1037 to 1093° C gives the optimum creep resistance[19]. This is shown for the El steel in Table 4-5 which has a strength of 13,500 psi for a creep rate of 0.1 per cent per 1000 hrs at 593° C (1100° F). These results are based on tests of 3000 hours' duration.

TABLE 4-6. 18CR-8NI STABILIZED WITH TI TYPE 321[1]

Chemical Composition

C	Mn	Si	P	S	Cr	Ni	Ti
0.08 max	2.0 max	1.0 max	0.04 max	0.03 max	17–19	8–11	5×C min

Short-time Tensile Strength

Temp (°C)	(°F)	Tensile Strength (psi)
Room	Room	83,500
426	800	59,000
482	900	58,000
538	1000	54,000
593	1100	50,000
650	1200	44,500
704	1300	36,500
760	1400	28,500

Rupture Strength

Temp (°C)	(°F)	Stress for Rupture in 1000 hrs (psi)
593	1100	27,000
650	1200	17,500
704	1300	10,000
760	1400	5500
815	1500	3700

Creep Strength

Temp (°C)	(°F)	Stress for 1% Creep in 10,000 hrs (psi)
538	1000	18,000
593	1100	13,000
650	1200	8000
704	1300	4500
760	1400	2000
815	1500	850

II. Stabilization of the 18Cr-8Ni by Small Percentages of Other Elements (Types 321, 347, 316)

The austenitic alloys of the 18Cr-8Ni class, namely Types 316, 321, and 347, are stabilized against many types of intergranular corrosion by the addition of small amounts of such elements as Mo, Ti, and Cb. These metals unite with the C to prevent the withdrawal of Cr-rich carbides from

solid solution, which precludes the formation of localized areas deficient in Cr. In all these alloys, Mn is present in small proportions to keep the alloy austenitic and prevent the formation of a second phase, thereby inhibiting corrosion.

TABLE 4-7.   18CR-8NI STABILIZED WITH CB TYPE 347[1]

Chemical Composition

C	Mn	Si	P	S	Cr	Ni	Cb
0.08 max	2.0 max	1.0 max	0.04 max	0.03 max	17–19	9–12	10×C min

Short-time Tensile Strength

Temp (°C)	(°F)	Tensile Strength (psi)
Room	Room	90,000
426	800	66,000
482	900	64,500
538	1000	61,500
593	1100	57,000
650	1200	50,000
704	1300	40,500
760	1400	31,500

Rupture Strength

Temp (°C)	(°F)	Stress for Rupture in 1000 hrs (psi)
593	1100	30,000
650	1200	17,000
704	1300	11,200
760	1400	7500
815	1500	4400

Creep Strength

Temp (°C)	(°F)	Stress for 1% Creep in 10,000 hrs (psi)
538	1000	19,000
593	1100	15,000
650	1200	9500
704	1300	5000
760	1400	2500
815	1500	1100

These alloys have excellent weldability, good forming properties and fair machinability. Their elevated-temperature properties are shown in Tables 4-6, 4-7, and 4-8 In general, their rupture strength and creep strength are higher than the stainless steel Type 304. In order of increasing strength at elevated temperature they fall as follows: Type 321, 347 and 316.

However, there are other tests which do not show this order for the 18Cr-

8Ni steels stabilized with Ti and Cb. In Table 4-5, elevated-temperature properties are shown for 3 steels, one with no additional elements and one each with Ti and Cb added[19]. Steel E3 with 0.82 per cent Cb has the highest creep strength of the three steels tested.

TABLE 4-8. 18CR-8NI STABILIZED WITH MO TYPE 316[1]

Chemical Composition

C	Mn	Si	P	S	Cr	Ni	Mo
0.10 max	2.0 max	1.0 max	0.04 max	0.03 max	16–18	10–14	2–3

Short-time Tensile Strength

Temp (°C)	(°F)	Tensile Strength (psi)
Room	Room	82,500
426	800	71,500
482	900	70,000
538	1000	67,500
593	1100	63,000
650	1200	56,500
704	1300	46,500
760	1400	35,000

Rupture Strength

Temp (°C)	(°F)	Stress for Rupture in 1000 hrs (psi)
593	1100	33,000
650	1200	25,000
704	1300	17,000
760	1400	11,000
815	1500	7000

Creep Strength

Temp (°C)	(°F)	Stress for 1% Creep in 10,000 hrs (psi)
538	1000	24,000
593	1100	18,000
650	1200	11,000
704	1300	7000
760	1400	4500
815	1500	2000

a. Magnetic and Impact Tests on Modified 18Cr-8Ni Steels. The change in properties of a modified 18Cr-8Ni steel is shown by magnetic and impact tests on specimens after prolonged heating[26]. The steel which exhibited deterioration has the following analysis:

C	Mn	Si	Ni	Cr	W	V	Ti
0.11	0.41	0.85	8.53	17.65	0.72	0.20	0.30

Due to the fact that creep tests at 600° C (1112° F) show a marked decrease in creep resistance after a few hundred hours, the magnetic and

impact properties are reported below for heating at 650° C (1202° F) in the unstressed state.

Magnetic Saturation

Material	Magnetic Saturation (gauss)
As received	203
1000 hrs at 650° C	325
2500 " " " "	1090
20% reduction, + 1000 hrs at 650° C	1880
" " + 2500 " " " "	2580

Impact Tests

Material	kgm/sq cm (results of 3 tests)
As received	29.9, 30.7, 32.4
1000 hrs at 650° C	23.2, 24.5, 24.9
2500 " " " "	13.5, 18.0, 16.5

The magnetic tests indicate that heating 1000 hrs and 2500 hrs at 650° C causes a decomposition of austenite to ferrite. The impact tests indicate a decrease in impact strength with increase in time of testing. These values are included here to show the possible value of magnetic tests in correlating decrease in creep strength with increase in time.

C. Moderately Alloyed Austenitic Steels

There are a number of modifications of the austenitic stainless steels which have higher creep strength and yet retain their good forming properties. Small additions of Mo, W, Ti, and Cb form such alloys as 19-9DL and 19-9W-Mo. Other similar alloys where the Ni is increased to 20 to 25 per cent are Gamma Columbium, 19-W, and 16-25-6.

These alloys recrystallize at temperatures above 926° C (1700° F) after working. They show their optimum creep and stress rupture properties when they are "hot-cold" worked in the range of 650 to 760° C (1200 to 1400° F). Forming in this intermediate temperature range renders them suitable for service at temperatures from 510 to 650° C. It is important that forming temperatures should be above those encountered in service so that no softening of the metal occurs later with lowering of the creep strength. These alloys find wide use as forgings for turbine disks and for blading in applications where temperatures do not exceed the limit specified for their use.

I. 19-9W-Mo Alloy*

The 19-9W-Mo alloy contains approximately 9 per cent Cr, 9 per cent Ni, 0.35 per cent Mo, 1.25 per cent W, 0.5 per cent Cb, and 0.35 per cent Ti.

* Universal Cyclops Steel Corp.

It consists of austenite with about 30 per cent of ferrite phase which is changed to sigma phase on heating in the range of 650 to 870° C (1200 to 1600° F) over extended periods[10]. This alloy is useful in gas turbine and supercharger wheels, ducts and gas turbine blades.

The room-temperature and stress-rupture properties at 650° C (1200° F) of the 19-9W-Mo alloy are shown in Table 4-9 after hot-rolling followed by 20 to 25 per cent "hot-cold" work at 650° C (1200° F). Its rupture strength after 1000 hrs at 650° C (1200° F) is 40,000 psi, with 22 per cent elongation. This value is extrapolated from a test period of 661 hrs. Samples representative of 2 other heats of a 19-9W-Mo alloy solution treated and then given 20 to 25 per cent "hot-cold" work at 650° C (1200° F) do not have a

TABLE 4-9. ELEVATED-TEMPERATURE PROPERTIES OF 19-9W-Mo ALLOY

Chemical Composition

C	Mn	Si	Cr	Ni	Mo	W	Cb	Ti
0.11	0.60	0.42	18.87	8.63	0.40	1.36	0.28	0.45

Manufacturing Procedure

This alloy is representative of a heat melted in a 20,000-lb basic arc furnace and cast into 12 ¼ in ingots. It was then hammer-cogged at 1137 to 926°C (2080 to 1700° F) to 4 by 4 in and rolled at 1150 to 1037°C (2100 to 1900° F) to ¾ by ¾ in. Finally, it was stress-relieved at 650°C (1200°F)[9].

19-9W-Mo Alloy 20 to 25% "Hot-Cold" Work at 650°C (1200°F) After Hot-Rolling[15]

Room-temperature Properties

Brinell Hardness	Tensile Strength (psi)	0.02% Offset Yield	Elong. % in 2"
275	122,900	79,000	26.7

Rupture Properties at 650°C (1200°F)

Rupture Strength		Longest Rupture Test	
100 Hrs	1000 Hrs	Time, Hrs	Elong % in 2"
53,000	40,000	661	22.0

higher rupture strength at 650° C (1200° F) and show a ductility of only 6 to 10 per cent[15].

Other short-time tensile and stress-rupture tests for a 19-9W-Mo alloy are shown in Table 4-10, which compares the properties of stress-relieved hot-rolled bar stock with (1) a weldment between hot-rolled bars and (2) a cast sample, quenched and stress relieved. The weldment and the cast sample have a gradual decrease in ductility up to the approximately 200 hr test period[10].

II. 19-9DL Alloy

The 19-9DL alloy is somewhat similar to the 19-9W-Mo in that it contains approximately 19 per cent Cr and 9 per cent Ni. However, the Mo

content is 1.25 per cent, the W 1.19, the Cb 0.30, and the Ti 0.20 approximately. In general the elevated-temperature properties of this alloy are superior to those of 19-9W-Mo. The 19-9DL alloy contains about 5 per cent ferrite[10].

TABLE 4-10. ELEVATED-TEMPERATURE PROPERTIES 19-9W-Mo ALLOY[10]

Chemical Composition

C	Mn	Si	Cr	Ni	Mo	W	Cb	Ti
0.10	0.60	0.50	19.00	9.00	0.40	1.25	0.40	0.35

Short-time Tensile and Stress-rupture Tests of 19-9W-Mo

Form	Temp (°C)	Temp (°F)	Stress (psi)	Time to Rupture (hrs)	Elong % in 2″	Reduction in Area (%)
Hot-rolled bar stock stress-relieved at 650°C	650	1200	60,000	S.T.T.S.*	27.0	62.3
			55,000	0.10	30.0	69.3
			52,000	5.40	24.0	65.6
			45,000	17.0	30.0	59.1
			36,418	285.00	31.5	53.0
			30,000	2109.00	32.0	56.8
	760	1400	44,700	S.T.T.S.*	41.5	75.1
			35,000	0.95	33.0	72.7
			28,000	15.25	35.0	70.6
			20,000	97.00	48.0	72.5
			17,000	330.50	34.5	69.3
			14,000	683.00	29.0	57.3
			12,500	936.00	24.0	47.8
			11,000	1533.00	32.0	53.0
Weldment between hot-rolled bars, stressed-relieved at 760° C (fractures in weld or at interface)	650	1200	40,900	S.T.T.S.	21.5	29.2
			30,000	3.50	15.0	22.3
			25,000	68.50	5.5	11.9
			23,000	271.50	8.5	10.4
Casting. Samples water-quenched from 1120° C. Stress-relieved at 760° C	650	1200	45,900	S.T.T.S.*	24.0	54.1
			35,000	13.00	15.0	32.1
			30,000	58.0	10.0	19.9
			26,000	174.00	4.0	8.9

S.T.T.S. Short Time Tensile Strength

Creep Strength[1]

Material	Temp (°C)	Temp (°F)	Stress, psi, for Min Creep Rate of 0.00001 % 1 hr
Rolled stock, stress-relieved 650° C	650	1200	6600

Hot Fatigue Strength[1]

Material	Temp (°C)	Temp (°F)	Endurance Strengh (psi) 10⁸ cycles	Endurance Strengh (psi) 2.5 × 10⁸ cycles
Heated 1093° C, water-quenched. Aged 4 hrs at 650° C	650	1200	37,000	35,000

<div align="center">TABLE 4-11. ELEVATED-TEMPERATURE PROPERTIES 19-9DL ALLOY</div>

Chemical Composition

C	Mn	Si	Cr	Ni	Mo	W	Cb	Ti
0.26	0.52	0.57	18.95	9.05	1.22	1.19	0.29	0.21

Manufacturing Procedure

19-9DL is representative of a 33-lb heat, hammer-forged at 1124 to 704° C (2055 to 1300° F) to ⅜th-in sq bar. The heat treatment consists of holding 1 hr at 1150° C (2100° F) and air-cooling. It is then heated to 650° C (1200° F) and reduced 21.3 per cent by rolling and stress relieved at 650° C (1200° F)[15]

Room-temperature Properties

Brinell Hardness	Tensile Strength (psi)	Yield Strength 0.02% offset	Yield Strength 0.2% offset	Elong % in 2"	Reduction in Area (%)
289	138,750	95,000	113,750	28.7	48.3

Stress Rupture and Elongation Values

Temp (C°)	(°F)	Rupture Strength (psi) 10 hrs	100 hrs	500 hrs	1000 hrs	Elong after Fracture % in 1 in 10 hrs	100 hrs	500 hrs	1000 hrs
650	1200	70,000	62,000	54,000	50,000	7	3	2	3
732	1350	—	35,000	24,000	20,500*	—	4	5	—

* Estimated

Chemical Composition

C	Mn	Si	Cr	Ni	Mo	W	Cb	Ti
0.3	0.6	0.7	19.0	9.0	1.3	1.2	0.4	0.2

Manufacturing Procedure

19-9DL alloy is representative of heating at 1232° C (2250° F) for ½ hr and oil-quenching followed by heating at 815° C (1500° F) for 50 hrs.[15]

Stress Rupture and Elongation Values

Temp (°C)	(°F)	10 hrs	Stress to Rupture and Elongation %	100 hrs	%	1000 hrs	%
815	1500	17,500	5.0	13,300	4.0	10,000	3.0

Creep Strength

Temp (°C)	(°F)	Stress for Minimum Creep Rate % per Hr 0.001	0.0001	0.00001
815	1500	10,400	7100	4800

Creep Strength[1]

Material	Temp (°C)	(°F)	Stress for Min Creep Rate (psi) 0.0001%/hr	0.00001%/hr
Annealed 1232° C oil-quenched, aged 50 hrs at test temperature	732	1350	13,000	——
	815	1500	6500	<5000

Hot Fatigue[1]

Material	Temp (°C)	(°F)	Endurance Strength (psi) 10⁸ cycles
1150° C 1 hr, air-cooled, cold-worked 15% at 650° C, aged 4 hrs at 650° C	650	1200	43,000

TABLE 4-11.—*Continued*

Hot Impact Strength[9]

Temp (°C)	(°F)	Charpy Impact Resistance (ft-lbs)
Room	Room	27
815	1500	39

Specimens: Keyhole notch

Thermal Expansion

(Temp °F)	Mean Coefficient of Linear Expansion (In/In/°F × 10^{-6})
70–600	9.31
70–800	9.59
70–1000	9.78
70–1200	9.97
70–1500	10.01

It finds wide use as gas turbine wheels and in ducts, collector rings and exhaust cones. It is especially useful in bolting materials as will be shown in the data which follow. At 650° C (1200° F) its rupture strength is about 20 per cent greater than that of 19-9W-Mo. Its use as a bolting material is satisfactory up to 650° C (1200° F), but falls off at 732° C (1350° F). At this temperature its relaxation stress for 10,000 hours has a factor of 5 to 1 greater than that of 19-9W-Mo[9,10,15].

The elevated-temperature properties of the 19-9DL alloy are given in Table 4-11. The results of relaxation tests are shown in Tables 4-12 and 4-13. Design curves for the 19-9DL alloy at 732° C (1350° F) for two different heat treatments are shown in Figs. 4-1 and 4-2.

III. 17W Alloy*

This alloy, containing approximately 13 per cent Cr and 19 per cent Ni with small additions of Mo, W, and Ta, is representative of an earlier analysis used in turbine wheels. It has been replaced by other alloys which have improved properties at elevated temperatures.

Chemical Composition

C	Mn	Si	Cr	Ni	Mo	W	Ta
0.49	0.61	0.61	13.12	19.11	0.58	2.36	0.03

20 to 25% "Hot-Cold" Work After Hot-rolling[15]

Room-temperature Properties

Brinell Hardness	Tensile Strength (psi)	Yield 0.02% Offset	Elong % in 2"
335	164,000	111,000	13.5

* Universal Cyclops Steel Corp.

TABLE 4-12. RELAXATION CREEP TESTS 19-9DL ALLOY[9]

Material	Temp. (°C)	(°F)	Stress (psi)	Creep Rate (% per hr)	Values for Computation of Residual Stress						Residual Stress (psi)	
					n	E	S_0	r_0	r_0E	t	1000 hrs	10000 hrs
19-9DL Hot-rolled stress re-lieved 2 hrs 650° C	565	1050	28,430	0.0009	21.93	22,250,000	25,000	0.00005%/hr	8.575	1000 and 10,000	22,470	20,130
			26,190	0.00016								
			24,400	0.000052								
	650	1200	21,680	0.003	16.03	18,070,000	16,500	0.000021%/hr	3.795	1000 and 10,000	15,215	13,055
			20,115	0.00053								
			18,550	0.00011								
			16,980	0.00003								
			15,415	0.000013								
	732	1350	14,990	0.00385	5.425	16,260,000	14,500	0.00053%/hr	86.178	1000 and 10,000	6925	4115
			13,420	0.00088								
			11,850	0.00025								
			10,285	0.00008								
			8715	0.000035								
			7150	0.000012								
	815	1500	8270	0.0055	4.547	14,400,000	5600	0.001%/hr	144	1000 and 10,000	1570	820
			6480	0.0020								
			4685	0.00045								

Rupture Properties at 650° C (1200° F)

Rupture Strength		Longest Rupture Test	
100 Hrs	1000 Hrs	Time (hrs)	Elong. (%)
37000	20500	456	9.0

TABLE 4-13. RELATIONSHIPS AT 650° C (1200° F) BETWEEN 19-9DL AND 19-9W-Mo FOR 10,000-HOUR RELAXATION STRESS, RESTRAINED AND UNRESTRAINED CREEP RATES[10]

	19-9DL	19-9W-Mo	Ratio
10,000-hr Relaxation Stress, (psi) (Rigid-frame Method)	10,000	2000	5:1
Stress, (psi) for Unrestrained Secondary Creep Rate of 1% in 10,000 hrs	22,000	17,000	1.3:1
Stress, (psi) for Unrestrained Secondary Creep Rate of 1% in 100,000 hrs	10,000	6500	1.54:1
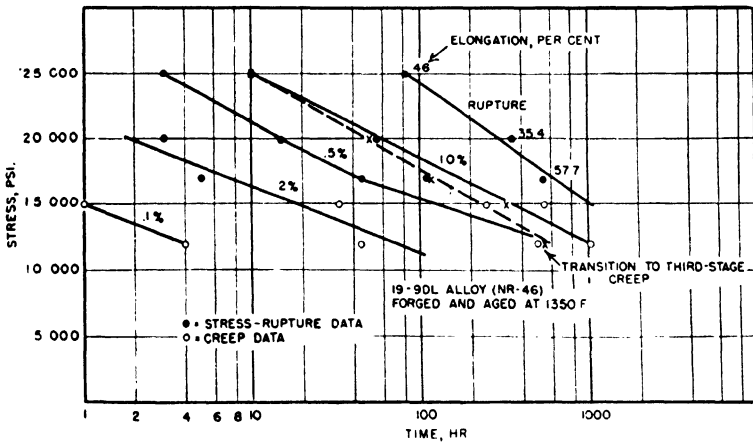
Fig. 4-1. Design Curves for Alloy 19-9DL at 732° C (1350° F). Forged and aged at 732° C (1350° F). (After Cross and Simmons)

IV. CSA Alloy*

This alloy, containing approximately 18 per cent Cr, 5 per cent Ni, and 4 per cent Mn with smaller percentages of Mo, W, and Cb, has also been developed for high-temperature service.

Chemical Composition

C	Mn	Si	Cr	Ni	Mo	W	Cb
0.38	4.17	0.30	18.52	4.55	1.35	1.34	0.57

Manufacturing Procedure

This alloy is representative of a hammer-forged 150-lb induction-furnace heat. It was finished at 650° C (1200° F) and stress-relieved 1 hr at 650° C (1200° F)[15].

* Crucible Steel Co. of America.

Room-temperature Properties

Brinell Hardness	Tensile Strength (psi)	Yield Strength		Elong % in 2"	Reduction in Area (%)
		0.02% Offset	0.2% Offset		
292	153,250	84,650	105,350	17.8	22.2

Rupture Properties

Temp		Rupture Strength (psi)				Estimated Elong after Fracture, % in 1 in			
(°C)	(°F)	10 hrs	100 hrs	500 hrs	1000 hrs	10 hrs	100 hrs	500 hrs	1000 hrs
650	1200	58,000	50,000	43,000	39,000	20	25	18	12
732	1350	—	22,500	16,000	12,500	—	25	25	20
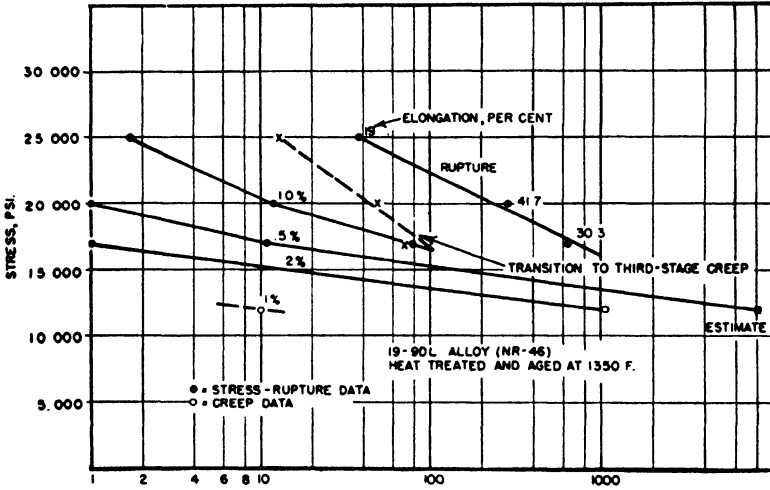
Fig. 4-2. Design Curves for Alloy 19-9DL at 732° C (1350° F). Heat treated and aged at 732° C (1350° F). (After Cross and Simmons)

V. Gamma Cb Alloy*

This alloy, containing approximately 15 per cent Cr, 25 per cent Ni, and 4 per cent Mo with small percentages of Cb and N, has also found use in turbosupercharger wheels.

Chemical Composition

C	Mn	Si	Cr	Ni	Mo	Cb	N
0.40	0.84	0.46	15.08	24.71	4.39	1.90	0.036

20 to 25% "Hot-Cold" Work at 650° C (1200° F) After Hot-rolling[15]

Room-temperature Properties

Brinell Hardness	Tensile Strength (psi)	Yield 0.02% Offset	Elong. % in 2"
333	160,900	118,000	13.2

* Allegheny Ludlum Steel Corp.; Universal Cyclops Steel Corp.

Rupture Properties at 650° C (1200° F)

Rupture Strength		Longest Rupture Test	
100 Hrs	1000 Hrs	Time (hrs)	Elong in 2″ (%)
51,000	37,200	612	2.0

VI. 16-25-6 Alloy*

This alloy contains 16 per cent Cr, 25 per cent Ni, 6 per cent Mo, and 0.08 to 0.10 per cent C. The high Ni content helps suppress the formation of the delta phase and the low C content preserves good forming and welding properties. Due to the wide usage of this material for turbosupercharger wheels and the fact that the published information is considerable, a description of its manufacturing methods and properties is given in detail.

Manufacturing Procedure

For jet engine turbine wheels, ingots are cast 19 or 21 inches in diameter and are forged into $8\frac{1}{2}$-inch square blooms. For supercharger wheels, the ingots may be cast 14 inches in diameter and then reduced to 8-inch blooms after being heated to 1093° C (2000° F). Hammer-forging reduces these to 5-inch square billets for forging into wheels. The blocking die for wheel forgings must be designed to control the cold work required in the finishing die to keep hardness gradients to a minimum across the surface of the wheel. The second or finishing operation is carried out at 650 to 732° C (1200 to 1350° F). Forging strains are eliminated by annealing at 650° C (1200° F) for 6 hours[12].

Microstructure

The 16-25-6 alloy undergoes certain changes under heat treatment, such as solution of the carbides on heating above 1093° C (2000° F) and precipitation of these microconstituents on reheating at lower temperatures. These are described here in some detail since they are typical of the changes which occur in many austenitic alloys. The structure of 16-25-6 alloy, after being hot-rolled, consists of austenite with a phase resembling carbides in banded form. Tempering the hot-rolled material for 12 hours at temperature ranges of 704 to 871° C (1300 to 1600° F) causes the carbides to migrate through the austenite grains and become quite uniformly dispersed. This tempering decreases the ductility of the hot-worked alloy in tests conducted at room temperature[12].

A solution treatment for 16-25-6 alloy involves heating to 1176° C (2150° F) and quenching in water. In the solution-quenched structure of Figs. 4-3 and 4-4, it is evident that the carbides are largely dissolved. Tempering the quenched alloy causes precipitation-hardening, which increases

* Timken Roller Bearing Co.
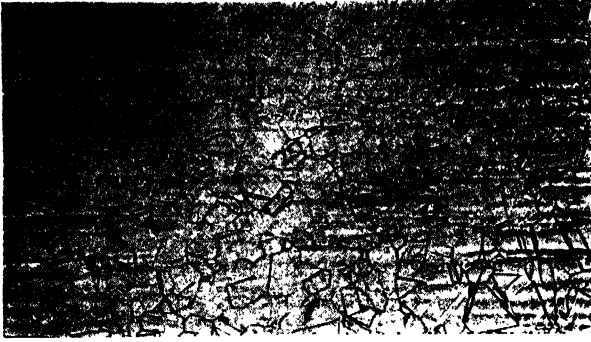
Fig. 4-3. Alloy 16-25-6 hot rolled, heated to 1176° C (2150° F) and water quenched· Magnification 100×. (After Fleischmann)

Fig. 4-4. Same as Figure 4-3. Magnification 1000×. (After Fleischmann)
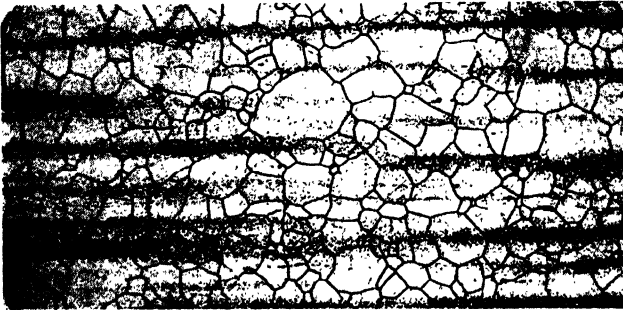
Fig. 4-5. Alloy 16-25-6 solution quenched and tempered for 12 hrs. at 815° C (1500° F). Magnification 100×. (After Fleischmann)

as the temperature is increased from 650 to 870° C (1200 to 1600° F). In Figs. 4-5 and 4-6, the solution-quenched and tempered alloy is shown after
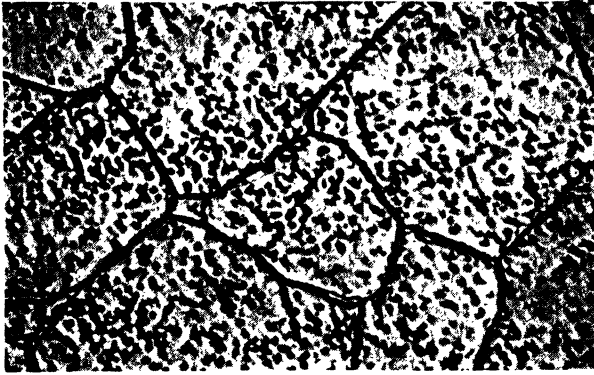
Fig. 4-6. Same as Figure 4-5. Magnification 1000×. (After Fleischmann)
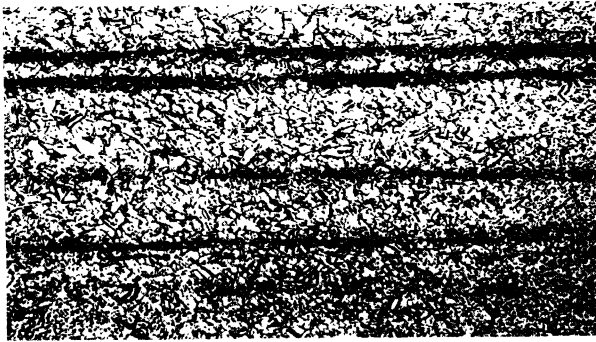
Fig. 4-7. Alloy 16-25-6 hot rolled, cold worked by 20% elongation, and tempered at 815° C (1500° F) for 72 hrs. Magnification 100×. (After Fleischmann)
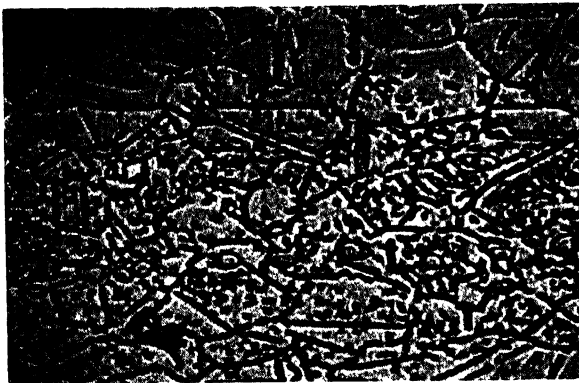
Fig. 4-8. Same as Figure 4-7. Magnification 1000×. (After Fleischmann)

12 hrs at 815° C (1500° F). At this temperature, the precipitate is more coarse-grained than that formed by tempering at 650° C (1200° F). It will be noted from the photomicrographs that tempering does not change the size of the austenitic grains formed on solution quenching from 1176° C (2150° F).

Fig. 4-9. Alloy 16-25-6 solution quenched, cold worked by 20% elongation, and tempered at 650° C (1200° F) for 72 hrs. Magnification 100×. (After Fleischmann)

Fig. 4-10. Same as Figure 4-9. Magnification 1000×. (After Fleischmann)

The difference in the effect of cold-working on two different treatments, namely, the hot-rolled alloy and the solution-quenched alloy, should be noted. If both types are elongated 20 per cent by cold work and tempered at 815° C (1500° F) for 72 hrs, their structures as shown in Figs. 4-7 to 4-10 are somewhat different. The original austenite grains are fine in the hot-worked alloy and very coarse in the solution-quenched alloy. The precipitate, on the other hand, is coarse in the hot-worked alloy and very fine in the solution-quenched alloy. The large austenite grains in Figs. 4-8 and

4-9 show distortion from the cold-working, which produced 20 per cent elongation. The banding in both samples is probably due to dendritic segregation, which is typical of alloys high in Ni. The fact that the solution-quenched sample has a very fine precipitate suggests that the treatment of 72 hrs at 815° C (1500° F) is still within the precipitation-hardening range.

High-temperature Properties: Short-time Tensile Strength

The tensile strength, elongation, and reduction in area for 16-25-6 alloy are shown in Fig. 4-11 for the hot-rolled alloy and an alloy water-quenched from 1176° C (2150° F) from room temperature to 926° C (1700° F). The results of short-time tensile tests indicate that up to 788° C (1450° F), the hot-rolled material has a slightly higher strength than the solution-quenched alloy. The dip in the ductility curve for the water-quenched sample at 704° C (1300° F) suggests that precipitation-hardening is taking place in this temperature range. This decrease does not occur in the hot-rolled samples.

Stress-Rupture Tests

The results of stress-rupture tests for 16-25-6 alloy shown in Fig. 4-12 cover the temperature range from 538 to 815° C (1000 to 1500° F) and extrapolations on the time axis up to 10,000 hours. At 650° C (1200° F), for tests of 1000 hours, the rupture strength is about 34,000 psi. On the same chart, values for the rupture strength of an 18Cr-8Ni alloy and a Sicromo 5-S alloy are included, to demonstrate the superior properties of 16-25-6 alloy. These curves represent values for both solution-quenched and annealed material. Above 650° C (1200° F) for long periods of service, differences in treatment are ineffective in increasing rupture strength[12].

Creep Strength

Time-elongation curves for 16-25-6 alloy are shown in Fig. 2-2 (Chapter 2) at 650° C (1200° F) under a constant load of 20,000 psi. The upper curve represents an alloy solution-quenched from 1176° C (2150° F) which has a creep rate, as indicated, of 0.32 per cent per 1000 hours. The lower curve represents an alloy finished at 815° C (1500° F) and tempered 6 hrs at 690° C (1275° F) under the same test conditions of 650° C (1200° F) and 20,000 psi. This alloy has a creep rate of 0.018 per cent per 1000 hours.

In Fig. 2-3 (Chapter 2) the same two alloys are subject to a creep test at 704° C (1300° F) under a load of 12,500 psi. The creep rate for the solution-quenched alloy is 0.05 per cent per 1000 hours and 0.021 per cent for the tempered alloy. These two sets of curves indicate the greater stability which results from 6 hours' tempering at 690° C (1275° F).
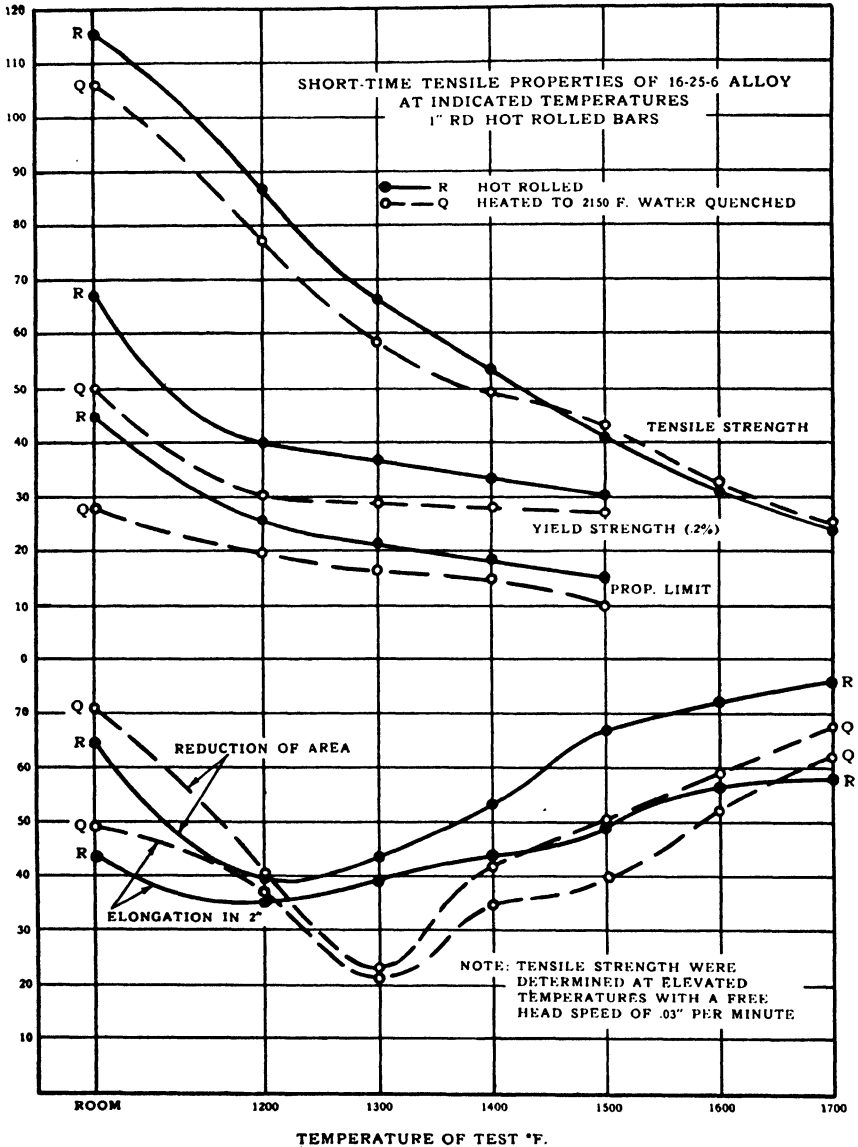
Fig. 4-11. Alloy 16-25-6. Short time tensile properties at indicated temperatures, 1 inch round bars. (After Fleischmann)

The results of creep tests of 16-25-6 alloy for average conditions are indicated in Fig. 4-13 for a temperature range of 650 to 815° C (1200 to 1500° F). These curves represent average conditions.
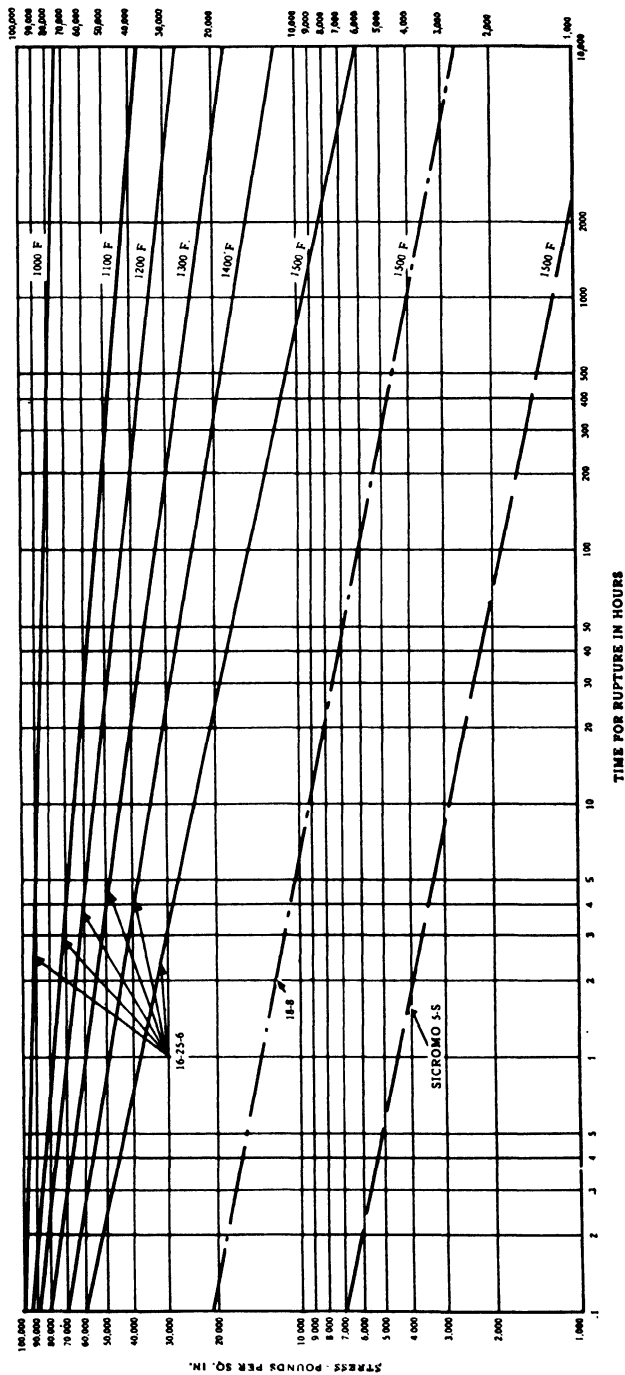
Fig. 4-12. Alloy 16-25-6 stress rupture strength. (After Fleischmann)

Design Curves

The total elongation after 1000 hours is shown in Fig. 4-14, where the stress to produce a certain deformation is plotted against the test temperature for the solution-quenched 16-25-6 alloy. The total elongations selected
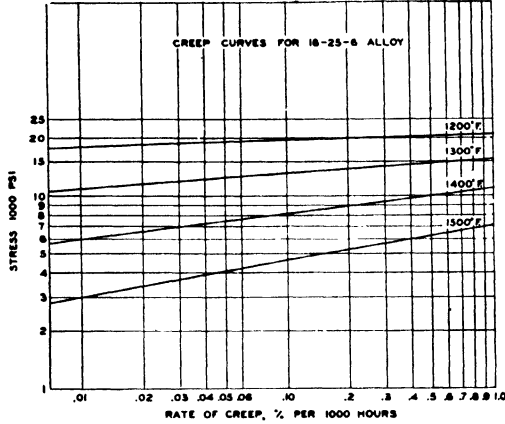
Fig. 4-13. Alloy 16-25-6. Creep curves at 650 to 815° C (1200° F to 1500° F). (After Fleischmann)
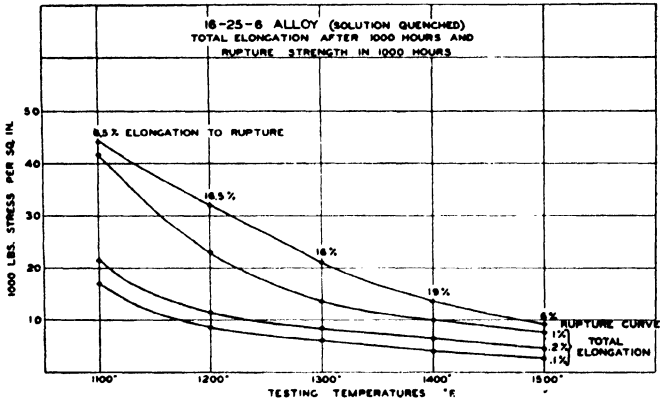
(*Courtesy Timken Roller Bearing Co.*)

Fig. 4-14. Alloy 16-25-6 (solution quenched). Total elongation after 1000 hours and rupture strength in 1000 hours.

are for a total of 1, 0.2, and 0.1 per cent, and are obtained from creep data. The upper curve represents the stress required for rupture in 1000 hours at the indicated temperature and the elongation measured on the broken specimen. The 16-25-6 alloy at 650 and 704° C (1200 and 1300° F) has an elongation of approximately 16 per cent in 1000-hour tests.

Hot Fatigue Tests

The hot fatigue strength of 16-25-6 alloy exceeds its rupture strength in periods up to 10,000 hours[12].

TABLE 4–14. ELEVATED-TEMPERATURE PROPERTIES OF 16–25–6 ALLOY[12]

Thermal Expansion

Temp (°F)	Mean Coefficient of Linear Expansion (In/In/°F × 10⁻⁴)
70–200	8.4
70–400	8.7
70–600	8.85
70–800	9.05
70–1000	9.2
70–1200	9.4
70–1400	9.5

Modulus of Elasticity Versus Temperature

Material	Temp (°C)	(°F)	Modulus × 10
a*	Room	Room	28.2
b†	Room	Room	32.5
a	650	1200	17.9
b	650	1200	17.9
a	704	1300	14.0
b	704	1300	14.9
a	760	1400	11.3
b	760	1400	14.2
a	815	1500	10.0
b	815	1500	13.8

* Forged, cold worked and tempered at 650° C (1250° F)

† Quenched, 1176° C (2150° F), cold worked, tempered 4 hrs at 650° C (1250° F)

Modulus of rigidity = 11,000,000 psi.

Poisson's ratio = 0.286 for test pieces cut from supercharger wheel forgings.

VII. Alloy G.18B.

This austenitic alloy contains about 13 per cent each of Ni and Cr, 10 per cent Co, 0.4 per cent C with additions of the strong carbide-forming elements W, Mo, and Cb (Nb). It is the most widely used forging heat-resistant alloy for disc and rotors at the present time in England. A typical analysis and some properties at elevated temperatures are shown in Table 4-15 and Fig. 4-15[23].

This alloy has the optimum creep strength when solution-treated at 1300° C (2372° F) followed by "warm working" or "hot-cold working" in the range of 650 to 800° C (1200 to 1472° F). During this warm-working operation precipitation of certain constituents as carbides occurs, which tends to increase creep strength. From experiments with austenitic alloys,

the addition of carbide-forming elements does not influence the solid solution matrix in increasing the creep strength[23].

VIII. Grain-size Effects of Austenitic Alloys

Many users of austenitic steels for seamless tubing specify a grain size of 5 or finer (A.S.T.M. grain size classification) in the belief that fine grains have better properties for high-temperature service. A comparison of aus-

STRESS TIME CURVES FOR STATED CREEP STRAINS OF G.18B STEEL AT 650°C.
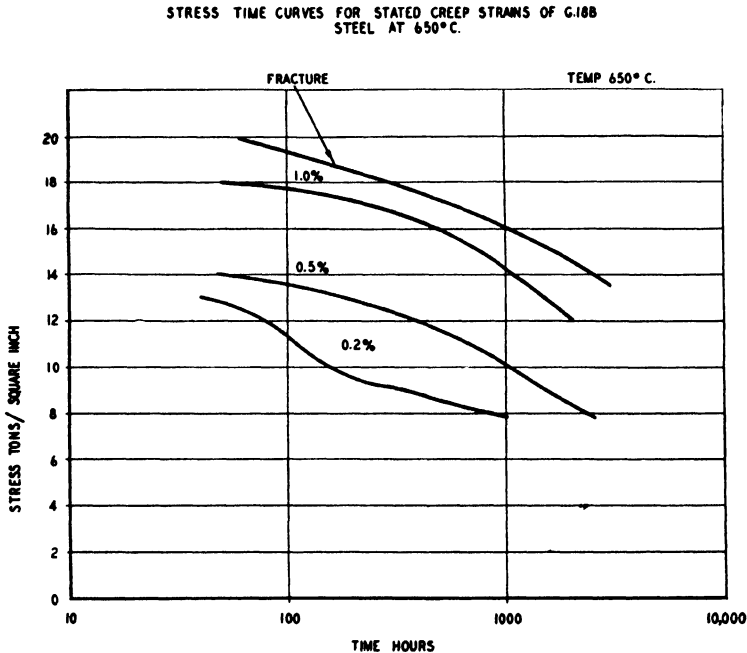
Fig. 4-15. Stress-time curves for stated creep strains of Alloy G.18B at 650° C. (After Oliver and Harris)

tenitic steels with varying grain size suggests that this factor is somewhat complicated.

The alloys for this study consist of (1) 18-8 quenched from 1093° C (2000° F); (2) 18-8 normalized at 926° C (1700° F); (3) 18-12 + Cb quenched from 1038° C (1900° F); (4) 18-12 + Cb quenched from 1232° C (2250° F); (5) 18-12 + Cb normalized at 926° C (1700° F); (6) 25-20 quenched from 1176° C (2150° F); (7) 25-20 normalized at 926° C (1700° F); (8) 25-12 water-quenched from 1038° C (1900° F); (9) 25-12 water-quenched from 1204° C (2200° F). The analysis of these alloys, their grain size and hardness are shown in Table 4-16[7].

The normalized samples are all fine-grained, size 8, and the water-quenched samples are coarser-grained, usually less than 5 except the sam-

TABLE 4–15. ELEVATED-TEMPERATURE PROPERTIES OF G. 18 B ALLOY[23]

Chemical Composition

C	Mn	Si	Ni	Cr	W	Mo	Cb (Nb)	Fe	Co
0.41	0.76	1.13	13.4	13.3	2.72	1.80	3.38	52.8	10.3

Physical Constants

Temp (°C)	Density (gms/cc)	(lb/cu in)	Mean Linear Thermal Expansion Coefficient (20°C − θ° C) per °C	Thermal Conductivity (c.g.s. units)	Young's Modulus (tons/sq in)
20	8.13	0.294	—	—	13,500
100	8.10	.293	15.6×10^{-6}	0.032	13,300
200	8.07	.292	15.8×10^{-6}	.036	13,000
300	8.02	.290	16.5×10^{-6}	.041	12,600
400	7.99	.289	16.9×10^{-6}	.045	12,000
500	7.94	.287	17.1×10^{-6}	.049	11,400
600	7.90	.286	17.3×10^{-6}	.053	10,600
700	7.85	.284	17.7×10^{-6}	.057	9800
800	7.80	.282	18.0×10^{-6}	.061	9100
900	7.75	.280	18.3×10^{-6}	.066	—

Hot Fatigue Data (Solution-treated 1300° C)

Temp (°C)	Endurance Limit (Zero Mean Stress) (tons per sq in)	Endurance Limit (Tensile Mean Stress) (tons per sq in)
600	± 18	20 ± 8.5
650	± 15	14 ± 10.0
700	± 13	12 ± 8.4
750	± 10	9 ± 8.7
800	± 8.5	6 ± 5.7

Charpy Impact Tests (Solution-treated 1300° C)

Temp (°C)	Hot Impact Strength (kg m/cm²)
20	15.0
200	10.1
400	8.0
500	9.5
600	12.3
700	10.4
800	9.5

ples quenched from under 1093° C (2000° F), which tend to the intermediate grain size range of 5 to 7.

The physical properties resulting from all these treatments show good

strength, varying from 83,000 to 98,000 psi, and satisfactory ductilities, as denoted by elongations of 40 to 61 per cent and reductions of area of 63 to 76 per cent. The normalized steels with the finest grain size of 8 have the best room-temperature strength properties. However, the difference be-

TABLE 4-16. COMPOSITION, HEAT TREATMENT AND ROOM TEMPERATURE PHYSICAL PROPERTIES OF FOUR AUSTENITIC STEELS[7]

Chemical Composition

Type Steel	C	Mn	P	S	Si	Cr	Ni	Cb
18-8 (Q)	0.06	0.50	0.008	0.008	0.61	17.75	9.25	....
18-8 (N)	0.056	0.50	0.010	0.015	0.47	18.68	10.21	....
18-12 + Cb (Q)	0.07	1.68	0.013	0.014	0.55	17.78	12.70	0.88
18-12 + Cb (N)	0.08	1.72	0.011	0.008	0.58	18.25	12.93	0.88
25-20	0.11	0.58	0.009	0.010	0.75	23.60	20.65	...
25-12	0.06	1.55	0.011	0.017	0.42	24.96	13.40	....

Heat Treatment*, Hardness and Grain Size

Type Steel	Heat Treatment, Deg. Fahr.		Brinell Hardness	Grain Size
18-8 (Q)	Water-quenched	2000	137	2–5
18-8 (N)	Normalized	1700	143	8+
18-12 + Cb (Q1)	Water-quenched	1900	144	4–6
18-12 + Cb (Q2)	Water-quenched	2250	148	2–4
18-12 + Cb (N)	Normalized	1700	163	8
25-20 (Q)	Water-quenched	2150	143	2–4
25-20 (N)	Normalized	1700	159	8+
25-12 (Q1)	Water-quenched	1900	183	5–7
25-12 (Q2)	Water-quenched	2200	178	3–5

Room Temperature Physical Properties

Type Steel	Tensile Strength	Yield Stress 0.2% Set	Proportional Limit	Elongation in 2 In.	Reduction of Area (%)
18-8 (Q)	85,200	27,900	12,500	61.0	74.0
18-8 (N)	87,500	33,500	15,500	54.0	75.0
18-12 + Cb (Q1)	83,350	33,500	12,500	54.0	72.5
18-12 + Cb (Q2)	81,800	32,000	12,500	54.0	73.0
18-12 + Cb (N)	91,750	41,500	22,500	46.0	66.0
25-20 (Q)	87,400	36,000	15,000	54.0	76.0
25-20 (N)	96,000	50,000	37,500	40.0	63.0
25-12 (Q1)	98,000	47,500	20,000	40.5	72.7
25-12 (Q2)	93,600	44,000	22,500	49.5	73.9

* Bars cold drawn to the desired degree before quenching or normalizing from designated temperature.

tween coarse and fine grains is small in the 18-8 alloy and quite marked in 18-12 + Cb and 25-20 compositions.

Short-time Tensile Properties

The short-time tensile strength of these alloys in the range of 538 to 982° C (1000 to 1800° F) is not greatly affected by changes in grain size.

The 25-20 alloy with coarse grains is superior in strength to the fine-grained sample in the temperature range of 538 to 815° C (1000 to 1500° F). There is also evidence that the fine-grained 25-12 alloy at 704° C (1300° F) is stronger than the coarse-grained.

Values of the yield stress obtained in short time testing are more consistent in that the fine-grained structure in all cases has the higher value. The difference is less marked in the 25-12 alloy.

Ductility of these steels is more dependent on grain size than is yield strength, and again finer grains are associated with greater ductility. The difference is quite marked in that the coarse-grained alloys have about 10 per cent elongation and the fine-grained steels have a minimum of 30 per cent elongation.

Stress Rupture

Stress-rupture tests in the temperature range of 538 to 982° C (1000 to 1800° F) indicate that coarse-grained steels are superior for alloys 25-20 and 25-12. Intermediate grain size is best for 18-12 + Cb. For 18-8 alloy, the difference in grain size does not appear to change the stress-rupture characteristics appreciably. The hot ductility obtained from the stress-rupture tests again shows the fine grains to be superior for all the alloys.

Creep Strength

Based on a creep rate of 0.01 per cent per 1000 hours, the alloys with coarse grains have a higher creep strength than those with fine grains. This is especially marked in 25-20 alloy and less evident in 18-8 and 25-12 alloys. In the case of 18-12 + Cb composition, the intermediate grain size 4 to 6 has the higher creep strength.

Conclusions

The microstructure of 18-8 alloy shows carbide precipitation after prolonged heating. The coarse-grained alloys 18-12 + Cb, 25-20, and 25-12 also show carbide precipitation at the grain boundaries after prolonged heating. This condition may well account for the decreased hot ductility displayed by the coarse-grained alloys from the short-time tensile tests.

The microstructures of the fine-grained steels, 18-12 + Cb, 25-20, and 25-12 are unusual in that heating at elevated temperature causes a very fine precipitate to form, which etches rapidly and increases in amount with increasing time and temperature. This may be the sigma phase. The decrease in the creep strength of the fine-grained structures is probably related to the appearance of this new phase.

The selection of an alloy with the corresponding optimum grain size is thus a compromise between the requirements of good creep strength as against a satisfactory hot ductility[7].

D. Austenitic Alloys for Valves and Valve Seats

Materials for valves and valve seats in contact with hot exhaust gases from gas engines must have high corrosion resistance and wear resistance. Corrosion in the hot exhaust gas is due to lead compounds, oxygen, carbon, and hydrocarbons from incomplete combustion of the gas. In automotive valves, operating temperatures may reach 982 to 1038° C (1800 to 1900° F). In aircraft, valves operate at lower temperatures because of internal cooling of the valve with sodium. Failures in valves may occur by sticking of the stem from cold corrosion in the presence of moisture condensed from the exhaust gases. Failures also may occur from heat shock if a valve operating at red heat is suddenly cooled with unburned gas. This condition may arise if a bus engine is used as a brake in the descent of a long hill in low gear[17].

Valve steels are for the most part medium- or high-C alloys to maintain high wear resistance against battering or upsetting at the valve seats and scuffing at the guides. Hot hardness tests are often specified, or a hardness may be indicated by mutual indentation of two short cylinders pressed together at the required temperature[17]. Corrosion tests are carried out by weight loss measurements from immersion in molten lead compounds or cyclic heating in hot exhaust gas atmospheres.

A list of alloys used in valves with their hot hardness, corrosion resistance and industrial applications is given in Table 4-17[17].

E. Casting Alloy 25Cr-12Ni, Type HH

Heat-resistant castings are classified as those which may be exposed to temperatures above 482° C (900° F) for continuous or intermittent operation. They are widely used for furnace parts exposed to high temperature and for applications in the oil refining and synthetic rubber industries. The composition of Type HH alloy may vary between 24 to 28 per cent Cr and 11 to 14 per cent Ni with varying C content. The superiority of this alloy over the 18Cr-8Ni composition in regard to its surface stability, elevated-temperature strength, and its moderate cost, has resulted in wide use of this alloy to the extent that it constitutes over 30 per cent of all industrial heat-resistant castings[4,30].

The composition limits, shown in Table 4-18, are wide owing to the fact that there are two types of alloys best classified according to their magnetic permeability: Type I, permeability between 1.05 and 1.70; Type II, permeability below 1.05. The fully austenitic Type II alloys maintain high ductility at elevated temperatures. The Type I alloys have a higher limiting creep stress but a lower ductility due to the presence of small amounts of a ferrite phase. The composition limits of the two types of alloys are indicated in the following formula:

$$\text{Ratio factor} \quad \frac{\text{Cr } (\%) - 16\text{C } (\%)}{\text{Ni } (\%)} \quad \text{must be less than 1.7}$$

TABLE 4-17

VALVES AND VALVE SEAT MATERIAL

From paper by S. D. Heron, O. E. Harder and M. R. Nestor before American Society for Testing Materials

No.	C	Si	Cr	Ni	W	Mo	Other	Rockwell Hardness — Natural	Rockwell Hardness — After 1475 F. Draw	Brinell Hardness, Hot (g) — At 930°F	Brinell Hardness, Hot (g) — At 1475°F
							Martensitic or Pearlitic Steels				
1	0.40-0.50	3.0-3.5	8.0-9.0	1.0-2.0				C-32 to 35	C-20 to 29	169-179	16-20
2	0.35-0.45	3.9-4.2	2.8-3.0	0.75-1.0							26
3	0.50	1.5	8.0			0.75					
4	0.60-0.85	1.25-2.75	19-23	<0.65	3.25-3.75			C-38	C-31	254	38 at 1600°
5	1.0-1.1	1.8-2.0	13-14			0.50-0.75		C-55			
6	1.27-1.43	<0.65	11.5-14	12-16	12-16	0.45-0.95	2.5-3.5 Co				
7	0.50-0.70		3.0-4.0								
8	1.0-1.2	<0.50	12-14	<0.50							
9	0.5	0.2	11.0	1.5			0.5 Mn 1.8 Al				
10	2.5-3.0	1.5-2.0	2.75-3.25			4.0-5.0	0.6-0.8 Mn	C-40	C-19		28
11	1.0	1.0	25.0								
							Austenitic Steels and Nickel-Chromium-Iron Alloys				
12	0.30-0.45	2.50-3.25	17.5-20.5	7.0-9.0				C-26	C-24	142	45
13	0.20-0.30	0.70-1.00	21-22	11-12				C-20 to 27	C-18 to 22	130-180	55-78
14	0.20-0.30	2.5-3.0	21-22	11-12				C-24	C-20	166	71
15	0.40-0.50	0.30-0.80	13-15	13-15	1.75-3.00	<0.50		C-25	C-23	162	55
16	0.40-0.50	2.75-3.25	13-15	13-15	1.75-3.00	<0.50		C-30	C-22	165	53
17	0.50	1.25	14	26	3.5			C-22	C-16	182	84
18	0.40-0.50	0.30-0.80	24-26	13-15				B-94	B-94		76
19	0.95-1.20	2.0-3.0	15-16	13-15		2.0-3.0		C-24	C-30	174	94
20	0.50	1.0	20	32			1.0 Mn	C-21	C-19	140	80
21	0.50-0.60	0.50	3.5	12			5.0 Mn	C-22	B-95	107	55
22	0.10	0.30	14	80				B-83	B-83	74	54
23	0.07	<0.75	18	8				B-81	B-80		49
							Transformation Hardening Steels				
24	0.25-0.35	2.0-3.0	12.0-13.5	7.0-7.75		2.5-3.5		C-42	C-41	244	98
25	0.40-0.50	<1.0	23.3-24.3	4.5-5.0				C-41	C-36	230	63
							Non-Ferrous Alloys				
26	1.25	2.7	27		4		65 Co			217 at 1200° F	132 at 1600° F
27	2.0	0.9	30		12		54 Co			314 at 1200° F	185 at 1600° F
28	0.20	0.30	21	Balance		0.90 Mn	0.60 Fe				
29	0.16	0.02	30.3 Cu	66.9	0.16 Al	0.90 Mn	1.6 Fe				
30			Bal. Cu	4.0-6.0	9.5 Al		0.5 Fe				
31			Bal. Cu		10.5-11.5 Al		4-6 Fe				
32				>99.0							

Table 4-17—Continued

No.	Scaling Loss (a) Oxidizing Atmosphere	Scaling Loss (a) Reducing Atmosphere	Corrosion Resistance in Exhaust Condensate	Relative Attack by Lead Compounds (b) PbO-PbBr₂ at 1550°F	PbO at 1800°F	2 PbO·PbSO₄ at 1800°F	Utility and Remarks
							Martensitic or Pearlitic Steels
1	50	140	Poor	41	100	200	Most widely used exhaust valve material.
2	160	360	Very bad	41	106	258	Cheaper variety; inferior as to burning and rusting.
3	10,000	12,000	Very bad	.	.	.	Unsatisfactory substitute for No. 1.
4	40	75	Complete	1	104	8	Rapidly replacing No. 1.
5	.	.	Very bad	.	.	.	Limited use replacing No. 6.
6	5,000	2,200	Very bad	16	136	6	Superseded No. 7 for aircraft use in early 1920's.
7	—	—	Very bad	—	—	—	High speed toolsteel; adopted in U.S. in 1911; much used in War; first valve with good hot strength.
8	19,000 (c)	19,000 (c)	Very bad	56	64	3	Cutlery stainless (modified); used in Europe for 1916-1918 aircraft.
9	.	.	(d)	26	113	5	Reputation for unreliability in automobiles.
10	18,000	17,000	.	36	240	520	Cast exhaust valve seats for passenger cars and trucks.
11	60	100	Complete	2	14	1	In experimental use.
							Austentic Steels and Nickel-Chromium-Iron Alloys
12	90	70	Complete	63	57	46	Wide use in automobiles for its hot strength.
13	30	60	Complete	37	43	2	Wide use in bus and truck engines.
14	50	90	Complete	48	48	17	Higher silicon than No. 13 does not improve resistance to burning.
15	2,600	1,600	(e)	20	126	26	U.S. aircraft exhaust valves, internally cooled and seat faced.
16	100	150	Complete	25	92	184	Too hard to drill, seat inserts in aluminum cylinders.
17	840	370	Complete	28	73	228	European aircraft exhaust valves.
18	50	40	(e)	12	47	0.3	Recently introduced to replace No. 15, about same in severe service; no intergranular attack by sodium.
19	140	160	Complete	.	.	.	Castings for both intake and exhaust valves on Ford motors.
20	60	40	Complete	.	.	.	Limited use, as cast, in auto, bus and truck valves.
21	11,000	11,000	(d)	.	.	.	Exhaust valve seats in European aircraft. High thermal expansion requires threaded design to remain tight.
22	60	50	Complete	40	42	254	Not used, despite interesting properties.
23	2,400	1,700	Complete	25	112	2	Not used, despite interesting properties.
							Transformation Hardening Steels
24	2,800	2,300	Very good	49	84	24	Had limited use in autos and wide use in aircraft.
25	40	50	Complete	2	35	1	Better wear and scuffing resistance than austenitic steels; embrittled by many cycles between 1400 and 1600° F.

TABLE 4-17—Continued

No.				Non-Ferrous Alloys			Remarks
				0.5	4	0.5	
26	20	15	Complete				Stellite No. 6, almost universal in U S. for welded-on seat facings in aircraft engines.
27	50	15	Complete	72	6	1	Valve seat inserts for bus and trucks, with higher hot hardness and wear resistance than No. 26.
28	45	15 gain	Complete	71	52	197	Brightray; used in Europe for welded-on seat facings.
29	13,000	30	Very good	.	.	.	Monel; used in Europe for some exhaust valve seat inserts.
30	1,000 (f)	.	Good	100	244	243	Formerly much used as extruded valve seat inserts in aluminum cylinders.
31	.	.	Good	.	.	.	Cast and heat treated substitute for No. 30. Neither good for leaded fuels.
32	250	70	Complete	3	340	504	Commercially pure nickel; has unusually high hot corrosion resistance.

Notes: (a) Loss in mg. on $\frac{7}{8}$ x 2-in. rod after 300 40-min. cycles between 1800° and 650° F. Fuel is a special kerosene with anti-knock additions, burned with 15½ lb. air per lb. for oxidizing atmosphere and 12½ lb. for reducing. Low results may be misleading.
(b) Calingaert test Relative loss after 6 min. in molten compound.
(c) After 250 cycles.
(d) Probably very bad.
(e) Complete if not nitrided; poor when nitrided.
(f) Maximum temperature on heating cycles: 1800° F.
(g) By mutual indentation.

TABLE 4-18. PROPERTIES OF THE IIH ALLOYS[30]

Composition Range

C %	Cr %	Ni %	Mn %	Si %	N %	P or S %
0.20–0.45	23–28	10–14	2.5 max.	1.75 max.	0.20 max.	0.05 max.

Room Temperature Mechanical Properties

(a) As Cast

Tensile Strength Psi	Yield Point Psi	Elongation in 2" %	Red. of Area %	Charpy Impact Ft. Lb.	Hardness BHN
70,000–95,000	35,000–50,000	15–35	20–40	10–35	160–180

(b) After Aging 48 Hours at 760° C (1400° F)

Tensile Strength Psi	Yield Point Psi	Elongation in 2" %	Charpy Impact Ft. Lb.	Hardness BHN
75–100.000	40–000–55,000	4–25	5-15	190–215

Elevated Temperature Tensile Properties

(a) Short Time Tests

Temperature °C	°F.	Tensile Strengsh Psi Average Value	Elongation in 2" % Average Value
760	1400	35,000	17
871	1600	20,000	22
982	1800	10,000	34
1093	2000	7,000	—

(b) Stress Rupture Tests

Alloy Type*	Temperature °C	°F.	Minimum Fracture Time Hours	Limiting Rupture Stress Psi
I	871	1600	16	5000
II	871	1600	16	8000

* Alloy types are identified in A.S.T.M. Specification B190-45T.

(c) Creep Tests

Temperature °C	°F.	Limiting Creep Stress for 1% Extension in 10,000 Hours
760	1400	7000 to 3000 psi
871	1600	4000 to 1700 psi
982	1800	2100 to 1000 psi

Thermal Expansion Coefficients

UNITS—INCHES/INCH/°F.

70–1300 °F.	70–1650 °F.	70–1800 °F.
9.9×10^{-6}	10.1×10^{-6}	10.5×10^{-6}

for maintenance of the wholly austenitic alloy Type II. For this relationship to hold, the minor elements present must be as shown in Table 4-18, and the nitrogen content must be approximately 0.09 per cent[30].

The heat-resistant castings are melted in both the electric furnace, acid or basic, and the high-frequency induction furnace. Many special techniques have been developed to insure the production of sound castings. Pouring is static or centrifugal as in the manufacture of tubing for radiant heating furnaces[1]. The 25Cr-12Ni alloy is suitable for welding by the usual processes applicable to the general class of austenitic compositions.

The relative machinability of Type HH alloy compares favorably with that of the other austenitic alloys, with the exception that castings may have segregated areas of coarser carbides which are more difficult to ma-
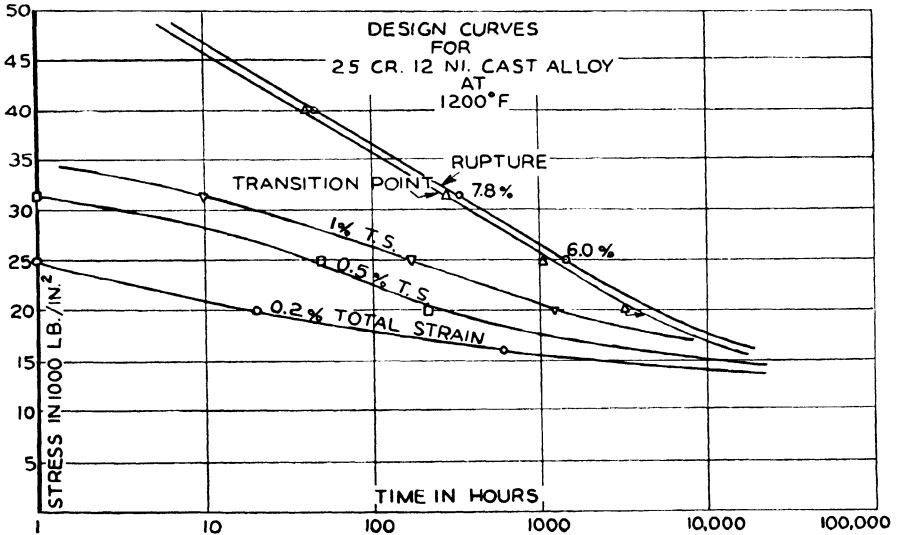
Fig. 4-16. Design curves of Alloy 25-12 at 650° C (1200° F). (After Manjoine)

chine. If the alloy is used below 650° C (1200° F) for corrosion resistance and the surface finish calls for cleaning by blasting, sand should be used in the process rather than shot-peening with steel balls, as the latter may contaminate the surface of the casting and decrease its corrosion resistance[30].

The microstructure of the 26Cr-12Ni alloy Type HH may consist of a number of constituents as austenite, ferrite, carbides, a lamellar structure resembling pearlite, and the Fe-Cr sigma phase. The stability of the material at elevated temperatures depends on precipitation of carbides and the possibility that the ferrite phase may change slowly to the brittle Fe-Cr sigma constituent. If the 25-12 alloy is heated to 760° C (1400° F) for 24 hours, the partial carbide precipitation which occurs increases room-

temperature tensile strength and decreases ductility. As a means of controlling the properties of the alloy during elevated-temperature service life, thus eliminating tendencies toward failure due to brittleness, a requirement for a heat-treating test may be as follows:

Type I: After heating at 760° C (1400° F) 24 hours, followed by slow cooling, the loss in ductility at room temperature shall not be greater than 9 per cent.

Type II: With the same heat treatment, the loss in ductility shall not be greater than 4 per cent (A.S.T.M. Specification B190-45T).
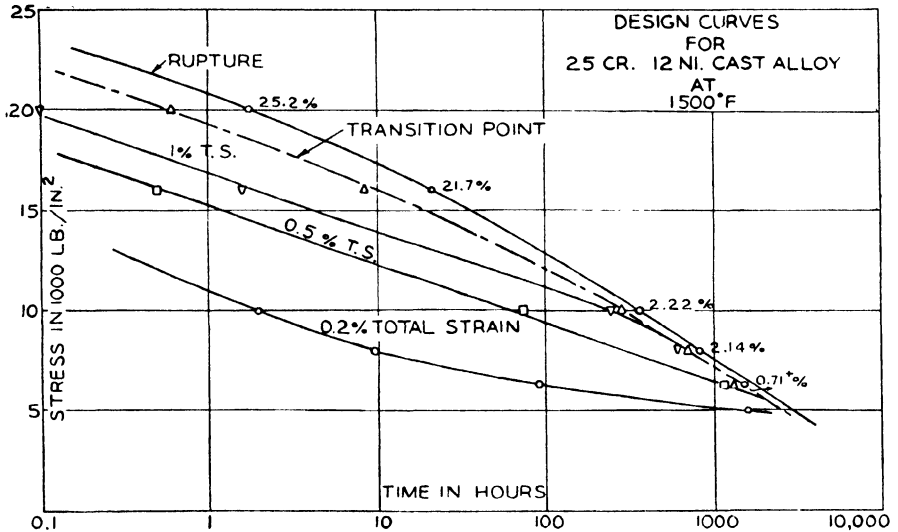
Fig. 4-17. Design curves of Alloy 25-12 at 815° C (1500° F). (After Manjoine)

In selecting the best alloy for a particular service, the temperature of operation is most important. For continuous operation above 871° C (1600° F), the question of embrittlement from either the formation of sigma phase or precipitation of carbide does not arise. An alloy for this service may be, for example, 0.35 to 0.40 per cent C, 10 to 12 per cent Ni, and 24 to 27 per cent Cr. For applications in the temperature range of 650° C to 871° C (1200 to 1600° F), the recommended composition is 0.40 per cent C, 11 to 14 per cent Ni, and 23 to 27 per cent Cr[1].

Design curves for the 25Cr-12Ni cast alloy are shown in Figs. 4-16 and 4-17 at 650° C and 815° C (1200° F and 1500° F). At 650° C (1200° F), for a rupture strength of 25,000 psi, the elongation is approximately 6 per cent after 1000 hours' test. For 0.2 per cent total strain after 1000 hours, the stress is approximately 15,000 psi. At 815° C (1500° F), for the same

time, the elongation at rupture is about 2 per cent and the stress for 0.2 per cent strain is 5000 psi[18].

References

1. Amer. Soc. Metals Handbook (1948).
2. Archer, R. S., Briggs, J. Z., and Loeb, C. M., Jr., "Molybdenum, Steels, Irons and Alloys," Hudson Press, N. Y. (1948).
3. Avery, H. S. and Wilks, C. R., "Cast 26% Cr-20% Ni Alloys," *Trans. Am. Soc. Metals*, **40**, (1948).
4. Avery, H. S., Cook, E., and Fellows, J. A., "Engineering Properties of Heat-resistant Alloys," *Metals Technology*, **9**, T. P. 1480 (Aug., 1942).
5. Babcock and Wilcox Tube Co., Tech. Bulls. 1-A (1940) and 6-E (1948).
6. Binder, W. O., "Alloys for High-temperature Service," *Iron Age*, **158**, 46 (1946).
7. Clark, C. L. and Freeman, J. W., "Apparent Influence of Grain Size on the High-temperature Properties of Austenitic Steels," *Trans. Am. Soc. Metals*, Preprint No. 19 (1946).
8. Cornelius, H., "Properties of Austenitic Valve Steels which are Alloyed with Manganese," *Luftfahrt Forschung*, **19**, 44 (1942); *Chemische Zentralblatt, II*, **95** (1942).
9. Cross, H. C. and Simmons, W. F., "Heat-resisting Metals for Gas Turbine Parts, Symposium on Materials for Gas Turbines," *A.S.T.M.*, 3 (June, 1946).
10. Evans, C. T. Jr., "Materials for Power Gas Turbines," *Trans. Am. Soc. Mech. Engrs.*, **69**, 601 (1947).
11. Feild, A. L., "Stainless Steel and High-temperature Alloys Produced by Germany during World War II," Fried. Krupp Co., Essen, PB 1635 (Apr., 1945).
12. Fleischmann, M., "16–25–6 Alloy for Gas Turbines," *Iron Age*, **157**, 44 and 50 (1946).
13. Freeman, J. W. and Cross, H. C., "A Metallurgical Investigation of a Large Forged Disk of Low Carbon N-155 Alloy," N.A.C.A., No. 5K20 (Dec., 1945).
14. Freeman, J. W., Reynolds, E. E., and White, A. E., "A Metallurgical Investigation of a Large Forged Disk of CSA (234-A-5) Alloy," N.A.C.A., ARR No. 5H17.
15. Freeman, J. W., Reynolds, E. E., and White, A. E., "High-temperature Alloys Developed for Aircraft Turbosuperchargers and Gas Turbines," Symposium on Materials for Gas Turbines, *A.S.T.M.*, 52 (June, 1946).
16. Grant, N. J., Taylor, M. E., and Frederickson, A. F., Heat-resisting Alloys from 1200 to 1800° F," Navships 250–330–12, Res. Memo No. 3–47 (Sept. 1, 1947).
17. Heron, S. D., Harder, O. E., and Nestor, M. R., "Gas Engine Valves," *Metal Progress*, **37–38**, 418 (1940); "Valves and Valve Seat Materials," *Metal Progress*, **37–38**, 541 (1940).
18. Manjoine, M. J., "New Machines for Creep and Creep-Rupture Tests," *Trans. Am. Soc. Mech. Engrs.*, **67**, 111 (1945).
19. Miller, R. F., Benz, W. G., and Day, M. J., "Creep Strength, Stability of Microstructure and Oxidation of Cr-Mo and 18 Cr-8 Ni Steels," *Trans. Am. Soc. Metals*, **32**, 381 (1944).
20. Monypenny, J. H. G., "Stainless Steels for Turbine Blading," *Trans. Inst. Marine Engrs.*, **57**, 129 (Dec., 1945).
21. Morlet, E., "Influence of Heat Treatment and Microstructure of Austenitic Heat Resisting Steels on the Scatter of Creep Test Results," *Rev. de Métallurgie, Mémoires*, **41**, 161, June; 284, Sept.; 346, Oct. (1944).
22. Newell, H. D., "Properties and Characteristics of 27% Chromium-Iron," *Metal Progress*, **49**, 977 (1946); "High-chromium Irons," *Metal Progress*, **51**, 917 (1947).

23. Oliver, D. A. and Harris, G. T., "High Creep Strength Austenitic Gas Turbine Forgings," *Trans. Inst. Marine Engrs.*, **59**, No. 5 (1947); "Ferritic Discs for Gas Turbines," *Metallurgia*, **34** (1946); *J. West of Scotland Iron & Steel Inst.*, **54**, 97 (1945–6).

24. Payson, P. and Savage, C. H., "Changes in Austenitic Chromium-Nickel Steels during Exposure at 1100 to 1700° F," *Trans. Am. Soc. Metals*, **39**, 404 (1947).

25. Rudorff, D. W., "Development of Austenitic Manganese-alloyed Steels for Aero Engine Exhaust Valves," *Metallurgia*, **27**, 205 (Apr., 1943).

26. Siegfried, W., "Observations on Conducting and Evaluating Creep Tests," *J. Iron and Steel Inst.*, **189** (June, 1947).

27. Thum, E. E., "Book of Stainless Steels," Am. Soc. Metals, Cleveland, Ohio (1935).

28. Timken Roller Bearing Co., Tech. Bulls., 33 (1945); 32 (1946).

29. Tofaute, W. and Bandel, G., "Strategic, Especially Low-nickel and Nickel-free Austenitic Exhaust Valve Materials," *Technische Mitteilungen Krupp, Forschungsberichte*, **5**, 192 (1942).

30. Wilson, E. F., "Heat-resistant Alloy Castings of the "HH" Type," *Alloy Casting Bull.*, No. 11 (Dec., 1947).

31. Zschokke, H., "Increasing Creep Limit by Cold Work," *Schweizer Arch.*, **12**, 297 (Oct., 1946).

Chapter 5

Highly Alloyed Austenitic Steels

The alloys discussed in Chapters 5, 6, and 7 are in many instances the results of investigations carried out during World War II under O.S.R.D., N.D.R.C., and N.A.C.A.* government sponsorship, which vigorously pursued the problem of finding suitable materials for operation of components stressed above 650° C (1200° F). The published data are considerable and in certain instances the discrepancies in the values obtained are wide. This is understandable on the basis of several difficulties, such as variation in composition, size of heats, and subsequent forming and heat treatment. Some of the tests are limited to controlled experimental conditions on small bar stock. In spite of these discrepancies, the designer has a wide range of materials, the selection of which will depend largely on the cost of the ingredients, especially where rupture and creep strength are reasonably close. With peacetime use of these heat-resistant alloys, they are finding application in high-temperature service where the results of long-time service are now available and the economics are justified in a competitive market.

The alloys considered in this chapter are the highly alloyed wrought stainless steels containing decreasing amounts of Fe, from approximately 50 per cent down to 15 per cent. The metals Co, Cr, and Ni replace Fe and are further stabilized by small amounts of W, Mo, and Cb and precipitation-hardened by such elements as Al and Ti.

A. Precipitation-hardened Alloys with Ti and Al

In the previous chapter, it appeared that the austenitic alloys are made suitable for high-temperature service by cold-working or by hot-cold working, provided that the service range of temperature is below that required for recrystallization in the first case and below the temperature of hot working in the second case.

There is a third method of increasing resistance to deformation in highly alloyed stainless steels, which takes advantage of the precipitation-harden-

* O.S.R.D. Office of Scientific Research and Development. N.A.C.A. National Advisory Committee for Aeronautics. N.D.R.C. National Defense Research Committee.

ing accomplished by the addition of one or more elements in small quantities. The fact that the precipitated particles are fine and tend to uniform distribution adds greatly to the uniformity in hardness and to greater stability under loading at high temperature.

Several elements offer possibilities as hardening agents for the austenites. C will increase the hardness of an austenitic structure, but since the resulting alloy does not respond to heat treatment, machining must be done on the hardened structure. C has the further disadvantage that it unites with Cr and tends to increase susceptibility to corrosion due to areas depleted in this element. Another element which gives effective precipitation-hardening is Be, but the temperature range at which the alloy ages is very low for service conditions required for many applications, such as gas turbines[15].

Both Ti and Al are widely used as precipitation agents for a large number of different austenitic alloys. The increase in hardness obtained provides remarkable stability in the use range of 593 to 760°C (1100 to 1400° F). In general with these alloys of Cr-Ni-Fe, the C content is maintained at 0.05 per cent, as this element readily combines with Ti and prevents effective hardening.

Three alloys in this class are "Discaloy," "Refractaloy" 26, and K42B*, with Fe contents varying from approximately 55 to 14 per cent. These alloys are forgeable at an upper temperature range of 1204° C (2200° F). Billet forging is started at 1065° C (1950° F) for "Discaloy," and 1150° C (2100° F) for K42B and "Refractaloy" 26. These materials are resistant to scaling in this temperature range and require no protective atmosphere in heating for forging. Their forming properties are good, since the C content is low and die wear is not excessive. However, close control of temperatures and reductions is necessary.

The alloys are solution-treated to a Brinell of 140 to 180 for machining. For rough machining, feeds and speeds similar to those used for stainless steels are satisfactory. Finish machining is carried out with high-speed tools after the alloys have been aged.

Welding of all three compositions is accomplished with austenitic rods and procedures used for stainless steels. A solution treatment for the whole structure after welding is recommended[16].

I. "Discaloy"

This alloy is in reality a stainless steel with about 55 per cent Fe, but it is included in this section because of the addition of Al and Ti as precipitation-hardening agents. The elevated-temperature properties are given in Table 5-1.

* Westinghouse Electric Mfg. Corp.

II. Alloys K42B and "Refractaloy" 26

Two other alloys, K42B and "Refractaloy" 26, are precipitation-hardened with Al and Ti. The Fe content is decreased to 14 and 18 per cent,

TABLE 5-1. ELEVATED-TEMPERATURE PROPERTIES OF "DISCALOY."[14]

Chemical Composition

NR No	C	Mn	Si	Cr	Ni	Fe	Mo	Al	Ti
78	.05	.7	.7	13	25	55	3	.2	1.8

Heat Treatment

The solution treatment for "Discaloy" is 1065° C (1950° F) for a period of 1 hour. The rate of cooling is not critical but in general oil-quenching is recommended[15] Aging at 732° C (1350° F) for 20 hours gives a hardness of 320 Vickers DPH (approximately Rockwell C 30) which is maximum for this alloy.

Density versus Heat Treatment

The density of "Discaloy" is highest in the heat-treated and aged condition as follows[15]:

Condition	Density gms/cm³
Hot-rolled	7.969
Solution-treated	7.960
Solution-treated and aged	7.989

Creep Strength

Temp (°C)	Temp (°F)	Specified Life (hrs)	Creep Strength (psi) for total strain of 0.5%	1.0%	Rupture Strength (psi)	Elong % in 2"
650	1200	100	39,200	42,500	52,000	6.0
650	1200	1000	35,200	36,000	38,200	5.5

The tests for creep and stress rupture represent specimens from a forged disk. The heat treatment consists of a solution treatment at 1065° C (1950° F) for 1 hour and aging at 732° C (1350° F) for 20 hours.

Design Curves

Fig. 5-1 shows the design curves for "Discaloy" at 650° C (1200° F) which is the maximum range recommended for the use of this alloy[15].

Thermal Expansion

Temp (°F)	Mean Coefficient of Linear Expansion (In/In/°F × 10⁻⁶)
70–200	8.5
70–400	8.7
70–600	9.1
70–800	9.4
70–1000	9.5

respectively, and Co substituted in amounts of 20 and 22 per cent. Their nominal compositions are given in Table 5-2[15].

These alloys are heat-treated by solution-treating at 1065° C (1950° F)

and aging can be at 732° C (1350° F) for 20 hours or at a somewhat higher temperature. In Fig. 5-2 is shown the effect of aging the alloy K42B at 732 to 815° C (1350 to 1500° F) for varying periods of time[15]. As in all
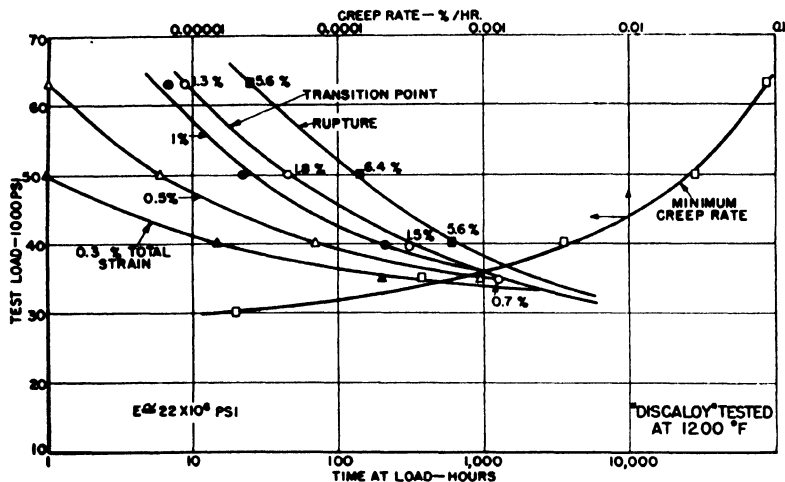
Fig. 5-1. Design curves for "Discaloy" at 650° C (1200° F). Specimens cut from a forged rotor. Heat treatment: solution treatment 1065° C (1950° F) 1 hr., furnace cooled, aged 732° C (1350° F) 20 hrs. (After Scott and Gordon)

TABLE 5-2. NOMINAL COMPOSITIONS OF TITANIUM HARDENED ALLOYS

Element	K42B	"Refractaloy" 26
Ni	42	37
Co	22	20
Cr	18	18
Mn	0.7	0.7
Si	0.7	0.7
Al	0.2	0.2
Fe	14	18
Mo	—	3
Ti	2.2	2.8
C	0.05	0.05

Effect of Heat Treatment on Density of K42B

Condition	K42B
Hot-rolled	8.180
Solution-treated	8.140
Solution-treated and aged	8.230

aging phenomena, the hardness rises rapidly and then falls off with time. The maximum hardness obtained is almost 320 Vickers DPH (about Rockwell C30). A conversion table of hardness values on the Vickers and Rockwell scales is given in Chapter 2.

Overaging these alloys by a fluctuation in temperature is shown by the fact that a variation of $\pm$ 50° F changes the Vickers number by $\mp$ 15
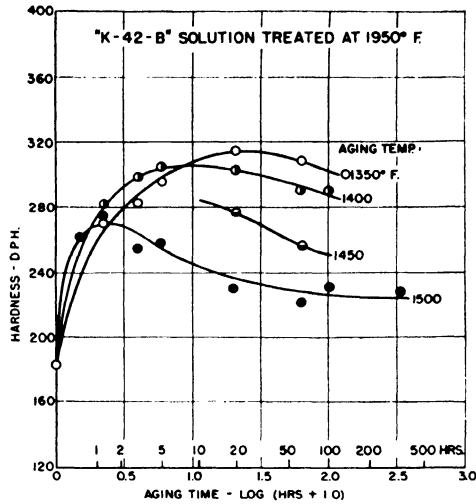
Fig. 5-2. Aging curves for a typical heat of K42B. (After Scott and Gordon)

TABLE 5-3. RUPTURE STRENGTH AND CREEP STRENGTH
OF ALLOYS K42B AND "REFRACTALOY" 26[15].

Alloy	Test Temp (°C)	(°F)	Specified Life (hrs)	Rupture Strength (1000 psi)	Elong % in 2"	Creep Strength 1000 psi for total strain of		
						0.2%	0.5%	1.0%
K42B	650	1200	100	66.0	1.0	36.8	60.0	—
	650	1200	1000	40.8	0.7	32.8	—	—
	732	1350	100	37.0	0.8	31.0	—	—
	732	1350	1000	26.8	0.8	21.2	—	—
	815	1500	100	17.2	6.0	11.0	15.0	—
	815	1500	1000	10.5	2.5	6.0	8.0	—
"Refractaloy" 26	650	1200	100	73.5	1.5	—	—	69.5
	732	1350	100	51.0	2.5	44.0	47.5	49.0
	815	1500	100	29.5	19.0	20.0	24.3	25.0
	*815	1500	100	28.7	20.0	21.7	23.2	24.6
	*815	1500	1000	18.1	17.0	15.1	15.5	16.1

Note: K42B tested as rolled bar, Refractaloy 26 tested as rolled bar with exception of samples marked * which are forged bars.
Heat treatment of K42B 1065° C (1950° F), 1 hr, oil-quenched;
732° C (1350° F), 20 hrs.
"Refractaloy" 26 1150° C (2100° F), 1 hr, oil-quenched;
815° C (1500° F), 20 hrs;
732° C (1350° F), 20 hrs.

points. Temperature fluctuations under service conditions can be expected to have similar effects.
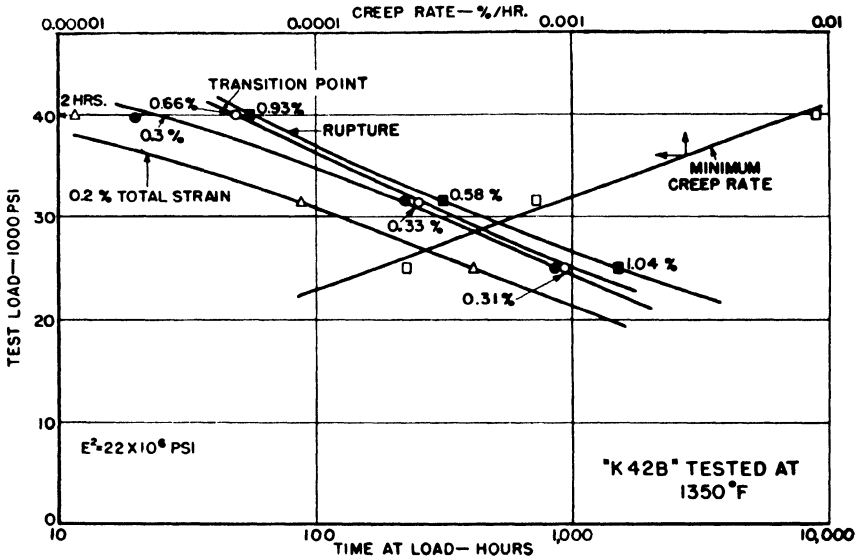
Fig. 5-3. Design curves for K42B at 732° C (1350° F). Specimens machined from hot rolled bar stock. Heat treatment: solution treatment 1065° C (1950° F) 1 hr., oil quenched, aged 732° C (1350° F) 20 hrs. (After Scott and Gordon)
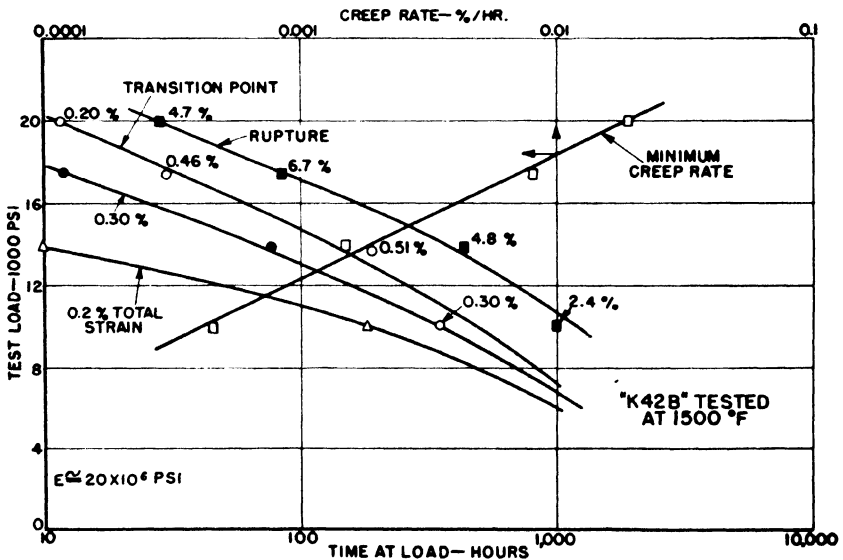
Fig. 5-4. Design curves for K42B at 815° C (1500° F). Specimens machined from hot rolled bar stock. Heat treatment: solution treatment 1065° C (1950° F) 1 hr. oil quenched, aged 732° C (1350° F) 20 hrs. (After Scott and Gordon)

It is also true that if these alloys are solution-treated at 1065°C (1950° F) and aged for 20 hours at 732° F (1350° F), they lose some hardness on being heated to 815° C to 871° C (1500° F to 1600° F). However, they will return close to the originally aged hardness value if they are heated again to 732° C (1350° F). This cycle can be repeated a second time with only small hardness variations.

On the other hand, slight changes in chemical composition or manufacturing procedure can change the final aging properties of these alloys.
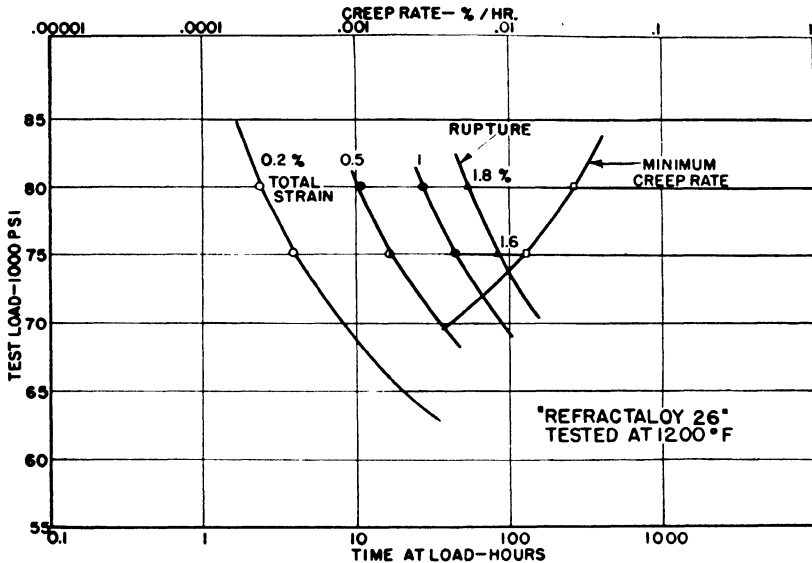
Fig. 5-5. Design curves for "Refractaloy 26" at 650° C (1200° F). Specimens machined from hot rolled bar stock. Heat treatment: solution treatment 1150° C (2100° F) 1 hr., oil quenched, aged 815° C (1500° F) 20 hrs., aged 732° C (1350° F) 20 hrs. (After Scott and Gordon)

If the maximum hardness has not been reached, the imposed stresses in service may cause failure of the part.

The effect of heat treatment on the density of alloy K42B is shown in Table 5-2[16].

Rupture Strength and Creep Strength

Values of the rupture strength and creep strength of alloys K42B and "Refractaloy" 26 from 650 to 815° C (1200 to 1500° F) are given in Table 5-3. Both materials are representative of quenched and aged heat treatments. The heat treatment for alloy K42B consists of solution-treating at 1065° C (1950° F) and tempering at 732° C (1350° F). The heat treat
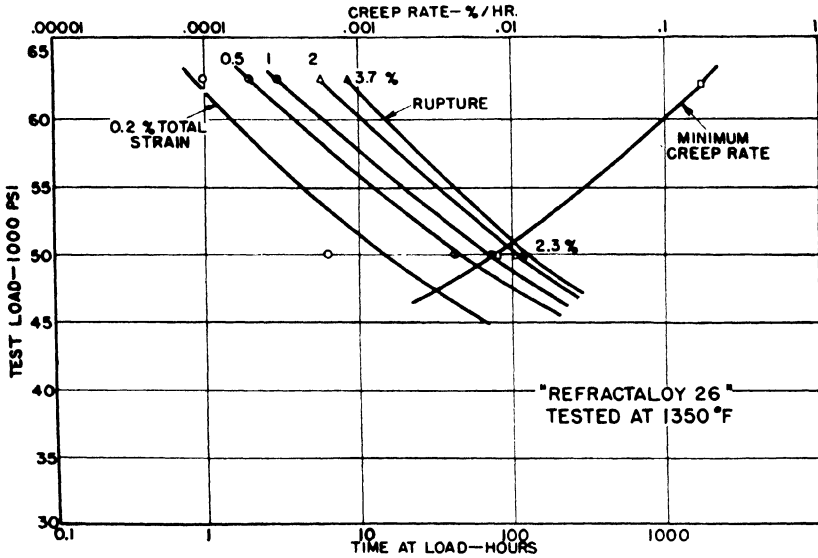
Fig. 5-6.   Design curves for "Refractaloy 26" at 732° C (1350° F).   Specimens machined from hot rolled bar stock.   Heat treatment: solution treatment 1150° C (2100° F) 1 hr., oil quenched, aged 815° C (1500° F) 20 hrs., aged 732° C (1350° F) 20 hrs.   (After Scott and Gordon)
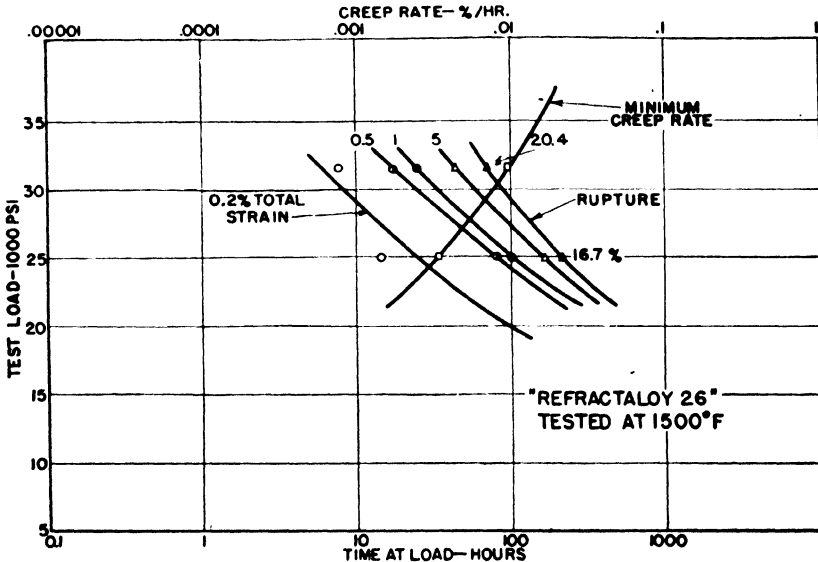
Fig. 5-7.   Design curves for "Refractaloy 26" at 815°' C (1500° F).   Specimens machined from hot rolled bar stock.   Heat treatment: solution treatment 1150° C (2100° F) 1 hr., oil quenched, aged 815° C (1500° F) 20 hrs., aged 732° C (1350° F) 20 hrs.   (After Scott and Gordon)

ment for "Refractaloy" 26 consists of solution-treating at 1150° C (2100° F), tempering at 815° C (1500° F) and tempering again at 732° C (1350° F). On the basis of rupture and creep tests, "Refractaloy" 26 has higher strength and greater ductility.

Design Curves

The design curves of K42B at 650° C (1200° F) in Fig. 2-19, (Chapter 2) and in Figs. 5-3 and 5-4 at 732 and 815° C (1350 and 1500° F) respectively in this chapter represent the same heat treatment as given in Table 5-3.
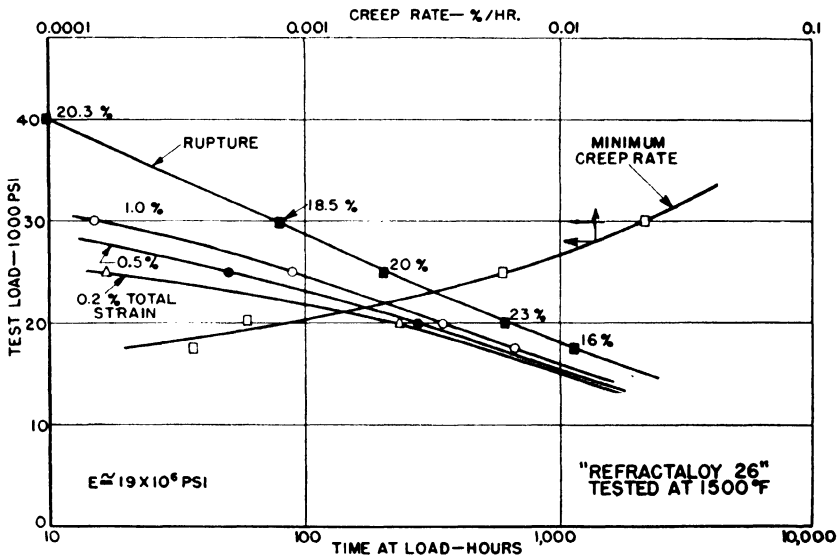
Fig. 5-8. Design curves for "Refractaloy 26" at 815° C (1500° F). Specimens machined from forged bar stock. Heat treatment: solution treatment 1150° C (2100° F) 1 hr., oil quenched, aged 815° C (1500° F) 20 hrs., aged 732° C (1350° F) 20 hrs. (After Scott and Gordon)

This alloy is satisfactory for service in the range of 732° C (1350° F) even though its ductility is less than 1 per cent.

The design curves of "Refractaloy" 26 in Figs. 5-5 to 5-7 from 650 to 815° C (1200 to 1500° F) respectively represent tests on specimens machined from hot-rolled stock. In Fig. 5-8, a design curve is given for "Refractaloy" 26 representative of specimens machined from forged bar stock. The heat treatment for both lots is the same as given in Table 5-3, namely, quenching in oil from 1150° C (2100° F), aging 20 hours at 815° C (1500° F), and finally aging 20 hrs at 732° C (1350° F). This alloy holds its strength well at 815° C (1500° F), but for long periods of service an upper limit of 760° C (1400° F) is recommended[3].

Fatigue Strength

For maximum creep strength at 815° C (1500° F), "Refractaloy" 26 is solution-treated for 1 hour at 1065° C (1950° F), aged 20 hours at 815° C (1500° F), and then aged 20 hours at 732° F (1350° F). At 650° C (1200° F), the fatigue strength of the alloy with such a heat treatment is 52,000 psi for 100 million cycles of reversed bending.

For hot-rolled stock, an endurance limit of 80,000 psi is obtained for "Refractaloy" 26 at 650° C (1200° F). Tests on turbine blades machined from hot-rolled stock give the same fatigue strength, but blades made by forging have a lower fatigue limit[16].

TABLE 5-4. THERMAL EXPANSION OF FULLY HEAT-TREATED ALLOY K42B.[16]

Temp (°F)	Mean Coefficient of Linear Expansion (In/In/°F × 10⁻⁶)
70–200	6.9
70–400	7.4
70–600	7.8
70–800	8.1
70–1000	8.3
70–1200	8.5

TABLE 5-5. THERMAL EXPANSION OF FULLY HEAT-TREATED ALLOY "REFRACTALOY" 26.[16]

Temp (°F)	Mean Coefficient of Linear Expansion (In/In/°F × 10⁻⁶)
70–200	7.8
70–400	7.9
70–600	8.0
70–800	8.1
70–1000	8.2

Thermal Expansion with Temperature

Tables 5-4 and 5-5 show the change of coefficient of thermal expansion with temperature[16].

B. ALLOY S-495*

This alloy contains Cr and Ni with small percentages of Mo, Cb, and W, and an Fe content of approximately 53 per cent. The composition in Table 5-6 is representative of the material on which the elevated-temperature tests are made. With only 15 per cent Cr, this composition cannot withstand temperatures of 815° C[5,6,9,10].

* Allegheny Ludlum Steel Corp.

C. Alloy ATV-3*

This alloy contains Cr, Ni, a small percentage of W and about 50 per

TABLE 5-6. ELEVATED-TEMPERATURE PROPERTIES OF S-495 ALLOY, FORGED.

Chemical Composition

NDRC	C	Mn	Si	Cr	Ni	Mo	Cb	Fe	W
8 & 34	.5	.7	.9	15	20	4	4	53	4

Short-time Tensile Properties: Finish-forged at 1400° F

Temp (°C)	(°F)	Tensile Strength (psi)	Yield Strength 0.2% offset	Elong % in 2"	Reduction of Area (%)
Room	Room	147,750	136,000	6.0	21.7
650	1200	87,625	72,200	24.0	34.3

Stress to Rupture and Elongation Values

| | Temp | | 10 hrs | | 100 hrs | | 1000 hrs | |
Treatment	(°C)	(°F)	Stress (psi)	% Elong in 2"	Stress (psi)	% Elong in 2"	Stress (psi)	% Elong in 2"
(1)	650	1200	47,000	25	35,000	18	26,000	6
(2)	732	1350	33,000*	28	28,000*	20	24,000*	—
(3)	815	1500	24,000	30	18,300	27	14,200	21

Treatment (1) Forged 1204° C (2200° F), air-cooled; finish-forged 760°C (1400° F).
　　　　　(2) 1232° C (2250° F), 2 hrs, water-quenched; 760° C (1400° F), 50 hrs.
　　　　　(3) 1232–1315° C (2250–2400° F), 2 hrs, water-quenched; 760–815° C (1400–1500° F), 16–50 hrs.

* Estimated.

Creep Data

| Temp (°C) | (°F) | Stress for Minimum Creep Rates, % per hr, of | | |
		0.001	0.0001	0.00001
732	1350	22,400	16,100	11,700
815	1500	12,900	10,400	8300
871	1600	7900	5300	3500

Thermal Expansion

Temp (°F)	Mean Coefficient of Linear Expansion (In/In/°F × 10⁻⁶)
70–600	8.94
70–800	9.0
70–1000	9.11
70–1200	9.29
70–1500	9.46

cent Fe. Its composition and elevated-temperature properties are given in Table 5-7[9,10].

* Midvale Steel Co.

D. Alloy N-155*, ("Multimet")†

This series of alloys, known as the N-155 or "Multimet" alloys, contains essentially 20 Cr, 20 Ni, and 20 Co, with small additions of other elements

TABLE 5-7. Elevated-temperature Properties of ATV-3 Alloy, Forged.

Chemical Composition

NDRC	C	Mn	Si	Cr	Ni	W	Fe
51 & 67	0.4	1.4	1.2	15	27.4	4	Bal (50)

Density (gm/cm³): 8.062

Short-time Tensile Tests

Material	Temp (°C)	(°F)	Tensile Strength (psi)	Yield Strength 0.1% offset	Elong % in 2″	Reduction of Area (%)
ATV-3	Room	Room	121,700	84,000	21.5	36.5
As rolled	650	1200	75,200	46,000	25.0	32.2
	732	1350	60,000	30,750	28.0	39.4
	815	1500	42,600	15,100	31.0	38.5
	926	1700	24,100	—	38.5	43

Stress to Rupture and Elongation Values

ATV-3 Alloy 1232° C (2250° F), 30 mins, air-cooled; 815° C (1500° F), 50 hrs.

Temp (°C)	(°F)	10 hrs Stress (psi)	% Elong in 2″	100 hrs Stress (psi)	% Elong in 2″	1000 hrs Stress (psi)
732	1350	29,000	7	18,000	3	11,300
815	1500	16,800	7	10,500	5.5	6600

TABLE 5-8. Physical Properties of "Multimet" (N-155) Alloy.

Chemical Composition (Nominal)

Trade Mark	Common Name	NDRC No.	C	Cr	Ni	Mo	Cb	W	Co	N
"Multimet" (Low-C)	N155	NR21	0.12–0.2	19–23	19–23	2.5–4	0.75–1.5	1.5–3.5	19–23	0.08–0.2
"Multimet" (Med-C)			0.3 –0.5	19–23	19–23	2.5–4	0.75–1.5	1.5–3.5	19–23	0.08–0.2

Material	Density gms/cm³
"Multimet" (Wrought)	8.20

Age-hardening Properties of "Multimet"

Material	As cast	Aged Temp (°F)	Rockwell A Hardness Hours 1	2	5	24	50	100
"Multimet" Low-C Wrought	61	1500	62	62.5	62	61.5	62	62
"Multimet" Med-C Wrought	61	1500	65	65	64.5	64	63.5	63

These alloys are aged after being cast.

and a base of Fe of about 34 per cent.　This is an important series which has received much attention in government-sponsored investigations and

* Universal Cyclops Steel Corp.
† Union Carbide and Carbon Co.

forms the basis of many Ni-Cr-Co-Fe alloys described in Chapter 8. The alloy is forged in both the low-C and medium-C grades. It finds use in sheet form in tail cones and other high-temperature applications. It has the advantage of being cheaper than certain of the alloys considered in

TABLE 5-9. SHORT-TIME TENSILE PROPERTIES OF "MULTIMET" (MEDIUM-C).

Temp (°C)	(°F)	Tensile Strength (psi)	Yield Strength 0.2% offset (psi)	Elong % in 2 in	Reduction of Area (%)	Modulus of Elasticity × 10⁶
Room	Room	82,100	53,600	10.0	10.9	24
		85,000	56,200	11.0	15.9	—
		82,400	55,400	12.0	14.3	—
		85,500	55,400	14.0	14.3	—
510	950	70,000	—	20.0	18.0	—
		71,200	—	19.0	18.8	—
		66,700	—	19.0	15.9	—
		68,400	—	16.0	15.9	—
621	1150	63,100	—	17.0	21.0	—
		63,100	—	18.0	20.2	—
		64,000	—	12.0	21.0	—
		64,100	—	17.0	22.5	—
745	1375	56,500	—	11.0	14.3	—
		55,600	—	16.0	13.7	—
		57,400	—	15.0	15.9	—
		55,400	—	14.0	16.6	—
815	1500	47,700	—	24.0	39.4	—
		45,600	—	25.0	39.4	—

TABLE 5-10. STRESS-RUPTURE DATA OF "MULTIMET" ALLOYS.

Material	Temp (°C)	(°F)	Stress (psi) for Rupture in 10 hrs	100 hrs	500 hrs	1000 hrs
"Multimet"						
Regular	815	1500	28,000	21,500	17,500	16,500
Low-C	815	1500	23,500	18,800	15,000	—
Modified (Med C)	815	1500	27,500	20,500	16,800	14,300
Modified (Low-C)	815	1500	26,000	19,000	15,000	13,000
Hot-worked & Aged (Low-C)	815	1500	—	20,000	14,500	12,500
Hot-worked & Aged (Med-C)	815	1500	29,000	22,000	18,000	16,500
Low-C Solution Heat-treated	926	1700	12,500	7600	5600	4800
Low-C Solution Heat-treated	982	1800	8700	4900	3300	2800
Hot-rolled Low-C	926	1700	10,000	5100	3200	2500

Chapter 6. Some typical compositions with their trade marks are shown in Table 5-8[18].

From the short-time tensile tests in Table 5-9, the medium-C grade maintains a strength of 45,600 psi at 815° C. The stress-rupture values at 815° C for 1000 hours range from 12,500 to 16,500 psi, as shown in Table 5-10. The hot fatigue strength at 815° C varies from 28,000 to 33,000

TABLE 5-11. CREEP DATA OF "MULTIMET", [18]

"Multimet"	Condition	Test Temp. (°C)	(°F)	Stress (psi)	Duration (hrs)	Deformation Upon Application of Load	Creep Rate Per Cent Per Hour At				Total Deformation Per Cent At			
							500 hours	1000 hours	1500 hours	2000 hours	500 hours	1000 hours	1500 hours	2000 hours
(Low C)	2	732	1350	20,000	2041	0.113	0.00031	0.000165	0.000125	0.0001	0.395	0.510	0.585	0.632
(Low C)	2	732	1350	15,000	2016	.094	.00032	.000268	.000361	.000612	.366	.563	.651	.893
(Med C)	1	732	1350	20,000	2016	.092	.00062	.00062	.000725	.000895	.671	.975	1.318	1.724
(Med C)	1	732	1350	15,000	2016	.073	.000116	.00079	.000053	.000038	.254	.298	.327	0.351
(Med C)	1	732	1350	12,000	2016	.058	.000042	.000025	.000017	.000013	.115	.130	.141	.148
(Low C)	1	815	1500	10,000	1590	.054	.0002	.00025	.00062	—	.308	.415	.607	—
(Low C)	1	815	1500	8000	2016	.065	.000063	.000043	.000047	.000048	.157	.180	.206	.230
(Low C)	1	815	1500	7000	2060	.041	.00005	.000035	.000025	.00002	.137	.154	.174	.182
(Low C)	1	815	1500	12,000	1750	.061	.000122	.000107	.000124	.000168(a)	.181	.238	.292	.323(a)
(Low C)	1	815	1500	9000	3400	.064	.00020	.00027	.0003	.00038(b)	.184	.310	.452	.627(b)

Condition 1: Aged 50 hrs at 871° C (1600° F).
Condition 2: Hot-worked and aged.
(a) When discontinued at 1705 hrs.
(b) When discontinued at 3400 hrs. Total deformation 1.34%, rate increasing.

psi, as shown in Table 5-11. Other high-temperature properties are given in Table 5-12.

E. Alloy S-497 Forged*

This alloy, with 15 per cent Cr as shown in Table 5-13, is not sufficiently oxidation-resistant to withstand temperatures of 815° C[5,6,9,10].

TABLE 5-12. ELEVATED-TEMPERATURE PROPERTIES OF "MULTIMET."

Endurance Properties

Specimens stressed in alternate bending at a frequency of 120 cycles per second.

Material	Temp (°C)	Temp (°F)	Heat Treatment Solution	Heat Treatment Aging	Endurance Strength psi At cycles 10^8	Endurance Strength psi At cycles 2.5×10^8
"Multimet" (Low-C)	650	1200	None	50 hrs, 650° C	66,000	—
	815	1500	None	50 hrs, 815° C	33,000	32,000
"Multimet" (Med-C)	815	1500	1204° C, water quench	50 hrs, 815° C	29,000	28,000

Thermal Expansion

Material	Temp (°F)	Mean Coefficient of Linear Expansion (In/In/°F $\times 10^{-6}$)
"Multimet"	70–600	8.70
Low-C	70–800	8.89
Wrought	70–1000	9.10
	70–1200	9.40
	70–1500	9.77
	70–1600	9.90
"Multimet"	70–600	7.96
Med-C	70–800	8.30
Cast	70–1000	8.46
	70–1200	8.58
	70–1500	9.01

F. S-590 Forged*[5,6,9,10]

This alloy is a modification of the composition N-155 with 20 Cr, 20 Ni, and 20 Co, and contains in addition 4 Mo, 4 W, and 4 Cb with about 26 per cent Fe. Its elevated temperature properties are given in Table 5-14.

G. "Refractaloy" 70

When temperatures for service are required above 815° C, alloys which have been precipitation-hardened by Ti are no longer stable. For this service, the refractory metals W and Mo have been alloyed with Co-Ni-

* Allegheny Ludlum Steel Co.

TABLE 5-13. ELEVATED-TEMPERATURE PROPERTIES OF ALLOY S-497, FORGED.

Chemical Composition

NDRC	C	Mn	Si	Cr	Ni	Co	Mo	W	Cb	Fe
45 & 2	0.4	0.5	0.6	15	20	20	4	4	4	Bal (32)

Density (gm/cm³): 8.570

Short-time Tensile Properties: Finish-forged 760° C

Temp (°C)	(°F)	Tensile Strength (psi)	Yield Strength 0.2% offset	Elong % in 2″	Reduction of Area (%)
Room	Room	154,750	138,500	10.5	25.5
650	1200	103,625	89,800	22	25.9

Stress to Rupture and Elongation Values

Treatment	°C)	(F°)	10 hrs Stress psi	Elong % in 2″	100 hrs Stress psi	Elong % in 2″	1000 hrs Stress psi	Elong % in 2″
(1)	650	1200	61,000	17	45,000	9	33,000	4
(2)	732	1350	37,500	23	29,000	26	23,000	—
(3)	815	1500	22,500	28	18,000	19	14,300	12
(4)	871	1600	14,800	23	11,500	15	9000	1

Treatment (1) Forged 1204° C (2200° F); finish-forged 760° C or 1093° C (1400° F or 2000° F), 1 hr, water-quenched; 704° C (1300° F), 16 hrs.
    (2) 1204 to 1232° C (2200 to 2250° F), 12 hrs, water-quenched; 815° C (1500° F), 4 to 50 hrs.
    (3) 1204 to 1232° C (2200 to 2250° F), 12 hrs, water-quenched; 815° C (1500° F), 4 to 50 hrs.
    (4) 1232° C (2250° F), 2 hrs, water-quenched; 871° C (1600° F), 50 hrs.

Creep Data

Temp (°C)	(°F)	Stress psi for Minimum Creep Rates, % per hr., of 0.001	0.0001	0.00001
732	1350	19,700	15,800	12,800
815	1500	12,400	10,000	8100
871	1600	7800	6200	5000

Thermal Expansion

Temp (°F)	Mean Coefficient of Linear Expansion (In/In/°F × 10⁻⁶)
70–600	7.92
70–800	8.08·
70–1000	8.26
70–1200	8.50
70–1500	8.80

Cr-Fe to produce precipitation-hardened structures which offer remarkable stability at this high temperature level. Such an alloy is "Refractaloy" 70* with the composition given in Table 5-15. It contains 30 per cent

* Westinghouse Electric Mfg. Corp.

TABLE 5-14. PROPERTIES OF S-590 ALLOY.

Chemical Composition

NDRC	C	Mn	Si	Cr	Ni	Co	Mo	W	Cb	Fe
74	0.5	0.9	0.6	20	20	20	4	4	4	Bal (26)

Density (gm/cm³): 8.313

Short-time Tensile Tests

Treat-ment	Temp (°C)	(°F)	Tensile Strength (psi)	Yield Strength 0.2% offset	Elong % in 2″	Reduc-tion of Area (%)
(1)	Room	Room	160,500	89,500	10	10.5
(2)	650	1200	81,600	49,000*	27	31
(3)	732	1350	66,875	58,500	27	33

Treatment (1) 1243° C (2270° F), 1 hr, water-quenched; 760° C (1400° F), 16 hrs.
   (2) 1260° C (2300° F), 1 hr, water-quenched; 760° C (1400° F), 16 hrs, air-cooled.
   (3) 1243° C (2270° F), 1 hr, water-quenched; 760° C (1400° F), 16 hrs.

 * 0.02% offset.

Stress to Rupture and Elongation Values

Stress to Rupture and Elongation

Treat-ment	Temp (°C)	(°F)	10 hrs Stress psi	Elong % in 2″	100 hrs Stress psi	Elong % in 2″	1000 hrs Stress psi	Elong % in 2″
(1)	650	1200	69,000*	33	52,000	35	40,000	37
(2)	732	1350	42,000	28	31,500	24	23,500	19
(3)	815	1500	25,500	16–20	20,000	16–20	15,500	8–12
(4)	871	1600	19,000	40–48	14,000	28	10,500	20–21
(5)	926	1700	13,000	60	9200	32	6500	13
(6)	982	1800	9000	56	5500	28	3400	—

 * Estimated

Treatment (1) 1273° C (2325° F), 1 hr, water-quenched; 760° C (1400° F), 16 hrs, air-cooled.
   (2) 1260° C (2300° F), 1 hr, water-quenched; 760° C (1400° F), 10 hrs, air-cooled.
   (3) 1232° C–1273° C (2250–2325° F), 1–2 hrs, water-quenched; 815° C (1500° F), 16–50 hrs, air-cooled.
   (4) 1260° C (2300° F), 1 hr, water-quenched; 871° C (1600° F), 16 hrs, air-cooled.
   (5) 1243° C (2270° F), 1 hr, water-quenched; 926° C (1700° F), 16 hrs.
   (6) 1243° C (2270° F), 1 hr, water-quenched; 982° C (1800° F), 16 hrs.

Creep Data

Temp (°C)	(°F)	Stress psi for Minimum Creep Rates, % per Hr 0.001	0.0001	0.00001
732	1350	—	19,000	14,300
815	1500	12,700	9600	7300

Thermal Expansion

Temp (°F)	Mean Coefficient of Linear Expansion (In/In/°F × 10⁻⁶)
70–600	8.47
70–800	8.43
70–1000	8.54
70–1200	8.61
70–1500	8.97
70–1600	9.20

Co, 20 per cent Ni, 20 per cent Cr, 15 per cent Fe, and smaller percentages of Mo and W to act as precipitation-hardening agents.

"Refractaloy" 70 is billet-forged from 1175° C. Die wear is more severe for this alloy than for those which have been precipitation-hardened by

TABLE 5-15.   ELEVATED-TEMPERATURE PROPERTIES OF "REFRACTALOY" 70.[15]

Chemical Composition (Nominal)[15]

C	Mn	Si	Cr	Ni	Co	Mo	W	Fe
0.05	2	0.2	20	20	30	8	4	15

Effect of Heat Treatment on Density

Condition	Density gm/cc
Hot-rolled	8.618
Solution-treated	8.611
Solution-treated and aged	8.626

Creep Strength (Condition: Forged Bar)

Test Temp (°C)	(°F)	Specified Life (hrs)	Creep Strength 1000 psi for total strain of 0.2%	0.5%	1.0%	Rupture Strength (1000 psi)	Elong % in 2"
650	1200	100	23	31.3	37.3	55.5	25
650	1200	1000	--	20	28.8	42	8
732	1350	100	16	19	22.1	33.4	23
732	1350	1000	—	—	17	23.8	28
815	1500	100	13	14.9	16	18.7	27
815	1500	1000	12	13.5	14.8	15	12
870	1600	100	9.8	—	10.9	11.6	15
870	1600	1000	9	—	9.6	10	6

Heat treatment "Refractaloy" 70: Heated to 1288° C 4 hrs, oil-quenched; heated to 815° C for 240 hrs.

Thermal Expansion of Fully Heat-treated Alloy

Temp (°F)	Mean Coefficient of Linear Expansion (In/In/°F × 10⁻⁶)
70–200	7.2
70–400	7.6
70–600	7.8
70–800	8.1
70–1000	8.3 ·
70–1200	8.4
70–1500	8.9
70–1600	9.1

Ti, as hardness is maintained fairly well at forging temperatures. Reheatings must be frequent and reductions in the die are small.

As would be expected this alloy is difficult to machine, as it work-hardens appreciably when solution-treated to 200 Brinell. A positive feed
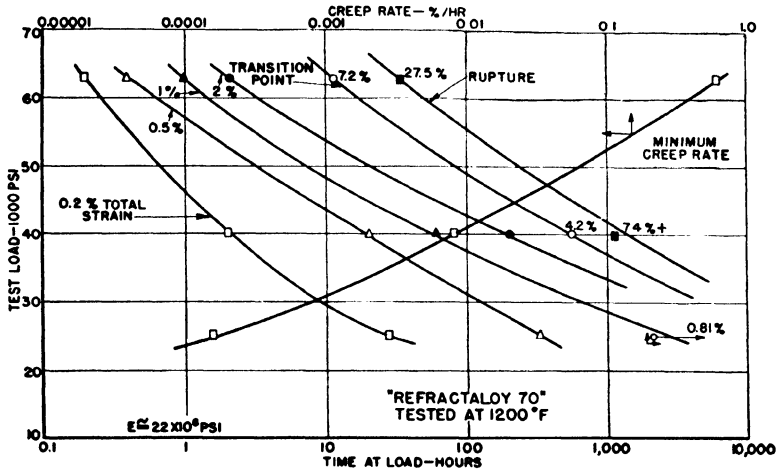
Fig. 5-9. Design curves for "Refractaloy 70" at 650°C (1200° F). Specimens machined from forged bar stock. Heat treatment: solution treatment 1288° C (2350° F) 4 hrs., oil quenched, aged 815° C (1500° F) 240 hrs. (After Scott and Gordon)
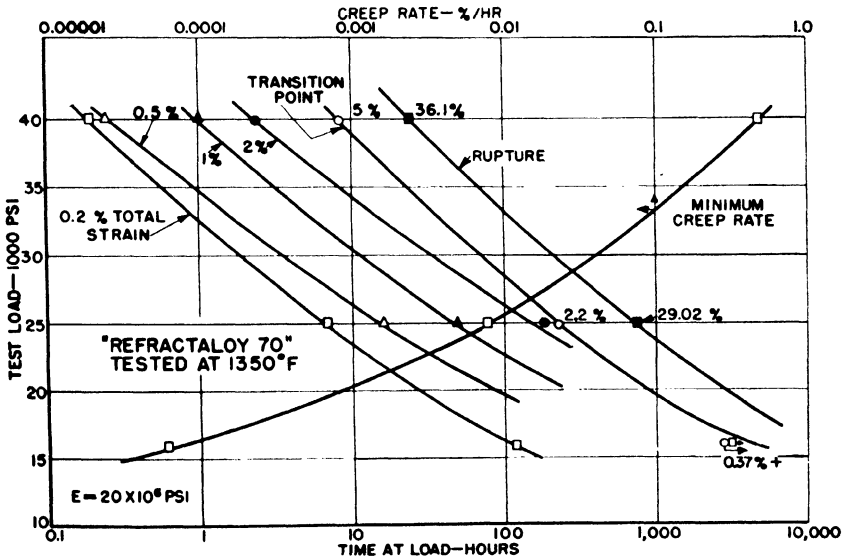
Fig. 5-10. Design curves for "Refractaloy 70" at 732° C (1350° F). Specimens machined from forged bar stock. Heat treatment: solution treatment 1288° C (2350° F) 4 hrs., oil quenched, aged 815° C (1500° F) 240 hrs. (After Scott and Gordon)
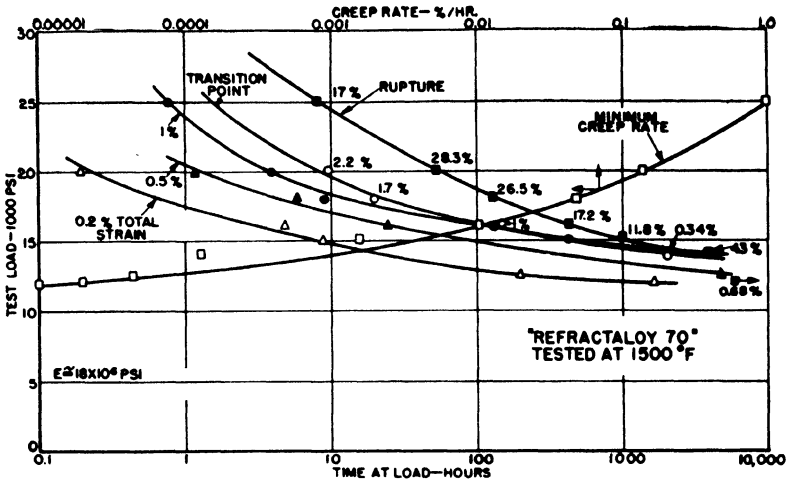
Fig. 5-11. Design curves for "Refractaloy 70" at 815° C (1500° F). Specimens machined from forged bar stock. Heat treatment: solution treatment 1288° C (2350° F) 4 hrs., oil quenched, aged 815° C (1500° F) 240 hrs. (After Scott and Gordon)
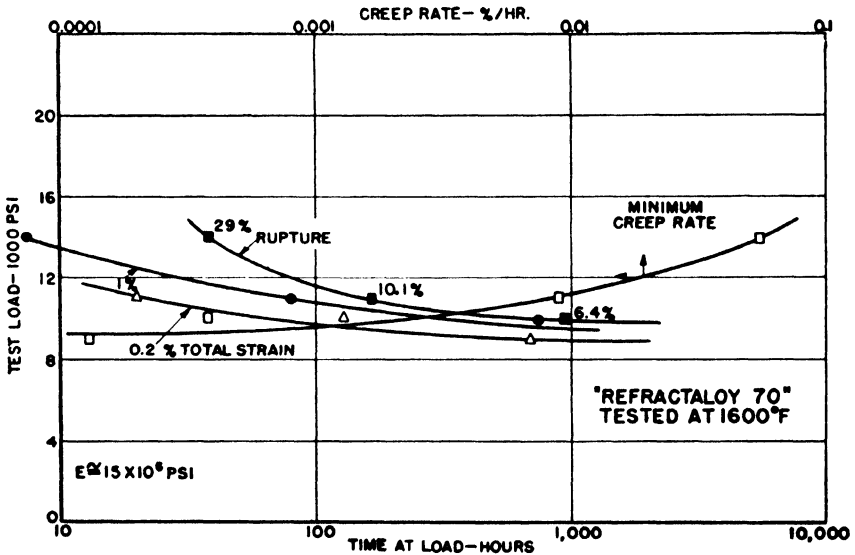
Fig. 5-12. Design curves for "Refractaloy 70" at 871° C (1600° F). Specimens machined from forged bar stock. Heat treatment: solution treatment 1288° C (2350° F) 4 hrs., oil quenched, aged 815° C (1500° F) 240 hrs. (After Scott and Gordon)

is recommended. The aged material can be machined with high-speed steel or W carbide tools.

"Refractaloy" 70 has remarkably stable properties at high temperatures as shown by the required heat treatment of 1288° C (2350° F) for 4 hrs for solution treatment and aging for 240 hrs at 815° C (1500° F). This procedure gives the maximum hardness obtainable, which is 325 Vickers (DPH).

Above a service temperature of 815° C, the alloy undergoes some structural changes which are slow up to 925° C[15,16]. The elevated-temperature properties of "Refractaloy" 70 are shown in Table 5-15. Design curves for this alloy at several temperatures are given in Figs. 5-9 to 5-11 inclusive.

SUMMARY

The alloys discussed in this chapter are all utilized as wrought materials, with the exception of the higher-C "Multimet," which is used in the cast condition. "Discaloy" is hot-rolled, alloy K42B is either hot-rolled or forged, and the other alloys are usually forged. All the alloys listed have optimum high-temperature properties after fairly long aging periods at temperatures of at least 732° C (1350° F).

"Discaloy" is suitable for use at 650° C (1200° F) and the other alloys at 732° C (1350° F) and higher. "Refractaloy" 26 shows the best rupture strength in periods up to 500 hrs at 815° C (1500° F)[5]. For 1000 hours, these alloys show rupture strengths of 15,000 to 18,500 psi. Alloys S-590 and N-155 have good creep strength at 732° C (1350° F); "Refractaloy" 26 has the lowest creep rate, or 0.00001 per cent per 1000 hours at 15,000 psi for the group. In general, these forged alloys are all superior in creep resistance at 732° C (1350° F) to the cast alloys discussed in the following chapter[5].

References

1. Amer. Soc. Metals, Metals Handbook (1948).
2. Austin, C. R. and Halliwell, G. P., "Some Developments in High-temperature Alloys in the Nickel–Cobalt–Iron System," *Trans. Am. Inst. Metallurgical Engrs.*, **99**, 78 (1932).
3. Binder, W. O., "Alloys for High-temperature Service," *Iron Age*, **158**, 46 (1946).
4. Brace, P. H., "A New Alloy for Working at High Temperature," *Metal Progress*, **41**, 354 (1942).
5. Cross, H. C. and Simmons, W. F., "Heat-resisting Metals for Gas Turbine Parts," *A.S.T.M. Symposium on Materials for Gas Turbines*, 3 (June, 1946).
6. Freeman, J. W., Reynolds, E. E., and White, A. E., "High-temperature Alloys Developed for Aircraft Turbosuperchargers and Gas Turbines," *A.S.T.M. Symposium on Materials for Gas Turbines*, 52 (June, 1946).
7. Freeman, J. W., Reynolds, E. E., and White, A. E., 'The Rupture Test Characteristics of Six Precision Cast and Three Wrought Alloys at 1700 and 1800° F," Nat. Advisory Committee for Aeronautics, ARR No. 5J16 (Nov., 1945).

8. Freeman, J. W., Rote, F. B., and White, A. E., "High-temperature Characteristics of 17 Alloys at 1200 and 1350° F," Nat. Advisory Committee for Aeronautics, ACR No. 4C22 (March, 1944).

9. Grant, N. J., Frederickson, A. F., and Taylor, M. E., "Heat-resistant Alloys from 1200 to 1800° F," Research Memo No. 3-47, Navships 250-330-12, Sept. 1 (1947).

10. Grant, N. J., Frederickson, A. F., and Taylor, M. E., "Heat-resistant Alloys from 1200 to 1800° F," *Iron Age*, **161**, Mar. 18, Apr. 8, Apr. 15 (1948).

11. Harder, O. E., "Materials for High-temperature Service," *Materials and Methods*, Manual 4 (Mar., 1945).

12. Knight, H. A., "Superalloys for High Temperature Service," *Materials and Methods*, **23**, 1557 (1946).

13. Newell, H. D., "Properties and Characteristics of 27% Chromium-Iron," *Metal Progress*, **49**, 967B (1946).

14. "Secret War Time High Temperature Alloys Now Available for Peace Time Use," *Machinery*, **52**, 183 (1946).

15. Scott, H. and Gordon, R. B., "Precipitation-hardened Alloys for Gas Turbine Service. II," *Trans. Am. Soc. Mech. Engrs.*, **69**, 583 (1947).

16. Scott, H. and Gordon, R. B., "Precipitation-hardened Alloys for Gas Turbine Service. II," *Trans. Am. Soc. Mech. Engrs.*, **69**, 593 (1947).

17. "Superalloys for High-temperature Service," Report on Cleveland Symposium, *Metal Progress*, **50**, 97 (1946).

18. Sweeney, W. O., "Haynes Alloys for High-temperature Service," *Trans. Am. Soc. Mech. Engrs.*, **69**, 569 (1947).

Chapter 6

Cobalt-base Alloys

Alloys high in Co have excellent wear resistance and are oxidation- and corrosion-resistant under extreme conditions encountered in highly corrosive media and elevated-temperature applications. These properties make them suitable in such diverse situations as valves operating at high temperature, in sheet form for searchlight reflectors, and in castings for the dental trades. During the early days of World War II, the development of the turbosupercharger depended on finding metals or alloys maintaining adequate strength at temperatures of 732° C (1350° F) and above. Attention was soon directed to the Co-base alloys, and their superior performance as gas turbine blades is one of the remarkable developments of the war.

Since forging capacity was low due to war activity, the precision casting process developed by the dental and jewelry trades offered an alternative method of manufacturing. The Co-base alloys in the cast form show remarkable strength at high temperature and are today foremost in the commercial alloys developed for gas turbine service. The precision casting process for their manufacture is described in Chapter 9.

The Co-base alloys considered in this chapter contain 30 to 65 per cent Co with Fe occurring as an impurity of not more than about 3 per cent. Cr is an essential ingredient and is present to the extent of 25 to 30 per cent. Ni is present as a minimum of 1.5 per cent or in amounts of 20 per cent to equal the amount of Cr. Additions of Mo, W, and Cb from 3 to 12 per cent add greatly to high-temperature stability.

While a vast amount of research has been carried out on the Co-base alloys, this chapter is restricted to the compositions which are commercially available. Classification of the Co-base alloys is open to several methods. Here they are considered on the basis of their alloy content as Co-Cr-Mo, Co-Cr-W, Co-Cr-Ni-Mo, Co-Cr-Ni-W. Further modification of the alloy content is the addition of small amounts of Cb to one of the alloys.

The Co-base alloys are obtainable in the form of bar or sheet stock, as forgings or as castings. They are all extremely sensitive to cold-work and thereby harden rapidly. In forming, small reductions and close tem-

perature control are requisites. Castings are sensitive to both sand-blasting and grinding; markings 0.003 in depth result from either of these operations. For certain blades which require shaving of the roll and neck, work-hardening is eliminated by annealing the castings at 1150° C (2100° F). Close temperature control is necessary as above 1176° C (2150° F), the carbides go into solution[3].

The Co-Cr alloys held at temperatures above 704° C (1300° F) age harden to Rockwell C55 to C60 after 50 hours of service. Such a high hardness may well endanger their serviceability at elevated temperatures. The addition of Ni in small amounts maintains a hardness of Rockwell C40 to C42 which decreases the tendency to brittleness[3].

For both the wrought and cast Co alloys, a heat treatment consisting of aging stabilizes the structure for periods of extended service at high temperatures. A generally successful treatment is an aging temperature of 732° C (1350° F) for a period of 50 hours[6]. Heating for longer periods does not increase the hardness to any appreciable extent.

Tests on the Co-base alloys considered in this chapter have been performed on cast specimens with the exception of alloy S-816, which is represented in both the forged and cast state. Much has been written about the advantages of castings over forgings in relation to rupture and creep properties at elevated temperatures. One of the obvious differences in cast and forged structures is the fact that hot-forming produces smaller grains. This difference in grain size is exaggerated by the fact that the precision casting method used in the production of components has required hot refractory molds resulting in slow cooling and very large grains. The effect of grain boundary conditions will be discussed later.

A. "VITALLIUM" (H.S. 21)* (NR-10)

The composition limits for this alloy are as follows[15]:

C	Cr	Ni	Mo	Fe	Co (bal)
0.20–0.35	25–30	1.5–3.5	4.5–6.5	2 max	60

The alloy "Vitallium" consisting of 28 Cr, 60 Co, 3 Ni, 6 Mo, 2 Fe, and 0.25 C, is typical of the first Co-base alloys used for turbosupercharger blading. Its initial success resulted in a wartime production of approximately 40 million blades by the precision casting process[3]. This alloy is subject to age-hardening from Rockwell A65 in the cast condition to Rockwell A69 after being aged at 732° C (1350° F) for a period of 50 hours as shown in Table 6-1. The subsequent tests for stress rupture and creep are representative of samples which have been given this treatment.

---

* Haynes Stellite Co.

The elevated-temperature properties of "Vitallium" are shown in Tables 6-1, 6-2, and 6-3.

TABLE 6-1. PROPERTIES OF "VITALLIUM"[15]

Room-temperature Density: 8.30 gm/cm³

Age-hardening Properties

As cast	Aged Temp (°C)	(°F)	Rockwell A Hardness (hours) 1	2	5	24	50	100
65	732	1350	65	66	66.5	68.5	69.5	71.5
65	815	1500	67	67	68	69	69	71
67	871	1600	69	69	68.5	69	69	70
64.5	871	1600	67.5	67.5	67.5	68.5	68.5	68.5
65	926	1700	66	66.5	67.5	67.5	68	69

Short-time Tensile Properties

Condition	Temp (°C)	(°F)	Tensile Strength (psi)	Yield Strength 0.2% strain (psi)	Elong % in 2 in	Reduction of Area (%)	Young's Modulus of Elasticity × 10⁶
As cast	Room	Room	101,300	82,300	8.2	9.0	36
As cast	538	1000	69,100	39,100	16.4	25.3	33.3
Aged 50 hrs, 732° C (1350° F)	538	1000	86,200	74,400	1.2	4.3	35
As cast	650	1200	74,200	38,000	15.7	36.9	33.7
Aged 50 hrs, 732° C (1350° F)	650	1200	89,300	71,300	2.0	6.0	23.9
Aged 50 hrs, 732° C (1350° F)	732	1350	79,300	61,500	3.8	9.0	24.2
Aged 50 hrs, 732° C (1350° F)	815	1500	59,000	49,000	6.8	19.7	16.8
Aged 50 hrs, 732° C (1350° F)	871	1600	41,600	32,800	19.3	23.6	15.4
As cast	926	1700	42,500	—	27.	52.4	—
As cast	982	1800	33,300	—	35.	52.4	—
Aged 16 hrs, 926° C (1700° F)	982	1800	32,900	—	49.	63.1	—

Average Stress Rupture

Temp (°C)	(°F)	Stress (psi) for Rupture in 10 hrs	100 hrs	500 hrs	1000 hrs
650	1200	70,000	51,900	—	44,200
704	1300	54,000	43,000	—	27,000
760	1400	42,000	24,000	—	15,000
815	1500	—	22,000	15,800	14,200
871	1600	—	16,700	13,400	13,200
926	1700	17,000	13,000	10,700	10,000
982	1800	12,500	9400	7700	7000
1093	2000	4200	—	—	—

During service life, aging of "Vitallium" occurs due to precipitation of certain constituents. As a result, turbosupercharger buckets, after several

TABLE 6-2. CREEP DATA ON "VITALLIUM" (H.S. #21)[16]

Condition	Test Temp (°C)	Test Temp (°F)	Stress (psi)	Duration (hours)	Deformation Upon Application of Load	Creep Rate Per Cent Per Hour At				Total Deformation Per Cent At			
						500 hours	1000 hours	1500 hours	2000 hours	500 hours	1000 hours	1500 hours	2000 hours
1	732	1350	10,000	1800	0.069	0.00013	0.0001	0.00008	0.00008(a)	0.220	0.275	0.318	0.338(a)
1	732	1350	15,000	2106	.068	.0003	.00019	.00007	.0001	.442	.540	.596	.662
2	815	1500	7000	2002	.036	.0001	.000205	.00011	.00009	.127	.208	.296	.344
2	815	1500	7000	2086	.046	.000224	.0001	.00006	.000065	.285	.354	.405	.439
3	871	1600	5500	1488	.063	.000036	.000031	.000031	—	.122	.130	.163	—
3	871	1600	7000	2184	.089	.000125	.000044	.000044	.000044	.258	.308	.330	.353
3	871	1600	10,000	2065	.120	.00033	.00013	.00013	.00013	.790	.900	.980	1.035

Condition 1—Aged 50 hrs at 732° C.
Condition 2—Aged 50 hrs at 815° C.
Condition 3—Aged 50 hrs at 871° C.
(a) When discontinued at 1800 hrs.

TABLE 6-3. DATA FOR DESIGN CURVES FOR "VITALLIUM"[6]

Stress for Indicated Deformation

	At 815°C (1500°F) for		
Transition	10 hrs	100 hrs	1000 hrs
	—	16,800	—
1.0%	25,500	17,800	11,500*
0.5%	21,100	1500	8900
0.2%	16,300	10,600	—
0.1%	—	600	—

* Estimated.

Variation of Grain Size with Modulus of Elasticity (Young's)[3]

Actual Average Grain Diam (in)	ASTM Grain Size	Modulus of Elasticity $\times 10^6$		
		Max	Min	Average
0.003	5	36.9	35.47	35.98
0.012	1	35.2	31.25	33.12
0.050	—	40.6	23.40	31.70

As the grain size becomes finer, the values of the modulus become more consistent. This suggests that a coarse grain structure does not average out the anisotropy as well as the fine grain structure.

Hot Fatigue

Temp		Endurance Strength (psi) at 10^8 cycles)
(°C)	(°F)	
Room	Room	35,000–40,000
650	1200	44,000
815	1500	33,000

Specimens stressed in alternate bending at a frequency of 120 cycles/sec. Material: Cast, no heat treatment.

Hot Impact of Cast "Vitallium"[6]

Temp	Charpy Impact Resistance, ft-lb V Notch
Room	2.9
815° C (1500° F)	11.0

Thermal Expansion[15]

Temp °F	Mean Coefficient of Linear Expansion In/In/°F $\times 10^{-6}$
70–600	7.83
70–800	7.96
70–1000	8.18
70–1200	8.38
70–1500	8.68

Thermal Conductivity (Watt/cm/°C)

Material	200°C (392°F)	300°C (572°F)	400°C (752°F)	500°C (932°F)	600°C (1112°F)
"Vitallium" Wrought	0.170	0.188	0.206	0.224	0.242
"Vitallium" Cast	0.145	0.160	0.175	0.190	0.205

TABLE 6-4. PROPERTIES OF ALLOY 61[15].

Room-temperature Density: 8.54 gm/cm^3

Age-hardening Properties[15]

	Aged Temp		Rockwell A Hardness Hours					
As cast	(°C)	(°F)	1	2	5	24	50	100
65	732	1350	66	68	69.5	71	71.5	71.5
	815	1500	70	69.5	70	70	69.5	69
	871	1600	68	68	67.5	68.5	69	69.5
	926	1700	68	68	69	69	69	71

Average Stress Rupture

Temp		Stress (psi) for Rupture in			
(°C)	(°F)	10 hrs	100 hrs	500 hrs	1000 hrs
650	1200	—	58,000	50,000	47,000
704	1300	50,000	39,000	32,300	30,000
760	1400	—	36,000	28,000	25,000
815	1500	—	27,200	22,500	21,800
871	1600	—	16,000	13,000	12,000
926	1700	17,000	14,000	12,200	11,500
982	1800	12,500	8600	6200	5400

Short-time Tensile Properties[15]

Condition	Temp (°C)	(°F)	Tensile Strength (psi)	Yield Strength 0.2% strain psi	Elong % in 2 in	Reduction of Area (%)	Young's Modulus of Elasticity × 10⁶
As cast	Room	Room	105,400	58,400	7.0	11.2	29
As cast	538	1000	77,100	41,400	14.8	24.1	27.9
Aged 50 hrs, 732° C (1350° F)	538	1000	97,500	72,500	1.7	4.1	27.6
As cast	650	1200	82,900	40,700	15.6	21.5	33.5
Aged 50 hrs, 732° C (1350° F)	650	1200	97,500	74,700	1.8	6.6	25.0
Aged 50 hrs, 732° C (1350° F)	732	1350	79,600	63,100	2.0	6.5	27.0
Aged 50 hrs, 732° C (1350° F)	815	1500	58,500	40,600	7.8	12.7	23.5
Aged 50 hrs, 732° C (1350° F)	871	1600	45,800	33,100	9.8	16.8	21.9
As cast	926	1700	37,500	—	7.0	35.7	—
Aged 16 hrs, 926° C (1700° F)	926	1700	43,600	—	18.0	35.7	—
As cast	982	1800	33,100	—	32.0	40.6	—
Aged 16 hrs, 926° C (1700° F)	982	1800	33,000	—	27.0	39.5	—

hundred hours of service, show little ductility when tested at room temperature. However, the ductility of this alloy at elevated temperatures under service conditions must be considerably higher as demonstrated by

TABLE 6-5. CREEP DATA OF ALLOY 61.[15]

tion	Test Temp (°C) (°F)	Stress (psi)	Duration (hours)	Deformation Upon Application of Load	Creep Rate Per Cent Per Hour At				Total Deformation Per Cent At			
					500 hours	1000 hours	1500 hours	2000 hours	500 hours	1000 hours	1500 hours	2000 hours
1	732 1350	15,000	1560	0.050	0.00025	0.00016	0.00014	—	0.234	0.310	0.379	—
1	732 1350	20,000	1300	.068	.00036	.00042	.00063(a)	—	.292	.518	.712(a)	—
2	815 1500	12,000	2780	.080	.000285	.00011	.000085	.000035(b)	.506	.608	.657	0.682(b)
2	815 1500	12,000	2136	.035	.000022	.000062	.000024	.000024	.176	.201	.205	.222
3	871 1600	5500	2184	.035	.000045	.000025	.000025	.000025(c)	.105	.127	.152	.164(c)
3	871 1600	7000	1536	.024	.00005	.000036	.000036	—	.173	.193	.207	—
3	871 1600	9000	833	.058	.0002	.0001(d)	—	—	.300	.332(d)	—	—

Condition 1: Aged 50 hrs at 732° C.
Condition 2: Aged 50 hrs at 815° C.
Condition 3: Aged 50 hrs at 871° C.

(a) Data for 1300 hrs, fractured after overheating to 900° C.
(b) When discontinued at 2780 hrs, rate 0.0000239%, per hr, total deformation 0.70%.
(c) When discontinued at 2184 hrs.
(d) Specimen broken while removing it from test unit because of burn-out of heating furnace at 833 hrs.

the fact that certain blades, when struck during operation by failure of another part, bent before breaking during test runs[4].

B. ALLOY 61 (H.S. 23)* (NR-63)

This alloy is in general similar to "Vitallium" except that approximately

TABLE 6-6. ELEVATED-TEMPERATURE PROPERTIES OF ALLOY 61[15]

Hot Fatigue

Temp (°C)	Temp (°F)	Endurance Strength (psi) At 10⁸ cycles	At 2.5 × 10⁸ cycles
650	1200	44,000	—
815	1500	38,000	38,000

Specimens stressed in alternate bending at a frequency of 120 cycles/sec.
Material: Cast, no heat treatment.

Hot Impact[6]

Temp	Charpy Impact Resistance, ft-lb V Notch
Room	2.4
815° C (1500° F)	10

Thermal Expansion[15]

Temp (°F)	Mean Coefficient of Linear Expansion In/In/°F × 10⁻⁶
70–600	7.64
70–800	7.96
70–1000	8.18
70–1200	8.48
70–1500	9.24

Thermal Conductivity (Watt/cm/°C)

200° C (392° F)	300° C (572° F)	400° C (752° F)	500° C (932° F)	600° C (1112° F)
0.154	0.176	0.180	0.189	0.212

the same amount of W replaces Mo. The composition limits are as follows[15]:

C	Cr	Ni	W	Fe	Co (bal)
0.35–0.50	23–29	1.5 max	4–7	2 max	65

A typical analysis on which many tests were conducted is as follows[6]:

Material	C	Mn	Si	Cr	Co	W
61	0.4	0.3	0.6	24	68	6

Age-hardening values for alloy 61 are shown in Table 6-4. Elevated-temperature properties are given in Tables 6-4, 6-5, and 6-6.

* Haynes Stellite Co.

TABLE 6-7. PROPERTIES OF ALLOY 6059[15]

Room Temperature Density: 8.21 gm/cm^3

Age-hardening Properties

As cast	Aged Temp (°C)	(°F)	Rockwell A Hardness Hours					
			1	2	5	24	50	100
61	732	1350	62	66	66.5	67	67.5	67.5
59	815	1500	65	64.5	65	65	64.5	65
59.5	871	1600	62.5	62.5	62.5	62.5	64	64.5
61	926	1700	62	62.5	63	63.5	64	66

Short-time Tensile Properties

Condition	Temp (°C)	(°F)	Tensile Strength (psi)	Yield Strength 0.2% strain psi	Elong % in 2 in	Reduction of Area (%)	Young's Modulus of Elasticity × 10^6
As cast	Room	Room	82,500	46,900	7.0	10.3	28.0
As cast	538	1000	50,500	36,600	4.3	10.3	26.2
As cast	650	1200	48,900	35,000	3.8	8.0	27.0
Aged 50 hrs 732° C (1350° F)	732	1350	66,200	50,800	3.2	4.6	20.2
Aged 50 hrs 732° C (1350° F)	815	1500	51,200	38,200	10.1	14.4	18.7
Aged 50 hrs 732° C (1350° F)	871	1600	41,400	30,800	11.5	20.1	18.2
As cast	926	1700	43,000	—	23.0	26.5	—
Aged 16 hrs 926° C (1700° F)	926	1700	45,400	—	16.0	34.0	—
As cast	982	1800	33,400	—	24.0	50.3	—
Aged 16 hrs 926° C (1700° F)	982	1800	33,700	—	26.0	41.7	—

Average Stress Rupture

Temp (°C)	(°F)	Stress (psi) for Rupture in 10 hrs	100 hrs	500 hrs	1000 hrs
650	1200	58,000	55,000	49,000	46,000
704	1300	45,000	37,000	31,500	29,000
760	1400	35,000	28,000	—	—
815	1500	29,200	23,400	19,700	18,400
871	1600	—	16,000	12,900	12,000
926	1700	16,000	12,000	9700	8600
982	1800	12,500	9300	7500	6800

C. ALLOY 6059 (H.S. 27)* (NR-60)

This alloy contains about 30 per cent each of Ni and Co and about 6 per cent Mo. The composition limits are as follows[15]:

C	Cr	Ni	Mo	Fe	Co
0.35–0.50	23–29	30+	5–7	2 max	30 min

* Haynes Stellite Co.

TABLE 6-8. Creep Data of Alloy 6059.[15]

Con-di-tion	Test Temp (°C)	(°F)	Stress (psi)	Duration (hours)	Deformation Upon Application of Load	Creep Data Per Cent Per Hour At				Total Deformation Per Cent At			
						500 hours	1000 hours	1500 hours	2000 hours	500 hours	1000 hours	1500 hours	2000 hours
1	732	1350	12,000	2348	0.042	0.000005	0.000002	0.000002	0.000002	0.135	0.137	0.140	0.140
1	732	1350	15,000	1656	.076	.0044	.0008	.0008	.00008(a)	.405	.479	.519	.533
1	732	1350	20,000	1536	.070	.0045	.0047	.00047	—	.446	.690	.950	—
2	815	1500	12,000	1778	.078	.00019	.0018	.0008	.00008(b)	.305	.500	.575	.600
3	815	1500	12,000	2016	.061	.00014	.000030	.000030	.000030	.170	.250	.256	.290
3	871	1600	7000	2187	.045	.00005	.0003	.00002	.00001	.141	.158	.169	.171
3	871	1600	9000	2070	.050	.00002	.000013	.00001	.00001	.143	.153	.162	.165
3	871	1600	11,000	2059	.060	.00036	.00031	.00026	.00025	.627	.784	.922	.105

Condition 1: Aged 50 hrs at 732° C.
Condition 2: Aged 50 hrs at 815° C.
Condition 3: Aged 50 hrs at 871° C.
(a) When discontinued at 1656 hrs.
(b) When discontinued at 1778 hrs.

A typical analysis is as follows[6]:

Material	C	Mn	Si	Cr	Ni	Co	Mo
6059	0.5	0.2	0.8	26	33	34	6

Age-hardening values of alloy 6059 are given in Table 6-7. Elevated-temperature properties are shown in Tables 6-7, 6-8, and 6-9.

TABLE 6-9. ELEVATED-TEMPERATURE PROPERTIES OF ALLOY 6059.

Hot Fatigue[15]

Temp (°C)	(°F)	Endurance Strength (psi) at 10^8 cycles	at 2.5×10^5 cycles
650	1200	41,000	—
815	1500	31,000	30,000

Specimens stressed in alternate bending at a frequency of 120 cycles/sec. Material: Cast, no heat treatment.

Hot Impact (Alloy 6059, Cast[6])

Temp	Charpy Impact Resistance, ft-lb V Notch
Room	2.3
815° C (1500° F)	3.6

Thermal Expansion[15]

Temp (°F)	Mean Coefficient of Linear Expansion In/In/°F $\times 10^{-6}$
70–600	7.53
70–800	7.79
70–1000	8.04
70–1200	8.29
70–1500	8.67
70–1600	8.84

Thermal Conductivity (watt/cm/°C)

200° C (392° F)	300° C (572° F)	400° C (752° F)	500° C (932° F)	600° C (1112° F)
0.141	0.155	0.166	0.181	0.198

D. ALLOY 422-19 (H.S. 30)* (NR-12)

This alloy is similar to Vitallium except that 15 per cent Ni replaces part of the Co. The composition limits are as follows[15]:

C	Cr	Ni	Mo	Fe	Co (bal)
0.35–0.50	23–29	13–17	5–7	2 max	50

A typical analysis is as follows[15]:

Material	C	Mn	Si	Cr	Ni	Co	Mo	Fe
422-19	0.4	0.5	0.5	25	16	52	6	0.65

* Haynes Stellite Co.

The age-hardening properties of alloy 422-19 are given in Table 6-10. Elevated-temperature properties of this alloy are given in Tables 6-10, 6-11, and 6-12.

TABLE 6-10. PROPERTIES OF ALLOY 422-19[15]

Room-temperature Density: 8.31 gm/cm^3

Age-hardening Properties

| | Aged Temp | | Rockwell A Hardness | | | | | |
As cast	(°C)	(°F)	1	2	Hours 5	24	50	100
65.5	815	1500	69	69.5	69.5	70.5	71	73
65.5	871	1600	68	68.5	69	69	70	72
65.5	926	1700	67.5	68.5	69	70	70	72

Short-time Tensile Properties

Condition	Temp (°C)	(°F)	Tensile Strength (psi)	Yield Strength 0.2% strain (psi)	Elong % in 2 in	Reduction of Area (%)	Young's Modulus of Elasticity × 10^6
As cast	Room	Room	98,100	55,100	5.0	11.9	33.0
As cast	538	1000	62,900	42,500	6.2	9.2	25.6
As cast	650	1200	59,900	37,600	6.3	10.7	27.5
Aged 50 hrs 732° C (1350° F)	732	1350	77,800	61,400	1.8	2.7	24.8
Aged 50 hrs 732° C (1350° F)	815	1500	64,000	47,600	3.0	3.4	25.6
Aged 50 hrs 732° C (1350° F)	871	1600	48,900	35,900	9.6	17.8	17.3
As cast	926	1700	45,200	—	17.0	26.6	—
Aged 16 hrs 926° C (1700° F)	926	1700	47,100	—	18.0	33.3	—
As cast	982	1800	36,300	—	24.0	33.7	—
Aged 16 hrs 926° C (1700° F)	982	1800	37,800	—	21.0	38.7	—

Average Stress Rupture

Temp (°C)	(°F)	Stress (psi) for Rupture in 10 hrs	100 hrs	500 hrs	1000 hrs
732	1350	—	47,000	—	—
815	1500	33,000	28,600	24,100	21,700
871	1600	24,200	18,800	15,500	14,800
926	1700	19,000	16,000	12,300	11,500
982	1800	14,000	10,000	7900	7100
1093	2000	5500	3000	—	—

E. ALLOY X-40 CAST* (NR-71)

This alloy contains 55 per cent Co, 25 per cent Cr, 10 per cent Ni, 7 per cent W, and Fe present as an impurity. A representative analysis is given in Table 6-13. It has had a wide use in many high-temperature com-

---

* General Electric Co.

TABLE 6-11. CREEP DATA OF ALLOY 422-19.[15]

Con-di-tion	Test Temp (°C)	(°F)	Stress (psi)	Duration (hours)	Deformation Upon Application of Load	Creep Rate Per Cent Per Hour At				Total Deformation Per Cent At			
						500 hours	1000 hours	1500 hours	2000 hours	500 hours	1000 hours	1500 hours	2000 hours
1	732	1350	15,000	2016	0.058	0.000210	0.000100	0.000020	0.000020	0.190	0.245	0.255	0.272
2	815	1500	12,000	1997	.069	.00021	.000068	.000035	.000035	.430	.487	.507	.523
2	815	1500	12,000	2082	.060	.000191	.000079	.000061	.000046	.397	.453	.489	.524
1	815	1500	12,000	2016	.065	.000090	.000053	.000015	.000015	.172	.190	.205	.212
3	871	1600	9000	2207	.044	.000065	.000015	.000015	.00001(a)	.230	.249	.256	.260
3	871	1600	11,000	2250	.051	.000085	.00002	.00002	.00002	.284	.301	.313	.325
3	871	1600	12,000	2035	.080	.00027	.00023	.00011	.00028	.700	.815	.880	.980

Condition 1: Aged 50 hrs at 732° C.
Condition 2: Aged 50 hrs at 815° C.
Condition 3: Aged 50 hrs at 871° C.

(a) When discontinued at 2207 hrs, rate less than 0.00001" per hr, elongation 0.26%.

ponents due to its excellent performance. The properties of this alloy
are given in Table 6-13. At 815° C (1500° F) this alloy has a rupture
strength of 23,200 psi after 1000 hrs with 7 per cent elongation. At the
same temperature, its creep rate is 0.00001 per cent per hr for a stress of
10,200 psi.

TABLE 6-12. ELEVATED-TEMPERATURE PROPERTIES OF ALLOY 422-19

Data for Design Curves[6]

Stress for Indicated Deformation

	871°C (1600°F) (psi)		
	10 hrs	100 hrs	1000 hrs
Transition	—	17,400	14,100
1.0%	19,900	16,000	13,250
0.5%	—	12,700	10,800*
0.2%	12,400	9800	—
0.1%	8750	—	—

* Estimated.

Hot Fatigue[15]

Temp	Endurance Strength (psi) at 10⁵ cycles
650° C (1200° F)	52,000

Specimens stressed in alternate bending at a frequency of 120 cycles/sec.
Material: Cast, no heat treatment.

Hot Impact[6]

Temp	Charpy Impact Resistance, ft-lb V Notch
Room	1.5
815° C (1500° F)	3.6

Thermal Expansion[15]

Temp (°F)	Mean Coefficient of Linear Expansion In/In/°F × 10⁻⁶
70–600	7.70
70–800	7.86
70–1000	7.91
70–1200	8.07
70–1500	8.42
70–1600	8.54

F. ALLOY X-50 CAST* (NR-72)

A typical analysis of alloy X-50 together with its properties at elevated
temperature is given in Table 6-14. It contains somewhat more C, Cr,
Ni, and W than alloy X-40.

* General Electric Co.

TABLE 6-13. PROPERTIES OF ALLOY X-40, CAST[15]

Chemical Composition

NDRC	C	Mn	Si	Cr	Ni	Co	Fe	W
71	0.5	0.6	0.7	25	10	55	0.6	7

Room-temperature Density: 8.608 gm/cm^3

Age-hardening Properties

As cast	Aged Temp (°C)	(°F)	Rockwell A Hardness Hours 1	2	5	24	50	100
64	815	1500	66	69.5	70	69.5	70	70
64	871	1600	66.5	67.5	67.5	67	68	70
64	926	1700	67	68	69	68.5	69.5	71

Short-time Tensile Properties[6]

Treatment	Temp (°C)	(°F)	Tensile Strength (psi)	Yield Strength 0.2% strain (psi)	Proportional Limit (psi)	Elong (% in 2")	Reduction of Area (%)
As cast	Room	Room	101,000	74,100	—	11	14.0
As cast	650	1200	76,800	37,400	23,400	18	28.1
As cast	650	1200	77,300	37,800	22,500	20	28.6
Aged 50 hrs 732° C (1350° F)	732	1350	82,200	53,400	31,300	7	8.1
Aged 50 hrs 732° C (1350° F)	732	1350	69,200	53,800	33,100	2.3	7.0
Aged 50 hrs 732° C (1350° F)	815	1500	57,500	42,000	26,200	14	15.4
Aged 50 hrs 732° C (1350° F)	815	1500	61,400	47,500*	32,400	5	12.1
Aged 50 hrs 732° C (1350° F)	871	1600	48,500	35,200	22,900	14.3	18.1
Aged 50 hrs 732° C (1350° F)	871	1600	48,600	37,300	24,000	—	—

* Estimated.

Stress-to-Rupture and Elongation Values[6]

Treatment	Temp (°C)	(°F)	10 hr Stress (psi)	Elong (%)	100 hr Stress (psi)	Elong (%)	1000 hr Stress (psi)	Elong (%)
(1)	650	1200	66,000	—	55,000	—	46,000	—
(2)	732	1350	59,000	20	44,800	31	34,000	37
(3)	815	1500	34,000	30	28,000	12	23,200	7
(4)	871	1600	25,000	36	21,300	19	18,500	7.5
(5)	926	1700	21,000	39	17,300	22	14,400	16
(6)	982	1800	13,300	46	11,300	24	9800	8

Treatment

(1) Not known.
(2) Aged 50 hrs, 732° C.
(3) Aged 50 hrs, 732 to 815° C.
(4) Aged 50 hrs, 871° C.
(5) As cast.
(6) As cast.

TABLE 6-13—*Continued*

Creep Data[16]

Temp (°C)	Temp (°F)	Stress for Minimum Creep Rates (% per hr) 0.001	0.0001	0.00001
815	1500	18,500	13,700	10,200
871	1600	15,700	11,700	8700

Thermal Expansion

Temp (°F)	Mean Coefficient of Linear Expansion In/In/°F $\times 10^{-6}$
70–800	7.88
70–1000	7.98
70–1200	8.18
70–1500	8.43
70–1600	8.79

Data for Design Curves[6]

Stress for Indicated Deformation

	815°C (1500°F) 10 hrs	100 hrs	1000 hrs	871°C (1600°F) 10 hrs	100 hrs	1000 hrs
Transition	27,500*	22,100*	21,500	20,400*	18,300*	18,200
1.0%	23,800	—	—	19,000	16,500	16,000†
0.5%	20,000	16,800	—	—	—	—
0.2%	17,600	14,200	11,200	14,400	12,500	9800
0.1%	13,500	10,700	—	12,000	7600	—

* Stress for 2% deformation, transition not reached.
† Stress for 2% deformation.

Hot Fatigue[16]

Temp	Endurance Strength (psi at 10^8 cycles)
650° C (1200° F)	56,000

Specimens stressed in alternate bending at a frequency of 120 cycles/sec.
Material: Cast, no heat treatment.

Hot Impact[6]

Temp	Charpy Impact Resistance, ft-lb V Notch
Room	2.3
815° C (1500° F)	5

G. ALLOY S-816* FORGED AND CAST

This alloy contains 45 per cent Co, 20 per cent Cr, 20 per cent Ni, 4 per cent W, 4 per cent Cb, 3 per cent Mo, and 0.4 per cent C (bal. Fe). The ratio of C to Cb is one of the important factors in maintaining a satisfactory composition[17]. In spite of the presence of this amount of C, alloy S-816 is produced in both forgings and castings and has excellent elevated-

* Allegheny Ludlum Steel Co.

temperature properties at 815 to 870° C (1500 to 1600° F). Because of its superior performance, manufacturing data are given here in some detail. It is commercially available in billets and bars and has been experimentally produced in sheet, wire and welded tubing. In spite of its high alloy content and the absence of Fe, except as in impurity, the alloy responds well to fabrication. It is also available in the cast form and as a precision

TABLE 6-14. ELEVATED-TEMPERATURE PROPERTIES OF ALLOY X-50[6]

Chemical Composition

NDRC	C	Mn	Si	Cr	Ni	Co	W	Fe
72	0.8	0.6	0.5	23	20	40	12	Bal (3)

Room-temperature Density: 8.855 gm/cm³

Stress-to-Rupture and Elongation Values

Treat-ment	Temp (°C)	(°F)	10 hrs Stress (psi)	Elong in 2″ (%)	100 hrs Stress (psi)	Elong in 2″ (%)	1000 hrs Stress (psi)	Elong in 2″ (%)
(1)	815	1500	38,400	28	29,200	14.5	22,500	5
(2)	871	1600	25,400	24	20,100	17	16,200	10
(3)	926	1700	19,700	27	16,300	16	13,800	2
(4)	982	1800	12,200	30	9700	15	7800	8

Treatment

 (1) Aged 50 hrs, 815° C.
 (2) Aged 50 hrs, 871° C.
 (3) As cast
 (4) As cast

Creep Data[6]

Temp (°C)	(°F)	Stress for Minimum Creep Rates, % per hr 0.001	0.0001	0.00001
815	1500	18,200	13,500	10,100
871	1600	13,200	10,500	8500

Hot Impact[6]

Temp	Charpy Impact Resistance, ft-lb V Notch
Room	2.4
815° C (1500° F)	3.1

cast product finds wide use at 815° C (1500° F). It has a further advantage in resisting corrosion in hot fuel gases. In production, care must be taken during welding, but both arc welding and atomic hydrogen welding are suitable methods[17].

Alloy S-816 in the forged condition is heat-treated by solution treatment in the range of 2150 to 2300° F followed by water-quenching. Time for heating may be ½ hour for thin sections as small turbine blades, sheet and strip, and 3 hours for heavier sections, such as turbine wheels 3 to 4 inches

TABLE 6-15. PROPERTIES OF ALLOY S-816[6, 17]

Chemical Composition

NDRC	C	Mn	Si	Cr	Ni	Co	Mo	W	Cb	Fe
76	0.4	0.6	0.3	20	20	45	3	4	4	Bal (2)

Room-temperature Density: 8.587 gm/cm³ (Forged alloy)

Hardness

Water Quenched From 1 Hour at:		Rockwell C*
(°C)	(°F)	
1176	2150	31
1204	2200	30
1232	2250	29
1260	2300	29
1290	2350	28

* These values are about 2 to 4 points above minimum.

Solution Treated 1260°C (2300°F) Aged 16 Hr. at:		Rockwell C
(°C)	(°F)	
538	1000	25–26
650	1200	25–26
704	1300	25–26
760	1400	24–25
815	1500	24–25
871	1600	25–26
926	1700	26
982	1800	26
1038	1900	23

Short-time Tensile Properties (Forged Alloy)

Treat-ment	Temp		Tensile Strength (psi)	Yield Strength 0.2% offset	Elong (% in 2″)	Reduction of Area (%)
	(°C)	(°F)				
(1)	Room	Room	175,000	73,000	39	45
(2)	650	1200	120,200	—	17	22
(3)	732	1350	98,900	—	15	22
(4)	815	1500	78,260	—	12	21
(5)	871	1600	59,770	—	18	20
(6)	926	1700	48,180	—	14	17

Treatment

(1) As rolled.
(2) 1260° C (2300° F), 1 hr, water-quenched; 760° C (1400° F), air-cooled.
(3) Same.
(4) Same.
(5) Same.
(6) Same.

TABLE 6-15—*Continued*

Short-time Tensile Properties (Cast alloy)

Treat-ment	Temp (°C)	(°F)	Tensile Strength (psi)	Elong (% in 2 in)	Reduc-tion of Area (%)
(1)	Room	Room	100,000	6.0	7.4
(1)	815	1500	61,780	17.0	18.0
(2)	Room	Room	104,400	1.0	1.5
(2)	815	1500	70,500	8.0	15.0
(3)	Room	Room	122,300	0.5	1.5
(3)	650	1200	100,500	3.5	10.5
(3)	815	1500	71,062	3.5	14.0

Treatment

(1) Cast.
(2) Aged 100 hrs at 815° C (1500° F).
(3) 1 hr at 1260° C (2300° F), water-quenched; aged 6 hrs at 760° C (1400° F).

Stress-to-Rupture and Elongation Values (Cast Alloy)

Treat-ment	Temp (°C)	(°F)	10 hrs Stress (psi)	Elong in 2" %	100 hrs Stress (psi)	Elong in 2" %	1000 Hrs Stress (psi)	Elong in 2" %
(1)	650	1200	72,000	---	58,000	—	46,000	—
(2)	732	1350	54,000	—	40,000	16	29,000	—
(3)	815	1500	35,500	15	28,500	3	22,000	1
(4)	871	1600	24,500	19	18,000	17	13,000*	11
(5)	926	1700	18,000	7	14,800	6	12,000*	2*
(6)	982	1800	14,000	16	10,500	10	8000	6

Treatment

(1) As cast.
(2) As cast.
(3) 1260° C (2300° F), 1 hr, water-quenched; aged 16–50 hrs, 732–815° C (1350–1500° F).
(4) As cast.
(5) Same.
(6) Same.

* Estimated

Forged, Heat-treated Alloy

Hours	Stress to Rupture in Time Indicated 650°C (1200°F)	732°C (1350°F)	815°C (1500°F)
100	63,000	41,500	25,500
1000	51,000	32,500	19,400
10,000	40,000	25,500	14,500
*100,000	31,500	19,700	10,900

* Extrapolated

TABLE 6-15—*Concluded*

Creep Data (Forged Alloy)

Temp		Stress for Minimum Creep Rates, % per hour		
°C	°F	0.001	0.0001	0.00001
732	1350	26,800	18,000	12,200
815	1500	16,400	11,500	8100
871	1600	8500	5800	4000

10,000-Hour Creep Tests at 815° C (1500° F)

Treat-ment	Stress (psi)	Creep Rate % per Hr at		Final Reading	Length of Test (hr)
		10,000 hrs	20,000 hrs		
1290° C (2350° F), water-quenched	8500	0.00003	0.000029	0.000113	10,103

Thermal Expansion

Temp (°F)	Mean Coefficient of Linear Expansion In/In/°F $\times$ 10⁻⁶
70–500	7.6
70–1000	8.0
70–1600	9.4

Hot Fatigue Strength (Cast Alloy)

Temp	Endurance Strength (psi at 10^8 cycles)
815° C (1500° F)	33,000

Specimens stressed in alternate bending at a frequency of 120 cycles/sec.

Hot Impact Properties (Forged Alloy)

Temp	Charpy Impact Resistance, ft-lb	
	Keyhole Notch	V Notch
Room	9	18
815° C (1500° F)	25	54

thick. If there are present very low strains of less than 1 per cent resulting from various types of previous working, either hot, warm, or cold, grain growth may occur at solution-treating temperatures above 1150° C (2100° F). It is for this reason that the final reductions during hot working must be of an order to prevent such an occurrence.

The subsequent heat treatment is aging in the range between 732 and 815° C (1350 to 1500° F). The amount of precipitation of the micro-constituents at this period is influenced by the time and the temperature. If the time of aging is too long, the ductility may fall to 1 per cent. The hardness of the alloy after heat treatment is a factor in obtaining optimum elevated-temperature properties. In certain instances a hardness of Rockwell C22 has resulted in an alloy which gave satisfactory service. However, a hardness of C26 or higher obtained by solution-treating at 1260° C (2300° F) and aging at 760° C (1400° F) is recommended. Higher hard-

nesses than this value can be obtained, as for example cold-working after solution treatment, which can produce an alloy above Rockwell C34. Also a 20 per cent cold reduction after solution treatment will result in an alloy with a hardness of C44 after the aging treatment. For many applications, the aging heat treatment consists of heating at 760° C (1400° F) for 6 hours. There is some difference of opinion as to whether cast S-816 alloy should be heat-treated by aging or used in the cast condition. The fatigue strength of S-816 at 815° C (1500° F) is 33,000 psi for 100 million cycles of stress. The elevated temperature properties of this alloy are shown in Table 6-15. Design curves which are approximations are shown in Fig. 6-1 at 732° C (1350° F).
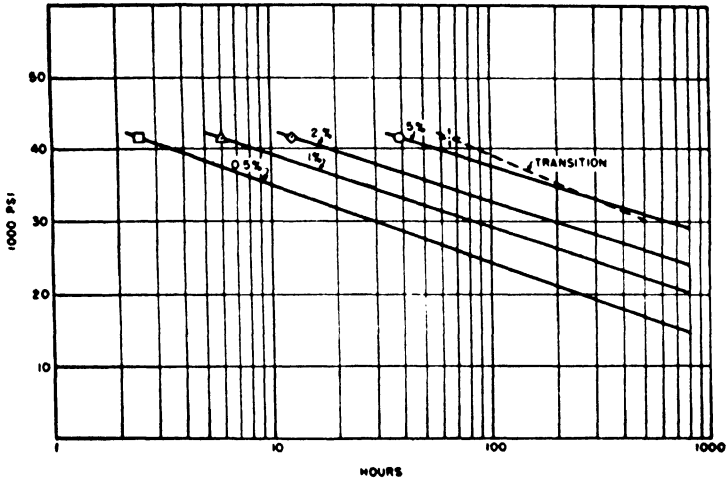
Fig. 6-1. Approximate design curves of forged alloy S-816 at 732° C (1350° F). (After Wilson)

The rupture strength at 815° C (1500° F) for 1000 hours is 19,400 psi for the forged alloy and 22,000 psi for the cast alloy. The creep strength at the same temperature is 8100 psi for a creep rate of 0.00001 per cent per hour. The alloy is also reported under test for 10,103 hours at 8500 psi at which period the creep rate is 0.00003 per cent per hour based on 10,000 hours.

Comparison of Properties of Cast Co-base Alloys

I. **Age-hardening.** All the cast alloys age-harden in the temperature range of 732 to 926° C (1350 to 1700° F) from Rockwell A 62 to 65 after 50 hours to Rockwell A 70 to 71 after 100 hours.

II. **Short-time Tensile Test.** *Tensile Strength.* In all the alloys, the

increase in hardness from aging also results in an increase in tensile strength over the cast condition. At 538 and 650° C (1000 and 1200° F), the cast alloy 61 and both cast and forged alloys S-816 show the highest tensile strengths. At 732, 815, and 871° C (1350, 1500 and 1600° F), the differences in short-time tensile strength are less marked, with the exception of S-816, which maintains a consistently higher value. Many of the tests represent strain rates of 0.02 in per min up to 0.2 per cent offset yield strength and then a strain rate of 0.06 in per min to rupture[6].

Ductility. At 732° C (1350° F), all the alloys have a decrease in ductility to less than 5 per cent.

Modulus of Elasticity. Very coarse grains cause variations in values of the modulus of elasticity. Fine grains tend to produce more uniform results.

III. Rupture Strength. The stress rupture tests on the cast specimens are reported for both 0.250 and 0.505 in diameter rods cast in refractory molds. Results of tests do not indicate any essential difference between the two sizes. Many of the early tests under government sponsorship determined only the time to rupture, the elongation, and the reduction in area. This procedure has been largely replaced by a complete time deformation curve to indicate the stress-time relationship up to failure[6].

At 815° C (1500° F), alloys 61, 422-19, X-40, S-816, and X-50 have stress-rupture values at 100 hours of 27,000 to 29,000 psi and at 1000 hours of 21,000 to 23,000 psi. Alloys "Vitallium" and 6059 fall below these values.

At 870° C (1600° F), all the cast Co-base alloys are definitely superior to the forged alloys described in the preceding chapter. The cast Co-base alloys "Vitallium", 61, 6059, 422-19, X-40, X-50, and S-816 have stress rupture values at 100 hours of 16,000 to 21,000 psi and at 1000 hours of 12,000 to 16,000 psi.

IV. Creep Strength. Creep data are difficult to evaluate, since the limitations of space do not allow the reproduction of time-deformation curves. A presentation is here given of the creep rate and the total deformation at periods of 500, 1000, 1500, and 2000 hours. The tests carried out at 732° C (1350° F) under government sponsorship are conducted for the most part at 15,000 and 20,000 psi. For alloys with creep rates greater than 0.00001 per cent per hour for 15,000 psi, tests are also given at 12,000 psi.

At 815° C (1500° F), many creep tests are reported. One specification required a material for a creep rate of 0.00001 per cent per hour at 7000 psi and at this temperature. With the exception of "Vitallium", all the cast Co-base alloys exceed this value[6].

V. Hot Impact Tests. The specimens for the Charpy impact tests

are the V notch type, since drilling a keyhole notch is very difficult in cast Co-base alloys. The room-temperature impact values are lower in all the cast Co-base alloys than the values at 815° C (1500° F). However, all the cast alloys have much lower impact strength at both room temperature and elevated temperature than do the wrought alloys. The amount of ductility required for high-temperature service is still in certain respects difficult to evaluate. The excellent service given by these relatively brittle alloys is surprising when considered on the basis of previous concepts regarding deformation under service conditions.

VI. Hot Fatigue Tests. The fatigue strength of the cast Co-base alloys at 650° C (1200° F) is above 40,000 psi for 100 million cycles of stress. Alloy 422-19 at this temperature has a fatigue strength of 52,000 psi and alloy X-40 has a fatigue strength of 56,000 psi. At 815° C (1500° F), the fatigue strength of those Co-base alloys tested is above 30,000 psi for 100 million cycles of stress.

H. STRUCTURE OF CO-BASE ALLOYS

Pure Co undergoes a transformation on cooling from a face-centered cubic to a close-packed hexagonal structure at a temperature of about 420° C (788° F). The existence of yet another change in the lattice structure of Co above the broad temperature range of 850 to 1050° C (1562 to 1922° F) is also a possibility. The Co-rich end of the binary Co-Fe system consists of a hexagonal lattice structure called the epsilon phase. The Co-rich end of the Co-Ni binary system also has a hexagonal lattice structure (beta phase).

In the Co-base alloys discussed in this group, Fe varies from about 1 to 3 per cent and Ni from about 2 to 32 per cent. Cr is present in amounts from about 19 to 27 per cent. Co itself also varies from 36 to 70 per cent. The outstanding characteristic of these various compositions is the sluggishness with which the structural transformations take place. From x-ray evidence to date, a face-centered cubic phase has been identified, as well as the presence of a hexagonal constituent in small amounts.

X-ray examinations of alloys "Vitallium", 61, and 6059 reveal diffraction patterns which vary with heat treatment. On a qualitative basis, the alloys undergo changes indicating the appearance or suppression of two lattices, one cubic and one hexagonal. The changes of structure with heat treatment are shown as follows[3]:

Material	Heat Treatment	Lattice	
		Hexagonal	Cubic
"Vitallium"	As cast	Some	Large amount
	Annealed 1163° C (2125° F)	None	All
	Aged 800° C (1475° F), 50 hrs	Present	Small amount
	Aged 800° C (1475° F), 100 hrs	More	Much less

Alloy 61	As cast	Small amount	Large amount
	Annealed 1163° C (2125° F)	Small amount	Large amount
	Aged 800° C (1475° F), 50 hrs	None	All
	Aged 800° C (1475° F), 100 hrs	None	All
Alloy 6059	As cast	None	All
	Annealed 1163° C (2125° F)	None	All
	Aged 800° C (1475° F), 50 hrs	None	All
	Aged 800° C (1475° F), 100 hrs	None	All

Microstructure

In these high-Co alloys containing 0.25 to 0.45 per cent C, three different carbides have been identified by x-ray diffraction and by chemical analyses of residues from the alloys obtained by electrolysis in a 10 per cent solution
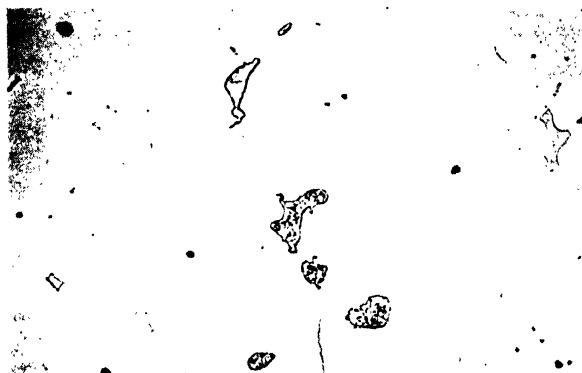
Fig. 6-2. "Vitallium" (H.S. 21) water quenched from 1300° C (2375° F). Etched with 6 per cent aqua regia. Magnification 250×. (After Badger and Sweeney)

of HCl. They are Cr_4C with a cubic lattice structure, Cr_7C_3 with a hexagonal structure, and a constituent considered as M_6C, where M may be Co, Cr, or Mo[3].

Etching techniques reveal these carbides in different colors under the microscope as follows: (1) a light etching is given in 2 per cent chromic acid, followed by (2) an immediate etching in alkaline potassium permanganate (20 per cent $KMnO_4$, 8 per cent NaOH) for 7 seconds. The chromium carbide, Cr_4C, is etched brown; the Cr_7C_3 is etched light yellow, and the third constituent varies in color between red and green tints, although, occasionally, it may have bluish tints. Another satisfactory etching solution for Co-base alloys is a 6 per cent aqua regia mixture applied electrolytically.

A series of photomicrographs of "Vitallium" illustrate some of the effects of heat treatment. In Fig. 6-2, heating "Vitallium" to 1300° C (2375° F) and water-quenching shows that the lamellar constituent is dissolved and

suppressed from appearing at the grain boundaries in a specimen etched with 6 per cent aqua regia. The same specimen in Fig. 6-3, etched in the alkaline permanganate solution described above, shows gray areas of Cr_4C, small areas where the film is cracked or reticulated, which is characteristic of the M_6C constituent, and very dark areas which comprise a
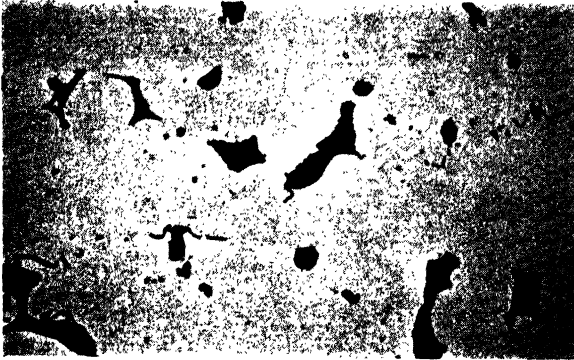
Fig. 6-3. Same as Fig. 6-2, but etched with alkaline permanganate. Magnification 250×. (After Badger and Sweeney)

Fig. 6-4. "Vitallium" (H.S. 21) furnace cooled from 1300° C (2375° F). Etched with 6 per cent aqua regia. Magnification 250×. (After Badger and Sweeney)

eutectic containing all the carbides. The background in both Figs. 6-2 and 6-3 is the Co-rich solid solution.

Furnace-cooling "Vitallium" from 1300° C (2375° F) results in a lamellar constituent at the grain boundaries, as shown in Fig. 6-4 with the 6 per cent aqua regia etch and in Fig. 6-5 with the alkaline potassium permanganate etch. In the latter photomicrograph, the light gray lamellar constituent is Cr_4C and the very dark areas, a eutectic containing all the

carbides.   A typical microstructure of "Vitallium", as cast and cooled in a refractory mold, is shown in Fig. 6-6, where only a moderate amount of lamellar constituent appears at the grain boundaries.
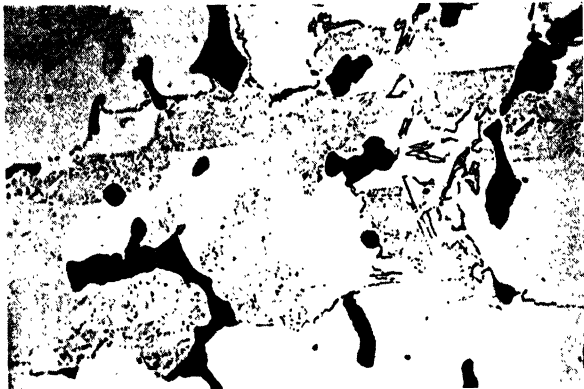
Fig. 6-5.   Same as Fig. 6-4, but etched with alkaline potassium permanganate. Magnification 250X.   (After Badger and Sweeney)
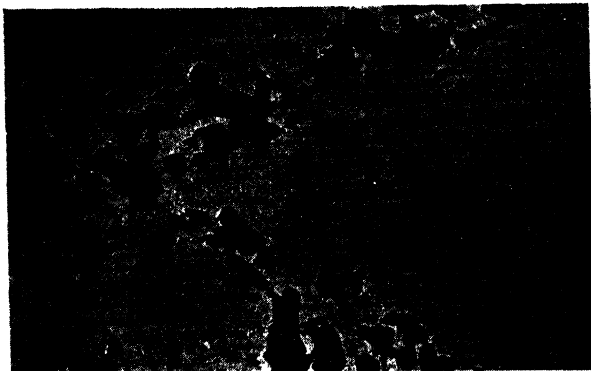
Fig. 6-6.   "Vitallium" (H.S. 21).   Structure typical of investment casting.   Magnification 100X.

I. Comparison of Forgings versus Castings

There are certain instances where the forged Cr-Ni-Co-Fe alloys have properties differing from Co-base alloys in the cast condition.

I. At room temperature, forgings have higher impact strength than castings[6]. At 815° C (1500° F), both forgings and castings have higher impact values than at room temperature.

II. The short-time tensile properties are higher for wrought than for cast alloys.

III. In stress-rupture tests at 815° C (1500° F), duplicate heats give more consistent results for forged than for cast alloys. This is not unexpected if the cast alloys are produced with variations in grain size.

IV. Stress-rupture tests at 815 and 871° C (1500 and 1600° F) indicate that cast alloys are superior to forged alloys.

V. Creep tests on cast alloys show superiority to forged alloys at 815 and 871° C (1500 and 1600° F).

VI. Hot fatigue tests at 650° C (1200° F) indicate that cast alloys are somewhat inferior to wrought alloys. At 815° C (1500° F) the alloys having optimum creep strength in both classes have about the same endurance strength.

VII. A word of caution is introduced here regarding creep rates at low stresses. In design curves at low values of total deformation, forged alloys are as good or somewhat better than the cast alloys. This is particularly noteworthy in the cases of S-590 and forged S-816.

VIII. The casting method in certain instances may be more economical than forging, especially in the alloys which maintain high hardness at elevated temperatures. This effect is enhanced in the alloys to which C is added for greater creep strength, as will be shown in a later chapter.

References

1. Badger, W. L., "Metallurgical Development of Materials for Turbosuperchargers and Aircraft Gas Turbines," *Iron Age*, **158**, (Jul. 25, Aug. 1, 1946).
2. Badger, F. S., Jr., (Letter), *Materials and Methods*, **24**, (Oct., 1946).
3. Badger, F. S. and Sweeney, W. O., "Metallurgy of High-Temperature Alloys used on Current Gas Turbine Designs," A.S.T.M. Symposium on Materials for Gas Turbines (June, 1946).
4. Bollenrath, F., "Further Development of Heat-resistant Materials for Aircraft Engines," *N.A.C.A.*, **14**, No. 1093, (Sept., 1946). Data from 1937.
5. Browne, L. E., "Cobalt-base High-temperature Alloys," *Steel*, **118**, 88 (1946).
6. Cross, H. C. and Simmons, W. F., "Heat-resisting Metals for Gas Turbine Parts," A.S.T.M. Symposium on Materials for Gas Turbines (June, 1946).
7. Freeman, J. W., Rote, F. B., and White, A. E., "High-temperature Characteristics of 17 Alloys at 1200 and 1350° F," *N.A.C.A.*, ACR No. 4C22 (Mar., 1944).
8. Freeman, J. W., Reynolds, E. E., and White, A. E., "Rupture Test Characteristics of Six Precision Cast and Three Wrought Alloys at 1700 and 1800° F," *N.A.C.A.*, ARR No. 5J16 (Nov., 1945).
9. Grant, N. J., Frederickson, A. F., and Taylor, M. E., "Heat-resistant Alloys from 1200 to 1800° F," *Iron Age*, **161**, (Mar. 18, Apr. 8, Apr. 15, 1948).
10. Hansen, M., "Der Aufbau der Zweistofflegierungen," Springer, Berlin (1936).
11. Hoffman, Harry D., "Information on Gas Turbine Developments," PB 1648 (1945).
12. Krisch, A., "Creep Strength of Nickel-Chromium-Cobalt and Iron-Chromium-Cobalt Alloys," *Mitteilungen aus dem K.W. Inst. für Eisenforschung*, **27**, 1 (1944).
13. Priolo, L. A., "Vitallium Turbosupercharger Buckets," PB 4598, Army Air Forces, Experimental Engineering Section, EXP-M-57-522-122 (1942).

14. Reynolds, E. E., Freeman, J. W., and White, A. E., "Evaluation of Two High-carbon Precision-cast Alloys at 1700 and 1800° F by the Rupture Test," *N.A.C.A.*, Tech. Note No. 1130 (Sept., 1946).
15. Sweeney, W. O., "Haynes Alloys for High-temperature Service," *Trans. Am. Soc. Mech. Engrs.*, 69, 569 (1947).
16. Sykes, W. P. and Graff, H. F., "The Co-Mo System," *Trans. Am. Soc. for Metals*, 23, 249 (1935).
17. Wilson, T. Y., "High-strength High-temperature Alloy S-816," *Materials and Methods*, 24, 885 (Oct., 1946).

Chapter 7

Nickel-base Alloys

A. WROUGHT AND CAST ALLOYS

The alloys included in this group are those with more than 35 per cent Ni which are suitable for service at elevated temperature. The presence of Ni in proportions from 55 to about 80 per cent imparts stability to the alloy at high temperature, with retention of good forming properties.

I. Ni-Mo Alloys

These series of alloys with or without Cr were developed for their resistance to chemical corrosion. Only subsequently did it appear that their performance under load at elevated temperature was superior to that of several other classes of heat-resistant alloys. Their cost and their elevated-temperature properties lie between those of the Fe-base and the Co-base alloys. The Ni-Mo compositions are available in both the wrought and cast form and in the latter category are especially suited to precision-casting techniques. They find wide use in furnace parts and in components for gas turbines.

a. Alloy "Hastelloy" B*. A series of Ni-Mo alloys, known as "Hastelloys", are resistant to HCl at all concentrations up to the boiling point. They are also resistant to H_2SO_4 up to 50 per cent concentration and to some salts, e.g., cuprous chloride.

"Hastelloy" B alloy consists of approximately 30 per cent Mo, 65 Ni, and 5 per cent Fe. It is especially satisfactory under reducing conditions, but must be limited to a maximum of 760° C (1400° F) under oxidizing conditions[7]. Forging is recommended in the limited range of 1038 to 1204° C (1900 to 2200° F). The elevated-temperature properties of "Hastelloy" B are shown in Table 7-1.

Microstructure and Heat Treatment. The "Hastelloy" compositions consist of a Ni-rich solid solution of Mo which appears under the microscope as a single phase. Dispersed throughout the grains are complex carbides which persist even after rapid cooling from a high temperature[6].

When heated in the range of 650 to 1090° C (1200 to 2000° F), the alloy

---

* Haynes Stellite Co.

TABLE 7-1. ELEVATED-TEMPERATURE PROPERTIES OF ALLOY "HASTELLOY" B[7,9]

Chemical Composition

C	Ni	Mo	Fe
0.02–0.12	62.5–66.5	26–30	4–5

Room-temperature Density: 9.24 gm/cm³

Short-time Tensile Properties (Precision-cast and Wrought)[7]

Test Temp. (°C)	(°F)	Tensile Strength, (psi)	Prop. Limit (psi)	Yield Strength, 0.1% Strain (psi)	Yield Strength, 0.2% Strain (psi)	Elong. % in 2"	Red. of Area, (%)	Young's Modulus of Elasticity
				As-Cast				
Room	Room[1]	84,200	399,00	52,600	57,800	11.9	13.9	28.5 × 10⁶
538	1000[1]	77,400	—	—	—	15.0	16.4	—
650	1200[1]	65,200	—	—	—	14.7	16.8	—
815	1500[1]	58,500	—	—	—	18.8	18.0	—
			Wrought; rolled and annealed at 2150°F.					
Room	Room	135,000	—	—	63,000	44.0	42.0	30.0 × 10⁶
482	900	115,000	—	—	—	39.0	30.0	—
704	1300	85,000	—	—	—	9.0	15.0	—
900	1650	50,000	—	—	—	17.0	20.0	—
982	1800	25,000	—	—	—	25.0	30.0	—

(1) Averaged results on ¼-in. diameter precision-cast test specimens with 1-in. gage length.

Stress-rupture Properties (Precision-cast and Wrought)

Test Temp. (°C)	(°F)	Condition	Stress, psi for Rupture in 10 Hours	100 Hours	1,000 Hours
		As-Cast			
815	1500	Heat-treated 30 minutes at 1163° C (2125° F); air-cooled; reheated to 926° C (1700° F) for 72 hours; air-cooled.	29,000	17,600	10,700
		Wrought			
650	1200	Heat-treated 30 minutes at 1163° C (2125° F); air-cooled; reheated to 926° C (1700° F) for 72 hours; air-cooled.	61,500	54,000	36,500
704	1300	Heat-treated 30 minutes at 1163° C (2125° F); air-cooled; reheated to 926° C (1700° F) for 72 hours; air-cooled.	60,000	37,000	23,000
760	1400	Heat-treated 30 minutes at 1163° C (2125° F); air-cooled; reheated to 926° C (1700° F) for 72 hours; air-cooled.	37,000	21,000	12,000
815	1500	Heat-treated 30 minutes at 1163° C (2125° F); air-cooled; reheated to 926° C (1700° F) for 72 hours; air-cooled.	26,100	16,200	10,000
815	1500	Aged 24 hours at 1038° C (1900° F); air-cooled.	—	17,000	—

TABLE 7-1—*Continued.*

Endurance Properties[9]

Temp. (°C)	(°F)	Heat Treatment Solution Treatment	Aging	Endurance Strength (psi)	
				10^8 cycles	2.5 × 10^8 cycles
650	1200	1093° C (2000° F) water-quench	4 hrs 650° C (1200° F)	66,000	64,000
815	1500	1121° C (2050° F) air-cooled	24 hrs 1038° C (1900° F)	34,000	—

Thermal Expansion (Wrought Alloy)

Temp (°F)	Mean Coefficient of Linear Expansion In/In/°F × 10^{-6}
70–600	6.41
70–800	6.57
70–1000	6.66
70–1200	6.73
70–1500	6.96
70–1600	7.78

Thermal Conductivity

Temp (°C)	Watts/sq cm/ cm/°C	Temp (°F)	BTU/sq ft/in/ hr/°F
200	0.122	392	85
300	.132	572	91
400	.142	752	98
500	.153	932	106
600	.164	1112	114

"Hastelloy" B age-hardens because of the formation of complex inter-metallic compounds of Ni, Mo, and C. Heating the alloy at 760° C (1400° F) for one week produces a hardness of Rockwell C45 to C50. To minimize the possibility of age-hardening in service, the alloy is given a heat treatment at 1065° C (1950° F) for 24 hrs. This stabilized structure is shown in Fig. 7-1[4]. The maximum hardness obtainable for this alloy is shown in the structure of Fig. 7-2 which represents the age-hardening occurring after an anneal at 732° C (1350° F) for one week.

b. Alloy Hastelloy C*. The "Hastelloy" C alloy contains approximately 15 per cent Cr, 17 per cent Mo, about 60 per cent Ni, and small percentages of W, Fe, and V. The presence of Cr makes this alloy resistant to oxidizing and reducing atmospheres up to 1150° C (2100° F). It finds use in furnace components operating up to 1093° C (2000° F), for conveyor belts up to 950° C (1750° F) and in carburizing equipment[1]. Forging is possible in the range of 1038 to 1204° C (1900 to 2200° F)[7]. The elevated-temperature properties of alloy "Hastelloy" C are shown in Table 7-2.

II. Alloys Containing Approximately 75 Per Cent Ni.

An important series of high-Ni alloys for high-temperature service are

* Haynes Stellite Co.

those containing approximately 75 per cent Ni. These are known as the "Inconel" series* in the United States and as the "Nimonic" series† in England. Unlike many austenitic alloys, these high-Ni alloys are precipi-

Fig. 7-1. "Hastelloy" B stabilized structure annealed 24 hrs. at 1065° C (1950° F). Etched with chrome regia. Magnification 100×. (After Badger and Sweeney)
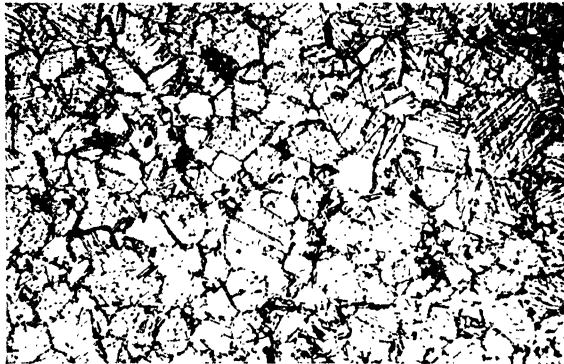
Fig. 7-2. "Hastelloy" B age hardened structure. Annealed 1 week at 732° C (1350° F). Etched with chrome regia. Magnification 100×. (After Badger and Sweeney)

tation-hardened due to the presence of a number of elements in very small percentages.

a. "Inconel" X. The alloy "Inconel" X contains 73 per cent Ni, 15 per cent Cr, 7 per cent Fe, with small additions of Cb, Ti, and Al[5]. It is available in sheet form for manifold assemblies, tail pipes, and other com-

* International Nickel Company
† Mond Nickel Company

ponents. It is recommended for all services up to 815° C (1500° F) and under certain conditions may be satisfactory at temperatures as high as

TABLE 7-2. ELEVATED-TEMPERATURE PROPERTIES OF ALLOY "HASTELLOY" C[7, 9]

Chemical Composition

C	Mo	Fe	W	Cr	V	Ni
0.04–0.15	15–18	4.5–7	3.75–5.25	13–15.5	0.2–0.4	55–60 (bal)

Room-temperature Density: 8.94 gm/cm³

Short-time Tensile Properties (Precision-cast and Wrought)

Test Temp., (°C)	(°F)	Tensile Strength, (psi)	Prop. Limit (psi)	Yield Strength, 0.1% Strain (psi)	Yield Strength, 0.2% Strain (psi)	Elong. % in 2″	Red. of Area, (%)	Young's Modulus of Elasticity
				As-Cast				
Room	Room[1]	81,200	35,600	48,600	50,800	10.2	12.2	24.5 × 10⁶
538	1000[1]	67,000	—	—	—	12.5	14.9	—
650	1200[1]	62,100	—	—	—	15.5	15.7	—
815	1500[1]	56,700	—	—	—	18.2	15.4	—
950	1750[1]	32,000	—	—	—	14.0	49.0	—
1065	1950[1]	15,000	—	—	—	27.5	60.0	—
		Sheet, 0.065 in. thick, annealed at 2225° F.						
Room	Room[2]	129,500	—	—	54,000	37.5	31.5	—
650	1200[2]	86,700	—	—	—	22.0	22.5	—
815	1500[2]	50,700	—	—	—	36.0	45.5	—
926	1700[2]	27,200	—	—	—	40.5	45.5	—
1038	1900[2]	14,200	—	—	—	35.5	39.5	—

(1) Averaged results on ¼-in. diameter precision-cast test specimens with 1-in. gage length.

(2) Averaged results on sheet specimens with 2-in. gage length. Specimens were held at temperature ½ hour before testing.

Stress-rupture Properties

Test Temp.,	Condition	Stress, psi for Rupture in		
		10 Hours	100 Hours	1,000 Hours
815° C (1500° F)	As-Cast	18,800	14,100	17,700

Mean Thermal Expansion Coefficient (in per in. per ° F. × 10⁻⁶)

70–600° F	70–800° F	70–1000° F	70–1200° F	70–1500° F	70–1600° F
7.02	7.35	7.44	7.73	8.07	8.20

Thermal Conductivity (Watts per sq. cm. per cm. per °C)

200° C	300° C	400° C	500° C	600° C
0.113	0.127	0.141	0.156	0.171

(B.t.u. per sq. ft. per in. per hr. per °F)

392° F	572° F	752° F	932° F	1112° F
78	88	98	108	118

870° C (1600° F). The fact that it contains no Co makes it an attractive substitute for Co-base alloys if this metal is not available.

Manufacturing and Heat Treatment

"Inconel" X is poured in 5000-lb ingots, formed into billets of 3000 lbs, and subsequently forged and rolled. Forging is recommended in the range of 982 to 1218° C (1800 to 2225° F), the higher side of the range being required for larger forgings. In sheet form, "Inconel" X is supplied in a stress-relieved condition, which is accomplished by a heat treatment at 1010° C (1850° F). After the sheet is fabricated, it is recommended that an aging heat treatment be given at 704° C (1300° F)[5].

Heat treatment for maximum strength in a service range below 538° C (1000° F) is as follows: Heat to 900° C (1650° F) for 20 hours, and air-cool or furnace-cool; age at 704° C (1300° F) for 20 hours. This rather low solution heat treatment at 900° C (1650° F) maintains a small grain size and provides a material suitable for use in rotors, bolts, and springs.

Heat treatment for maximum creep resistance above 538° C (1000° F) requires the following procedure: Heat to 1150° C (2100° F) for 2 to 4 hours, and cool in air. Heat to 843° C (1550° F) for 24 hours, cool in air or allow the furnace to cool to the lower temperature. Age at 704° C (1300° F) for 20 hours, cool in air. The variation in hardness obtained by different heat treatments is shown in Table 7-3[5]. The elevated-temperature properties of alloy "Inconel" X, given in Table 7-3, indicate that the material maintains its strength well up to a temperature of 593° C (1100° F). Above this temperature, the stress-rupture values decrease

TABLE 7-3. ELEVATED-TEMPERATURE PROPERTIES OF ALLOY "INCONEL" X[5, 8]

Chemical Composition

C	Mn	Si	Cr	Ni	Cb	Ti	Al	Fe
0.04	0.50	0.40	15.0	73.0	1.0	2.5	0.7	7.0

Melting Range: (1395–1425° C) 2540–2600° F
Room-temperature Density: 8.3 gm/cm³; 0.3000 lb/cu in
Electrical Resistance: 122.8 microhms/cu cm
Magnetic Permeability: 1.0028

Hardness at Room Temperature

Condition	Temp (°C)	(°F)	Treatment	BHN*	Rockwell
Solution-treated	1150	2100	4 hrs, air-cooled	140–180	77Rb-8Rc
Annealed	1010	1850	30 mins, air-cooled	140–180	77Rb-8Rc
Equalized	900	1650	24 hrs, air-cooled	140–230	77Rb-21Rc
Equalized and aged	900	1650	24 hrs, air-cooled;	320–400	34Rc-42Rc
	704	1300	20 hrs, air-cooled		
Fully heat treated	1150	2100	2–4 hrs, air-cooled;	280–340	28Rc-35Rc
	843	1550	24 hrs, air-cooled;		
	704	1300	20 hrs, air-cooled		

* BHN: Brinell Hardness Number.

TABLE 7-3—*Continued.*

Short-time Tensile Tests

Condition	Temp (°C)	(°F)	Tensile Strength (psi)	Yield Strength 0.2% Strain (psi)	Elong. % in 2 in	Reduction in Area (%)
(a)	26	80	167,000	102,000	21	26
(a)	650	1200	120,000	79,000	11	14
(a)	732	1350	93,000	77,000	6	12
(a)	815	1500	60,000	50,000	19	25
(b)	26	80	184,000	132,000	26	41
(b)	482	900	164,000	118,000	25	39
(b)	650	1200	142,000	111,000	12	17

(a) Hot-rolled 1150° C (2100° F) 4 hrs air-cooled
 Annealed 843° C (1550° F) 24 hrs air-cooled
 Annealed 704° C (1300° F) 20 hrs
(b) Hot-rolled and aged at 704° C (1300° F)

Stress Rupture

Temp (°C)	(°F)	Rupture Strength at 100 hrs (psi)	500 hrs (psi)	1000 hrs (psi)
650	1200	80,000	72,000	69,000
732	1350	58,000	48,000	42,000
815	1500	28,000	21,500	18,000

Creep Strength

Temp (°C)	(°F)	0.00001%/hr Creep Rate Stress (psi)	Total Plastic Deformation 100 hrs	1000 hrs	0.0001%/hr Creep Rate Stress (psi)	Total Plastic Deformation 100 hrs	1000 hrs
650	1200	48,000	0.001	0.010	60,000	0.030	0.18
732	1350	30,000	.001	.015	37,500	.014	.20
814	1500	15,000	.001	.20	18,000*	—	—

* Estimated: A test at 20,000 gave 0.025 total plastic deformation in 100 hrs.

Hot Fatigue

Temp (°C)	(°F)	10⁶ Cycles (psi)	10⁷ Cycles (psi)	10⁸ Cycles (psi)
650	1200	67,800	60,100	53,800
732	1350	51,500	49,500	48,500
815	1500	53,000	39,500	35,000

Hot Impact Strength

Temp (°C)	(°F)	Charpy Impact Resistance, ft-lb V Notch	Keyhole Notch
Room	Room	42	36
204	400	68	—
315	600	73	—
538	1000	77	—
650	1200	72	33
732	1350	59	28
760	1400	54	—
815	1500	82	42

TABLE 7-3—*Concluded.*

Thermal Expansion

Temp (°F)	Mean Coefficient of Linear Expansion In/In/°F × 10⁻⁶ (from 3 melts)
100–200	7.6
100–500	7.8
100–700	8.0
100–900	8.1
100–1000	8.2
100–1200	8.4
100–1350	8.7
100–1500	9.0
100–1600	9.2

Thermal Conductivity

Temp	BTU/sq ft/°F	Cm-cm-sec Units
Room	87	0.03
900° C (1652° F)	189	.065

Moduli of Elasticity

Temp (°C)	(°F)	Young's Modulus × 10⁶	Shear Modulus × 10⁶
26	80	31	11
260	500	28.7	10.2
538	1000	25	9
650	1200	23	8.1
732	1350	21	—
815	1500	18.5	—

to a value of 18,000 psi for a test period of 1000 hours at 815° C (1500° F). The results of fatigue tests shown in Fig. 7-3 and Table 7-3 are tentative as they represent only a comparatively few experiments.

b. Alloy "Nimonic" 80. Alloy "Nimonic" 80 containing approximately 75 per cent Ni, 21 per cent Cr with Al and Ti, is used widely in England for extremely severe service for turbine blading and other gas turbine components. Much of the information on manufacturing, heat treatment, and creep resistance remains on the restricted list and is not available for publication.

B. Cast Ni-base Alloys

A series of Ni-Fe-Cr alloys generally utilized as castings which have a Ni content varying from 33 to 68 per cent are included in this chapter, as it is this element which imparts the quality of a closely adherent scale as well as structural stability at elevated temperature. These alloys comprise about one-half of all the cast heat-resistant metals manufactured and are widely used in furnace components. Their resistance to carburizing is excellent and it increases with the Ni content. The fact that the scale

Fig. 7-3. Hot fatigue strength "Inconel" X at 650° C (1200° F), 732° C (1350° F) and 815° C (1500° F).
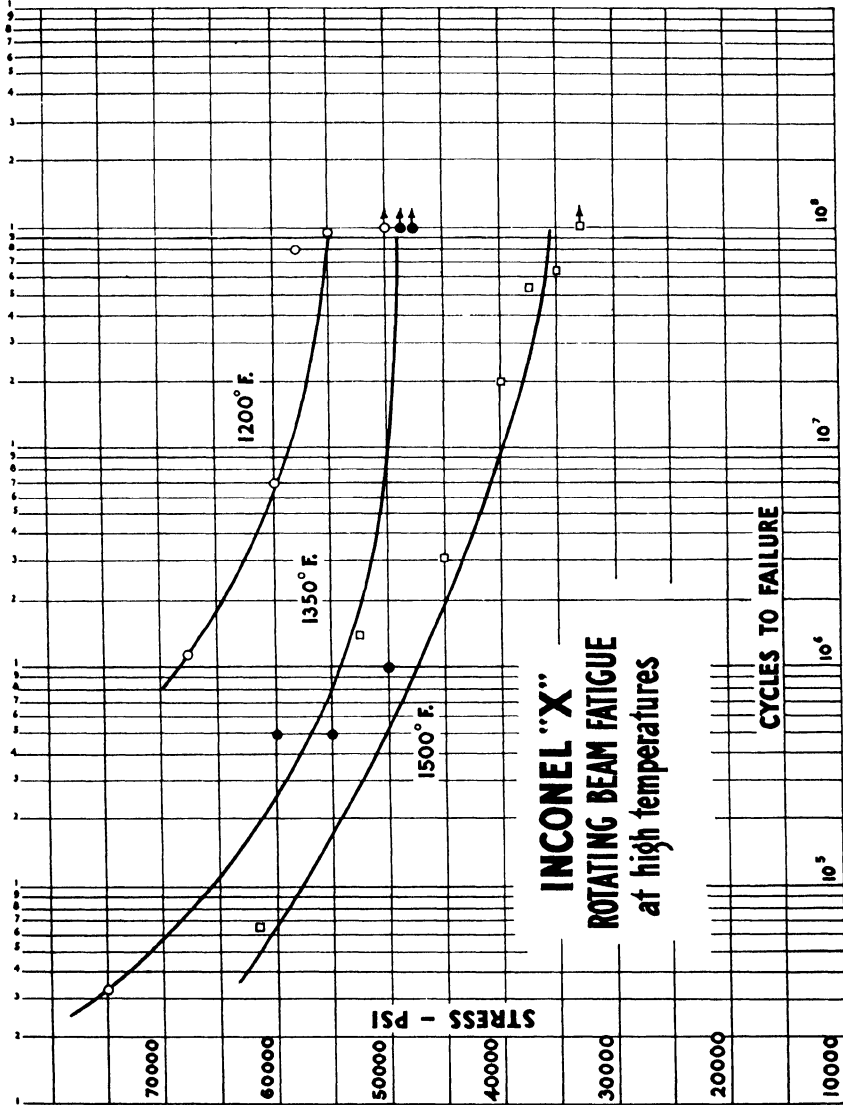
(Courtesy International Nickel Co.)

formed is adherent makes them suitable for enamelling operations. These alloys high in Ni are more stable than the high-Cr alloys, Type HH, discussed in a previous chapter, and are subject to less deterioration in the rapid heating and cooling occurring in many furnace parts[1, 2, 3].

I. Alloy Type HT

This alloy ranges from 34 to 37 per cent Ni and 13 to 17 per cent Cr with a typical foundry analysis as follows[3]:

C	Mn	Si	Ni	Cr
0.35–0.75	2.0 max	2.0 max	33–37	13–17

TABLE 7-4. ELEVATED-TEMPERATURE PROPERTIES ALLOY "NIMONIC" 80.[5]

Chemical Composition

C	Mn	Si	Cr	Ni	Al	Ti
0.04	0.56	0.47	21.18	74.23	0.63	2.44

Manufacture

These tests are taken from a heat melted in a 1000-lb Moore direct-arc furnace and cast into a 14-in sq ingot. Reductions consist of forging at 1226° C (2240° F) to 3 by 3-in billets and rolling at 2240° to ⅝-in diameter bar stock. The alloy is heat-treated by heating at 1065° C (1950° F) 4 hours, followed by water-quenching.

Room-temperature Density: 8.192 gm/cm³

Stress-rupture Tests

	Stress Rupture		Estimated Elong in 2″ for Rupture in	
Temp	10 hrs	100 hrs	10 hrs	100 hrs
815° C (1500° F)	29,000	17,200	2%	1.5%

Impact Resistance

	Charpy Impact Resistance, ft-lbs	
Temp	Keyhole Notch	V Notch
Room	24	59
815° C (1500° F)	23	—

The composition limits of Ni and Cr are not critical except in the presence of hot gases. However, both C and Si are important in regard to ductility and high-temperature strength. This alloy remains consistently austenitic because of its high Ni content and is therefore free from the deterioration which may be caused by formation of a ferrite or a sigma phase. The presence of N in amounts of 0.02 to 0.06 per cent, which is usual in foundry melting practice, does not influence the properties of this alloy[3].

The effect of temperature on the short-time tensile properties of an alloy Type HT shown in Table 7-5 shows a strength of about 18,000 psi at 871° C (1600° F). The ductility on the basis of these short-time tests increases with increase in temperature.

A comparison of two alloys, Types HT and HH in Table 7-6, indicates the life and elongation at fracture of stress-rupture tests conducted at

TABLE 7-5. SHORT-TIME TENSILE PROPERTIES OF ALLOY TYPE HT.[3]

		Composition, %			
C	Mn	Si	Ni	Cr	N
0.33	0.60	1.29	35.8	16.3	0.04

Temp °C	Temp °F	Tensile Strength (psi)	Elongation % in 2 in.	Reduction in Area (%)
26	80	68,750	14.0	18.9
760	1400	34,800	13.5	18.5
760	1400	34,380	13.5	20.4
800	1472	27,560	17.5	29.3
870	1600	19,350	26.0	42.3
870	1600	18,200	27.5	35.0
910	1670	15,100	25.5	40.2
982	1800	10,850	19.0	40.3
982	1800	10,700	23.0	31.4
1040	1905	8,020	30.0	33.2
1093	2000	5,720	37.0	45.1
1250	2282	2,970	42.5	65.7

Note: Rate of application of the load corresponds to a free crosshead speed of 0.03 in. per min.

TABLE 7-6. COMPARATIVE STRESS-RUPTURE PROPERTIES OF ALLOY TYPE HT AND ALLOY TYPE HH.[3]

16% Cr-35% Ni (HT) and 26% Cr-12% Ni (HH) Alloys

Alloy	Composition, %						Structure
	C	Mn	Si	Ni	Cr	N	
			26% Cr-12% Ni Series				
HH-31	0.31	0.42	0.42	11.4	26.5	0.07	Partially Ferritic
HH-42	0.42	0.45	0.45	11.3	26.1	0.05	Partially Ferritic
HH-52	0.52	0.53	0.47	11.4	26.4	0.07	Wholly Austenitic
HH-61	0.61	0.31	0.48	11.4	26.3	0.07	Wholly Austenitic
			16% Cr-35% Ni Series				
HT-35	0.35	0.67	1.28	34.4	16.0	0.05	Austenitic
HT-36	0.36	0.81	1.19	34.8	16.0	0.04	Austenitic
HT-44	0.44	0.74	1.17	35.0	16.2	0.05	Austenitic
HT-47	0.47	0.82	1.23	34.9	16.0	0.04	Austenitic
HT-56	0.56	0.71	1.22	34.7	16.4	0.04	Austenitic
HT-56	0.56	0.80	1.27	34.8	15.9	0.04	Austenitic
HT-61	0.61	0.76	1.29	34.6	16·1	0.05	Austenitic
HT-70	0.70	0.81	1.26	34.7	16.5	0.05	Austenitic
HT-92	0.92	0.78	1.17	34.6	16.2	0·05	Austenitic

|	1400°F—20,000 psi.				1800°F—6000 psi			
	Life in Hours		Elong.—%		Life in Hours		Elong.—%	
Alloy	16-35	26-12	16-35	26-12	16-35	26-12	16-35	26-12
HH-31	..	3	..	20	..	3	..	56
HT-35	29	..	16	..	..	..	..	..
HT-36	32	..	23	..	24	..	9	..
HH-42	..	10	..	10	..	21	..	11
HH-44	60	..	14	..	70	..	7	..
HT-47	50	..	14	..	50	..	6	..
HH-52	..	36	..	3	..	52	..	1
HT-56	37	..	14	..	22	..	17	..
HT-56	52	..	21	..	52	..	11	..
HH-61	..	42	..	2	..	47	..	2
HT-61	14	..	19	..	..	..	..	..
HT-70	16	..	19	..	..	..	..	..
HT-92	16	..	19	..	..	..	..	..
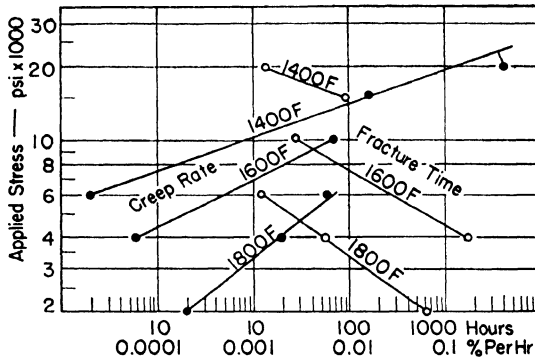
Fig. 7-4. Log-log plot of creep characteristics of 16% Cr 35% Ni 0.29% C alloy (Type HT-29).   (After Avery and Matthews)
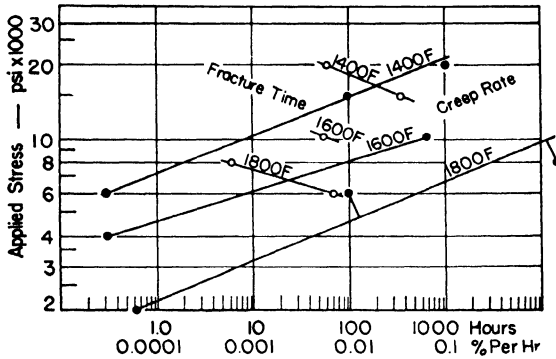
Fig. 7-5. Log-log plot of creep characteristics of 16% Cr 35% Ni 0.44% C alloy (Type HT-44.)   (After Avery and Matthews)
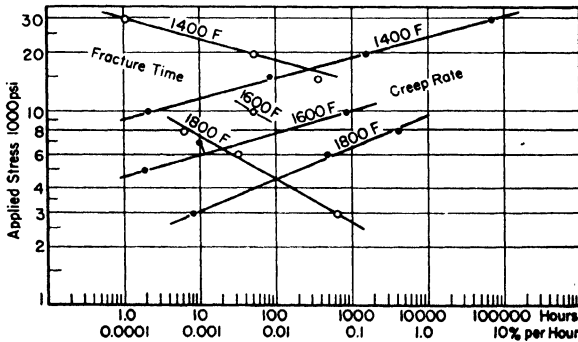
Fig. 7-6. Log-log plot of creep characteristics of 16% Cr 35% Ni 0.56% C alloy (Type HT-56).   (After Avery and Matthews)

20,000 psi at 760° C (1400° F) and 6000 psi at 982° C (1800° F). The letters after each alloy designate the C content, and the series are arranged in increasing percentages of C. The HH Type, or 26 Cr-12 Ni alloy, shows a decrease in elongation with increase in C content. The HT Type, or 16 Cr-35 Ni alloy, on the other hand, has a fairly constant elongation of 14 to 23 per cent at 760° C (1400° F) regardless of the C content, and at 982° C (1800° F) the elongation increases with C content.

This tendency toward hot ductility as the C content increases is an outstanding factor in the suitability of the Type HT alloys for carburizing
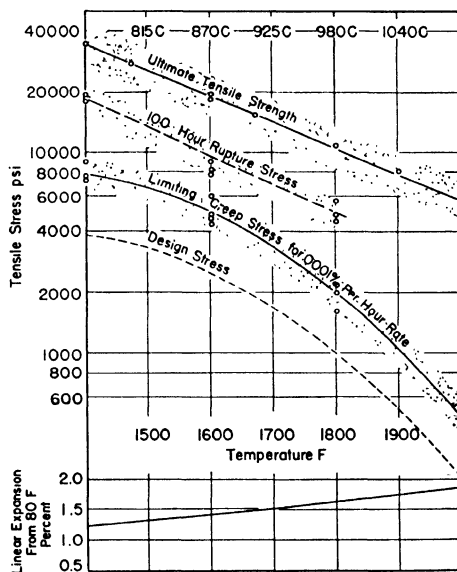
Fig. 7-7. Elevated temperature characteristics of 16% Cr 35% Ni alloys under constant temperature conditions. Type HT. (After Avery and Matthews)

boxes, retorts and muffles subject to such atmospheres. This wholly austenitic alloy, although slow to absorb C compared to the ferritic alloys, will finally carburize up to 2 per cent C. The attainment of this proportion of C throughout the entire cross-section may be the signal for failure of furnace components in service[3].

The effect of increasing C content on the creep strength of alloy Type HT is shown in Figs. 7-4, 7-5, and 7-6. The low C content of 0.29 in Fig. 7-4 indicates that creep strength is decreased with decrease in C. The alloys with 0.44 and 0.56 per cent C in Figs. 7-5 and 7-6, respectively, display better creep resistance. The combined high-temperature properties of alloy Type HT are shown in Fig. 7-7 for short-time stress rupture, and creep strengths at temperatures of 815 to 1038° C (1500 to 1900° F).

A dotted curve recommending design stresses for this temperature range is also indicated on the graph[3]. These values derived from laboratory tests are considerably in excess of earlier values which have appeared in the literature. The values in Fig. 7-7 are based on a consideration of 50 per cent of a limiting creep stress for a deformation rate of 0.0001 per cent per hour. A useful life of 2 to 8 years (17,000 to 70,000 hrs) seems reasonable for furnace applications. The stresses to be used in design data must also be considered in the light of the decrease in ductility which occurs when materials are subject to low stresses over long periods. It is

TABLE 7-7. HOT HARDNESS OF 16% CR 35% NI ALLOYS[3]

30-sec. load, mutual indentation method with 1-cm. dia. x 1-cm. cylinders

Heat No.	Chemical Analysis, %						Tens. Str.—psi × 1000		Brinell Hardness				
Temperature—F:							75	1200	1400	1600	1800		
Load—Kilograms:							3000	2000	1500	1000	500		
	C	Mn	Si	Ni	Cr	N	R.T.	1800 F					
A	0.50	0.81	1.34	35.8	15.3	0.06	68	10.8	169	127	86	36	32
H	0.52	0.74	0.53	34.9	15.2	0.04	67	11.8	167	109	97	58	37
F	0.49	0.93	0.93	35.4	15.2	0.06	65	10.4	166	117	86	55	34
E	0.54	0.99	0.91	34.6	15.1	0.02	64	11.7	169	122	101	58	40
I	0.46	0.92	0.92	34.7	15.7	0.02	65	11.5	167	109	82	58	43
F	0.49	0.93	0.93	35.4	15.2	0.06	65	10.0	168	111	82	51	34

R.T.　Room Temperature

TABLE 7-8. CHARPY IMPACT RESISTANCE OF 16% CR 35% NI ALLOYS.[3]

V-notched Charpy Specimens, Superheated 30 to 70 F to Compensate
Temperature Drop Before Impact

Heat No.	Chemical Analysis, %								Impact in Ft-Lbs. Temperature, F				
	C	Mn	Si	Ni	Cr	N	Mo		75	1200	1400	1600	1800
E	0.54	0.99	0.91	34.6	15.1	0.02	...	As Cast	3.5	6.0	6.5	7.0	7.5
I	0.46	0.92	0.92	34.7	15.7	0.02	...	As Cast	5.5	8.5	10.5	11.0	13.5
J	0.54	0.74	1.06	34.5	14.9	0.05	0.76	As Cast	3.0	7.0	7.0	7.5	10.0
								As Cast—Average	4.0	7.0	8.0	8.5	10.5
E		(Same heats as above except							3.5	6.5	6.0	6.5	7.0
I		aged 48 Hrs. at 1600 F							7.0	10.0	10.5	13.0	12.0
J		before testing.)							4.0	7.0	7.5	7.0	7.5
		Aged 1600 F—48 Hrs.—Average							5.0	8.0	8.0	9.0	9.0

here that the danger of extrapolation of the data on the time axis must not be overlooked.

In Tables 7-7 and 7-8 the hot hardness and Charpy impact resistance for various temperatures are given.

Summary

The creep strength of the HH Type alloy, 16 per cent Cr-35 per cent Ni ranges from about 8000 psi at 760° C (1400° F) to 180 psi at 1176° C (2150° F) for a minimum creep rate of 0.0001 per cent per hour. The presence of C does not reduce hot ductility. A Si content of 0.5 to 1.5 per

cent is recommended for the usual furnace construction but 1.5 to 2.3 per cent Si helps prevent carburization in conjunction with C. Temperature fluctuations above 815° C (1500° F) may lower the safety factor involved in allowable working stresses. The HT Type alloy remains austenitic and is therefore less sensitive to changes in composition and manufacturing conditions than the HH Type alloy[3]. The scaling resistance of these alloys will be shown in a later chapter.

II. Alloys Types HU, HW, and HX

These alloys are similar to Type HT except that Ni and Cr are uniformly increased as follows[1]:

Type	C	Mn	Si	Cr	Ni
HU	0.35–0.75	2.0 max	2.5 max	17–21	37–41
HW	.35– .75	2.0 max	2.5 max	10–14	58–62
HX	.35– .75	2.0 max	2.5 max	15–19	64–68

The increase in Ni content of the above alloys decreases the tendency to carburization and increases the resistance to thermal shock. Higher Cr contents increase resistance to oxidation at the higher temperatures. All these alloys with higher percentages of Cr and Ni are only substituted for the Type HH where demands of service are severe, since their cost is higher. Type HU has about the same properties at elevated temperature as Type HT but its corrosion resistance is superior. Types HW and HX do not warp or crack on repeated heating and cooling and give excellent service where carburization is severe. They also withstand cyanide salts, tempering salts, and molten Pb.

References

1. Am. Soc. Metals, "Metals Handbook" (1948).
2. Avery, H. S., "Properties of HT Type Alloys, A Summary," *Alloy Casting Bull* (Oct., 1946).
3. Avery, H. S. and Matthews, N. A., "Cast Heat-resistant Alloys of the 16% Cr 35% Ni Type," *Trans. Am. Soc. Metals*, **38,** 957 (1946).
4. Badger, F. S., Jr. and Sweeney, W. O., Jr., "Metallurgy of High-temperature Alloys used on Current Gas Turbine Designs," A.S.T.M. Symposium on Materials for Gas Turbines (June, 1946).
5. Crawford, C. A., "Nickel-Chromium Alloys for Gas Turbine Service," *Trans. Am. Soc. Mech. Engrs.*, **69,** 609 (1947).
6. Cross, H. C. and Simmons, W. F., "Heat-resisting Metals for Gas Turbine Parts," A.S.T.M. Symposium on Materials for Gas Turbines (June, 1946).
7. "Haynes Alloys for High-temperature Service," Haynes Stellite Co. (1948).
8. International Nickel Co. Inc., "Inconel X, a High-strength High-temperature Alloy" (Jan., 1949).
9. Sweeney, W. O., "Haynes Alloys for High-temperature Service," *Trans. Am. Soc. Mech. Engrs.*, **69,** 569 (1947).

Chapter 8

Non-Commercial Alloys

A. CONDITIONS FOR CONDUCTING TESTS. From 1940 through the war years, government-sponsored research investigated thousands of alloy compositions in an effort to find materials suitable for high-temperature service. The problem at first was to find a material to function at 815°C (1500°F) with a creep rate of 0.00001 per cent per hour under a stress of 7000 psi. Later the temperature range for study became 732 and 870°C (1350 and 1600°F) and subsequently materials to operate at 1093°C (2000°F) were included.

Due to the pressure of the war effort and the many unknown variables which determine flow properties of metals in these high-temperature ranges, certain stages of the investigations concentrated on alloy composition in the hope that by some miracle, a specific material with superior creep strength and corrosion resistance would be evolved. It so happened that the results probably justified the means of a trial and error method, in that several alloy compositions showed remarkable properties. In the exceptionally wide range of alloys in both the forged and cast states, an attempt was made to evaluate the effect of each element by small increments with the remaining constituents held constant. No discussion of metals for high-temperature service is complete unless it takes into account the extensive investigations undertaken under government sponsorship, and it is for this reason that the results are presented herewith in considerable detail.

I. Limitations

a. Composition. In examination of the data, it is important to appreciate some of the limitations which characterize the results of the tests. The compositions are for the most part nominal as the raw materials are not themselves pure. The Co contains 98.5 ± 0.3 per cent Co; Ni and Fe are also present as impurities. The Cr contains 98 ± 0.5 per cent Cr with Fe as the chief impurity. The ferroalloys contribute a number of impurities such as N, which is present in the ferrochromium. In the Co-Cr base alloys, up to 2 per cent Ni and 0.5 per cent Fe may be present, but are not shown in the nominal composition[5]. The variation in composition

may therefore be considerable and yet in many instances, the effect may not be great. It is known, however, that the effect of small changes in C and N are especially important in determining formability of the alloy and its physical properties at high temperatures.

b. Melting and Casting. For the most part, the heats in these laboratory tested compositions are very small, varying from 2 to 5 lbs. This again is a necessary concomitance justified by the expensive ingredients and the thousands of heats produced. Control of composition and duplication of results are therefore necessarily limited. In the series of alloys cast by the precision investment method, the small melting furnaces are provided with about 5 to 15 lbs air pressure. Such melting practice does not give sufficient pressure to fill a refractory mold at room temperature. As a result, the molds are preheated and the metal cools slowly after being poured. Slow cooling rates obviously produce coarse-grained castings. The effect of grain size on stress rupture and creep strength was not appreciated until 1945 after much of the experimental data on these alloys had been reported. This lack of control of pouring temperature and cooling rate must be taken into consideration in an appraisal of the results of many of these tests.

Subsequently, the effect of mold temperature on the more promising alloy systems is reported as follows: If the mold is held at a constant temperature of 1010°C (1850°F), a uniform grain size is produced in a wide group of refractory alloys, such as "Vitallium" with varying C content, the Cr-Ni-Co-Fe series of alloys, and several others. If the mold temperature is varied over a range from 100 to 1010°C (1850°F), the grain size increases from 30 to 40 grains per inch to 4 or 5 grains per inch. This grain-size variation versus mold temperature is established for several alloy series. Variations in grain size versus high temperature properties are considered under the section on design data[3, 4].

II. Effect of Minor Elements

C is the chief element which in variations of as small as 0.1 per cent influences the stress rupture and creep properties. It will be seen from the data in this chapter that C increasing through a specified range strengthens the alloy for high-temperature service. The presence of C also decreases formability and may require a change in the method of manufacturing from forging to casting. In alloys where the C content is specified in 2 decimal places, this figure represents an actual analysis; otherwise, it may only be nominal.

Nitrogen is especially effective in changing the forging properties of alloys high in Cr. For compositions containing 20 per cent Cr which are not protected by slags, N is dissolved from the atmosphere up to 0.07 per

cent. The effect of N depends upon the presence of nitride-forming elements. The relation of C is also important, as an increase in this element decreases the solubility of N.

The effect of Mn is important especially in the Co-Cr-Mo series of alloys. The effect of Si in amounts of 2 to 4 per cent is important. When Si is present in amounts of less than 1 per cent, its influence is uncertain[4].

B. Properties of the Laboratory Series, Non-Commercial Alloys

The compositions selected for tests cover several extensive ranges within which the minor elements are varied in small increments. One classification is the broad composition of alloys, either forged or cast, with Fe present in amounts of about 20 to 35 per cent. These are called the Ni-Cr-Co-Fe base alloys and may have 20 per cent Ni, 20 per cent Cr and 20 per cent Co. By far the larger group of compositions, however, have a base of 30 per cent Ni, 20 per cent Cr and Co up to 20 per cent. The second large classification is the alloys which are tested only in the cast state and which contain Co in amounts greater than 60 per cent, about 20 per cent Cr, while Fe is present only as an impurity. For the most part these alloys are too brittle to be forged, especially because of their higher C contents. The numbers placed before the letter in the compositions listed under the two broad alloy classifications indicate the C content. This value represents the results of chemical analysis. The other figures or alloy composition not in bold face are only nominal.

I. Ni-Cr-Co-Fe Base Alloys

a. Forged Series. This series of alloys with a composition as shown in Table 8-1 have less than 0.2 per cent C, except for a few which have as high as 0.45 per cent C. The lower-C range is designed to retain hot-forming properties. They all contain about 30 per cent Ni, 20 per cent Cr, 4 to 6 per cent Mo with or without Ta, Cb, W and N. Certain compositions also contain small proportions of elements such as V, Zr, and B as age-hardeners.

Stress-Rupture Properties. This series of forged Ni-Cr-Co-Fe base alloys receives in all cases a heat treatment of water-quenching from a solution treating temperature of 1150 to 1260°C (2100 to 2300°F). Tempering subsequently at 815°C (1500°F) for 50 hrs is optional. The time for rupture of this series, shown in Table 8-2 for a test temperature of 815°C (1500°F), is shown for two loads, namely, 15,000 and 20,000 psi. At 15,000 psi, alloy MT-11A quenched from 1260°C (2300°F) lasts the longest, 936 hours, with an elongation at fracture of 9.2 per cent[2].

Creep Properties. Creep test results at 815°C (1500°F) for loads of 7000

to 10,000 psi for the forged series are presented in Table 8-3. For the standard set of 7000 psi at 815°C (1500°F) with a creep rate of 0.00001 per cent per hr, only alloy TE meets the requirement[2].

TABLE 8-1. NON-COMMERCIAL ALLOYS TESTED IN THE FORGED AND HEAT-TREATED CONDITION[2]

(Boldface values are analyzed, others are nominal values)

Alloy	C	Mn	Si	N_2	Ni	Cr	Co	Mo	Ta	Cb	W	Others
TA (1)	**0.10**	0.7	1.0	**0.143**	30.0	20.0		6.0	**2.97**	**5.10**		
TA (2)	**0.09**	0.7	1.0	0.15	30.0	20.0		6.0	**4.07**	**5.25**		
TB (1)	**0.06**	0.7	0.5	**0.135**	29.7	19.76	21	5.6	**2.77**			
TB (2)	**0.09**	0.7	0.5	0.15	30.0	20.0	21	6.0	**2.10**			
TC (1)	**0.11**	1.3	1.2	**0.10**	28.9	19.97	20	5.5		**5.22**		
TC (2)	**0.14**	0.9	1.5	0.15	30.0	20.0	20	6.0		**5.78**		
TD (1)	**0.12**	0.7	1.0	0.15	30.0	20.0	18	6.0	**2.75**	**4.20**		
TE (1)	**0.09**	0.7	0.5	**0.137**	30.0	20.0		4.0	**1.90**		**4.10**	
TF (1)	**0.09**	0.4	0.9	0.15	29.2	20.0		**4.08**	...	**4.47**	**3.60**	
TG (1)	**0.09**	0.7	1.0	0.15	30.0	20.0		4.0	**1.97**	**4.04**	**4.00**	
TAA(1)	**0.10**	0.7	1.0	0.15	30.0	20.0		6 0	**1.92**	**4.10**		
SX (1)	**0.07**	0.7	1.0	0.15	27.5	17.5		6.0		**4.19**		
SY (1)	**0.15**	0.7	0.5	0.12	35.0	12.5	23	5.0		...	**2.50**	
SY (2)	**0.21**	0.7	0.5	0.12	35.0	12.5	23	5.0			**2.20**	
SZ (1)	**0.07**	0.5	0.5	**0.143**	29.5	**20.0**		6.1	**1.15**	...		
TE-O	**0.04**	0.7	0.7	0.15	30.0	20.0		4.0	**3.67**	..	**3.87**	
TE-C1	**0.23**	0.7	0.7	0.15	30.0	20.0	..	4.0	**3.26**	...	**3.87**	
TE-C2	**0.45**	0.7	0.6	0.15	30.0	20.0		4.0	**3.32**	....	**3.87**	
TE-OA	**0.07**	0.7	0.5	0.15	30.0	20.0		4.0	**5.83**	.	**4.00**	
TE-OB	**0.09**	0.7	0.5	0.15	30.0	20.0		4.0	**3.51**		**4.00**	
TE-OC	**0.08**	0.7	0.5	0.15	30.0	20.0		4.0	**4.48**	.	**4.00**	
TE-T	**0.09**	0.7	0.5	0.15	30.0	20.0	.	4.0	**7.64**	..	**4.00**	
MT-1	**0.08**	1.0	1.0	.	30.0	20.0	5	6.0	1.00	2.00	4.00	0.5 V. 0.5 Zr. 0.5 U
MT-2	**0.33**	2.0	1.0		30.0	20.0	5	6.0	1.00	2.00	4.00	same
MT-3	**0.33**	2.0	1.0		30.0	20.0	5	6.0	1.00	2.00	4.00	same + 2 Ti
MT-4	**0.34**	2.0	1.0	.	30.0	20.0	5	5.0	1.00	2.00	4.00	...
MT-5	**0.34**	2.0	1.0	.	30.0	20.0	5	5.0	1.00	2.00	4.00	0.5 V
MT-6	**0.34**	2.0	1.0		30.0	20.0	5	5.0	1.00	2.00	4.00	15 V. 1.5 Ti
MT-7	**0.34**	2.0	1.0		30.0	20.0	5	5.0	1.00	1.00	4.00	...
MT-7	**0.34**	2.0	1.0		30.0	20.0	5	5.0	1.00	2.00	4.00	0.5 V. 1.5 Ti. 0.1 B
MT-8	**0.33**	2.0	1.0	0.15	31.0	21.0		4.0	2.1		4.00	....
MT-9	**0.37**	2.0	1.0	0.15	31.0	21.0	5	4.0	1.95	..	4.00	....
MT-10	**0.37**	2.0	1.0	0.15	30.0	20.0	5	4.0	1.70	0.92	4.00	.
MT-11	**0.43**	2.0	1.0	0.15	30.0	20.0	11	4.0	1.59	0.92	4.00	
MT-11A	**0.28**	1.0	0.5	0.15	30.0	20.0	12	4.0	2.43	0.78	4.00	
MT-12	**0.16**	1.0	0.5	0.15	30.0	20.0	12	4.0	6.35	.	4.00	
MT-13	**0.11**	1.0	0.5	0.15	30.0	20.0	12	4.0	3.0		4.00	
MT-14	**0.11**	1.0	0.5	0.15	30.0	20.0	12	4.0	2.77	1.29	4.00	.

b. Cast Series. The cast Ni-Cr-Co-Fe base alloys have a wider variation in composition than the forged series. The Ni content varies from 20 to 31 per cent, the Cr from 15 to 21 per cent and the Co from 0 to 21 per cent. Since the alloys are cast, the C content varies from 0.15 to 1.56 per cent and for most of the alloys is about 1 per cent. The composition ranges are shown in Table 8-4[2]. The cast alloys are water-quenched between 1150

TABLE 8-2. RUPTURE TEST RESULTS AT 815°C (1500°F) ON FORGED BARS[2]

Alloy	Heat Treatment[1]	Aging Treatment[1]	Stress Psi	Hours to Fracture	Elong. % in 2″	R. A. %	Creep Rate % per hr	
							Total	Min.
TB	2200° WQ	50 hr 1500°	20,000	14.0	13.2	14.9	0.94	....
	2200° WQ	50 hr 1500°	20,000	11.0	15.8	14.1	1.43	....
	2250° WQ	50 hr 1500°	15,000	100.0	17.8	. ...	0.178	....
TE	2200° WQ	50 hr 1500°	20,000	15.5	19.8	30.0	1.27	....
	2200° WQ	50 hr 1500°	20,000	13.5	30.8	26.7	1.60	....
	2300° WQ	None	20,000	52.4	12.1	17.3	0.23	...
	2200° WQ	50 hr 1500°	15,000	213.0	20.2	.	0.093	....
	2300° WQ	None	15,000	380.0	17.2	27.3	0.045	....
TE-O	2200° WQ	50 hr 1500°	20,000	21.5	7.9	6.4	0.37	....
	2200° WQ	50 hr 1500°	20,000	13.8	35.9	20.9	2.82	....
TE-OA	2150° WQ	50 hr 1500°	20,000	7.5	29.2	29.6	3.90	...
	2150° WQ	50 hr 1500°	20,000	6.5	49.8	29.0	7.70	....
	2250° WQ	50 hr 1500°	20,000	9.0	18.1	17.2	2.01	....
	2250° WQ	50 hr 1500°	15,000	105.0	17.2	15.1	0.16	....
TE-OB	2200° WQ	50 hr 1500°	20,000	14.0	17.2	21.6	1.23	....
	2250° WQ	None	20,000	24.5	11.8	18.0	0.46	....
	2300° WQ	None	20,000	39.6	8.8	11.1	0.22	....
	2250° WQ	None	15,000	120.0	14.0	14.7	0.116	..
TE-OC	2200° WQ	50 hr 1500°	20,000	13.5	30.8	25.5	2.28	....
	2250° WQ	None	20,000	15.0	15.2	20.3	1.01	....
	2250° WQ	None	15,000	110.0	23.4	19.6	0.212	....
TE-T	2150° WQ	50 hr 1500°	20,000	6.0	36.2	24.5	6.04	....
	2250° WQ	50 hr 1500°	20,000	8.0	25.0	20.3	3.12	....
	2250° WQ	50 hr 1500°	15,000	36.0[2]	2.2	14.5	0.61	....
TE-C1	2200° WQ	50 hr 1500°	20,000	18.5	2.6	3.2	0.14	....
	2200° WQ	50 hr 1550°	20,000	4.3	19.8	27.0	4.65	....
	2200° WQ	None	20,000	11.5	18.4	19.7	1.60	....
SX	2200° WQ	50 hr 1500°	20,000	4.5	14.5	26.8	3.22	....
SY	2200° WQ	50 hr 1500°	20,000	6.0	6.6	4.8	1.10	....
SZ	2200° WQ	50 hr 1500°	20,000	17.0	19.8	18.2	1.17	....
	2200° WQ	50 hr 1500°	20,000	10.0	13.2	23.2	1.32	....
MT-2	2200° WQ	50 hr 1500°	20,000	11.0	18.3	41.5	1.66	....
	2200° WQ	None	20,000	13.0	27.6	47.5	2.12	....
	2000° WQ	None	20,000	6.5	30.6	42.4	4.70	....
MT-4	2200° WQ	50 hr 1500°	20,000	7.0	33.0	33.5	4.70	....
	2250° WQ	50 hr 1550°	20,000	13.0	21.0	27.2	1.62	....
	2250° WQ	50 hr 1500°	15,000	56.0	22.4	....	0.34	....
MT-5	2200° WQ	50 hr 1500°	20,000	9.0	13.2	28.0	1.47	....
	2250° WQ	50 hr 1550°	20,000	8.0	14.2	34.8	1.78	....
	2200° WQ	50 hr 1500°	15,000	27.0	28.2	23.5	1.05	....

TABLE 8–2 *Continued*

Alloy	Heat Treatment[1]	Aging Treatment[1]	Stress Psi	Hours to Fracture	Elong. % in 2″	R. A. %	Creep Rate % per hr	
							Total	Min.
MT-8	2200° WQ	50 hr 1500°	20,000	11.0	10.5	14.8	0.95	...
	2200° WQ	None	20,000	8.0	16.1	11.6	2.01	...
	2200° WQ	50 hr 1500°	15,000	157.0	14.0	12.8	0.089	..
MT-9	2200° WQ	None	20.000	27.0	11.7	8.0	0.43	....
	2200° WQ	None	20,000	30.0	7.0	7.2	0.23	....
	2200° WQ	50 hr 1500°	20,000	16.0	7.9	7.6	0.49	....
MT-10	2100° WQ	50 hr 1500°	20,000	8.5	31.0	31.3	3.65	....
	2100° WQ	None	20,000	7.0	23.6	22.8	3.37	....
	2100° WQ	50 hr 1500°	15,000	79.0	44.5	31.3	0.56	....
MT-11	2100° WQ	50 hr 1500°	20,000	20.0	21.4	22.5	1.07	. .
	2100° WQ	None	20,000	22.0	24.2	23.2	1.01	....
MT-11A	2150° WQ	50 hr 1500°	20,000	10.6	25.6	36.1	2.41	....
	2200° WQ	None	20,000	20.0	37.2	25.7	1.86	....
	2300° WQ	None	20,000	60.5	2.6	3.6	0.04	....
	2200° WQ	None	15,000	119.0	21.8	....	0.183	....
	2300° WQ	None	15,000	936.0	9.8	9.6	...	0.0065
MT-12	2150° WQ	50 hr 1500°	20,000	17.0	30.5	22.1	1.79	. .
	2150° WQ	None	20,000	24.5	16.6	15.2	0.68	....
	2200° WQ	None	20,000	16.7[2]	16.2	13.4	0.97	....
	2300° WQ	None	20,000	25.0	8.0	8.0	0.32	. . .
	2300° WQ	None	20,000	24.3	16.5	10.0	0.68	....
	2300° WQ	None	20,000	122.0[3]	15.9	14.7	0.13	....
	2150° WQ	None	15,000	85.0	24.2	.	0.284	....
MT-13	2150° WQ	50 hr 1500°	20,000	10.5	26.5	30.0	2.52	....
	2200° WQ	None	20,000	17.0	43.5	25.5	2.56	....
	2300° WQ	None	20,000	31.0	18.5	14.0	0.60	....
	2200° WQ	None	15,000	211.0	24.8	....	0.12	....
	2300° WQ	None	15,000	210.0[2]	19.1	15.6	0.09	....
MT-14	2150° WQ	None	20,000	31.5	23.3	15.7	0.74	....
	2300° WQ	None	20,000	36.3[4]	31.5	22.0	0.87	....
	2300° WQ	None	20,000	58.6	20.0	14.0	0.34	....
	2150° WQ	None	15,000	116.0	26.1	....	0.23	....

[1] All temperatures in °F.
[2] Failed in fillet.
[3] Temperature 25°F high.
[4] Temperature 25°F low.

and 1260°C (2100 to 2300°F) and for the most part are not aged except for a few which are tempered at 815 to 871°C (1500 to 1600°F) for 24 or 200 hours.

Stress-Rupture Properties. The results of stress-rupture tests at 815°C (1500°F) to 982°C (1800°F) for loads of 15,000 to 30,000 psi are given in Table 8-5. At 815°C (1500°F) and 15,000 psi, the best alloy is 93N-2

with a time of 3450 hours for fracture. At 815°C (1500°F) and 20,000 psi alloys 93N-2, 108N-2, 111N-2, 104NT-2, 109N-1, and 92NT-2 all last for more than 1000 hours. The elongation is low, not over 3.3 per cent, in all these alloys under the condition of test mentioned. This is typical of cast materials compared to forged. The NT-2 series is promising enough to show at 926 and 982°C (1700 and 1800°F). At 982°C (1800°F)

TABLE 8-3. CREEP TESTS ON FORGED ALLOYS AT 815°C (1500°F)

Alloy	Heat Treatment[1]	Aging Treatment[1]	Load Psi	Total Creep		Minimum Creep Rate		Remarks
				Hours	Elong. in. per in.	Hours	Pct per hr	
TB	2200° WQ	50 hr 1500°	10,000	186	.0614	0 186	0.033	Discontinued
	2200° WQ	50 hr 1500°	7,000	2015	.0333	1370 2015	0.00190	Final
TE	2200° WQ	50 hr 1500°	10,000	221	.0238	0 221	0.010	Discontinued
	2200° WQ	50 hr 1500°	7,000	2435	.00248	1370 2435	0.00006	Final
	2200° WQ	50 hr 1500°	7,000	2360	.00104	1400 2360	0.000014	Final
	2200° WQ	50 hr 1500°	8,500	2110	.00133	1380 2110	0.000031	Final
	2300° WQ	None	8,500	2100	.00095	1000 2100	0.000010	Final
TE O	2200° WQ	50 hr 1500°	7,000	2100	.00131	1000 2100	0.000006	Final
	2250° WQ	50 hr 1500°	8,500	2000	.00115	1200 2000	0.000023	Final
TE-OB	2250° WQ	50 hr 1500°	7,000	600	.00245	200 600	0.000214	Discontinued
SX	2200° WQ	50 hr 1500°	10,000	219	.0520	0 219	0.024	Discontinued
SY	2200° WQ	50 hr 1500°	10,000	170	.0168	Forge crack failure		
	2200° WQ	50 hr 1500°	7,000	270	.0009	120 270	0 00032	Forge crack
SZ	2200° WQ	50 hr 1500°	10,000	171	.1581	0 171	0.092	Discontinued
MT-11A	2300° WQ	None	8,500	2200	.0020	1400 2200	0.00006	Final
	2300° WQ	None	10,000	1400	.00030	500 1400	0.0000001[2]	Final
MT-12	2150° WQ	None	7,000	500	.00276	100 500	0.00032	Discontinued
MT-13	2200° WQ	None	7,000	2000	.00205	1200 2000	0.000027	Final
MT-14	2150° WQ	None	7,000	1000	.00178	500 1000	0.000065	Discontinued
MT-14	2300° WQ	None	8,500	1780	.00450	Power interruptions		Discontinued

[1] All temperatures in °F.
[2] 1 in. gage length.

and 13,000 psi, alloy 97NT-2 has a life of 490 hours and 3 per cent elongation at fracture[3].

Creep Strength. The creep strength of the cast Ni-Cr-Co-Fe base alloys at 815 and 871°C (1500 and 1600°F) is shown in Table 8-6. Alloys 30TA-1 and 15TG-1, containing no Co, are included to indicate the lower values associated with this omission. Results are shown here for the better

TABLE 8-4. COMPOSITION OF CAST ALLOYS TESTED[2]

Alloy	C	Mn	Si	N₂	Ni	Cr	Co	Mo	Ta	Cb	W
30TA-1	0.38	0 7	1	0.12	30	20		6	4.07	5.25	..
24TA-1	0.24	0.7	1	0.12	30	20		6	4.07	5.25	.
17TA-1	0.17	0.7	1	0.122	30	20		6	4.07	5.25	
24TD-1	0.24	0.7	1	0.15	30	20	18.0	6	2.75	4.20	..
22TD-1	0.22	0.7	1	0.15	30	20	18.0	6	2.75	4.20	...
18TD-1	0.18	0.7	1	0.15	30	20	18.0	6	2.75	4.20	
18TG-1	0.18	0.7	1	0.168	30	20		4	1.97	4.04	4
15TG-1	0.15	0.7	1	0.149	30	20		4	1.87	4.04	4
15TG-2	0.15	0.7	1		30	20		4	4	4	4
17TG-2	0.17	0.7	1		30	20		4	4	4	4
13TEOB-1	0.13	0.7	1	0 15	30	20		4	3.51	..	4
42MT9-1	8.42	2.0	1	0.12	31	21	5.0	4	1.95	....	4

N-2 Series of Alloys

(Unless otherwise indicated the analyses are the same as the first listed)

Alloy	C	Mn	Si	N₂	Ni	Cr	Co	Mo	Ta	Cb	W
19N-2	0.19	1.5	1.0		30	21	21	3.0		1.0	2.2
59N-2	0.59										
61N-2	0.61										
86N-2	0.86			0.063							
87N-2	0.87										
93N-2	0.93			0.069							
104N-2	1.04			0.072							
108N-2	1.08							..			
111N-2	1.11			0.063							
115N-2	1.15										
151N-2	1.51										
156N-2	1.56			0.052							

P-2 Series of Alloys

Alloy	C	Mn	Si	N₂	Ni	Cr	Co	Mo	Ta	Cb	W
30P-2	0.30	1.5	1.0		21	21	21	3.0		1.0	2.2
95P-2	0.95										
116P-2	1.16										
117P-2	1.17										

S-2 and SA-2 Series of Alloys

Alloy	C	Mn	Si	N₂	Ni	Cr	Co	Mo	Ta	Cb	W
40S-2	0.40	0.	0.4		20	15	20	4.0		4.0	4.0
76S-2	0.76					15					
80S-2	0.80					15					
37SA-2	0.37					20					
82SA-2	0.82					20					

M-1 Series of Alloys

Alloy	C	Mn	Si	N₂	Ni	Cr	Co	Mo	Ta	Cb	W
75M-1	0.75	1.0	0.5	0.15	30	20	12	4.0	2.0	1.0	4.0
107M-1	1.07							.	.		....
123M-1	1.23							.			...
125M-1	1.25						..	.	.	.	
136M-1	1.36		..			.	..	..	..	.	

257

TABLE 8-4. *Continued*

NT-2 Series of Alloys

Alloy	C	Mn	Si	N₂	Ni	Cr	Co	Mo	Ta	Cb	W
32NT-2	0.32	1.5	1.0	....	30	20	21	3.0	2.0	....	2.2
86NT-2	0.86	...	....	...	..	....	....	....	....	....	....
92NT-2	0.92	....	....	....	....	....	..	....	....	....	....
93NT-2	0.93	..	...	0.070	..	....	....	....	....	....	....
94NT-2	0.94		..	..	...	....	....	....	....	....	....
96NT-2	0.96	(mold casting temp. at 2250°)									
97NT-2	0.97	....	....	0.057	....	....	..	....	....	....	....
102NT-2	1.02	.	.			....	. .	....	....	....	....
104NT-2	1.04	....	.	0.066		....	....	. .	....	....	....
107NT-2	1.07	...	....	. .	.	....	....	....	....	....	....
112NT-2	1.12	....	....	....	..	....	....	..	....	....	....

N-1 Series of Alloys

Alloy	C	Mn	S	N₂	Ni	Cr	Co	Mo	Ta	Cb	W
102N-1A	1.02	1.5	1.0	0.093	30	20	21	0.0	....	1.0	2.2
89N-1B	0.89		...	0.097	...	....	....	....	.. .	....	....
105N-1B	1.05	.	. .	. .	....	....	....	....	....	....	....
109N-1B	1.09	..	...	0.120	..	....	....	....	....	....	....
121N-1B	1.21	...	...	0.090	....	....	....	. .	....	....	....
124N-1B	1.24	....	...	0.085	....	....	....	. .	....	....	....
134N-1B	1.34	....	...	0.090	....	. .	....	. .	....	....	....
106N-1C	1.06	..	....	0.076	..	. .	....	..	....	....	....
107N-1C	1.07	...	....	0.086	..	...	....	.	....	....	....
114N-1C	1.14	...	....	0.110	..	..	. .	.	....	....	....
110N-1D	1.10	.	....	0.089		....	....	.	. .	....	....
111N-1D	1.11	...	...	0.085	..	....	.	. .	....	....	....
115N-1D	1.15	....	....	0.083	.	....	.	. .	..	....	....
122N-1D	1.22	...	....	0.133	..	.	.	.	....	....	....
128N-1B	1.28	.	...	0.105	(cast into a room temp. mold)						

NT-1B Series of Alloys

Alloy	C	Mn	Si	N₂	Ni	Cr	Co	Mo	Ta	Cb	W
90NT-1B	0.90	1.5	1.0	0.110	30	20	21	3.0	2.0	....	2.2
93NT-1B	0.93	....	....	0.101	....	....	....	....	....	....	....
94NT-1B	0.94	....	....	0.090	....	....	....	....	....	....	....
99NT-1B	0.99	. .	....	0.071	....	....	....	....	....	....	....
101NT-1B	1.01	....	...		....	....	....	....	....	....	....
102NT-1B	1.02	....	....	0.081	....	.	....	....	....	....	....
103NT-1B	1.03	....	...		....	....	....	....	....	....	....
111NT-1B	1.11	....	....	0.112	....	..	....	....	....	....	....
115NT-1B	1.15	....	.	0.096	....	. .	....	·.	....	....	....
124NT-1B	1.24	....	. .	0.097	. .	....	....	....	....	....	...

alloy series, namely, N-1, N-2, and NT-2. These selected alloys tested at 815°C (1500°F) and 10,000 to 15,000 psi have creep rates of 0.00002 per cent per hour.

In Table 8-7 the results of analyses for nitrogen are shown on a number of alloys in the N-1, N-2, NT-1, and NT-2 series. Melting in the arc furnace used in these experimental heats results in 0.06 per cent nitrogen on the

Aging Treatment: None unless otherwise specified as follows:

    (1) Aged 24 hrs at 815°C (1500°F)
    (2) Aged 24 hrs at 843°C (1550°F)
    (3) Aged 24 hrs at 870°C (1600°F)
    (4) Aged 200 hrs at 815°C (1500°F)

Test Temperature: 815°C (1500°F) except as follows:

    (5) Tested at 870°C (1600°F)
    (6) Tested at 926°C (1700°F)
    (7) Tested at 982°C (1800°F)

Alloy	Heat Treatment†	Stress Psi	Hours to Fracture	% Elong. in 2"	% R. of A.	%/Hr. Min. Creep Rate
30TA-1	2250, WQ	20,000	33.8	10.7	19.2	....
	2300, WQ	20,000	11.5	1.3	2.2	....
	2250, WQ	15,000	256.0	14.1	23.4	....
24TA-1	2250, WQ	20,000	35.0	12.1	17.6	....
	2250, WQ	15,000	232.0	13.5	18.2	....
17TA-1	2300, WQ (1)	20,000	0.3	Recrystallization at 2300°		
	2300, WQ	20,000	2.5	F; see other poor results		
	2300, WQ (1)	20,000	0.5	at 2300°F in this series.		
24TD-1	2250, WQ	20,000	31.0	8.1	27.8	....
	2300, WQ	20,000	54.3	6.0	27.0	....
	2350, WQ	20,000	17.1	4.1	13.2	....
	2300, WQ	15,000	420.0	11.2	24.5	....
18TD-1	2300, WQ	20,000	0	Recrystallization		
	2300, WQ	20,000	0			
18TG-1	2300, WQ	20,000	62.0	16.8	30.6	0.040
	2300, WQ (3)	20,000	40.0	14.2	24.1	....
15TG-1	2300, WQ (2)	20,000	10.0	14.5	20.4	....
	2300, WQ (1)	20,000	23.3	15.4	20.6	....
15TG-2	2300, WQ	20,000	16.8	12.9	24.0	....
17TG-2	2300, WQ	20,000	22.0	16.0	21.3	....
	2300, WQ	20,000	19.0	17.1	9.8	....
	2250, WQ	20,000	28.0	12.5	14.8	....
13TEOB-1	2300, WQ	20,000	42.0	10.0	....	....
42MT9-1	2300, WQ	20,000	1.5	Recrystallized		
	2250, WQ	20,000	204.6	4.6	4.4	0.017
	2280, WQ	20,000	>240.0	Incomplete		0.023
	2280, WQ	20,000	198.6	7.1	2.4	....
19N-2	2260, WQ	30,000	1.2	14.4	11.8	10.0
	2250, WQ	20,000	68.5	16.0	15.8	0.047
	2300, WQ	20,000	60.8	11.4	7.6	....
61N-2	2250, WQ	30,000	21.3*	7.0	3.0	....
	2260, WQ	30,000	28.6	5.6	1.7	0.073
	2250, WQ	20,000	341.0	7.8	2.4	0.017
86N-2	2250, WQ	30,000	55.0	4.8	2.0	0.036
	2250, WQ	30,000	47.5	4.0	1.0	0.036
	2250, WQ	30,000	69.5 HP	4.8	2.0	0.041
	2250, WQ (4)	20,000	828.0	3.1	1.7	0.0020

TABLE 8-5.   *Continued*

Alloy	Heat Treatment†	Stress Psi	Hours to Fracture	% Elong. in 2″	% R. of A.	%/Hr. Min. Creep Rate
87N-2	2300, WQ	20,000	0.2	Recrystallization		
	2300, OQ	20,000	191.8	4.0	1.6	....
	2280, WQ	20,000	>281.5	Incomplete		
	2250, WQ	20,000	960.0	3.6	1.6	0.0018
	2250, WQ	15,000	>3450.0	Discontinued		0.00015
93N-2	2250, WQ	30,000	101.2	7.1	1.6	0.035
	2250, WQ (4)	30,000	22.3	5.4	4.4	....
	2250, WQ	20,000	1200.0	3.5	0.5	0.0007
104N-2	2260, WQ	30,000	72.0	4.6	1.0	0.037
	2260, WQ	30,000	44.5*	....	....	....
108N-2	2250, WQ	20,000	>590.0	Broke in grip failure		
	2250, WQ	20,000	1080.0	1.8	0.0	0.00050
111N-2	2250, WQ	30,000	27.2	7.2	3.2	....
	2250, WQ	30,000	52.7	6.0	1.0	0.027
	2250, WQ	20,000	1841.0	3.3	0.5	0.00027
115N-2	2260, WQ	30,000	52.7	4.0	1.0	0.027
	As cast	30,000	7.0	12.0	7.8	1.71
151N-2	2250, WQ	30,000	9.1	2.5	2.3	0.30
	2250, WQ	30,000	9.5	4.7	2.0	0.30
156N-2	2300, WQ	20,000	112.3	Recrystallization		
	2250, WQ	20,000	534.0	3.0	0.5	0.0040
	2300, WQ	15,000	293.0	3.5	Recrystallization	
30P-2	2250, WQ	30,000	4.7	5.0	2.0	1.00
	2260, WQ	30,000	2.8	4.0	2.0	....
	2250, WQ	20,000	155.0	8.0	2.5	0.035
95P-2	2260, WQ	30,000	30.7	3.0	1.0	0.072
	2260, WQ	30,000	32.0	2.5	1.0	0.050
117P-2	2260, WQ	30,000	70.6	1.6	0.8	0.020
116P-2	2260, WQ	20,000	885.0	2.8	0.5	0.015
40S-2	2250, WQ	30,000	4.6	4.0	0.5	....
	2250, WQ	20,000	174.5	8.9	1.3	0.013
76S-2	2250, WQ	30,000	15.1	4.0	1.0	....
80S-2	2250, WQ	30,000	11.1*	....	....	....
	2300, WQ	30,000	0.0	Recrystallization		
	2250, WQ	20,000	302.5	2.0	0.5	0.0054
37SA-2	2260, WQ	30,000	2.0	8.0	3.7	4.0
	2260, WQ	30,000	2.0	11.2	6.1	....
	2260, WQ	30,000	2.0 HP	6.4	8.6	....
82SA-2	2250, WQ	30,000	5.4	2.4	1.0	0.136
	2260, WQ	30,000	3.3 HP	1.5	0.5	....
	2250, WQ	25,000	22.7	2.8	0.5	....
75M-1	2300, WQ	30,000	0.0	Recrystallization		
	2280, WQ	30,000	17.0	2.4	1.0	....
107M-1	2280, WQ	30,000	0.5	Appears recrystallized		
	2260, WQ	30,000	15.7	1.5	0.5	....
	2260, WQ	30,000	26.3 HP	4.8	2.4	0.015

TABLE 8-5. *Continued*

Alloy	Heat Treatment†	Stress Psi	Hours to Fracture	% Elong. in 2″	% R. of A.	%/Hr. Min. Creep Rate
123M-1	2320, WQ	30,000	4.7	Appears recrystallized		
	2300, WQ	30,000	88.0	3.6	0.5	0.040
	2250, WQ	30,000	31.3	8.8	5.6	....
	2300, WQ	20,000	6.8	Recrystallized		
	2280, WQ	20,000	848.0	1.5	0.5	0.0011
125M-1	2260, WQ	30,000	38.5	5.6	1.2	0.027
	2260, WQ	30,000	34.6	4.0	1.0	0.050
136M-1	2260, WQ	30,000	5.7*	2.5	0.5	....
32NT-2	2260, WQ	30,000	2.0	....	....	••••
	2300, WQ	20,000	0.0	Recrystallized		
	2280, WQ	20,000	182.0	1.5	1.6	....
	2250, WQ	20,000	295.0	8.5	2.5	0.023
	2300, OQ	20,000	0.2	Recrystallized		
	2250, OQ	15,000	956.0	5.6	1.0	0.00206
86NT-2	2250, WQ	30,000	55.0	5.0	2.0	....
	2275, WQ	20,000	898.0	6.0	1.6	....
92NT-2	2260, WQ	30,000	52.8	4.0	1.6	0.032
	2250, WQ	30,000	51.8	5.6	1.2	0.050
	2250, WQ	25,000	390.5	3.0	1.6	0.0023
	2260, WQ	20,000	1606.0	3.0	1.0	0.00035
93NT-2	2260, WQ	30,000	76.2	5.3	2.8	0.026
	2200, WQ	30,000	40.2	6.0	2.3	0.073
	2100, WQ	30,000	23.5	9.2	9.0	0.333
94NT-2	2260, WQ	30,000	80.0	4.8	. ..	....
	2200, WQ	30,000	45.5	5.7	3.2	0.075
	2100, WQ	30,000	29.7	9.7	4.3	0.320
	2100, WQ	25,000	211.8	4.7	2.6	0.0081
	2100, WQ	25,000	116.6	7.0	5.1	0.032
97NT-2	2260, WQ	30,000	79.8	4.8	2.2	0.034
	2260, WQ	30,000	99.0	5.7	4.0	0.021
	2260, WQ	25,000	489.0	3.1	1.3	0.0017
	2200, WQ	25,000	310.0	4.0	1.3	0.0078
	2260, WQ (6)	27,000	1.4	22.0	18.3	....
	2260, WQ (6)	19,000	88.0	7.0	11.5	....
	2260, WQ (6)	17,000	134.5	5.0	8.5	....
	2260, WQ (6)	15,000	412.0	2.0	3.9	....
	2260, WQ (7)	21,000	1.4	20.0	34.0	....
	2260, WQ (7)	15,000	48.6	8.0	12.1	....
	2260, WQ (7)	14,000	61.0	3.0	7.1	....
	2260, WQ (7)	13,000	490.0	3.0	4.9	....
	2260, WQ (7)	11,000	329.5	4.0	10.9	....
99NT-2	2260, WQ	30,000	109.5	4.3	1.2	0.013
	2260, WQ	25,000	542.4	3.2	1.8	0.0041(?)
	2200, WQ	25,000	412.3	3.5	2.0	0.0028
	2260, WQ (5)	20,000	289.0	2.0	1.0	0.0195

TABLE 8-5. *Continued*

Alloy	Heat Treatment†	Stress Psi	Hours to Fracture	% Elong. in 2″	% R. of A.	%/Hr. Min. Creep Rate
102NT-2	2260, WQ	30,000	105.0	5.2	1.2	0.017
	2260, WQ (5)	30,000	17.2	6.3	4.1	0.230
	2260, WQ (5)	25,000	148.0	2.8	1.2	0.012
	2260, WQ (5)	20,000	805.0	2.8	1.0	0.0013
104NT-2	2260, WQ	30,000	69.3	6.8	1.6	0.030
	2260, WQ	30,000	100.0 HP	4.0	1.7	0.021
	2260, WQ	20,000	2100.0	3.3	1.2	0.00026
107NT-2	2260, WQ	30,000	61.0	5.6	2.4	0.033
	2260, WQ	30,000	86.4 HP	4.8	1.6	0.028
112NT-2	2260, WQ	30,000	85.0 HP	5.0	2.8	0.029
102N-1	2260, WQ	30,000	70.7	4.0	1.0	0.025
	As cast	30,000	6.5	10.4	7.3	1.60
89N-1	2250, WQ	30,000	39.5	4.6	1.3	0.036
	2250, WQ	30,000	38.0	4.0	1.0	0.036
	2260, WQ	30,000	47.3 HP	4.0	1.7	0.046
	As cast	30,000	10.3	14.2	7.8	1.38
109N-1	2260-½-WQ	30,000	69.4	7.2	2.5	0.035
	2260-1-WQ	30,000	68.0	6.4	1.7	0.063
	2260-2-WQ	30,000	43.0	5.6	2.0	....
	2260, WQ	20,000	2240.0	3.3	1.0	0.00008
121N-1	2260, WQ	30,000	44.0	4.8	2.4	0.075
	2260, WQ	30,000	72.0 HP	6.5	3.3	0.054
	2260, WQ	30,000	92.7	5.6	2.8	0.034
124N-1	2260, WQ	30,000	35.2	6.5	3.5	0.154
134N-1	2260, WQ	30,000	48.2	8.8	4.8	0.091
106N-1	2260, WQ	30,000	80.0	4.8	2.0	0.032
	2260, WQ	25,000	377.0	4.0	1.0	0.0028
107N-1	2260, WQ	30,000	56.7	5.2	3.2	0.051
	2260, WQ	30,000	52.4*	3.2	2.0	0.047
	2260, WQ	30,000	53.4	4.3	1.6	0.029
114N-1	2260, WQ	30,000	32.6*	5.6	2.5	0.101
110N-1	2260, WQ	30,000	105.0	5.6	1.4	0.019
	2260, WQ	25,000	411.3	3.3	1.0	0.0028
	2260, WQ	25,000	364.0	3.0	0.8	0.0026
111N-1	2260, WQ	30,000	79.4	5.2	2.0	0.042
	2260, WQ	30,000	62.0*	3.1	1.8	0.028
	2260, WQ	25,000	349.5	2.8	1.8	0.0021
115N-1	2260, WQ	30,000	124.7	4.3˙	2.4	0.019
	2260, WQ	20,000	257.3	4.3	1.0	0.020
122N-1	2260, WQ	30,000	23.0	5.6	3.6	....
90NT-1	2260, WQ	30,000	20.3	4.8	2.4	....
	2260, WQ	30,000	35.5	5.6	4.0	....
	2260, WQ	30,000	3.5*	...	...	....
93NT-1	2260, WQ	30,000	65.3	6.2	1.8	0.045
94NT-1	2260, WQ	30,000	72.0	6.1	2.4	0.045
	2260, WQ	25,000	315.0	3.0	2.0	0.0028
	2260, WQ	25,000	365.6	3.0	1.0	0.0056

TABLE 8-5—*Continued*

Alloy	Heat Treatment†	Stress psi	Hours to Fracture	% Elong. in 2″	% R. of A.	%/Hr. Min. Creep Rate
99NT-1	2260, WQ	30,000	154.0 HP	4.0	1.6	0.015
	2260, WQ	30,000	50.8 HP	2.8	2.0	0.046
	2260, WQ	25,000	200.0 HP	2.5	0.5	0.0064
101NT-1	2260, WQ	30,000	101.3	6.1	4.6	0.027
	2260, WQ	30,000	97.9	6.4	2.4	0.034
	2260, WQ (5)	25,000	98.0	4.8	1.6	0.021
	2260, WQ (5)	20,000	400.0	3.2	1.2	0.0010
102NT-1	2260, WQ	30,000	42.3	5.6	2.0	0.040
	2260, WQ	30,000	50.0	4.0	2.0	0.042
	2260, WQ	30,000	89.8	4.4	3.1	0.019
103NT-1	2260, WQ	30,000	27.7	3.2	2.4	....
111NT-1	2260, WQ	30,000	34.6*	4.0	2.0	....
	2260, WQ	30,000	18.5*	<2.0	...	....
	2260, WQ	30,000	9.5*	<1.0	...	....
115NT-1	2260, WQ	30,000	60.1	7.5	4.5	0.085
	2260, WQ	25,000	200.0	4.0	2.0	0.011
	2260, WQ	25,000	294.8	3.5	1.6	0.0036
124NT-1	2260, WQ	30,000	41.0	7.2	5.2	0.126
	2260, WQ	30,000	27.3 HP	7.0	5.7	0.204
	2260, WQ	25,000	209.0	4.6	3.1	0.015
102NA-2	2260, WQ	30,000	29.4	5.7	4.9	....
	2260, WQ	30,000	63.8	6.5	4.4	0.060
101NA-2	2260, WQ	30,000	25.5	7.0	6.8	....
	2260, WQ	30,000	22.7	4.0	3.6	....
94NC-2	As cast	30,000	8.5	22.3	12.7	....
	As cast	30,000	7.5	10.4	12.9	....
	2260, WQ	30,000	28.0	5.7	3.6	0.115
	2260, WQ	30,000	15.3	4.1	5.2	....

* Failure occurred in the fillet section.

HP These letters following the hours-to-rupture figure indicate that the specimen was highly polished prior to testing instead of testing with the as-cast and sand-blasted surface.

† All temperatures in °F.

average. Additional nitrogen raises the value to a maximum of 0.095 per cent. With increase in C content, the solubility of nitrogen decreases. In the lower C ranges, the presence of nitrogen increases creep strength. A carbon range of 1.0 to 1.5 per cent is recommended for these alloys.

In comparing alloys of the same composition in the forged and cast states, the forged alloys in many cases have the higher ductility in stress-rupture tests. The cast alloys have longer life to rupture in spite of their lower ductility. This is shown for the forged alloy MT-9 in Table 8-10 at 815°C (1500°F) 20,000 psi, with a rupture life of 27 hrs and 11.7 per cent elongation. The cast alloy 42MT9-1 in Table 8-5 at 815°C (1500°F) and 20,000

psi has a rupture life of 204.6 hrs and an elongation of 4.6 per cent. In this alloy, there is a marked difference between the microstructures of the cast and forged states which may account for some of the differences in properties. A comparison of the forged alloy TE-OB in Table 8-2 with the cast alloy 13TEOB-1 in Table 8-5 at 815°C (1500°F) and 20,000 psi does not show very different properties.

II. Co-Cr-Mo Base Alloys, Cast

These alloys are selected on the basis of improving the highly successful "Vitallium", especially by increasing the C content. They contain a

TABLE 8-6. CREEP RESTS RESULTS AT 815°C AND 871°C (1500 AND 1600°F) ON Ni-Cr-Co-Fe BASE ALLOYS[2]

Temperature of Test: 815°C (1500°F) except as follows; (1) 870°C (1600°F)

Alloy	Heat Treatment†	Load Psi	Total Creep		Minimum Creep Rate		Remarks
			Hours	Elong. In./In.	Hours	%/Hr.	
30TA-1	2250, WQ	7,000	670	0.00350	200-670	0.000198	Discontinued
15TG-1	2300, WQ	8,500	650	0.00215	200-650	0.000130	Discontinued
61N-2	2260, WQ	10,000	1030	0.00118	200-1030	0.0000023	Holder failed. Final
93N-2	2250, WQ	12,000	2030	0.00155	1100-2030	0.000007	Final
93N-2*	2260, WQ	13,500	2230	0.0020	1600-2230	0.000012	Final
108N-2	2260, WQ	13,500	2230	0.0023	1300-2230	0.00002	Final
108N-2	2260, WQ	15,000	1700	0.0035	800-1700	0.000012	Holder failed. Final
151N-2	2260, WQ	12,000	800	0.0037	300-800	0.00012	Discontinued
116P-2	2260, WQ	12,000	2000	0.0033	1200-2000	0.000028	Final
104NT-2	2260, WQ	13,500	2500	0.0016	1600-2500	0.000019	Final
104NT-2	2260, WQ	15,000	2400	0.0022	1400-2400	0.000030	Final
112NT-2	2260, WQ	16,000	650	Poor temperature control			Discontinued
121N-1	2260, WQ	15,000	2600	0.0018	1400-2600	0.00001	Final
99NT-1	2260, WQ	15,000	2100	0.0023	1100-2100	0.000024	Final
100NT-2	2260, WQ	15,000	1500	0.0023	600-1500	0.000028	Final
100NT-2	2260, WQ (1)	10,000	2520	0.0020	1300-2500	0.000019	Final
102NT-2	2260, WQ (1)	10,000	2320	0.0029	1100-2320	0.000057	Final
102NT-2	2260, WQ (1)	12,000	2000	0.0030	900-2000	0.000103	Final

† Temperatures °F

minimum of 61 per cent Co, in all cases 23 per cent Cr and 6 per cent Mo. The compositions of the V-2, V-1, VN, VT, etc. series are given in Table 8-8[2]. For the most part they are tested in the cast condition except for those with the lower C contents, which may be aged.

Stress-Rupture Properties. These alloys are so strong at 815°C (1500°F) that a load of 25,000 psi results in a life of over 1000 hours for alloys 111VT2-2, 113VT2-2, and 108VTN2-2. Elongations at fracture vary from 3.9 to 7 per cent, as shown in Table 8-9[2].

Creep Properties. The minimum creep rate of alloy 111VT2-2 shown in Table 8-10 at 815°C (1500°F) and a load of 13,500 psi is 0.000034 per cent per hour.

TABLE 8-7. RESULTS OF ANALYSIS FOR NITROGEN[2]

Alloy	% N₂ Added	Analyzed		Alloy	% N₂ Added	Analyzed	
		% N₂	% O			% N₂	% O
86N-2	0	0.063	0.013	93NT-2	0	0.070	0.005
93N-2	0	0.069	0.010	97NT-2	0	0.057	0.005
104N-2	0	0.072	0.013	99NT-2	0	0.057	0.004
111N-2	0	0.053	0.005	104NT-2	0	0.066	0.009
156N-2	0	0.052	0.020	90NT-1*	0.15	0.110	0.011
102N-1	0.08	0.093	0.005	93NT-1	0.15	0.101	0.005
89N-1	0.15	0.097	0.008	94NT-1	0.15	0.090	0.004
109N-1	0.15	0.120	0.006	99NT-1	0.15	0.071	0.006
121N-1	0.15	0.090	0.005	102NT-1	0.15	0.081	0.006
124N-1	0.15	0.085	0.005	111NT-1	0.15	0.112	0.009
134N-1	0.15	0.090	0.005	115NT-1	0.15	0.096	0.005
106N-1	0.20	0.076	0.005	124NT-1	0.15	0.097	0.005
107N-1	0.20	0.086	0.005				
114N-1*	0.20	0.110	0.004				
110N-1	0.23	0.089	0.007				
111N-1	0.23	0.085	0.006				
115N-1	0.23	0.083	0.007				
122N-1*	0.23	0.133	0.005				
128N-1	0.23	0.105	0.006				

* Hot top or riser of casting was very badly puffed up, indicating that nitrogen was still in excess of the solubility and was in the process of being released by the alloy.

Average Nitrogen Content (in %) of the N-2 and NT-2-Type Alloys

N-2 (No N₂ Added)	N-1 (0.08 and 0.15% Added)	N-1 (0.20% Added)	N-1 (0.23% Added)
0.072	0.090	0.076	0.089
0.053	0.090	0.086	0.083
0.063	0.120	0.110	0.085
0.052	0.085	———	0.133
0.065	0.097	0.091 avg.	0.105
———	0.093		———
0.061 avg.	———		0.099 avg.
	0.096 avg.		

NT-2 (No N₂ Added)		NT-1 (0.15% N₂ Added)		
0.070	0.057	0.101		0.090
0.057	0.066	0.081	0.097	0.096
0.062 avg.		0.093 avg.		

As a result of the laboratory tests described in this chapter, the series of alloys giving the most promise are the cast Ni-Cr-Co-Fe base alloys N-2,

TABLE 8-8. "VITALLIUM" BASE CAST ALLOYS[2]

(Unless otherwise indicated, the analyses are the same for the entire series, as shown by the first in each group)

Alloy	C	N₂	Cr	Co	Mo	Others
84V-2	0.84	....	23	69	6	None
89V-2	0.89	....	..	..	..	....
90V-2	0.90	....	..	..	..	....
93V-2	0.93	0.064	..	..	..	....
94V-2	0.94	....	..	..	..	....
110V-2	1.10	....	..	..	..	....
112V-2	1.12	....	..	..	..	....
116V-2	1.16	....	..	..	..	....
127V-2	1.27	....	..	..	..	....
133V-2	1.33	....	..	..	..	....
134V-2	1.34	....	..	..	..	....
147V-2	1.47	....	..	..	..	....

V-I Series

Alloy	C	N₂	Cr	Co	Mo	Others
82V-1	0.82	0.118	23	62	6	6 Fe (0.15 N₂ added)
114V-1	1.14	*	23	69	6	(N₂ gas bubbled in)
116V-1	1.16	0.086	23	68	6	(0.04 N₂ added)

VN Series

Alloy	C	N₂	Cr	Co	Mo	Others
104VN2-2	1.04	....	23	67	6	2 Ni
95VN8-2	0.95	....	23	61	6	8 Ni

VT Series

Alloy	C	N₂	Cr	Co	Mo	Others
40VT2-2	0.40	....	23	67	6	2 Ta
70VT2-2	0.70	...	..	..	..	....
77VT2-2	0.77	....	..	..	..	....
91VT2-2	0.91	....	..	..	..	....
95VT2-2	0.95(No.1)	....	..	..	..	....
95VT2-2	0.95(No.2)	....	..	..	..	....
96VT2-2	0.96	....	..	..	..	....
99VT2-2†	0.99	....	..	..	..	....
100VT2-2††	1.00	....	..	..	..	....
101VT2-2	1.01	....	..	..	..	....
102VT2-2*	1.02	....	..	..	..	....
103VT2-2**	1.03	....	..	..	..	....
111VT2-2	1.11	0.062	..	..	..	....
113VT2-2	1.13	....	..	..	..	....
117VT2-2	1.17	....	..	..	..	....
120VT2-2	1.20	....	..	..	..	....
125VT2-2	1.25	....	..	..	..	....
117VT4-2	1.17	....	23	65	6	4 Ta

TABLE 8-8—*Concluded*

Other Alloys

Alloy	C	N₂	Cr	Co	Mo	Others
85VB-2	0.85	....	23	67	6	0.5 Boron added as FeB
97VZ2-2	0.97	....	23	67	6	2 Zr
109VW2-2	1.09	....	23	67	6	2 W

† Mold temperature at 1500°F
†† Mold temperature at 2250°F
* Fine tungsten powder spray applied to wax pattern before investing
** Mold temperature at 75°F (room temperature)

NT-2 and the cast "Vitallium" base alloys, VT2-2 series. The VT-2 series with 1 per cent C has a higher rupture strength at 815°C (1500°F), but is weaker than the VT-2 series at 982°C (1800°F). The creep strength of the N-2 series is greater at 815 and 871°C (1500 to 1600°F). The microstructure of both alloys consists of a network structure of carbides in an austenitic matrix. Increase of C from 0.2 to 1.5 per cent results in an increase in the network structure which corresponds in a general way with increase in rupture strength.

III. Chromium-base Alloys

In any survey of metals for use at temperatures in the range of 871°C (1600°F), both availability and cost of the alloy are factors. For large-scale production the extensive application of rare or noble metals is eliminated. Thus, for the qualities of high melting point and stability at 871°C (1600°F), consideration must be given to alloys based on the metals W, Mo, or Cr. Alloys of W in combination with Cr are not practical, as they are extremely fragile, and W-base alloys are difficult to melt and cast[8].

Cr as a base for heat-resistant alloys is attractive because of its oxidation resistance, high strength at elevated temperatures, and lower specific gravity than the Co-base alloys. Some of the properties of Cr which are of importance in its resistance to heat are as follows[8]:

Properties of Chromium

Melting point 1890°C ± 10 (3430°F ± 20)
Hardness at 70°F—108–193 Brinell
        at 1600°F—142 DPH
Density 7.138 gm per cu cm
Coefficient of Thermal Expansion 3.2×10^{-6} to 5.7×10^{-6} from 70°F to 1290°F
Stress rupture at 1600°F, at 20,000 psi, time for rupture 1 min, elong. 3.5%, reduction of area 3.7% in 1 inch gage length.
Oxidation resistance: Similar to that of 24 per cent Cr steel. The loss in weight when heated in air at 1600°F is 0.00338 gm per sq in per 100 hr.

TABLE 8-9. STRESS-RUPTURE TEST RESULTS AT 815 TO 982°C (1500 TO 1800°F) AT VARIOUS STRESSES FOR "VITALLIUM" TYPE ALLOYS[2]

Aging Treatment: None unless otherwise specified as follows:

    (1) Aged 24 hrs at 732°C (1350°F)
    (2) Aged 50 hrs 815°C (1500°F)
    (3) Aged 42 hrs 815°C (1500°F)
    (4) Aged 16 hrs 815°C (1500°F)

Temperature of Test: 815°C (1500°F) except as follows:

    (5) Test temperature 870°C (1600°F)
    (6) Test temperature 926°C (1700°F)
    (7) Test temperature 982°C (1800°F)

Alloy	Heat Treatment†	Stress Psi	Rupture Time, Hrs.	% Elong. in 2″	% R. of A.	Minimum Creep %/Hr.
84V-2	As cast	30,000	82.8	15.3	9.3	0.048
93V-2	As cast	30,000	118.5	13.6	6.9	0.045
	As cast	25,000	457.5	11.9	7.3	0.026
	As cast (5)	20,000	421.3	8.0	5.3	0.014
94V-2	As cast	30,000	197.0	10.4	4.8	0.025
	As cast	25,000	900.5	6.5	2.8	0.0039
	As cast (5)	25,000	101.0	9.5	5.3	0.047
110V-2	As cast	30,000	138.1	15.3	9.7	0.049
	As cast	30,000	176.0	10.5	5.2	....
112V-2	As cast	30,000	90.6	15.3	6.5	0.112
	As cast	30,000	127.1	13.6	7.0	0.065
116V-2	As cast	30,000	226.3	6.5	2.4	0.016
	As cast	25,000	425.0	12.1	5.3	0.012
	As cast	25,000	669.0	10.8	4.5	0.0056
116V-2	As cast (5)	25,000	138.3	11.3	6.1	0.039
124V-2	As cast	30,000	120.0	18.0	....	....
	As cast	30,000	102.0	16.1	11.1	0.120
127V-2	As cast	30,000	372.0	8.8	2.0	0.013
	As cast	25,000	535.0	9.1	4.0	....
	As cast	25,000	543.7	8.5	2.8	0.0069
	As cast (5)	20,000	347.3	10.2	6.8	....
134V-2	As cast	30,000	74.0	13.7	10.8	....
	As cast	30,000	62.4	12.8	9.0	....
147V-2	As cast	30,000	192.0	12.0	5.1	0.034
	As cast	25,000	658.5	13.3	5.7	0.0082
	As cast (5)	20,000	724.7	11.0	7.3	0.0079
82V-1	As cast	30,000	14.0	17.7	-11.5	....
	2260, WQ	30,000	0.0	Broke while loading		
	As cast	30,000	25.0	8.0	5.7	....
114V-1	As cast	30,000	150.0	13.7	6.5	0.033
	As cast	30,000	130.5	11.0	5.3	....
	As cast	30,000	95.4	8.7	4.9	....
116V-1	As cast	30,000	138.7	12.9	5.3	0.093
	As cast	30,000	277.0	10.2	4.9	0.018
	As cast (5)	25,000	>60.0	Clock not registering		
	As cast (5)	25,000	78.4	15.3	8.9	0.037

TABLE 8-9. *Continued*

Alloy	Heat Treatment†	Stress Psi	Rupture Time, Hrs.	% Elong. in 2″	% R. of A.	Minimum Creep %/Hr.
104VN2-2	As cast	30,000	76.9*	8.0	....	
	As cast	30,000	185.5	8.5	2.0	0.038
	As cast	30,000	200.0	5.3	3.6	0.015
105VN4-2	As cast	35,000	70.8	8.7	6.2	0.060
	As cast	30,000	130.3	10.0	7.7	0.037
	As cast	30,000	91.7	4.7	5.3	..
	As cast	30,000	140.6	5.6	....	0.030
109VN4-2	As cast	30,000	169.4	18.9	9.7	0.065
	As cast (1)	30,000	157.6	14.4	11.3	....
	As cast (5)	25,000	25.2	22.2	13.4	0.119
95VN8-2	As cast	30,000	34.7	8.8	3.6	....
	As cast	30,000	51.4	11.9	7.6	0.144
40VT2-2	As cast (2)	30,000	44.0	6.5	4.0	....
	As cast	30,000	27.4	8.1	4.0	..
	2300, FC	30,000	10.6	7.2	2.8	.
70VT2-2	As cast	30,000	47.5	8.1	4.9	..
	As cast	30,000	58.3	12.7	7.3	0.087
77VT2-2	As cast	30,000	45.5*	7.2	5.7	0.093
	As cast	30,000	57.2	8.1	4.4	0.092
	As cast	30,000	77.0	14.7	8.0	....
91VT2-2	As cast	30,000	180.0	7.9	4.1	0.032
	As cast (3)	30,000	174.3	15.3	8.6	0.035
95VT2-2	2300, AC (2)	30,000	23.0	2.4	0.5	....
	2350, FC	30,000	0.0	0.0	Complete recrystallization	
	2300, FC	30,000	189.0	7.2	4.1	0.020
	2300, FC	30,000	106.1	2.1	0.5	....
	2200, FC	30,000	85.0	14.2	14.2	0.150
	2100, FC	30,000	79.4	10.2	10.1	0.071
	2100, FC	30,000	48.6	16.8	11.2	0.196
	2000, FC	30,000	65.0	17.4	11.4	0.135
	2000, FC	30,000	37.0	18.4	11.7	0.250
	1800, FC	30,000	121.5	10.0	7.7	0.035
	As cast	30,000	180.0	8.7	10.2	0.021
	As cast	30,000	175.0	9.9	7.8	0.024
96VT2-2	As cast	30,000	>175.0	Poor temperature control		
101VT2-2	As cast	30,000	220.0	7.8	.	...
	As cast	30,000	207.0	7.9	3.6	0.025
	2200, FC	30,000	66.0	6.4	0.5	0.018
	2300, FC	30,000	78.3	1.6	0.8	0.006
102VT2-2	As cast	30,000	219.1	7.3	2.4	0.013
102VT2-2	As cast	30,000	174.0	6.4	4.1	..
111VT2-2	As cast	35,000	<91.0	10.3	6.9	0.048
	As cast	30,000	297.3	8.3	3.7	0.013

TABLE 8-9. *Continued*

Alloy	Heat Treatment†	Stress Psi	Rupture Time, Hrs.	% Elong. in 2″	% R. of A.	Minimum Creep %/Hr.
111VT2-2	2300, FC	30,000	12.6	0.0	Brittle failure	
	As cast	25,000	1093.4	6.5	2.0	0.0035
	As cast (5)	25,000	122.2	6.8	3.2	0.031
	As cast (5)	25,000	136.7	7.9	4.9	0.029
	As cast (5)	20,000	960.0	8.9	2.0	0.0027
113VT2-2	As cast	35,000	69.0	11.1	10.6	0.080
	As cast	35,000	65.2	9.6	8.1	0.078
	As cast	30,000	321.0	7.1	9.7	0.010
	As cast	25,000	1304.0	7.0	7.0	0.0024
	As cast (5)	30,000	85.4	8.8	8.1	0.054
	As cast (5)	25,000	197.0	8.1	7.8	0.022
	As cast (5)	25,000	188.0	8.3	4.9	0.027
	As cast (5)	20,000	890.0	8.1	4.9	0.0053
	As cast (6)	24,000	6.0	20.0	18.0	....
	As cast (6)	17,000	108.0	14.0	20.5	....
	As cast (6)	15,000	173.0	19.0	25.7	....
	As cast (6)	14,000	252.0	12.0	20.2	....
	As cast (6)	13,000	651.0	9.0	12.8	....
120VT2-2	As cast	30,000	159.2	7.3	4.5	0.040
	As cast	30,000	250.0	7.2	5.6	0.020
	As cast (5)	25,000	78.6	7.3	6.9	0.060
	As cast (5)	25,000	141.6	10.5	7.6	0.060
125VT2-2	As cast	30,000	152.0	7.9	3.7	0.021
	As cast	30,000	247.5	7.1	2.5	0.018
	As cast (5)	25,000	135.0	6.4	3.5	0.031
	As cast (5)	25,000	129.7	8.2	4.1	0.036
128VT2-2	As cast (7)	20,000	1.3	22.0	29.0	....
	As cast (7)	12,500	66.5	16.0	33.0	....
	As cast (7)	11,000	102.0	20.0	37.0	....
	As cast (7)	9,000	300.0	20.0	30.9	....
117VT4-2	As cast	30,000	150.0	Poor temperature control		
	As cast	30,000	195.2	7.2	3.6	0.017
	As cast	25,000	444.6	7.0	4.5	0.0062
	As cast (5)	25,000	161.5	8.0	4.5	0.027
	As cast (5)	20,000	801.1	6.8	1.2	0.0061
114VT6-2	As cast	30,000	123.2	7.2	5.3	0.036
	As cast	30,000	114.6	7.2	4.5	0.022
	As cast (1)	30,000	101.7	6.4	4.1	0.040
108VTN2-2	As cast	30,000	330.0	6.4	3.3	0.010
	As cast	30,000	304.8	7.2	4.1	0.012
	As cast	28,000	604.7	6.3	4.9	0.0063
	As cast	25,000	1554.0	3.9	2.4	0.00092
111VT2-0	As cast	35,000	57.0	20.2	17.1	0.123
	As cast	30,000	177.5	17.5	10.5	0.041
	As cast	28,000	274.0	16.8	14.9	0.042
	As cast	25,000	902.3	13.7	10.8	0.0063

TABLE 8-9. *Concluded*

Alloy	Heat Treatment†	Stress Psi	Rupture Time, Hrs.	% Elong. in 2″	% R. of A.	Minimum Creep %/Hr.
97VZ2-2	As cast	30,000	95.9	7.2	5.2	0.027
	As cast	30,000	83.3	8.8	7.7	0.087
	As cast (5)	25,000	160.0	12.9	7.6	0.043
	As cast (5)	20,000	803.0	4.7	4.0	0.0037
109VW2-2	As cast	30,000	122.7	8.8	5.1	0.035
	As cast	30,000	86.3	10.4	2.6	0.065
	As cast (5)	25,000	94.5	9.5	4.9	0.065
45VS2-2	As cast	30,000	28.0	5.6	6.1	....
	As cast	30,000	13.1	9.7	5.3	....
47VS4-2	As cast	30,000	6.1	11.1	12.3	....
108VS2-2	As cast (4)	30,000	87.0	25.4	10.6	0.188
	As cast	30,000	87.3	11.2	12.0	0.067
111VS4-2	As cast	30,000	22.5	18.3	9.9	....
109VX2-2	As cast	30,000	17.6	12.2	18.4	....
	As cast	30,000	29.4	11.1	15.3	....
103VA-2	As cast	30,000	105.8	8.7	2.9	....
	As cast	30,000	75.3	8.0	4.8	....
110VA-2	As cast	30,000	172.3	13.9	10.6	0.046
	As cast	30,000	196.7	18.5	11.7	....
107W8-2	As cast	35,000	90.0	5.6	2.9	0.030
	As cast	35,000	59.9	5.4	2.0	0.049
	As cast	35,000	176.8	6.3	2.8	0.017
	As cast	30,000	232.4	4.8	2.0	....
	As cast	30,000	182.5	8.7	2.9	0.027
	As cast	28,000	340.1	6.6	3.2	0.011

* Broke in fillet.
† Temperature in °F.

TABLE 8-10. CREEP RESULTS AT 815 AND 871°C (1500 AND 1600°F) AT VARIOUS STRESSES[2]

Alloy	Heat Treatment	Aging Treatment	Temp. F	Load Psi	Total Creep		Minimum Creep Rate	
					Hours	Elong. In./In.	Hours	%/Hr.
111VT2-2	As cast	None	1500	13,500	2000	0.00192	800–2000	0.000034
111VT2-2	As cast	None	1500	12,000	2020	0.00170	700–2000	0.000037
111VT2-2	As cast	None	1600	10,000	2130	0.0028	1000–2130	0.000078
116V-1	As cast	None	1500	13,500	2020	0.00330	600–2000	0.000091
127V-2	As cast	None	1500	13,500	2320	0.00360	800–2300	0.000078
97VZ2-2	As cast	None	1600	10,000	2160	0.0039	1100–2160	0.000038
111VT2-0	As cast	None	1500	10,000	2410	0.0027	1100–2400	0.000053
109VT2-2*	As cast	None	1500	13,500	800	0.0029	300–800	0.000154
109VT2-2*	As cast	None	1600	10,000	2500	0.0031	1300–2500	0.000062

* Cast to produce very large grains—these contained essentially single grains across any cross section of the test bar.

In an investigation of binary and ternary alloys of Cr with Be, Co, Cb, Fe, Mo, Ni, Pt, Ta, Th, Ti, W, V, and Zr, many experimental compositions

TABLE 8-11. ELEVATED-TEMPERATURE PROPERTIES OF ALLOY CM469[6,8]

*Chemical Composition**

C	Cr	Mo	Fe
0.03	60	25	14

* Vacuum cast.

Stress-Rupture and Elongation Values

Temp		10 Hrs		100 Hrs		1000 Hrs	
(°C)	(°F)	Tensile Strength (psi)	Elong % in 1″	Tensile Strength (psi)	Elong % in 2″	Tensile Strength (psi)	Elong % in 2″
871	1600	67,000	17	37,800	12.5	21,400	..

* As cast.

Thermal Expansion

Temp °F	Mean Coefficient of Linear Expansion In/In/°F $\times 10^{-6}$	
	As Cast	Aged*
75–300	3.56	3.17
75–600	3.76	3.75
75–900	4.16	4.11
75–1200	4.50	4.52
75–1500	4.81	5.02
75–1800	5.10	5.49

* Heated to 871°C (1600°F) in vacuum for 200 hrs, air cooled.

Hot Hardness

Temp		DPH
(°C)	(°F)	
Room	Room	498
600	1112	430
700	1292	396
871	1600	296
926	1700	274

are eliminated by a hot hardness test carried out at 815°C (1500°F). A requirement of at least 200 DPH for these alloys is a satisfactory lower limit, and further study is prevented if the alloys fall below this value.

In the preparation of Cr-base alloys, melting and casting in vacuum is necessary to eliminate the chief impurities, C, N, and O. The raw materials must be low in Si and Al. Crucibles of beryllia are recommended. The high vapor pressure of molten Cr is a serious factor in the preparation of these alloys. The loss of Cr from vaporization is held at 2 per cent if the time for melting is held at a minimum, if the crucible is designed to have a minimum of exposed surface, and if the temperature is only slightly above the melting point of the alloy being made. Another requisite is maintaining the pressure during melting below 0.1 mm to accelerate deoxidation. Casting of the alloy is in steel or copper molds[8].

TABLE 8-12. ELEVATED-TEMPERATURE PROPERTIES OF 36J ALLOY CAST[5]

Chemical Composition

C	Mn	Cr	Ni	Co	Mo	Ta
0.36	1	23	6	60	6	2

Tensile Properties at Room Temperature

Tensile Strength (psi)	Elongation % in 2"
120,000	10.2

Stress-Rupture and Elongation Values*

Temp	10 hrs		100 hrs		1000 hrs	
	Tensile Strength (psi)	Elong. % in 2"	Tensile Strength (psi)	Elong. % in 2"	Tensile Strength (psi)	Elong. % in 2"
815°C (1500°F)	37,500	18	29,200	12	23,000	5

* Aged 48 hours at 732°C (1350°F).

Of the above-mentioned alloy systems, the most favorable on the basis of stress rupture, density, availability, and cost is the ternary system Cr-Fe-Mo at about 60 per cent Cr, the Fe varying from 15 to 25 per cent and the Mo varying from 25 to 15 per cent. For the optimum strength and ductility, the following conditions must be met: C is less than 0.05 per cent and Si less than 0.2 per cent. Both the O and N are at a minimum. The alloys are chilled cast and annealed 90 hrs at 871°C (1600°F). If the ratio of Fe to Mo is less than 3:5, the alloy cannot be machined, but only ground.

The high-temperature properties of Alloy CM 469 are shown in Table 8-11. This alloy with a nominal composition of 60 per cent Cr, 25 per cent Mo, and 15 per cent Fe has a density of 7.87 gm per cu cm[6,8].

The alloy CM 469 can be machined with "Carboloy" tools and may be finished by grinding. This series of alloys is extremely interesting, but for the present is too brittle to be used in commercial applications. It may be that improved techniques in vacuum melting and casting will improve its ductility.

TABLE 8-13. ELEVATED-TEMPERATURE PROPERTIES OF 73J ALLOY CAST[5]

Chemical Composition

C	Mn	Cr	Ni	Co	Mo	Ta
0.73	1	23	6	60	6	2

Tensile Properties at Room Temperature

Material	Tensile Strength (psi)	Elong % in 2″	Reduction of Area (%)
70J*	111,000	3.0	1.5

* Alloy contained 0.70 C.

Stress-Rupture and Elongation Values*

Temp		10 hrs		100 hrs		1000 hrs	
(°C)	(°F)	Tensile Strength (psi)	Elong % in 2″	Tensile Strength (psi)	Elong % in 2″	Tensile Strength (psi)	Elong % in 2″
732	1350	69,000	7	52,500	7	40,500	7
815	1500	43,500	14	34,800	13	28,200	10
871	1600	33,500	16	26,400	11	21,000	6
926	1700	24,800	20	17,200	13	12,300	6
982	1800	18,000	20	12,800	10	9300	3

* Aged 48 hours at 732°C (1350°F).

Creep Strength

Temp °F	Stress psi for Minimum Creep Rate (% per hr)			
	0.00001	0.0001	0.001	0.01
815°C (1500°F)	10,100	14,300	20,400	28,800

IV. Alloy J Series

The cast alloy J series containing 23 per cent Cr, 6 per cent Ni, 60 per cent Co, 6 per cent Mo, 2 per cent Ta, and 1 per cent Mn represents a more recent laboratory development. Its properties are listed below in Tables 8-12 and 8-13 for two compositions, Alloy 36J with 0.36 per cent C

and Alloy 73J with 0.73 per cent C[5]. At 815°C (1500°F) for 100 hours rupture life, Alloy 73J has a strength of 34,800 psi and 13 per cent elongation. For a rupture life of 1000 hours, the strength is 28,200 with 10 per cent elongation. These excellent results represent a substantial increase over the materials previously tested.

C. Aging Characteristics

Attempts to link microstructural changes with elevated-temperature properties have been made in many instances. All heat-resistant alloys show aging effects on prolonged heating, but any consistent explanation in connection with rupture life or creep life is still uncertain. For alloys operating in the temperature range of 732 to 982°C (1350 to 1800°F), aging is one of the characteristics which may decrease creep strength. The factors which influence aging are temperature, time, strain rate, and length of service at high temperature.

A selection of four cast alloys with wide variation in chemical analysis and good high temperature properties has been made to show the similarity in aging characteristics after exposure at elevated temperature[7]. Aging characteristics are established for four alloys with the following compositions[7]:

Material	CHEMICAL COMPOSITION %									
	C	Mn	Si	Ni	Cr	Co	Mo	W	Ta	Fe
100NT-2	1.0	1.5	0.5	30	20	20	3	2.2	2	bal (20)
"Vitallium"	0.25	1.0	...	..	23	68	6	...	.	....
6059	0.45	1.0	...	32	26	32	6	...	.	....
111VT2-2	1.1	...	...	..	23	67	6	...	2	....

Alloy 100NT-2 is essentially a modified high-C N-155 alloy and the 111VT2-2 is a modified high-C "Vitallium".

The microstructure of alloy 100NT-2 is shown in Figs. 8-1 to 8-5 in the as cast stage and after aging for 48 hrs at 538 and 732°C (1000 and 1350°F), 24 hours at 871°C (1600°F), and 3 hrs at 1204°C (2200°F). The increase of C content from 0.25 to 1 per cent is shown in the microstructure by an increase in the carbide network or mesh structure. Fig. 8–1 has a typical mesh structure characteristic of a 1 per cent C alloy of this type. In general the background or matrix is an austenitic continuous phase with a face-centered structure, although there may be a coexisting hexagonal phase where the Co content is high. Fig. 8-2 of the alloy NT-2 after being heated at 538°C (1000°F) for 48 hrs shows no signs of precipitation. However, after 48 hrs at 732°C (1350°F), precipitation is marked, as in Fig. 8-3 and coarsening or coalescence has occurred after 24 hours at
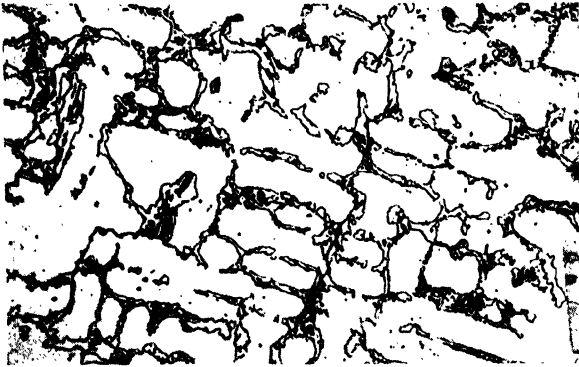
Fig. 8-1. Alloy 100NT-2. As cast. Magnification 250×. (After Grant)
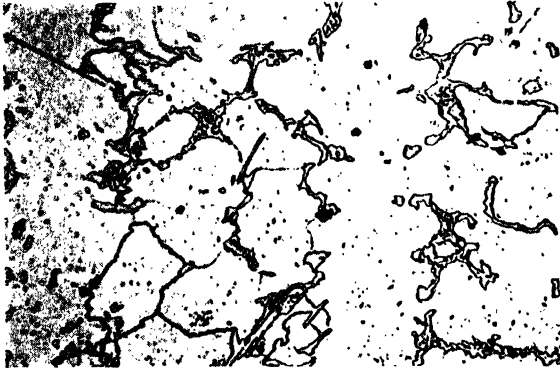
Fig. 8-2. Alloy 100NT-2. Heated 48 hrs. at 538°C (1000°F). Magnification 250×. (After Grant)

Fig. 8-3. Alloy 100NT-2. Heated 48 hrs. at 732°C (1350°F). Magnification 250×. (After Grant)

871°C (1600°F), as in Fig. 8-4. Heating this alloy to 1204°C (2200°F) for 3 hours only dissolves the precipitate formed at the lower temperatures, as in Fig. 8-5.

Figure 8-4. Alloy 100NT-2. Heated 24 hrs. at 871°C (1600°F). Magnification 250×. (After Grant)
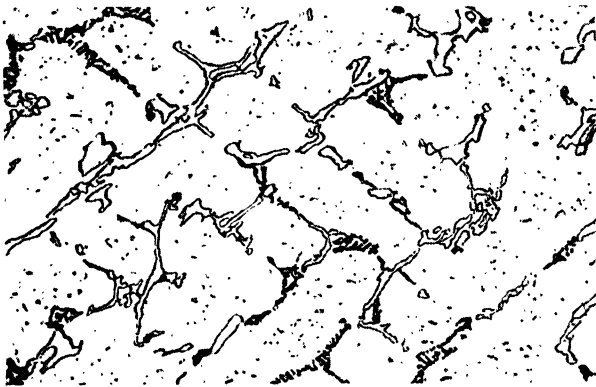
Fig. 8-5. Alloy 100NT-2. Heated 3 hrs. at 1204°C (2200°F). Magnification 250×. (After Grant)

From a study based on changes in microstructure, x-ray diffraction, electrical resistivity, and dilatometry, the aging characteristics are shown to be remarkably similar, even though the alloys range in composition from 0.25 to 1.1 per cent C, 20 to 68 per cent Co and notwithstanding the presence or absence of Fe and Ni. These alloys include the widely divergent compositions, 100NT-2, "Vitallium", 6059, and 111VT2-2.

The following conditions summarize the aging characteristics of the four alloys listed above[7]:

1. All the alloys are stable up to 538°C (1000°F).
2. The first precipitate forms close to 732°C (1350°F).
3. In the low-C alloys the maximum precipitation occurs in the range of 843 to 871°C (1550 to 1600°F). In the high-C alloys it occurs in the range of 871 to 926°C (1600 to 1700°F).
4. Agglomeration of the precipitate before re-solution starts at about 926°C (1700°F). For all the alloys, solution is complete by 1204°C (2200°F).
5. The rate of precipitation is a maximum for all alloys at 732°C (1350°F).
6. Precipitation causes a break in the curves showing expansion coefficients, which suggests the advisability of pre-aging turbine blade materials before assembly and application of stress.

TABLE 8-14. PROPERTIES OF 110N-2 ALLOY CAST[6]

Chemical Composition

C	Mn	Si	Cr	Ni	Co	Mo	W	Cb	N_2
1.10	1.5	1	21	30	21	3	2.2	1	0.07

Creep Strength

Temp °F	Stress psi for Minimum Creep Rate (% per hr) of			
	0.00001	0.0001	0.001	0.01
815°C (1500°F)	14,800	18,000	21,900	26,600

D. COMPARISON OF COMMERCIAL ALLOYS WITH LABORATORY-DEVELOPED ALLOYS

The commercial alloys in actual service for temperatures above 650°C (1200°F) are the results of limitations imposed by manufacturing conditions and economic considerations, coupled with the best possible flow properties obtainable with these requirements. The alloys developed from laboratory tests are not in general so limited, although it is obvious that manufacturing conditions must be met with eventually if they are to be produced in quantity. An attempt is made here to evaluate all the metals available from both sources suitable for operation, especially at 815°C (1500°F) and above. The conclusions are tentative in all cases and are presented as a summary and a comparison.

Prior to such a comparison, a summary of several of the properties of the best noncommercial alloys, 110N-2, 100NT-2, 36VT 2-3, 111VT2-2, and 31V-4, is given for comparison with commercial alloys in Tables 8-14 to 8-18[6].

TABLE 8-15. PROPERTIES OF 100NT-2 ALLOY CAST[6]

Chemical Composition

C	Mn	Si	Cr	Ni	Co	Mo	W	T a
1	1.5	0.5	20	30	20	3	2.2	2

Tensile Properties at Room Temperature*

Tensile Strength (psi)	Reduction of Area (%)	Elong % in 2″
100,000	1.5	1.0

* Alloy heated to 1238°C (2260°F), water-quenched.

Stress-Rupture and Elongation Values*

Temp		10 hrs		100 hrs		1000 hrs	
(°C)	(°F)	Tensile Strength (psi)	Elong % in 2″	Tensile Strength (psi)	Elong % in 2″	Tensile Strength (psi)	Elong % in 2″
815	1500	40,500	8	30,500	5	22,800	3
871	1600	35,000	7	26,100	4	19,300	2
926	1700	25,800	20	18,200	6	13,100	2
982	1800	18,800	20	13,600	7	9900	2.5

* Alloy heated to 1238°C (2260°F) for ½ hr, water-quenched.

Creep Strength

Temp		Stress psi for Minimum Creep Rate (% per hr)			
(°C)	(°F)	0.00001	0.0001	0.001	0 01
815	1500	13,800	17,400	21,800	27,100
871	1600	8500	11,700	16,000	22,000

Thermal Expansion

Temp (°F)	Mean Coefficient of Linear Expansion In/In/°F × 10⁻⁶
70–1200	8.5
70–1350	8.8
70–1500	9.0
70–1600	9.0
70–1800	9.3

TABLE 8-16. PROPERTIES OF ALLOY 36VT2-3 CAST[6]

Chemical Composition

C	Mn	Cr	Co	Mo	Ta
0.26	2	23	65	6	2

Tensile Properties at Room Temperature*

Tensile Strength (psi)	Elong % in 2″	Reduction of Area (%)
102,800	5.9	10.7

* Alloy as cast.

Stress-Rupture and Elongation Values*

Temp	10 hrs		100 hrs		1000 hrs	
	Tensile Strength (psi)	Elong % in 2″	Tensile Strength (psi)	Elong % in 2″	Tensile Strength (psi)	Elong % in 2″
815°C (1500°F)	39,000	28	27,800	25	19,200	6

* Alloy aged 48 hours at 815°C (1500°F).

TABLE 8-17. PROPERTIES OF ALLOY 111VT2-2 CAST[6]

Chemical Composition

C	Cr	Co	Mo	Ta
1.11	23	67	6	2

Tensile Properties at Room Temperature*

Tensile Strength (psi)	Elong % in 2″	Reduction of Area (%)
120,000	3.8	1.0

* Alloy as cast.

Stress-Rupture and Elongation Values*

Temp		10 hrs		100 hrs		1000 hrs	
(°C)	(°F)	Tensile Strength (psi)	Elong % in 2″	Tensile Strength (psi)	Elong % in 2″	Tensile Strength (psi)	Elong % in 2″
815	1500	43,000	11	33,200	10	25,800	6
871	1600	37,000	10	27,300	8	20,000	8
926	1700	22,400	22	16,800	16	12,100	8
982	1800	15,300	22	11,100	20	8000	20

* Alloy as cast.

TABLE 8-17—*Concluded*

Creep Strength

Temp		Stress psi for Minimum Creep Rate (% per hr) of			
(°C)	(°F)	0.00001	0.0001	0.001	0.01
815	1500	11,000	15,000	20,400	27,500
871	1600	7200	10,300	15,100	

Thermal Expansion

Temp (°F)	Mean Coefficient of Linear Expansion In/In/°F $\times 10^{-6}$
70–1200	8.8
70–1350	8.9
70–1500	9.0
70–1600	9.0

TABLE 8-18. PROPERTIES OF 31V-4 ALLOY CAST[6]

Chemical Composition

C	Mn	Cr	Co	Mo
0.31	4	23	65	6

Tensile Properties at Room Temperature*

Tensile Strength (psi)	Elong % in 2″	Reduction of Area (%)
136,300	3.3	6.0

* Alloy aged 48 hrs at 732°C (1350°F).

Stress to Rupture and Elongation Values*

Temp	10 hrs		100 hrs		1000 hrs	
	Tensile Strength (psi)	Elong % in 2″	Tensile Strength (psi)	Elong % in 2″	Tensile Strength (psi)	Elong % in 2″
815°C (1500°F)	36,000	7	26,500	4	19,500	3

* Alloy aged 48 hrs at 732°C (1350°F).

I. Results of Stress-Rupture Tests

a. Rupture Strength. *1. Forged Alloys*

At 650°C (1200°F) "Inconel" X shows the highest rupture strength. The other alloys with superior properties are N-155, N-153, S-816, and "Nimonic" 80.

At 732°C (1350°F) "Inconel" X still is superior, followed by S-816, N-155, and K42B.

At 815°C (1500°F) the strength of "Inconel" X decreases with time, suggesting that overaging is taking place. S-816 is best, followed by "Refractaloy" 26, high-C N-155, S-590, and low-C N-155.

At 871°C (1600°F) the forged alloys decrease in strength, except for the highly alloyed groups such as N-155, S-590, S-816, S-497, and S-495.

At 926 and 982°C (1700 and 1800°F) the forged alloys are generally unsuitable.

2. Cast Alloys

At 650°C (1200°F) there are only a few tests made on cast alloys, as the forged compositions dominate the field. The cast alloy 36J after 1000 hours has a rupture strength of over 55,000 psi which is higher than alloys 61, X-40, and 6059.

At 732°C (1350°F) there are still only a few tests on the cast alloys. Alloy 73J is highest, followed by Nr-90 and X-40. The series of J compositions are higher than any forged alloys at 650 and 732°C (1200 and 1350°F), with the exception of "Inconel" X.

At 815°C (1500°F) alloy 73J is best of the cast group and is much better than the forged alloys. The other outstanding cast alloys are 111VT2-2, NR-88, X-40, 100NT-2, and X-50.

At 871°C (1600°F) alloy 73J is still superior, followed by 111VT2-2, 100NT-2, and X-40. The Cr-base alloy CM-469 has high-stress rupture, but it is too brittle for commercial application.

At 926°C (1700°F) alloys X-40, X-50, and 100NT-2 are best.

At 982°C (1800°F) alloy X-40 is best after 1000 hours stress rupture.

b. Results of Elongation Measurements from Stress-Rupture Tests. Elongation values show many discrepancies that are unexplainable, but it is generally true at these high temperatures that ductility falls off with time. Certain alloys are especially subject to decrease in ductility. It is also true that as the temperature is raised above 650 to 982°C (1200 to 1800°F), the ductility decrease is more marked.

Cast and Forged Alloys

At 650°C (1200°F) alloys N-155 and S-590 show a minimum decrease of ductility with time. Alloys K42B, "Nimonic" 80, "Inconel" X, and 19-9DL all have low ductilities.

At 732°C (1350°F) alloys S-590, low-C N-155, 73J, 6059, and X-40 show slight change of ductility with time. The alloys K42B, "Nimonic" 80, and "Inconel" X all have low ductility.

At 815 to 982°C (1500 to 1800°F) alloy S-590 shows up well, followed by X-40 and 111VT2-2. Alloys K42B, "Nimonic" 80, and "Inconel" X continue to display low ductility.

II. Results of Creep Tests

The creep tests represent on the order of a test of a minimum of 2000 hours' duration. This is not long enough to establish a minimum creep rate for tests which will last for 20,000 hrs, but it is a conservative estimate since in general the creep rate diminishes with time under the assumption that no structural changes occur in the material.

Cast and Forged Alloys

At 650°C (1200°F) alloy K42B has the highest creep strength.

At 732°C (1350°F) alloy S-590 and low-C N-155 have the highest values.

Most of the creep testing is carried out at a temperature of 815°C (1500°F). The best cast alloys for 1 per cent creep in 10,000 hours are 110N-2, 100NT-2, and 93N-2 with a stress of 16,000 to 18,000 psi. The best forged alloys for this creep rate have a stress of about 11,000 psi, as shown by alloys "Inconel" X, S-816, and "Refractaloy".

At 871°C (1600°F) the best cast alloys are 100NT-2, X-40, and 422-19 which require a stress of about 11,000 psi for a minimum creep rate of 1 per cent per 10,000 hours. For this creep rate, the forged alloys fall to about 6000 psi.

References

1. Epremian, E., "Development of a Turbosupercharger Bucket Alloy," *Am. Soc Metals*, Preprint No. 1 (1946).
2. Grant, N. J., "High-temperature Alloys," *Iron Age*, **157**, May 23, May 30, June 6, June 20 (1946).
3. Grant, N. J., "Stress Rupture and Creep Properties of Heat-resistant Gas Turbine Alloys, "*Am. Soc. Metals*," **39**, 281 (1947).
4. Grant, N. J., "Effect of Composition and Structural Changes on the Rupture Properties of Certain Heat-resistant Alloys at 1500°F," *Trans. Am. Soc. Metals*, **39**, 368 (1947).
5. Grant, N. J., "Cobalt-Chromium J Alloys at 1350 to 1800°F," Bur. Ships Research Memo No. 2–47 (May 1, 1947).
6. Grant, N. J., Frederickson, A. F., and Taylor, M. E., "Heat-resistant Alloys from 1200 to 1800°F," Res. Memo No. 3-47, Navships 250-330-12, Sept. 1 (1947); *Iron Age*, **161**, Mar. 18, Apr. 8, Apr. 15 (1948).
7. Grant, N. J., Lane, J. R., and Taylor, M. E., "Aging Characteristics of Gas Turbine Type Alloys," Bur. Ships Research Memo, No. 1-47, Navships 250-330-8, Test B-3254 (Jan, 1947).
8. Parke, R. M. and Bens, F. P., "Chromium-Base Alloys," A.S.T.M., Symposium on Materials for Gas Turbines, (June, 1946).
9. Reynolds, E. E., Freeman, J, W., and White, A. E., "Evaluation of Two High-Carbon Precision-Cast Alloys at 1700°F and 1800°F by the Rupture Test," National Advisory Committee for Aeronautics, Tech. Note No. 1130 (Sept., 1946).

Chapter 9

Manufacturing Processes

A. CASTING

The casting method for production of metal components for high-temperature service is now widely accepted, for several reasons. With the increase of such elements as W, Mo, and Cr in the alloys and a decrease in the Fe content, forming has become more difficult. When carbon is increased from 0.1 per cent to about 1 per cent, certain compositions such as the alloys 110N-2 and 73J discussed in the preceding chapter can no longer be forged but must be cast. In those alloys which have good forming properties, the wear of forging dies may be severe with resulting higher fabrication costs.

In the meantime, the remarkable fact is that a cast structure has proved itself capable of withstanding stresses at high temperature by a large body of evidence from creep and stress rupture testing and from long periods of operation. It must not be overlooked that a cast structure free from porosity does not have the directional properties of a formed piece.

In any casting process, the problem of grain size control is an important one. The only factor in changing the size of a metal crystal in an aggregate is the cooling rate which implies pouring temperature of the molten metal, temperature of the mold, shape of the casting, and other factors which determine how fast heat is given off to the surroundings.

I. Effect of Grain Boundaries

The literature on refractory alloys for use at high temperature contains many statements that "coarse-grained" material has a higher creep strength than "fine-grained" material if testing is carried out above the equicohesive temperature, or in that range where fracture occurs by grain boundary sliding. These comparisons are made on cast alloys versus forged alloys. It is unfortunate that there are no published data of the optimum grain size or grain size distribution of any particular alloy in relation to elevated-temperature service.

From the discussion in Chapter 1 on grain boundary conditions, it is reasonable to assume that at elevated temperatures grain boundaries are weaker than the grains themselves, so that failure for many metals under

these conditions is intercrystalline. Grain boundaries are sources for viscous behavior or they may be areas where microcracks occur or imper-
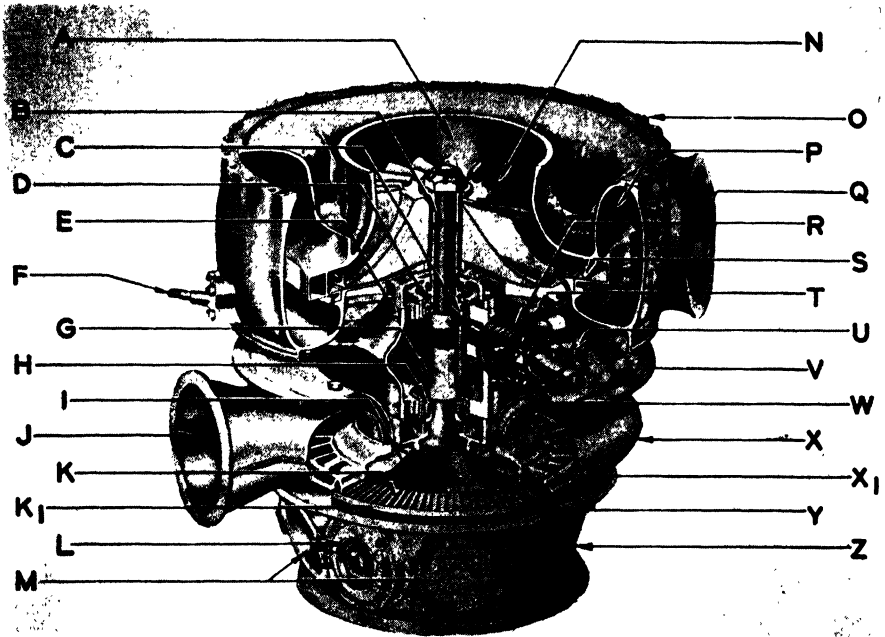
Fig. 9-1. Turbosupercharger for airliner, Model 377, Stratocruiser, Boeing Aircraft.

A   Compressor air inlet
B   Rotor shaft
C   Oil jet
D   Ball bearing
E   Bearing and pump casing
F   Turbo mounting trunnion
G   Pump drive sleeve
H   Roller bearing
I   Sealing plate assembly
J   Exhaust gas inlet
K   Buckets
K_1 Bucket wheel
L   Cooling cap blast tube exit
M   Inspection ports
N   Impeller
O   Compressor casing
P   Diffuser
Q   Compressor discharge outlet
R   Oil pump
S   Diffuser vane
T   Oil pressure and scavenge lines
U   Plugged oil filter line connection
V   Baffle ring
W   Screw (oil by pass)
X   Nozzle box
X_1 Nozzle box diaphragm
Y   Nozzle box L ring
Z   Exhaust shroud

fections start cracking. If the grain size in a casting is too large, the boundaries are unquestionably planes of weakness. On the other hand, very fine grains provide too many areas where viscous behavior may induce
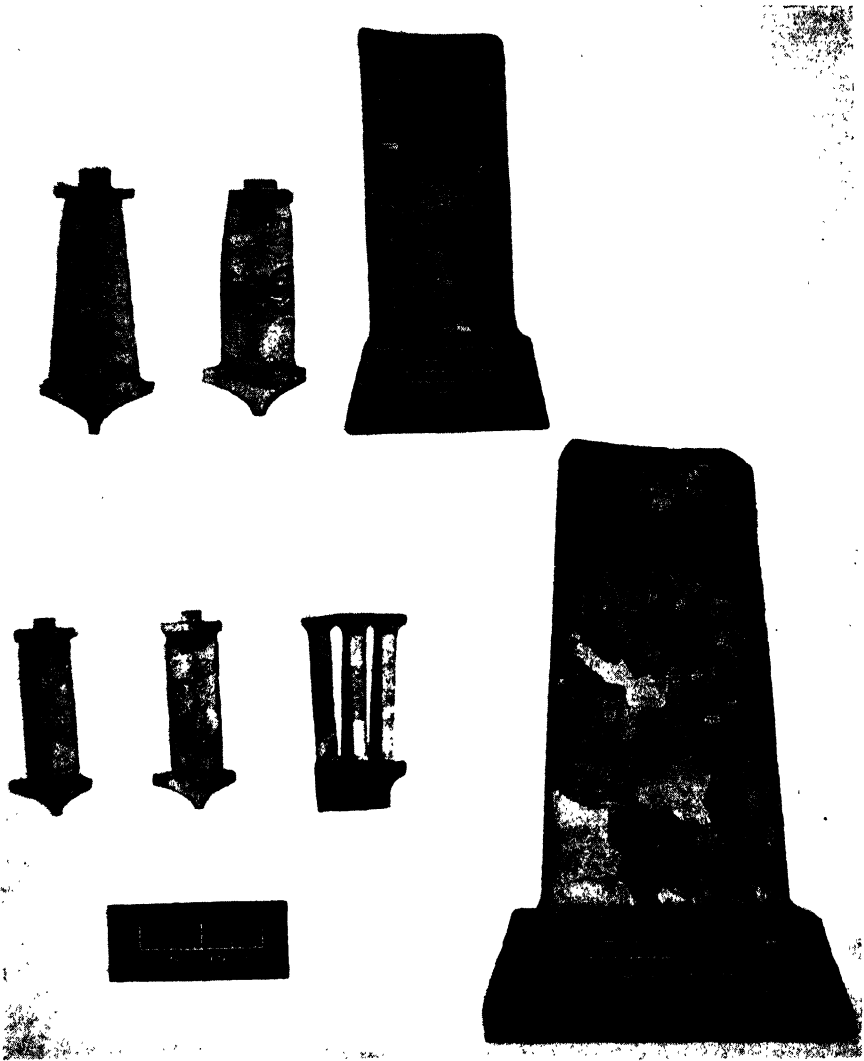
Fig. 9-2. Variations in grain size of cast turbine blades due to lack of uniformity in cooling rate. (After Badger)

a lower creep strength. It seems only reasonable that somewhere between extremely fine grains and excessively coarse grains, there must exist an optimum grain size or grain size distribution.

In Fig. 9-2, the large grain structure of turbine blades cast from "Vital-

lium" alloy is typical of commercial production from casting the metal in hot refractory molds[1]. The analysis of the blades is as follows:*

C	Cr	Mo	Co	Ni	Fe	Mn	Si
0.30-0.45	25.0-29.0	5.0-6.0	Bal	1.75-3.75	2.0 max	1.0 max	1.0 max

The variation in grain size is due to the wedge shape of the part, which causes difference in cooling rates of thin and thick sections. The many sharp corners visible at the grain boundaries may well be areas of stress concentration when the blade is stressed at elevated temperature.

II. Casting Techniques

Foundry methods employed for large-scale commercial production of heat-resistant castings are satisfactory for components used in furnaces and parts required in the petroleum and allied industries. The dimensional accuracies for such castings depend on the quality of the sand mold, and, with the special techniques employed in certain instances, the casting may have superior surface qualities. In the production of compressor and turbine blades, smooth surfaces are required which may be attained by the use of refractory molds of very fine silica. This practice eliminates machining which produces a worked layer of metal and in consequence a surface which may flow in service when stressed at high temperature.

With the necessity of producing turbosupercharger blades early in 1940, casting techniques developed in the dental and jewelry trades were adapted overnight to large-scale production of turbine blades. The techniques of precision casting are not new, but their rapid expansion in a short time and the remarkable performance of the blades thus produced was one of the outstanding achievements of wartime metallurgical research. Approximately 50 million blades were precision-cast during the war.

a. Precision Casting†. This type of investment casting involves the use of a pattern which is a positive replica of the part with proper dimensions, its investment with a fine-grained refractory, burning out the pattern, firing the refractory mold, and casting the metal in the mold cavity.

1. Dies. Dies for producing patterns are made of low-melting alloys or of steel, depending upon the type of material used for patterns and the production requirements for the part in question. They are single-cavity or multiple-cavity dies, depending on the size and shape of the part to be produced.

* Specification B50R99, General Electric Co.
† See Cady, E. L., "Precision Investment Castings," New York, Reinhold Pub. Corp., 1948.

2. Patterns. The pattern material widely used consists of a mixture of low-melting waxes which are formed readily under low pressures. In the dental and jewelry trades, special wax mixtures are in use which have given excellent service over many years, especially in regard to burning out in the mold and leaving no residue to contaminate the molten metal during casting. Waxes have the difficulty of deforming readily, which inhibits rapid assembly methods and makes storage difficult. The reaction of waxes during hot weather can be circumvented only by air-conditioning the surroundings. The high cost of waxes has a marked influence on the final price of the casting.

To overcome these difficulties, the field of plastics offers many attractive possibilities for pattern materials. Plastics which are commercially available must have a minimum distortion after being injection-molded. It is obvious that plastic patterns are more easily stored and assembled without injury than wax patterns. Certain polystyrene compositions have had experimental trials, but distortion of the pattern is difficult to control.

Success is reported in the development of a low molecular weight plastic which is injection-molded in steel dies at pressures less than $\frac{1}{10}$ of those ordinarily used for commercial plastics. The distortion of the pattern is sufficiently low and it is readily stored and assembled. Its cost is only a fraction of the cost of waxes. Injection-molding speeds are higher than those used in molding wax, although this difference is not inherent in the two processes. A high-speed injection-molding machine equipped with a steel die and plastic pattern is shown in Fig. 9-3[19]. This press produces 40 impressions per hr.

The patterns are next mounted in a flask which consists of a steel shell of about 8 inches in diameter. For economic production, patterns should be assembled in as large units as possible depending on the shape and size of the part and the size of the flask.

3. Investment. A material which is satisfactory for an investment must be fine-grained to give a smooth surface to the finished casting, it must have expansion and contraction coefficients which are reproducible, it must be free from cracks or other imperfections after being fired, and it must be cheap. There are many refractory materials that would fill the above requirements, but the low cost of silica flour gives it a preference over other refractories.

The treatment of the silica to provide a strong investment is varied. It may be bonded with ethyl silicate in alcohol and water mixtures, with colloidal silicate in a water suspension, or with phosphoric acid. Other additions may be asbestos, crystobalite, and gypsum.

In some instances the pattern mounted in its flask is precoated with a mixture of silica flour (200 mesh), sodium silicate, hydrochloric acid, and water. A vibrating screen dusts silica sand (100 mesh) over the pattern coated with the primary slurry. A backing is then added to fill the remainder of the flask. It is made of ground firebrick, natural silica sand (60 mesh), ground silica (80 mesh), tetraethyl silicate, alcohol, water, hydrochloric acid, and magnesium oxide as an accelerator[16].
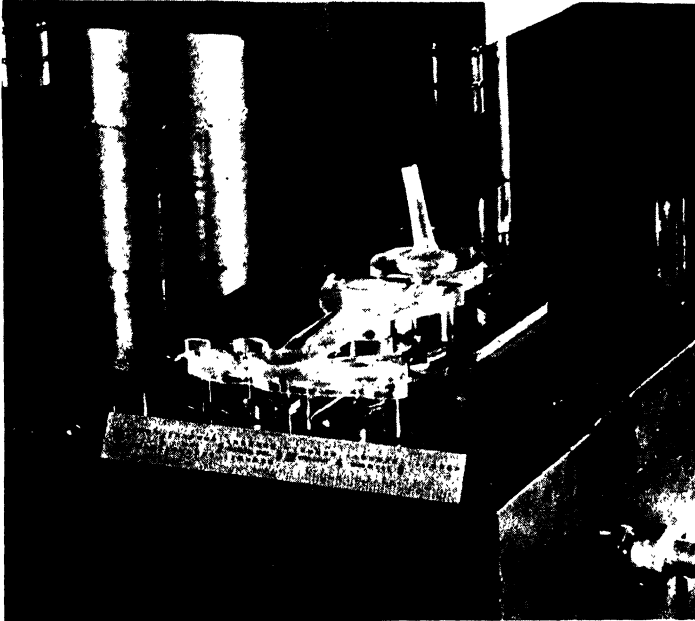
Fig. 9-3. Ejection of plastic pattern from die. (After Valyi)

One installation provides automatic weighing and mixing of the slurry in batches of 3000 lbs per hour and the filling of the flasks from a hose at the bottom of the mixing unit, as shown in Fig. 9-4[19]. Two mixing units are convenient as one is cleaned and filled with a fresh batch while the other dispenses slurry. In this way, a continuous flow of slurry fills the waiting flasks.

Some processes require vacuuming of the slurry to eliminate air bubbles and some do not. If the investment entraps air on the surface of the mold cavity, the resulting casting will have pinholes on its surface.

The flasks are now heated at a low temperature to drive off the moisture first and then melt out the wax which may be recovered at this stage. The flask may then be transferred to a firing furnace where remnants of the

wax or plastic pattern are burned out.   The final firing cycle must be controlled to produce a strong, crack free investment capable of withstanding erosion from the hot metal.   A firing cycle may be 5 to 8 hrs and reach a temperature of 1010°C.

4. Casting.   From this stage, precision casting follows standard foundry procedures.   Melting may be done in a carbon arc furnace of 15-lb capacity, or in an induction furnace of 35-lb capacity, or in a carbon resistance furnace of approximately 100-lb capacity[16, 19].   If casting is done under low
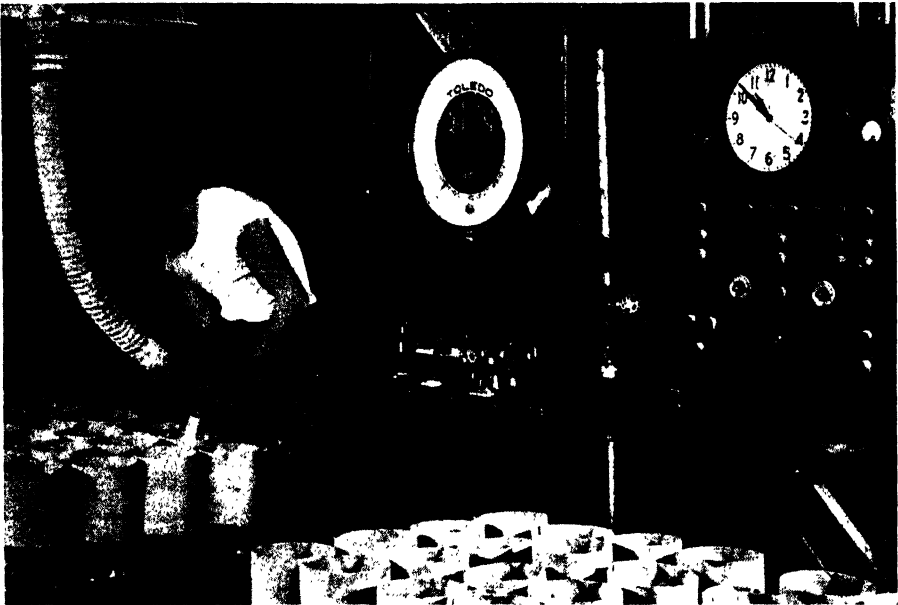
Fig. 9-4. Filling flasks with slurry from automatically prepared batches.   (After Valyi)

pressures, it is necessary to use hot molds in order to fill the mold cavity. If pouring is by centrifugal methods, the molds may or may not be heated.

The casting table has a square pour block in the center with holes radiating out to connect with the sprues of 4 flasks.   All surfaces are given a fire clay wash.   For castings larger than 8 in diameter, no pour block is required but a central sprue hole allows the metal to flow radially into the flasks[19].

After being poured the flasks are allowed to cool and subsequently the investment is knocked out by air hammers.   This brings up the problem of the economics of cleaning the castings.   An investment must be strong

enough to contain the molten metal and not crack during casting; but it can be made too strong so that removal during the knock-out stage is difficult and expensive. The ideal material lies between these two hazards.

5. Accuracy and Properties. Much has been written about the tolerances that can be obtained on precision cast parts. Dimensions must be controlled during the following steps: injection-molding die, dimensional changes and distortion of patterns, dimensional changes of the investment, and shrinkage characteristics of the metal being cast. The surface smoothness of a casting free from porosity and other defects depends largely on the fineness of particle size of the silica refractory. This is the principal reason for the closer tolerances of precision castings over sand castings. For small castings, certain dimensions may be held to 0.003 inch per in.
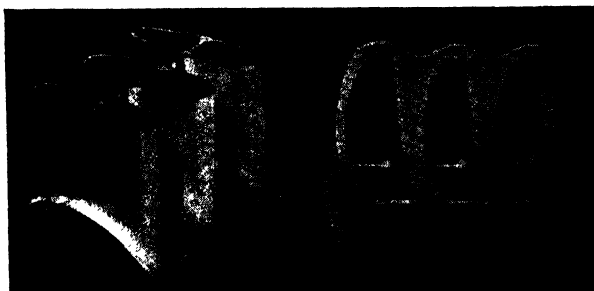
Fig. 9-5. Cast jet outlet nozzle tested in alloys Vitallium and Hastelloy C. (After Sweeney)

The absence of directional properties which is characteristic of casting processes tends to increase the strength of a turbine stator when casting is substituted for forging[22]. This component weighs 12 lbs and is cast complete with blades $8\frac{1}{2}$ inches in diameter. The blade contours require no machining and the spacing between them has a total variation of 0.003 inch. The faces of the stator are however machined. Precision casting of this part is considerably cheaper than forging. Another part suitable for casting is the jet outlet nozzle shown in Fig. 9-5.

Much testing needs to be done to determine the physical properties of precision cast parts to compare them with those produced by forming. A conservative estimate is that they lie somewhere between the transverse and longitudinal figures prevailing in rolled bars[22].

B. FORMING

Forging and Rolling

With the decrease in Fe content and the increase in such elements as Co and Cr, the problem of fabricating alloys for high-temperature service is

serious.   It is a great tribute to the ingenuity and effort of the metal-working industries that so many metals are successfully formed that are high in Co, Cr, Mo, and W.

This increased difficulty in forming as the Fe content decreases is compared in the following operations.   In the manufacture of exhaust collector rings for jet engines, a flat is shaped into a cup by press forming.   The steps involved depend upon the particular alloy selected[4].   The number of draws and anneals required for several different alloys is shown below:

Material	No. of draws	No. of anneals
Stainless steel	2	2
19-9 alloy	3	3
N-155 or "Hastelloy" C	4	4

Techniques for forging and rolling require close temperature regulation of ranges for hot working.   Each step of the reduction schedule must also be held within close tolerances.   It is remarkable that all the Co-base alloys, including N-155 and S-816 as well as the Ni-base compositions "Inconel" X and "Nimonic" 80, are available in formed shapes.   It is mainly the introduction of C for increased creep strength that has resulted in the necessity for casting many of these alloys.

In forging turbine wheels, the sluggishness of the alloys in their response to heat treatment makes it difficult to obtain uniform hardness throughout the disk.   The metal is restrained at the center of the disk during upsetting of the cylinder.   As a result, the hardness is a maximum along diagonals through the perimeter of the wheel.   Heat treating for fairly long periods is required to decrease these hardness gradients as much as possible[7].

The precision forging of turbine blades to very close tolerances requires experience and control of operating conditions.   At the thin edge of the wedge-shaped blade, there is not sufficient metal to protect the two halves of the forging die.   To prevent die wear in this section reductions are of necessity small.   Cracking of the blade during forging is also a hazard.

Powder Metallurgy Techniques

The field of powder metallurgy offers some interesting possibilities in the development of naterials suitable for elevated temperatures.   For temperatures above 1000°C where metals have lower creep strengths, powder metallurgy methods suggest several unconventional channels for experiment.   This technique is based primarily on the mixing of separate constituents which are then pressed into shape and sintered to give sufficient strength for the particular use for which the parts are designed.   Such

a procedure immediately suggests that materials can be brought together by powder metallurgical methods which can not be produced by conventional melting, casting, and forming.

The other outstanding technique that can be accomplished by powder metallurgy procedures is the use of controlled porosity. A turbine blade designed with a cavity for cooling by some medium as air is an attractive means of decreasing weight and lowering temperatures. It is possible that a blade with a cavity could be formed by powder metallurgy methods.

Metal powders can also be formed and sintered to provide a well distributed porosity throughout the mass and with the size distribution of pores held within specified limits. Many types of porous filters of Cu base and corrosion resistant metals as Ni are in commercial production. A porous metallic structure can be immersed in a molten metal to produce a bimetallic structure as developed in the electrical contact field. As an example, porous W is immersed in molten Cu or Ag. Such techniques suggest that there may be a combination of metallic materials that would withstand the stresses encountered by turbine blades above 1000°C.

In the sintering of dissimilar constituents, the range available for selection of unusual combinations is almost unlimited. The refractory metallic carbides, nitrides, and borides are all possible for experimentation. Certain of these compounds can be eliminated because of their recognized instability. For instance, W carbide is no longer stable above 900°C and Ti carbide decomposes in O at 1150°C[8]. Cr boride is known to be as oxidation- and corrosion-resistant as Cr. Such a compound could be sintered with some other refractory metal as Cr itself with the possibility of the desired strength at high temperatures. Another approach to unconventional combinations is the use of ceramics with metal powders, but this is so much more a problem in the field of ceramics that it will not be considered here.

The experimenter should be acquainted with some of the inherent difficulties in powder metallurgy techniques. For example, diffusion of one metal into the structure of another cannot be carried out to produce an alloy with a uniform structure. With elements of the corrosion and heat-resistant class such as Cr, Co, and Ni, this property of low diffusion rates is enormously exaggerated. Powder metallurgy techniques should be directed toward taking advantage of dissimilarity in a structure.

The other outstanding problem is the difficulty in forming powders in a die to complicated shapes with a uniform density throughout the structure. This is especially manifest in a shape such as a turbine blade which is thick at the base and decreases in a wedge to a thin edge. Die wear is always excessive if high pressures are used and refractory powders are being pressed. The trend then should be to develop techniques which would

produce the required shape at very little or no pressure as is done in the manufacture of porous metal filters.

In spite of these obstructions, the techniques offered by powder metallurgy are unique and suggest exceedingly interesting methods for developing materials suitable for high-temperature use. It is for this reason that such extensive research programs are under way in many laboratories.

C. Welding

The welding of highly alloyed heat-resistant metals presents special problems which depend primarily on the characteristic properties of the materials. Compared to plain-C steels, these alloys have higher electrical resistivities, lower heat conductivities, and generally lower melting points. In many instances, the welding method suitable for the austenitic alloys is applicable to these special compositions if allowance is made for the different characteristics suggested above. Considerations such as shortening the time at welding heat and confining the heat to minimum areas to avoid distortion and cracking are generally advisable.

I. Types of Welding

With the exception of fire welding, which is unsuitable for stainless steel, many types of welding may be used for joining heat-resistant alloys if proper precautions are maintained. Both resistance welding and oxyacetylene welding are suitable for stainless steel and are applicable for such Co-base alloys as "Vitallium" and "Hastelloy" C. Various types of arc welding are suitable, including metal arc welding, atomic hydrogen arc welding and inert gas-shielded arc welding. In the last method, argon is superior to helium in supplying an inert atmosphere for welding thin sheet stock such as No. 24 gage[4].

The submerged arc welding method (Unionmelt) also offers excellent protection from oxidation during welding, due to deep penetration of the weld metal and the few passes required. In this process, bare weld rods are submerged in a molten mineral material. Used in joining turbine blades to wheels, this method welds with speeds of 18 to 30 inches per minute on 12 inch diameter wheels carrying 144 blades. In this application, the rods are $\frac{1}{8}$ inch diameter and the welding requires only one pass on either side of the wheel. At this speed 350 to 600 amps and 30 volts are required[4].

II. Weldability

Difficulty in the weldability of heat-resistant alloys when joined to other alloys by a particular welding rod has occurred in turbine blades fastened to wheels of a different alloy by means of a welding electrode

which may consist of a third alloy composition. It is unfortunate that certain combinations of such assemblies were selected and manufacturing undertaken without consideration as to the weldability of the various components. In actual practice, some combinations of wheel, bucket, and welding rod show greater tendencies to crack than others. Test methods to produce various types of failure in the laboratory to simulate manufacturing conditions are described below.

An analysis of failures due to cracking of an assembly of buckets welded to turbine wheels discloses three types of cracks which may occur: (a) weld metal cracking, (b) underbead cracking, and (c) notch extension cracking. The last type is by far the most frequent failure. It is a crack that is initiated at the junction between the buckets and extends radially into the wheel itself. Certain combinations of wheel, bucket, and filler metal produce extensive and severe cracking at the junction between the buckets, while other alloy compositions produce only slight notch extension cracking which may possibly be tolerated in the structure during service.

Wheel and Bucket Design Weld Test. A laboratory test method for reproduction of the manufacturing methods encountered in joining blades to wheels should reproduce the various types of cracking especially notch extension cracking, since this type occurs most frequently. For two types of welding, namely, manual metal arc welding and submerged arc welding, a test piece can be devised, as shown in Figs. 9-6 and 9-7. In this design, 8 test buckets are welded to a straight piece, which is more convenient for welding and sampling than having the test piece conform to the curvature of an actual wheel[13, 14, 6].

The single solid plate in Fig. 9-6 represents the wheel. The $\frac{1}{2}$-inch segments welded on the plate represent the buckets. The weld consists of a straight line double preparation butt joint. The cut out section indicated by a dotted line in the flat plate of the illustration is designed to reduce the thermal capacity adjacent to the weld metal at the top and bottom surfaces. This relief is actually unnecessary as all types of cracking can be produced in the design specimen whether the cut out is present or not. The joint preparation for submerged arc welding is a double-V with a $\frac{1}{8}$-inch root face shown in the upper portion of Fig. 9-6; that for manual arc welding is a double-U with a $\frac{3}{32}$-inch root face shown in the lower portion of Fig. 9-6.

Detail drawings of the segments themselves for the two types of welding tests are shown in Fig. 9-7. They are both reduced in thickness from $\frac{3}{4}$ to $\frac{1}{2}$ inch through a $\frac{1}{8}$-inch radius fillet. The base of the segment is similar to the base of an actual turbine blade. The section $\frac{1}{2}$ inch in thickness opposite the weld is reduced at the bottom and top surface to lower the heat capacity adjacent to the weld metal. This is because some heat-resistant alloys are susceptible to cracking in a fusion zone which may be overheated.

The submerged arc-welding equipment consists of a head and carriage*
supplied by 60-cycle AC from two 500-amp transformers.   The manual arc
welding equipment suitable for use with this design test weld is a 400-amp
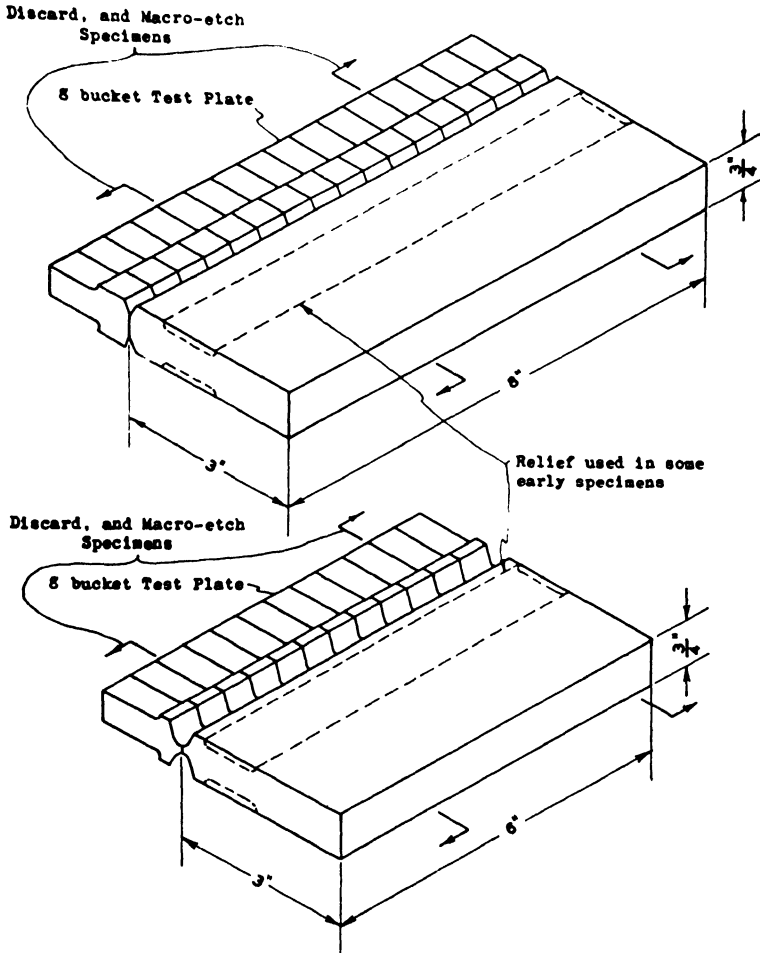
Fig. 9-6. Wheel and bucket design weld test.   (After Linnert)

motor-generator welding machine.   The manual arc method uses a DC-
reversed polarity.   A jig is required to hold the plate and line up the
8 segments.   The jig fixture and all accessory equipment are nonmagnetic
to minimize the possibility of magnetic effects during welding[14].

* Unionmelt, Type U, Union Carbide and Carbon Corp.
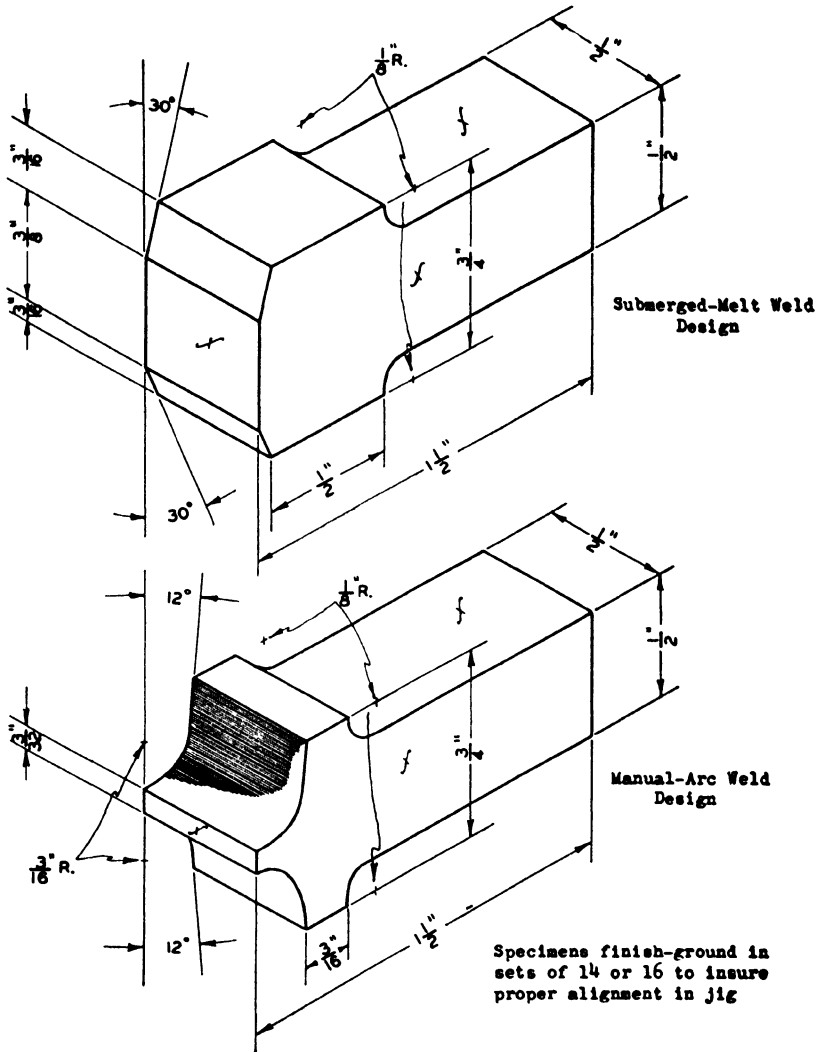
Fig. 9-7. Bucket base replica for wheel and bucket design weld test. (After Linnert)

Examination of Weld Test Piece. The weld test piece described above reproduces all types of cracking which occur during commercial welding of wheels and buckets. A survey of the different types of failures is as follows:

Weld Metal Fissures: Cracks in the weld metal sometimes occur in austenitic stainless steel, as shown in Fig. 9-8 with a wheel of alloy 16-25-6 welded to a bucket of alloy X-40 with Type 316 filler welding rod. The nominal composition of Type 316 filler rod is as follows:

C	Mn	Cr	Ni	Mo	Fe
0.07	1.7	17.5	12.5	2.2	Balance

Compositions of the other alloys are given in earlier sections of the text. Higher P contents tend to increase the susceptibility of weld metal fissures. The presence of delta ferrite in the austenite probably decreases the tendency to cracking. The weld metal in Fig. 9-8 shows a typical crack formed in a wholly austenitic matrix.

Fig. 9-8. Typical intergranular micro-fissure in austenitic weld metal. (Timken Wheel, X40 buckets, Type 316 filler). Etchant: Mixed acids in glycerol. Magnification 100×. (After Linnert)

Base Metal to Weld Metal Crack: This type of defect originates in the base metal and extends into the weld metal. It occurs so rarely that it will not be considered here.

Fusion Line Crack: This defect follows the fusion line between the bucket and the weld metal. It is observed to extend only short distances and it is probably initiated within the complex alloy structure where the weld metal and bucket diffuse.

Interbucket Notch Extension Crack: This type of failure is by far the most frequent in the welding of buckets to turbine wheels. The weld test piece as designed reproduces in laboratory tests notch extension cracks. From cracks thus produced, it is apparent that the interbucket junction in the

bucket side of the weld joint creates a gap which disturbs the flow of heat during solidification. The weld metal opposite the gap may fail due to (1) the junction of liquid and solid weld metal or (2) the segregation of

Fig. 9-9. Stringer-like segregation associated with a severe junction extension crack. (S816 Wheel, X40 Buckets, "Hastelloy B" Filler). Average extension cracking value, 13.5. Etchant: Mixed acids in glycerol. Magnification 100X. (After Linnert)

Fig. 9-10. Severe extension crack (Timken Wheel, S816 Bucket, Type 316 Filler). Note stringer-like segregation along edge of crack. Etchant: mixed acids in glycerol. Magnification 500X. (After Linnert)

low-melting constituents at the junction during slower cooling. The presence of longitudinal stress increases the liability to cracking. A typical notch extension crack is shown in Fig. 9-9 at 100X obtained from welding

an S-816 alloy wheel to an X-40 bucket with "Hastelloy" B alloy filler rod. The small irregular stringers are areas of segregated material such as complex carbides. Proof that the stringers carry segregates is demonstrated in Fig. 9-10 which shows the segregation in a stringer at 500× associated with a notch extension crack in a 16-25-6 wheel welded to an S-816 bucket with a Type 316 filler rod. The stringer-like segregation is accompanied by severe junction extension cracking.

The association of the microstructure with cracking suggests that the interdendritic segregation of lower melting compounds is a factor in this type of failure. These compounds lie transversely in the weld deposit and promote severe extension cracking.

TABLE 9-1.   DEPTH OF NOTCH EXTENSION CRACKING[14]

| Bucket Alloy | Average Cracking Value (64ths Inches) | | | |
| | Submerged Arc Welded | | Manual Arc Welded | |
	16-25-6	19-9DL	16-25-6	19-9DL
1. 16-25-6	1.0	....	...	...
2. "Hastelloy" B	1.8	....	2.0	4.4
3. "Vitallium"	7.3	....	2.8	...
4. 422-19	10.3	19.4	2.8	8.0
5. 6059	12.4	....	...	...
6. S-816	14.6	10.5	5.1	7.0
7. X-40	15.7	19.5	5.7	8.9

Note: Values listed above are the average of all tests with Type 316 filler metal.

Summary of Notch Extension Cracking. The most frequent type of failure in welding buckets to wheels with filler rods by means of manual arc metal welding or by submerged arc welding is notch extension cracking at the junction of the buckets.

Table 9-1 shows the depth of cracking measured in 64ths of an inch of different alloy combinations welded by the two methods, manual arc metal and submerged arc welding. The simpler types of alloys which are mainly austenitic in structure are less subject to notch extension cracking. Alloys S-816 and X-40 which contain larger amounts of Cb, Mo, W, Co, and others are more subject to this failure and the depth of cracking is greater.

Influence of the Welding Method. Where the metal combination is prone to cracking, the submerged arc welding method produces deeper extension cracks than the manual arc deposit. In combinations of metals which show little susceptibility to cracking, the welding method employed makes little difference.

Influence of the Preheat Temperature. Regardless of the welding method, preheating from 25 to 550°C with narrow deposits does not influence the amount of cracking in a combination of 16-25-6 wheel, S-816 bucket, and Type 316 filler material. However, if the weld deposit is wide and submerged arc welded, preheating to 550°C is beneficial.

D. Inspection

X-rays. For parts such as turbine blades operating under high stresses, porosity must be eliminated at all costs. Inspection by x-rays is required for all precision cast blades. The wedge shape of the blade makes it difficult for the rays to penetrate the heavier section to produce as clear a photograph as for the thinner section at the edge. If necessary, separate exposures can be made to correct this difference in thickness.

Surface Inspection. To detect surface cracks in turbine blading, the Zyglo, Magnaflux, and supersonic reflectoscope methods of testing are used. These methods are especially applicable to forgings where incipient cracks may form.

Hardness. Hardness testing for certain alloys may be required for inspection to indicate the degree to which heat treatment, especially aging, has been effective.

E. Design Data

Many factors complicate the problem of selection of materials for high-temperature service and the designer must of necessity follow a difficult course in evaluation of the available information. The requirements for materials to operate at high temperature depend on a number of factors and classification can be considered from several points of view. These may be the allowable deformation or flow during service life, temperature fluctuations, or corrosion resistance. The classification suggested below covers certain high temperature applications on the basis of physical requirements. A tabulation of a number of industries which utilize metals at elevated temperatures follows.

CLASSIFICATION OF HIGH TEMPERATURE APPLICATIONS[3]

I. On the basis of physical requirements:
    A. Permissible deformation during service
        1. Decidedly limited
            a. Gas turbines, blades, rotors, nozzles
            b. Steam turbines
            c. Valve parts
            d. Bolting
        2. Up to 5.0%
            a. Cracking still tubes
            b. Superheater tubes
            c. Heat exchangers

    B. Constant versus varying temperature
        1. Constant
            a. Steam turbines
            b. Steam lines
            c. Bolting
        2. Varying
            a. Cracking still tubes
            b. Superheater tubes

    C. Relative importance of strength and stability
        1. Petroleum industry
            a. Sweet crude
                i. Strength
                ii. Oxidation resistance
            b. Sour crude
                i. Corrosion resistance
                ii. Strength
        2. Central stations
            a. Strength
            b. Oxidation resistance
            c. Corrosion resistance (steam)

II. On the basis of industry:
    A. Central stations
        1. Superheater tubes—1000 to 1300°F (537 to 704°C)
        2. Steam lines—850 to 1050°F (454 to 565°C)
        3. Steam turbines—850 to 975°F (454 to 524°C)
    B. Petroleum
        1. Liquid-temperature varies with cycle
        2. Vapor-temperature varies with cycle
    C. Aircraft
        1. Turbo supercharger
        2. Jet engine
    D. Miscellaneous
        1. Chemical equipment
        2. Furnace parts
        3. Heat treating equipment

I. Use of Information from Elevated-temperature Tests

Many test methods are still controversial especially in regard to the time factor. Below are set forth some of the more arbitrary features involved in the use of design data.

(a) In many laboratories conducting creep tests, the transition from second stage to third stage creep is arbitrarily taken at the point where the deformation becomes 10 per cent greater than the minimum creep rate.

(b) In general, design stresses are based mainly upon stress rupture, creep rates, and fatigue life. A figure of 50 to 60 per cent of the stress

required for rupture in the life of the part is generally used[9, 17]. The value of the stress selected is then compared with the maximum allowable deformation in that time.

A comparison of creep strength with hot fatigue strength for various alloys is recommended in order that the lower value may be used in designing parts for elevated-temperature service. The relation of these values to each other may change depending upon the material and the temperature in question. At reasonable values of stress, plain-C steels have a higher fatigue resistance than creep resistance. This is also the case for 18-8 stainless steel at 650°C. In general, the alloys considered superior in the temperature range of 650 to 815°C have higher fatigue resistance than stress-rupture strength in 1000-hour tests.

For aircraft requirements, tests of materials based on a life of 500 hours are reasonable estimates; whereas for stationary gas turbine installations, a life of 10 years is hoped for. Naturally, the tendency to wring out data from short testing periods to cover a long life expectancy is an every recurrent problem for the designer.

II. Stresses Encountered in Service

In a gas turbine rotor, the principal stress is due to the centrifugal force on the wheel. This value is more readily determined than the bending moment on the blades from impingement of the hot gases. There are also the vibratory stresses from the wheel itself. Other factors which are to be considered are the method of fastening of the blade to the wheel and the natural frequency of the blade in motion[9]. Changes in design which tend to decrease the weight of the blade, as in the use of hollow air cooled blades, may be advantageous in decreasing the stresses in service.

III. Temperatures Encountered in Service

(a) Surface deterioration is very important in plain-C and low-alloy steels where scaling is appreciable. The addition of Cr is one of the chief elements in decreasing susceptibility to scaling. With the highly alloyed refractory metals, high-temperature oxidation and scaling are much less important. Certain alloys form a tough, adherent scale at 815°C which makes them suitable for bolting, as for example alloys K42B, "Refractaloy" 26 and 70, and others. Factors in scaling will be considered in the next chapter.

(b) The method in use of plotting of stress versus rupture life on log log or semi log graphs is still controversial. The fact that one method or another produces a straight line must not be taken as magical in any sense.

Slight changes in aging, precipitation, or coalescence, oxidation at grain boundaries, and other unknown conditions may result in a deterioration of the material and a drop in stress on the time axis. Extrapolations always present this danger.

(c) A warning is also given here against assuming that high-temperature properties of forged disks and rolled bar stock are comparable as the effects of working may result in very different creep rates and stress rupture values. As a case in point, two heat-resistant metals in forged disks each have a minimum creep rate of 0.1 per cent per 1000 hours at 650°C for a stress of 28,000 psi. However, these same two alloys in bar stock at 650°C have the same creep rate in one case at 36,000 psi and in the other case at only 22,000 psi[18].

(d) Temperatures encountered in gas turbines are variously estimated. The gas turbine driven supercharger installed in bombers has an inlet temperature of approximately 870°C[10]. The gas turbine for jet propulsion has an inlet temperature of about 815°C. In order to compete with a contemporary stationary steam plant or Diesel plant, it is estimated that a turbine inlet temperature must be not less than 815°C.

Aside from the estimated temperatures encountered in jet engine operation, there are the other uncertain factors which may result in higher temperatures. "Hot starts" raise the temperature of any exhaust part to at least 1900°F (1037°C). Tail pipe flame or "after burning" in auxiliary bursts of speed raises appreciably the temperature of the hot exhaust gases, which condition is especially severe on the sheet metal components[4]. It is estimated that in a life of 1000 hours, an aircraft gas turbine may undergo 200 or more cycles of starting, running and stopping. Perhaps 20 times there may be hot starts with actual flame impingement on the blades[17].

IV. Ductility

The measurements of total elongation now generally recorded on both creep testing and stress rupture are of great value in determining what materials are most suitable for high temperature service. If the efficiency of the gas turbine is low, greater deformations are possible as clearances are larger. In such cases, the stress rupture test offers data which is applicable for use by the designer. The most important factor in the determination of ductility is the relation of ductility to time over extended periods of service. Certain installations require 5 per cent ductility as in blade root fastenings and bolts which should yield locally to avoid failure. Such elongations are satisfactory if determined in testing periods of 2000 hrs. In other instances, a ductility of 2 per cent is accepted in the use of nickel base alloys such as "Nimonic" 80 and "Inconel" X.

V. Evidences from the Microstructure

Above 815°C service range, the coarser grains found in cast structures are generally superior to the finer grains obtained from forgings. Aging in service is followed in many cases by microstructural changes which are predictable under specifically controlled conditions.

In certain of the heat-resistant alloys hardened by additions of Al and Ti, their hardness after service is sometimes a criterion as to the temperature they have encountered in service.

VI. Thermal Expansion and Specific Gravity

Those alloys highest in Fe have in general the largest thermal expansion. Alloys with a Cr base have somewhat lower specific gravities than other heat resistant alloys.

All the cast Co-base alloys require aging for at least 48 hours at 732°C before fitting and assembly in order to stabilize the structure and maintain a constant coefficient of linear expansion.

VII. Availability and Costs

The production method to be selected as casting, forging, or rolling into bar stock may depend upon the availability of the equipment if large scale operations are needed. The cost of parts produced by different methods is sometimes a second consideration as in the case of wartime necessities.

All the special alloying elements added for improved creep strength are costly, but Co, Cb, and Ta are especially so. The availability of Ni in England has added greatly to the widespread development and use of the "Nimonics". It should also be pointed out here that there exist many applications for materials with much lower alloy content such as compressor blades of 13 per cent Cr (Types 403, 405, 410) and that the number of compressor blades manufactured is many times greater than the rotor blades.

VIII. Applications

When more information as to service life is known about many of these heat-resistant alloys, it is probable that increased uses will be found for them in applications not connected with gas turbines. One such possibility is in exhaust collector rings in reciprocating engines[4].

IX. Failures

Failures in most types of turbine blades occur in the middle or about one third from the end of the blade due to bending stresses from the impinging gases. Fatigue cracks generally start at the leading edge of the blade

(towards the stationary diaphragm nozzle blading) or sometimes in the center of the blade itself. Fatigue cracks following grain boundaries between large dendrites in cast "Vitallium" blades have been observed.

Fatigue failures are decreased by careful design of the contour, and by reduction of sources of vibration. Fretting failures (seizure) may be alleviated by arranging small air gaps at susceptible junctions. Failures from flame impingement and poor heat distribution in the flame tubes are deceased by eliminating thin metal parts in the flame region and with improved fuel injection. Failures in blades are decreased by more accurate manufacturing, by providing small radii at root junctions, by avoiding turbine vibration, and by improving the material itself as regards strength and ductility.

F. Machining Heat-resistant Alloys

Machining heat-resistant alloys is in many instances difficult and may require low feeds and low speeds. Heat treatment can in some cases be utilized to improve the conditions for machining. For those alloys which are heat-treatable, the age-hardened condition is often best for machining, since the rate of work hardening is less than if the alloy is in the quenched state. It is better, however, that drilling be done in the solution quenched condition when the metal is probably softer. Recommendations are given below for the optimum conditions and the tools required for machining several heat-resistant alloys:

S816 Alloy. This alloy may be machined in the age-hardened condition with high-speed tools operating at 10 to 15 surface feet per minute. The substitution of tungsten carbide tools increases machining speeds to 30 to 45 surface feet per minute[20].

Cr-base Alloys. These alloys can for the most part be machined with cemented carbide cutting tools. Alloys of the compositions between 60 per cent Cr, 25 per cent Fe, 15 per cent Mo and 60 per cent Cr, 15 per cent Fe, 25 per cent Mo are machined in the as-cast conditions at hardnesses up to 600 Vickers pyramid number with standard high-speed steel tools. Alloys containing more than 15 per cent Mo or W and more than 15 per cent Fe are turned and ground to stress-rupture specimens, the threads being ground by means of a thread-grinding attachment on an engine lathe and the gage section being turned.

It may be said that, in general, Cr-base alloys containing about 60 per cent Cr and having the Fe-Mo or Fe-W ratio equal to, or greater than, 5:3 can be machined with high-speed steel tools. Cr-base alloys containing about 60 per cent Cr and having the Fe-Mo or Fe-W ratio between 5:3 and 3:5 can be machined with cemented carbide cutting tools or by grinding.

Alloys containing 60 per cent Cr and having Fe-Mo ratios less than 3:5 can only be ground to shape[15].

Other alloys for which machining data are available are included here as follows[5a]:

19-9 DL Alloy
Part Machined Turbine Disk
Sources of Data Universal Cyclops Steel Corp.
                  Turbo Engineering Corporation
                  Westinghouse Electric and Manufacturing Company
Rough Machining
    Firthite T-04
    Rex AAA (18-4-1 plus 5 % cobalt), 210 S.F.M., $\frac{1}{4}''$ cut, .015″ feed, no coolant used.
    Cobalt High Speed Steel, 125 S.F.M., $\frac{1}{8}''$ Cut, 0.031″ feed.
    "Carboloy", 650 S.F.M., $\frac{3}{32}''$–$\frac{1}{8}''$ cut, 0.0015″ feed, soluble oil.
Finish Machining (medium)
    Firthite T-04
Finish Machining (Fine)
    Cobalt High Speed Steel (10% cobalt), ground to feather edge.
Milling
    High speed steel (18-4-1), Rex AA, soluble oil.

25 Cr 20 Ni Stainless Alloy (Type 310)
Part Machined Cast Diaphragms
Source of Data General Electric Co., Allis-Chalmers Mfg. Co.
Rough Machining
    "Carboloy" 883, about 25–30 S.F.M., 0.04–0.6″ cut, soluble oil ⚡5014
    High-speed steel for intermittent cuts, 0.005-0.008″ feed
Finish Marhining
    "Carbology" 883, about 55 S.F.M., 0.01–0.02″ cut, 0.005–0.008″ feed, soluble oil
        ⚡5014
Formed Tool (Skiving)
    High-speed Steel, soluble oil

Timken 16-25-6 Alloy (Hot-Cold Worked)
Part Machined Supercharger Wheel
Source of Data General Electric Co., Allis-Chalmers Mfg. Co.
Rough Machining
    "Carboloy" 78B, 55 to 135 S.F.M., $\frac{1}{4}''$ to 1″ cut, .007″ feed.
    Soluble oil ⚡5014
    "Kennametal" and "Carboloy," dry (Allis Chalmers)
Rough Machining Weld
    "Carboloy" 78B, 45 to 85 S.F.M., 0.0029–0.0075″ feed, soluble oil ⚡5014
    "Stellite" 98 M-2
Finish Machining
    "Carboloy" 78B, 170 S.F.M., $\frac{1}{8}''$ cut, 0.008″ feed, soluble oil ⚡5014
    "Carboloy" 78B, 125 to 250 S.F.M., 0.0039″ feed, soluble oil ⚡5014
Form Cutting Tool
    "Carboloy" 78C or 55A, 50 to 60 S.F.M., 0.007–0.012″ feed
    High-speed Steel, 15 S.F.M., 0.005–0.007″ feed (Better for large tools)

Radius Cutting
  "Carboloy" 78B
Drilling
  High-speed Steel, $\frac{31}{64}$″ diameter, 180 r.p.m., 0.009″ feed, soluble oil ⚡5014
Reaming
  High-speed Steel, 0.506″ diameter, 180 r.p.m., 0.005″ feed
Rough and Finish Grinding (Outside Diameter of Wheel)
  Wheel: Norton No. 36 CL, Size: 14″ x 1½″ x 5″
  Spindle Speed: 1500 r.p.m.
  Work Speed: 250 r.p.m. approximately
  Feed: 0.005″
  Soluble oil ⚡5014
Grinding (Faces on Sides of Wheel) (Stop on Rim)
  Wheel: Norton No. 1980 L6 BE, Serial 16-8, Size: 16″ x 1″ x 8″
  Spindle Speed: 900 r.p.m., Table Speed: Approximately 50 r.p.m.
Finish Grinding (Rims Both Sides)
  Wheel: "Carborundum" No. S 10 K 10, Serial 11-2, Size: 11″ x 5″ x 9″
Broaching (4 and 5 Section Broaches)
  High-speed Steel (18-4-2) and Mo-W-V High-speed Steel (6-6-2)
  Speed: 6½ ft per minute
  Coolant: Continental Broaching, also Tycol 660 using 15 to 25% carbon tetra-
    chloride by volume with either of the two oils
  Life: 54 slots per wheel, 5 to 7 wheels per grind

65 Ni, 15 Cr Alloy (Circle L41)
Part Machined   Turbine Parts
Source of Data   Turbo Engineering Corp.
Rough and Finish Machining
  "Carboloy" or "Vascoloy"—375 S.F.M.

"Hastelloy" B Alloy
Part Ground   Special Supercharger Buckets
Source of Data   General Electric Co.
Side Grinding
  Wheel: Norton 1960—L-5-T "Resinoid Bond"
  Speed: 9000 S.F.M., Rough grind in one machine leaving 0.007″ on side for
    finishing.
  Coolant: Thread grinding oil

K42B Alloy
Part Machined   Turbine Blading
Source of Data   Westinghouse Electric and Mfg. Co.
Machining is practically limited to the base portion of the blade.   Blades pass through
two milling cutters simultaneously.   Cutters are 5″ diameter, run at 26 r.p.m., with
feed of ⅜ to ¼″ per minute.   Milling cutters are of high-speed steel.

References

1. Badger, W. L., *Iron Age*, **158** (Aug. 1, 1946).
2. Cady, E. L., "Precision Investment Casting," Reinhold Publishing Corp., 1948.
3. Clark, C. L., "Requirements for High-temperature Service," *Metal Progress*, **50**, 897 (1946).

4. Chisholm, C. G., Welding and Fabrication of High-temperature Alloys, *Welding J.*, **27**, 217 (1948).

5. Cross, H. C., "Alloys and Ceramic Materials for High-temperature Service," A.S.T.M. Symposium on Materials for Gas Turbines (June, 1946). (a) "Machining Data on Heat Resisting Metals for Gas Turbine Parts," PB 16743 (N-102), Progress Report (OSRD Rept. 4554), (Dec., 1945).

6. Feild, A. L., Bloom, F. K., and Linnert, G. E., "Weldability of Heat-resisting Alloys" (N-102), OSRD, No. 6389, Serial No. M-626, Dec. 5 (1945).

7. Fleischmann, M., "16-25-6 Alloy for Gas Turbines," *Iron Age*, **157**, 44 and 50 (1946).

8. Goetzel, C. G., "High-temperature Materials," *Iron Age*, **161**, 78 (1948).

9. Hughes, A. D., "Design and Operation of Some Experimental High-temperature Gas Turbine Units," *Trans. Am. Soc. Mech. Engrs.*, **69**, 549 (1947).

10. Judge, A. W., "Modern Gas Turbines," Chapman and Hall, Ltd., London (1947).

11. Kihlgren, T. E. and Lacy, C. E., "Control of Weld Hot Cracking in Ni-Cr-Fe Alloys," *Welding J.*, **25**, 769-S (1946).

12. Lardge, H. E., "Resistance Welding of Heat-resisting Materials for Aircraft," *Aircraft Production*, **8**, 107 (Mar., 1946).

13. Linnert, G. E., "Weldability of Alloys for High-temperature Service," (N5-ori-111), Office of Naval Research, Navy Dept., May (1947).

14. Linnert, G. E., "Weldability of Alloys for High-temperature Service," Welding Research Supplement, *Welding Research Council*, **8**, 385-S (1948).

15. Parke, R. M. and Bens, F. P., "Chromium-base Alloys," A.S.T.M. Symposium on Materials for Gas Turbines (June, 1946).

16. "Precision Casting at Allis-Chalmers," *Iron Age*, **161**, 82 (1948).

17. Schweizer, C. I., "Drop Forgings for Gas Turbine Applications," *Materials and Methods*, **24**, 642 (1946).

18. Smith, R. H., "Selection of High-temperature Materials for Gas Turbines," *Iron Age*, **161**, 56 (1948).

19. Valyi, E. I., "Precision Casting with Plastic Patterns," *Iron Age*, **162** (Oct. 8, 1948).

20. Wilson, T. Y., "High-strength, High-temperature Alloy S-816," *Materials and Methods*, **24**, 885 (1946).

21. Woldman, N., "Metal Process Engineering," Reinhold Publishing Corp., New York, 1948.

22. Wood, R. L. and Ludwig, D. von, "Critical Survey of Investment Casting," *Iron Age*, **161**, 72 (1948); 90 (1948).

Chapter 10

Lower Melting Alloys

A. LEAD AND LEAD ALLOYS.

Creep tests at room temperature indicate that single crystals of Pb are subject to deformation at a critical resolved shear stress of approximately 250 psi[2]. The specimens tested are commercially pure Pb sheath of the following spectrographic analysis:

Bi	Cu	Ag
0.005	0.0001	0.0003

The samples are heat-treated prior to the test by holding at 282°C (540°F) for 100 hours, followed by slow cooling. Any stress above 250 psi causes a relatively rapid creep in the single crystal sample. At the fracture of the single crystal of Pb, newly formed grains appear near the break which are due to recrystallization from localized heat effects[2].

Creep tests at room temperature on polycrystalline Pb indicate that, in the early stages, strain-hardening occurs with slip lines observed at extensions as small as 0.1 per cent. As is to be expected, the slip lines change direction at the grain boundary. With increase in time of the creep test, a new system of slip lines may occur and extend across the original grain boundaries, indicating a reorientation of the crystals. If elongation is plotted on a graph against time, the early portions of the curve show a normal strain hardening followed by a break in the curve due to the recrystallization. The reoriented grains are sometimes larger than the original ones and may be 10 times greater[2, 16, 17, 26, 27].

The purer the Pb, the smaller is the deformation required for recrystallization. On annealed electrolytic Pb of extremely high purity, a constant stress of 500 psi causes recrystallization after extensions of 1.3 to 2 per cent[16]. Certain commercially pure Pb samples do not exhibit such a reorientation when creep tested at room temperature. The change is repressed if the metal is heated to 120 to 130°C and cooled quickly[16].

In Table 10-1, the results of creep tests on pure polycrystalline lead at room temperature are given[24]. Coarse-grained samples have a greater creep strength than fine grained samples.

TABLE 10-1. CREEP TESTS ON PURE POLYCRYSTALLINE LEAD
AT ROOM TEMPERATURE[24]

Spectropic Analysis of Pure Lead

Grain	Sn	Sb	Cd	Cu	Ag	Bi	Zn
Coarse	nil	<0.002	0.00002	<0.0005	<0.0005	0.0005	nil
Fine	nil	nil	0.0001	0.001	0.001	0.001	0.001

Both samples contain 0.0005 Fe. As, Te, Al not detected.

Room temperature variations: 23.5° C summer maximum.

12.5° C winter minimum.

For 24-hour period variation not greater than 3° C.

Creep Tests on Virgin Pb at Room Temperature

	Stress (psi)	Life (days)	Extension (%)	Reduction Area (%)	Min Creep Rate (Strain/Day × 10^{-4})
Coarse-grained	200	660	0.33*	..	0.04
	300	942	2.0 U	..	0.17
	400	1482	21.0 U	..	0.72
	500	585	19.0 B	50	1.44
	600	210	24.0 B	72	4.17
	700	66	30.5 B	97	13.8
Fine-grained	500	311	87 B	94	10.6
	600	70	60 B	98.5	47.7

* Test discontinued   U Unbroken   B Broken.

Coarse-grained: Av. grain area per sq mm at beginning of test 0.84.

Fine-grained: Av. grain area per sq mm at beginning of test 0.01.

Coarse-grained lead: extruded rod, specimens machined from 1¼ in diam rod.

Fine-grained lead: extruded rod, specimens machined from 1¼ in diam rod.

B. MG-BASE ALLOYS

Mg-base alloys in the form of heat-treated castings and die castings find wide use for operation over a modest range of temperature as they are relatively stable up to at least 150°C (300°F). The alloys described below are commercially available except for the Mg alloys containing cerium used in German aircraft. Solution heat treated sand castings and hard-rolled Mg alloy sheet are not included in these tests as they are unstable above 150°C (300°F).

In Table 10-2 are listed a series of Mg alloys containing Al, Ce, Mn, and Zn with their nominal compositions and room temperature physical properties. The tensile strengths of these alloys at room temperature vary from 24,000 to 50,000 psi and the yield strength from 14,000 to 34,000 psi, with elongations of 2 to 17 per cent[28].

TABLE 10-2. PROPERTIES OF MAGNESIUM BASE ALLOYS[28]

Designation		Nominal Composition				Typical Properties at Room Temperature		
ASTM	Dow	Al	Ce	Mn	Zn	Tensile (psi)	Yield (psi) 0.2% strain	Elonga-tion (%) in 2"
Castings								
AZ92	C-S[a]	9	0	0.2	2	24,000	14,000	2
AZ92	C-HTA[b]	9	0	0.2	2	40,000	23,000	2
AZ92	C-HTS[c]	9	0	0.2	2	40,000	20,000	3
AZ63	H-S[a]	6	0	0.2	3	29,000	14,000	5
AZ63	H-HTA[b]	6	0	0.2	3	40,000	19,000	5
AZ63	H-HTS[c]	6	0	0.2	3	40,000	17,000	7
AZ90	R[d]	9	0	0.2	0.7	33,000	22,000	3
E10	..	.	10	..	..	....	....	.
Forgings								
M1	M	..	.	1.5	..	36,000	23,000	7
AZ80	0-1HTA[b]	8.5	.	0.2	0.5	50,000	34,000	5
EM22	..	..	2	2	..	....	....	
Extrusions								
M1	M	.	.	1.5	.	38,000	26,000	10
AZ31	FS-1	3	.	0.2	1	40,000	30,000	15
AZ61	J-1	6	.	0.2	1	40,000	32,000	15
AZ80	0-1HTA[b]	8.5	.	0.2	0.5	50,000	34,000	7
Sheet								
M1	Ma	..	.	1.5	..	33,000	15,000	17
M1	Mh	..	.	1.5	..	37,000	29,000	8

(a) Sand-cast and stabilized 4 hrs at 260°C (500°F).
(b) Heat-treated and aged 16 hrs at 177°C (350°F).
(c) Heat-treated and stabilized 4 hrs at 260°C (500°F).
(d) Die-cast.

I. Short-time Tension Tests

Short-time tension tests on the alloys given in Table 10-3 were conducted under ASTM specifications E21-43 on round bars of 0.505 in diameter and under ASTM specifications E8-42 for sheet stock with standard sheet tension specimens. Samples held 10 mins at temperature prior to testing have a temperature variation through the reduced section of less than 1°F. The tests represent a rate of straining determined by a cross head speed of 0.05 in per min up to the yield point and 0.25 in per min from this point to rupture. Test temperatures range from 35°C to 315°C (95°F

TABLE 10-3. SHORT-TIME TENSILE PROPERTIES MG-BASE ALLOYS[28]

Material	Temp (°C)	(°F)	Tensile Strength (psi)	Yield Strength (psi) 0.2% strain	Elongation (%) in 2″
Sand Castings					
C-S	35	95	24,000	18,900	0.3
	94	200	24,100	16,400	0.9
	150	300	24,100	13,500	3.6
	232	450	15,500	9600	31.9
	315	600	9100	5100	60.7
C-HTS	35	95	40,700	22,000	3.2
	94	200	39,300	18,700	7.7
	121	250	35,300	17,600	35.0
	150	300	27,500	15,700	26.0
	232	450	15,100	9900	41.4
	315	600	8600	5400	76.2
C-HTA	35	95	43,400	26,000	2.0
	94	200	41,300	22,000	25.0
	121	250	35,600	20,000	29.7
	150	300	28,000	18,000	35.0
	205	400	16,900	10,900	36.0
	260	500	11,300	7400	33.0
	315	600	7800	5100	49.0
H-S	35	95	28,300	17,700	3.7
	94	200	29,600	15,100	7.5
	121	250	29,400	14,400	9.2
	150	300	26,100	12,700	32.7
	232	450	14,100	7800	42.9
	315	600	7800	4400	65.2
H-HTS	35	95	38,700	17,800	7.6
	94	200	38,000	16,500	15.2
	121	250	33,400	15,700	19.5
	150	300	27,000	14,200	40.3
	232	450	14,900	8600	33.2
	315	600	7300	3700	77.2
H-HTA	35	95	38,700	17,700	5.5
	94	200	36,000	17,300	11.0
	121	250	32,400	16,500	11.0
	150	300	24,500	15,000	15.0
	205	400	17,500	12,000	17.0
	260	500	12,000	8800	15.0
	315	600	8200	5600	20.0
E10-HTA	35	95	19,100	....	0.5
	150	300	20,100	18,200	1.0
	205	400	21,300	18,400	..
	260	500	16,700	10,200	2.0
	315	600	15,500	7400	10.0

TABLE 10-3. *Continued*

Material	Temp (°C) (°F)		Tensile Strength (psi)	Yield Strength (psi) 0.2% strain	Elongation (%) in 2"
Die Casting					
R	35	95	34,200	21,900	4.0
	94	200	32,700	21,100	5.0
	150	300	27,600	16,200	14.7
	232	450	14,600	9800	17.0
	315	600	7000	3600	20.7
Forgings					
M	35	95	33,600	18,800	11.6
	94	200	23,100	13,800	25.7
	121	250	22,400	16,000	25.5
	150	300	19,900	12,000	30.7
	205	400	17,200	9100	34.2
	260	500	10,100	5900	87.5
	315	600	6000	3800	140.0
0-1HTA	35	95	52,900	39,500	4.5
	150	300	31,000	20,700	30.3
EM22	35	95	36,400	26,000	11.5
	150	300	25,400	20,600	19.0
Extrusions					
M	35	95	39,600	30,900	7.6
	94	200	27,000	21,300	15.0
	121	250	24,400	18,800	20.2
	150	300	21,300	15,700	18.7
	205	400	18,800	11,700	25.0
	260	500	13,000	7500	60.0
	315	600	9000	5400	93.0
FS-1	35	95	39,900	28,600	16.6
	94	200	34,800	22,000	20.2
	121	250	30,600	18,300	29.0
	150	300	24,700	14,500	38.2
J-1	35	95	45,800	33,100	14.3
	94	200	42,300	26,400	21.0
	121	250	39,000	25,800	30.7
	150	300	30,400	20,200	40.5
	205	400	21,400	14,700	42.0
	260	500	12,900	8200	64.0
	315	600	7900	5100	70.0

<div align="center">TABLE 10-3. *Continued*</div>

Material	Temp (°C) (°F)	Tensile Strength (psi)	Yield Strength (psi) 0.2% strain	Elongation (%) in 2″
	Extrusions *Continued*			
0-1HTA	35 95	56,500	40,500	4.5
	94 200	48,500	32,100	20.0
	121 250	42,000	26,600	33.0
	150 300	33,600	21,400	41.2
	205 400	21,600	14,700	49.0
	260 500	13,600	7800	83.0
	315 600	8700	4700	123.0
	Sheet			
Ma	35 95	33,000	20,200	17.7
	94 200	24,200	16,200	31.0
	121 250	21,600	14,700	40.5
	150 300	19,300	12,700	44.0
Mh	35 95	36,000	27,000	10.0
	94 200	29,700	26,700	7.7
	121 250	27,300	24,500	11.7
	150 300	25,000	21,200	16.0

to 600°F). As with other alloy systems, Mg-base alloys have lower tensile and yield strengths and larger elongation with increase in temperature under short time tension tests. The E10-HAA alloy has the highest strength at 205°C (400°F) of 21,300 psi[28].

II. Stress-Rupture Tests

Stress-rupture values for the same Mg-base alloys are given in Table 10-4 which represents tests carried out to a limit of about 1000 hours. Included also in the data is the time to reach the beginning of third-stage creep, the elongation at the beginning of third-stage creep, the elongation at rupture, and the rupture time. The test methods for both stress rupture and creep conform to ASTM specifications E22-41 for conducting long-time high-temperature tension tests. The chief difference in the two methods is in the accuracy of strain measurements.

At 35°C (95°F), the alloys can withstand stresses for 1000 hours which are fairly close to the short-time tensile strength. At 150°C (300°F), however, it is only the Ce-bearing alloys that maintain a reasonable strength after 1000 hours[28].

TABLE 10-4.   STRESS-RUPTURE TESTS OF MG-BASE ALLOYS[28]

Material	Temp (°C)	(°F)	Stress (psi)	Hours to Third Stage Creep*	Extension Third Stage (%)	Hours to Rupture	Extension at Rupture % in 2"
Sand Castings							
C-S	35	95	25,000	No rupture in 1000 hrs			
			26,000	Broke in loading			
	150	300	11,000	300	2.3	890	20.1
			12,000	168	2.3	550	20.5
C-HTS	35	95	37,000	720	9.6	1176	21.0
			40,000	140	7.2	265	15.6
	150	300	9000	430	3.5	910	29.6
			10,000	145	2.0	354	33.7
C-HTA	35	95	34,000	480	7.4	1156	28.8
			40,000	115	9.0	233	26.8
	121	250	12,000	495	2.7	1080	30.5
			14,000	120	5.7	290	30.9
	150	300	8000	405	2.5	1181	32.9
			10,000	84	2.1	288	35.7
H-S	35	95	27,000	No rupture in 1000 hrs			
			28,000	Broke in loading			
	150	300	10,000	285	3.6	660	30.2
			12,000	78	4.3	183	29.6
H-HTS	35	95	39,000	730	7.6	840	14.7
	150	300	9000	540	4.5	915	34.0
			10,000	180	5.5	450	26.7
H-HTA	150	300	9000	330	2.4	728	10.8
			10,000	90	1.4	310	11.0
Forgings							
0-1HTA	150	300	10,000	310	3.5	794	30.5
			12,000	160	3.5	356	26.7
EM22	150	300	23,000	420	0.55	1258	19.3
			24,000	230	1.4	578	17.3
Extrusions							
M	35	95	24,000	1300	16.6	1420	21.1
			25,000	340	13.5	477	22.1
	150	300	12,000	680	14.7	1115	38.5
			14,000	..	....	232	41.8
FS-1	35	95	31,000	570	15.1	866	30.4
			32,000	330	15.9	418	28.9
	150	300	7000	390	10.5	900	55.0
			8000	180	9.5	410	54.0
J-1	35	95	42,000	660	8.4	1158	24.7
			44,000	210	9.1	299	21.9
	150	300	6000	360	4.2	1174	71.0
			10,000	114	3.2	312	44.4

TABLE 10-4. *Continued*

Material	Temp (°C) (°F)		Stress (psi)	Hours to Third Stage Creep*	Extension Third Stage (%)	Hours to Rupture	Extension at Rupture (%)
			Extrusion	*Continued*			
0-1HTA	35	95	40,000	610	8.4	1228	24.8
			42,000	116	12.0	284	23.2
	121	250	12,000	180	3.2	780	50.4
			14,000	90	4.4	370	41.5
	150	300	8000	300	3.5	1148	43.9
			Sheet				
Ma	35	95	22,000	265	9.3	630	39.8
	150	300	9000	625	2.9	996	64.0
			10,000	285	2.1	531	73.0
Mh	35	95	25,500	1190	1.6	1645	10.6
			26,000	130	0.9	290	14.5
	150	300	12,000	190	5.1	800	47.7
			14,000	90	3.5	176	35.0

* The beginning of third stage creep is taken as the point of inflexion on the curve.

III. Creep Tests

Creep data for the above Mg-base alloys carried out under ASTM specifications E22-41 are presented in Table 10-5 taken at various temperatures for 0.1, 0.5, and 1.0 per cent creep in 100 hrs. The sand-cast alloy H-HTS has a yield strength at 94°C (200°F) of 16,500 psi and for 100 hours has a 1 per cent creep rate under a stress of 17,500 psi. At 150°C (300°F), the Mg alloy with Ce, EM22, has the highest creep strength for 1000 hours, 17,800 psi. Mg alloys are unusual in that they break with a ductile fracture after long periods of loading. Large deformations in service before failure of the part may serve as a warning.

C. Al and Al Alloys

I. Pure Al

Pure Al tested in creep at elevated temperature may fail with either transcrystalline or intercrystalline fractures depending on the amount of elongation that occurs. At 250°C, Al poly-crystals stressed to produce failure in 20 mins have 4 per cent elongation and a transcrystalline fracture. At this same temperature if the stress is lowered so that failure occurs after 220 hrs with 20 per cent elongation, the fracture is intercrystalline[18, 19]. The transition from one type of fracture to the other occurs at about 10 per cent elongation.

Single crystals of Al heated to 250°C and creep tested in tension show

TABLE 10-5.   CREEP DATA WITHOUT RUPTURE OF MG-BASE ALLOYS[28]

Material	Temp (°C) (°F)		Stress (psi) in Extension 0.1%		Stress (psi) for Extension 0.5 % 1000 hrs	Stress (psi) for Extension 1% 1000 hrs
			100 hrs	1000 hrs		
Sand Castings						
C-HTS	35	95	21,800	16,000	....	....
	94	200	9400	7400	12,800	....
	121	250	6900	3900	8100	....
	150	300	3400	1500	3800	....
C-HTA	35	95	19,000	17,900	....	....
	94	200	8600	6800	11,200	....
	150	300	3100	1900	3800	....
H-S	94	200	9600	6800	....	....
	121	250	6500	....	....	....
	150	300	4200	2200	5300	....
H-HTS	35	95	20,100	17,400	....	....
	94	200	11,000	7100	15,400	17,500
	121	250	8600	4200	10,200	11,700
	150	300	4100	1700	4200	6200
H-HTA	35	95	22,000	18,200	....	....
	94	200	11,000	8900	....	....
	150	300	3500	1600	4200	6300
E10-HTA	205	400	....	7300	....	....
	260	500	4800	3400	....	....
	315	600	1800	....	....	....
Forgings						
0-1HTA	150	300	....	....	3000	5300
	177	350	....	....	....	4400[a]
EM22	150	300	....	17,800	....	....
Extrusion						
M	35	95	16,800	14,300	16,600	....
	94	200	13,900	13,800	....	....
	121	250	13,000	10,700	11,800	12,200
						14,000[a]
	150	300	....	5700	7400	8200
Sheet						
Ma	35	95	13,900	13,500	14,000	....
	121	250	....	7600	....	....
	150	300	....	....	4800	....

(a) Stress for 5 per cent extension

normal slip lines in the early stages of deformation. If the load is maintained over a sufficiently long time, heavy deformation bands appear which are not characteristic of polycrystalline Al. This effect is detected in single crystals of Al at 250°C stressed at a creep rate of 1.15 per cent per day. Under these conditions failure occurs at the end of 719 hours with a total elongation of 37 per cent. If the creep rate for stressing single crystals of Al is lowered to 0.1 per cent per day, the first appearance of slip bands is delayed considerably and is observed after greater extensions of the crystal.

II. Al Alloys

a. **Commercial Al Alloys.**—*1. Elevated-temperature Properties.* The high-temperature properties of a series of commercial Al alloys in sheet form tested from 23 to 190°C (75 to 375°F) are shown below. The composition, heat treatment, grain size and tensile properties at 23°C (75°F) of the alloys are listed in Table 10-6[15]. Alloy 24S is a naturally aged alloy whereas the other alloys are artificially aged. Natural aging is the increase in hardness which occurs at room temperature.

The elevated-temperature properties of the above commercial Al alloys in sheet form are shown combined in a series of graphs (Figs. 10-1 to 10-6)[13, 15].

The results of short-time tensile tests on alloys 24S-T, 24S-T81, 24S-T86, and 75S-T are shown in Fig. 10-1 for test temperatures from 35 to 190°C (94 to 375°F). All samples were exposed 1000 hours at the test temperature in the unstressed condition before the short-time tensile test. All samples are stressed transverse to the direction of rolling. The tests represent strain rates of 0.06 inch per min of the cross head of the tensile machine. However, in the 2-inch gage length of the specimen, the strain rate varies considerably during the test due to plasticity in this region. Average values of observed strain rates obtained from samples with a 2-inch gage length and expressed as inch per inch per minute are as follows[13]:

Stress	¼ Hr at 100°C (212°F)	1000 Hrs at 190°C (375°F)
Zero stress to yield stress	0.0028	0.0046
Yield stress to fracture	.019	.026
Zero stress to fracture	.014	.021

The short-time tensile properties of all four alloys after 1000 hours' exposure to the test temperature in the unstressed condition remain high at temperatures up to 121°C (250°F). The alloy 75S-T has a sharp drop at this temperature which is not unexpected, since this is also the temperature for artificial aging of this alloy as shown in Table 10-6.

TABLE 10-6. ROOM-TEMPERATURE PROPERTIES OF SOME
COMMERCIAL ALUMINUM ALLOYS[15]

Nominal Composition

Material	Cu	Mn	Mg	Si	Zn	Cr	Al
24S	4.5	0.6	1.5				Bal
75S	1.6	0.2	2.5		5.6	0.3	Bal
R301	4.5	0.8	0.4	1.0			Bal

Standard Heat Treatments

24S-T   24S alloy solution-heat-treated at 488°C to 500°C (910°F to 930°F) followed by quenching in cold water and aging at room temperature.

24S-T81   24S-T stretched 1 per cent and aged 10 hrs at 190°C (375°F) or 12 hrs at 185°C (365°F).

24S-T86   24S-T strain-hardened by rolling to a reduction of about $5\frac{1}{2}$ per cent and aged $5\frac{1}{2}$ hrs at 190°C (375°F) or $8\frac{1}{2}$ hrs at 185°C (365°F).

R301-T   R301 alloy solution-heat-treated at 500°C to 510°C (930°F to 950°F) followed by quenching in cold water and aging at 177°C (350°F), or 18 hrs at 160°C (320°F).

75S-T   75S alloy solution-heat-treated at 460°C to 500°C (860°F to 930°F) followed by quenching in cold water and aging 24 hrs at 121°C (250°F).

In accordance with commercial procedure, straightening by stretching or roll-flattening is carried out by a cold deformation of about 1 per cent.

*Grain Size**

Material	Rolling Direction (grains per mm)	Thickness Direction (grains per mm)
24S-T "Alclad"	19	60
24S-T81 "	22	65
24S-T86 "	17	44
75S-T "	16	54
R301-T (clad)	48	89

* Number of grains per mm cut by a straight line. All counts made in plane parallel to rolling direction and perpendicular to surface of sheet.

Tensile Properties at 23°C (75°F)

All materials in form of 0.04 in clad sheet.

Material	Tensile Strength (psi)	Yield Strength (psi) 0.2% strain	Elong % in 2"
24S-T "Alclad"	63,000	47,400	16.5
24S-T81 "	66,100	62,200	5.7
24S-T86	67,300	64,000	5.3
75S-T "Alclad"	75,500	67,700	10.5
R301-T (clad)	66,000	59,900	9.5
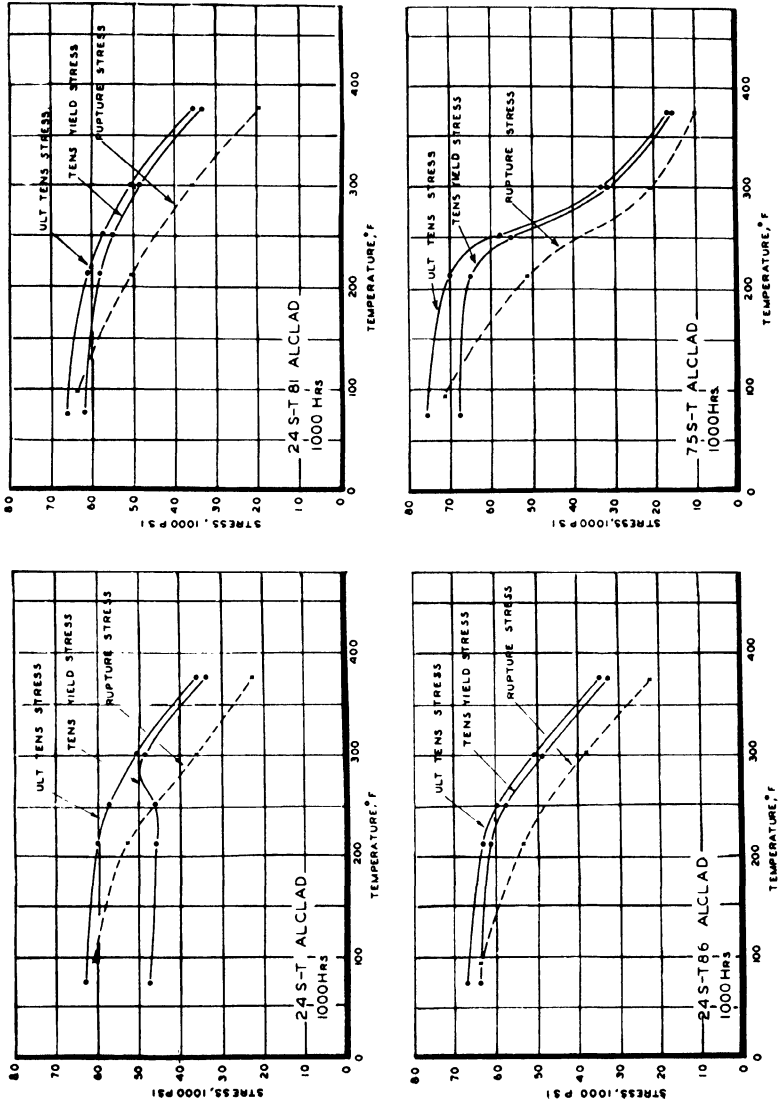
Fig. 10-1. Comparison of rupture stress with yield and ultimate stresses determined in short time tensile tests at elevated temperatures. Rupture stress: Stress required for fracture in 1000 hrs. under constant load. Tensile data: Determined after 1000 hrs. exposure in unstressed condition. Direction of stress: Cross-grain. (After Flanagen, Tedsen, and Dorn)
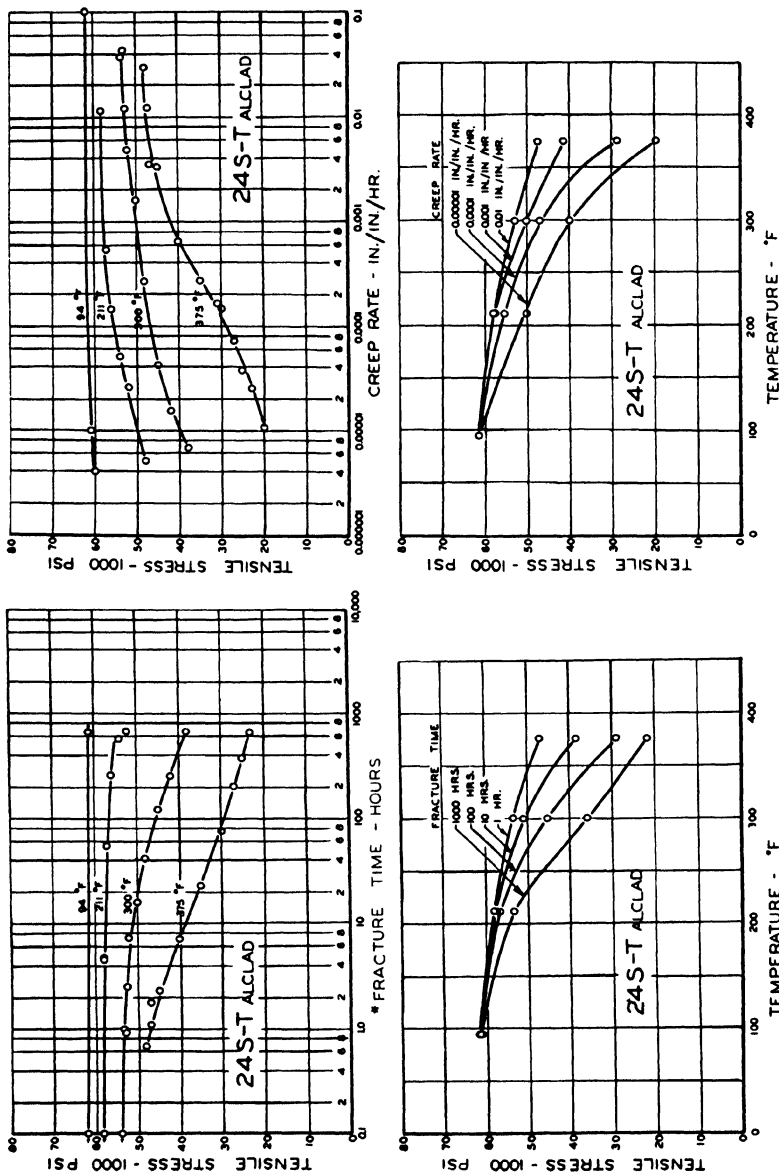
Fig. 10·2. Effects of temperature and tensile stress on fracture time and creep rate—24S-T Alclad sheet. Direction of stress: Cross-grain Gage length: 6 inches. Sheet thickness: 0.040 inches. Time in furnace before application of load: 1 hr. (includes 45 min. to reach temperature). (After Flanagen, Tedsen, and Dorn) *Time measured from attainment of full load.*
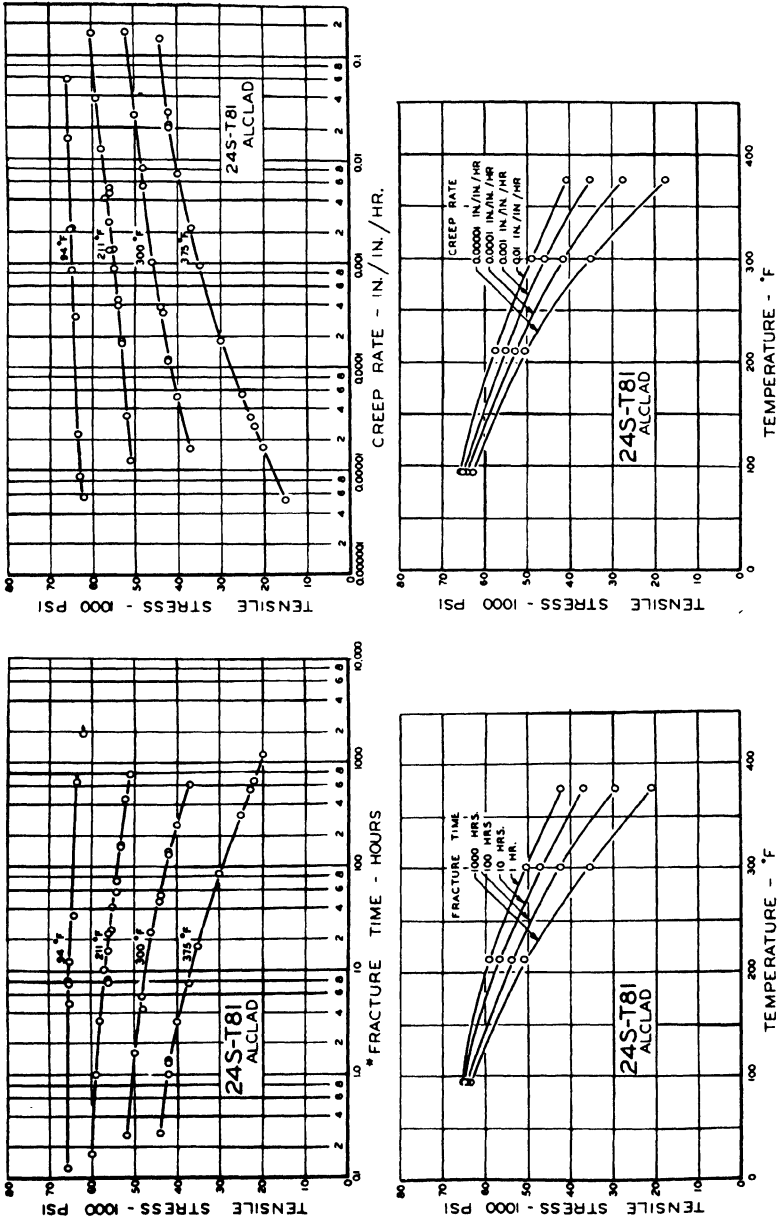
Fig. 10-3. Effects of temperature and tensile stress on fracture time and creep rate—24S-T81 Alclad sheet. Direction of stress: Cross-grain. Gage length: 6 inches. Sheet thickness: 0.040 inches. Time in furnace before application of load: 1 hr. (includes 45 min. to reach temperature). (After Flanagen, Tedsen, and Dorn) *Time measured from attainment of full load.*
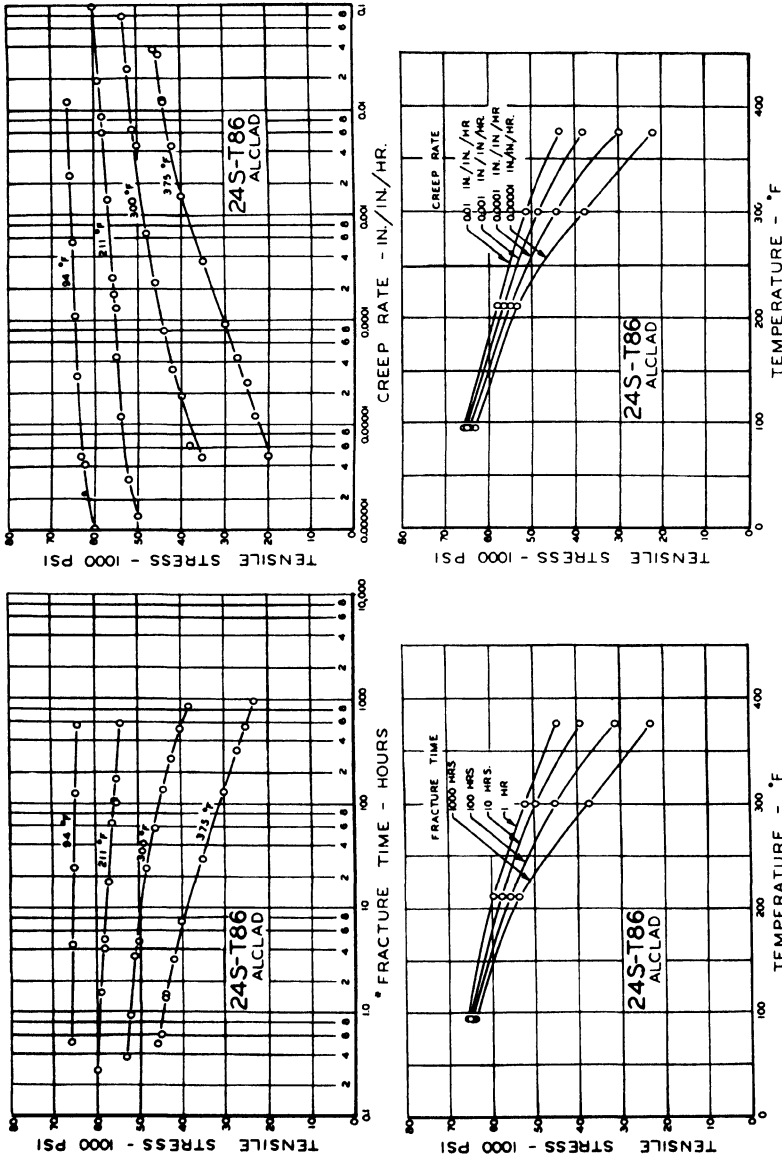
Figure 10-4. Effects of temperature and tensile stress on fracture time and creep rate—24S-T86 Alclad sheet. Direction of stress: Cross-grain. Gage Length: 6 inches. Sheet thickness: 0.040 inches. Time in furnace before application of load: 1 hr. (includes 45 min. to reach temperature). (After Flanagen, Tedsen, and Dorn) *Time measured from attainment of full load.
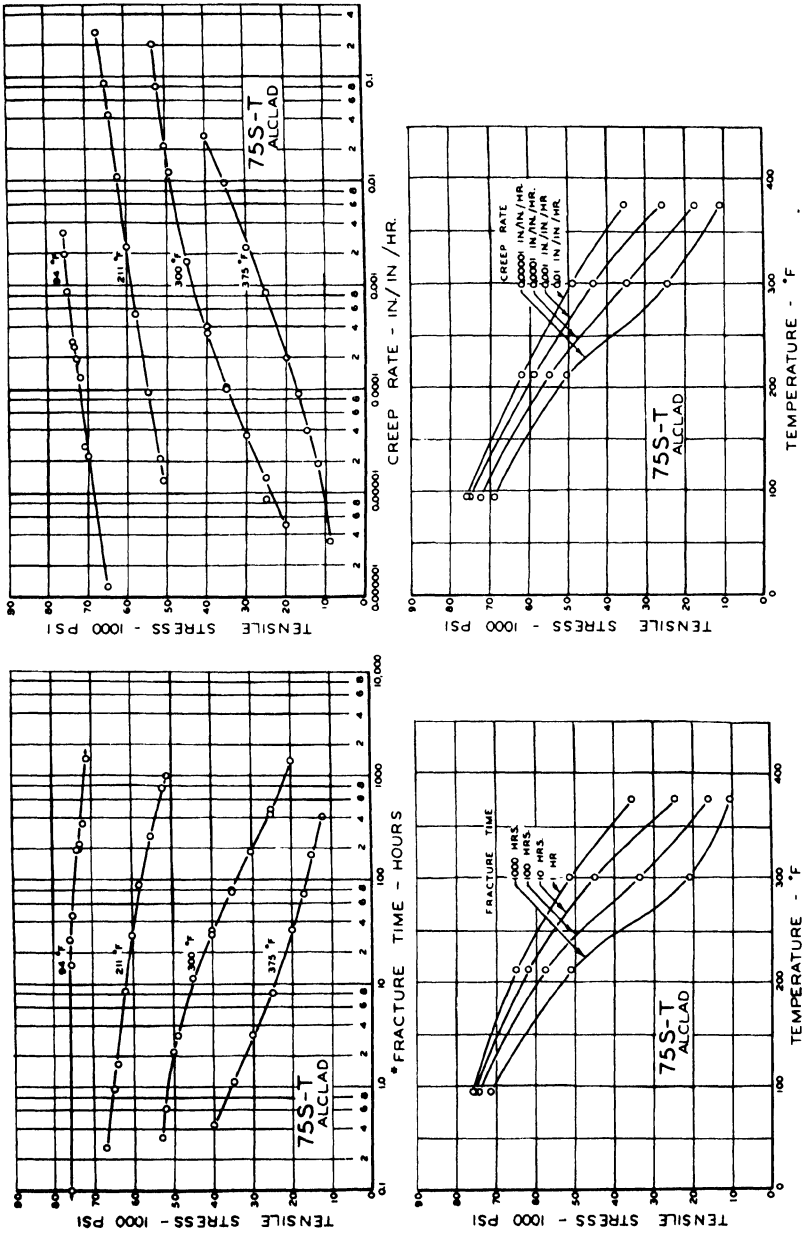
Figure 10-5. Effects of temperature and tensile stress on fracture time and creep rate—75S-T Alclad sheet. Direction of stress: Cross-grain. Gage length: 6 inches. Sheet thickness: 0.040 inches. Time in furnace before application of load: 1 hr. (includes 45 min. to reach temperature). (After Flanagen, Tedsen, and Dorn) *Time measured from attainment of full load.*
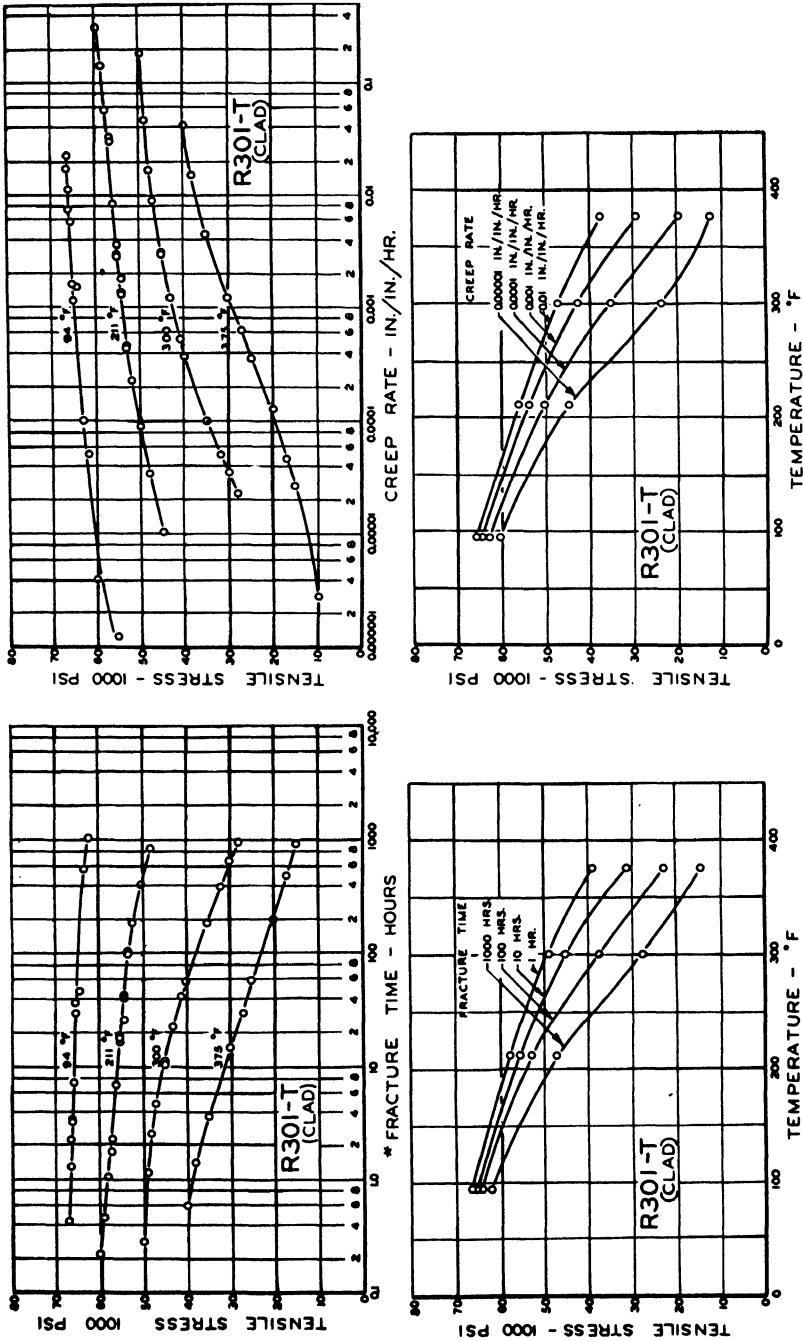
Fig. 10-6. Effects of temperature and tensile stress on fracture time and creep rate—R301-T (clad) sheet. Direction of stress: Cross-grain. Gage length: 6 inches. Sheet thickness: 0.040 inches. Time in furnace before application of load: 1 hr (includes 45 min. to reach temperature). (After Flanagen, Tedsen, and Dorn) *Time measured from attainment of full

Clad Al alloys show a primary and a secondary modulus of elasticity due to the separate effects of the cladding and core, the former having the lower yield stress. With increase in temperature these moduli are lowered but the effect of time at temperature appears to be insignificant. The values of the primary and secondary moduli tend to approach each other as the temperature is increased.

In Al alloys subject to buckling in service, it is sometimes desirable to know the shape of the stress strain curve in the plastic region. The modulus thus determined from stress strain curves in both tension and compression is the tangent modulus. The tangent modulus is lowered by both increase in temperature and exposure time.

2. Stress-Rupture Tests. Stress-rupture tests for alloys 24S-T, 24S-T81, 24S-T86 and 75S-T at temperatures from 35 to 190°C (94 to 375°F) for 1000-hour tests are shown in Fig. 10-1 for comparison with short-time tensile data. At 23°C (75°F) the charts indicate that the rupture stress equals or exceeds the yield stress and is only slightly lower than the ultimate stress. But above 65°C (150°F) the rupture stress falls off compared to the short-time tensile stress except in the case of the 24S-T where the rupture stress does not fall below the tensile yield stress until the temperature of 121°C (250°F) is reached.

The effect of time on the rupture strength of the above alloys and also on alloy R301-T is shown in Figs. 10-2 to 10-6[15]. Exposure periods are 1, 10, 100, and 1000 hours. In the range of 35 to 99°C (94 to 211°F), the 75S-T alloy has the highest values. Above this range the alloy 24S-T86 is superior. These stress-rupture curves are useful especially in showing the decrease in strength with increase in time at the higher temperatures. For alloys displaying this deterioration, the use of the tangent modulus in designs is untenable .

Comparisons of elongations at fracture of four alloys, 24S-T, 24S-T81, 24S-T86, and 75S-T with elongation in the short time tensile test at 35 to 190°C (94 to 375°F) are shown in Table 10-7. The rupture time for the stress-rupture tests is the same as the time of exposure in the unstressed condition prior to the short time tensile test. An increase in time generally lowers the ductility of the alloys in both test methods. Values for elongation are for the most part lower at the higher temperatures.

3. Characteristic Fractures. The Al sheet test pieces show two types of fractures (a) one perpendicular to the axis of the specimen and (b) one with a fracture inclined at about a 60· angle to the axis. Alloy 75S-T at 94° F breaks according to type a; at higher temperatures it breaks according to type b. For the other alloys, the reverse is generally true Such effects depend on the anisotropy of the sheet.

4. Creep Strength. In Figs. 10–2 to 10-6 the tensile stress is plotted

TABLE 10-7.   COMPARISON OF ELONGATIONS AT FRACTURE IN STRESS RUPTURE AND SHORT TIME TENSILE TESTS* OF AL ALLOYS[15]

24S-T "Alclad"   24S-T81 "Alclad"

Temp (°C) (°F)		Time (hrs)	Elong % in 2"		Time (hrs)	Elong % in 2"	
			Stress Rupture	Tensile		Stress Rupture	Tensile
35	94	..	....	....	5	6.5	5.0
					12	6.0	5.0
					34	6.0	5.0
99	211	5	19.0	15.5	10	7.5	7.0
		54	17.5	16.0	57	7.0	7.0
		258	16.0	16.5	456	7.0	7.0
		570	10.0	16.5	790	9.5	7.5
		668	10.0	16.5	..	..	..
150	300	7	15.5	18.0	6	8.0	7.5
		41	7.0	14.0	24	7.0	7.5
		124	5.5	11.0	128	6.0	7.5
		253	2.5	9.0	253	4.5	7.5
		658	3.5	8.0	611	3.0	8.0
190	375	7	6.5	12.0	8	9.0	9.5
		75	6.0	8.0	311	7.0	9.5
		381	5.5	10.5	562	6.0	9.5
		671	5.0	11.5	664	5.0	9.0
35	94	4	5.0	4.0	26	13.5	10.5
		126	5.5	4.0	197	15.0	10.5
		545	5.5	4.0	347	15.0	10.5
99	211	5	7.0	6.0	9	16.5	14.0
		18	7.5	6.0	90	15.5	12.0
		101	6.0	6.0	276	11.5	12.0
		583	4.0	6.0	992	13.0	11.5
150	300	5	6.0	7.0	2	15.5	14.0
		25	7.5	7.0	30	11.5	11.0
		140	5.0	7.0	189	12.0	11.0
		508	4.0	7.5	479	9.5	13.0
		865	2.0	8.0	1452	13.0	17.0
190	375	3	6.0	8.0	33	14.0	16.5
		317	3.0	9.0	74	16.5	18.5
		....	....	....	500	....	26.5
		959	3.5	10.5	1000	....	29.0

* Direction of stress: Cross grain.   Sheet thickness 0.04 in.   Tensile tests performed after indicated exposures in unstressed condition.   Tensile and stress rupture samples taken from different sheets.

against the log of the creep rate for the four alloys mentioned above. Many of the alloys tested at higher temperatures do not show straight lines in these graphs due to precipitation effects.

5. *Properties of Wrought Al Alloys 205 to 426°C (400 to 800°F).*   Tests

on Al alloys are extended to higher temperatures since it has been estimated that parts of reciprocating aircraft engines, such as pistons and cylinder heads, may develop localized areas which reach 370 to 425°C

TABLE 10-8. PROPERTIES OF WROUGHT AL ALLOYS[20]

Chemical Composition

Material	Si	Fe	Cu	Mg	Mn	Ni	Zn	Cr	Pb	Bi	Ti
XB18S	0.58	0.31	3.89	1.43	0.01	2.14	0.02	0.01	0.01	0.01	0.03
18S	.58	.45	3.98	0.64	.05	2.01	.02	.01	.01	.01	.01
24S	.10	.25	4.41	1.41	.67	0.01	.02	.02	.01	.01	.01
32S	12.18	.41	.89	1.20	.01	.87	.02	.01			.01

Heat Treatment to Produce T-Temper

XB18S   Hold for 1 hr, water-quench, temper at 171°C (340°F) for 10 hrs.
18S   Same as for Alloy XB18S.
24S   Hold at 493°C (920°F) for 1 hr, water-quench, temper at room temp 4 days.
32S   Hold at 515°C (960°F) for 1 hr, water-quench, temper at 171°C (340°F) for 12 hrs.

Nominal Room Temperature Properties in T-Temper

	Tensile Strength (psi)	Yield Strength (psi)	Elong (% in 2 in)	Reduction of Area (%)	Brinell Hardness
XB18S*	45,600	61,200	14.5	28.4	117
18S	47,000	63,000	17.0	....	115
24S	46,000	68,000	22.0	....	120
32S	46,000	56,000	8.0	....	125

* Actual properties

Grain Size*

Material	Fabrication	Solution Treatment		Average Grain Diam (in)	Range of Grain Size (in)
		Time (hrs)	Temp (°F)		
XB18S-T	Hot-rolled	1	960	0.0006	Fairly uniform
XB18S-T	Forged	1	960	.0020	0.00165 to 0.00236
XB18S-T	Hot-rolled	10	960	.0013	Fairly uniform
32S-T	Hot-rolled	1	960	.0011	0.00079 to 0.00118
24S-T	Hot-rolled	1	920	.0027	0.00158 to 0.00315 Some very large grains
18S-T	Hot-rolled	1	960	.0013	0.00099 to 0.00197

* Average of 25 to 40 measurements.

(700 to 800°F). The alloys selected for this study are shown in Table 10-8[20]. Included are the composition, heat treatment and room-temperature properties. Test samples are taken from 1-inch hot-rolled rods.

In the case of the X̄B18S-T, some samples are representative of rod forged to ⅞-inch rounds.

6. Short-time Tension Tests of Wrought Al Alloys.   The results of short-time tension tests are shown in Table 10-9 for the wrought alloys XB18S-T, 24S-T, and 32S-T at 205 to 426°C (400 to 800°F).   The values of the

TABLE 10-9.   SHORT-TIME TENSILE PROPERTIES OF AL ALLOYS[20]

(All bars held 1 hr at temperature before being pulled.   Bars pulled 0.02 in per min to 0.02 per cent offset yield, then 0.10 in per min to rupture.)

Material	Number	Temp (°F)	Tensile Strength (psi)	Yield Strength (psi)		Elong (% in 2 in)[a]	Reduction of area (%)	Apparent Modulus of Elasticity × 10⁶
				0.1% offset	0.2% offset			
XB18S-T	A6J	400	47,400	40,000	41,500	14.4	29.3	9.65[b]
	A6K	400	48,300	39,200	40,800	15.9	33.4	9.10[b]
	A4J	500	30,500	28,500	30,000	24.0	55.4	9.5
	A4K	500	27,900	22,800	24,300	12.0	35.7	9.7
	A4L	600	14,000	12,000	12,250	41.0	74.7	9.0
	A4M	600	14,700	11,600	12,200	33.0	74.9	8.4
	A8F	700	7250	5500	6000	55.0	83.0	5.5
	A8G	700	7650	6100	6300	64.0	86.0	3.5
	A5L	800	2940	1340	1430	. . .	. . . .	1.6[c]
	A8H	800	2700	1700	1800	. . . .	. . . .	1.45
24S-T	G1H	400	51,700	44,000	45,000	19.0	46.0	9.8
	G1J	400	52,500	32,500	34,500	26.0	46.0	9.8
	G1K	500	28,700	23,000	24,600	28.0	75.0	8.4
	G1L	500	27,400	22,900	23,800	20.0	82.0	8.7
	G1M	600	17,700	15,140	15,300[d]	25.0	81.0	9.6
	G2A	600	18,700	16,000	16,500	29.0	81.0	8.3
	G2B	700	10,800	9300	9500	36.0	84.0	9.1
	G2C	700	9550	8200	8400	54.0	92.0	4.9
32S-T	L1P	500	27,200	24,200	25,000	9.0	18.0	9.6
	L1Q	500	27,200	24,500	25,800	10.0	28.0	7.4

(a) Specimens were not broken.   Elongation is greater than stroke of machine under normal conditions.

(b) Bars pulled 0.02 in per min to 0.02 per cent offset yield, then 0.06 in per min to rupture.

(c) Held for 2 hrs at temperature.

(d) Estimated.

modulus of elasticity which are included are only approximations as the stress-strain curves for Al alloys at these high temperatures indicate plastic flow at relatively low loads[20].

7. Creep Tests of Al Alloys.   The results of creep tests on Al alloys XB18S-T both hot-rolled and forged, as well as the hot-rolled Al alloys 24S-T, 32S-T, and 18S-T are shown in Table 10-10[20].   They represent

TABLE 10-10. CREEP TESTS OF AL ALLOYS[20]

Material	No.	Temp (°C) (°F)		Stress (psi)	Initial Deformation (%)	Min Creep Rate (% per hr)	Final Creep Rate (% per hr)	Total Deformation (%)	Contraction on Release of Load (%)	Duration (hr)
XB18S-T	A6L	205	400	10,000	0.069	0.000160	0.000160	0.240	..	478
	A6M	205	400	15,000	.406	.000900	.002200	1.440	0.120	697
	A3K	260	500	5000	.052	.000360	.001250	0.636	.064	501
	A3J	260	500	10,000	.138	.022000	a	a	a	a
	A8C	315	600	1000	.017	.000310	.000310	.365	.009	618
	A8B	315	600	2500	.017	.006100	b	b	b	b
24S-T	G1B	205	400	10,000	.117	.000025	.000025	.148	.117	524
	G1C	205	400	15,000	.175	.000130	.000140	.304	.181	572
	G1F	315	600	1200	.013	.000040	.000040c	.035	.023	526
	G1E	315	600	2000	.015	.000080	.000080c	.076	.018	553
	G1G	315	600	3000	.030	.000120	.000120	.152	.023	528
32S-T	L1B	205	400	10,000	.119	.000300	.000470	.443	.122	722
	L1C	205	400	8000	.062	.000120	.000140	.195	.077	528
	L1D	315	600	1500	.041	.000270	.000270	.240	.019	497
	L1F	315	600	2500	.021	.002200	d	d	d	d
	L1E	315	600	3000	.047	.006000	e	e	e	e
18S-T	J1N	315	600	1000	.017	.000090	.000090	.076	..	498
	J1L	315	600	2000	.024	.000330	.000330	.295	.021	500
XB18S-Tf	F4C	205	400	15,000	.170	.000450	.000720	.506	.180	502
	F3B	315	600	1000	.015	.000350	.000350	.212	.009	503

(a) Broke at 96.8 hrs; 38.8 per cent elongation; 61.2 per cent reduction of area.

(b) Broke at 257.8 hrs; 84.7 per cent elongation; 90.9 per cent reduction of area.

(c) Average creep rate between 100 and 150 hrs. Rate varied somewhat during test.

(d) Broke at 552 hrs; 48.5 per cent elongation; 81.3 per cent reduction of area.

(e) Broke at 244 hrs; 38.9 per cent elongation; 78.0 per cent reduction of area.

(f) Forged. All other specimens from rolled alloy. These specimens were run at the same temperatures and stresses as rolled XB18S-T specimens A6M and A8C so that a direct comparison of the results of rolled and forged fabrication could be made.

TABLE 10-11. TENSILE STRESS FATIGUE TESTS ON AL ALLOYS.[20]

Temp (°C) (°F)		Stress (pi)	Cycles for Failure			
			XB18S-T	32S-T	24S-T	18S-T
205	400	30,000	1,754,800	3,477,460	476,300	233,500
			3,299,500a		432,900	236,700
260	500	15,000	3,826,000	791,200	1,760,000	793,000
			86,000a			
			10,000,000a			
315	600	7000	4,200,600a	5,103,500	1,866,000	7,973,000
					18,433,300	
371	700	3000	2,986,400	4,155,900	19,101,100b	3,000,000
			241,000a			

(a) Forged specimen.

(b) Unbroken.

tests conducted at temperatures from 205 to 315°C (400 to 600°F) and times of approximately 500 hours.

The effect of grain size for the 18S alloy rod in relation to creep rate is given below[15]:

PER CENT CREEP OF 18S ROD [10 HRS. AT 515° C (960° F), BWQ—12 HRS AT 171° C (340° F)] AT 400° F AND AT END OF 50 HRS

Structure (¾ in rod)	15,000 psi	20,000 psi
Coarse grain	0.056	0.10
Medium grain	.10	.20
Fine grain	.32	.81

BWQ: Boiling water quench

These results are consistent with those determined for other metals where fine grains are associated with higher creep rates.

8. Hot Fatigue Tests of Al Alloys. Fatigue tests shown in Table 10-11 are representative of measurements of tensile repeated stress on specimens subjected to axial loading at temperatures from 205 to 371°C (400 to 700·F).* The temperature control of the furnaces is ± 10° F and the rate of application of the load is 1500 cycles per minute. The tests are conducted on the basis of continuous heating of the specimen over a 24-hr period but fatigue testing is carried out only during a 10-hr period of the day. Thus for 10 days operation at the selected temperature, the specimen receives 9 million cycles of stress.

Above 205°C (400°F) two types of fracture are observed, one which is typical of fatigue failures, and the other which is ductile and resembles a static failure[20].

9. Thermal Expansion of Al Alloys. The thermal expansion and contraction coefficients of several Al alloys are shown in Table 10-12. The coefficients of expansion of the 32S alloy are nearly 15 per cent less than for alloys 18S, XB18S, and 24S. Samples aged at 371 and 426°C (700 and 800°F) show smaller dimensional changes after being heated and cooled than alloys aged at lower temperatures as indicated in the last column of Table 10-12.

10. Compressive Properties of Al Alloy Sheet. With the method of de-icing aircraft structures by heating them from exhaust gases to temperatures up to 150°C (300°F), the effect of buckling on commercial Al alloys at this temperature becomes important. The yield strength determined from compression testing of sheet stock at high temperatures is of value in selecting materials for this type of service.

* Krouse tensile stress fatigue-testing machine. The mean stress in the tensile stress method is about ½ the maximum stress.

The results of compression testing a series of commercial Al alloys in sheet form of a nominal thickness of 0.125 inch are given below from experiments conducted in compression testing equipment of special design to

TABLE 10-12. COEFFICIENTS OF EXPANSION AND CONTRACTION OF ROLLED ALUMINUM ALLOYS*

	Sample No										
	1776	1776A	1776B	1777	1777A	1778	1778A	1778B	1779	1779A	1779B
	Material										
	$18S\text{-}T^a$	$18S\text{-}T^b$	$18S\text{-}T^c$	$XB18S\text{-}T^a$	$XB18S\text{-}T^b$	$24S\text{-}T^a$	$24S\text{-}T^b$	$24S\text{-}T^c$	$32S\text{-}T^a$	$32S\text{-}T^b$	$32S\text{-}T^c$
Average Coefficient of Expansion per ($°F \times 10^{-6}$)											
68 to 200° F	12.8	12.5	12.7	12.8	12.5	12.8	12.7	12.6	11.1	10.9	10.8
68 to 400° F	13.1	12.9	13.1	13.0	13.1	13.0	13.1	13.2	11.7	11.3	11.4
68 to 600° F	14.1	13.4	13.7	13.7	13.6	13.3	13.7	13.6	12.5	11.6	11.7
68 to 800° F	14.4	13.9	14.2	14.6	.	14.0	14.6	14.3	13.0	12.2	12.2
Average Coefficient of Contraction per °F $\times 10^{-6}$)											
800 to 68° F	14.0	14.1	14.1	14.0		14.7	14.6	14.4	12.1	12.0	11.9
600 to 68° F	....	....	.		13.6	.	.	...	..	11.4	....
400 to 68° F	13.0	13.0	13.0	13.1		13.1	13.2	13.3	11.0	....	10.9
200 to 68° F	12.4	12.3	12.3	12.5	12.4	12.4	12.6	12.6	10.3	. ..	10.3
†Change in Length after Heating and Cooling %	0.03	−0.01	0.01	0.04	0.00	−0.05	0.00	−0.01	0.06	0.02	0.02

(a) T-temper.
(b) T-temper and aged at 700° F for 100 hrs.
(c) T-temper and aged at 800° F for 500 hrs.
* Data from National Bureau of Standards.
† Determined at 20° C from the expansion curve on heating and the contraction curve on cooling. Positive values indicate an increase in length; negative values, a decrease in length.

minimize friction and control the temperature. The alloys are basically 24S, R301, and 75S as listed in Table 10-13 with standard commercial heat treatments and room-temperature strength properties. Alloy 301-T is
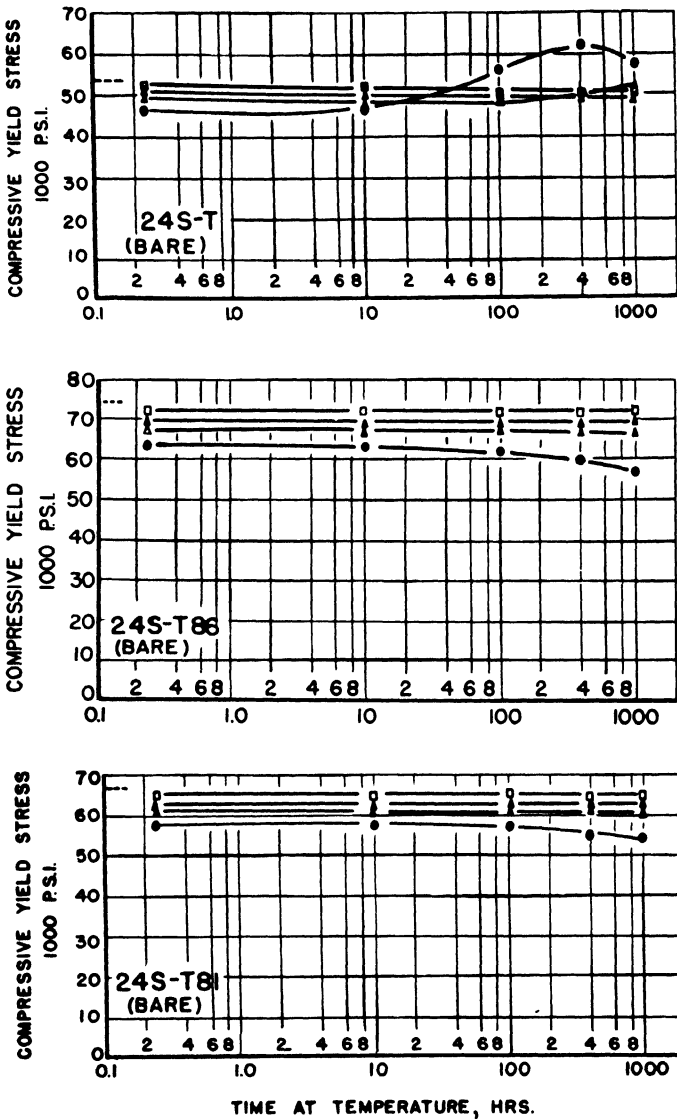
Fig. 10-7. Effects of temperature and exposure time on compressive yield stress at elevated temperatures. (After Flanagen, Tedsen, and Dorn)
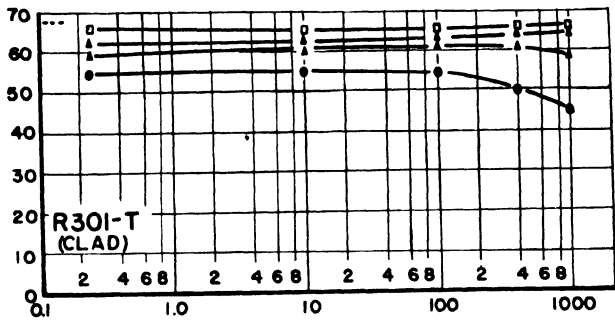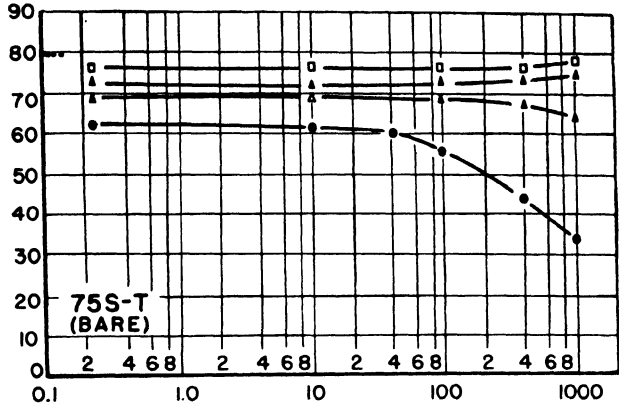
FIG. 10-7. Continued

DIRECTION OF STRESS: CROSS GRAIN

STRAIN RATE: 0002 IN./IN. PER MIN

MATERIAL: 0125 IN SHEET

EACH POINT REPRESENTS AN AVERAGE VALUE BASED ON 2 OR MORE TESTS

--- 78°F
□ 150
▲ 212
▲ 250
● 300

is clad with 2.3 per cent by weight of pure Al, but the other alloys are bare. Alloy 24S-T is solution-treated and aged at room temperature. The other alloys are all artificially aged at higher temperatures. Since

TABLE 10-13. PROPERTIES OF AL ALLOYS AT ROOM TEMPERATURE.[14]

Nominal Composition

Material	Cu	Mn	Mg	Si
24S	4.5	0.6	1.5	...
R301	4.5	0.8	0.4	1.0
75S	Principal hardening agents are Zn and Mg with smaller additions of Cu and other elements.			

Note: In each case the remainder consists of Al and normal impurities.

Heat Treatment

Material	Heat Treatment
24S-T	24S alloy solution heat-treated at 488 to 500° C (910 to 930° F) followed by quenching in cold water and aging at room temperature.
24S-T81	24S-T stretched 1 per cent and aged 10 hrs at 190° C (375° F) or 12 hrs at 185° C (365° F).
24S-T86	24S-T strain hardened by rolling to a reduction of about 5½ per cent and aged 5½ hrs at 190° C (375° F) or 8½ hrs at 185° C (365° F).
R301-T	R301 alloy solution heat treated at 500 to 510° C (930 to 950° F) followed by quenching in cold water and aging 6 hrs at 177° C (350° F) or 18 hrs at 160° C (320° F).
75S-T	75S alloy solution heat treated at 460 to 500° C (860 to 930° F) followed by quenching in cold water and aging 24 hrs at 121° C (250° F).

Tensile Properties at Room Temperature

Material	Tensile Strength (psi)	Yield Strength 0.2% offset (psi)	Elong (% in 2 in)
24S-T bare	70200	50500	20.0
24S-T81 "	70400	65900	7.0
24S-T86 "	75500	71500	5.5
75S-T "	83700	75400	11.0
R301-T clad	69800	63600	10.0

Average cross grain values based on four tests for each material at 23° C (75° F).

these alloys may age with exposure to high temperature, it is also important to determine the effect of exposure with time. To accomplish this end the alloys are subject to exposure at the test temperature for periods of time from 1 to 1000 hours[14].

11. Compressive Yield Stress. The compression tests are conducted at a

constant strain rate of 0.002 in per in per min with continuous loading of the specimen throughout the test. The compressive yield stress for each alloy at the test temperature is plotted in Fig. 10-7 against the log time of exposure of the alloy in the unstressed condition. The 24S-T alloy shows an increase in the compressive yield strength at 150°C (300°F) which is to be expected since it was aged originally at room temperature. Alloys 24S-T86 and 24S-T81 show the greatest stability at elevated temperature on the basis of compression testing. The 75S-T alloy loses strength most rapidly due to the fact that its artificial aging temperature is lower than that for the other alloys. In general, the effects of prior exposure at the test temperature and the compressive properties at elevated temperature are comparable to the same tests derived from tension data. The modulus of elasticity in compression decreases with increase in temperature and is especially marked with alloy 75S-T[14].

References

1. Andrade, E. N. daC., "On the Viscous Flow in Metals and Allied Phenomena,' *Proc. Roy. Soc. (A)*, **84,** 1 (1911).
2. Andrade, E. N. daC., "Flow in Metals under Large Constant Stresses," *Proc. Roy Soc.*, **90,** 329 (1914).
3. Baker, J. B., Betty, B. B., and Moore, H. F., "Creep and Fracture Tests on Single Crystals of Lead," *Am. Inst. Min. Metall. Engrs.*, **128,** 118 (1939).
4. Beck, A., "Technology of Magnesium and its Alloys," F. A. Hughes, Ltd., London, 1940.
5. Beckinsale, S. and Waterhouse, H., "Deterioration of Lead Cable Sheathing by Cracking and its Prevention," *J. Inst. Metals*, **39,** 375 (1928).
6. Betty, B. B., "Making and Testing Single Crystals of Lead," *Am. Soc. Testing Materials*, *II*, **35,** 193 (1935).
7. Boas, W. and Schmid, E., "Über die Temperaturabhängigkeit der Kristallplastizität," *Z. f. Phsik.*, **61,** 767 (1930); **64,** 845 (1930); **71,** 703 (1931).
8. Chalmers, B., "Microplasticity of Tin," *Proc. Roy. Soc.*, **156-A,** 427 (1936).
9. Chalmers, B., "Precision Extensometer Measurements on Tin," *J. Inst. Metals,* **61,** 103 (1937).
10. Davis, E. A., "Creep and Relaxation of Oxygen-Free Copper," *J. Applied Mechanics*, **10,** A-101 (1943).
11. Dix, E. H., Jr., "New Developments in High Strength Aluminum Alloy Products," *Trans. Am. Soc. Metals*, **35,** 130 (1945).
12. Elam, C. F., "Distortion of Metal Crystals," Oxford, Clarendon Press, 1935.
13. Flanagen, A. E., Tedsen, L. F., and Dorn, J. E., "Tensile Properties of Aluminum-alloy Sheet at Elevated Temperatures," *Metals Tech.*, T. P. 1929 (Dec., 1945).
14. Flanagen, A. E., Tedsen, L. F., and Dorn, J. E., "Compressive Properties of Aluminum-alloy Sheet at Elevated Temperatures," A.S.T.M. Symposium on Materials for Gas Turbines, p. 161 (June, 1946).
15. Flanagen, A. E., Tedsen, L. F., and Dorn, J. E., "Stress Rupture and Creep Tests on Aluminum-alloy Sheet at Elevated Temperature," *Am. Inst. Min. Metall. Engrs.*, **171,** 213 (1937).

16. Greenwood, J. N. and Worner, H. K., "Types of Creep Curves obtained with Lead and its Dilute Alloys," *J. Inst. Metals*, **64,** 135 (1939).

17. Hanffstengel, K. v. and Hanemann, H., "*Z. Metallkunde*," **30,** Pt. 2, 51 (1938).

18. Hanson, D., "Creep of Metals," *Am. Inst. Min. Metall. Engrs.*, **133,** 15 (1939).

19. Hanson, D. and Wheeler, M. A., "Deformation of Metals under Prolonged Loading, Part I. Flow and Fracture of Aluminum," *J. Inst. Metals*, **45,** 229 (1931).

20. Jackson, L. R., Cross, H. C., and Berry, J. M., "Tensile, Fatigue, and Creep Properties of Forged Aluminum Alloys at Temperatures up to 800° F," Nat. Advisory Com. for Aeronautics, Tech. Note 1469 (March, 1948).

21. Kanter, J. J., "Interpretation and Use of Creep Results," *Trans. Am. Soc. Metals*, **24,** 870 (1936).

22. Leontis, T. E. and Murphy, J. P., "Properties of Cerium Containing Magnesium Alloys at Room and Elevated Temperatures," T. P. 1995, *Metals Tech.* (April, 1946).

23. Leontis, T. E., "Room and Elevated Temperature Properties of Some Sand Cast Mg-base Alloys Containing Zinc," *Metals Tech.*, T. P. 2371, **15** (June, 1948).

24. McKeown, J., "Creep of Lead and Lead Alloys, Part 1. Creep of Virgin Lead," *J. Inst. Metals*, **40,** 201 (1947).

25. Moore, H. F., and Alleman, N. J., "Creep of Lead and Lead Alloys used for Cable Sheathing," Bull. No. 243, Univ. Illinois (1932).

26. Moore, H. F., Betty, B. B., and Dollins, C. W., "Creep and Fracture of Lead and Lead Alloys," Bull. No. 272, Univ. Illinois (Feb., 1935).

27. Moore, H. F., Betty, B. B., and Dollins, C. W., "Investigation of Creep and Fracture of Lead and Lead Alloys for Cable Sheathing," Bull. No. 306, Univ. Illinois (Aug., 1938).

28. Moore, A. A. and McDonald, J. C., "Tensile and Creep Strengths of Some Magnesium-base Alloys at Elevated Temperature," A.S.T.M. Symposium on Materials for Gas Turbines, p. 180 (June, 1946).

29. Nadai, A. and Manjoine, M. J., "High-speed Tension Tests at Elevated Temperatures: Parts II and III," *Am. Soc. Mech. Engrs.*, **63,** A-77 (1941).

30. Phillips, A. J., "Some Creep Tests on Lead and Lead Alloys," *Am. Soc. Testing Materials*, **36,** 170 (1936).

31. Rosenhain, W. and Humphrey, J., "The Crystalline Structure of Iron at High Temperatures," *Proc. Roy. Soc.*, **83,** 200 (1909).

32. Wyman, L. L., "High-temperature Properties of Light Alloys (NA-137). I— Aluminum," OSRD No. 3607, Serial No. M-251, War Metallurgy Div., NDRC (April 15, 1944).

Chapter 11

Scaling

A. SCALE FORMATION

The resistance of metals to surface attack on exposure to elevated temperatures depends largely upon the type of scale formed. The physical properties of the film, such as its adherence to the base metal, its porosity, and its tendency to crack, determine the ability of the metal to withstand surface attack. The type of scale formed depends also upon chemical properties, such as its composition, density, melting and boiling points. On a clean metallic surface exposed to an atmosphere containing oxygen molecules, oxygen forms in layers up to about 0.0002 mm. under conditions which differ from those governing the formation of heavier layers. The rate of formation and the nature of these very thin films will not be considered here.

There are many conditions in film formation which tend to increase the thickness of oxide layers. Films formed on metallic surfaces may volatilize rapidly; they may be porous; they may crack intermittently; or they may increase in thickness by diffusion of metal or oxygen atoms through the layer. All these conditions have been substantiated in scale formation and they may all occur at the same time. Other factors governing the formation of oxides in relation to the base metal on which they form are determined by their heats of formation, their dissociation pressures, their densities relative to the base metal, and the diffusivity of the films formed.

I. Noble Metal Oxides

Noble metals represent a class where the metal base has little affinity for oxygen; the oxide, if formed, is relatively unstable and decomposes on being heated. The dissociation pressures of these oxides are below that of the partial pressure of oxygen in the atmosphere and they decompose when their dissociation pressures approach the partial pressure of oxygen. Silver oxide (Ag_2O) decomposes at 190°C (375°F). Pd oxide dissociates at 800°C (1472°F); Rh oxide dissociates at 1100°C (2012°F).

II. Oxides that Volatilize Readily

The metal Mo remains bright when exposed to a stream of oxygen at high temperature and loses weight continuously. The oxide being formed

is volatile and passes off as a gas leaving fresh metal exposed beneath for further attack. Other metals such as Ir, Ru, and Os form volatile oxides and thus lose weight when heated in air. Pt loses weight on being heated to 1000 to 1200°C. At high temperatures, the oxides of W also volatilize[10].

III. Volume Relations of Scale and Metal

A tough, adherent scale is formed on a metal surface if the specific volume of the scale is equal to or greater than the specific volume of the metal. If the molecular weight of the oxide formed on a metal is M and its density is D, the volume occupied by 1 gm-molecular weight is M/D. For the metal destroyed by this weight of oxide, if its atomic weight is m and its density is d, the volume of 1 gm-atomic weight is m/d. If the volume of the oxide has not changed in relation to the volume of the metal

TABLE 11-1

Metal	Md/mD[10]	Md/mD[2]
Na	0.57	0.57
K	0.41	0.45
Mg	0.79	0.79
Ca	0.64	0.65
Al	1.24	1.28
Be	1.70	1.59
Cu	1.71	1.68
Zn	1.58	1.52
Ni	1.60	1.52
Fe	2.16	1.77

from which it was formed, (M/D divided by m/d equals 1), the film may be considered to cover the surface. But for metals forming less dense oxides ($Md/mD < 1$), the oxide film may be stretched across the metal surface with a tension that results in cracking or crumbling of the film. This argument is not valid for formation of the first layer as pointed out above.

If, on the other hand, the oxide volume is greater than that of the metal from which it was formed ($Md/mD > 1$), then the oxide layer is in compression on the metal surface. This condition also may be a cause of cracking if the compressive strength of the film is low. Table 11-1 shows a list of metal oxides classified as to their relative densities[2, 10].

These values represent data from two different sources, and though they do not agree exactly, the order of the metals is the same. The first four metals listed (Na, K, Mg, and Ca) are characterized by oxides occupying low volumes where $Md/mD < 1$. These metals are very reactive to

oxygen and, moreover, their oxide films are known to be porous, so that oxidation is rapid. On the other hand, although Al is very reactive to oxygen, the value of Md/mD is greater than unity, or about 1.24. The film which forms also has a high compressive strength. These facts can well account for the protective nature of Al oxide. The other metals listed above which have relative densities greater than unity form adherent scales. They are not, however, necessarily considered as oxidation-resistant. In general, this rule of relative densities appears to hold more consistently for the metals with relative densities less than unity[22].

IV. Diffusion through Oxide Films

If impervious films are formed on the heavy metals Cu and Fe, they should protect the surface from further oxidation. Since, however, the scale continues to form on these metals, the theory of diffusion through films is postulated as follows[18, 25]: The radius of the metal cation being smaller than that of the oxygen ion, it is possible that diffusion of the metal cation through the lattice takes place. It is characteristic of both Cu_2O and FeO that they have slightly less metal than the oxide formulas require, which suggests that vacant spaces on the oxide lattice exist through which the metal cation moves. Furthermore, electrons are free to move outward through the film, which tends to prevent an accumulation of an electrical charge. At the surface the electrons can react with oxygen to produce O'' and permit further oxide formation. This phase of the theory is supported in the case of Cu, as observations show that increasing the oxygen pressure in the atmosphere increases the electrical conductivity of the Cu_2O film.

The mechanism of film formation by passage of metal cations outward due to metal deficit in the oxide lattice appears likely for the case of film formation on iron. The Fe ions move outward through the film to the oxide-gas interface and react with the oxygen. The process is compared to an electrolytic cell with its metal-base cathode and gas-atmosphere anode short-circuited by an external resistance, which is the electron conduction through the oxide. The emf of the cell is determined by the free energy of formation of the oxide[22].

Many metals appear to form oxides by this mechanism of metal deficit. A study of the electrical conductivities of metallic oxides shows a close correlation to the protective qualities of film formation. In the case of Al and Be, which have a fixed valency, the oxides Al_2O_3 and BeO have accurate compositions, low electrical conductivities and are highly protective to the metal beneath.

With metals of more than one valency, the higher oxides are likely to be free of metal deficiencies. Fe_2O_3 has more Fe than the formula requires

and Cr_2O_3 has more Cr than is required. This is probably also true of ZnO, as its conductivity decreases as the pressure of oxygen is increased[10]. The more refractory or higher melting oxides have lower electrical conductivities and have lower scaling rates. They are therefore more suitable for alloying with other metals for oxidation resistance.

V. Weak Films and Susceptibility to Cracking

Many oxide films may fail to protect the metal beneath due to mechanical weakness. It is known that both ZnO and Fe_2O_3 are not hard and they may be weak as well. Any film of sufficient thickness may crack and permit oxygen to penetrate to the metal. Such a mechanism may be the primary cause of oxidation rather than metal deficit in the oxide lattice.

VI. Multiple Oxidation Films

Certain metals have more than one oxide in the films built up under oxidizing conditions. Cu forms an inner layer of Cu_2O, and an outer layer of CuO. If the oxygen is reduced sufficiently in the atmosphere, the CuO layer does not form[10].

The temper colors formed on iron at relatively low temperatures are produced by interference films of Fe_2O_3 which lie directly on the metallic base. As the temperature of the metal is raised, magnetite (Fe_3O_4) forms as an inner layer beneath the Fe_2O_3. This condition persists up to about 575°C. In this temperature range an inner layer of FeO forms which is stable above 575°C. The electrical conductivity of the FeO layer is the highest of the three, which suggests that the thickness of the layers and the diffusivity of the iron ion in each phase are related. At 1022°F (550°C), the relative thickness of the layers is[22]:

Layer	Thickness %
FeO	85–90
Fe_3O_4	10–15
Fe_2O_3	0.5–2

If scale is removed mechanically from iron, it can be separated into the following layers:

(a) An inner layer consisting of FeO, where the inner side is next to the adsorbed oxygen layer and the outer side of the FeO is the original surface of the iron.

(b) A middle layer consisting of FeO, where the inner side is the original surface of the iron and the outerside is next to the Fe_3O_4.

(c) An outer layer consisting of Fe_3O_4 and Fe_2O_3.

The composition of each of the three oxides of Fe is not exactly that required by the chemical formulas. All three oxides show a deficit in Fe content which is higher at the inner layer. At 1832°F (1000°C), the Fe contents of the oxide layers at equilibrium are[24]:

	Outer Interface	Inner Interface	Theoretical (%)	
Outer layer	....	70.3	Fe_2O_3	69.9
Middle layer	72.35	72.6	Fe_3O_4	72.35
Inner layer	75.6	76.9	FeO	77.75

The innermost portion of the scale on Fe becomes porous after a short time. This fact suggests that if the Fe ion moves outward at a rate faster than the rate of oxidation of the Fe core, porosity of the inner side of the film is to be expected.

VII. Effect of Time on Scaling of Metals

The incidence of cracks in films on metals during oxidation at high temperature changes markedly the rate of film formation. Intermittent cracking also occurs in a number of metals such as Cu and Al. Experimental observations show that at constant temperature oxide films form on metals at rates which vary in three ways expressed by (1) a linear relation, (2) a logarithmic relation, and (3) a parabolic relation[10]. If y is the thickness of the film and t is the time required for its formation, then at constant temperature:

$$\text{Linear} \qquad y = k_1 t + k_2 \qquad (1)$$
$$\text{Logarithmic} \qquad y = k_3 \log (k_4 t + k_5) \qquad (2)$$
$$\text{Parabolic} \qquad y^2 = k_6 t + k_7 \qquad (3)$$

At constant temperature, the metal Ca oxidizes at a constant rate expressed by a linear function with time. This can be explained on the basis that cracks form in the film readily and expose fresh metal to the action of the atmosphere. In metals where this relation holds, the film offers no protection against oxidation.

The increase of film thickness with time is varied for any metal by many factors. At lower temperatures, when films are thinner, the effect of flaws or cracks is more important and the formation of the film is likely to proceed logarithmically with time. As the temperature is raised and film thicknesses increase, the metal may change its response to time, and the film thickness may increase as a parabolic function. This is the characteristic relation by which film thickness increases for many metals expressed by $x^2 = kt$, where x is the weight or thickness of the metal consumed in scale

formation, t the time and k the rate constant. The formation of any film which is permeable, whether due to movement of metal out or oxygen inward, or both, leads to the expression of a parabolic function. Ni, W, and Cu at ordinary pressures form oxides for a wide range of temperatures at rates which are parabolic functions. In the case of Fe, calculations of the constant k from values of the conductivities of the oxide and the relative mobilities of the positive and negative ions agree with experimentally determined values[14].

VIII. Effect of Temperature on Film Formation

The increase in rate of film formation with increase in temperature is expressed by an exponential function which is characteristic of diffusion processes. To move through a film, a particle requires a certain critical energy, E, which is proportional to $e^{-E/RT}$, or the energy for the diffusing particle to jump from one position of low potential energy to the next. The general expression for variations in the rate of film formation with temperature, or the rate constant k is

$$k = Ae^{-Q/RT}$$

A and Q are constants, R is the gas constant, and T the absolute temperature. In this formula, a straight-line relation exists for log k plotted against $1/T$, which is consistent for experimental observations in the examples of Cu and brass. Plotting log k against $1/T$ for Fe results in two straight lines which intersect at about 930°C due to the transformation of alpha to gamma Fe[27].

B. Measurement of Scale Formation

I. Microscopic Examination

A qualitative examination of the process of oxidation in many metals is frequently visible under a microscope. Scale formation may proceed along grain boundaries at first and the oxides diffuse later through the grain itself. In the case of Fe, intergranular attack is readily observed and is often associated with lowered ductility of the material in service. The decrease in C in carburized layers due to oxidation may also be observed under a microscope.

II. Changes in Weight

The decrease in weight of a specimen after removal of the scale is a means of measuring scale formation. The difficulties here are that removal of all the scale may not be complete, especially in the case where diffusion of the oxygen into the base metal has occurred. It is useful in evaluating pickling methods or in ascertaining damage to the surface finish.

The increase in weight of a specimen during oxidation is an extremely useful method of measuring scale formation. It is usually carried out at constant temperature for specified periods of time. For films that are liable to spalling, a means for collecting the non-adherent scale is required and the non-adherent scale weighed. For films that volatilize at higher temperatures, this method is useless.

III. Tests on Wires

Wires designed for electrical heating units may be tested by determining the period for burning out at a specified temperature[4]. Alternate heating and cooling of a wire dipping into a pool of Hg is established as a severe life test for intermittent heating by an electrical current with a cycle of 2 mins off and 2 mins on. Such a test uses a 12-inch long sample of wire of No. 20 or No. 22 gage (A.S.T.M. B76-39). The temperature may be adjusted to 1120 to 1170°C (2050 to 2150°F) as measured by an optical pyrometer[2]. Such a test is valuable in determining the life of the alloy under the specific conditions of the test for comparative purposes only.

C. Composition of Scale Formed on Alloys

The composition of the scale formed on a metallic surface may bear little relation to the amount of the element present in the base metal. The determining factor is the activity of the alloying element to oxygen compared to that of the base metal with oxygen. If the activity of the alloying element is greater than that of the base metal, its oxide appears in the scale and may be present in very large percentages. If the activity of the element with oxygen is less than that of the base metal, the oxide of the alloying element may appear in segregated areas.

This situation is exemplified in the case of elements added to Fe to form alloy steels. Elements which form refractory oxides and have greater affinity for oxygen, as Cr, Si, and Al, appear in the inner layer as the refractory oxide or as a double oxide with FeO[22]. As scaling progresses these elements may build up concentrations four times that represented in the composition of the steel base. In the outer oxide layers, the concentration of the added element decreases and may be as low as 10 per cent of its composition in the steel. With highly alloyed steels, the oxide layers may consist almost entirely of the refractory oxide. This condition tends toward low diffusion rates in the film and results in a highly protective layer.

Elements which are less reactive to oxygen than Fe, such as Ni, appear in the inner oxide layer but in patches or segregated areas and provide little protection. A 5 per cent Ni steel contains particles in the scale which may have a Ni content of 30 per cent.

Grain boundaries often play an important role in determining the extent of attack on a metal as oxygen diffuses into the base metal by these channels.

Certain metals as Ni, Co, and Mo increase the solubility of oxygen in Fe and the penetration of oxygen is thereby enhanced, especially along grain boundaries. Such increased solubilities may lead to surface cracking of the metal during hot-working or cracking during pickling.

The composition of scale being formed on a metal surface should not result in the appearance of a eutectic which has a lower melting point. As an example, the addition of 0.04 per cent B to a 30 per cent Cr steel destroys its resistance to scaling at 2200°F (1200°C)[12]. Steels with more than 5 per cent Si are readily attacked above 2200°F because of the formation of $FeO-SiO_2$ eutectic melting at 2250°F (1240°C).

In protecting Cu from oxidation, it is important that a film should be formed wholly of the oxide of the alloying constituent and that no CuO exist in the protective layer. Such additions as Al, Be, and Mg offer some

TABLE 11-2. *INCREASE IN WEIGHT FROM 4 HRS AT 800° C IN DRY OXYGEN

Material	Mg/Dm^2	Type of Scale
Pure Cu	1624	Black oxide, freely scaling
Cu + 5% Al (not treated)	15.6	Tenacious black oxide
Cu + 5% Al (treated in H)	3.1	No visible oxidation

* Milligrams per square decimeter.

resistance to the oxidation of Cu[11]. The best protection is obtained if a means is devised to form a thin film of alumina or beryllia free from CuO. With an alloy of Cu containing 5 per cent Al, heating the sample at 800°C for 15 minutes in pure hydrogen which contains water vapor forms a thin film of alumina on the surface of the Cu alloy[26]. This procedure gives excellent oxidation resistance as shown in Table 11-2.

The pure Cu forms a heavy scale after 4 hours at 800°C in dry oxygen. The Cu with 5 per cent Al has an adherent scale with a smaller increase in weight. The same alloy pretreated to form an alumina film shows no visible oxidation under the same heating conditions.

I. Properties of a Good Scale

The properties required for a protective scale on a metallic surface may be summed up as follows[10]:

Good adhesion
Sufficient elasticity
No volume change from that of the base metal
Low electrical conductivity
High melting and boiling points
No eutectic formation
Small permeability for metal or oxygen
Sufficient alloy constituent to maintain proper alloy content of the scale

D. Effect of Various Elements in Oxidation Resistance of Fe

The element Cr is the single most effective one in increasing oxidation resistance of Fe at high temperatures. Amounts as low as 2 per cent Cr show a perceptible corrosion resistance over plain-C steels. In Fig. 11-1, the effect of increasing Cr content on Cr-Fe alloys is shown in various atmospheres of H₂S and oils at elevated temperatures. The penetration of the film is seen in the chart to decrease with increase in Cr content.
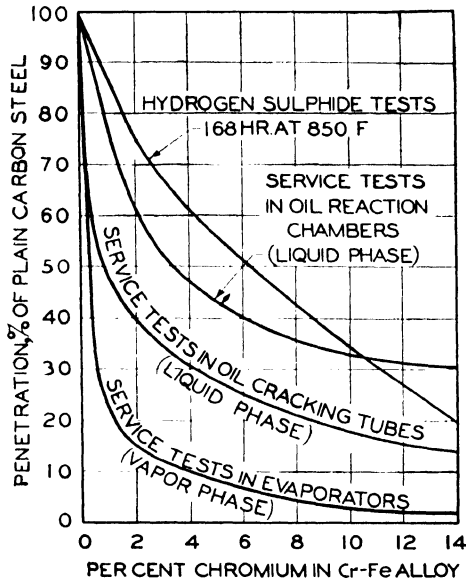
(Courtesy Babcock and Wilcox Tube Company)

Fig. 11-1. The effect of chromium on corrosion of Cr-Fe alloys

The maximum temperature for the effective protection of a series of alloy steels with varying amounts of Cr is shown in Table 11-3[2]. These values indicate only that excessive scaling will not occur at these temperatures in the unstressed condition.

E. Effect of Atmospheres

I. Oxidation in Air

A comparison of scaling of any metal or alloy under different conditions leads to many inaccuracies, as slight changes in impurities in the metal or in the atmosphere, or rate and time of heating may lead to very different values. Any attempt to indicate the temperature range for stability of various metals and alloys is for the purpose of comparison only. Exact duplication of the experimental conditions is required for checking results. On this basis, the temperature for stability of some common metals in air

is suggested in Table 11-3A for a loss in weight from scaling less than 0.0002 to 0.0004 gm per sq cm per hr[17].

TABLE 11-3. TEMPERATURE RANGE FOR SATISFACTORY
OPERATION WITHOUT EXCESSIVE SCALING*

Material		Max Temp in Oxidizing Atmosphere	
		(°F)	(°C)
501	5Cr-Mo	1150	621
	7Cr-Mo	1200	648
	9Cr-Mo	1250	676
403, 410	12Cr	1300	704
430	17Cr	1550	843
442	21Cr	1750	954
446	27Cr	2000	1093
302, 304	18-8	1650	899
302B	18-8 Si	1800	982
309	24-12	2000	1093
310	25-20	2100	1149
316	18-8 Mo	1650	899
321	18-8 Ti	1650	899
347	18-8 Cb	1650	899

* Compiled by Subcommittee on Wrought Heat Resisting Alloys.[2]

TABLE 11-3A. STABILITY OF METALS IN AIR*

Material	Max Temp for Stability	
	°C	°F
Cu	450	842
Fe	500	932
Brass (70Cu, 30Zn)	700	1292
Ni	800	1472
Cr	900	1652

* Loss in weight from scaling less than 0.0002 to 0.0004 gm per sq cm per hr.[17]

II. Gaseous Atmospheres

The effects of gas atmospheres at elevated temperature on scale formations depend on such factors as pressure, velocity of flow, composition, and oxidizing or reducing conditions. No attempt is made here to cover this problem rigorously as the actual test conditions must be duplicated for check results and slight changes in impurities, or heating and cooling cycles, cause great differences in film formation. A few general conditions outlining the factors involved are suggested below.

a. Composition of Gas. The following gases oxidize steels at increasing rates in the order named: CO_2, dry air, oxygen, and steam. The stability of steel in steam at 925°F (500°C) is equivalent to air at 1200°F (650°C). At higher temperatures for exposure of steel, steam at 1750°F (950°C) is equivalent to air at 2200°F (1200°C)[22].

The effect of S in the atmosphere is especially injurious. Ni and its alloys are embrittled in its presence. For some metals, S compounds in the atmosphere change the rate of film formation from a parabolic to a linear relation and the scale becomes completely pervious to penetration[10].

The oxidation of steel is doubled by the addition to an atmosphere of air of 5 per cent CO_2 and 5 per cent H_2O, and is trebled by the addition of 5 per cent SO_2 and 5 per cent H_2O[15].

For an 18-8 steel the oxidation rate is increased, 7 times by 5 per cent H_2O added to the atmosphere, 8 times by 5 per cent SO_2 plus 5 per cent H_2O, and 10 times by 5 per cent CO_2 plus 5 per cent H_2O[22].

b. Velocity of Gas. The rate at which gas flows does not change the rate of scale formation at lower temperatures particularly if the early stages of film formation have occurred. However, at higher temperatures this factor may play a very important part in the life of the material[10].

III. Stress-Rupture Tests in Steam

In power plant installations, increases in steam pressures and temperatures give rise to more exacting conditions for materials used in this type of service. A reasonable appraisal of the life of materials in steam is difficult since most of the high temperature testing is conducted in air.

Stress-rupture tests and the thickness of the scale formed in steam at 1200°F (650°C) are shown for a series of alloy steels. The steam pressures are varied to produce both laminar and turbulent flow. The steels ranging in composition from plain C, low alloy, to stainless steel are shown with their various heat treating procedures in Table 11-4[1].

The rupture strength for the series of steels after 10 hours and 1000 hours and extrapolated values for 10,000 hours are shown in Table 11-5, arranged in the order of decreasing magnitude for each test period. For the 1000-hour test period, 18-8 steel has the highest value, followed by 12Cr steel and 25-20Cr steel.

In a comparison of tests for rupture strength in air at 650°C for the same periods, values are taken from current literature for extrapolations in 10,000 hours[22]. In all cases, the rupture strength in steam is as great or greater than that in air as indicated in Table 11-6. The low-C steel and the 12Cr steel have ratios of more than 3 for the strength in steam over air. Such comparisons must of course be viewed as comparative especially since they represent extrapolated values on the time axis.

The tests in steam appear generally comparable to tests conducted in air at 650°C in that log-log relationships of stress versus time produce straight lines with no deterioration of the material due to the atmosphere of steam[1].

No difference in the effect of turbulence versus laminar flow of steam is seen either in relation to rupture strength or scale formation.   In these

TABLE 11-4[1]

Chemical Analysis

Type	Steel No.	C	Mn	P	S	Si	Mo	Cr	Ni	Ti
Low-C	1	0.16	0.47	0.084	0.023	0.20	....	....	....	....
C-Mo	2	.20	.53	.01	.016	.24	0.50	....	....	....
2.25Cr-1Mo	3	.16	.39	.03	.03	.33	.90	2.24	....	....
5Cr-Mo-Si	4	.10	.38	.03	.03	1.55	.51	4.83	....	....
9Cr-Mo-Si	5	.12	.44	.03	.03	.67	.95	9.5	....	....
12Cr	6	.11	.41	.014	.013	.286	....	12.66	0.385	....
25-20	7	.11	.58	.03	.03	.75	...	23.6	20.65	....
18-8	8	.06	.50	.03	.03	.61	....	17.75	9.25	....
5Cr-Mo-Ti	9	.10	.44	.03	.03	.38	.50	4.98	....	0.51

Heat Treatment

Type	Steel No.	Heat Treatment
Low-C	1	Air-cooled from 1650°F (900°C)
C-Mo	2	Normalized, tempered 1202°F (650°C)
2.25Cr-1Mo	3	Annealed 1550°F (843°C)
5Cr-Mo-Si	4	Annealed 1550°F (843°C)
9Cr-Mo-Si	5	Oil-quenched 1742°F (950°C), tempered 1500°F (815°C)
12Cr	6	Air-cooled from 1166°F (630°C)
25-20	7	Normalized at 1700°F (926°C)
18-8	8	Water-quenched from 2000°F (1093°C)
5Cr-Mo-Ti	9	Annealed 1650°F (900°C)

tests the depth of scale is measured by mounting for metallographic examination under a microscope.   The scaling characteristics follow a normal pattern in that the plain-C steel has excessive scaling and the higher alloys have reduced scaling.

As regards the thickness or the depth of corrosion, the Cr content appears to be the determining factor, as previously observed by many investigators. The steels fall generally into four classes on the basis of the type of scale formed.   The plain-C and C-Mo steels have a thick, porous, and tightly adhering scale and are the most severely corroded.   The next most corroded steels having a brittle, flaky scale are the 2.25Cr-1Mo, the 5Cr-Mo-Si, and the 5Cr-Mo-Ti compositions.   The third class of steels with only a

small amount of corrosion are the 9Cr-Mo-Si and the 12Cr steels. In the fourth class are the 18-8 and the 25-20 alloys where the corrosion is very slight. All scaling tests are reported on the basis of depth of scale due to the fact that the samples are small and their shape is not suitable for electrolytic stripping tests to show depth of penetration.

TABLE 11-5. STRESS REQUIRED TO CAUSE RUPTURE OF
VARIOUS STEELS AT 650°C (1200°F)[1]

Steel No.	Type	In 10 hrs	Steel No.	Type	In 1000 hrs	Steel No.	Type	In 10,000 hrs*
8	18-8	35,000	8	18-8	16,800	8	18-8	11,600
7	25-20	25,000	6	12Cr	12,000	6	12Cr	9400
2	C-Mo	21,500	7	25-20	11,200	7	25-20	7550
6	12Cr	19,500	3	2.25Cr-1Mo	9400	3	2.25Cr-1Mo	7000
3	2.25Cr-1Mo	17,000	2	C-Mo	8600	5	9Cr-Mo-Si	6800
4	5Cr-Mo-Si	15,500	5	9Cr-Mo-Si	8500	2	C-Mo	5450
1	Low-C	13,500	4	5Cr-Mo-Si	7600	4	5Cr-Mo-Si	5300
5	9Cr-Mo-Si	13,200	1	Low carbon	6900	9	5Cr-Mo-Ti	5000
9	5Cr-Mo-Ti	11,500	9	5Cr-Mo-Ti	6700	1	Low-C	4900

* Extrapolated.

TABLE 11-6. RATIO OF STRESS IN STEAM AND STRESS IN AIR REQUIRED FOR RUPTURE
IN 10,000 HOURS OF VARIOUS ALLOYS AT 650°C (1200°F)[1]

Type of Steel	Ratio of Stresses in Steam to Air
Low-C	3.6
12Cr	3.2
C-Mo	1.8
25-20	1.4
5Cr-Mo-Si	1.2
18-8	1.2
2.25Cr-1Mo	1.2
9Cr-Mo-Si	1.1
5Cr-Mo-Ti	0.98

In the plain C and C-Mo steels, graphitization may occur in heating periods of less than 1000 hours at temperatures considerably lower than that represented by these tests, especially if the steel is abnormal. No evidence of graphitization appears in these tests conducted in steam[1].

F. SCALING OF Ni-Cr-Fe ALLOYS

Since the basis of many heat-resistant alloys is dependent upon the Ni-Cr-Fe system, the scale formation from heating in air as influenced by composition is presented here in some detail.

The effect of Ni and Cr on a series of Ni-Cr-Fe alloys in relation to resistance to scaling is shown by weight losses of samples maintained for stipulated periods of time at temperatures between 1600°F (870°C) and 2200°F (1200°C)[6]. The alloys are melted in a basic lined induction furnace, and sand cast into wedges 1 in thick at the bottom, 2⅜ inches thick at the top, 6 inches wide, and 8 inches high. The test samples are machined from areas 1 to 3 inches from the bottom into sizes 0.375 inch diameter by 1.000 inch long with a ground finish.

The corrosive atmosphere consists of air saturated with water vapor at 90°F (32°C) preheated to furnace temperature before its introduction into the furnace at 200 cu cm per min. Temperature fluctuations are maintained at ±10°F. The samples are placed on refractory blocks within the furnace and held for 100-hour and 1000-hour periods.

At the conclusion of the test, the specimens are removed from the furnace and treated as follows:

(a) Cathodically descaled in a molten caustic salt bath (60 per cent NaOH, 40 per cent Na_2CO_3) with a current density of 400 amps per sq ft maintained for 1 to 4 mins, then water-quenched.

(b) To remove the caustic, samples are dipped in concentrated HCl (saturated with arsenic trioxide, As_2O_3) and finally washed.

I. Corrosion Tests of 100 Hours

The composition of a series of Ni-Cr-Fe alloys and their loss in weight are recorded in Table 11-7 for 100 hours' exposure at 1600°F (870°C), 1800°F (980°C), 2000°F (1090°C), and 2200°F (1200°C). The alloys consist of a plain-C steel and two steels with 4 to 6 per cent Cr. These are compared to a series of steels containing 11 per cent Cr with Ni varying up to 70 per cent and to a series of 16, 21, 26, 31, and 36 per cent Cr, all with Ni varying over a wide range. The weight loss of gm per sq in per day from these 100-hour tests is plotted on a logarithmic scale against the per cent Ni on a linear scale at the various levels of Cr and for the four test temperatures as shown in Figs. 11-2 and 11-3. The curves indicate the influence of Ni on scaling of the various alloys by an arbitrary value of 0.05 gm per sq in per day metal loss. If scaling is above this amount, it is indicated as excessive and below this figure as satisfactory[6].

a. Effect of Ni. *1. 11 per cent Cr.* At this level of Cr, additions of Ni from zero to 20 per cent have little influence in the prevention of excessive scaling. The most effective range is 20 to 50 per cent Ni.

2. 16 per cent Cr. The most effective addition is in the range of zero to 40 per cent Ni for scaling resistance.

3. 21 per cent Cr. This series of alloys has a marked resistance to scaling due to the high Cr content. The effect of Ni is therefore less pronounced

TABLE 11-7. SUMMARY OF METAL-LOSS DATA OF Fe-Ni-Cr ALLOYS BY AIR CORROSION AT 1600°F (870°C), 1800°F (980°C), 2000°F (1090°C), AND 2200°F (1200°C)[6]

| Alloy No. | Composition of Alloys, per cent | | | | | | Metal Loss by Corrosion | | | | | | | |
| | Carbon | Nickel | Chromium | Silicon | Manganese | Nitrogen | Grams per sq. in. per day | | | | Inches Penetration per year | | | |
							1600 F.	1800 F.	2000 F.	2200 F.	1600 F.	1800 F.	2000 F.	2200 F.
							Zero per cent Cr alloy							
C-99	0.85	0	0	0.2	0.4	…	0.4799	1.267	2.28	…	1.34	3.55	6.38	…
							5 per cent Cr alloys							
CA-11b	0.19	0	6.00	0.48	0.66	…	0.4451	0.7552	…	…	1.25	2.12	…	…
CA-12b	.19	0	4.71	.34	.68	…	.5197	.7189	…	…	1.54	2.01	…	…
							11 per cent Cr alloys							
C-70	0.45	0.13	11.0	1.31	0.78	0.05	0.2291	0.4552	1.0380	…	0.641	1.27	2.91	…
C-71	.45	3.0	10.9	1.30	.76	0.05	.1843	.3315	1.3982	2.3795	.516	0.928	3.92	6.67
C-72	.45	8.3	11.0	1.28	.75	0.06	.1511	.3441	0.9263	…	.423	.963	2.59	…
C-73	.45	12.1	11.0	1.22	.78	0.05	.14	.2873	.7577	…	.39	.804	2.12	…
C-74	.40	16.1	11.0	1.20	.72	0.05	.1593	.2857	.7512	2.2344	.449	.800	2.10	6.31
C-1	.34	20.13	11.21	1.21	.76	0.046	.0925[a]	.3055	…	…	.259[a]	.855	…	…
C-2	.34	23.66	11.01	1.21	.76	0.046	.0612[a]	…	.5680	…	.171[a]	.566	1.59	…
C-3	.33	27.37	10.84	1.21	.76	0.046	.0522[a]	.0897	.62	…	.146[a]	.251	1.74	…
C-4	.35	31.84	11.12	1.28	.82	0.035	.0245[a]	.0262	.4303[a]	…	.069[a]	.073	1.20[a]	…
C-5	.35	35.57	11.06	1.28	.82	0.035	.0030	…	.3033[a]	0.3564	.008	…	0.849[a]	0.998
C-6	.39	39.31	10.77	1.28	.82	0.035	.0028[a]	.0047[a]	.1081[a]	…	.008[a]	.013	.303[a]	…
C-7	.31	47.34	11.09	1.28	.84	0.022	.0014	…	.0415[a]	…	.004	…	.116[a]	…
C-8	.37	55.09	11.21	1.28	.84	0.022	.0014[a]	.0032	.0191	0.0275	.004[a]	.009	.053	0.077
C-9	.32	63.03	10.98	1.36	.90	0.008	.0013[a]	.0025	.0103[a]	0.0224	.004[a]	.007	.029[a]	0.063
C-10	.37	69.07	10.87	1.36	.90	0.008	.0011[a]	.0027	.0088[a]	…	.003[a]	.008	.025[a]	…

TABLE 11-7. *Continued*

Alloy	Composition of Alloys, per cent						Metal Loss by Corrosion							
							Grams per sq. in. per day				Inches Penetration per year			
	Carbon	Nickel	Chromium	Silicon	Manganese	Nitrogen	1600 F.	1800 F.	2000 F.	2200 F.	1600 F.	1800 F.	2000 F.	2200 F.
16 per cent Cr alloys														
C-75	0.47	0.11	16.0	1.26	0.78	0.03	(0.0059)	(0.1238)	0.7610	...	(0.017)	(0.347)	2.13	...
C-76	.43	3.0	16.1	1.23	.75	0.04	.0281	.2360	.7020	...	.079	.661	1.97	...
C-77	.45	8.2	15.7	1.20	.75	0.06	.0180	.1783	.9374	...	.050	.499	2.63	...
C-78	.46	12.0	15.8	1.22	.77	0.06	.0022	.0793	.5216	...	.006	.222	1.46	...
C-79	.44	16.2	15.8	1.18	.69	0.06	.0022	.0497	.3031	...	.006	.139	0.849	...
C-11	.47	20.00	16.17	1.16	.80	0.050	.0014a	.0194	.1406a	...	.004a	.054	.394a	...
C-12	.48	24.10	16.02	1.16	.80	0.050	.0012a	.0195	.0359a	...	.003a	.055	.101a	...
C-13	.50	27.55	16.25	1.16	.80	0.050	.0016a	.0076	.0803a	...	.004a	.021	.225a	...
C-14	.45	32.20	15.98	1.24	.80	0.075	.0015a	.0087	.0705a	0.0916	.004a	.024	.197a	0.256
C-15	.45	36.43	15.98	1.24	.80	0.075	.0015a	.0036	.0287a	.0615	.004a	.010	.080a	.172
C-16	.46	40.34	15.98	1.24	.80	0.075	.0015a	.0040	.0118a	.0353	.004a	.011	.033a	.099
C-17	.40	47.95	15.73	1.25	.84	0.057	.0017a	.0037	.0162a	.0290	.005a	.010	.045a	.081
C-18	.40	56.07	15.86	1.25	.84	0.057	.0014a	.0034	.0140a	.0249	.004a	.010	.039a	.070
C-19	.39	60.95	15.73	1.24	.84	0.032	.0012a	.0028	.0077a	...	.004a	.008	.022a	...
C-20	.42	68.13	15.90	1.24	.84	0.032	.0011a	.0026	.0130a	...	.003a	.007	.036a	...
21 per cent Cr alloys														
C-80	0.44	0.14	20.8	1.31	0.78	0.05	0.0026	(0.0052)	0.0348	0.1210	0.007	(0.015)	0.097	0.339
C-81	.43	3.0	21.0	1.28	.73	0.03	.0040a	.0292	.0347	.0544a	.011a	.082	.097	.152a
C-82	.45	8.2	21.1	1.25	.75	0.07	.0019	.0259	.0333	.0295a	.005	.073	.093	.083a
C-83	.47	12.1	20.8	1.23	.76	0.06	.0015	.0144	.0274	.0218a	.004	.040	.077	.061a
C-84	.44	16.3	20.7	1.18	.73	0.06	.0021	.0049	.0285	.0187a	.006	.014	.080	.052a
C-31	.46	19.95	20.96	0.76	.73	0.058	.0035a	.0055a	.0182	...	.010a	.015a	.051	...
C-32	.46	24.08	20.92	0.76	.73	0.058	.0026a	.0054a	.0163	.0672	.007a	.015a	.046	.188
C-33	.47	28.34	20.85	0.76	.73	0.058	.0020	.0052	.0128	.0576	.006	.015	.036	.161
C-34	.47	32.32	20.92	1.21	.77	0.072	.0023	.0040	.0109	.0719a	.006	.011	.031	.201a
C-35	.47	36.02	21.03	1.31	.77	0.064	.0016	.0036	.0136	.0502	.004	.010	.038	.141

TABLE 11-7. *Continued*

21 per cent Cr alloys. *Continued*

C-36	.46	40.08	20.98	1.29	.76	0.064	.0041a	.0033	.0144	.0468a	.011a	.009	.040	.131a
C-37	.46	47.90	21.00	1.27	.77	0.080	.0019a	.0032	.0101a	.0274a	.005a	.009	.028a	.077a
C-38	.45	55.92	20.77	1.35	.81	0.067	.0014	.0035	.0111	.0301	.004	.010	.031	.084
C-39	.45	61.84	21.22	1.17	.78	0.054	.0023	.0032	.0103	.0206	.006	.009	.029	.058

26 per cent Cr alloys

C-85	0.45	0.16	25.8	1.34	0.78	0.04	0.0035a	0.0204	0.0353	0.1135a	0.010a	0.057	0.099	0.318a
C-86	.43	3.0	25.9	1.32	.73	0.03	.0029	.0262	.0418	.0598a	.008	.073	.117	.167a
C-87	.45	8.2	25.8	1.30	.75	0.07	.0024	.0084	.0320	.0215a	.007	.024	.090	.060a
C-88	.47	12.1	25.6	1.23	.77	0.05	.0013	.0061	.0190	.0198a	.004	.017	.053	.055a
C-89	.45	16.0	25.8	1.15	.74	0.06	.0014	.0036	.0115	.0188a	.004	.010	.032	.053a
C-41	.46	20.12	25.47	1.12	.68	0.046	.0026a	.0058a	.0117	.0183	.007a	.016a	.033	.051
C-42	.47	23.48	26.00	1.23	.73	0.126	.0037a	.0038	.0166a	.0594a	.010a	.011	.046a	.166a
C-43	.47	27.40	25.78	1.22	.75	0.139	(.0101)	.0042	.0133	.0521	(.028)	.012	.037	.146
C-44	.45	31.80	25.64	1.22	.72	0.074	.0042	.0051a	.0129	.0658	.012	.014a	.036	.184
C-45	.49	35.94	25.92	1.22	.74	0.093		.0047	.0137	.0303		.013	.038	.085
C-46	.45	40.15	26.08	1.24	.74	0.087	.0043	.0041a	.0115	.0254	.012	.011a	.032	.071
C-47	.49	48.04	25.93	1.17	.77	0.083	.0025a	.0045a	.0120a	.0256	.007a	.013a	.034a	.072
C-48	.42	55.82	25.94	1.27	.73	0.079	.0031	.0029	.0113	.0208	.009	.008	.032	.058

31 per cent Cr alloys

C-90	0.47	0.20	30.9	1.30	0.77	0.05	0.0042	0.0186	0.0100	0.0379	0.012	0.052	0.028	0.106
C-91	.44	3.0	30.9	1.22	.72	0.04	.0037a	.0126	.0139	.0493	.010a	.035	.039	.138
C-92	.43	8.2	31.0	1.28	.77	0.07	.0017	.0043	.0061	.0471	.005	.012	.017	.132
C-93	.44	12.1	30.8	1.24	.77	0.06	.0026	.0038	.0104	.0337	.007	.011	.029	.094
C-94	.46	15.9	30.8	1.19	.73	0.06	.0027	.0037	.0257	....	.008	.010	.072	....
C-51	.43	20.12	30.71	1.12	.73	0.062	.0063a	.0092	.0142	.0388	.018a	.026	.040	.109
C-52	.44	23.81	30.98	1.13	.72	0.058	.0050a	.0126	.0120a	.0474	.014a	.035	.034a	.133
C-53	.43	27.44	31.09	1.17	.73	0.057	.0076a	.0100	.0219	.0259	.021a	.028	.061	.073
C-54	.44	31.28	30.79	1.19	.73	0.083	.0081	.0098	.0131	.0285	.023	.027	.037	.080
C-55	.43	36.42	30.35	1.10	.71	0.081	.0046a	.0080	....	.0305	.013a	.022	....	.085
C-56	.48	40.25	30.68	1.18	.70	0.114	.0040a	.0080	.0183a	.0184	.011a	.022	.051a	.052
C-57	.44	48.35	30.62	1.25	.67	0.093	.0081	.0083	.0221	.0199	.023	.023	.062	.056

TABLE 11-7. *Continued*

Alloy No.	Composition of Alloys, per cent						Metal Loss by Corrosion							
							Grams per sq. in per day				Inches Penetration per year			
	Carbon	Nickel	Chromium	Silicon	Manganese	Nitrogen	1600 F.	1800 F.	2000 F.	2200 F.	1600 F.	1800 F.	2000 F.	2200 F.
36 per cent Cr alloys														
C-64	0.45	31.85	35.50	1.15	0.68	0.079	0.0139	0.0110	0.0152[a]	0.0377	0.039	0.031	0.043[a]	0.106
C-65	.45	36.18	35.40	1.26	.69	0.114	.0072	.0082	.0299	.0391	.020	.023	.084	.109
C-66	.45	39.80	35.68	1.29	.70	0.091	.0067[a]	.0095	.0121	.....	.019[a]	.027	.034	.....
Control specimens														
C-22 HT	0.48	35.50	16.15	1.33	0.80	0.069	0.0021	0.0056	0.0156[a]	0.0485[a]	0.006	0.016	0.044[a]	0.136[a]
C-21 HH	.33	11.45	26.01	0.56	.49	0.122	.0050	.0096[a]	.0181[a]	.0191	.014	.027[a]	.051[a]	.053
C-26 HH	.44	11.58	26.20	1.28	.68	0.073	.0011	.0143	.0130	.0155[a]	.003	.040	.036	.043[a]

[a] Averages of two or more tests.

[b] Alloys CA-11 and CA-12 also contain 0.56 per cent molybdenum.
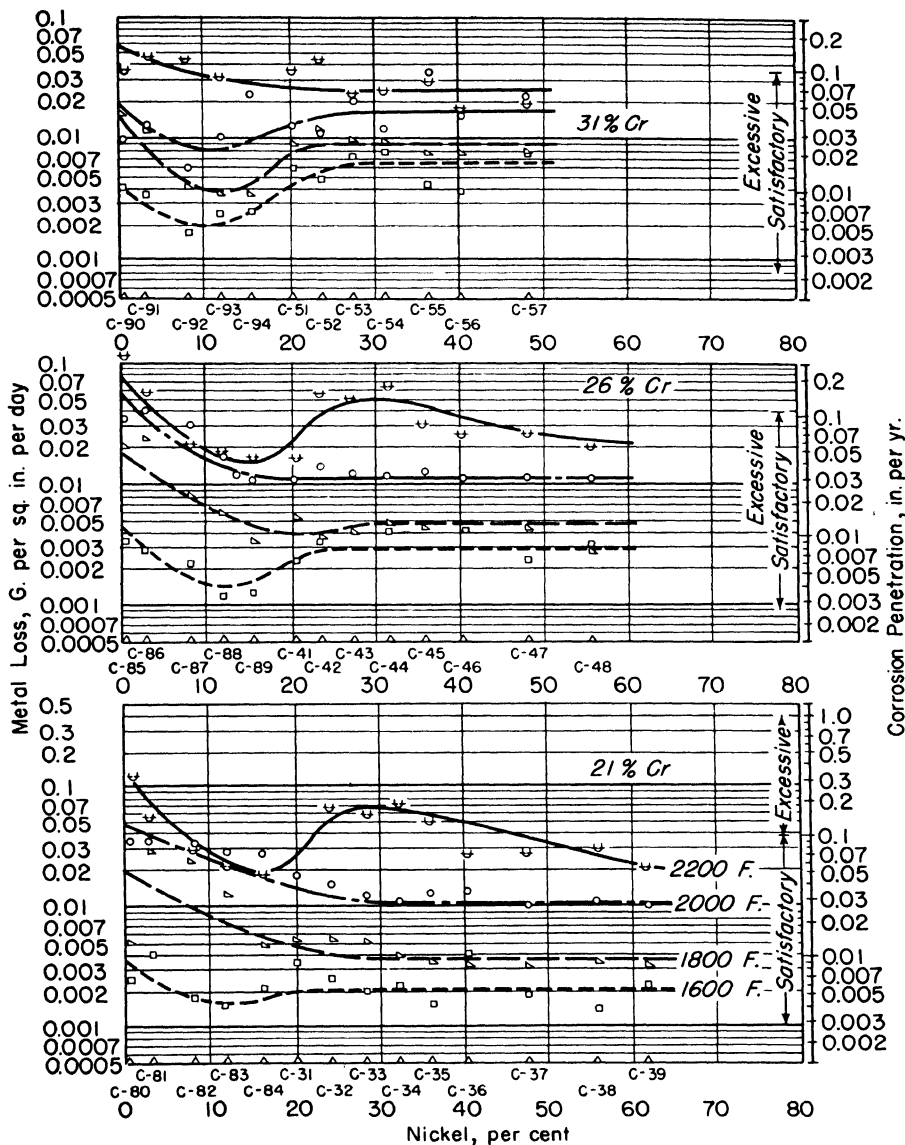
Fig. 11-2. Influence of increasing amounts of Ni at the 11 and 16 per cent Cr levels on air corrosion of alloys at 1600°F (870°C), 1800°F (980°C), 2000°F (1090°C), and 2200°F (1200°C), as determined in 100 hr. tests. (After Brasunas, Gow, and Harder)

than in the series with lower Cr contents. At 1800°F (980°C), there is a moderate improvement in corrosion by the addition of Ni up to 20 per cent. At 2200°F (1200°C), where corrosion is more severe, Ni up to 20 per cent is effective in reducing weight loss.
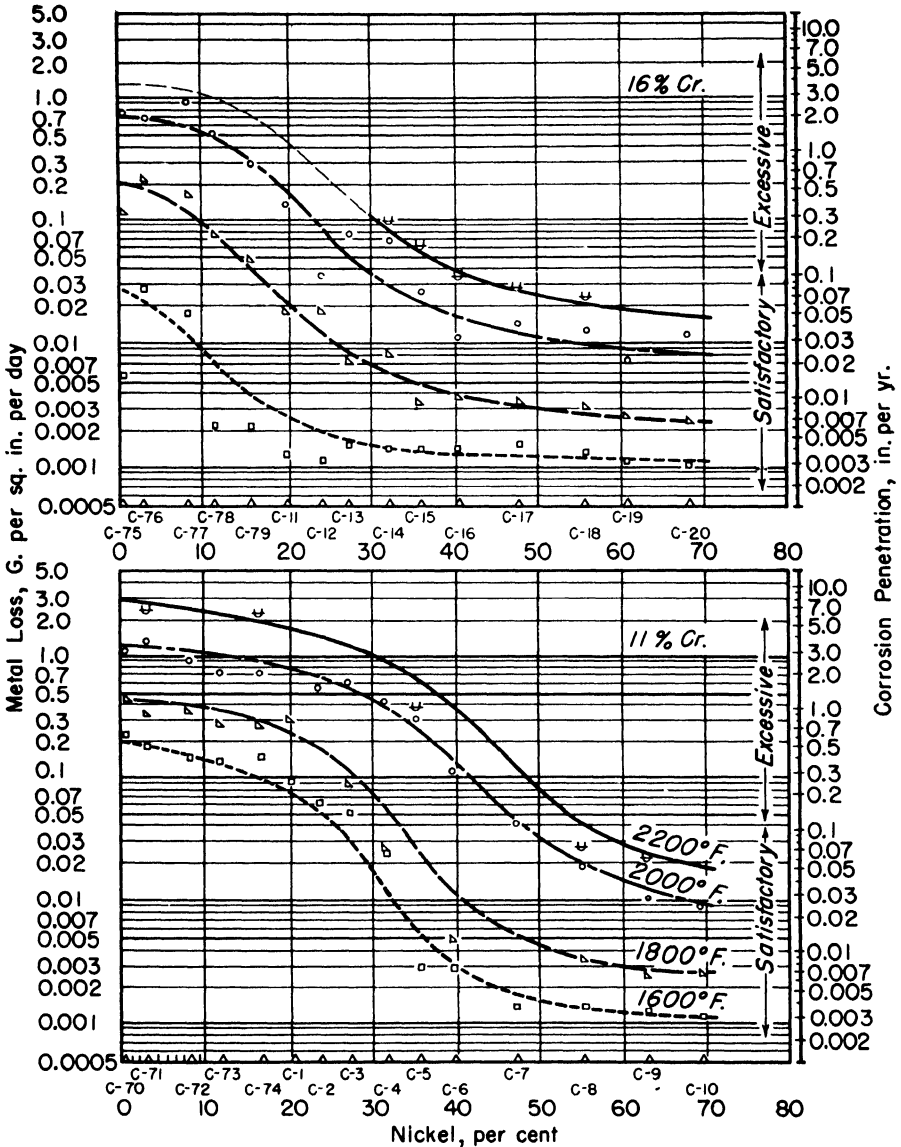
Fig. 11-3. Influence of increasing amounts of Ni at the 21, 26, and 31 per cent Cr levels on air corrosion of alloys at 1600°F (870°C), 1800°F (980°C), 2000°F (1090°C) and 2200°F (1200°C), as determined in 100 hr tests. (After Brasunas, Gow, and Harder)

4. 26 per cent. Ni does not have any great effect in this series except at 2000°F (1090°C) where 15 per cent Ni decreases corrosion.
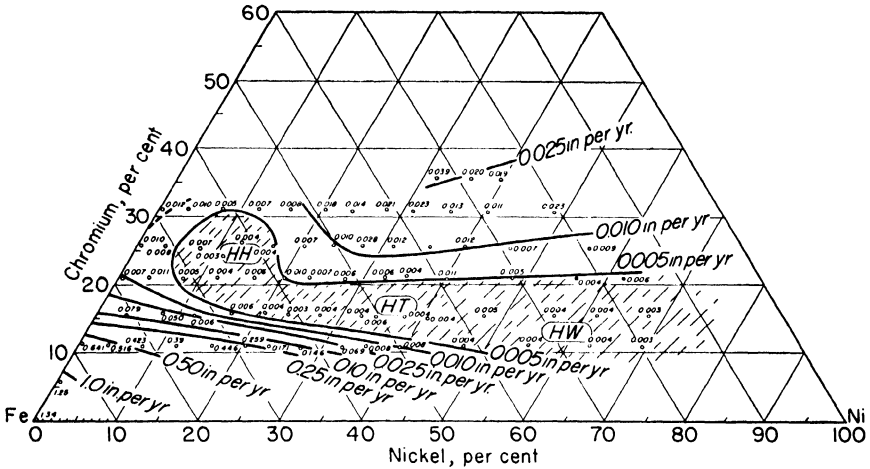
Fig. 11-4. Metal loss in air atmosphere at 1600°F (870°C) with corrosion expressed in inches penetration per year. Alloys also contain about 0.4 per cent C, 1.25 per cent Si, 0.75 per cent Mn, balance Fe. Above data are based on 100 hr. tests. (After Brasunas, Gow, and Harder)
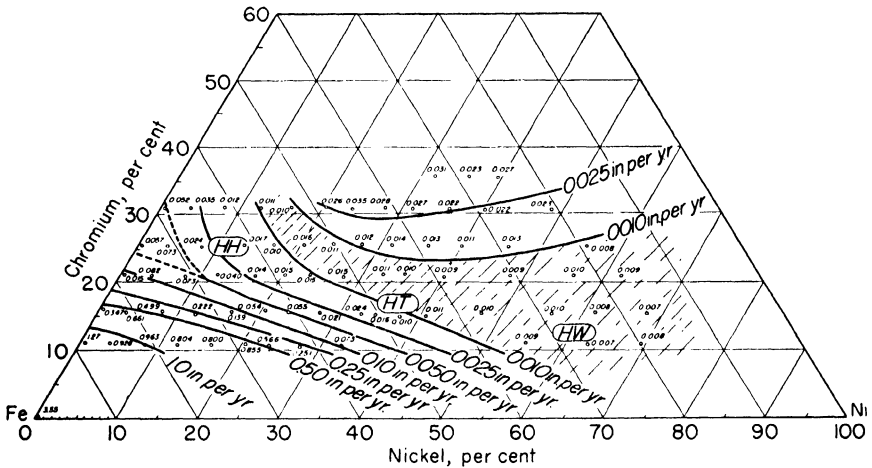
Fig. 11-5. Metal loss in air atmosphere at 1800°F (980°C) with corrosion expressed in inches penetration per year. Alloys also contain about 0.4 per cent C, 1.25 per cent Si, 0.75 per cent Mn, balance Fe. Above data based on 100 hr. tests. (After Brasunas, Gow, and Harder)

5. Higher Cr Contents, 31 and 36 per cent. For these two series of alloys, Ni contents of 10 to 20 per cent are the optimum levels for corrosion resistance.
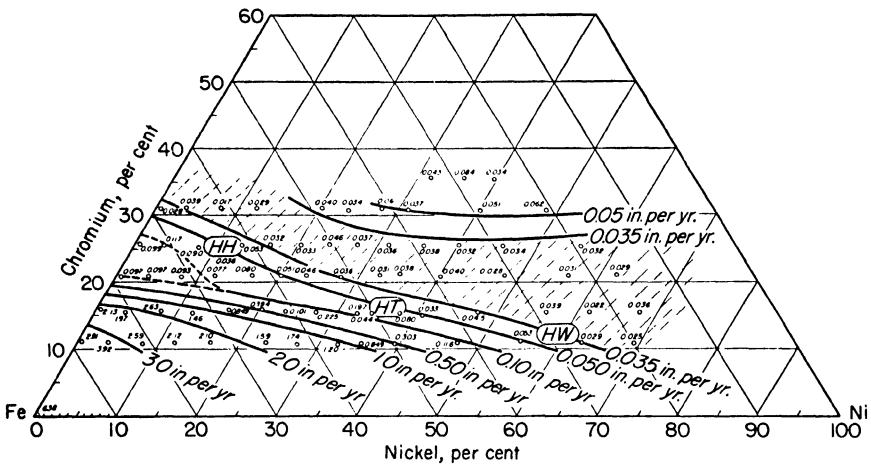
Fig. 11-6. Metal loss in air atmosphere at 2000°F (1090°C) with corrosion expressed in inches penetration per year. Alloys also contain about 0.4 per cent C, 1.25 per cent Si, 0.75 per cent Mn, balance Fe. Above data are based on 100 hr. tests· (After Brasunas, Gow, and Harder)
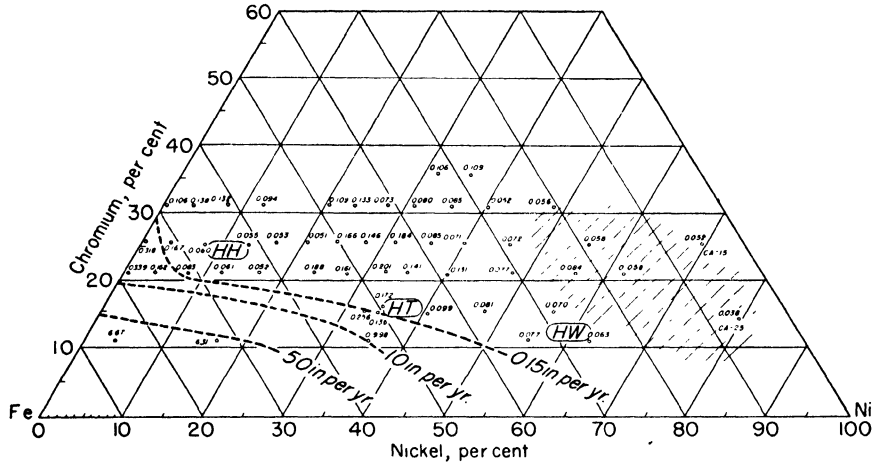
Fig. 11-7. Metal loss in air atmosphere at 2200°F (1200°C) with corrosion expressed in inches penetration per year. Alloys also contain about 0.4 per cent C, 1.25 per cent Si, 0.75 per cent Mn, balance Fe. Above data are based on 100 hr. tests. (After Brasunas, Gow, and Harder)

b. Effect of Cr. Cr contents up to 20 per cent in the absence of Ni are very effective in decreasing corrosion. At higher amounts of Cr, the advantages are small except at 2200°F (1200°C), where 25 per cent Cr is beneficial.

Contour curves of metal loss on the basis of air corrosion for 100-hour tests at temperatures of 1600°F (870°C), 1800°F (980°C), 2000°F (1090°C) and 2200°F (1200°C) are shown in Figs. 11-4, 11-5, 11-6 and 11-7 in ternary diagrams where the Ni and Cr contents are plotted for the various alloys. The loss in weight expressed as inches penetration per year is located at the point for the alloy composition. Lines are drawn to indicate isocorrosion contours or alloys which show the same loss in weight. On the graphs, the symbol HH designates the 25 per cent Cr, 12 per cent Ni casting alloy; HT represents 36 per cent Ni, 16 per cent Cr; and HW represents 60 per cent Ni, 12 per cent Cr. Aside from the Ni and Cr contents shown on the ternary diagrams, the other constituents for all the alloys are approximately 0.4 per cent C, 1.25 per cent Si, 0.75 per cent Mn, and the balance Fe.

c. Effect of Temperature. *At 1600°F (870°C).* At this temperature, the penetration varies from 0.641 to 0.003 inch per year. The slope of the curves downward towards the Ni base line suggests that Cr is more effective than Ni in oxidation resistance. The cross-hatched area shows alloys which have the lowest penetration of scale. Beyond this region corrosion rates increase. The three casting alloys, HH, HT, and HW mentioned earlier have compositions in this range.

At 1800°F (980°C). Penetration at the 1800°F (980°C) level varies from 1.27 to 0.007 in per year. In Fig. 11-5, a raising of the Cr level is shown for the alloys more resistant to corrosion.

At 2000°F (1090°C). Penetration at the 2000°F (1090°C) level varies from 3.92 to 0.022 inches per year. The corrosion rates are fairly uniform in the low Ni range where the Cr content is 20 to 30 per cent.

At 2200°F (1200°C). Penetration varies from 6.67 to 0.055 inches per year. At this high level only a few of the more resistant alloys are tested. The dotted lines indicate that there are gaps in the composition range since fewer tests were conducted at this temperature.

Tests on the Ni-Cr-Fe series carried out for periods of 1000 hours are not included here, but the trends for the most part are similar to the 100-hour tests. Intermittent heating and cooling tests show certain differences in the alloys. Where corrosion rates are higher, the loss in weight is sometimes due to cracking of the scale in the cooling operation.

This series of 100-hour tests must be regarded as indications of scale formation only for material under no load. In this respect the tests do not necessarily predict service life and are not intended for that purpose. Moreover, such studies of scale formation do not furnish data on tendencies for intergranular oxidation or interdendritic penetration of oxides for materials exposed to elevated temperatures. They are valuable, however, in obtaining information of penetration under controlled conditions of atmosphere, temperature, and weight measurements.

References

1. Agnew, J. T., Hawkins, G. A., and Solberg, H. L., "Stress-Rupture Character-
   istics of Various Steels in Steam at 1200°F," *Trans. Am. Soc. Mech. Engrs.*, **68**,
   309 (1946); Eng. Bull. 101, Purdue University.
2. Amer. Soc. Metals Handbook (1948).
3. Babcock and Wilcox Tube Co., Tech. Bull. 6-E (1948).
4. Bash, F. E. and Harsch, J. W., "Life Tests on Metallic Resistor Materials for
   Electrical Heating," *Proc. A.S.T.M.*, Part 2, **29**, 506 (1929).
5. Bauer, O., Kröhnke, O., and Masing, G., "Die Korrosion Metallischer Werk-
   stoffe," V. I. Hirzel, Leipsig, 1936.
6. Brasunas, A. deS., Gow, J. T., and Harder, O. E., "Resistance of Iron-Nickel-
   Chromium Alloys to Corrosion in Air at 1600 to 2200°F," A.S.T.M. Symposium
   on Materials for Gas Turbines (June, 1946).
7. Cornelius, H., "Scaling Behavior of Hard Alloy Welded Deposits with Different
   Cobalt Contents," *Stahl und Eisen*, **64**, 529 (Aug. 17, 1944); Iron and Steel Inst.,
   Translation Series No. 250.
8. Darken, L. S., "Diffusion in Metal Accompanied by a Phase Change," *Trans.
   Am. Inst. Min. Metall. Engrs.*, **150**, 157 (1942).
9. Dunn, J. S., "Oxidation of Some Copper Alloys," *J. Inst. Metals*, **46**, 25 (1931).
10. Evans, Ulick, "Metallic Corrosion, Passivity and Protection," Longmans, Green
    and Co., N. Y., 1946.
11. Frölich, K. W., "Die Zunderung von reinem und von legierten Kupfer," *Z. für
    Metallkunde*, **28**, 368 (1936).
12. Fry, A., "Erhohung des Korrosions-widerstandes durch Legieren," *Technische
    Mitteilungen Krupp*, **1**, 1 (1933).
13. Griffiths, R., "Blistering of Iron Oxide Scales and the Conditions for the Forma-
    tion of a Nonadherent Scale," *J. Iron and Steel Inst.*, **130**, 377 (1934).
14. Gulbransen, E. A., and Hickman, J. W., "An Electron Study of Oxide Films
    formed on Iron, Cobalt, Nickel, Chromium, and Copper at Elevated Tempera-
    tures," *Metals Technology*, T. P. 2068 (Oct., 1946).
15. Hatfield, W. H., "Heat-resisting Steels," *J. Iron and Steel Inst.*, **115**, 483 (1927).
16. Heindlhofer, K. and Larsen, B. M., "Rates of Scale Formation on Iron and a Few
    Alloys," *Trans. Am. Soc. Steel Treating*, **21**, 865 (1933).
17. Hessenbruch, W., "Metalle und Legierungen für hohe Temperaturen, Part 1—
    Zunderfeste Legierungen," Springer, Berlin, 1940.
18. Houdremont, E., "Handbuch der Sonderstahlkunde," Springer, Berlin, 1943.
19. Jost, W., "Diffusion und Chemische Reaktion in festen Stoffen," T. Steinkopf,
    1937.
20. Keller, F., and Edwards, J. D., "Formation of the Natural Oxide Film on Alumi-
    num," *Metal Progress*, **54**, 35 (1948).
21. Kornilov, I. I. and Spilekmann, A. I., "Rate of Oxidation of Chromium-Nickel-
    Iron-Austenitic Alloys," *Reports Acad. Sci. U.S.S.R.*, **54**. 515 (Nov. 21, 1946);
    Metals Rev., **20** (Mar., 1947).
22. Lustman, B., "Resistance of Metals to Scaling," *Metal Progress*, **50**, 850 (1946).
23. Matsunaga, Y., "Nickel-Chromium Alloys," *Japan Nickel Rev.*, **1**, 347 (1933).
24. Pfeil, L. B., "Oxidation of Iron and Steel at High Temperatures," *J. Iron and
    Steel Inst.*, **119**, 501 (1929).
25. Pilling, N. B. and Bedworth, R. E., "Oxidation of Metals at High Temperatures,"
    J. Inst. Metals, **29**, 529 (1923).

26. Price, L. E. and Thomas, G. F., "Oxidation Resistance in Copper Alloys," *J. Inst. Metals,* **63,** 21 (1938).

27. Scheil, E., Über das Zundern von Metallen und Legierungen, *Z. für Metallkunde,* **29,** 209 (1937).

28. Scheil, E. and Kiwit, K., "Einfluss von Legierungszusaten auf das Zundern des Eisens," *Arch. für das Eisenhüttenwesen,* **9,** 405 (1935–36).

29. Scheil, E. and Schulz, E. H.,"Hitzebeständige Chrom-Aluminium-Stähle," *Arch. für das Eisenhüttenwesen,* **6,** 155 (1932–33).

30. Smithells, C. J., Williams, S. V., and Avery, J. W., "Laboratory Experiments on High-temperature Resistance Alloys," *J. Inst. Metals,* **40,** 269 (1928).

31. Smithells, C. J., Williams, S. V., and Grimwood, E. J., "Melting Nickel-Chromium Alloys in Hydrogen," *J. Inst. Metals,* **46,** 443 (1931).

32. Thum, E. E., "Book of Stainless Steel," Am. Soc. Metals, 1935.

33. Timken Roller Bearing Co., "Digest of Steels for High Temperature Service".

34. Wetternik, L., "Method of Testing the Scaling Resistance of Heat-resistant Alloys," *Korrosion und Metallschutz,* **18,** 130 (Apr., 1942).

35. Ziegler, N. A., "Resistance of Iron-Aluminum Alloys to Oxidation at High Temperatures," *Trars. Am. Inst. Min. Metall. Engrs.,* **100,** 267 (1932).

INDEX

DATE OF ISSUE